

# **Functional Poly(phosphoester)s: Variation of Solubility, Thermal Stability, Film Formation and Gelation**

**Dissertation**

zur Erlangung des akademischen Grades eines

“Doctor rerum naturalium (Dr. rer. nat.)“

des Fachbereiches Chemie, Pharmazie und Geowissenschaften (FB 09)

der Johannes Gutenberg-Universität Mainz

vorgelegt von

**Dipl.-Chem. Greta Becker**

geboren in Goslar

Mainz, September 2017



JOHANNES GUTENBERG  
UNIVERSITÄT MAINZ



Max-Planck-Institut  
für Polymerforschung  
Max Planck Institute  
for Polymer Research





Die vorliegende Arbeit wurde im Zeitraum von Juli 2014 bis September 2017 am Max-Planck-Institut für Polymerforschung im Arbeitskreis von Prof. Dr. Katharina Landfester unter der Betreuung von Priv.-Doz. Dr. habil. Frederik R. Wurm angefertigt.

1. Gutachter: Priv.-Doz. Dr. habil. Frederik R. Wurm
2. Gutachter: Prof. Dr. Pol Besenius

#### Erklärung

Hiermit versichere ich, die vorliegende Arbeit selbstständig und ohne Benutzung anderer als der angegebenen Hilfsmittel angefertigt zu haben. Alle Stellen, die wörtlich oder sinngemäß aus Veröffentlichungen oder anderen Quellen entnommen sind, wurden als solche eindeutig kenntlich gemacht. Diese Arbeit ist in gleicher oder ähnlicher Form noch nicht veröffentlicht und auch keiner anderen Prüfungsbehörde vorgelegt worden.

Greta Becker

Mainz, September 2017



*Für meine Eltern*

***“Wir sehen nie, was wir getan haben;  
wir können nur sehen, was noch zu tun bleibt.“***

Marie Curie in einem Brief an ihren Bruder (1894)





## Danksagung

Mein besonderer Dank gilt PD Dr. habil. Frederik R. Wurm für die Möglichkeit meine Dissertation in seiner Arbeitsgruppe anzufertigen, für die Bereitstellung der Projekthemen, die hervorragende Betreuung in den letzten drei Jahren und die zahllosen wissenschaftlichen Diskussionen und Hilfestellungen. Vielen Dank für ein jederzeit offenes Ohr.

Bei Frau Prof. Dr. Katharina Landfester bedanke ich mich für die Möglichkeit die Doktorarbeit in ihrem Arbeitskreis durchzuführen und für wissenschaftliche Diskussionen.

Mein Dank gilt auch der MAINZ Graduiertenschule „Materials Science in Mainz“ für die finanzielle Unterstützung während meiner Arbeit. Die Förderung ermöglichte mir meine Projekte zu realisieren, meinen wissenschaftlichen Horizont auf Konferenzen und Sommerschulen zu erweitern und in einen wissenschaftlichen Austausch mit der Fachgemeinschaft zu treten. Das große Workshopangebot und Mentorenprogramm ermöglichte mir eine Weiterentwicklung meiner persönlichen Kompetenzen. Allen Mitarbeitern des Koordinationsbüros danke ich für jegliche organisatorische Unterstützung, insbesondere Edeltraud Eller und Michael Fuchs für viele gute Diskussionen und ihre Unterstützung. Die Graduiertenschule wird mir noch lange in Erinnerung bleiben durch zahlreiche schöne gemeinschaftliche Veranstaltungen als den auch wissenschaftlichen Austausch mit den MAINZ Studenten.

Bei meinen zahlreichen Kooperationspartnern möchte ich mich für die gute Zusammenarbeit bedanken, ohne die die Umsetzung meiner Projekte nicht möglich gewesen wäre. Die wissenschaftlichen Diskussionen mit PD Dr. habil. Karen Lienkamp, Prof. Dr. Aránzazu del Campo und Prof. Dr. Sigfried Waldvogel haben einen wichtigen Beitrag zu meinen Projekten geleistet. Danke möchte ich auch Prof. Dr. Wolfgang Tremel, Prof. Dr. Markus Klapper und Prof. Dr. Filip E. du Prez. Mein Dank gilt Lisa-Maria Ackermann, Eugen Schechtel, Laetitia Vlaminck, Zhuoling Deng, Maria Vöhringer, Oya Ustahüseyin für die technische und synthetische Unterstützung und analytische Messungen, und Dr. Günter K. Auernhammer für die Benutzung seines Piezorheometers.

Für ihre Unterstützung bei analytischen Messungen danke ich der Gruppe der Polymeranalytik, Dr. Manfred Wagner, Stefan Spang und Kathrin Kirchhoff. Angelika Manhardt, Tizian Passow, Katja Weber, Tristan A. Marquetant und Chiara Pelosi danke ich für die synthetische Unterstützung im Labor.

Weiterhin bedanke ich mich bei Dr. Tobias Steinbach, Kristin Bauer, Hisaschi Tee, Thomas Wolf, Maria Valencoso und Alper Cankaya für wissenschaftliche und synthetische Diskussionen über Poly(phosphoester).

Ein großer Dank gilt allen (ehemaligen) Mitgliedern der Arbeitsgruppe Wurm, meinen lieben Labor- und Bürokollegen und (ehemaligen) Kollegen im Arbeitskreis Landfester für ein gemeinsames Arbeiten im Labor, vor allem aber für eine tolle gemeinsame Zeit, viele schöne Erlebnisse miteinander, eine tolle Arbeitsatmosphäre und gute Zusammenarbeit.

Mein persönlicher Dank gilt meiner Mentorin Frau Dr. Ursula Loggen für ihre persönliche Unterstützung durch zahlreiche Gespräche und Ratschläge.

Mein größter Dank gilt schließlich meiner Familie, die mich immer unterstützt hat meine Ziele zu erreichen, mich in schwierigen Phasen unermüdlich ermutigt weiterzumachen und immer ein offenes Ohr für mich hat. Hendrik danke ich für seine persönliche Unterstützung und Verständnis in der letzten Phase meiner Doktorarbeit. Meinen Freunden danke ich dafür, dass ich in den letzten Jahren auch noch ein soziales Leben und viele schöne Erlebnisse und Erinnerungen außerhalb der Arbeit genießen durfte.

## Table of Contents

<b>Motivation and Objectives</b> .....	<b>4</b>
<b>Abstract</b> .....	<b>8</b>
<b>Zusammenfassung</b> .....	<b>10</b>
<b>Graphical Abstract</b> .....	<b>13</b>
<b>1 Introduction: Synthetic biodegradable polymers from ring-opening polymerization: Insight in the toolbox of orthogonally reactive cyclic monomers</b> .....	<b>17</b>
1.1 Abstract.....	18
1.2 Introduction.....	18
1.3 Degradation.....	19
1.4 Overview on orthogonally reactive groups.....	22
1.5 Poly(ester)s.....	25
1.6 Poly(amide)s.....	43
1.7 Poly(carbonate)s.....	58
1.8 Poly(phosphoester)s.....	71
1.9 Poly(organophosphazene)s.....	76
1.10 Conclusions and Outlook.....	78
<b>2 Joining two natural motifs: catechol-containing poly(phosphoester)s</b> .....	<b>91</b>
<b>3 Investigation on catechol-containing poly(phosphoester)-hydrogels</b> .....	<b>137</b>
<b>4 Multifunctional poly(phosphoester)s for reversible Diels-Alder postmodification to tune the LCST in water</b> .....	<b>173</b>
<b>5 Toward surface-attached poly(phosphoester)-networks as coatings</b> .....	<b>225</b>
<b>6 Breathing air as oxidant: Optimization of 2-chloro-2-oxo-1,3,2-dioxaphospholane synthesis as a precursor for phosphoryl choline derivatives and cyclic phosphate monomers</b> .....	<b>279</b>
<b>7 Triazolinedione-“clicked” poly(phosphoester)s: Systematic adjustment of thermal properties</b> .....	<b>295</b>
<b>8 Conclusions</b> .....	<b>319</b>
<b>9 Appendix</b> .....	<b>320</b>
9.1 List of Publications.....	320
9.2 Curriculum Vitae.....	321



## Motivation and Objectives

Synthetic polymers, inspired by natural biopolymers, are of great interest in materials science. A broad range of polymer classes, including poly(ester)s, poly(amide)s, and poly(phosphoester)s, has been developed mimicking binding motifs within their backbone from biopolymers, e.g. polyhydroxyalkanoates, polypeptides or (desoxy)ribonucleic acids (DNA and RNA).

Oligomeric poly(phosphoester)s (PPEs) from polycondensation initially gained interest as niche products for flame-retardants in the middle of the last century. Ever since the development of modern organocatalysts for the anionic ring-opening polymerization (AROP), which also produces well-defined PPEs with high molecular weights and narrow polydispersities from cyclic phosphates, PPE-based materials became attractive especially for biomedical applications. They exhibit good biocompatibility and -degradation profiles. The nature of carbon spacers in the backbone of PPEs, the binding motif around the phosphorus atom and nature of pendant chains strongly influence the material properties, alter their solubility, change their degradation profiles and allow introduction of functional groups (Figure 1).

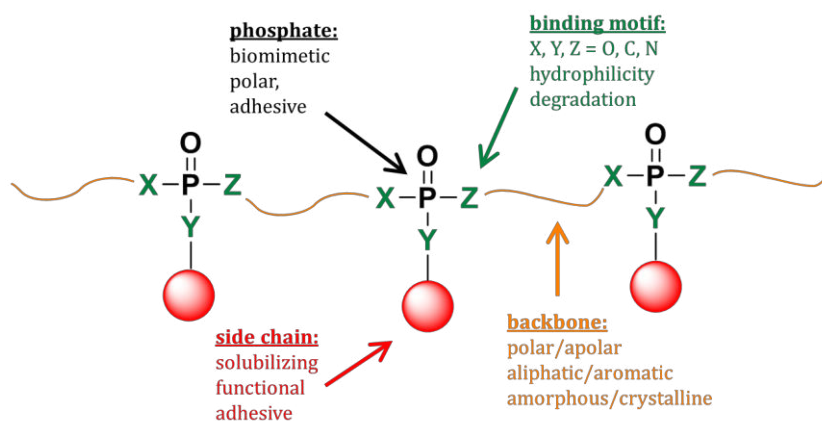


**Figure 1.** The platform of poly(phosphoester)s and their parameters influencing the materials' properties.

Advanced polymeric materials often require incorporation of chemical functionalities, e.g. to further tune their properties and to attach labels or other molecules along the backbone. However, polymerization methods only tolerate a limited number of functionalities, not interfering with the polymerization mechanism or applied catalysts. Different approaches include (i) protection of the active functional group in monomers during polymerization and a later release of the functionality, (ii) the use of orthogonal functionalities which are reactive itself, e.g. photo- or redox-reactive and (iii) the use of orthogonally reactive functions, which are accessible for post-modification reactions. Modification can occur on functional end groups, functions within the backbone of polymers or in the pendant chains. Prominent modification reactions include concepts as thiol-ene, thiol-yne or alkyne-azide click reaction, cycloaddition, Michael-addition, nucleophilic substitution of

alkylhalogenides, esterification of activated esters and acid chlorides and radical reactions mainly for cross-linking purposes.

With the pendant group in PPEs, the introduction of functional groups in each repeating unit is possible. Besides a number of protected functional cyclic phosphate monomers for ROP, including protected hydroxyl, amino, or guanidyl groups, only a few orthogonally reactive monomers have been reported with alkyne, alkene, or vinyl ether functions, allowing irreversible post-modification. The development of novel functional phosphate monomers will give excess to advanced PPE-based materials and broaden their areas of application. The objectives of the current thesis are therefore the **extension of the toolbox of functional phosphate monomers** suitable for ROP or ADMET polymerization (Figure 2), **their polymerization to chemically functional PPEs** and extensive **investigations on the variation of their properties for novel possible applications** to broaden the scope of PPEs.

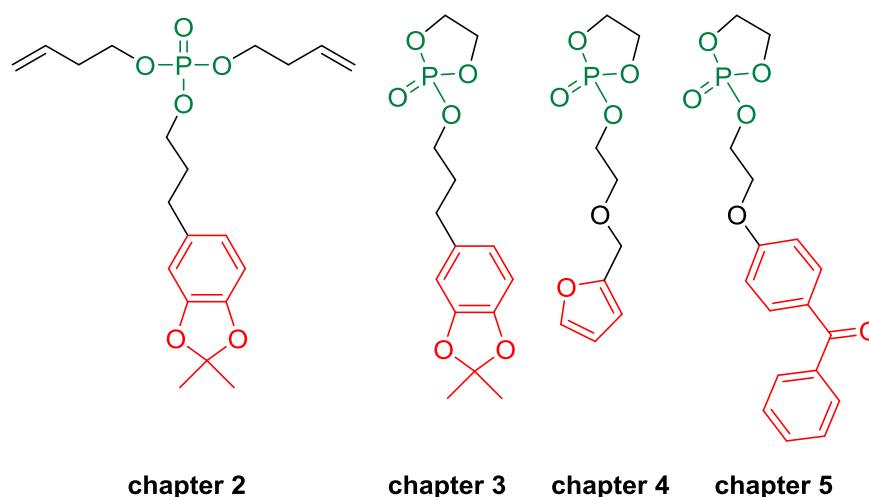


**Figure 2.** Novel functional phosphate monomers developed in the current thesis, suitable for ROP or ADMET polymerization.

**Catechol-functionalized PPEs (chapter 2&3):** The combination of catechols and PPEs has been studied. Mussel-inspired catechol-modified polymers are currently heavily discussed as bioadhesives, hydrogels or anchor groups, due to their ability to coordinate metal ions/oxides and to react with amines, thiols and other catechols under oxidative alkaline conditions. Phosphate groups in PPEs exhibit adhesive properties.

Two phosphate monomers, an acyclic phosphate suitable for ADMET polycondensation and a cyclic phosphate for ROP, both carrying a protected catechol group, have been developed. Multicatechol-PPEs were prepared after polymerization and acidic hydrolysis of the protecting group. These PPEs are promising materials due to the combination of two adhesive motifs. The polymers prepared by ADMET polycondensation were studied with respect to their adhesive properties. They bound to magnetite nanoparticles (NPs) and were attractive to stabilize them in

polar organic solvents, which might be interesting for biomedical imaging based on metal oxide NPs or nanocarrier functionalization. They are also interesting for tissue engineering, due to their additionally cohesive properties. An increasing market share demands of the development of novel wound sealants for soft tissue and bioadhesives for hard bone tissue. Oxidative cross-linking of the multicatechol-PPEs produced organo- and hydrogels. The curing time and mechanical properties of the more hydrophilic PPEs from ROP were investigated, which are crucial for potential application of the PPE-networks as “bone glue”.

**Furan-functionalized PPEs (chapter 4):** The combination of furans and PPEs has been studied with respect to their thermoresponsive properties. Thermoresponsive PPEs are promising materials for future drug delivery and temperature-responsive devices. While homopolymers exhibit a certain cloud point (CP), copolymerization allows adjustment of the CP depending on the comonomer ratio. However, the CP of copolymers cannot be altered after synthesis. Post-modification allows further adjustment of the solubility and thermoresponsive properties of the same copolymer. The [4+2] Diels-Alder (DA) cycloaddition is attractive for post-modification, because it is a catalyst-free reaction with typically high conversions, a broad substrate spectrum and exhibits thermal reversibility at elevated temperatures.

The development of a furan-functionalized cyclic phosphate monomer and corresponding copolymers gave access to PPEs, which exhibited a thermoresponsive behavior in water, depending on the furan content. Further adjustment of the solubility and thermoresponsive properties of the same copolymer was possible by post-modification of the PPE-copolymers via the DA reaction with maleimides of different hydrophilicity. It also allowed the synthesis of PPE-polyelectrolytes and is the first reversible post-modification for PPEs.

**Benzophenone-functionalized PPEs (chapter 5):** Photo-reactive PPEs have been studied with respect to their film formation. PPEs are biocompatible and might be potential anti-fouling coatings for biomedical devices as implants or catheters due to their stealth effect. Benzophenones can photochemically cure polymer films by a C,H-insertion cross-linking reaction (CHic process) with methylene groups.

A benzophenone-functionalized cyclic phosphate monomer has been developed and studied in the ROP to prepare hydrophilic and multibenzophenone-PPEs. Film formation and the first covalently surface-attached and cross-linked PPE-networks has been achieved by spin-coating and UV-irradiation. The PPE-coatings were physically characterized in detail.

**Optimization of the preparation of COP (chapter 6):** 2-chloro-2-oxo-1,3,2-dioxaphospholane (COP) is an important intermediate and the precursor for the synthesis of cyclic phosphate monomers for ROP. Although commercially available, high demands on purity, pricing and delivery issues of COP still require in-house synthesis. Established synthesis protocols include an oxidation

reaction with molecular oxygen from a gas bottle, lavish a high amount of unreacted oxygen due to slow consumption and may cause an explosive atmosphere.

Optimization of the reaction set up using oxygen from air and a catalyst avoided wasting of oxygen and reduced reaction times from days to several hours, making the synthesis more convenient and a safer alternative in university labs.

**TAD-clicked PPEs (chapter 7):** The combination of 1,2,4-triazoline-3,5-diones (TADs) and PPEs have been studied with respect to their thermal properties. PPEs usually exhibit low glass transition temperatures ( $T_g$ 's) between -40 and -60 °C, which limit the range of applications. Post-modification of unsaturated polymers with TADs is quantitative at room temperature, increases their  $T_g$ 's and alters the thermal degradation profiles.

Unsaturated PPEs with different main- and side chains were modified with several TAD-derivatives, which is the first report on the post-modification of PPEs from ADMET polycondensation *via* the internal double bonds of the backbone and the TAD-clicked PPEs. Examination of thermal properties revealed significantly increased  $T_g$ 's and improved thermal stability and char yields, contributing to the current discussion of PPEs as potent, halogen-free flame retardants.

The corresponding Outlook and Supporting Information for the chapters are always at the end of each chapter.

---

## Abstract

Synthetic poly(phosphoester)s (PPEs) are inspired by the most important natural biopolymer desoxyribose nucleic acid (DNA). They are rarely noticed, in spite of their versatile properties. Modern polymerization methods, e.g. acyclic diene metathesis polymerization (ADMET) and especially ring-opening polymerization (ROP) by organocatalysis, provide well-defined PPEs with controllable molecular weights and narrow polydispersities, which has increased the attention as potential materials for biomedical or flame-retardant applications. Functionalization and post-modification is often required in advanced polymeric materials to further fine-tune their properties, but is still limited for PPEs. The aim of this thesis is the introduction of novel functional PPEs to improve their properties and broaden the range of applications.

**Chapter 1** gives an insight into available, orthogonally reactive cyclic monomers and corresponding functional synthetic and biodegradable polymers, obtained from ROP. Functionalities in the monomer are reviewed, which are tolerated by ROP without further protection and allow further post-modification of the corresponding chemically functional polymers after polymerisation. Synthetic concepts to these monomers are summarized in detail, preferably using precursor molecules. Post-modification strategies for the reported functionalities are presented and selected applications highlighted.

**Chapter 2** focuses on catechol-containing PPEs from ADMET polycondensation. The combination of catechol and phosphate functions displayed adhesive and cohesive properties and turned out to be an attractive strategy for the generation of hydrogels or functionalization of metal oxide nanoparticles (NPs). A novel acetal-protected catechol phosphate was copolymerized with a phosphoester comonomer and the release of catechols was quantitative by acidic hydrolysis without backbone degradation. The PPEs revealed complete and statistical degradation of the phosphotri- to phosphodiester under basic conditions. Catechol-modified PPEs, P-OH-functional poly(phosphodiester)s and unfunctionalized poly(phosphotriester)s bound to magnetite NPs, due to the phosphoester groups in the backbone, and enhanced the stability of NPs in polar organic solvents. Significantly higher binding affinity of multicatechol-PPEs was observed, because of additional binding of the catechols. Multicatechol-PPEs were further used to generate organo- and hydrogels by oxidative cross-linking, due to cohesive properties of catechols.

In **Chapter 3**, the catechol function was further extended to more hydrophilic PPEs from ROP. A novel acetal-protected cyclic catechol phosphate was copolymerized and deprotected. The curing time and mechanical properties of oxidatively cross-linked PPE-networks were examined with respect to potential properties for bone adhesives.

**Chapter 4** focuses on the first functional PPEs, which can be reversibly post-modified. A furfuryl-carrying cyclic phosphate was designed. Variation of the furan content in copolymers

allowed adjustment of the cloud points. Post-modification of the thermoresponsive copolymers by Diels-Alder reaction with maleimides of different hydrophilicity and charge further altered the solubility profile and created a library of completely water-soluble or -insoluble PPEs. Thermal reversibility of the post-modification has been shown in kinetic studies, and the biodegradable PPE backbone remained unaffected. The approach allowed access to PPE-electrolytes, which pH-dependently differed their solubility in water.

**Chapter 5** describes the development of PPE-films as potential coatings for biomedical devices. A benzophenone-carrying cyclic phosphate and corresponding copolymers were synthesized. The incorporation kinetic of different comonomers into photo-active PPE-terpolymers with additional furan, alkene or alkyl functions has been studied. Film formation of covalently surface-attached and cross-linked PPE-networks was achieved by photochemical reaction of the benzophenone functions with methylene groups. Their physical characteristics have been studied. Additional furan or alkene functions in the networks present an addressable platform to further tune the properties of PPE-films.

**Chapter 6** describes an optimization of the synthetic protocol of 2-chloro-2-oxo-1,3,2-dioxaphospholane (COP), a precursor molecule for cyclic phosphate monomers. The oxidation of 2-chloro-1,3,2-dioxaphospholane (CP) to COP was improved using oxygen from air instead of molecular oxygen from a gas bottle, overcoming the release of high amounts of unreacted oxygen and being a safer alternative in university labs. Catalytic amounts of cobalt(II)chloride increased the reaction kinetics remarkably from days to several hours, resulting in COP with a very high purity and good yields.

**Chapter 7** describes the first post-modification of unsaturated PPEs from ADMET polycondensation *via* the internal double bonds within their backbone using 1,2,4-triazoline-3,5-diones (TADs), which altered their thermal properties. TAD-modification was quantitative at room temperature. A systematic study with structural variation of the main and side chains of PPEs and modification with several TADs showed significant increase of the glass transition temperatures and improved the thermal stability with respect to their decomposition temperatures, degradation profiles and char yields. The improvement of thermal properties has a positive impact, using PPEs as potent, halogen-free flame retardants.

---

## Zusammenfassung

Synthetische Poly(phosphoester) (PPEs) sind von dem wichtigsten natürlichen Biopolymer, der Desoxyribonukleinsäure (DNA), inspiriert. Trotz ihrer vielfältigen Eigenschaften werden sie in der Fachliteratur wenig beachtet. Moderne Polymerisationsverfahren, wie z.B. die azyklische Dienmetathese-Polymerisation (ADMET) und insbesondere die organokatalytische Ringöffnungspolymerisation (ROP), liefern definierte PPEs mit kontrollierbaren Molekulargewichten und engen Molekulargewichtsverteilungen. Mit der Entwicklung dieser Verfahren stieg die Aufmerksamkeit für PPEs als potenzielle Materialien für biomedizinische Anwendungen und als flammenhemmende Zusätze. Wie bei allen modernen polymeren Werkstoffen sind auch bei den PPEs Funktionalisierungen und Modifizierungsmöglichkeiten häufig erforderlich, um ihre Eigenschaften zu verfeinern und den jeweiligen Anwendungen anpassen zu können. Diese Möglichkeiten sind für PPEs allerdings noch begrenzt. Das Ziel dieser Doktorarbeit ist daher die Entwicklung neuartiger funktioneller PPEs zur Verbesserung ihrer Eigenschaften und der Erweiterung des Anwendungsspektrums.

**Kapitel 1** umfasst einen Einblick in verfügbare, orthogonal reaktive und zyklische Monomere, aus denen durch die ROP funktionelle, synthetische und bioabbaubare Polymere erhalten werden können. Zunächst werden Funktionalitäten in den Monomeren betrachtet, die ohne weitere Schutzgruppen von der ROP toleriert werden und eine Modifizierung der entsprechenden funktionellen Polymere nach der Polymerisation erlauben. Die synthetischen Konzepte zu diesen Monomeren, bei denen bevorzugt Vorläuferverbindungen verwendet werden, werden detailliert zusammengefasst. Außerdem werden nachträgliche Modifikationsstrategien für die betrachteten Funktionalitäten vorgestellt und ausgewählte Anwendungsbeispiele hervorgehoben.

**Kapitel 2** befasst sich mit Catechol-haltigen PPEs aus der ADMET-Polykondensation. Die Kombination aus Catechol- und Phosphatfunktionen zeigte adhäsive und kohäsive Eigenschaften und erwies sich als eine attraktive Strategie zur Erzeugung von Hydrogelen oder zur Funktionalisierung von Metalloxid-Nanopartikeln (NPs). Ein neuartiges Acetal-geschütztes Catecholphosphat wurde mit einem Phosphoester-Comonomer copolymerisiert. Die Freisetzung der Catechole durch saure Hydrolyse und ohne Abbau des Polymerrückgrats war quantitativ. Die PPEs zeigten einen vollständigen und statistischen Abbau der Phosphotriester zu -diestern unter basischen Bedingungen. Catechol-modifizierte PPEs, P-OH-funktionelle Poly(phosphodiester) und unfunktionalisierte Poly(phosphotriester) banden aufgrund der Phosphoestergruppen im Rückgrat an Magnetit-NPs und erhöhten ihre Stabilität in polaren organischen Lösungsmitteln. Eine deutlich höhere Bindungsaffinität der Multicatechol-PPEs wurde aufgrund der zusätzlichen Catechole beobachtet. Die Multicatechol-PPEs wurden zusätzlich zur Herstellung von Organo- und Hydrogelen durch oxidative Vernetzung verwendet, welche auf die kohäsiven Eigenschaften von

Catecholen zurückzuführen ist. Die Betrachtung der Catecholfunktionen wurde in **Kapitel 3** auf hydrophilere PPEs aus der ROP ausgeweitet. Ein neuartiges Acetal-geschütztes zyklisches Catecholphosphat wurde copolymerisiert und entschützt. Die Aushärtungszeit und mechanische Eigenschaften von oxidativ vernetzten PPE-Gelen wurden hinsichtlich möglicher Eigenschaften für Knochenklebstoffe untersucht.

**Kapitel 4** konzentriert sich auf die ersten funktionalen PPEs, die nachträglich reversibel modifiziert werden können. Es wurde ein Furan-haltiges zyklisches Phosphat entwickelt. Die Änderung des Furangehaltes in Copolymeren erlaubte eine Anpassung der Trübungspunkte. Die Modifizierung der thermoresponsiven Copolymere durch eine Diels-Alder-Reaktion mit Maleinimiden unterschiedlicher Hydrophilie und Ladung veränderte weiterhin das Löslichkeitsprofil und schuf eine Bibliothek vollständig wasserlöslicher oder -unlöslicher PPEs. Die thermische Reversibilität der Nachmodifikation konnte in kinetischen Studien nachgewiesen werden, bei denen das Rückgrat der biologisch abbaubaren PPEs unbeeinflusst blieb. Die Herangehensweise ermöglichte zusätzlich den Zugang zu PPE-Elektrolyten, die ihre Wasserlöslichkeit in Abhängigkeit vom pH-Wert änderten.

**Kapitel 5** beschreibt die Entwicklung von PPE-Filme als potenzielle Beschichtungen für biomedizinische Geräte. Ein Benzophenon-haltiges zyklisches Phosphat und entsprechende Copolymere wurden hergestellt. Die Einbaukinetik verschiedener Comonomere in photoaktive PPE-Terpolymere mit zusätzlichen Furan-, Alken- oder Alkylfunktionen wurde untersucht. Die Filmbildung von kovalent-oberflächengebundenen und -vernetzten PPE-Netzwerken wurde durch photochemische Reaktion der Benzophenon-Funktionen mit Methylengruppen erreicht und physikalisch charakterisiert. Zusätzliche Furan- oder Alkenfunktionen in den Netzwerken stellen eine adressierbare Plattform für eine Nachmodifizierung dar, um die Eigenschaften der PPE-Filme zu optimieren.

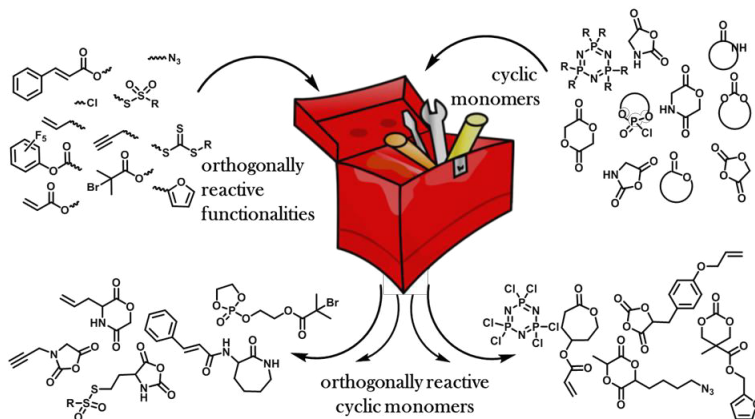
**Kapitel 6** konzentriert sich auf die Optimierung des synthetischen Protokolls zur Herstellung von 2-Chloro-2-oxo-1,3,2-dioxaphospholan (COP), einem Vorläufermolekül für die Synthese zyklischer Phosphatmonomere. Die Synthese von COP durch Oxidation von 2-Chloro-1,3,2-dioxaphospholan (CP) wurde unter Verwendung von Sauerstoff aus der Luft anstelle von molekularem Sauerstoff aus einer Gasflasche optimiert. Die Freisetzung von großen Mengen nicht reagierten Sauerstoffs wird so vermieden und das Protokoll stellt eine sicherere Synthesealternative in akademischen Laboren dar. Cobalt(II)chlorid in katalytischen Mengen erhöhte die Reaktionskinetik deutlich von mehreren Tagen auf einige Stunden und COP mit sehr hoher Reinheit und guten Ausbeuten wurde erhalten.

**Kapitel 7** beschreibt die erste Nachmodifizierung ungesättigter PPEs aus der ADMET-Polykondensation an deren internen Doppelbindungen in ihrem Rückgrat mit 1,2,4-Triazolin-3,5-

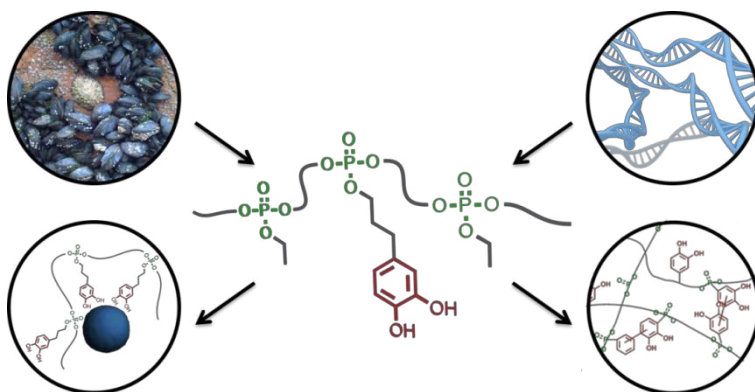
dionen (TADs), wodurch ihre thermischen Eigenschaften verändert wurden. Die TAD-Modifizierungen waren quantitativ bei Raumtemperatur. Eine systematische Studie mit strukturellen Änderungen der Haupt- und Seitenketten von PPEs und Modifizierung mit verschiedenen TADs zeigte einen signifikanten Anstieg der Glasübergangstemperaturen und verbesserte die thermische Stabilität in Bezug auf Zersetzungstemperaturen und -profile sowie Verkohlungsausbeuten. Die Verbesserung der thermischen Eigenschaften ist ein positiver Aspekt, PPEs als wirksame und halogenfreie, flammenhemmende Zusätze zu verwenden.

## Graphical Abstract

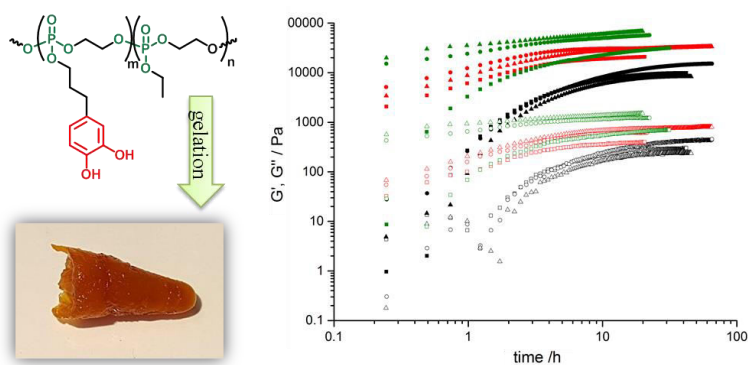
### 1 Introduction: Synthetic biodegradable polymers from ring-opening polymerization: Insight in the toolbox of orthogonally reactive cyclic monomers.....17



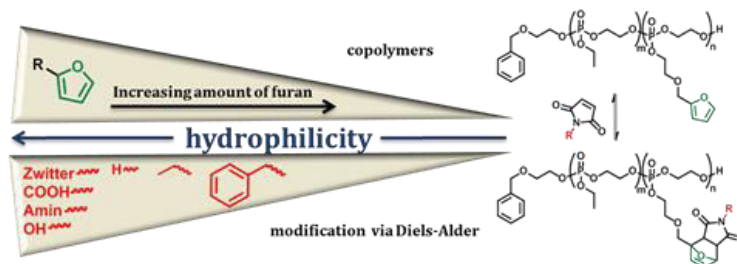
### 2 Joining two natural motifs: catechol-containing poly(phosphoester)s.....91



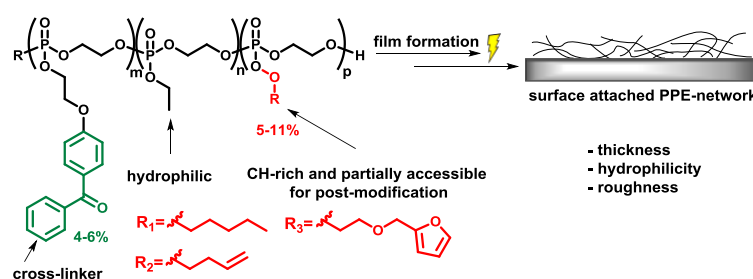
### 3 Investigation on catechol-containing poly(phosphoester)-hydrogels.....137



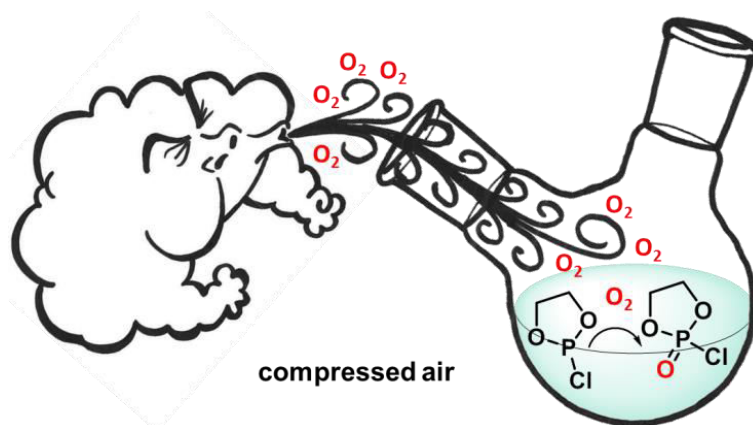
#### 4 Multifunctional poly(phosphoester)s for reversible Diels-Alder postmodification to tune the LCST in water.....173



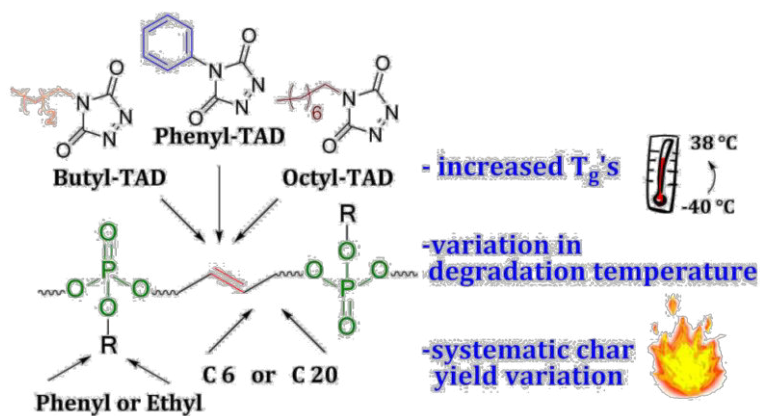
#### 5 Toward surface-attached poly(phosphoester)-networks as coatings.....225



#### 6 Breathing air as oxidant: Optimization of 2-chloro-2-oxo-1,3,2-dioxaphospholane synthesis as a precursor for phosphoryl choline derivatives and cyclic phosphate monomers.....279



**7 Triazolinedione-“clicked” poly(phosphoester)s: Systematic adjustment of thermal properties.....295**



## 1. Introduction:

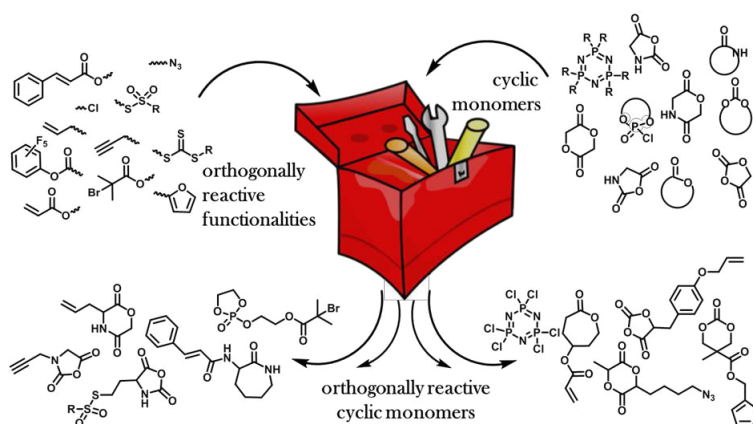
### Synthetic biodegradable polymers from ring-opening polymerization: An insight in the toolbox of orthogonally reactive cyclic monomers

Greta Becker,<sup>1,2</sup> Frederik R. Wurm<sup>1</sup>

<sup>1</sup>Max Planck Institute for Polymer Research, Ackermannweg 10, 55128 Mainz, Germany

<sup>2</sup>Graduate School Materials Science in Mainz, Staudinger Weg 9, 55128 Mainz, Germany

Unpublished review.



## 1.1 Abstract

Biodegradable polymers are of current interest and chemical functionality in such materials is often demanded in advanced biomedical applications. Functional groups often are not tolerated in the polymerization process of ring-opening polymerization (ROP) and therefore protective groups need to be applied. Advantageously, many orthogonally reactive functions are available, which do not demand protection during ROP. We give an insight into available, orthogonally reactive cyclic monomers and corresponding functional synthetic and biodegradable polymers, obtained from ROP. Functionalities in the monomer are reviewed, which are tolerated by ROP without further protection and allow further post-modification of the corresponding chemically functional polymers after polymerization. Synthetic concepts to these monomers are summarized in detail, preferably using precursor molecules. Post-modification strategies for the reported functionalities are presented and selected applications highlighted.

## 1.2 Introduction

Biodegradable polymers are of great current interest for biomedical applications, e.g. for drug and gene delivery systems, bioengineering scaffolds or as bioadhesives. They employ binding motifs within their backbone, inspired by natural biopolymers, e.g. polysaccharides, polyhydroxyalkanoates, polypeptides or (desoxy)ribonucleic acids (DNA and RNA). A broad range of synthetic biodegradable polymer classes has been developed so far, including poly(ester)s, poly(amide)s, poly(carbonate)s, poly(phosphoester)s, poly(phosphazene)s, poly(ester amide)s, poly(ester ether)s, poly(ester anhydride)s, poly(ester urethane)s, poly(ester urea)s, poly(acetal)s, poly(orthoester)s, poly(dioxanone)s and poly(iminocarbonate)s, which can be obtained by step-growth polycondensation or -addition or chain-growth polymerization.<sup>1</sup> Especially, when it comes to advanced applications, chemical functionality in such materials is demanded, e.g. to attach labels or other molecules along the backbone.

With a plethora of modern catalysts, the chain growth approach has a higher control over molecular weights and polydispersities. Different mechanisms are available, including cationic, anionic, enzymatic, coordinative and radical ring-opening polymerization (ROP). Copolymerization of different cyclic monomers with pendant alkyl or aryl groups gives access to a variety of polymeric materials with a broad range of different physical properties, e.g. varying hydrophilicity/hydrophobicity, crystallinity, solubility, mechanical strength, degradation behavior or thermal stability. Properties and features, as well as their advantages and drawbacks of the different classes of synthetic biodegradable polymers are beyond our scope and are extensively discussed in several reviews.<sup>2-4</sup>

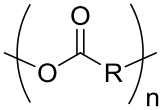
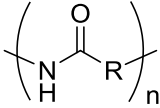
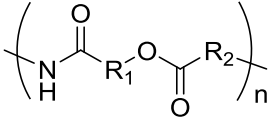
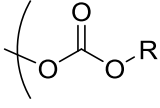
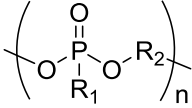
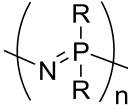
While copolymerization of alkylated and arylated monomers adjusts the materials properties, fine-tuning of the polymers is often demanded for specific applications: additional attachment of bioactive molecules, redox- or pH-sensitive functionalities or cross-linkable groups might be required for their applications. On the one hand, (especially) ionic ROP might be sensitive to impurities and tolerates only certain chemical functionalities. The sensitivity to moisture and thereby the exclusion of water as reaction solvent is a drawback. On the other hand, also bioactive molecules (e.g. carbohydrates, peptides or proteins) can be sensitive or undergo side-reactions that they do not tolerate the polymerization process or conditions, e.g. organic solvents, high temperatures or required catalysts. Great effort has been made in the last decades, developing cyclic monomers with orthogonal chemical functions, which do not interfere the polymerization process. These monomers can be divided into two groups: (I) orthogonally reactive groups that do not interfere with the polymerization, but can be post-modified afterwards; (II) active groups, e.g. photo- or redox-active.

In this review, we summarize synthetic strategies to orthogonally reactive cyclic monomers reported in the literature that allow subsequent post-polymerization modification. We highlight the general concepts, preferably using precursor molecules, which can be used to prepare these monomers and thereby chemically functional biodegradable polymers by ROP (Table 1.1). A comparison on the synthetic ease of the different monomer classes will be given, that helps to choose the polymer class of choice for the desired application. We further display post-modification strategies with selected applications. The scope of the review is to be a handbook on the preparation of orthogonally reactive cyclic monomers to deliver a “toolbox” on how functional synthetic biodegradable polymers are prepared and post-modified.

### 1.3 Degradation

All the herein discussed polymer classes are degradable, due to certain linkages in the backbone. The degradation profile is one of the most important features of these polymers, depending on their area of application. Several of the examples given in this review are claimed to be degradable, due to labile ester or amide linkages in the backbone, although degradation behavior was not studied in detail. Degradation is possible by acidic, alkaline, enzymatic, microbial or oxidative hydrolysis of ester/amide bonds. The comparison of degradation rates and conditions is difficult, as the degradation profiles depend on various factors: the hydrophilicity or hydrophobicity, water-solubility, crystallinity, glass transition, and/ or glass transition temperature, processing, size, geometry (in bulk, as foams, thin fibers, nanoparticles, micelles, in solution, etc.), porosity and water diffusion. In addition, the degree of polymerization, steric of any substituents, polymer architecture, and solubility of degradation products have a strong impact on

**Table 1.1.** Overview on the monomers and polymer classes discussed in this review.

polymer class	general structure	cyclic monomers
<b>poly(ester)s</b>		lactone macrolactone glycolide lactide hemilactide <i>O</i> -carboxyanhydride (OCA)
<b>poly(amide)s</b>		lactam $\alpha$ - <i>N</i> -carboxyanhydride ( $\alpha$ -NCA) $\gamma$ - <i>N</i> -carboxyanhydride ( $\gamma$ -NCA) <i>N</i> -substituted <i>N</i> -carboxyanhydride (NNCA)
<b>poly(ester amide)s</b>		esteramide
<b>poly(carbonate)s</b>		trimethylene carbonate (TMC)
<b>poly(phosphoester)s</b>		phosphate H-phosphonate phosphonate
<b>poly(phosphazene)s</b>		hexachlorophosphazene

the degradation rates as well. Another factor that makes comparison even in one polymer class difficult are additional post-modifications, e.g. with hydrophobic, polar or charged groups that further alter the degradation profiles.

The protocols for polymer degradation are diverse and lack standardized conditions, which makes most degradation studies non-comparable with each other. Most common degradation mechanism for the polymers discussed herein is hydrolysis of the polymer backbone. In most cases both acidic or basic hydrolysis are conducted under non-physiological conditions, i.e. at very low or high pH values that do not occur in natural environments. Furthermore, the chemical nature of the buffer solution, buffer-capacity, temperature, and concentration of polymer (if water-soluble) or shape of the specimen is different for most studies. For the enzymatic degradation different enzymes can be applied, which may stem from different organisms and vary in their activity. Even batch to batch variations of the very same enzyme make standardization of *in vitro* degradations difficult (overview on parameters shown in Table 1.2).

Trying to summarize some general aspects of degradation profile, herein we give some examples of nonfunctionalized polymers. While polycaprolactone shows rather slow degradation

**Table 1.2.** Overview on parameters influencing the degradability of polymers and polymeric materials.

degradation	Influencing parameters of the...		
	polymer	sample	procedure
-hydrolytic: - acidic - basic	- hydrophilicity/ hydrophobicity -water-solubility	-processing -size/geometry: - bulk	-choice of enzyme: - origin - activity
-enzymatic	-degree of polymerization	- foam	- selectivity
-microbial	-glass transition	- fibers	-physiological/ non-physiological
-oxidative	temperature -crystallinity -steric of substituents -architecture (linear/ branched/ crosslinked) -solubility of degradation products -post-modifications	- nanoparticles - micelles - in solution -porosity -water diffusion	conditions -pH: - acidic - basic - molarity -buffer: - buffer-system - capacity -concentration -temperature - <i>in vitro/ in vivo</i>

rate (within 2-3 years), due to its crystallinity, polylactide (depending on the chirality and composition) undergoes loss of mass within 6-16 months; polyglycolide (45-55% crystallinity) is known to lose mass within 6-24 months. Copolymers of poly-D,L-lactide-co-glycolide are reported to degrade faster, depending on the composition ratio, within 5-6 months. Polyesters hydrolyze under acidic and basic conditions<sup>5</sup>; in contrast, some poly(phosphoester)s can be very stable under acidic conditions, but degrade in the presence of base. For poly(phosphate)s, a typical water-soluble example is poly(methyl ethylene phosphate); while being stable at low pH, degradation of triester to diester bonds occurs under alkaline conditions within 5 h (at pH 12.3) to 21 months (pH 7.3) (*Note:* These are degradation times for 50% cleavage of the ester bonds in the main chain of the polymer).<sup>6</sup> Poly(phosphonate)s with the P-C bond in the side chain show similar degradation profiles under neutral and basic conditions. Complete degradation was observed after 1 hour at pH 12.<sup>7</sup> Contrary, poly(phosphoramidate)s undergo hydrolysis in basic and acidic media.<sup>8-12</sup> While hydrolysis almost exclusively proceeds at the P-N bond under acidic and nearly neutral conditions, P-O as well as P-N bond cleavage occurs under basic conditions, still with a higher probability for P-N cleavage.<sup>11</sup> 94% cleavage of main-chain poly(phosphoramidate)s to diesters has been shown at pH 3.0 within 12.5 days.<sup>8</sup> The degradation profile of polyphosphazenes strongly depends on the substituents and ranges from hydrolytically stable (with hydrophobic, bulky alkoxy side groups) to hydrolytically unstable (with hydrophilic amino substituents). Degradation of the P=N-backbone is commonly accelerated in acidic media, but they are rather inert under basic conditions.<sup>13-14</sup> The biodegradation of synthetic aliphatic poly(amide)s is known

to be low due to high crystallinity. Enzymatic or microbial degradation has been shown.<sup>15</sup> While poly(peptide)s are enzymatically degradable, this is hindered for poly(peptoid)s because of the tertiary amides. Oxidative degradation by reactive oxygen species (ROS) is the major mechanism for them.<sup>16</sup> Figure 1.1 gives a rough overview on the systematic order of degradability of the discussed polymer classes, however the data has to be taken as estimation only, as many factors as mentioned above may influence absolute values. We refer the interested reader to separate reviews concentrating on degradation of synthetic polymers.<sup>2-3, 13-14, 17-20</sup>

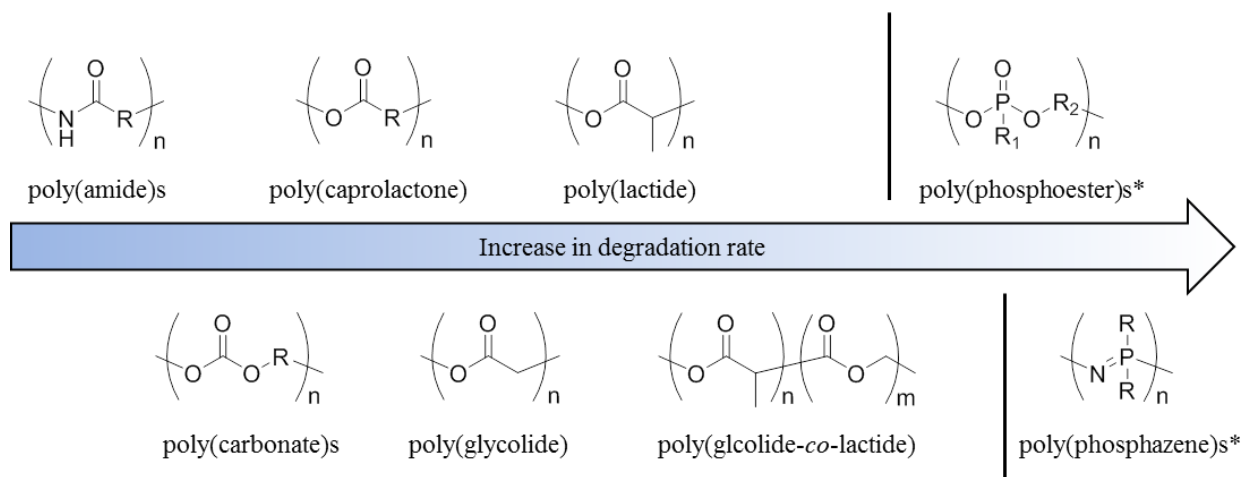


**Figure 1.1.** Overview on the systematic order of degradability of the discussed polymer classes.

\*Note: degradation profiles of poly(phosphazene)s and poly(phosphoester)s depend strongly on the nature of the substituents.

## 1.4 Overview on orthogonally reactive groups

ROP only tolerates some additional chemical functionalities in the monomers. Since alcohols, thiols, amines or carboxylic acids interfere with the propagation and serve as initiators or terminating agents, they need to be protected before polymerization. Commonly used protecting groups, e.g. benzyl, benzoyl, ethers, silyl ethers, acetals, urethanes, sulfonamides or esters are applied in cyclic monomers for ROP. Removal of protection groups is conducted after the polymerization under alkaline or acidic conditions, or by hydrogenation and often demands harsh conditions, which might also degrade the polymer backbone. We do not further consider these protected monomers in the review and concentrate exclusively on orthogonally reactive functionalities (Figure 1.2). For protected monomers we refer to other reviews, specializing on the respective polymer class.<sup>21-24</sup>

For the orthogonal functions, alkynes and alkenes are by far most frequently reported in literature. Alkynes undergo the copper(I)-catalyzed azide-alkyne cycloaddition (CuAAC, Huisgen

1,3-dipolar cycloaddition) with azides or can react in a thiol-yne reaction with thiols in often quantitative yield and mild conditions. Also azides as the “counterpart” are reported as functionality in monomers. Besides CuAAC, they can be additionally modified with DBCO derivatives in a strain-promoted alkyne-azide cycloaddition (SPAAC),<sup>25</sup> which turns the reaction into a copper-free functionalization and is especially interesting for biomedical applications. Alkenes are accessible for probably the most modification reactions: besides thiol-ene reaction and Michael addition, epoxidation (e.g. by mCPBA), dihydroxylation, hydroboration, ozonolysis, hydrazination, hydrogenation, bromination, hydrobromination, and others are applicable. Especially epoxidation opens a platform for diverse further reaction. Also few monomers are reported that directly carry an epoxide, which under certain conditions does not interfere during ROP. Epoxides can cross-link the materials, react with thiols, be dihydroxylated or further polymerized. If alkene functions are vinylidenes, the cyclic monomers are bifunctional for radical polymerization or can serve as cross-linkers as well. They furthermore can be used for olefin cross-

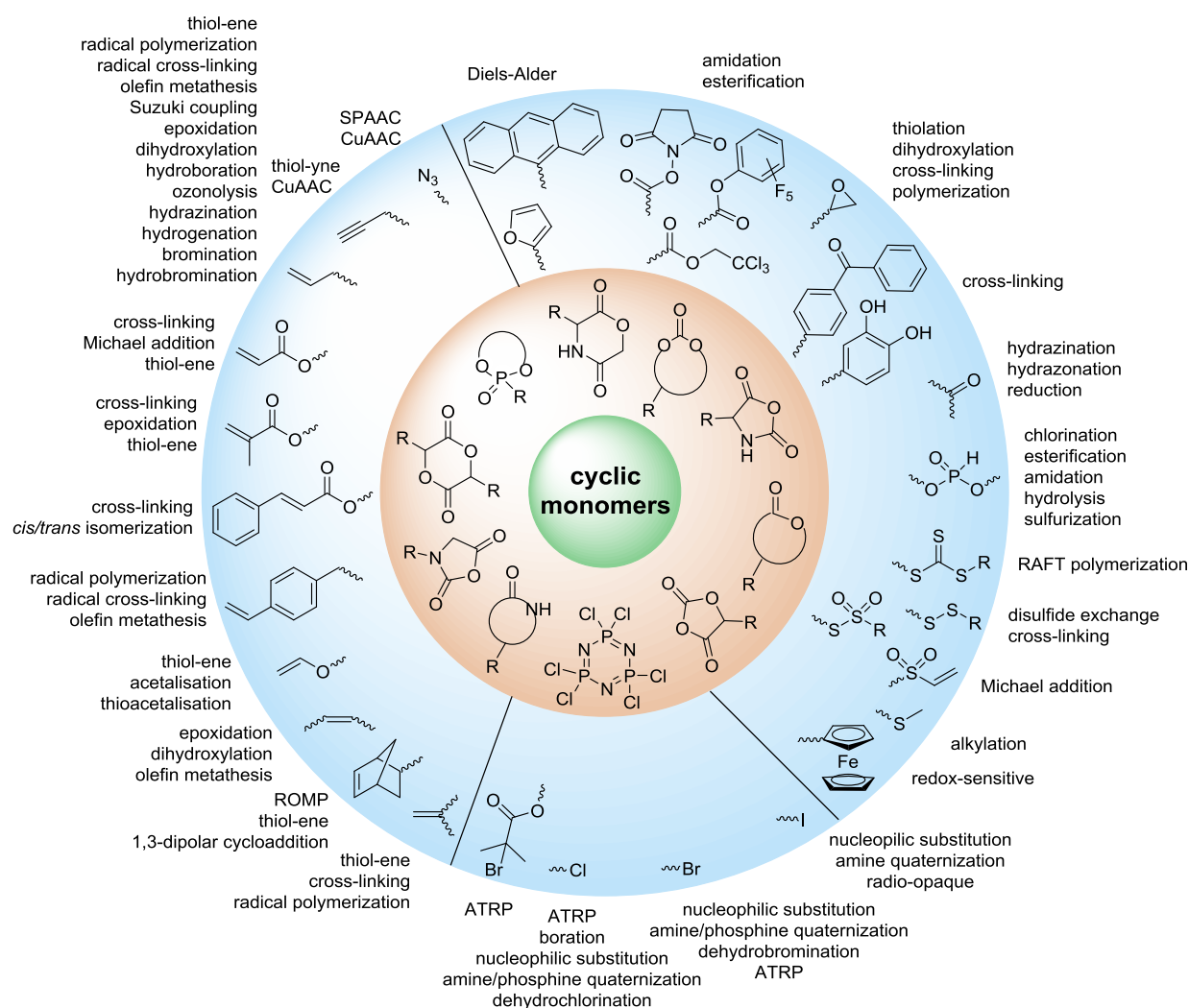


**Figure 1.2.** Overview on cyclic monomers discussed in the review with orthogonally reactive groups.

metathesis or Suzuki coupling. Acrylate, methacrylate and styrenic functions likewise can be radically polymerized, cross-link the materials, undergo thiol-ene reaction and Michael addition or are accessible for olefin cross-metathesis. Cinnamoyl groups serve as cross-linkers. Likewise, methyldiene functions can be polymerized or cross-link materials and undergo thiol-ene reaction, which can be also achieved with norbornene groups, additionally suitable for 1,3-dipolar cycloadditions and ring-opening metathesis polymerization (ROMP). Completing the group of double bond containing functionalities, internal double bonds are accessible for epoxidation, dihydroxylation and cross-metathesis, while vinyl ethers are interesting reaction partners for thiol-ene reaction, acetal- and thioacetalisation.

Halogenated monomers are a second important category, especially with bromide or chloride substituents. Nucleophilic substitution e.g. with sodium azide, and quaternization of tertiary amines or phosphines, has been reported, as well as dehydrohalogenation or boration. Iodide substituted monomers play a minor part, but can also be used for nucleophilic substitution and quaternization of amines, or are used as radio-opaque function, e.g. for contrast agents. Such halogenated polymers have also been used extensively as initiators for atom transfer radical polymerization (ATRP) to prepare graft or brush (co)polymers. Several bromo isobutyrate containing monomers were developed for the same purpose, as well as trithiocarbonate monomers for reversible addition-fragmentation chain-transfer polymerization (RAFT).

A third category includes more exotic, but at the same time very interesting and partly unexpected chemical functionality: besides the trithiocarbonate-containing monomers for RAFT polymerization, several further sulfur-containing monomers are introduced, bearing disulfide or S-sulfonyl groups. The functional groups do not interfere with ROP and can be considered as “protected thiols”. Functionalization is achieved with thiols by disulfide exchange reaction without any prior deprotection reaction: dynamic and redox-responsive cross-linking is accessible. Methyl-thioether functions can undergo reversible alkylation reaction, additionally implementing cationic charges. Vinyl sulfonyl moieties can react in Michael addition reactions. P-H bonds of cyclic H-phosphonate monomers are suitable for modification by esterification, amidation (after chlorination), hydrolysis and sulfurization. The P-H bond has not been reported yet in pendant chains. Ketones within the ring the cyclic monomer are accessible for reduction, hydrazination and hydrazone formation reactions. Benzophenone groups can be used as photo-cross-linkers by a C,H-insertion crosslinking reaction (CHic mechanism<sup>26-27</sup>) with CH groups. Cross-linking can also be achieved by catechol functions (1,2-dihydroxybenzene), either reversible by metal ion complexation or covalently by reaction with amine, thiols or other catechols after oxidation to quinone intermediates. In addition, active ester-containing monomers have been reported, such as trichloroethyl-, NHS- (*N*-hydroxysuccinimide) and pentafluorophenyl-ester groups, which undergo

amidation and esterification reactions with alcohols or amines after polymerization. Finally, anthracene and furan derivatives are suitable for [4+2] cycloaddition Diels-Alder reactions. However, reports on this thermally reversible modification by additive/catalyst-free cycloaddition are rare, which might be a further potential for future applications.

## 1.5 Poly(ester)s

Aliphatic poly(ester)s from ROP probably display the broadest group of fully synthetic biodegradable polymers. A variety of lactones with different ring sizes are available resulting in poly( $\epsilon$ -caprolactone)s, poly( $\delta$ -valerolactone)s, poly( $\gamma$ -butyrolactone)s, poly( $\beta$ -butyrolactone)s, poly( $\beta$ -propiolactone)s, and poly( $\alpha$ -propiolactone)s. Macrolactone monomers are likewise polymerizable. Furthermore, cyclic diesters (lactides, glycolides and *O*-carboxyanhydrides (OCAs)) produce the commercialized poly( $\alpha$ -hydroxyacid)s (PAHAs) poly(lactide)s (PLAs) and poly(glycolide)s (PGAs). Several reviews about functional aliphatic poly(ester)s have been published and might be considered for further reading.<sup>23, 28-29</sup>

A less explored synthetic route to poly(ester)s is the radical ring-opening polymerization (RROP) of cyclic ketene acetals (CKAs), which was summarized recently<sup>30</sup> and is not further considered in this review. Some methylened- or chloride-substituted CKAs are reported, resulting in halogenated poly(ester)s or polymers with internal double bonds. They have not been post-modified so far. Poly(ester)s can also be obtained by alternating ring-opening copolymerization (ROCOP) of epoxides and anhydrides. We exclude the technique of polyaddition of orthogonally reactive epoxides or anhydrides and point to several recent reviews<sup>28, 31-32</sup>

### 1.5.1 Lactones

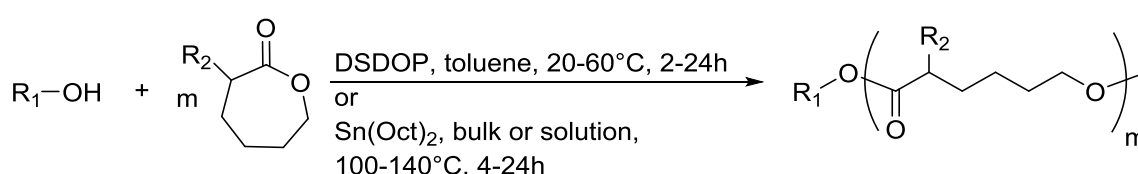
**$\epsilon$ -Caprolactones.** Functional  $\epsilon$ -caprolactones  $\epsilon$ -(CL) can be divided into three subgroups, substituted in  $\alpha$ -,  $\beta$  or  $\gamma$ -position, depending on the synthesis strategy for each monomer (overall yields: 19-70%). CLs are commonly polymerized with 2,2-dibutyl-2-stanna-1,3-dioxepane (DSDOP) as catalyst (in toluene at 20°C for 24h<sup>33</sup> or at 60°C for 2h) or with tin(II) 2-ethylhexanoate (SnOct<sub>2</sub>) in bulk or solution at 100-140°C for 4-24h (Scheme 1.1). For detailed polymerization conditions of lactones and lactides/glycolides and applied catalysts we refer to separate literature.<sup>34</sup>

**$\alpha$ -Substituted- $\epsilon$ -Caprolactones.**  $\alpha$ -Halogenated caprolactones can be prepared by the Baeyer-Villiger oxidation of 2-halogenated-cyclohexanone with *meta*-chloroperoxybenzoic acid (mCPBA) (yield: 45-70%, Scheme 1.2A).<sup>33</sup> Mohamod and coworkers<sup>35</sup> polymerized  $\alpha$ -fluoro caprolactone

(A1) as homo- or copolymer with caprolactone.  $\alpha$ -Chloro- (A2)<sup>33</sup> and  $\alpha$ -bromo-caprolactone (A3)<sup>36</sup> was polymerized and substituted with azides, which allowed further post modification with alkynes in a Huisgen 1,3-dipolar cycloaddition.<sup>36</sup> These graft-polymers were used as macroinitiators for ATRP of methyl methacrylate (MMA)<sup>37</sup> or hydroxyethylmethacrylate (HEMA)<sup>38</sup> with the chlorides or bromides as initiating sites. Azide-functional poly( $\epsilon$ -CL) was also directly synthesized by an  $\alpha$ -azido- $\epsilon$ -CL (A4),<sup>39</sup> which was prepared by substitution of A2 or A3 with sodium azide.

A further general strategy is the functionalization of the  $\alpha$ -position of  $\epsilon$ -caprolactone by deprotonation with LDA (lithium diisopropylamide) and subsequent reaction with an electrophile (Scheme 1.2B).  $\alpha$ -Iodo-caprolactone (A5) was obtained in this way by iodination with ICl (yield: 29%).<sup>40</sup> The authors claimed the resulting copolymers to exhibit radio-opacity properties with potential application in temporary reconstructing material or drug delivery because of visualization via routine X-ray radiology.

$\alpha$ -Alkene and -alkyne functionalized caprolactones are used for the purpose of thiol-ene reaction and click reaction, introducing charged functionalities or bulky molecules, such as dyes or sugars. Following the described strategy, deprotonated  $\epsilon$ -caprolactone reacts with allyl bromide, propargyl bromide or propargyl chloroformate to yield  $\alpha$ -allyl- $\epsilon$ -caprolactone (A6, yield: 65%),<sup>41</sup>  $\alpha$ -propargyl- $\epsilon$ -caprolactone (A7)<sup>42</sup> and  $\alpha$ -propargyl carboxylate- $\epsilon$ -caprolactone (A8).<sup>43</sup> After copolymerization of A6 with  $\epsilon$ -CL, Coudane and coworkers<sup>41</sup> attached Boc-protected-amines as the pendant chains by radical thiol-ene reaction. They proved deprotection of the amine without degradation of the backbone and subsequent reaction with fluorescein isothiocyanate (FITC). They claimed the water-soluble cationic polyesters as interesting materials for gene delivery. Maynard and coworkers<sup>44</sup> recently reported trehalose- and carboxybetaine-substituted poly(CL) and used it as a polymeric excipient for the stabilization of the therapeutic protein G-CSF for storage at 4°C and at heat stressor temperatures of 60 °C. Copolymers of A7 were functionalized with the clinically used diethylenetriaminepentaacetic acid (DTPA)/Gd<sup>3+</sup> complex, resulting in a MRI-visible polymers as a hydrophobic contrast agent.<sup>45</sup> PEG-block copolymers of  $\alpha$ -propargyl carboxylate- $\epsilon$ -caprolactone formed micelles, which were core-cross-linked by a difunctional azide-cross-linker.<sup>43</sup> An alternative strategy to produce  $\alpha$ -propargyl- $\epsilon$ -caprolactone (A7, yield: 14%) starts with deprotonation of cyclohexanone and subsequent substitution with propargyl bromide,

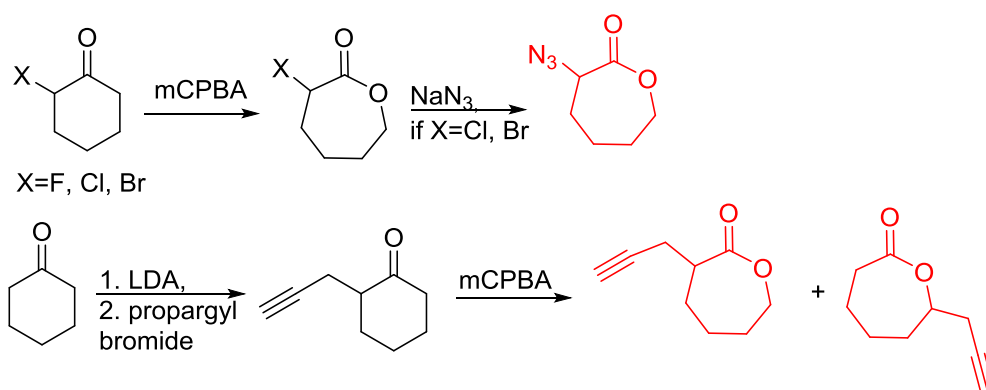


**Scheme 1.1.** General polymerization scheme of caprolactones to poly(ester).

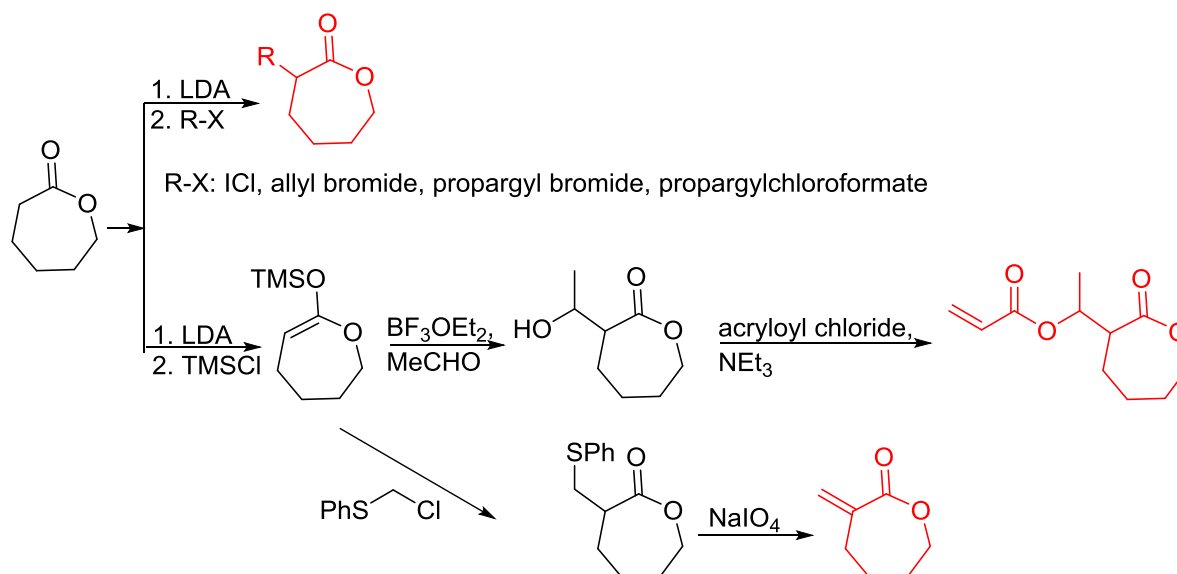
followed by the Baeyer-Villiger oxidation to expand the ring to  $\epsilon$ -caprolactone (Scheme 1.2A).<sup>46</sup> However, a mixture of  $\alpha$ - and  $\epsilon$ -substituted caprolactones (**A7** and **A7b**, isomeric mixture yield: 30/70) were obtained. Ritter and coworkers prepared polymers and attached cyclodextrines via click reaction to form supramolecular organogels.<sup>42</sup>

Lecomte and coworkers<sup>47</sup> reported an acrylate-substituted CL (**A9**) using it as endchain comonomer to form macrocyclic poly(ester)s. The macrocycles were formed by UV-crosslinking of the acrylates. **A9** was synthesized in three steps (Scheme 1.2B): deprotonation of caprolactone and addition of trimethylsilyl chloride formed a trimethylsilylketene acetal, which further reacted in a Mukaiyama aldol reaction with acetaldehyde. Esterification of the formed hydroxylactone with acryloyl chloride yielded the final monomer  $\alpha$ -(1-acryloyloxyethyl)- $\epsilon$ -caprolactone (**A9**). Ritter and coworkers<sup>48</sup> reported the ROP of  $\alpha$ -methylidene- $\epsilon$ -caprolactone (**A10**), while the monomer has been polymerized at the vinyl functionality before. Homopolymerization yielded only low

**A:  $\alpha$ -substituted CL's by ring-expansion**



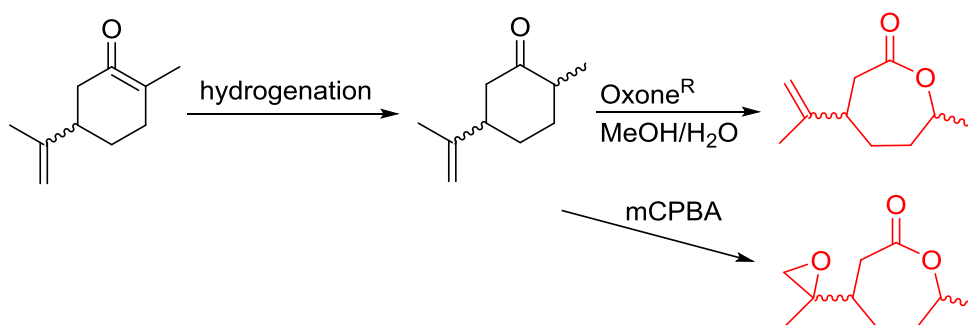
**B:  $\alpha$ -substituted CL's from CL**



**Scheme 1.2.** Synthetic strategies for synthesis of  $\alpha$ -substituted  $\epsilon$ -caprolactones: A) by ring-expansion via the Baeyer-Villiger oxidation of cyclohexanones; B) by substitution of  $\epsilon$ -caprolactone.

molecular weights, copolymerization with caprolactone clearly higher molecular weight polymers. They claimed the polymers to be radically cross-linkable, however did not report on further details. The monomer was synthesized by O-silylation, followed by thioalkylation with  $\alpha$ -chloro thioanisole and completed by oxidative sulfur (Scheme 1.2B) removal (overall yield: 39%).<sup>49</sup>

**$\beta$ -Substituted- $\epsilon$ -Caprolactones.** Hillmyer and coworkers reported two  $\beta$ -substituted CLs derived from natural carvone: 7-methyl-4-(2-methyloxiran-2-yl)oxepan-2-one (**A11**)<sup>50</sup> and dihydrocarvide (**A12**)<sup>51</sup> (Scheme 1.3). **A11** was synthesized in two steps: hydrogenation of carvone resulted dihydrocarvone; epoxidation and ring-expansion yielded the final monomer (second step 25% yield). The monomer was homo- and copolymerized with CL, however both rings reacted under the reported polymerization conditions (in bulk or solution, 20-120 °C, diethyl zinc (ZnEt<sub>2</sub>) or tin(II) 2-ethylhexanoate (SnOct<sub>2</sub>) catalyst). To obtain polymers with epoxides as pendant groups, monomer **A12** was obtained by ring-expansion of dihydrocarvone using Oxone® (triple salt 2·KHSO<sub>5</sub>·KHSO<sub>4</sub>·K<sub>2</sub>SO<sub>4</sub>).<sup>51</sup> Poly(dihydrocarvide-*co*-carvomenthide) was subsequently epoxidized and crosslinked with a dithiol to prove the possibility of post-modification.



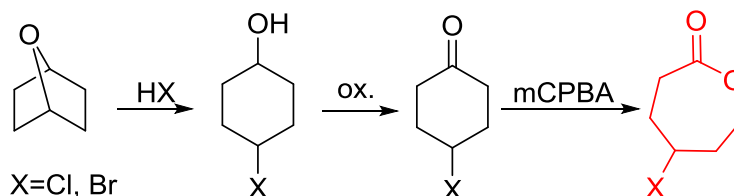
**Scheme 1.3.** Synthetic route to  $\beta$ -substituted CLs from carvone.

**$\gamma$ -Substituted- $\epsilon$ -Caprolactones.**  $\gamma$ -Halogenated caprolactones are synthesized starting from 4-halogenated-cyclohexanol (obtained by halogenation of 7-oxabicyclo[2.2.1]heptane); the alcohol was oxidized to a cyclic ketone to yield the monomer  $\gamma$ -chloro- $\epsilon$ -caprolactone (**A13**)<sup>52</sup> or  $\gamma$ -bromo- $\epsilon$ -caprolactone (**A14**)<sup>53</sup> after a Bayer-Villiger oxidation (yield for last step: 62%; Scheme 1.4A). Hegmann and coworkers<sup>52</sup> used **A13** in a copolymerization with caprolactone and lactide, substituted the chloride by an azide and attached cholesterol derivatives. The copolymers were used as cell scaffolds and foams. Jérôme and coworkers<sup>54</sup> quaternized copolymers of caprolactone and **A14** with pyridine, applied a debromination or epoxidation, and subsequent ring-opening to obtain hydrophilic poly(CL) substituted with diols in the backbone. P(**A14**) was substituted by an azide and amine-groups were then coupled by click chemistry to obtain pH-sensitive star-shaped pol(ester)s.<sup>55</sup> A  $\gamma$ -azide- $\epsilon$ -caprolactone has not been reported yet to the best of our knowledge.  $\gamma$ -Keto- $\epsilon$ -caprolactone (**A15**) was reported by the same group,<sup>56</sup> obtained by ring extension of 1,4-cyclohexanedione (Scheme 1.4B). Qiao and coworkers<sup>57</sup> functionalized the keto groups by

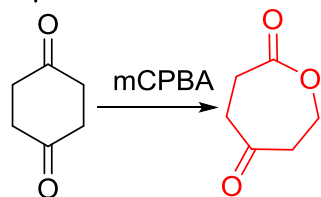
hydrazine chemistry to introduce hydroxyl groups and coupled 4-nitrophenyl chloroformate. The activated ester was reacted with primary amines, e.g. of the cell adhesive peptide GRGDS. Lang and coworkers<sup>58</sup> reduced the carbonyl group in copolymers to hydroxyl groups, using them as macroinitiator for further grafting of lactide.

$\gamma$ -Acryloyloxy  $\epsilon$ -caprolactone (**A16**), a bifunctional monomer for ROP and radical polymerization,<sup>59</sup> was prepared in two or three steps (Scheme 1.4C): 1,4-cyclohexanediol reacted with acryloyl chloride. The resulting monoalcohol was oxidized and the ring extended to yield the monomer (in an overall yield of 36%). A shorter alternative strategy started with the reaction of acryloyl chloride with 2-hydroxycyclohexan-1-one and subsequent ring extension (overall monomer yield 24%).<sup>60</sup> Besides using the monomer for both ROP and ATRP, copolymers were

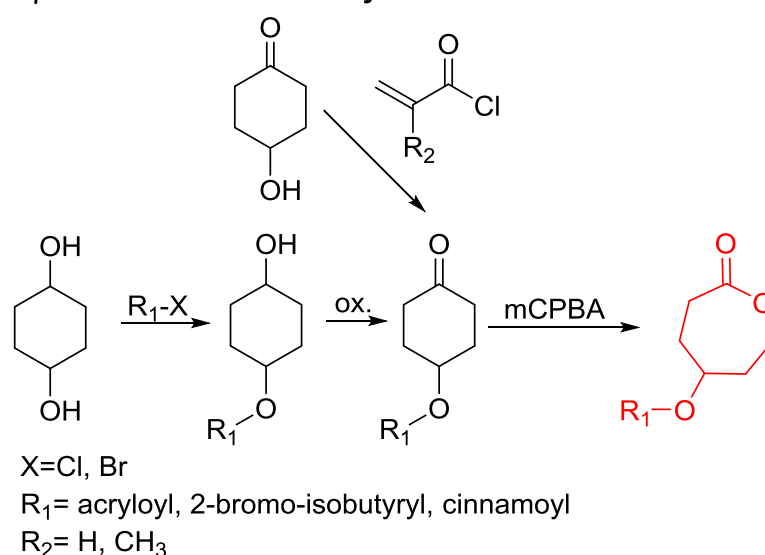
**A:  $\gamma$ -halogenated CLs**



**B:  $\gamma$ -keto CL**



**C:  $\gamma$ -substituted CLs from cyclohexanols**



**Scheme 1.4.** Synthetic strategies for synthesis of  $\gamma$ -substituted  $\epsilon$ -caprolactones: A) for  $\gamma$ -halogenated CLs; B) for  $\gamma$ -keto CL; C) for  $\gamma$ -substituted CLs from cyclohexanols.

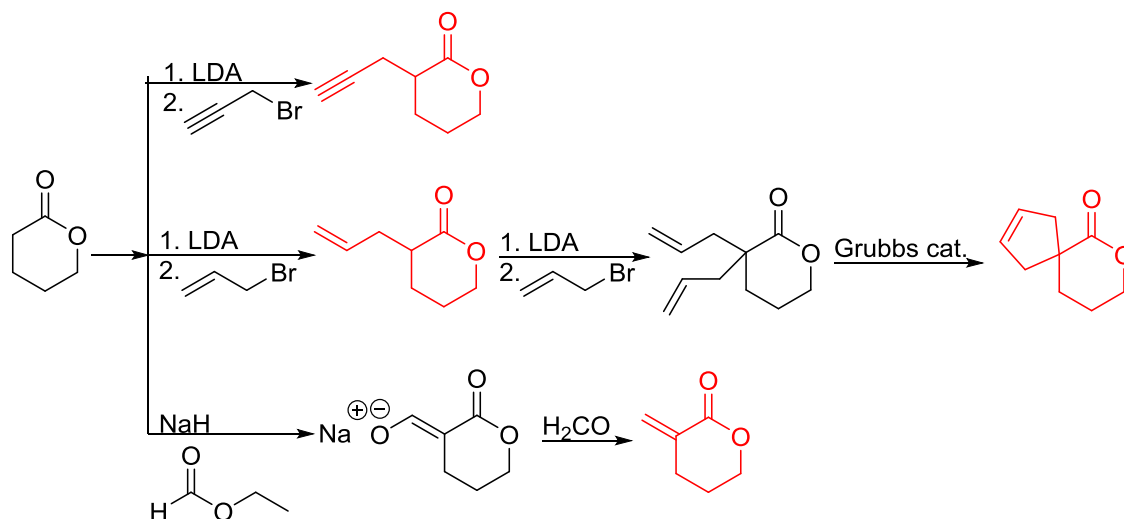
grafted onto metal surfaces,<sup>61</sup> used as 2D or 3D microstructured resins<sup>60</sup> or were post-modified by Michael-addition of thiols.<sup>62</sup> A similar monomer,  $\gamma$ -methacryloyloxy- $\epsilon$ -caprolactone (**A17**), was prepared by the same method, using methacryloyl chloride instead (overall monomer yield 29%),<sup>60</sup> which were cross-linked upon UV-irradiation e.g. to form microparticles.<sup>63</sup>  $\gamma$ -(2-Bromo-2-methylpropionate)- $\epsilon$ -caprolactone (**A18**) carries a classical ATRP initiating group and was presented by Hedrick and coworkers.<sup>64</sup> A  $\gamma$ -cinnemate-modified caprolactone (**A19**) was recently reported by Budhlall and coworkers,<sup>65</sup> which can undergo *cis/trans* isomerization and [2+2] cycloaddition upon UV-irradiation. Homo- or copolymers were used as thermoresponsive semicrystalline networks after photochemical cross-linking.

**$\delta$ -Valerolactones.** Poly( $\delta$ -valerolactone)s have been much less studied compared to poly( $\epsilon$ -caprolactone)s and the number of orthogonally reactive  $\delta$ -valerolactone monomers is very limited to a few examples of  $\alpha$ -substituted  $\delta$ -valerolactone. Examples for substitution in other positions are only available for alkylated substituents.  $\delta$ -Valerolactones are polymerized under similar conditions as caprolactones, e.g. with and an alcohol as initiator and Sn(Oct)<sub>2</sub> as catalyst in bulk at 100°C for 16h,<sup>66</sup> or with Sn(OTf)<sub>2</sub> as catalyst in bulk or THF at room temperature for 24h.<sup>67</sup>

Emrick and coworkers<sup>67</sup> reported the first functionally substituted monomer,  $\alpha$ -allyl- $\delta$ -valerolactone (**A20**), synthesized by the same strategy as  $\alpha$ -substituted  $\epsilon$ -caprolactones: lithiation of  $\delta$ -valerolactone in  $\alpha$ -position with LDA and subsequent reaction with allyl bromide yielded **A20** in one step (yield: 71%, Scheme 1.5). **A20** was copolymerized with  $\epsilon$ -caprolactone or  $\delta$ -valerolactone, as well as homopolymerization obtained polymers in good conversion and narrow molecular weights distributions. The alkenes were quantitatively dihydroxylated with NMO/OsO<sub>4</sub> to obtain more hydrophilic poly(ester)s. The group also introduced a  $\alpha$ -cyclopentene- $\delta$ -valerolactone (**A21**)<sup>68</sup>: **A20** was lithiated and allylated to yield  $\alpha,\alpha$ -diallyl- $\delta$ -valerolactone. Ring-closing metathesis using a Grubbs catalyst gave **A21**. The cyclopentene substituted lactone was not able to homopolymerize; copolymerization with  $\epsilon$ -caprolactone was realized with incorporation of ca. 20% of **A21**. The pendant group was converted to *cis*-1,2-diols by dihydroxylation with OsO<sub>4</sub> and showed longer bench-life stability compared to the diol-containing poly(ester)s from pendant allyl groups probably due to higher rigidity of the monomer units. PEG was grafted onto the copolymers. Finally, Emrick and coworkers<sup>69</sup> also used  $\alpha$ -propargyl- $\delta$ -valerolactone (**A22**)<sup>70</sup> (synthesized by the same strategy as **A21**) and obtained homo- as well as copolymers with  $\epsilon$ -caprolactone. They functionalized the polymers by click chemistry with a PEG-azide, a oligopeptide-azide (GRGDS-N<sub>3</sub>), a phosphorylcholine derivative<sup>71</sup> or a benzophenone group, to produce photopatternable aliphatic poly(ester).<sup>66</sup> Harth and coworkers<sup>72</sup> used **A20** and **A22** to form multifunctional poly(ester) nanoparticles.

$\alpha$ -Methylidene- $\delta$ -valerolactone (**A23**) has usually been polymerized as “vinyl monomer”. Ritter and coworkers<sup>73</sup> reported the first polymerization by ring-opening. Formylation of  $\delta$ -valerolactone, subsequent formyl transfer and elimination of a carboxylate anion yielded **A23** (yield: 57%, Scheme 1.5). The monomer was copolymerized with  $\delta$ -valerolactone, and networks obtained by free radical polymerization of the methylidene functionality with different methacrylates.

Diaconescu and coworkers reported a series of three different  $\alpha$ -ferrocenyl- $\delta$ -valerolactones (**A24-A26**) and six ferrocenyl-substituted trimethylene carbonate (TMC) monomers (**C5-C10**), all obtained by click chemistry of azide functionalized ferrocene to **A22**, 5-(propynyl)-1,3-dioxan-2-one and propargyl 5-methyl-2-oxo-1,3-dioxane-5-carboxylate (**C11**) (*see also below*).<sup>74</sup> While all TMC monomers were polymerizable with DBU/TU as the catalyst (1,8-diazabicycloundec-7-ene and 1-(3,5-bis(trifluoromethyl)phenyl)-3-cyclohexylthiourea), **A24-A26** were not able to be polymerized neither as homo- nor copolymers.

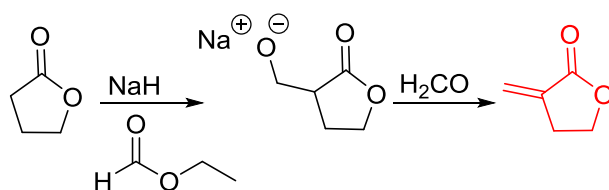


**Scheme 1.5.** Synthetic strategy for the synthesis of substituted  $\delta$ -valerolactones.

**$\gamma$ -Butyrolactones.**  $\gamma$ -Butyrolactone is often considered to be the “non-polymerizable” lactone, due to its low ring strain.<sup>75</sup> It can oligomerize using a lipase catalyst<sup>76</sup> or under high pressure (20,000 atm) and can be copolymerized with other lactone monomers.<sup>77</sup> Chen and coworkers<sup>78</sup> recently successfully obtained poly( $\gamma$ -butyrolactone) via ROP with a  $\text{La}[\text{N}(\text{SiMe}_3)_2]_3/\text{R-OH}$  catalyst system at  $-40^\circ\text{C}$  in THF with a number molecular weight of 30 kg/mol, 90% monomer conversion and control over linear or cyclic topology.

Since polymerization of  $\gamma$ -butyrolactone remains difficult, only few functional monomers have been reported so far.  $\alpha$ -Methylidene- $\gamma$ -butyrolactone (**A27**) is widely used as vinyl-comonomer; Ritter and coworkers<sup>79</sup> reported copolymerization with caprolactone in a ROP for the first time, Chen and coworkers<sup>80</sup> recently reported homopolymerization. They used the methylidene function for crosslinking of the polymers with a methacrylate to transparent polyester networks. The

monomer was synthesized in two steps by same strategy as **A23** (Scheme 1.6): formylation of  $\gamma$ -butyrolactone, subsequent formyl transfer and elimination of a carboxylate anion yielded **A27**.<sup>81</sup> Albertsson and coworkers<sup>82</sup> recently reported the copolymerization of  $\alpha$ -bromo- $\gamma$ -butyrolactone (**A28**), which is commercially available at Sigma Aldrich. Due to the high selectivity and reactivity of modern organocatalysts at ambient reaction temperatures, the authors were able to polymerize co- and terpolymers, with trimethylene carbonate (TMC), **C47** or  $\epsilon$ -caprolactone with an alcohol as the initiator and diphenyl phosphate (DPP) as the catalyst at 30°C for 48h. Grafting of methyl acrylate via Cu(0)-mediated CRP (controlled radical polymerization) on the copolymers was demonstrated.



**Scheme 1.6.** Synthetic strategy for synthesis of  $\alpha$ -methylidene- $\gamma$ -butyrolactone.

**$\beta$ -Propiolactones and  $\beta$ -Butyrolactones.** Substituted  $\beta$ -propiolactones and  $\beta$ -butyrolactones are synthesized by three general synthetic strategies, following a “ketene”, “epoxide”, or “aspartic” route (Scheme 1.7).

Mono-, di-, and tri-halogenated propiolactones and their polymerization are reported extensively in literature. Modification after polymerization has not been reported so far. Tani and coworkers<sup>83</sup> synthesized  $\beta$ -chloromethyl- (**A29**),  $\beta$ -dichloromethyl- (**A30**)  $\beta$ -trichloromethyl- $\beta$ -propiolactone (**A31**) by [2+2] cycloaddition from ketene and the corresponding mono-, di- or trichlorinated acetaldehyde and intensively investigated in their polymerization behavior and tacticity of obtained polymers (Scheme 1.7, 1A). Prud’Homme and coworkers further introduced several chlorinated and fluorinated propiolactones (**A32-A36**),<sup>84-86</sup> partially being  $\beta$ -disubstituted at the lactone ring (Scheme 1.7, 1A-3A). For racemic mixtures of the monomers, they used the corresponding halogenated aldehyde (or halogenated acetone or butanone for  $\beta$ -di substituted lactones), acetyl chloride and triethylamine, for optically active monomers they used the synthetic route using ketene and the chiral catalyst quinidine. Li and coworkers<sup>87-88</sup> copolymerized  $\alpha$ -chloromethyl- $\alpha$ -methyl-propiolactone (**A37**) with caprolactone (Scheme 1.7, E). Quaternization with pyridine resulted in polymers with increased hydrophilicity. Chlorination of 2,2'-bis(hydroxymethyl)propionic acid with thionyl chloride, hydrolysis of the formed acyl chloride and cyclization under basic conditions yielded the monomer. A  $\alpha,\alpha$ -bischloromethyl-propiolactone monomer (**A38**) has been reported by Kuriyama and coworkers<sup>89</sup> and copolymerized with  $\beta$ -propiolactone. Post-modification has not been shown.

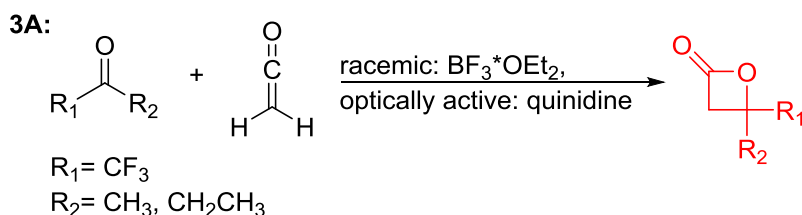
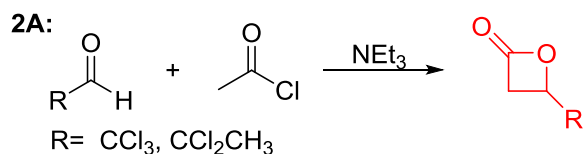
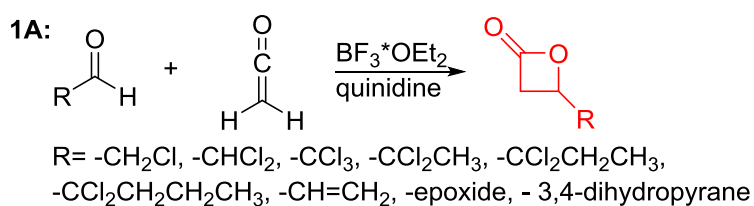
Cherdron and coworker<sup>90</sup> presented several  $\beta$ -substituted lactones, carrying pendant groups suitable for other polymerization techniques (epoxide (**A39**), 3,4-dihydropyran (**A40**), vinyl (**A41**)). They showed selective lactone polymerization, but also did not use the further functionality for post-modification reactions. They followed the general synthetic strategy using ketene and a corresponding aldehyde (Scheme 1.7, 1A).

The polymerization of  $\beta$ -heptenolactone (**A42**) (or also called allyl- $\beta$ -butyrolactone) is only rarely reported in literature, which is probably due to an inconvenient synthetic route of the monomer or use of special zinc or yttrium catalysts for polymerization. But-3-en-1-yl-epoxid reacted with carbon monoxide in the presence of a Co-based catalyst at 6.2 MPa /80°C<sup>91</sup> or an active Cr-catalyst at 1 atm /22°C<sup>92</sup> to the monomer (Scheme 1.7, B). While Guillaume and coworkers<sup>93</sup> functionalized poly( $\beta$ -heptenolactone) by hydroboration, Shaver and coworkers<sup>94</sup> recently post-modified the polymer by olefin cross-metathesis with 15 different alkene cross-partners producing a whole library of poly(ester)s with different functionalities.

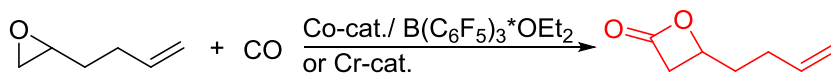
Guérin and coworkers<sup>95-96</sup> developed three functional monomers for unsaturated poly( $\beta$ -maleic acid) derivatives: allyl malolactonate (4-allyloxycarbonyl-2-oxetanone, **A43**), 3-methyl-3-butenyl malolactonate (4-[3-methyl-3-butenyloxycarbonyl]-2-oxetanone, **A44**) and 2-methylethenoxyethyl malolactonate (4-[2-methylethenoxyethyl-oxycarbonyl]-2-oxetanone, **A45**). While the ketene route gave only low yields, the “aspartic route” was applied (Scheme 1.7, C): aspartic acid was brominated and bromosuccinic acid anhydride formed. Esterification with an appropriate alcohol (allyl alcohol, 3-methyl-3-buten-1-ol or 2-hydroxyethyl methacrylate) opened the anhydride and formed a mixture of the corresponding mono-bromo succinic acid esters, and the major product was lactonizable. Epoxidation and subsequent sulfonation has been carried out. The copolymers were able to induce new bone formation and muscle regeneration in *in vivo* models.<sup>97-98</sup> Thiol-ene reaction with mercaptoethanol converted the copolymers into macroinitiators to “graft from” poly(caprolactone).<sup>99</sup>

Lu and coworkers<sup>100</sup> recently reported a novel methylene functionalized monomer,  $\alpha$ -methylidene- $\beta$ -butyrolactone (**A46**), synthesized from carbon dioxide and 2-butyne in four steps (Scheme 1.7, D). After formation of tiglic acid, catalyzed by NiCl<sub>2</sub>\*glyme and bathocuproine, an allylic peroxide was formed by photooxygenation. Dehydration formed a peroxy lactone, which yielded **A46** after deoxygenation. The vinylidene functional group was used for radical cross-linking or thiol-ene reaction.<sup>101</sup>

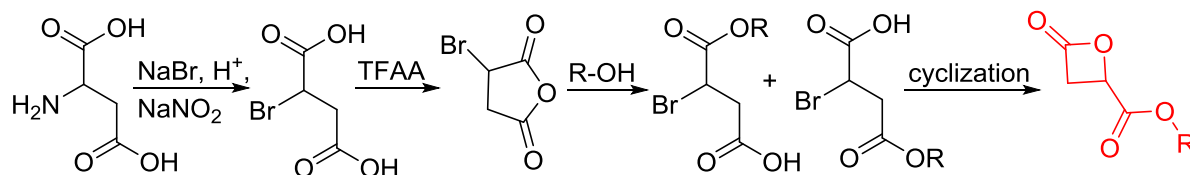
**A: "Ketene" route**



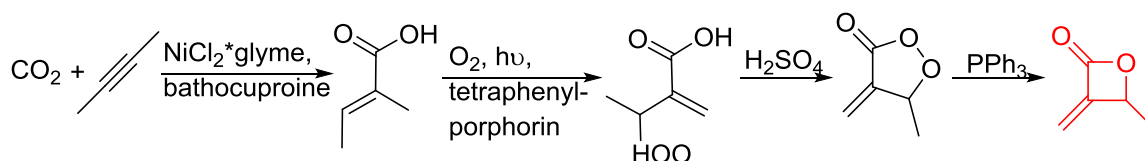
**B: "Epoxide" route**



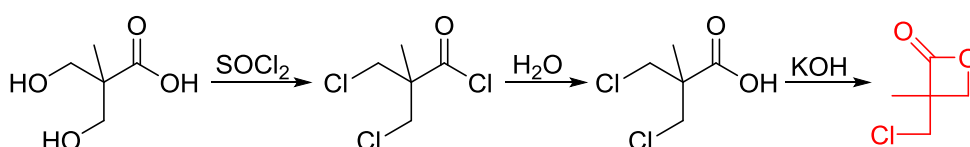
**C: "Aspartic" route**



**D:  $\alpha$ -methylene- $\beta$ -butyrolactone:**



**E:  $\alpha$ -chloromethyl- $\alpha$ -methyl-propiolactone**



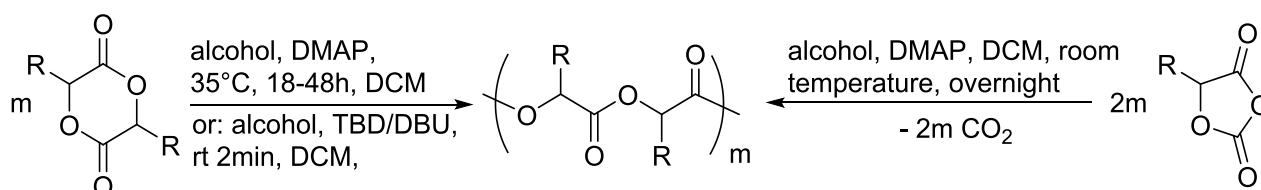
**Scheme 1.7.** Synthetic strategies to substituted of  $\beta$ -propio- and  $\beta$ -butyrolactones: A) "ketene" route, e.g. for halogenated lactones; B) "epoxide" route yielding  $\beta$ -heptenolactone; C) "aspartic" route; D) synthesis of  $\alpha$ -methylene- $\beta$ -butyrolactone; E) synthesis of an  $\alpha$ -disubstituted propiolactone.

**Macrolactones.** Mainly two macrolactones, globalide (**A47**) and ambrettolide (**Am**, **A48**) are used to prepare long-chain aliphatic polyesters by ROP. **A47** is a natural unsaturated 16-membered lactone, **A48** a 17-membered lactone used in the fragrance industry. 14-19-membered lactones can be extracted from natural sources including angelica plant root. The ring-strain is the driving-force for ROP of smaller cycles and increases from 5- to 7-membered lactones, exhibiting the maximum for  $\epsilon$ -caprolactone.<sup>102-103</sup> Macrolactones have a low ring-strain and their ROP is entropy-driven instead of enthalpy-driven, as for the strained lactones.<sup>103</sup> Macrolactones can be polymerized enzymatically by lipases, e.g. Novozyme 435 (Candida Antarctica lipase B (CALB) immobilized on acrylic resins).<sup>104</sup> For further details we refer to excellent reviews of Kobayashi<sup>104-105</sup> and the work of the Heise group.<sup>106-111</sup>

Heise and coworkers functionalized the olefins in poly(globalide) via thiol-ene reaction with different thiols.<sup>107, 109</sup> In another study, dithiol-cross-linked poly(globalide) films were further reacted with mercaptohexanol to attach ATRP initiators.<sup>106</sup> Such films were further grafted with *tert*-butyl acrylate and proteins were conjugated to the deprotected grafts. Möller and coworkers<sup>112</sup> polymerized **A48** and oxidized the internal double bonds by Baeyer-Villiger oxidation using mCPBA to the epoxides. They showed, that a strategy vice versa is also possible: after epoxidation of **A48**, the monomer **A49** (AmE) was polymerized with Novozyme 435, while the epoxides remained intact. Kobayashi and coworkers<sup>113</sup> reported already in 2001 the enzymatic ROP of 2-methylene-4-oxa-12-dodecanolide (**A50**) by lipase and subsequent radical crosslinking of the polymers.

### 1.5.2 Cyclic Diester Monomers

Poly( $\alpha$ -hydroxyacid)s (PAHAs) are obtained from cyclic diester monomers (Scheme 1.8). Poly(lactic acid) (PLA), poly(glycolic acid) (PGA), and their copolymers (PLGA) are accessible from renewable resources. They are typically prepared by ROP of the cyclic dimers of lactic and glycolic acid (lactides and glycolides). However, the lack of structural diversity of lactides and glycolides limits the preparation of functional poly( $\alpha$ -hydroxyacid)s. Synthesis of substituted 1,4-dioxane-2,5-diones can be complicated and reactivity in ROP is often poor. They are usually polymerized with



**Scheme 1.8.** General scheme for the polymerization of lactides/glycolides and *O*-carboxyanhydrides (OCAs) to poly( $\alpha$ -hydroxyacid)s (PAHAs).

$\text{Sn}(\text{Oct})_2$  at 110-130 °C for 2- 24 h in bulk<sup>114</sup> or toluene<sup>123</sup>, with 4-dimethylaminopyridine (DMAP) at 35 °C for 18-48 h in DCM,<sup>115-116</sup> or with TBD or DBU at room temperature for 2min to 24 h in DCM,<sup>122,117-118</sup> using primary alcohols as initiator. *O*-carboxyanhydrides (OCAs) are suitable alternatives for the preparation of functionalized PAHAs under mild conditions, and were recently summarized in an excellent article.<sup>119</sup>

**Lactide and Glycolide Monomers.** A general synthetic procedure to mono- or difunctional orthogonally reactive glycolide or lactide monomers was reported by Hennink and coworkers<sup>114</sup> in three steps (Scheme 1.9A). Starting from an appropriate alkylbromide (e.g. propargyl bromide), a Barbier-type addition to glyoxylic acid/ester (and cleavage of the ester, if used) resulted in a glycolic acid derivative which further reacted with 2-bromoacetyl bromide (or 2-bromopropanoyl bromide in case of a lactide monomer<sup>116, 120-122</sup>). Intramolecular cyclization in diluted solution yielded the monomer (yields typically 15-45%). Difunctional monomers can be formed by dimerization and cyclization of the glycolic acid derivative.<sup>123</sup>

Hennink and coworkers<sup>114</sup> polymerized an allyl functional glycolide (**A51**), and showed epoxidation with NMO/ $\text{OsO}_4$  and subsequent hydrolysis to diols. The allyl lactide analogue **A52** has been reported by Cheng and coworkers.<sup>120</sup> They photochemically crosslinked PEG-PLA-block copolymers via thiol-ene reaction with a dithiol-crosslinker to obtain nanoparticles. Pfeifer and coworkers<sup>122</sup> used cationic modified PEG-PLA-block copolymers for gene delivery. The monomer was also further functionalized by olefin cross-metathesis with an epoxy alkene and further hydrogenated to the saturated epoxy lactide (**A53**).<sup>121</sup> An orthogonal reactive iron-based catalyst was applied for the polymerization of **A53**, which selectively polymerizes the diester cycle, if the catalyst is in the an iron(II) form. The oxidized catalyst (iron(III)-species) instead selectively polymerizes the epoxide. The bifunctional epoxy diester was selectively polymerized to an epoxy-functional polyester (Figure 1.3). After oxidation of the catalyst and removal of solvent, the epoxy-functions were polymerized to cross-link the polymers.

Coudane and coworkers<sup>115</sup> reported an alkyne functional glycolide (3-(2-propynyl)-1,4-dioxane-2,5-dione, **A54**), and modified PLGA-copolymers with PEG-azides. Cheng and coworkers<sup>116</sup> reported the analogous alkyne lactide **A55**. They grafted PEG-paclitaxel-azide conjugates onto PLA-copolymers. A disubstituted alkynated glycolide (**A56**) has been used by Baker and coworkers<sup>123</sup> for the polymerization of homopolymers and random or block copolymers, which were functionalized by click chemistry with PEG550-azide and azidododecane, to obtain thermoresponsive materials exhibiting lower critical solution temperatures (LCST) from room temperature to >60 °C. A facilitated synthesis for difunctional halogenide monomers was reported by Collard and coworkers to yielding 3,6-bis(chloromethyl)-1,4-dioxane-2,5-dione (**A57**):<sup>124</sup> 3-Chloropropane-1,2-diol was oxidized to the glycolic acid derivative and subsequently dimerized

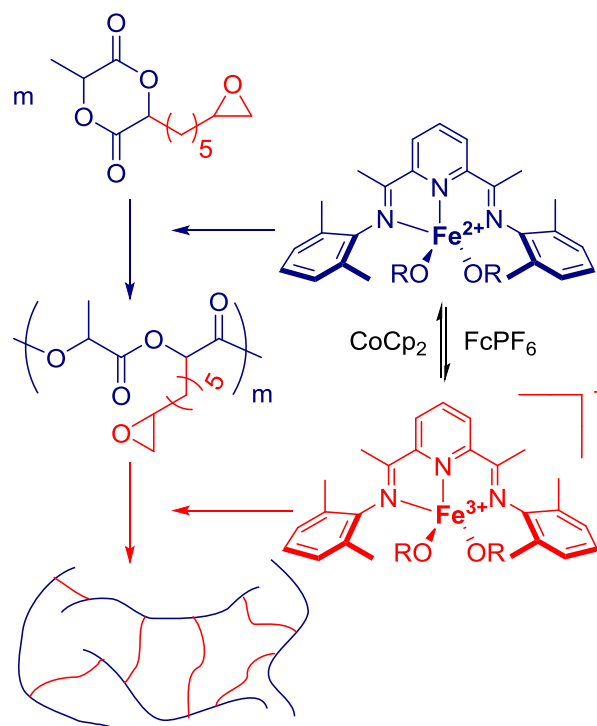


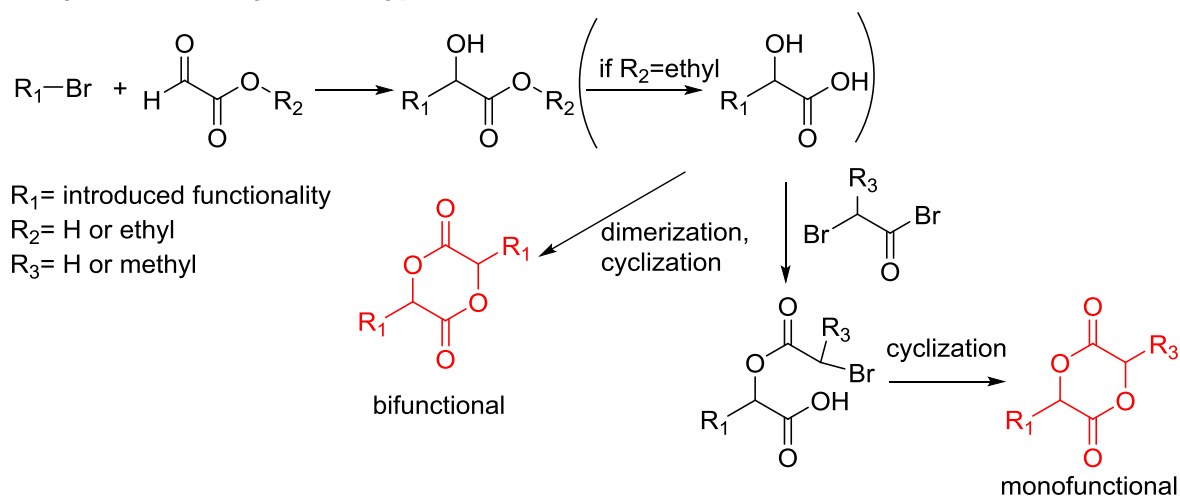
**Figure 1.3.** Selective polymerization of a bifunctional monomer by a redox-controlled iron catalyst. Adapted from Ref<sup>121</sup> with permission of The Royal Society of Chemistry.

and cyclized. Polymers were modified by dehydrochlorination to methyldene functions and further reacted with thiol derivatives by radical or nucleophilic thiol addition.

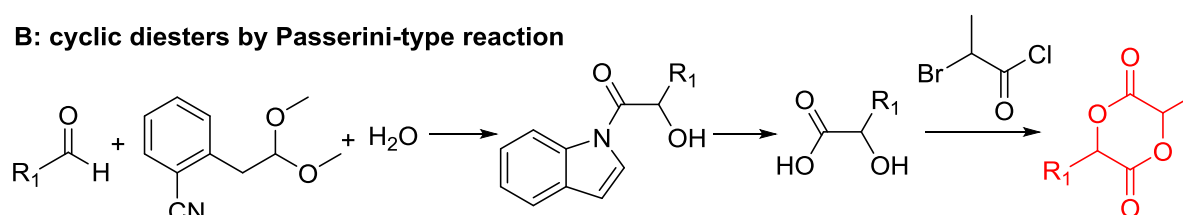
Yang and coworkers<sup>125</sup> reported a further alkyne-functionalized lactide **A58**, synthesized by an alternative route: several commercially available aldehydes were reacted in a Passerini-Type condensation to obtain the glycolic acid derivative (Scheme 1.9B). PLA-copolymers of **A58** were modified with dansyl-azide as prove of concept. They additionally reported two azide functionalized monomers (**A59** and **A60**), synthesized by the same route. Copolymers were modified with dansyl alkyne. Overall yields for the synthetic strategy of **A58-A60** were 6-16%. Weck and coworkers<sup>126</sup> introduced an azido-tri(ethylene glycole) functional lactide (**A61**). Polymers were modified with a fluorescent dye (7-nitrobenzoxadiazole, NBD) and a cell internalization peptide gH625 by click chemistry, and proved cellular uptake. The group as well showed modification by Staudinger condensation with Tap-GRGDS.<sup>127</sup>

Modification of lactides without ring-opening is rare. Hillmyer and coworkers<sup>118</sup> realized a bifunctional norbornene/lactide monomer (**A62**) suitable for ROP as well as ROMP by bromination and elimination of a lactide with an overall yield of 35% (Scheme 1.9C). The formed alkene reacted in a Diels-Alder reaction with cyclopentadiene and formed the bifunctional monomer. Dove and coworkers<sup>117</sup> showed that the norbornenes in such copolymers were able to react with tetrazine derivatives. The norbornene-tetrazine reaction allowed post-modification under mild conditions at

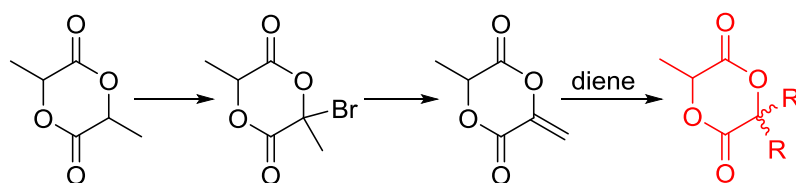
**A: cyclic diesters by Barbier-type addition**



**B: cyclic diesters by Passerini-type reaction**



**C: functional cyclic diesters from lactide**



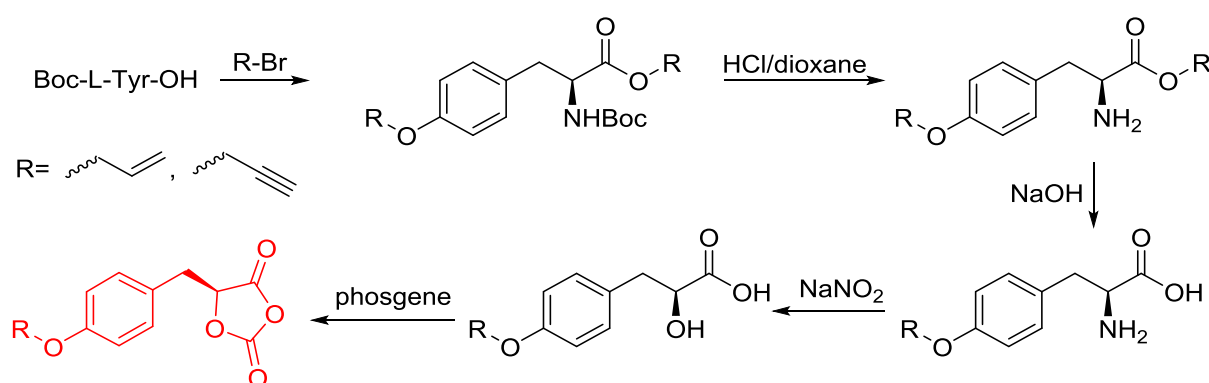
**Scheme 1.9.** Synthetic strategies to functional lactides and glycolides: A) by a Barbier-type addition; B) by a Passerini-type reaction, C) by functionalization of lactide.

room temperature and without the addition of a catalyst or additives. The monomer was further functionalized with azide derivatives (**A63**), e.g. PEG- $N_3$ <sup>128</sup> and polymerized. Two more lactides were realized by the same strategy using cyclohexa-1,3-diene (**A64**) and isoprene (**A65**) as diene for the Diels-Alder reaction, but the corresponding polymers were not further post-modified.<sup>129</sup>

**O-Carboxyanhydrides (OCAs).** In 1976, the first *O*-carboxyanhydride (OCA), 5-methyl-5-phenyl-1,3-dioxolan-2,4-dione, has been thermally polymerized.<sup>130</sup> OCAs are a readily available monomers from  $\alpha$ -hydroxy acids (with yields up to 28-75%, depending on the number of synthesis steps) and are a suitable alternative to lactides and glycolides, yielding PAHAs. Preparation of OCA monomers follows a general synthetic strategy:  $\alpha$ -hydroxy acids are carbonylated using phosgene, di- or triphosgene as carbonylating agent. In case of the latter two agents, activated charcoal is often used to promote the decomposition to phosgene and a tertiary amine is added as an acid scavenger (Scheme 1.10). Thermodynamically the ROP of OCAs is favored compared to lactide, both enthalpically and entropically. During the ROP,  $CO_2$  is released by decarboxylation from every

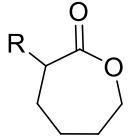
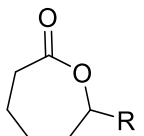
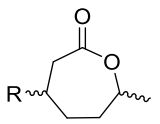
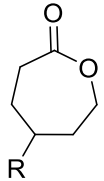
monomer unit and thus polymerization is more entropically driven than by release of ring strain.<sup>131</sup> Bases and nucleophiles like pyridine, DMAP, NHCs or zinc complexes (with an external protic initiator) are able to promote the polymerization of OCAs in organic solvents as dichloromethane at room temperature in a few minutes to several hours, acid catalysts fail. Enzymatic polymerization showed higher polymerizability for OCAs than for lactides (molecular weights up to  $10^4$  g/mol within 24 h at 80°C for OCAs, and 5-7 days at 80-130°C for lactide).<sup>119</sup>

The class of monomer has mainly been explored in the last decade and two orthogonally reactive OCAs have been reported so far: L-Tyr-alkynyl- (**A66**)<sup>132</sup> and L-Tyr-allyl-OCA (**A67**).<sup>133</sup> Cheng and coworkers used boc-protected L-Tyr-OH and reacted it with propargyl bromide to introduce the alkyne (or allyl bromide for the analogues alkene, Scheme 1.10).<sup>132</sup> After the release of the amine group and formation of the  $\alpha$ -hydroxy acid by diazotation with sodium nitrite, carbonylation and cyclization yielded the final monomer. PEG-block copoly(ester) of **A66** were core-crosslinked with a di-azide-cross-linker to redox-<sup>134</sup> or light-responsive<sup>135</sup> poly(ester) micelles; homopolymers were post-modified by thiol-yne reaction with cysteamine to polyelectrolytes for gene delivery and cell-penetration.<sup>136</sup> L-Tyr-allyl-OCA (**A67**) has not been used for post-modification so far.

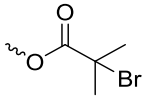
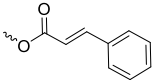
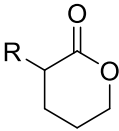
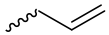
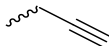
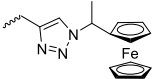
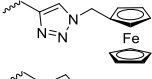
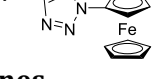
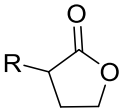
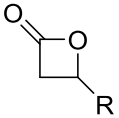


**Scheme 1.10.** Synthetic route to O-carboxyanhydrides (OCAs) from amino acids.

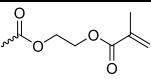
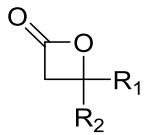
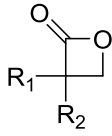
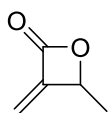
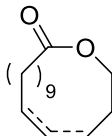
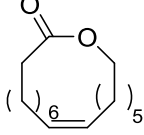
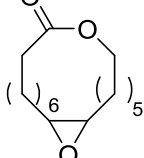
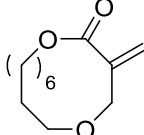
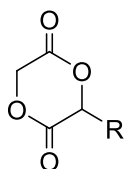
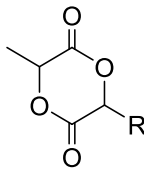
**Table 1.3.** Orthogonally functional cyclic monomers for the synthesis of poly(ester)s.

Monomer	R=	No	Post-Modification	Ref.
<b><u>ε-Caprolactones</u></b>				
<b><u>α-substituted</u></b>				
	~F	<b>A1</b>	-no modification	35
	~Cl	<b>A2</b>	-nucleophilic substitution with sodium azide and click chemistry	33, 37
	~Br	<b>A3</b>	-ATRP macroinitiator for “grafting from” of MMA -nucleophilic substitution with sodium azide and click chemistry	36, 38
	~I	<b>A5</b>	-radio-opaque properties	40
	~N <sub>3</sub>	<b>A4</b>	-click chemistry	39
	~C≡C	<b>A7</b>	-click reaction with cyclodextrin or Gd <sup>3+</sup> -complexes	42, 45-46
	~C≡C-CH <sub>2</sub> -C(=O)-O-	<b>A8</b>	-click reaction to core-cross-linked micelles	43
	~CH=CH <sub>2</sub>	<b>A6</b>	-thiol-ene reaction with amines, dyes, sugars or zwitterions	41, 44
	~CH=CH <sub>2</sub> -C(=O)-O-	<b>A9</b>	-end-chain cross-linker for macrocyclic polyester	47
	~C=C	<b>A10</b>	-no modification	48
<b><u>ε-substituted</u></b>				
	~C≡C	<b>A7b</b>	-click reaction to couple cyclodextrin	42, 46
<b><u>β-substituted</u></b>				
	~C≡C	<b>A11</b>	-no modification	50
	~C=C	<b>A12</b>	-epoxidation and thiol-ene reaction to cross-link	51
<b><u>γ-substituted</u></b>				
	~Cl	<b>A13</b>	-nucleophilic substitution with sodium azide and click chemistry with a cholesterol derivative for cell scaffolds and foams	52
	~Br	<b>A14</b>	-quaternization with pyridine -elimination, epoxidation and ring-opening to diols -nucleophilic substitution with sodium azide and click chemistry	53-55
	=O	<b>A15</b>	-hydrazination or hydrazone formation -reduction to alcohols and use as macroinitiator or coupling of maleic anhydride	56-58, 137-138
	~C(=O)-CH=CH <sub>2</sub>	<b>A16</b>	-bifunctional polymerization -electrografting onto metal surfaces -2D- and 3D-microstructured resins	59-62
	~C(=O)-C(=C) <sub>2</sub>	<b>A17</b>	-Michael-addition of thiols -photo-cross-linking	60, 63

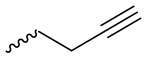
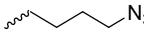
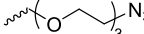
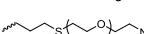
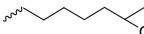
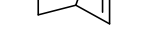
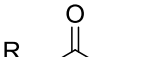
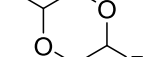
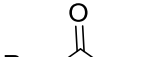
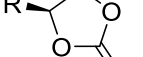
**Table 1.3.** Orthogonally functional cyclic monomers for the synthesis of poly(ester)s (*continued*).

Monomer	R=	No	Post-Modification	Ref.
		A18	-ATRP initiator or macroinitiator	64
		A19	-photo-cross-linking	65
<b><math>\delta</math>-Valerolactones</b>				
		A20	-dihydroxylation with NMO/OsO <sub>4</sub>	67,72
		A22	-click chemistry with PEG-, GRGDS-, phosphorylcholine or benzophenone-azides	66, 69, 71-72
		A21	-dihydroxylation and PEG "grafting to"	68
		A23	-radical copolymerization with methacrylates to form networks	73
		A24	-no polymerization	74
		A25	-no polymerization	74
		A26	-no polymerization	74
<b><math>\gamma</math>-Butyrolactones</b>				
		A27	-copolymerization with CL and cross-linking with methacrylate	79-80
		A28	-co- and terpolymerization with CL or TMCs and grafting from of methacrylates	82
<b><math>\beta</math>-Propiolactones</b>				
		A29	-tacticity studies	83
		A30	-tacticity studies	83
		A31	-tacticity studies	83,85
		A32	-tacticity and property studies	85
		A33	-tacticity and property studies	86
		A34	-tacticity and property studies	86
		A39	-selective polymerization studies	90
		A40	-selective polymerization studies	90
		A41	-selective polymerization studies	90
		A42	-hydroboration or olefin cross metathesis	91-94
		A43	-epoxidation and sulfonation to polymers inducing bone formation; thiol-ene reaction to macroinitiator for "grafting from"	95,97-98 99
		A44	-epoxidation	95

**Table 1.3.** Orthogonally functional cyclic monomers for the synthesis of poly(ester)s (*continued*).

Monomer	R=	No	Post-Modification	Ref.
		<b>A45</b>	-no modification	96
<b>β-Butyrolactones</b>				
	$R_1 = \text{CF}_3$ $R_2 = \text{wavy line}$	<b>A35</b>	-tacticity and property studies	84
	$R_1 = \text{CF}_3$ $R_2 = \text{wavy line}$	<b>A36</b>	-tacticity and property studies	84
	$R_1 = \text{Cl}$ $R_2 = \text{wavy line}$	<b>A37</b>	-quaternization with pyridine	87-88
	$R_1 = \text{Cl}$ $R_2 = \text{wavy line}$	<b>A38</b>	-polymerization studies	89
		<b>A46</b>	-radical cross-linking or thiol-ene reaction	100-101
<b>Macrolactones</b>				
		<b>A47</b>	-thiol-ene reaction for functionalization with pendant chains, cross-linking or functionalization with ATRP initiators for "grafting from" of <i>tert</i> -butyl acrylate	106, 109
		<b>A48</b>	-epoxidation	112
		<b>A49</b>	-no modification	112
		<b>A50</b>	-radical cross-linking	113
<b>Mono-substituted glycolides</b>				
	$\text{wavy line} - \text{CH=CH}_2$	<b>A51</b>	-epoxidation, dihydroxylation	114
	$\text{wavy line} - \text{C}\equiv\text{C}$	<b>A54</b>	-click chemistry with PEG-azide	115
<b>Mono-substituted hemilactides</b>				
	$\text{wavy line} - \text{CH=CH}_2$	<b>A52</b>	-thiol-ene reaction with amines for gene delivery	120, 122
	$\text{wavy line} - \text{C}\equiv\text{C}$	<b>A55</b>	-photo-cross-linking of nanoparticles/capsules -click chemistry with PEG-/Paclitaxel-azide	116

**Table 1.3.** Orthogonally functional cyclic monomers for the synthesis of poly(ester)s (*continued*).

Monomer	R=	No	Post-Modification	Ref.
		<b>A58</b>	-click chemistry with dansyl-azide	125
		<b>A59</b>	-click chemistry with dansyl-alkyne	125
		<b>A60</b>	-click chemistry with dansyl-alkyne	125
		<b>A61</b>	-click chemistry with dye/cell internalizing peptide -Staudinger condensation with Tap-GRGDS	126-127
		<b>A53</b>	-cross-linking	121
		<b>A62</b>	-ROMP -click reaction with tetrazine derivatives	117-118
		<b>A64</b>	-no modification	129
		<b>A65</b>	-no modification	129
		<b>A63</b>	-no modification	128
		<b>A63</b>	-no modification	128
<b>Di-substituted glycolides</b>				
		<b>A56</b>	-click chemistry with azide derivatives	123
		<b>A57</b>	-formation of double bonds -thiol-ene reaction	124
<b>O-Carboxyanhydrides (OCAs)</b>				
		<b>A66</b>	-cross-linking with di-azides to redox- or light-responsive micelles -thiol-yne reaction to form polyelectrolytes for gene delivery	132, 134-136
		<b>A67</b>	-no modification	133

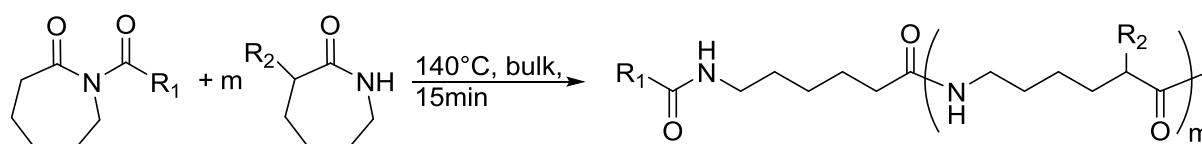
## 1.6 Poly(amide)s

Poly(amide)s from cyclic monomers can be obtained from cyclic lactams (polyamide-3 to polyamide-6), from  $\alpha$ -N-carboxyanhydrides (NCAs) (poly(peptide)s or polyamide-2) and N-substituted glycine N-carboxyanhydrides (NNCAs) (poly(peptoid)s), or from cyclic diamides and esteramides. They are known to show poor biodegradability.

### 1.6.1 Lactams

$\beta$ -Lactam (2-azetidinone),  $\gamma$ -butyrolactam (2-pyrrolidone),  $\delta$ -valerolactam (2-piperidone) and  $\epsilon$ -caprolactam (2-azepanone) are the main unsubstituted lactams used in the ROP. The number of orthogonally reactive lactam monomers is very limited so far. This might be attributed to the low

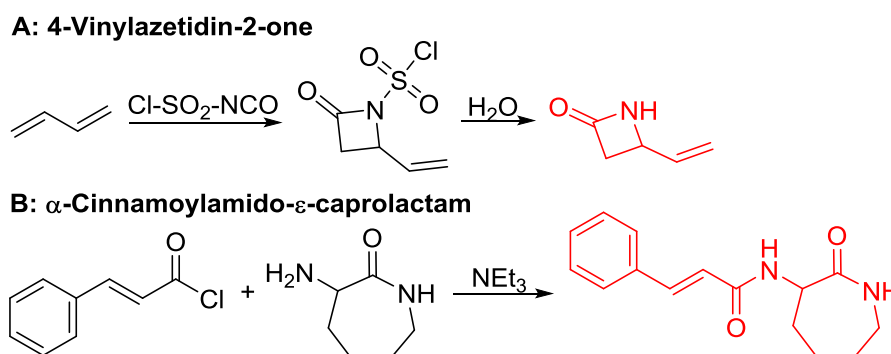
solubility of the products in most common organic solvents, due to H-bonding or crystallization.  $\epsilon$ -Caprolactam is typically polymerized in anionic ROP in bulk at temperatures of 140 °C above the melting point of the monomer (70 °C) within 15min, with the polymer precipitating from the melt (Scheme 1.11).<sup>139</sup> *N*-acyl or *N*-carbamoyl lactams as activators like hexamethylene-1,6-dicarbamoylcaprolactam are commonly added to promote the polymerization. For more details we refer to an excellent book chapter.<sup>140</sup>



**Scheme 1.11.** General polymerization protocol for caprolactams to poly(amide)s with an *N*-acyl lactam as an activator.

Vinyl lactam monomers are reported for all lactams, however, were only used for polymerization of the vinyl functionality. 4-Vinylazetid-2-one (**B1**) is the only bifunctional monomer, whose anionic ROP was reported (in DMSO with potassium 2-pyrrolidone, at 25-30 °C, 2h).<sup>141</sup> **B1** was synthesized by reaction of 1,3-butadiene with chlorosulfonyl isocyanate and subsequent saponification (Scheme 1.12A).<sup>142</sup> However, no post-modification has been reported.

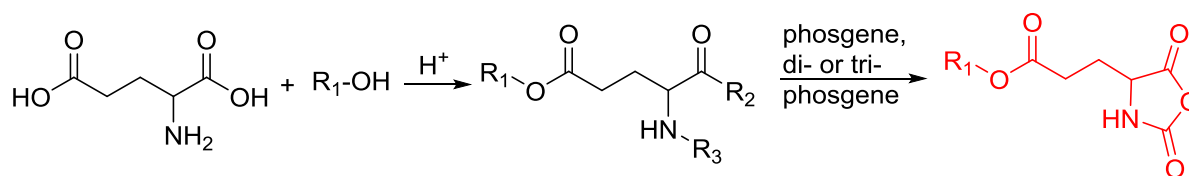
While a few protected functional  $\epsilon$ -caprolactam monomers (with amine, carboxy and carbonyl groups) are reported, Carlotti and coworkers<sup>139</sup> synthesized a reactive monomer, bearing a cinnamoyl functionality.  $\alpha$ -Cinnamoylamido- $\epsilon$ -caprolactam (**B2**) was synthesized in one step from cinnamoyl chloride and  $\alpha$ -amino- $\epsilon$ -caprolactam (yield: 80%) (Scheme 1.12B). Copolymers with  $\epsilon$ -caprolactam were cross-linked thermally (at 140 °C) or photochemically (at 364 nm) and again de-cross-linked photochemically (at 254 nm). The authors highlighted the potential of  $\alpha$ -amino- $\epsilon$ -caprolactam as an interesting precursor for other  $\epsilon$ -caprolactams. Poly(amide)s can also be post-modified at the amide group by *N*-alkylation with formaldehyde,<sup>143</sup> by epoxides or 2-bromoethylamine,<sup>144</sup> isocyanates or acid chlorides.<sup>145</sup>



**Scheme 1.12.** Synthetic route to functional lactams: A) 4-vinylazetid-2-one **B1** and B)  $\alpha$ -cinnamoylamido- $\epsilon$ -caprolactam **B2**.

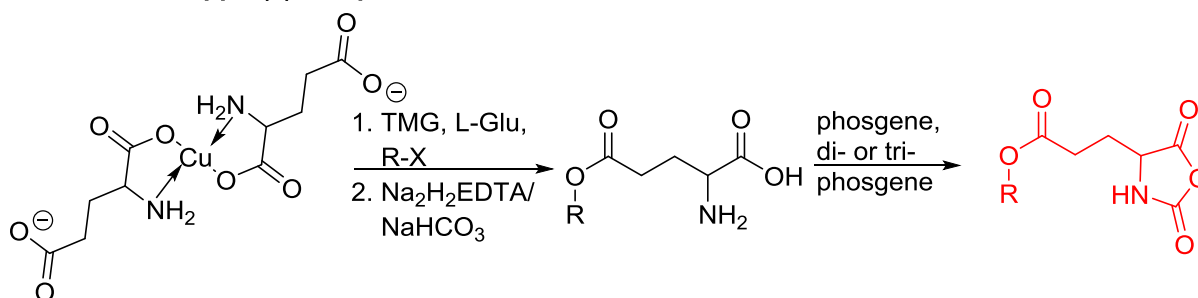


**A: General synthetic route**



R<sub>1</sub>= pendant chain  
 R<sub>2</sub>= -Cl or -OH  
 R<sub>3</sub>= -H, -Boc or Cbz

**B: General "Copper(II)-complex" method**



R= pendant chain  
 X= Cl or -O-C=O-O-R

**Scheme 1.14.** General synthetic routes to functional NCAs, depicted with glutamic acid.

**Glutamic acid- and tyrosine- based NCAs.** The majority of orthogonally functional NCA monomers are based on glutamic acid. Hammond and coworkers<sup>153</sup> reported  $\gamma$ -propargyl-L-glutamate NCA (**B3**), with homopolymers being functionalized by click chemistry with PEG-azides of different chain lengths to form grafted brushes,<sup>153</sup> different azide-functionalized carbohydrates,<sup>154</sup> primary to quaternary amines to form antimicrobial polypeptides,<sup>155</sup> or with cyclodextrin.<sup>156</sup> Chen and coworkers<sup>157</sup> introduced carboxy groups by photochemical thiol-yne reaction. The polymers were used to control biomineralization of calcium carbonate.<sup>157</sup> Tang and coworkers<sup>158</sup> reported a second alkyne functionalized monomer,  $\gamma$ -(4-(propargoxycarbonyl)-benzyl)-L-glutamate NCA (**B4**), synthesized by the Cu(II)-complex method, using 4-(chloromethyl)benzoyl chloride (Scheme 1.14B). Obtained polypeptides were functionalized by click chemistry with alkyl chains of different lengths and the UCST-behavior extensively analyzed in aqueous mixtures. Cheng and coworkers<sup>159</sup> reported a similar monomer,  $\gamma$ -(4-propargyloxybenzyl)-L-glutamate NCA (**B5**), also obtained by the Cu(II)-complex method, using 4-propargyloxybenzyl chloride. The polypeptides were amine/guanidine functionalized by click chemistry and their transfection efficiency for gene delivery examined.

Several alkene-functionalized NCAs have been reported to date. Daly and coworkers<sup>160</sup> prepared  $\gamma$ -allyl-L-glutamate (**B6**) and  $\gamma$ -(9-decenyl)-L-glutamate NCA (**B7**) and studied their homo- and copolymerization and epoxidation of the double bonds with mCPBA. Gelation was obtained by cross-linking of the epoxides with TFA, oxidation to carboxylic acids was shown with

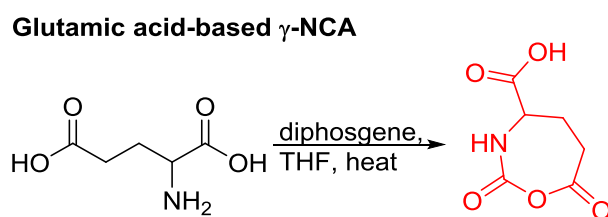
KMnO<sub>4</sub>/NaHCO<sub>3</sub>. Zhang and coworkers<sup>161</sup> used **B6** in copolymers for photochemical thiol-ene reaction and introduction of carboxy groups.  $\gamma$ -(4-Allyloxybenzyl)-L-glutamate NCA (**B8**) has been reported by Cheng and coworkers,<sup>162</sup> using the copper(II)-complex method and 4-allyloxybenzyl chloride. Thiol-ene reaction in homopolymers of **B8** with cysteamine to poly( $\gamma$ -(4-aminoethylthiopropoxy)benzyl-L-glutamate) exhibited a charge-backbone distance of 17  $\sigma$ -bonds. Remarkably high helicity of 81% was observed for polypeptides with a DP of 10 at pH 2. Compared to the polymer with elongated charge-backbone distance of 17  $\sigma$ -bonds, poly( $\gamma$ -(4-(1-hexanol-6-aminomethyl))benzyl-L-glutamate) with a DP of 10 and a charge-backbone distance of 11  $\sigma$ -bonds showed mixed conformation of  $\beta$ -sheets and only 26%  $\alpha$ -helices.  $\gamma$ -(4-vinylbenzyl)-L-glutamate NCA was introduced by the group of Schouten.<sup>163</sup> The olefins were used for radical cross-linking of terpolymer surface-grafted films,<sup>163</sup> or transformation by ozonolysis into alcohols<sup>164</sup> or aldehydes<sup>165</sup> and subsequent hydroamination with primary amines, to yield polypeptides suitable for gene transfection.<sup>166</sup> Oxidation to diols or carboxyl functionalities by osmiumtetroxide, olefin metathesis reaction with *cis*-1,4-dichlorobutene and Suzuki coupling were shown by Cheng and coworkers.<sup>164</sup>

Kamogawa and coworkers<sup>167</sup> reported already in 1975 a whole library of photoreactive glutamic acid, tyrosine and lysine based NCAs with pendant acryloyl, methacryloyl and cinnamoyl groups (**B10-B18**). They showed polymerization of all NCAs and photochemical cross-linking of films, whereas the photosensitivity decreased for acryloyl  $\approx$  methacryloyl > cinnamoyl, and poly(glutamate) > poly(lysine) > poly(tyrosine). A further photo-cross-linkable monomer, also containing a cinnamoyl function,  $\gamma$ -cinnamoyl-L-glutamate NCA (**B19**), was already reported before by Iwakura and coworkers in 1974.<sup>168</sup> Jing and coworkers<sup>169</sup> photochemically crosslinked self-assembled polypeptide-block-PEG micelles of **B19**, loaded with paclitaxel as stable drug carriers. Iwakura and coworkers reported a further potentially photoactive benzophenone-containing NCA,  $\gamma$ -*p*-benzoylbenzyl-L-glutamate NCA and its homo- and copolymerization with  $\gamma$ -*p*-benzyl-L-glutamate NCA (**B20**).<sup>170</sup> They studied the orientation of benzophenone groups in the side chains and conformation of polymers. Further photochemical reaction of the pendant groups has not been shown so far.

Several chlorinated monomers with varying length of alkyl spacers and suitable for nucleophilic substitution were reported: homo- and copolymers of a  $\gamma$ -(2-chloroethyl)-L-glutamate NCA (**B21**) were used as ATRP macroinitiator to graft oligoethylene methacrylate or to form nanogels for drug delivery.<sup>171</sup> Cross-linking of the gels was achieved through quaternization reaction of 2,2'-dithiobis(*N,N*-dimethylethylamine) (dTbDEA) with the chloride functionalities.<sup>172</sup> Polymers with the analogous  $\gamma$ -(3-chloropropyl)-L-glutamate (**B22**),  $\gamma$ -(6-chlorohexyl)-L-glutamate (**B23**), and  $\gamma$ -(8-chlorooctyl)-L-glutamate NCA (**B24**) were further derivatized to the respective azides and

modified with carbohydrates,<sup>173</sup> arginine,<sup>174</sup> or imidazolium<sup>175</sup> derivatives by click chemistry. These poly(arginine) mimics with hydrophobic side chains of different lengths exhibited helix-related cell-penetrating properties and high DNA and siRNA delivery efficiencies in various mammalian cells. Quaternization of the chloride substituted polypeptides with triethylphosphine yielded cell-penetrating peptides,<sup>176</sup> quaternization with pyridinium salts UCST-type polypeptides,<sup>177</sup> and with 1-methylbenzimidazole helical antimicrobial polypeptides.<sup>178</sup> Tang and coworkers<sup>179</sup> reported  $\gamma$ -(4-chloromethylbenzyl)-L-glutamate NCA (**B25**), synthesized by the copper(II) complex strategy. These chloride-substituted polypeptides were modified with 1-alkylimidazolium (methyl or *n*-butyl) and various counter-anions (i.e. Cl<sup>-</sup>, F<sup>-</sup>, BF<sub>4</sub><sup>-</sup>). The polypeptides exhibited LCST- or UCST-type behavior in organic solvents or in water. Poly(peptide)s of an active ester functionalized monomer,  $\gamma$ -trichloroethyl-L-glutamate NCA (**B26**)<sup>180</sup> were post-modified by amidation with different amine derivatives and their properties examined as gene delivery vectors.<sup>181</sup>

Higashi and coworkers<sup>146</sup> reported already in 1978 a carboxylated  $\gamma$ -NCA (**B27**), after the reaction of glutamic acid with diphosgene (Scheme 1.15). They proved successful polymerization by viscosity measurements and characteristic amide signals in IR spectra, which are also observed for Nylon-4. Modification of the carboxyl function has not been reported.



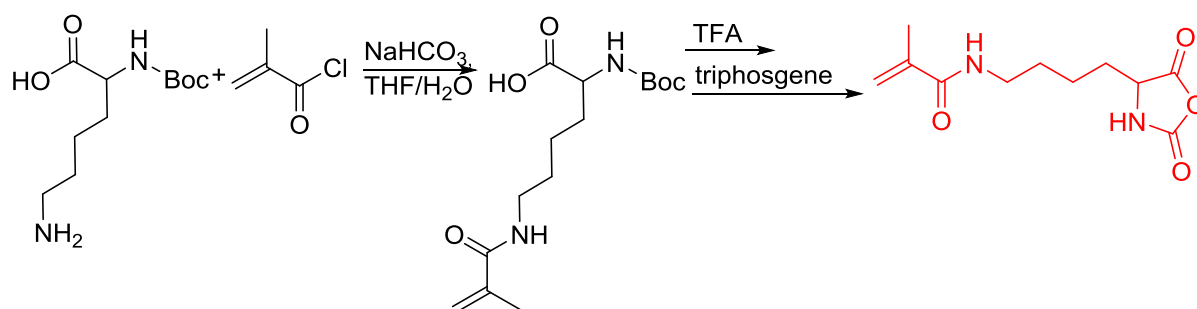
**Scheme 1.15.** Synthetic strategy to a glutamic acid-based  $\gamma$ -NCA **B27**.

**Lysine- and ornithine-based NCAs.** Besides the photoreactive investigations of **B16-B18** from Kamogawa<sup>167</sup> (*see above*), Lei and coworkers<sup>182</sup> recently used **B16** for complex mussel-inspired thermoresponsive polypeptide-pluronic copolymers as surgical adhesives and for hemostasis. Chen and coworkers<sup>183</sup> prepared copolymers of **B17** (Scheme 1.16A) and **B3**. Both groups applied thiol-ene reaction with high efficiency for post-modification.

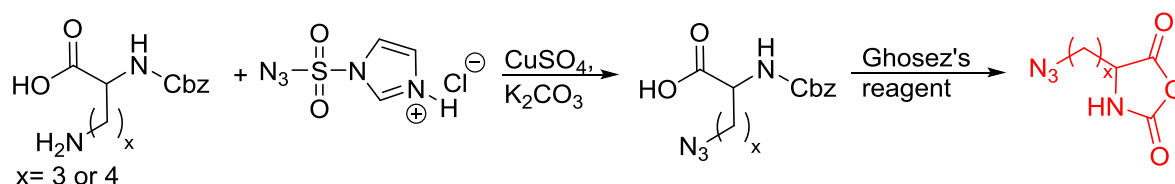
Polymers of  $\epsilon$ -*N*-bromoisobutyryl-L-lysine NCA (**B28**) were used as ATRP macroinitiators by Li and coworkers,<sup>184</sup> and two polypeptide bottlebrushes with polystyrene or poly(oligoethylene glycol methacrylate) prepared, exhibiting an  $\alpha$ -helical conformation in appropriate solvents.

Deming and coworkers<sup>185</sup> reported azide containing monomers: azido-norleucine (**B29**) and azido-norvaline NCAs (**B30**).  $\alpha$ -*N*-Carboxybenzyl lysine or ornithine were reacted with imidazole-1-sulfonyl-azide-HCl, CuSO<sub>4</sub> and K<sub>2</sub>CO<sub>3</sub> to form the azide derivative (Scheme 1.16B). The

**A: Lysine-based NCAs**



**B: Lysine/ornithine-based azide- NCAs**



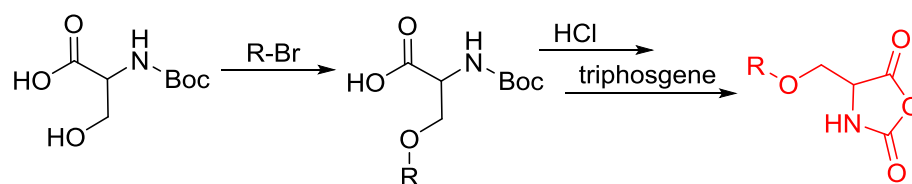
**Scheme 1.16.** Synthetic routes to lysine/ornithine-based NCAs.

derivatives were converted to NCAs, using the Ghosez's reagent (1-chloro-*N,N'*-2-trimethyl-1-propenylamine). Various alkyne derivatives were attached to azide-substituted poly(peptide)s through click chemistry with >95% conversion.

**Serine- and homoserine-based NCAs.** Cheng and coworkers<sup>186</sup> synthesized *O*-pentenyl-L-serine NCA (**B31**) (Scheme 1.17A) and prepared block copolymers with PEG. Modification by thiol-ene reaction with cysteamine gave water-soluble copolymers with elongated and charged side chains exhibiting cell-penetrating properties. Deming and coworkers<sup>187</sup> reported two phosphate containing monomers, *O*-2-bromoethylbenzylphospho-L-serine NCA (**B32**) and *O*-2-bromoethylbenzylphospho-L-homoserine NCA (**B33**) (Scheme 1.17B). While poly(L-phosphorylcholine serine) was not obtained after amination of the bromides in polymer P(**B32**) due to  $\beta$ -elimination and chain degradation, the use of poly(L-phosphorylcholine homoserine) overcame the side reaction. Both, deprotection and amination, were achieved in one step. **B32** and **B33** were synthesized from homoserine or serine and benzyl (2-bromoethyl) diisopropylphosphoramidite. Cyclization was achieved by Ghosez's reagent.

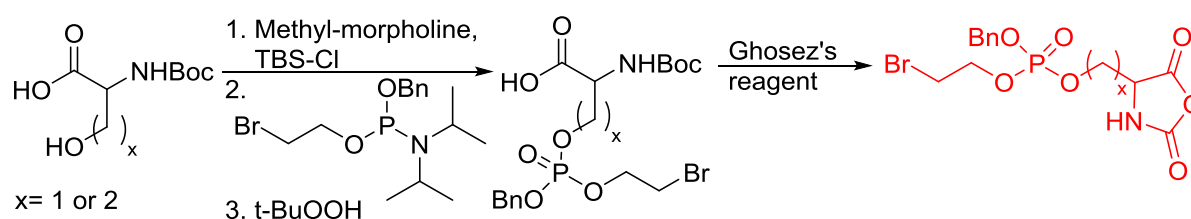
**Cysteine-based NCAs.** A vinyl sulfone-substituted L-cysteine NCA (**B34**) was reported by Zhong and coworkers,<sup>188</sup> synthesized from divinyl sulfone and L-cysteine hydrochloride (Scheme 1.18A). Post-modification of vinyl sulfone-functionalized polypeptides with different thiols (polar, charged, carbohydrates) through nucleophilic addition produced glycopolypeptides, functional polypeptide coatings, or hydrogels. Tang and coworkers<sup>189</sup> reported a *S*-(2-(3-chloropropoxycarbonyl)ethyl)-L-cysteine NCA (**B35**) from 3-chloropropyl acrylate. The poly(peptide)s were substituted with imidazolium salts and their UCST-behavior was investigated.

**A: Serine-based NCAs**



R= 5-pentenyl

**B: Serine/homoserine-based NCAs**

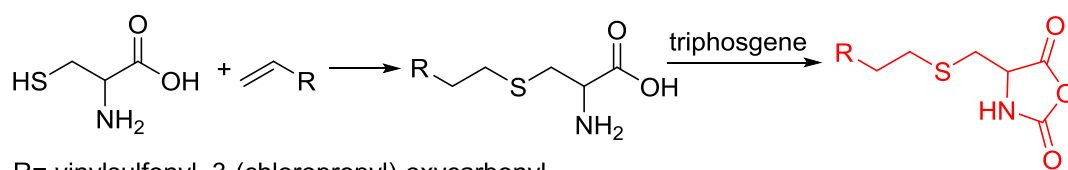


**Scheme 1.17.** Synthetic routes to serine/homoserine-based NCAs.

Barz and coworkers<sup>190</sup> recently reported two interesting *S*-sulfonyl based NCA monomers: *S*-(ethylsulfonyl)-L-cysteine NCA (**B36**) and *S*-(isopropylsulfonyl)-L-cysteine NCA (**B37**) (Scheme 1.18). Disulfides are bioreversible and therefore attractive for biomedical applications. They are stable under extracellular conditions, but cleavable inside of cells. Usually, disulfide formation has been achieved by oxidation of thiols (with long reaction times, often not 100% conversion and the lack of formation of asymmetric disulfides) or by formation of reactive thiols (chlorinated or nitroso-thiols). A major drawback of activated thiols is the limited stability against aminolysis and hydrolysis. The group of Barz introduced two monomers with a protective and at the same time activating group, which was stable during ROP. Asymmetric disulfide formation was chemoselectively achieved by post-modification with appropriate thiols. An alkylsulfonyl chloride was hydrolyzed to an alkylsulfonic acid sodium salt and reacted with *S*-nitrosocysteine (generated in situ from L-cysteine) forming a thiosulfonate, which reacted with diphosgene to yield the final NCAs (**B36** and **B37**) (Scheme 1.18B). Quantitative post-modification of polymers from **B36** with benzylmercaptane was proven within 60s, without degradation or side reactions. The approach opens a way to reversible conjugation of drugs as well as cross-linking to form nanostructures.<sup>191</sup>

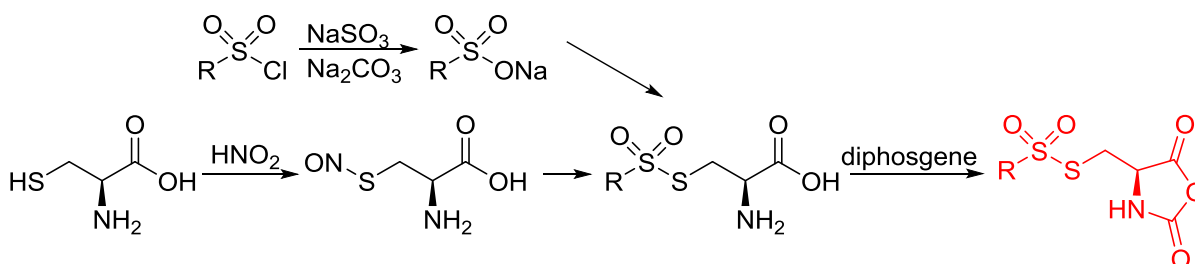
**Methionine-based NCAs.** Deming and coworkers<sup>192</sup> reported L-methionine NCA (**B38**). Beneficially, L-methionine NCA was synthesized in one step with high yield (91%)<sup>192</sup> proceeding from L-methionine. L-methionine is readily available and the amino acid with the highest production rate due to its use in animal feed. Methionine in homo- and copolypeptides were chemoselectively and efficiently (>90%) alkylated with a broad range of bromide, iodide, triflate and epoxide<sup>193</sup> (pH<3) derivatives yielding stable sulfonium or  $\beta$ -alkyl- $\beta$ -hydroxyethyl sulfonium products. Poly(methionine) was compatible with deprotection of other functional groups. Sulfur nucleophiles dealkylated the polypeptides again, and triggered release of therapeutics or tagged

**A: Cysteine-based NCAs through Michael addition**



R= vinylsulfonyl, 3-(chloropropyl)-oxycarbonyl

**B: Cysteine-based NCAs through sulfonyl halides**



R= Ethyl, isopropyl

**Scheme 1.18.** Synthetic protocols for cysteine-based NCAs.

protein digests from affinity columns were achieved.<sup>194</sup> Oxidation of sulfur in poly(L-methionine) to poly(L-methionine sulfoxide) or poly(L-methionine sulfone) influences the conformation of the polypeptides: poly(L-methionine) is hydrophobic forming an  $\alpha$ -helix, poly(L-methionine sulfoxide) is water-soluble with a disordered conformation (Figure 1.4) poly(L-methionine sulfone) exhibits a slightly water-soluble mainly  $\alpha$ -helical structure. Deming and coworkers<sup>195</sup> designed poly(L-methionine)-*b*-poly(L-leucine-*stat*-L-phenylalanine) copolymers and the oxidized sulfoxide copolymers self-assembled to stable vesicles. Upon reduction of the sulfoxides by methionine sulfoxide reductase A and B (MSR enzymes, found within human cells) and DTT as surrogate reductant, the hydrophilic disordered segments became hydrophobic and changed to rigid  $\alpha$ -helical conformation. Change of conformation stiffened the vesicle membranes by forming a crumpled sheet-like morphology and eventually caused vesicle membrane rupture. Triggered release of an encapsulated model cargo (Texas Red labeled dextran) by enzymatic reduction of the sulfoxides segments has been demonstrated.

**DOPA-based NCAs.** In recent years, catechol-containing polymers, inspired by mussel foot proteins (mfp) gained increasing interest for biomedical applications. Catechols complex metal-ions pH-dependently and reversible with high binding affinities, react with amines and thiols or covalently cross-link with each other under oxidizing conditions. *O,O'*-dicarbobenzyloxy-<sup>196</sup> and *O,O'*-acetyl-protected<sup>197</sup> L-DOPA NCAs were reported in literature. The unprotected L-dihydroxyphenylalanine NCA (**B39**) was introduced from the group of Qiao<sup>198</sup> by reaction of L-DOPA with triphosgene. They stated, that the phenolic hydroxyl groups did not initiate ROP of NCAs, however used the NCA immediately after synthesis for polymerization, probably due to instability during storage. Block copolymers of L-glutamic acid and **B39** showed reversible vesicle

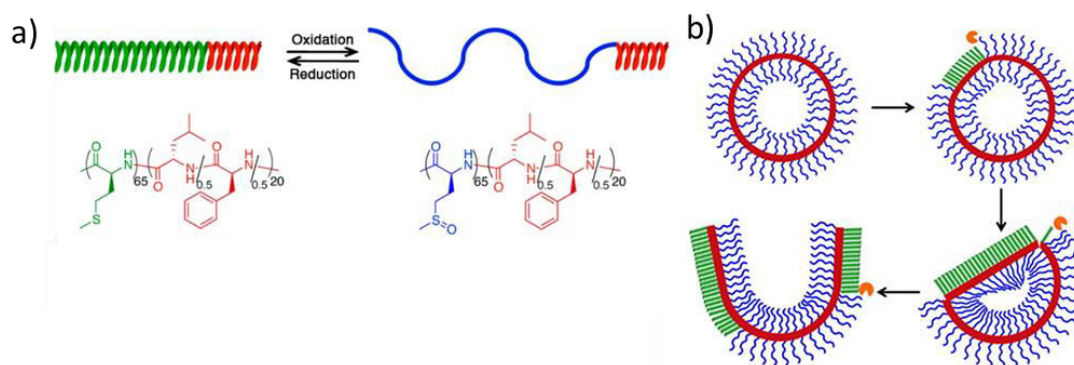


**Figure 1.4.** Enzyme-triggered release of cargos from methionine sulfoxide containing vesicles: a) structure, redox properties, and conformation of poly(l-methionine)-*b*-poly(l-leucine-*stat*-l-phenylalanine) peptides, b) the possible effect of enzymatic reduction of vesicle surface of sulfoxide segments to methionine segments for change of conformation and cause of vesicle ruptures.

Adapted with permission from Ref<sup>195</sup>; copyright 2017 American Chemical Society.

formation with ellipsoidal morphology at pH 3 and hollow vesicles at pH 12. Oxygen-mediated oxidation of DOPA groups at pH 12 stabilized the vesicles by cross-linking. Lei and coworkers<sup>182, 199</sup> recently applied the **B39** in L-arginine- and L-DOPA-containing copolypeptides as surgical adhesives.

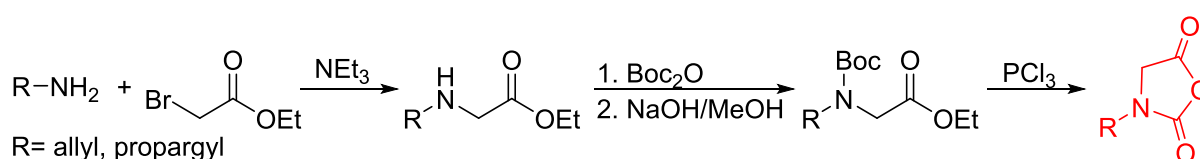
**Unnatural amino acid-based NCAs.** In 1945, Schlögl et al.<sup>200</sup> already introduced D,L-allylglycine NCA (**B40**) and its polymerization. Post-modification at that time was only conducted via hydrogenation, hydrobromination and bromination. Schlaad and coworkers<sup>201-202</sup> showed glycosylation by radical and photochemical thiol-ene reaction to enhance helical stability and solubility of poly(D,L-allylglycine) and poly(D,L-allylglycine-*co*-L-glutamate). A further unsaturated NCA, 5-pentenyl-D,L-glycine NCA (**B41**), was reported by Blanch and coworkers,<sup>203</sup> post polymerization modification has not been reported.. In 1960, Schlögl et al.<sup>204</sup> reported the synthesis of D,L-propylglycine NCA (**B42**) from D,L-propylglycine and phosgene, and its polymerization. Post-modification was only reported decades later in 2010 by Heise and coworkers<sup>205</sup> with glycosylation by click chemistry,<sup>206</sup> and in 2012 by Schlaad and coworkers<sup>202</sup> with glycosylation by photochemical thiol-yne reaction. Bioactivity of the polymers, micelles or polymersomes was proven by selective lectin binding by the groups of Heise and Schlaad. Block copolypeptides with one glycosylated segment were found to be efficient stabilizers (completely based on renewable building blocks) in the emulsion polymerization of styrene.<sup>207</sup> Alkene- or alkyne-substituted NCAs from unnatural amino acids compared to analog NCAs from natural amino acid display the distinct benefit, that ester or amide linkages are absent in the pendant chains. Pendant chains in polypeptides from naturally amino acid-based NCAs might be cleaved by hydrolysis or aminolysis at these linkages and thereby molecules introduced by post-modification detached. A challenging

drawback of unnatural amino acid-based NCAs is the synthesis of the needed amino acids, which might be the reason for only few reported monomers in literature.

### 1.6.3 *N*-Substituted *N*-Carboxyanhydrides

Compared to the variety of functional NCAs, only few *N*-substituted *N*-carboxyanhydrides NNCA monomers with a substitution at the nitrogen atom are reported, yielding poly(peptoid)s, typically under similar conditions as the NCA counterparts. Although structurally similar to poly(peptide)s, poly(peptoid)s is not able to form  $\beta$ -sheets by hydrogen bonding, due to the *N*-alkylation. They are therefore more soluble and better processable, but only oxidatively degradable.

Schlaad and coworkers<sup>208-209</sup> and Zhang and coworkers<sup>210-211</sup> reported the synthesis, polymerization and post-modification of two functional monomers, *N*-allyl glycine NCA (**B43**)<sup>208, 211</sup> and *N*-propargyl glycine NCA (**B44**) (overall yields 21-70%).<sup>209-210</sup> The synthetic route differs from the general strategies for NCAs (Scheme 1.19): allylamine or propargylamine and  $\alpha$ -bromo ethylacetate reacted in a substitution reaction. The newly formed secondary amine was protected and cyclization was achieved by using phosphorus trichloride (Leuch's method). 1,4-diallylpiperazine-2,5-dione was isolated as byproduct in the case of **B43** (yield: 58% main product, 31% byproduct).<sup>208</sup> Alkene containing polymers were successfully modified by photochemical thiol-ene reaction with 1-thioglycerol and -glucose in high conversion yields,<sup>208</sup> alkyne-containing polymers by click chemistry with PEG-azide.<sup>210</sup> The later ones were also cross-linked upon heating, however a precise mechanism is not confidently assigned so far.<sup>212</sup>



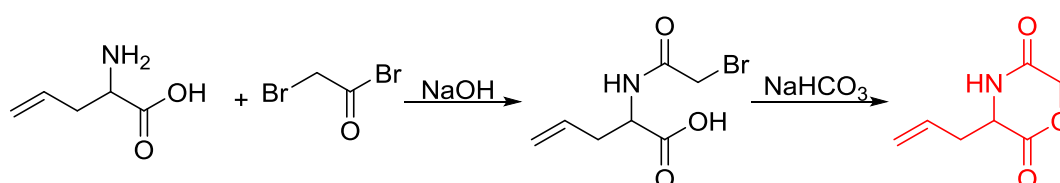
**Scheme 1.19.** Synthetic route to NNCA monomers.

### 1.6.4 Cyclic Diamide Monomers

To the best of our knowledge, no orthogonally functional cyclic diamides suitable for ROP have been reported so far. They are usually used for polycondensation reaction, where the ring remains in the backbone of the polymer. Elias and coworkers copolymerized the unfunctionalized monomer 2,5-dioxopiperazine (DOP) with caprolactam,<sup>213</sup> Hildgen and coworkers with allyl glycidyl ether.<sup>214</sup>

### 1.6.5 Cyclic Esteramide Monomers

Morpholine-2,5-diones, resulting poly(depsipeptide)s, have been functionalized with different alkyl chains or protected groups. However, they are less reactive as lactides.<sup>215</sup> To the best of our knowledge, Klok and coworkers<sup>216</sup> reported the only orthogonally reactive esteramide monomer, L-allylglycine-morpholine-2,5-dione (**B45**). Further functional morpholine-2,5-diones employ protecting groups. The synthetic strategy is analog to the synthesis of functional glycolides and lactides: a corresponding  $\alpha$ -amino acid and 2-bromoacetyl bromide reacted and the final monomer was realized by intramolecular cyclization of the intermediate in 13% yield (Scheme 1.20). Klok and coworkers showed modification by thiol-ene reaction with different fluorinated, carboxylated, aminated or dihydroxylated thiols with conversions between 15-100%.

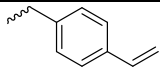
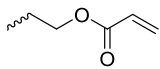
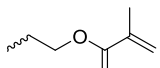
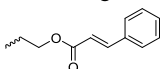
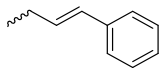
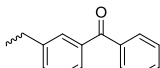
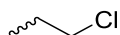
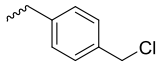
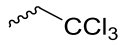
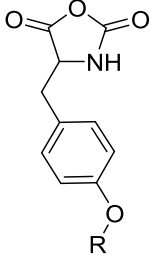
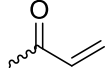
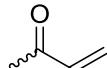
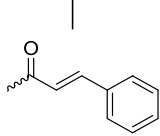


**Scheme 1.20.** Synthetic strategy to functional morpholino-2,5,-dione monomer (**B45**).

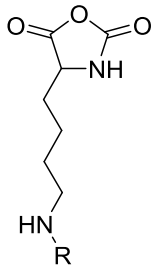
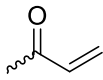
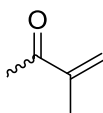
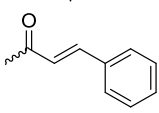
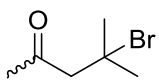
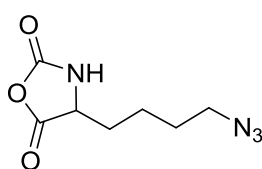
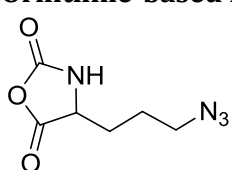
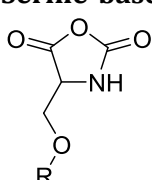
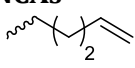
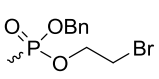
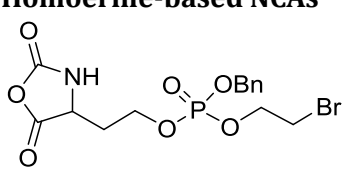
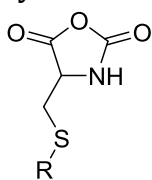
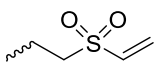
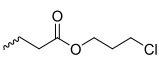
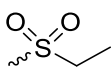
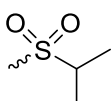
**Table 1.4.** Orthogonally functional cyclic monomers for the synthesis of poly(amide)s and poly(esteramide)s.

Monomer	R=	No	Post-Modification	Ref.
<b>Lactams</b>				
		<b>B1</b>	-no modification	141-142
		<b>B2</b>	-thermal or photochemical cross-linking	139
<b>Glutamic acid-based NCAs</b>				
		<b>B3</b>	-click chemistry with PEG-, carbohydrate-, amine- or cyclodextrin-azides; photochemical thiol-yne reaction to introduce carboxy groups	153-157
		<b>B4</b>	-click chemistry to introduce alkyl chains of different lengths	158
		<b>B5</b>	-click reaction with amine/guanidines for gene delivery	159
		<b>B6</b>	-epoxidation and cross-linking; oxidation to carboxy functionalities; photochemical thiol-ene reaction to introduce carboxy groups	160-161
		<b>B7</b>	-epoxidation and cross-linking	160
		<b>B8</b>	-oxidation to carboxy functionalities	162
			-thiol-ene reaction with cysteamine to elongate the distance between charged groups and backbone	162

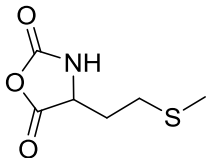
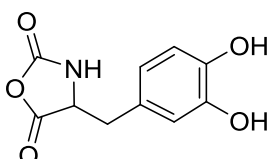
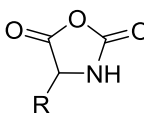
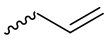
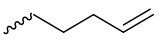
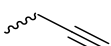
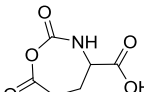
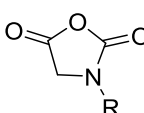
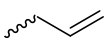
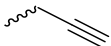
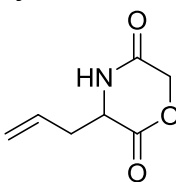
**Table 1.4.** Orthogonally functional cyclic monomers for the synthesis of poly(amide)s and poly(esteramide)s (*continued*).

Monomer	R=	No	Post-Modification	Ref.
		<b>B9</b>	-radical cross-linking -ozonolysis to alcohols and aldehydes and hydroamination -oxidation to diols and carboxy groups -olefin metathesis -Suzuki coupling	163-166
		<b>B10</b>	-formation of films by photo-cross-linking	167
		<b>B11</b>	-formation of films by photo-cross-linking	167
		<b>B12</b>	-formation of films by photo-cross-linking	167
		<b>B19</b>	-photo-cross-linking to stable micelles for drug delivery	168-169
		<b>B20</b>	-no modification	170
		<b>B21</b>	-ATRP macroinitiator -quaternization with diamines to form nanogels for drug delivery	171-172
		<b>B22</b>	-derivatization with NaN <sub>3</sub> and click chemistry with carbohydrates, arginine or imidazolium	173-177
		<b>B23</b>	-derivatization with NaN <sub>3</sub> and click chemistry with arginine	174, 176, 178
		<b>B24</b>	-derivatization with NaN <sub>3</sub> and click chemistry with arginine	174
		<b>B25</b>	-nucleophilic substitution with 1-alkylimidazolium salts to LCST- and UCST-type polypeptides	179
		<b>B26</b>	-amidation with amines for gene delivery	180-181
<b>Tyrosine-based NCAs</b>				
		<b>B13</b>	-formation of films by photo-cross-linking	167
		<b>B14</b>	-formation of films by photo-cross-linking	167
		<b>B15</b>	-formation of films by photo-cross-linking	167

**Table 1.4.** Orthogonally functional cyclic monomers for the synthesis of poly(amide)s and poly(esteramide)s (*continued*).

Monomer	R=	No	Post-Modification	Ref.
<b>Lysine-based NCAs</b>				
		<b>B16</b>	-formation of films by photo-cross-linking -thiol-ene reaction for cross-linking	167, 182
		<b>B17</b>	-formation of films by photo-cross-linking -thiol-ene reaction	167, 183
		<b>B18</b>	-formation of films by photo-cross-linking	167
		<b>B28</b>	-ATRP macroinitiator	184
		<b>B29</b>	-click chemistry	185
<b>Ornithine-based NCAs</b>				
		<b>B30</b>	-click chemistry	185
<b>Serine-based NCAs</b>				
		<b>B31</b>	-thiol-ene reaction with cysteamine to cell-penetrating peptides	186
		<b>B32</b>	-modification degrades the polymer	187
<b>Homoerine-based NCAs</b>				
		<b>B33</b>	-amination to form poly(L-phosphorylcholine homoserine)	187
<b>Cysteine-based NCAs</b>				
		<b>B34</b>	-Michael-type addition of polar-, charged- or carbohydrate-thiols forming glycopeptides, coatings and hydrogels	188
		<b>B35</b>	-nucleophilic substitution with imidazolium salts	189
		<b>B36</b>	-reaction with thiols to form asymmetric disulfides	190-191
		<b>B37</b>	-reaction with thiols to form asymmetric disulfides	190

**Table 1.4.** Orthogonally functional cyclic monomers for the synthesis of poly(amide)s and poly(esteramide)s (*continued*).

Monomer	R=	No	Post-Modification	Ref.
<b>Methionine-based NCAs</b>				
		<b>B38</b>	-alkylation with bromide, iodide and triflate derivatives and triggered dealkylation with sulfur nucleophiles -oxidation to sulfoxides causing change of copolymer conformation -reaction with epoxides to $\beta$ -alkyl- $\beta$ -hydroxyethyl sulfonium products	192-195
<b>DOPA-based NCAs</b>				
		<b>B39</b>	-oxidative cross-linking and tissue adhesion	182, 198-199
<b>Unnatural amino acid based NCAs</b>				
		<b>B40</b>	-reduction or bromination -glycosylation by thiol-ene reaction	200-202
		<b>B41</b>	-no modification	203
		<b>B42</b>	-glycosylation by click chemistry -photochemical thiol-yne reaction	202, 204-207
<b><math>\gamma</math>-NCAs</b>				
		<b>B27</b>	-no modification	146
<b>NNCAs</b>				
		<b>B43</b>	-thiol-ene reaction with thioglycerol and -glucose	208, 211
		<b>B44</b>	-click chemistry with PEG-azide -thermal cross-linking	209-210
<b>Cyclic esteramides</b>				
		<b>B45</b>	-thiol-ene reaction with charged or polar thiols	216

## 1.7 Poly(carbonate)s

Aliphatic polycarbonates find broad application in biomedical devices and drug delivery. They are typically prepared by phosgene condensation or ester exchange, by addition polymerization of epoxides with carbon dioxide in ring-opening copolymerization (ROCOP)<sup>217</sup> or by ROP of 6-membered cyclic carbonates, i.e. trimethylene carbonate (TMC). Poly(trimethylene carbonate) (PTMC) and poly(dimethyl trimethylene carbonate) (PDTC) display poor hydrophilicity and slow degradation rates. A broad range of functional TMCs, which we present here, has been explored to alter these properties and increase hydrophilicity and degradation. Polymerization of the five-membered cyclic carbonates is thermodynamically unfavorable.<sup>218</sup> Polymerization above 150°C results in poly(ether-carbonate)s and decarboxylation. Five-membered vinylene carbonate<sup>219</sup> and vinyl ethylene carbonate<sup>220</sup> are radically polymerized at the vinyl function, while the cyclic carbonate remains unaffected. Polymerization of seven-membered rings is possible, but less relevant. Reported functional monomers are limited to alkyl- or aryl-pendant chains, or protected functionalities; reactive functionalities have not been reported up to date. For more details, we also refer to a review of Rokicki.<sup>218</sup>

### 1.7.1 Trimethylene Carbonates

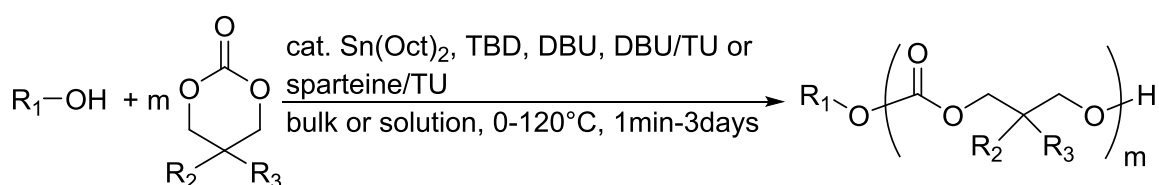
Various mono- and disubstituted trimethylene carbonate (TMC) monomers have been reported in literature. Dove and coworkers published an excellent review about TMCs in 2013,<sup>22</sup> including general synthetic strategies, functional monomers and their polymerization, as well as post-modification reactions and applications. Here, we restrict to general synthesis strategies for orthogonally-reactive monomers and selected some representative examples for further applications.

While homopolymerization of the most functional monomers is possible, often copolymerization with alkyl-chain containing TMCs is conducted to adjust the functional group density. Furthermore, disubstituted monomers mostly contain a methyl or ethyl substituent, which has an impact on the thermal properties and solubility of the products. Alcohols are commonly used as initiators. A variety of synthetic protocols for the polymerization of TMCs are reported, including the polymerization with tin(II) octoate in bulk at ca. 110-120°C for 4-48h. Modern synthesis protocols rely on organocatalysis with 1,8-diazabicyclo[5.4.0]undec-7-ene (DBU) in bulk or solution at temperatures between 25 and 110°C for 1-3 days, with a catalytic system of DBU or sparteine with a thiourea cocatalyst *N*-cyclohexyl-*N'*-(3,5-bis(trifluoromethyl)phenyl)thiourea (TU) at room temperature and in solution for 2-4h or with the more reactive base 1,5,7-triazabicyclo[4.4.0]dec-5-ene (TBD) in bulk or solution at temperatures ranging from 0-25°C

over a period of 1min to 2h (Scheme 1.21). Commonly used solvents are dichloromethane, chloroform or toluene, depending on the solubility of TMCs and applied reaction temperatures.

A variety of synthetic strategies has been reported for the synthesis of substituted TMCs, including 2-5 steps with overall yields between 17-70%. A synthetic strategy relies on 2,2-bishydroxy(methyl)propionic acid (bis-MPA) as feedstock (Scheme 1.22), which was esterified to introduce the functional group, e.g. with alkylhalogenides (Scheme 1.22, route I). Following cyclization with ethyl chloroformate under basic conditions produced the TMCs. Hedrick and coworkers<sup>221</sup> introduced an alternative route for a versatile precursor (5-methyl-5-carboxy-2-oxo-1,3-dioxane), yielding functional monomers in one further step (Scheme 1.22, route II). The carboxyl function of bisMPA was protected with benzyl bromide, cyclization achieved, e.g. with triphosgene, and the carboxylic acid functionality deprotected again by hydrogenation (overall yield of precursor 59%). The precursor was either directly esterified again to introduce functionalities as pendant chains or transformed into a more reactive acid chloride and then esterified (over all yields: 15-41%). An alternative precursor, carrying a pentafluorophenyl ester protecting group,<sup>222-223</sup> was synthesized on a gram to kilogram scale, easily handled and stored (yield: 75% Scheme 1.22, route III). It was reacted with suitable nucleophiles, as alcohols or amines in a transesterification reaction to functional TMCs. A further alternative is the use of imidazole intermediates using 1,1'-carbonyldiimidazole (CDI) as a key reagent (yield of intermediate: 67% Scheme 1.22, route IV). The intermediates were robust and benchstable.<sup>224</sup> Alternatively, the hydroxyl functions of bis-MPA was first protected, e.g. with 2,2-dimethoxypropane (DMP) (Scheme 1.22, route V). Esterification of the carboxyl group introduced subsequently the pendant functionality. After deprotection of the hydroxyl groups, cyclization was achieved with ethyl chloroformate under basic conditions to yield the final monomers.

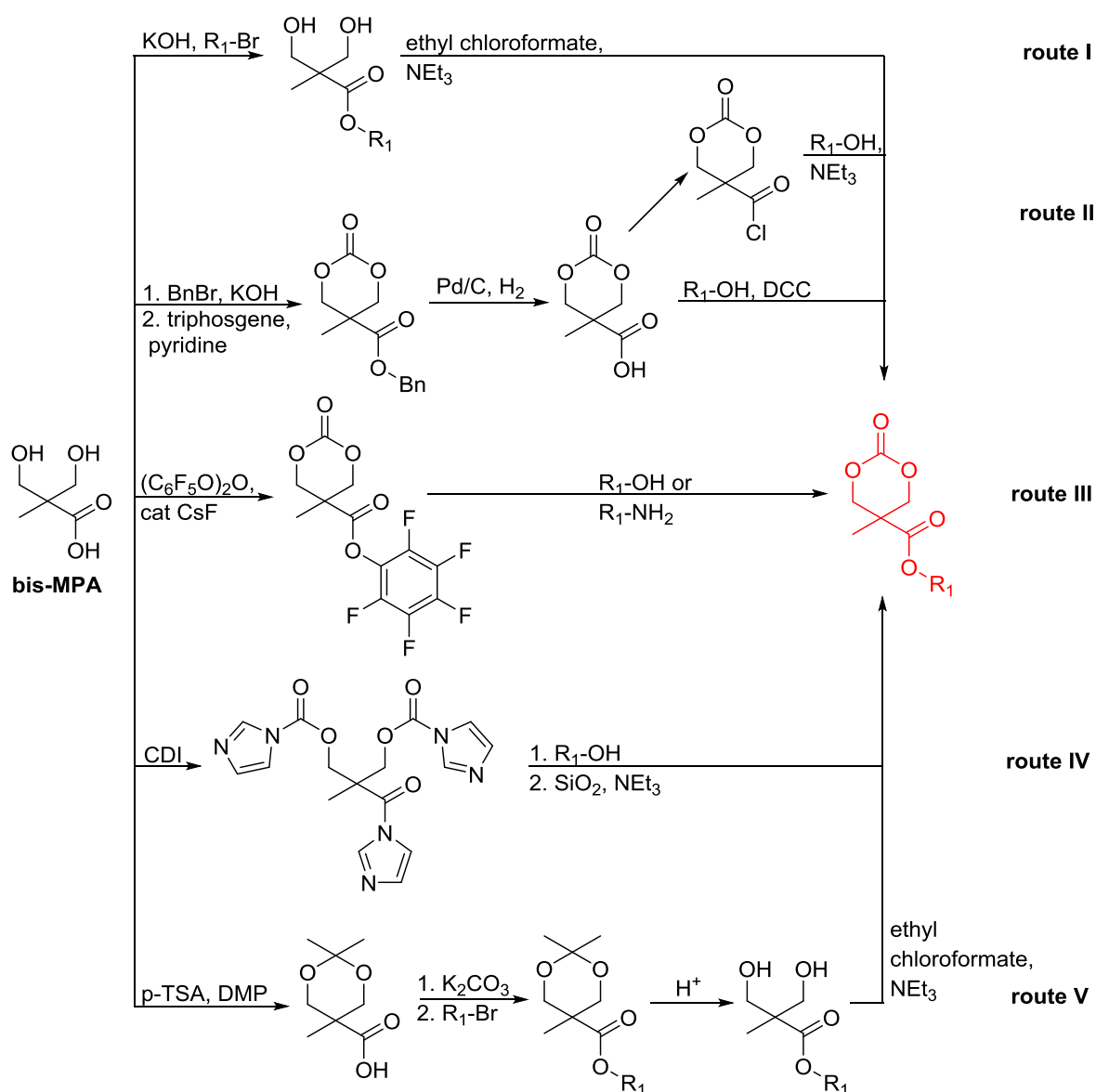
Another general route uses glycerol or trimethylolalkanes (such as trimethylolpropane) as feedstock (Scheme 1.23), which are protected as acetals with benzaldehyde (Scheme 1.23, route VI), acetone, or 2,2-dimethoxypropane (DMP) (Scheme 1.23, route VII). The pendant hydroxyl group was substituted with alkylhalogenides or acid chlorides, the acetal hydrolyzed, and the final monomer formed by reaction with triphosgene or ethyl chloroformate under basic conditions.<sup>225</sup> Alternatively, the starting compound was either directly transformed to the cyclic carbonate and



**Scheme 1.21.** General protocol for the organocatalytic polymerization of TMCs to poly(carbonate)s with alcohols as initiators.

afterwards esterified to introduce the pendant functionality (Scheme 1.23, route VIII) or first an oxetane-ring was generated (Scheme 1.23, routes IX-XI). After halogenation of the remaining hydroxyl group and ring-opening of the oxetane, cyclization was achieved, e.g. with ethyl chloroformate or 1,1'-carbonyldiimidazole (CDI) ( overall yield: 31-47%, Scheme 1.23, route IX). Alternatively, the alkyl halogenide was reacted with sodium hydrogensulfide and the resulting thiol modified either by thiol-ene reaction or disulfide formation (Scheme 1.23, routes X (yield: 16%) and XI (yield:16%)). For more details we also refer to the review of Dove<sup>22</sup>.

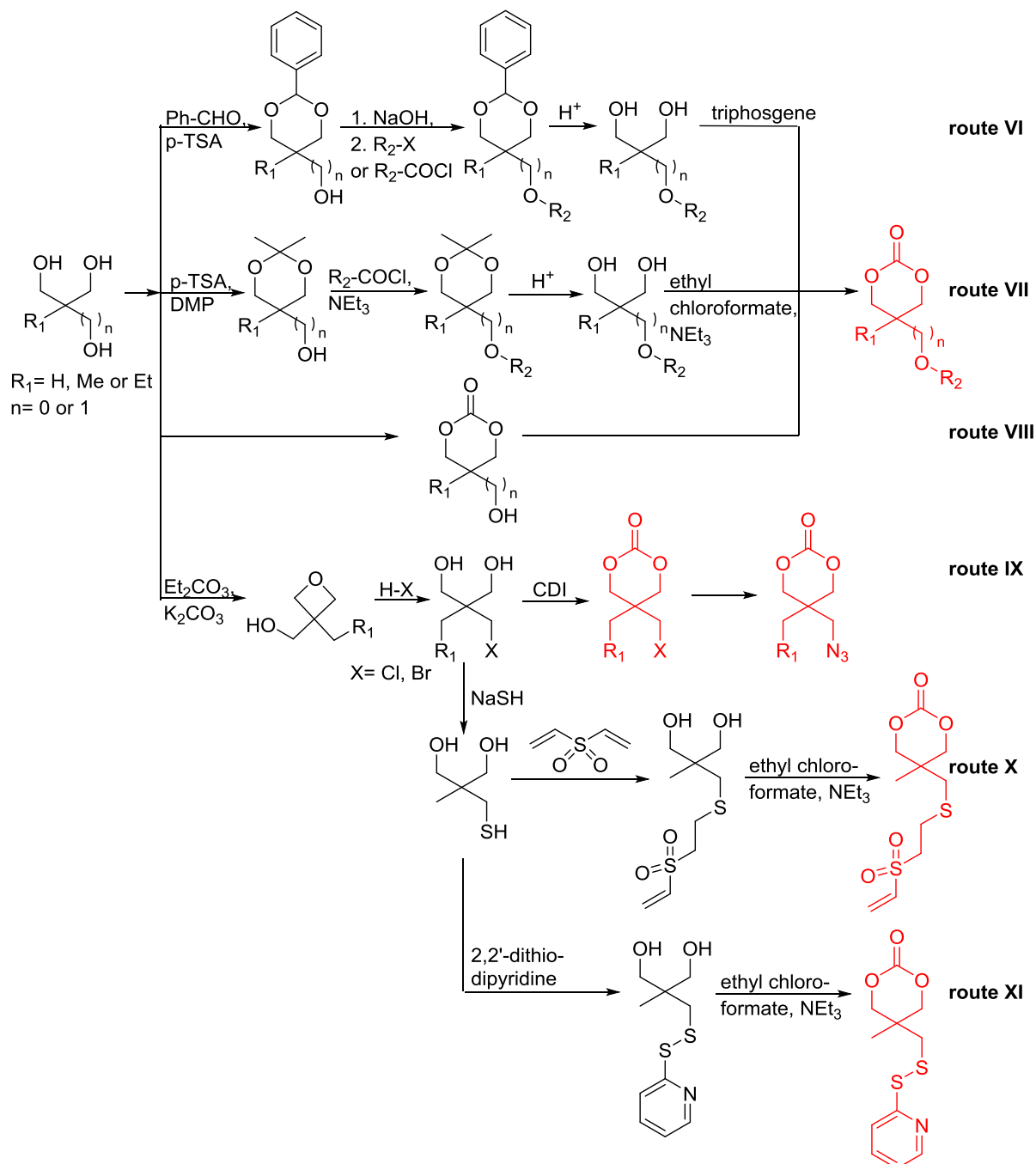
Yang and coworkers<sup>226</sup> reported a strategy synthesizing monosubstituted TMCs from 2-aminopropane-1,3-diols (serinol) (Scheme 1.24, route XII; yields: 32-69%). Substitution of the



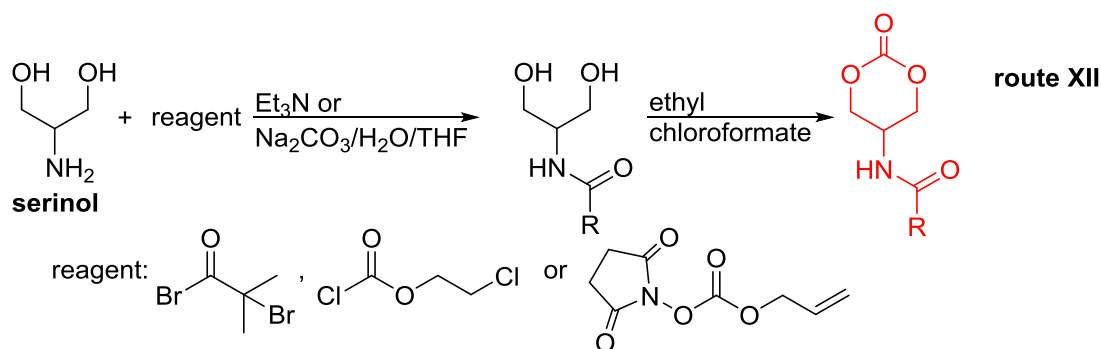
**Scheme 1.22.** Synthetic strategies to trimethylene carbonates (TMCs) from 2,2-bishydroxy(methyl)propionic acid (bis-MPA).

amine with chloroformates, acyl halides or *N*-carbonyloxy succinimide derivatives introduced the pendant chain, followed by cyclization with ethyl chloroformate.

**5-Monosubstituted Trimethylene Carbonates.** Zhuo and coworkers<sup>225, 227-228</sup> reported an allyl-containing monomer, 5-(allyloxy)-1,3-dioxan-2-one (**C1**). Homo- or amphiphilic block copolymers with PEG were functionalized by photochemical thiol-ene reaction with cysteamine<sup>229</sup> or by epoxidation, subsequent hydrazination and attachment of doxorubicin for drug delivery.<sup>230</sup> Yang and coworkers<sup>226</sup> reported allyl- (**C2**) and chloro- (**C3**) functional carbamate TMCs from



**Scheme 1.23.** Synthetic strategies to trimethylene carbonates (TMCs) derived from trimethylolalkanes .



**Scheme 1.24.** Synthetic strategy to trimethylene carbonates (TMCs) derived from serinol.

serinol (Scheme 1.24, route XII), however, post-modification of polymers was not shown by the authors. Dai and coworkers<sup>231</sup> reported recently a monomer with an ATRP initiating group, 2-(2-bromoisobutyrylamido) trimethylene carbonate (**C4**), using an analogous route with 2-bromoisobutyryl bromide. Hydroxyethyl methacrylate (HEMA) was grafted from copolymers as macroinitiator, and the amphiphilic polymers self-assembled in micelles.

Diaconescu and coworkers<sup>74</sup> reported several ferrocene containing TMCs (5-substituted (**C5-C7**) and 5-methyl-5'-substituted (**C8-C10**)), polymerized them and studied their redox potential for biological studies. Proceeding from 2-(prop-2-yn-1-yl)-propane-1,3-diol, cyclization was achieved with triphosgene. Ferrocene-azide derivatives were attached by click chemistry.

**5-Methyl-5'-Substituted Trimethylene Carbonates.** A variety of alkyne-, alkene-, vinylidene-, and acrylate-functionalized 5-methyl-5'-substituted trimethylene carbonates (MTCs) has been reported with versatile applications so far. Jing and coworkers reported an alkyne monomer (**C11**), where lactide-copolymers were functionalized with sugars-azides<sup>232</sup> and lectin-interactions has been proved, the protein TSP50 has been immobilized on polymer fibers,<sup>233</sup> or amphiphilic triblock copolymers were self-assembled into core-shell micelles and conjugated with hemoglobin as artificial oxygen carriers.<sup>234</sup> Reversibly light-responsive poly(carbonate) micelles functionalized with an azide-modified spiropyran were shown by Xu and coworkers.<sup>235</sup> Dove and coworkers<sup>236</sup> additionally showed quantitative radical thiol-yne functionalization. Carborane-conjugated amphiphilic PEG-block copolymers nanoparticles were used as drug delivery platform for doxorubicin and boron neutron capture therapy (BNCT) at the same time.<sup>237</sup> The functionalization with decaborane was shown for the monomer (**C12**) and subsequent polymerization.<sup>238</sup> An analogous allyl monomer (**C13**) was reported by Storey and coworkers<sup>239</sup> and lactide-copolymers were epoxidized and hydrolyzed to diols, reacted with alcohols, poly(ethyleneimine) as gene delivery vector,<sup>240</sup> or with diamines/dithiols to nanosponges for potentially controlled release.<sup>241</sup> Thiol-ene reaction was applied to attach folic acid,<sup>242</sup> or nucleobases<sup>243</sup> (for core-crosslinking of micelles by base pairing)<sup>244</sup> for drug delivery applications, to cross-link hydrogels,<sup>245</sup> to microstereolithography resins as biocompatible 3D extracellular constructs,<sup>246</sup> or to attach

dopamine for self-healing gels via Fe<sup>3+</sup>-ion complexation.<sup>247</sup> After ozonolysis and reductive work up, Wooley and coworkers<sup>248</sup> were able to isolate PCs with aldehydes: formation of oximes with hydroxylamine derivatives was shown with several model compounds.

Zhong and coworkers reported (meth)acrylated MTCs **C14** and **C15**. The acrylate was copolymerized with lactide or caprolactone and modified by Michael-addition with thiols of varying polar and charged groups,<sup>249</sup> or folate-conjugated paclitaxel loaded PEG-PC-PLA-triblock copolymer micelles photo-crosslinked for drug delivery.<sup>250</sup> Amsden and coworkers<sup>251</sup> electrospun lactide-copolymers of **C14** and photo-crosslinked them yielding fibrous crimped scaffolds to culture cells. Hedrick and coworkers<sup>252</sup> introduced additional (meth)acrylated and styrene functionalized monomers (**C16-C18**), synthesized from the pentafluorophenyl ester precursor (Scheme 1.24, route III). They showed polymerization of **C16** and **C18**, but no further chemical modification. Jing and coworkers<sup>253</sup> introduced a cinnamate- functionalized monomer (**C19**), which was photo-crosslinked after the ROP. A vinylsulfone monomer (**C20**) was synthesized by Zhong and coworkers<sup>254</sup> from 3-methyl-3-oxetanemethanol and divinylsulfone (Scheme 1.24, route X). Copolymers and coatings were functionalized by selective Michael-type reaction with thiol-containing molecules to introduce polar and charged groups, GRGDC peptide, or thiolated poly(ethylene glycol) (PEG-SH).

Bowden and coworkers<sup>255</sup> synthesized a series of 5-methyl or 5-ethyl-5'-halide-functional MTCs (halide=chloride or bromide, **C21-C24**) (Scheme 1.24, route IX), however, they did not perform post-functionalization. In another report, the bromide monomer **C21** was transformed to an azide monomer (**C25**)<sup>256</sup> and used as precursor for modification by click reaction with alkyne derivatives and subsequent ROP. Hedrick and coworkers<sup>257</sup> further reported 2-iodo-ethyl (**C26**), 3-chloro-propyl (**C27**) and 3-bromo-propyl (**C28**) MTC monomers, synthesized from the acid chloride MTC precursor (route II). Copolymers were functionalized with a bis-tertiary amine (TMEDA). While for the quaternization of the 3-chloropropyl substituted polymers from **C27** 90°C were required, the 3-bromo-propyl (**C28**) and 2-iodo-ethyl (**C26**) substituted polymers were functionalized at room temperature in high conversion >90%. Chloride substituted polymers (**C27**) showed no gel formation because of the low reactivity of chlorine substituents. The iodide and bromide substituted polymers from **C26** and **C28** were more difficult to handle as undesired cross-linking occurred. Bromide-substituted copolymers from **C28** with 50% 5-methyl-5-ethyloxycarboxyl-1,3-dioxan-2-one comonomer instead did not show cross-linking. The cationic polycarbonate was able to bind and complex DNA for generating nanoparticles and application as gene delivery vector were studied.<sup>257</sup> Coatings of surface grafted diblock copolymers of PEG and bromide substituted-polycarbonates from **C28**, quaternized with trimethylamine, exhibited antibacterial and antifouling properties and effectively killed staphylococcus aureus (MSSA) and methicillin-resistant S. aureus (MRSA) on the coatings.<sup>258</sup> The polymer coating prevented blood protein adhesion and no

significant hemolysis was observed. Nanoparticles of cationic polycarbonates disrupted microbial walls/membranes selectively and efficiently and thus inhibited the growth of gram-positive bacteria (MRSA and fungi).<sup>259</sup> Galactose-functionalized cationic polycarbonates were applied for targeted gene delivery to hepatocytes.<sup>260</sup> Yang and coworkers investigated in different pyridines and imidazoles as quaternizing agents<sup>261</sup> for polycarbonates or the effect of hydrophobicity<sup>262</sup> of the polymers from 3-chloropropyl (**C27**), -hexyl (**C29**) or -octyl (**C30**) and 3-bromopropyl (**C28**) or -hexyl (**C31**) MTCs, and their impact on antimicrobial properties.<sup>261</sup> In other studies, cationic (co)polymers of a benzylchloride-substituted MTC (5-methyl-5-(4-chloromethyl)benzylcarboxyl-1,3-dioxan-2-one, **C32**), again quaternized with different amines, were investigated with respect to their antimicrobial behavior,<sup>263</sup> activity, and selectivity.<sup>264</sup> Here, functionalization was faster compared to 3-bromopropyl substituted polymers from **C28**. Polymers were additionally functionalized by quaternization with phosphines, the chloride in polymers from **C32** was substituted with NaN<sub>3</sub> and subsequently clicked to various alkynes,<sup>265</sup> or functionalized with boronic acid derivatives.<sup>266</sup>

Besides the use of a pentafluorophenyl ester MTC (**C33**) as precursor for preparation of functionalized monomers (Scheme 1.22, route III),<sup>222</sup> **C33** itself was polymerized to highly reactive PCs. Hedrick and coworkers proved post-modification with different amines<sup>267-268</sup> to use them e.g. as stealth materials,<sup>269</sup> with persistent radicals, or with boronic acid derivatives.<sup>266</sup> They self-assembled them to nanoparticles or used them as MRI agents.<sup>270</sup> Liu and coworkers<sup>271</sup> reported a further active ester MTC monomer, functionalized with a NHS ester (5-methyl-5'-(succinimide-*N*-oxycarbonyl)-1,3-dioxan-2-one, **C34**), which was copolymerized with caprolactone and the copolymers modified by aminolysis with ethylene diamine to yield hydrophilic amido-amine pendant chains. They proposed facilitated attachment of bioactive molecules, targeting ligands, and covalent incorporation of prodrugs for the active ester copolymers.

A thioether-substituted monomer **C35** was recently reported by Hedrick and coworkers,<sup>272</sup> that was incorporated into homo-, di- and triblock copolymers, which were functionalized with epoxides, yielding sulfonium-functionalized PCs. Alkene functionalities, polar groups, galactose, tocopherol, and carbazols were introduced in the pendant chains. Zhong and coworkers reported a pyridyl disulfide-functionalized monomer (**C36**, Scheme 1.24, route XI), which was copolymerized with caprolactone. The polymers were functionalized in a thiol-disulfide exchange reaction with PEG-SH<sup>273</sup> and self-assembled into reduction-sensitive micelles for active intracellular drug release or with thiolated lactobionic acid<sup>274</sup> to reduction-sensitive shell-sheddable glyco-nanoparticles for efficient hepatoma-targeting delivery of doxorubicin. Two dithiolane-functionalized monomers **C37** and **C38** were recently synthesized by Waymouth and coworkers from 5-methyl-5'-carboxylic acid trimethylene carbonate, oxalylchloride, and 2-hydroxyethyl 4-carboxylate-4'-methyl-1,2-dithiolane<sup>275</sup> (**C37**) or 2-hydroxyethyl-5-(1,2-dithiolan-3-yl)pentanoate (**C38**).<sup>276</sup> Water-soluble

triblock PEG-PC-copolymers were cross-linked with dithiols or with each other by reversible ring-opening of the pendant 1,2-dithiolanes and dynamic hydrogels obtained,<sup>275</sup> or self-assembled into core-crosslinked (flower-bridged) micelles (Figure 1.5).<sup>276</sup> Depending on the pendant dithiolane chains, the hydrogels were dynamic, adaptable, and self-healing or rigid, resilient, and brittle. Cross-linked flower micelles dissociated upon the addition of acetone. Micelles cross-linked by a thiol and capped with maleimide persisted in acetone, and micelles cross-linked by a thiol, capped with maleimide, and then treated with dithiothreitol dissociated in acetone. Two trithiocarbonate functionalized monomers **C39**<sup>277</sup> and **C40**<sup>278</sup> were reported, serving as RAFT macroinitiator after ROP. *N*-Isopropylacrylamide (NiPAAm) (or methyl acrylate and tetrahydropyran acrylate)<sup>278</sup> were grafted from the poly(carbonate)s.

Tunca and coworkers<sup>279</sup> reported an anthracene containing MTC monomer (**C41**), suitable for Diels-Alder reactions with dienophiles. Polymers were grafted with a furan-protected maleimide-terminated-poly(methyl methacrylate) or poly(ethylene glycol) or a mixture of both to yield well-defined polycarbonate graft or hetero graft copolymers with an efficiency over 97%. Nelson and coworkers<sup>280</sup> chose a similar approach, using a furfuryl-containing TMC monomer (**C42**). They provided copolymers with a second counterpart monomer: a Diels-Alder-protected maleimide-containing comonomer (**C43**). The maleimide was thermally deprotected and furan released at 130°C. At 90°C furfuryl functionalities in the copolymers reacted with the maleimide functions and

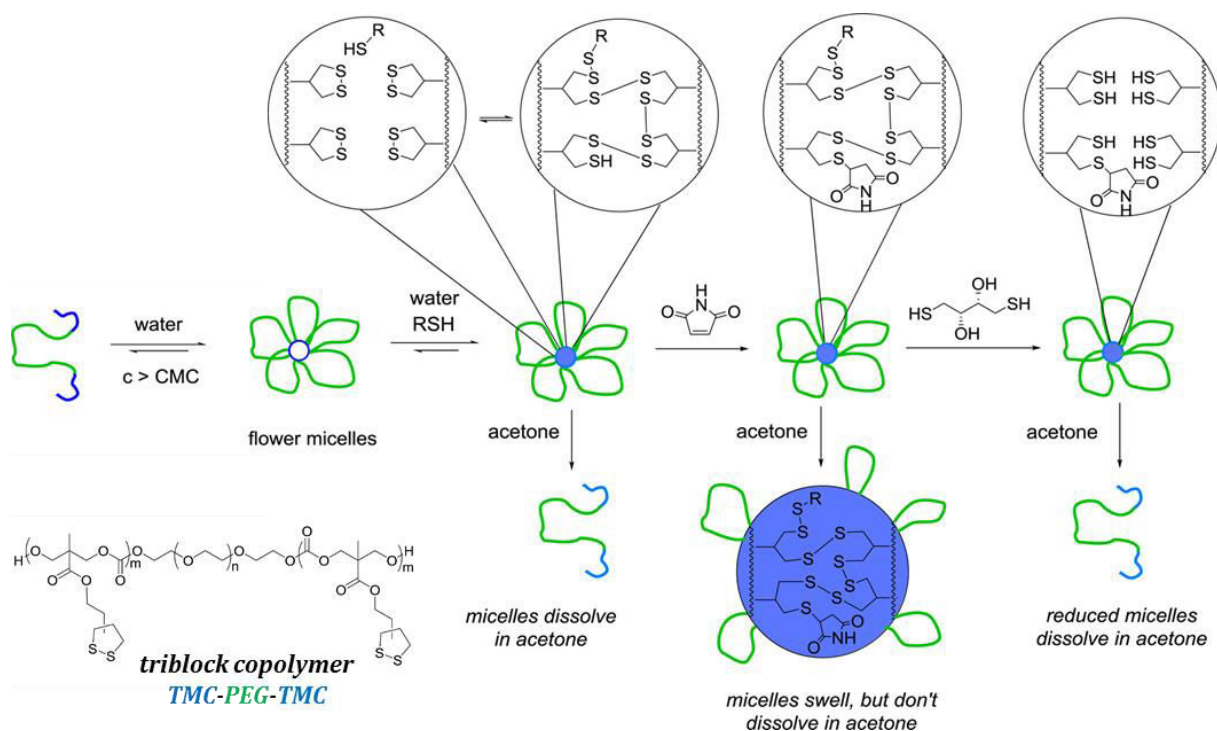


**Figure 1.5.** Self-assembly of dithiolane-functionalized TMC-PEG-TMC block copolymers into flower micelles and thiol-initiated cross-linking of the micelles. Adapted with permission from Ref<sup>276</sup>; copyright 2017 American Chemical Society.

covalently cross-linked the material. The polymer films were used for thermally induced nanoimprinting process. Dove and coworkers<sup>281</sup> introduced a monomer with a norbornene-functionality (**C44**). They presented different post-modification reactions on the homopolymers: (i) functionalization with azides via a 1,3-dipolar cycloaddition, (ii) inverse electron demand Diels-Alder reaction with tetrazines and (iii) radical thiol-ene coupling.

**5-Ethyl-5'-Substituted Trimethylene Carbonates.** Malkoch and coworkers<sup>224</sup> reported on alkyne- (**C45**) and alkene- (**C46**) functionalized 5-ethyl-5'-substituted TMCs, synthesized via imidazole intermediates (analog to Scheme 1.22, route IV with trimethylolpropane as starting material). They showed polymerization of the monomers, post-modification has not been reported so far. Höcker and coworkers<sup>282</sup> studied the polymerization of 5-allyloxymethyl-5'-ethyl TMC (**C47**), cross-linked the polymers and investigated their thermal behavior. Brandell and coworkers<sup>283</sup> used UV-cross-linked homopolymers as electrolytes in solid-state Li batteries. Dove and coworkers<sup>284</sup> modified homopolymers of **C47** via photochemical thiol-ene reaction, e.g. with PEG-SH of different chain lengths, and showed a linear increase of LCST in correlation with increasing length of PEG chains. They further transformed the monomer to an oxirane ether carbonate (**C48**) by epoxidation with mCPBA.<sup>285</sup> Homopolymers were functionalized in a thiol-epoxy reaction in presence of LiOH or DBU as catalyst. While the degree of functionalization with aliphatic and benzylic thiols was rather low (<1-56%), thiophenol showed effective modification (50-94%) without polymer degradation in the presence of DBU as catalyst. Functionalization with primary amines in the presence of Lewis acid catalysts was reported to be challenging, because the Lewis acids promoted degradation of the polymers. Functionalization without a catalyst and increased temperature (50°C) showed conversion >95% with benzylamine, but also formation of some cross-linked material was observed. A styrene-functionalized TMC (**C49**) was introduced by Endo and coworkers,<sup>286</sup> polymerized and radically cross-linked in the presence of styrene. The cross-linked polymer network was cleaved under basic conditions with potassium *tert*-butoxide and linear, soluble polystyrene with TMC functionalities were obtained.

Bowden and coworkers<sup>255</sup> reported two 5-ethyl-5'-halide-functional TMCs (halogenide=chloride (**C23**) or bromide (**C24**)). **C24** was transformed to an azide functionalized monomer<sup>256</sup> (**C50**) allowing further click chemistry. The authors showed selected monomers to be polymerizable, e.g. an  $\alpha$ -methyl vinyl triazole monomer (**C51**). However, post-polymerization modification has not been shown so far.

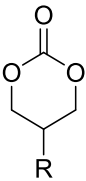
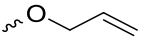
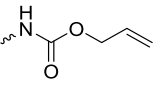
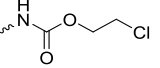
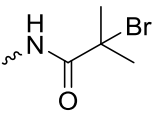
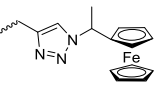
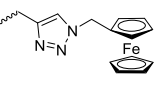
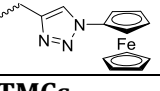
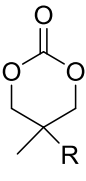
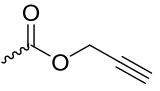
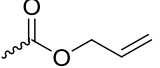
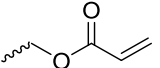
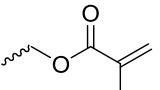
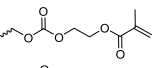
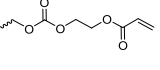
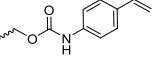
**5,5'-Disubstituted Trimethylene Carbonates.** Shen and coworkers<sup>287</sup> reported a dibromo-substituted monomer (**C52**), obtained by transesterification between 2,2-bis(bromomethyl)propane-1,3-diol and ethyl chloroformate. Caprolactone-carbonate copolymers were functionalized by quaternization with tertiary amines and their antimicrobial properties were examined.<sup>288</sup> Copolymers were quantitatively functionalized by azidation and click

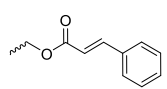
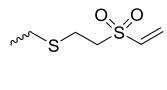
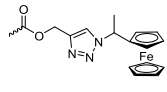
chemistry with PEG-alkyne of different chain length, to achieve amphiphilic graft copolymers with PEG as hydrophilic branches.<sup>287</sup> From such materials, aggregation<sup>287, 289</sup> and paclitaxel-loaded redox-responsive core-crosslinked micelles for drug delivery were investigated.<sup>290</sup> In contrast to Shen and coworkers, Zhuo and coworkers<sup>291</sup> reported only poor conversions for the azidation of bromide copolymers. They introduced a diazido-substituted TMC (**C53**, 2,2-bis(azidomethyl)trimethylene carbonate) by transesterification of 2,2-bis(azidomethyl)propane-1,3-diol with ethyl chloroformate. Functionalization of polymers with different alkynes was achieved in quantitative yields. Amphiphilic PEG-*b*-P(**C53**-*r*-DTC) copolymers were cross-linked with disulfide containing dialkyne-crosslinkers. The core-crosslinked redox-responsive micelles were investigated with respect to their drug release of methotrexate (MTX).<sup>292</sup> Song and coworkers<sup>293</sup> prepared hydrogels from PEG-PC-PEG triblock copolymer, containing azide substituents, and crosslinked them via copper-free ring-strain driven click reaction (SPAAC). Encapsulated bone marrow stromal cells exhibited high cell viability in the hydrogels and they exhibited higher cytocompatibility than hydrogels cross-linked by methacrylate functionalities.

Meng and coworkers<sup>294</sup> introduced a dithiolane TMC (**C54**), synthesized from 2,2-bis(bromomethyl)-1,3-propanediol and NaSH and subsequent cyclization with ethyl chloroformate. PEG-PC copolymers self-assembled to micelles and crosslinked by disulfide exchange reaction, encapsulating doxorubicin (DOX). *In vivo* studies of the micelles in malignant B16 melanoma-bearing C57BL/6 mice with a dosage of 30 mg DOX equiv./kg effectively suppressed tumor growth, prolonged mice survival time and did not cause systemic toxicity. The drug was released within the tumor cells after reductive cleavage by glutathione.

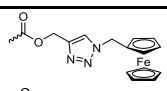
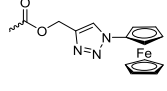
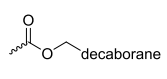
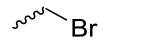
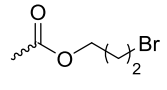
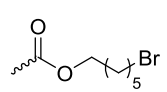
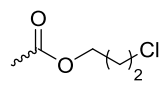
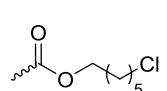
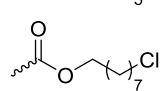
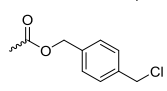
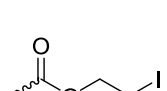
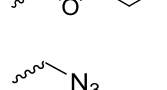
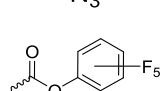
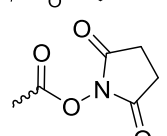
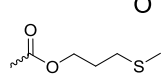
Gross and coworkers<sup>295</sup> reported 2,2-(2-pentene-1,5-diyl)trimethylene carbonate (**C55**), synthesized in one step from cyclohexene-4,4-dimethanol and ethyl chloroformate. They extensively studied the polymerization behavior and showed epoxidation of the pendant vinyl group with pCPBA (22-95% conversion, <2% hydrolysis of epoxides to diols). They suggested further hydrolysis to diols, reaction with alcohols or amines or initiation of ring-opening polymerization.<sup>296</sup>

**Table 1.5.** Orthogonally functional cyclic TMCs for the synthesis of poly(carbonate)s.

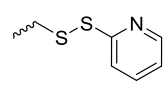
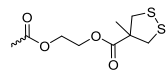
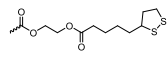
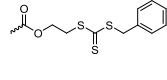
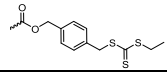
Monomer	R=	No	Post-Modification	Ref.
<b>5-Monosubstituted TMCs</b>				
		<b>C1</b>	-epoxidation with mCPBA, hydrazination and doxorubicin attachment for drug delivery -photochemical thiol-ene reaction with mercaptoethanol	225, 227-230
		<b>C2</b>	-no modification	226
		<b>C3</b>	-no modification	226
		<b>C4</b>	-macroinitiator for ATRP polymerization of HEMA	231
		<b>C5</b>	-study of redox potential	74
		<b>C6</b>	-study of redox potential	74
		<b>C7</b>	-study of redox potential	74
<b>Disubstituted TMCs</b>				
		<b>C11</b>	-click chemistry with carbohydrates, immobilization of TSP50 proteins or hemoglobin as oxygen carrier or reversible light-responsive micelles with spiropyran modification -thiol-yne reaction -functionalization with decaborane for BNCT	232-237
		<b>C13</b>	-epoxidation and hydrolyzation to diols or reaction with alcohols, amines or thiols -thiol-ene reaction to attach folic acid, nucleobases, for cross-linking and gelation -ozonolysis and reduction to aldehydes and aldehyde-aminoxy click reaction	239-248
		<b>C14</b>	-modification by Michael-addition with polar and charged groups, -photo-cross-linking to obtain micelles and fibers	249-251
		<b>C15</b>	-no modification	249
		<b>C16</b>	-no modification	252
		<b>C17</b>	-no modification	252
		<b>C18</b>	-no modification	252

	<b>C19</b>	-photo-cross-linking	253
	<b>C20</b>	-Michael-type reaction to attach polar or charged groups, GRGDC peptide or PEG-SH	254
	<b>C8</b>	-study of redox potential	74

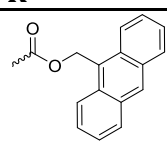
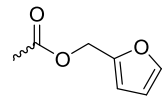
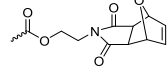
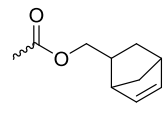
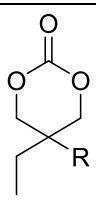
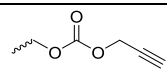
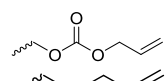
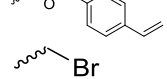
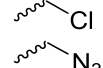
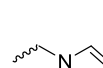
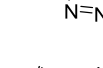
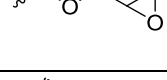
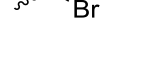
**Table1.5.** Orthogonally functional cyclic TMCs for the synthesis of poly(carbonate)s (*continued*).

Monomer	R=	No	Post-Modification	Ref.
		<b>C9</b>	-study of redox potential	74
		<b>C10</b>	-study of redox potential	74
		<b>C12</b>	-PEG-copolymer nanoparticles as boron vector for BNCT	238
		<b>C21</b>	-no modification	255
		<b>C28</b>	-nucleophilic substitution with bis-tertiary amines, pyridines or imidazoles as gene delivery vector and for antimicrobial applications	257-258, 260-261, 263
		<b>C31</b>	-nucleophilic substitution with pyridines or imidazoles for antimicrobial applications	261
		<b>C22</b>	-no modification	255
		<b>C27</b>	-nucleophilic substitution with bis-tertiary amines, pyridines or imidazoles as gene delivery vector and for antimicrobial applications	257, 259, 261-262
		<b>C29</b>	-nucleophilic substitution with pyridines or imidazoles for antimicrobial applications	261-262
		<b>C30</b>	-nucleophilic substitution with primary amines for antimicrobial applications	262
		<b>C32</b>	-nucleophilic substitution with primary amines for antimicrobial applications	263-266
		<b>C26</b>	-nucleophilic substitution with bis-tertiary amines as gene delivery vector	257
		<b>C25</b>	-click reaction with alkyne derivatives, -no polymerization shown of azide monomer	256
		<b>C33</b>	-functionalization with different amines	266-270
		<b>C34</b>	-functionalization with amines to introduce charged groups or bioactive molecules	271
		<b>C35</b>	-functionalization with epoxide derivatives to introduce galactose, tocopherol or carbazols	272,

1 Synthetic biodegradable polymers from ring-opening polymerization  
 1.7 Poly(carbonate)s

	<b>C36</b>	-thiol-disulfide exchange reaction with thiols to reduction-sensitive self-assembled micelles or nanoparticles	273-274
	<b>C37</b>	-thiol-disulfide exchange reaction for formation of dynamic, stimuli-responsive and self-healing hydrogels	275-276
	<b>C38</b>	-thiol-disulfide exchange reaction for formation of core-cross-linked micelles or hydrogels	276
	<b>C39</b>	-RAFT macroinitiator	277
	<b>C40</b>	-RAFT macroinitiator	278

**Table 1.5.** Orthogonally functional cyclic TMCs for the synthesis of poly(carbonate)s (*continued*).

Monomer	R=	No	Post-Modification	Ref.
		<b>C41</b>	-Diels-Alder reaction with maleimide-polymer derivatives to grafted copolymers	279
		<b>C42</b>	-cross-linking with maleimide-comonomers by Diels-Alder reaction to materials for nanoimprinting	280
		<b>C43</b>	-cross-linking with furfuryl-comonomers by Diels-Alder reaction to materials for nanoimprinting	280
		<b>C44</b>	-click reaction with azides -thiol-ene reaction -inverse electron demand Diels-Alder reaction with tetrazines	281
		<b>C45</b>	-no modification	224
		<b>C46</b>	-no modification	224
		<b>C47</b>	-thermal or photochemical cross-linking -thiol-ene reaction with PEG-SH for formation of LCST-type polycarbonates	282-284
		<b>C49</b>	-cross-linking with styrene	286
		<b>C23</b>	-no modification	255
		<b>C24</b>	-no modification	255
		<b>C50</b>	-click reaction with alkynes -no polymerization shown of azide monomer	256
		<b>C51</b>	-no modification	256
	<b>C48</b>	-functionalization with thiols or benzylamine	285	
	<b>C52</b>	-quaternization with tertiary amines for antimicrobial applications	287-290	

		-azidation and click reaction to form amphiphilic graft copolymers, micelles or nanoparticles for drug delivery	
	<b>C53</b>	-click reaction with alkynes core-cross-linked micelles or hydrogels for drug delivery or cell tissue engineering	291,292-293
	<b>C54</b>	-self-cross-linking of micelles for drug delivery and intracellular de-cross-linking	294
	<b>C55</b>	-epoxidation with <i>p</i> -CPBA	295,296

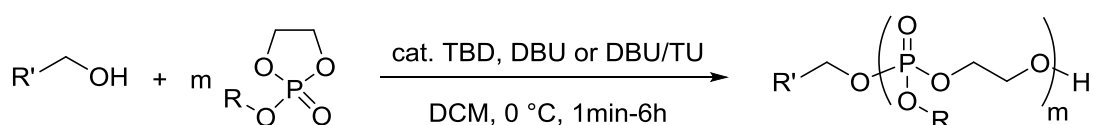
---

## 1.8 Poly(phosphoester)s

Poly(phosphoester)s (PPEs) have gained interest in the last two decades for biomedical applications due to their biocompatibility and -degradability. Depending on the number of methylene spacers in the backbone, PPEs with a broad range between hydrophobic to hydrophilic properties have been reported with various degradation behavior. The binding motif around the phosphorus atom (P-O, P-H, P-C or P-N) divides PPEs into further subclasses of poly(phosphate)s, -(phosphite)s, -(phosphonate)s, or -(phosphoramidate)s. The pentavalency of the phosphorus atom allows facile introduction of alkyl-, aryl- or functional side chains and thus further tuning of the polymer properties. PPEs can be obtained by ROP from 5- and 6-membered cyclic phosphates, H-phosphonates, phosphonates or phosphoramidates. Orthogonally functional cyclic phosphoramidates has not been reported so far. We refer to two recent reviews for detailed information on PPEs.<sup>297-298</sup>

**Cyclic Phosphates.** PPEs can be prepared from 5-membered cyclic phosphates. Most monomers are prepared via 2-chloro-2-oxo-1,3,2-dioxaphospholane (COP) as the precursor. COP is either commercially available or can be synthesized in two steps by the reaction of phosphorus trichloride with ethylene glycol, followed by oxidation (Scheme 1.26A). We recently optimized the reaction, using  $\text{CoCl}_2$  as catalyst and oxygen from dried air instead of elemental oxygen, making the synthesis process more convenient and shorten the reaction time from days to hours.<sup>299</sup> The final monomers are obtained by esterification of COP with an appropriate alcohol (yield for esterification step 30-70%). Some orthogonally reactive monomers have been reported in literature up to date. Because of a growing interest in PPEs for biomedical applications, we expect the report of several further monomers in the common years.

Modern polymerization techniques for PPEs rely on the use of organocatalysts such as TBD, DBU, or an additional use of a thiourea cocatalyst (TU), but also classical basic, acidic or metal-based catalysts ( $\text{Sn}(\text{Oct})_2$ ) may be applied.<sup>300</sup> Primary alcohols are typically used as initiator. Depending on the reactivity of catalyst, polymerizations can be conducted in dichloromethane at  $0^\circ\text{C}$  for a period of 1 min to several hours. Reaction is terminated after ca. 80% conversion of monomers to avoid transesterification side reactions during later stage of polymerization (Scheme 1.25).



**Scheme 1.25.** General protocol for the ROP of cyclic phosphates to poly(phosphoester)s

A propargyl-functionalized phosphate monomer (2-(prop-2-yn-1-yloxy)-2-oxo-1,3,2-dioxaphospholane, **D1**) was reported by Wang and coworkers,<sup>301</sup> block copolymers with caprolactone were synthesized and PEG-N<sub>3</sub> clicked on the alkyne. The polymers self-assembled to nanoparticles with high biocompatibility. Contrary, Wooley and coworkers<sup>302</sup> reported the unsuccessful synthesis of **D1** with isolated yield <20%, and suspected the reaction via a S<sub>N</sub>2' mechanism to be responsible for decomposition of the monomer (nucleophilic attack at the acetylene proton and subsequent loss of the pendant chain at the phosphate group). They pointed out the absence or loss of the terminal acetylene proton in the <sup>1</sup>H-NMR spectra provided by Wang and coworkers, and suggested loss or partial loss of the alkynyl functionality. Instead, Wooley et al. installed an additional methylene spacer and reported the butynyl monomer 2-(but-3-yn-1-yloxy)-2-oxo-1,3,2-dioxaphospholane (**D2**) with high yield and purity.<sup>302</sup> The monomer was polymerized (homopolymers or copolymers with caprolactone or cyclic phosphates) and post-modification by click chemistry or thiol-yne reaction was applied to prepare non-ionic, cationic, anionic, and zwitterionic micelles,<sup>303-304</sup> covalently labeled core-shell polymeric nanoparticles with fluorescent contrast agents for theranostic applications,<sup>305</sup> PEG-*b*-PPE-based paclitaxel conjugates for ultra-high paclitaxel-loaded multifunctional nanoparticles,<sup>306-307</sup> or silver-bearing degradable polymeric nanoparticles showing *in vitro* antimicrobial activity (Figure 1.6).<sup>308-309</sup> For this purpose, silver cations were chelated into the corona or incorporated into the core using AgOAc (depicted as blue balls in Figure 1.6), or SCC22 or SCC10 (depicted as yellow balls). The placements of the silver species within the nanoparticle frameworks are proposed locations that have not been confirmed experimentally. Frank and coworkers used **D2** to form anionic hydrophilic PPE-copolymers as efficient templating agent for calcium carbonate particles.<sup>310-311</sup>

Wang and coworkers<sup>312</sup> reported a cyclic phosphate carrying an allyl pendant group (2-(prop-2-en-1-yloxy)-2-oxo-1,3,2-dioxaphospholane, **D3**), which was polymerized with a PEG-macroinitiator. The block copolymers self-assembled into nanoparticles and the allyl groups were post-modified by thiol-ene reaction with cysteamine and partially further reacted with dimethyl maleic anhydride to introduce pH-responsivity. Additionally doxorubicine was conjugated to the polymers by hydrazine chemistry or the polymers were used for siRNA delivery.<sup>313</sup> In contrast, Lecomte and coworkers<sup>314</sup> used the pendant allyl chain of **D3** as a protective group to produce polyphosphodiester after selective deprotection with 1.5 eq. sodium benzene-thiolate. Quantitative deprotection without degradation was reported within 2h in DMF/H<sub>2</sub>O (50:50, v/v) at room temperature. A butenyl monomer (2-butenoxy-2-oxo-1,3,2-dioxaphospholane, **D4**) was reported by Lecomte and coworkers<sup>300</sup> and block copolymers with 2-isobutoxy-2-oxo-1,3,2-dioxaphospholane were prepared to demonstrate the control over copolymerizations of cyclic phosphates. Further post-modification has not been shown. Wooley and coworkers<sup>315</sup> synthesized PEG-*b*-PPE of **D4** and conjugated Paclitaxel with acid-labile linkages by thiol-ene reaction for drug

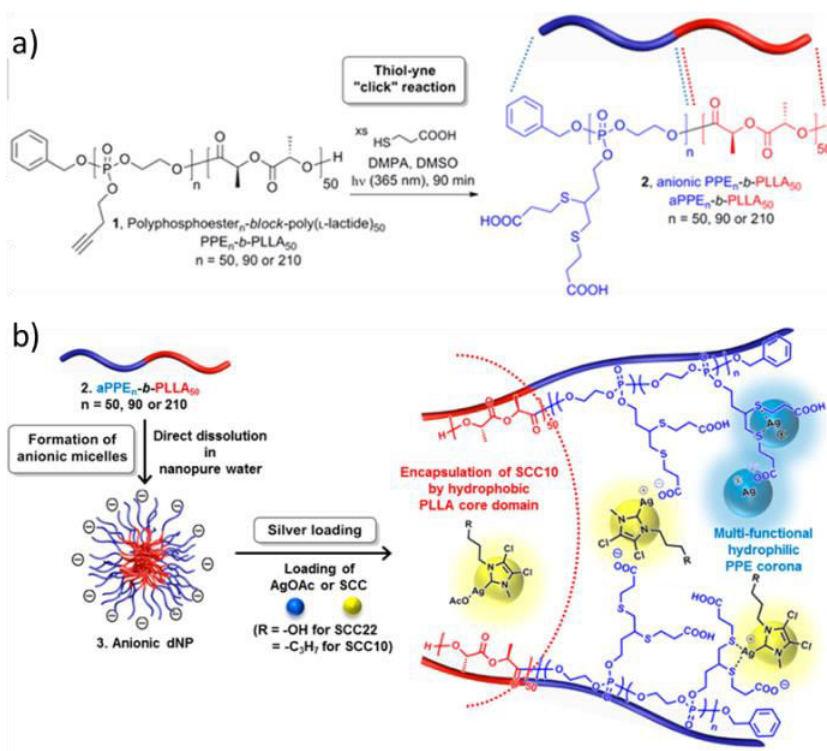


**Figure 1.6.** Synthetic route to silver-bearing degradable polymeric nanoparticles: a) post-polymerization modification of alkyne-functionalized PPE-*b*-PLLA *via* thiol-yne "click" reaction to prepare anionic amphiphilic diblock copolymer, b) self-assembly of diblock copolymers into anionic micelles and silver loading. Adapted with permission from Ref<sup>308</sup>; copyright 2017 American Chemical Society.

delivery. Junkers and coworkers<sup>316</sup> developed a flow microreactor to attach thiols upon UV-irradiation to butenyl-containing PPEs of **D4**. Wooley and coworkers<sup>317</sup> also introduced a monomer with a reactive vinyl ether moiety (**D5**), which was either reacted in a thiol-ene reaction, thio-acetalization with thiols or acetalization with alcohols. While they reported quantitative conversion for thiol-ene reaction, acetalization and thio-acetalization resulted in rather low conversions of 18% and 8%, respectively. Ni and coworkers<sup>318</sup> reported a functional acryloyl phosphate monomer (**D6**) and prepared block copolymers with caprolactone. The pendant acryloyl groups were quantitatively functionalized by nucleophilic addition chemistry with thiols to introduce hydrophilic chains with hydroxyl, carboxyl, amine, and amino acid functionalities with low cytotoxicity. Stable micelles in aqueous solution, loaded with doxorubicin, opened the way to drug delivery carriers. While after 2 days at 37 °C, 30% release of cargo was observed in PBS-buffer (pH 7.4, 0.01M), over 70% was reported in the presence of 0.2 mg/mL phosphodiesterase I. Iwasaki et al.<sup>319</sup> used a methacryloyl phosphate monomer (**D7**) to obtain copolymers with 2-isopropyl-2-oxo-1,3,2-dioxaphospholane. They were used as cross-linker and copolymerized with 2-methacryloyloxyethyl phosphorylcholine (MPC) to prepare hydrogels. 100% degradation of the PPE-crosslinker polymer was observed within 6 days at pH 11, and 50% within 15 days at pH 7.4.

50% of the hydrogels degraded after 44 days at pH 7.4 (PBS-buffer).<sup>320</sup> As highly porous hydrogels, they are suitable for 3D cell cultivation and increased proliferation of mouse osteoblastic cell (MC3T3-E1) was reported with increasing amount of PPEs in the hydrogels.<sup>321</sup> The methacrylates as well were photo-cross-linked to obtain hydrogels.<sup>322</sup>

Iwasaki et al.<sup>323-324</sup> copolymerized a cyclic bromoisobutylate phosphate (2-(2-oxo-1,3,2-dioxaphosphoroyloxyethyl-2-bromoisobutylate), **D8**) with 2-isopropyl-2-oxo-1,3,2-dioxaphospholane. The polymer was used as macroinitiator for ATRP polymerization, to form amphiphilic PPEs with poly(2-methacryloyloxyethyl phosphorylcholine)-grafted chains.

6-membered phosphate monomers are synthesized by a similar strategy, using 2-chloro-2-oxo-1,3,2-dioxaphosphorinane as precursor, which is further substituted with an appropriate alcohol (Scheme 1.26B). Penczek and coworkers<sup>325</sup> reported in 1977 three potentially orthogonally reactive monomers with 2,2,2-trichloroethyl (**D9**), 2,2,2-trifluoroethyl (**D10**) or 2-cyanoethyl (**D11**) functionalities as pendant chains (yields were not reported), but did not further modify the corresponding polymers, which were obtained by cationic polymerization in bulk. 6-membered cyclic phosphates as monomers are less considered in literature compared to 5-membered phosphates, due to a lower ring strain.

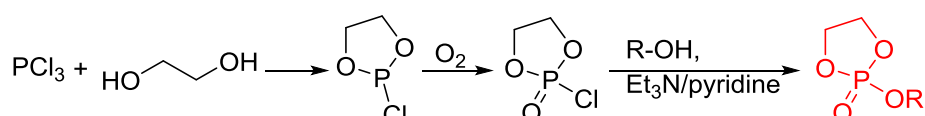
**Cyclic H-Phosphonates.** A cyclic 5-membered H-phosphonate monomer, 4-methyl-2-oxo-2-hydro-1,3,2-dioxaphospholane (**D12**), was polymerized by Vogl and coworkers,<sup>326</sup> starting from 1,2-propandiol and  $\text{PCl}_3$ . 4-methyl-2-chloro-1,3,2-dioxaphospholane was oxidized by a mixture of water/dioxane to obtain the phosphite (yield has not been reported) (Scheme 1.26C). The monomer was also synthesized from optically active propandiol. The polymer **p(D12)** was converted by various strategies to (i) poly(phosphoric acid)s by oxidation with dinitrogen tetroxide, (ii) poly(phosphoramidate)s<sup>327-328</sup> by an Atherton-Todd reaction with primary or secondary amine (30-60% conversion), and (iii) poly(phosphate)s<sup>329</sup> by chlorination and subsequent substitution with an appropriate alcohol (quantitative conversion), e.g. to poly(2-aminoethyl propylene phosphate) (PPE-EA). Leong and Mao used the poly(phosphate)s<sup>329-330</sup> and poly(phosphoramidate)s<sup>328, 331</sup> (with charged groups<sup>332</sup>) in several reports as gene carrier and transfection agent, or to form plasmid-templated DNA-block copolymer nanoparticles.<sup>333</sup>

A 6-membered H-phosphonate monomer, 2-hydro-2-oxo-1,3,2-dioxaphosphorinane (**D13**),<sup>334</sup> was polymerized by Penczek and coworkers<sup>335</sup> (Scheme 1.26D). It was prepared by transesterification from dimethyl phosphite and 1,3-propylene glycol (yield: 79%<sup>334</sup>). Penczek showed conversion to poly(phosphoric acid)s by oxidation with dinitrogen tetroxide, to poly(phosphoramidate)s by chlorination with gaseous chlorine and subsequent reaction with

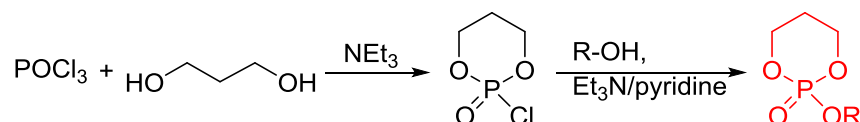
primary amines (C- or N-substituted imidazoles, adenine or uracil),<sup>336-338</sup> or to poly(phosphorothioate)s<sup>339</sup> by sulfurization with sulfur in the presence of lutidine.

**Cyclic Phosphonates.** A 5-membered cyclic allyl phosphonate monomer (2-allyl-2-oxo-1,3,2-dioxaphospholane, **D14**) was recently reported by Wurm and coworkers.<sup>7, 340</sup> For cyclic phosphonates the pendant group was introduced in the first step of a three step reaction (Scheme 1.26E): after reaction of allyl bromide with triethyl phosphite, allyl phosphonic acid dichloride was formed by reaction with chlorotrimethylsilane and oxalyl chloride. Ring-closing reaction with ethylene glycol formed the final phosphonate monomer with an overall yield of 28%. Terpolymers were quantitatively modified with cysteine by a thiol-ene reaction and their thermoresponsive behavior analyzed.<sup>340</sup> PEG-*b*-PPEs were modified with 3-mercaptopropionic acid. The block copolymers exhibited UCST behavior and were self-assembled into temperature-dependent dynamic aggregates.<sup>7</sup> Poly(phosphonate)s are realized by using the organocatalyst DBU and primary alcohols as initiator in dichloromethane at 0°C for 16 hours with monomer conversions of 90-96%.<sup>340-342</sup>

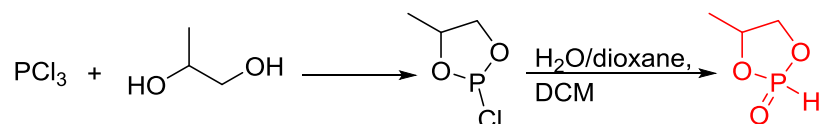
**A: 5-membered phosphate monomers**



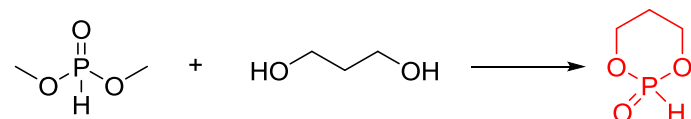
**B: 6-membered phosphate monomers**



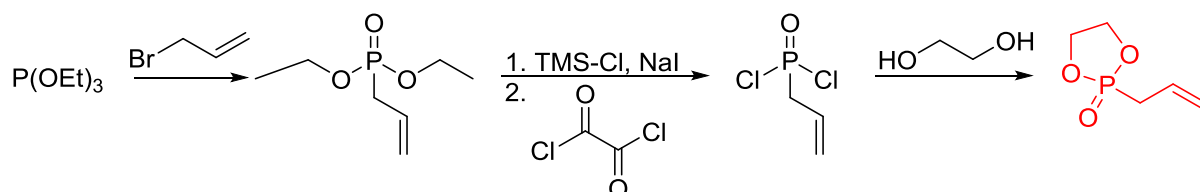
**C: 5-membered H-phosphonate monomer**



**D: 6-membered H-phosphonate monomer**



**E: 5-membered phosphonate monomers**



**Scheme 1.26.** Synthetic strategies for cyclic phosphate, phosphonate and H-phosphonate monomers.

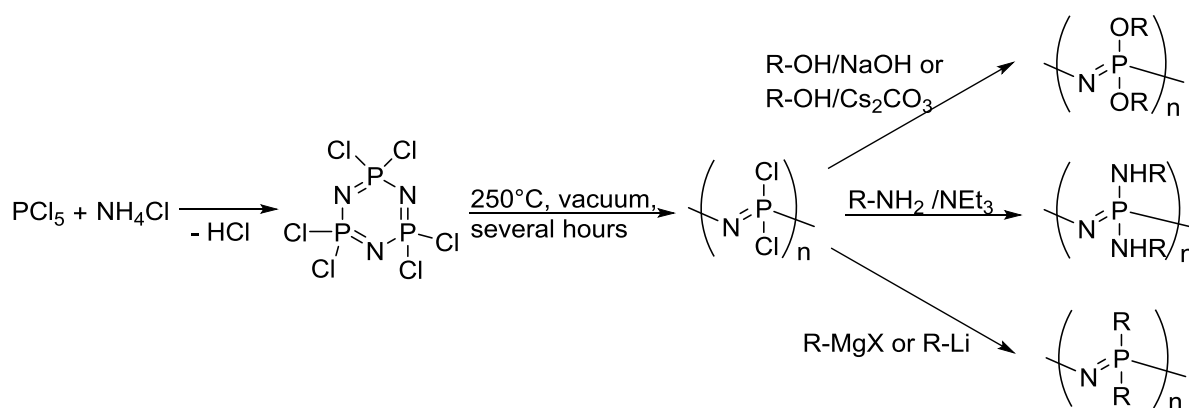
## 1.9 Poly(organophosphazene)s

Poly(organophosphazene)s are a polymer class of inorganic-organic hybrid polymers and exhibit high diversity of properties due to the high versatility of possible organic substituents. The phosphorus-nitrogen backbone is substituted by two organic side groups on the phosphorus atoms. Polymerization techniques and application of poly(organophosphazene)s were recently summarized in two excellent reviews.<sup>13, 343</sup>

The most widely used method to prepare poly(organophosphazene)s is the thermal ROP of hexachlorophosphazene (**D15**) with no control over the molecular weight and thus generally high molecular weights ( $> 10^6$  Da) and broad molecular weight distributions to the precursor poly(dichloro-phosphazene)  $[\text{N}(\text{PCl}_2)]_n$ . Living cationic polymerization of trichlorophosphoranimine  $(\text{Cl}_3\text{PNSiMe}_3)_n$  with two equivalents of phosphorus pentachloride by a chain growth mechanism in solution at room temperature results in higher control of molecular weight via the feed monomer to initiator ratio with lower polydispersities. We refer the reader to a separate review.<sup>13</sup>

**D15** is commercially available (at Sigma Aldrich) or can be synthesized from phosphorous pentachloride and ammonium chloride and subsequent sublimation from a mixture of oligomers (Scheme 1.27). The precursor rapidly hydrolyses in the presence of water, but can be completely post-modified under dry conditions with amines, alcohols, thiols or alkylation agents such as  $\text{RMgX}$  or  $\text{RLi}$ . Mixed, stepwise substitution with two or more organic substituents on the same macromolecule was possible and gives access to a library of polymers with varied properties.<sup>13</sup> Complete modification is important to prevent uncontrolled cross-linking or degradation due to unreacted P-Cl groups. ROP was achieved with partially or completely substituted cyclophosphazene, but side reactions as ring expansion, decomposition or no reaction at all were observed. Generally, the probability for polymerization decreased with increasing number of organic substituents.<sup>344</sup>

Several further cyclic phosphazene monomers with a substitution of a phosphorus atom by carbon or sulfur were reported yielding cyclocarbophosphazene  $\text{N}_3\text{P}_2\text{CCl}_5$  (**D16**) from phosphorous pentachloride, ammonium chloride and cyanamide (10% yield)<sup>345</sup> or cyclothiophosphazene  $\text{N}_3\text{P}_2\text{SCl}_5$  (**D17**) (yield 40-50%).<sup>346</sup> Poly(chlorocarbophosphazene)s<sup>347</sup> and poly(chlorothiophosphazene)s<sup>323</sup> were obtained by thermal polymerization (120 °C, 4-6h and 90 °C, 4h, respectively), and were more reactive to nucleophilic substitution by aryloxides than classical poly(phosphazene)<sup>345-346, 348</sup>. Poly(carbophosphazene)s exhibited higher glass transition temperatures than poly(phosphazene) analogues due to less torsional mobility in the backbone,<sup>345, 348</sup> poly(thiophosphazene)s<sup>346</sup> less hydrolytic stability. Polymerization (165-180 °C, 4h) of cyclothionylphosphazenes  $\text{N}_3\text{P}_2\text{SOCl}_5$  (**D18**) and  $\text{N}_3\text{P}_2\text{SOFCl}_4$  (**D19**) yielded hydrolytically stable poly(thionylphosphazene)s.<sup>349-350</sup>

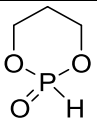
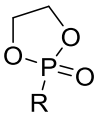
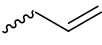
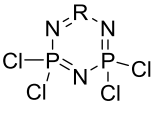


**Scheme 1.27.** Synthetic route to hexachlorophosphazene and poly(organophosphazene)s.

**Table 1.6.** Orthogonally functional cyclic phosphorus-containing monomers for the synthesis of poly(phosphoester)s or poly(phosphazene)s.

Monomer	R=	No	Post-Modification	Ref.
<b>Phosphates</b>				
		<b>D1</b>	-click chemistry with PEG-azide to self-assembled block copolymers	301
		<b>D2</b>	-click chemistry or thiol-yne reaction to form charged micelles, silver- or paclitaxel-loaded nanoparticles, or block copolymers as templating agent for calcium carbonate particles	302-311
		<b>D3</b>	-thiol-ene reaction to attach cysteamine for siRNA delivery or subsequent attachment of doxorubicin by hydrazine chemistry and dimethyl maleic anhydride for pH-responsivity	312-314
		<b>D4</b>	-thiolene reaction to conjugate paclitaxel with an acid-labile linker for drug delivery	300, 315-316
		<b>D5</b>	-thiol-ene reaction, acetalization or thio-acetalization	317
		<b>D6</b>	-Michael-type addition of charged thiols	318
		<b>D7</b>	-copolymers as cross-linker for copolymerization with 2-methacryloyloxyethyl phosphorylcholine (MPC) to hydrogels	319-322
		<b>D8</b>	-photo-cross-linking to hydrogels	323-324
		<b>D9</b>	-ATRP-macroinitiator to graft poly(2-methacryloyloxyethyl phosphorylcholine)	325
		<b>D10</b>	-no modification	325
		<b>D11</b>	-no modification	325
<b>H-Phosphonates</b>				
		<b>D12</b>	-oxidation with N <sub>2</sub> O <sub>4</sub> to poly(phosphoric acid)s -reaction with amines to poly(phosphoramidate)s as gene carrier -chlorination and reaction with alcohols to poly(phosphate)s as gene carrier	326-333

**Table 1.6.** Orthogonally functional cyclic phosphorus-containing monomers for the synthesis of poly(phosphoester)s or poly(phosphazene)s (*continued*).

Monomer	R=	No	Post-Modification	Ref.
		<b>D13</b>	-oxidation with N <sub>2</sub> O <sub>4</sub> to poly(phosphoric acid)s -chlorination and reaction with amines to poly(phosphoramidate)s -sulfurization to poly(phosphorothioate)s	334-339
<b>Phosphonates</b>				
		<b>D14</b>	-thiol-ene reaction with cysteine or 3-mercaptopropionic acid to form thermoresponsive terpolymers	7, 340
<b>Phosphazenes</b>				
		<b>D15</b>	-nucleophilic substitution with alcohols and amines	13, 343
		<b>D16</b>	-nucleophilic substitution with alcohols and amines	345, 347
		<b>D17</b>	-nucleophilic substitution with alcohols and amines	346, 323
		<b>D18</b>	-nucleophilic substitution with alcohols and amines	349-350
		<b>D19</b>	-nucleophilic substitution with alcohols and amines	349-350

## 1.10 Conclusions and Outlook

The ring-opening polymerization is an established method to obtain well-defined degradable polymers with narrow molecular weight distributions. Poly(ester)s, poly(amide)s and poly(carbonate)s are the prominent material classes prepared by ROP. The reaction conditions for ROP typically do not tolerate nucleophiles and need inert conditions (in most cases), many functional groups in the monomer structure need to be protected. The deprotection step after the polymerization can be challenging, when also the polymer backbone is built from degradable units. Orthogonally reactive groups that do not interfere with the polymerization conditions are efficient alternatives to protective group chemistry. They can be post-modified by efficient reactions, which do not degrade the polymer backbone. Besides alkene, alkyne and halogen functions, several further functions have been reported in literature and were summarized in this review.

The presented general concepts of post-modification, e.g. nucleophilic substitution of halides, alkyne-azide click chemistry, thiol-ene and -yne reaction or Diels-Alder reaction can be generally applied for all monomer classes. Post-modification strategies with quantitative conversion yields, and protocols using mild conditions (e.g. excluding acidic or alkaline conditions) seems to be most

convenient and reliable. Photoinduced or thermal modification e.g. in the case of Diels-Alder reactions, are promising alternatives without the use of toxic compounds/catalysts.

The described monomers are usually synthesized in several reaction steps. Pendant functionalities are mostly introduced in the first step, making the synthesis of functional monomers lengthy. The use of “precursor monomers” would be beneficial, introducing the desired functionality in the last reaction step. This is e.g. the case for cyclic phosphate monomers, all being based on 2-chloro-2-oxo-1,3,2-dioxaphospholane (COP). Development of such precursors is an important futuristic endeavor, to facilitate the access to functional monomers.

An interesting approach might be the synthesis of monomers from natural and renewable sources, e.g. macrolactones or carbohydrates. However, only a limited number of such examples is available up to date. Only few functional OCA monomers for the synthesis of poly(ester)s are reported, and expansion the monomer class is promising. Since reaction conditions for lactams are inconvenient, the number of functional monomers is very limited. Carlotti and coworkers<sup>139</sup> reported a functional monomer, synthesized from the precursor  $\alpha$ -amino- $\epsilon$ -caprolactam which might be an interesting precursor for future poly(amide)s with additional chemical functions

The radical ROP of cyclic ketene acetals to poly(ester)s is excluded in this review. However, it can be an interesting alternative, especially for the synthesis of poly(ester)s on an industrial scale, if development of functional monomers can be promoted. To the best of our knowledge only chlorinated monomers are reported so far.<sup>30</sup> The copolymerization of epoxides with anhydrides or carbon dioxide (and its sulfur analogues) to poly(ester)s and -(carbonate)s as well is an attractive strategy. Functional epoxides and their synthetic protocols are well-established,<sup>351</sup> and the potential of the combination with carbon dioxide<sup>217</sup> or anhydrides<sup>32</sup> is still exploited. The combination of polyaddition and ring-opening of different cyclic monomers offers a further strategy to novel functional materials with tunable properties: reaction of lactone monomers with diamines is under exploration,<sup>352</sup> as well as cyclic carbonates with diamines to poly(hydroxyurethane)s.<sup>353</sup>

Less explored polymer classes from ROP also seem to be promising to us as poly(ester ether)s, and poly(thioester)s. Five-, six- as well as seven-membered cyclic lactone ethers can be polymerized via ROP to poly(ester ether)s. Reported substituents are mainly alkyl- or aryl chains or protected functions. To the best of our knowledge, orthogonally reactive monomers are not available so far, but should be considered as a further development of lactone monomers. E-Thiolactones and  $\beta$ -thiolactones can be polymerized by a base-catalyzed ring-opening polymerization to poly(thioester)s. However, no functional reactive monomers have been reported to the best of our knowledge.<sup>354</sup> Finally, the class of poly(phosphoester)s offers much potential for new functional phosphate and phosphonate monomers.

To sum up, a broad variety of orthogonally reactive functionalities for cyclic monomers for the ROP and post-modification opportunities has been reported so far, which give access to diverse chemically functional biodegradable polymers and promising applications. There is still plenty of scope for further developments.

### 1.11 References

1. Okada, M., *Prog. Polym. Sci.* **2002**, *27* (1), 87-133.
2. Ulery, B. D.; Nair, L. S.; Laurencin, C. T., *J. Polym. Sci., Part B: Polym. Phys.* **2011**, *49* (12), 832-864.
3. Nair, L. S.; Laurencin, C. T., *Prog. Polym. Sci.* **2007**, *32* (8-9), 762-798.
4. Guo, B.; Ma, P. X., *Sci. China: Chem.* **2014**, *57* (4), 490-500.
5. Rahman, M., Degradation of Polyesters in Medical Applications. In *Polyester*, Saleh, H. E.-D. M., Ed. InTech: Rijeka, 2012; p Ch. 05.
6. Baran, J.; Penczek, S., *Macromolecules* **1995**, *28* (15), 5167-5176.
7. Wolf, T.; Rheinberger, T.; Simon, J.; Wurm, F. R., *J. Am. Chem. Soc.* **2017**, *139* (32), 11064-11072.
8. Wang, H.; Su, L.; Li, R.; Zhang, S.; Fan, J.; Zhang, F.; Nguyen, T. P.; Wooley, K. L., *ACS Macro Lett.* **2017**, *6* (3), 219-223.
9. Zhang, S.; Wang, H.; Shen, Y.; Zhang, F.; Seetho, K.; Zou, J.; Taylor, J.-S. A.; Dove, A. P.; Wooley, K. L., *Macromolecules* **2013**, *46* (13), 5141-5149.
10. Cankaya, A.; Steinmann, M.; Bulbul, Y.; Lieberwirth, I.; Wurm, F. R., *Polym. Chem.* **2016**, *7* (31), 5004-5010.
11. Baran, J.; Kaluzynski, K.; Szymanski, R.; Penczek, S., *Biomacromolecules* **2004**, *5* (5), 1841-1848.
12. Steinmann, M.; Wagner, M.; Wurm, F. R., *Chem. - Eur. J.* **2016**, *22* (48), 17329-17338.
13. Rothmund, S.; Teasdale, I., *Chem. Soc. Rev.* **2016**, *45* (19), 5200-5215.
14. Teasdale, I.; Brüggemann, O., *Polymers* **2013**, *5* (1), 161.
15. Rydz, J.; Sikorska, W.; Kyulavska, M.; Christova, D., *Int. J. Mol. Sci.* **2015**, *16* (1), 564.
16. Ulbricht, J.; Jordan, R.; Luxenhofer, R., *Biomaterials* **2014**, *35* (17), 4848-4861.
17. Leja, K.; Lewandowicz, G., *Pol. J. Environ. Stud.* **2010**, *19* (2), 255-266.
18. Woodruff, M. A.; Hutmacher, D. W., *Prog. Polym. Sci.* **2010**, *35* (10), 1217-1256.
19. Banerjee, A.; Chatterjee, K.; Madras, G., *Mater. Sci. Technol.* **2014**, *30* (5), 567-573.
20. Pathak, V. M.; Navneet, *Bioresour Bioproc* **2017**, *4* (1), 15.
21. Tian, H.; Tang, Z.; Zhuang, X.; Chen, X.; Jing, X., *Prog. Polym. Sci.* **2012**, *37* (2), 237-280.
22. Tempelaar, S.; Mespouille, L.; Coulembier, O.; Dubois, P.; Dove, A. P., *Chem. Soc. Rev.* **2013**, *42* (3), 1312-1336.
23. Jérôme, C.; Lecomte, P., *Adv. Drug Delivery Rev.* **2008**, *60* (9), 1056-1076.
24. Lou, X.; Detrembleur, C.; Jérôme, R., *Macromol. Rapid Commun.* **2003**, *24* (2), 161-172.
25. Dommerholt, J.; Rutjes, F. P. J. T.; van Delft, F. L., *Top. Curr. Chem.* **2016**, *374* (2), 16.
26. Pandiyarajan, C. K.; Prucker, O.; Rühle, J., *Macromolecules* **2016**, *49* (21), 8254-8264.
27. Prucker, O.; Naumann, C. A.; Rühle, J.; Knoll, W.; Frank, C. W., *J. Am. Chem. Soc.* **1999**, *121* (38), 8766-8770.
28. Tong, R., *Ind. Eng. Chem. Res.* **2017**, *56* (15), 4207-4219.
29. Seyednejad, H.; Ghassemi, A. H.; van Nostrum, C. F.; Vermonden, T.; Hennink, W. E., *J. Controlled Release* **2011**, *152* (1), 168-176.
30. Agarwal, S., *Polym. Chem.* **2010**, *1* (7), 953-964.
31. Paul, S.; Zhu, Y.; Romain, C.; Brooks, R.; Saini, P. K.; Williams, C. K., *Chem. Commun.* **2015**, *51* (30), 6459-6479.
32. Longo, J. M.; Sanford, M. J.; Coates, G. W., *Chem. Rev.* **2016**, *116* (24), 15167-15197.

33. Riva, R.; Schmeits, S.; Jérôme, C.; Jérôme, R.; Lecomte, P., *Macromolecules* **2007**, *40* (4), 796-803.
34. Duda, A., 4.11 - ROP of Cyclic Esters. Mechanisms of Ionic and Coordination Processes A2 - Matyjaszewski, Krzysztof. In *Polymer Science: A Comprehensive Reference*, Möller, M., Ed. Elsevier: Amsterdam, 2012; pp 213-246.
35. Al-Azemi, T. F.; Mohamod, A. A., *Polymer* **2011**, *52* (24), 5431-5438.
36. Xu, N.; Wang, R.; Du, F.-S.; Li, Z.-C., *J. Polym. Sci., Part A: Polym. Chem.* **2009**, *47* (14), 3583-3594.
37. Lenoir, S.; Riva, R.; Lou, X.; Detrembleur, C.; Jérôme, R.; Lecomte, P., *Macromolecules* **2004**, *37* (11), 4055-4061.
38. Massoumi, B., *Polym. Sci., Ser. B* **2015**, *57* (2), 85-92.
39. Riva, R.; Schmeits, S.; Stoffelbach, F.; Jerome, C.; Jerome, R.; Lecomte, P., *Chem. Commun.* **2005**, (42), 5334-5336.
40. Habnoui, S. E.; Darcos, V.; Coudane, J., *Macromol. Rapid Commun.* **2009**, *30* (3), 165-169.
41. Darcos, V.; Antoniacomi, S.; Paniagua, C.; Coudane, J., *Polym. Chem.* **2012**, *3* (2), 362-368.
42. Jazkewitsch, O.; Mondrzyk, A.; Staffel, R.; Ritter, H., *Macromolecules* **2011**, *44* (6), 1365-1371.
43. Garg, S. M.; Xiong, X.-B.; Lu, C.; Lavasanifar, A., *Macromolecules* **2011**, *44* (7), 2058-2066.
44. Pelegri-O'Day, E. M.; Paluck, S. J.; Maynard, H. D., *J. Am. Chem. Soc.* **2017**, *139* (3), 1145-1154.
45. El Habnoui, S.; Nottelet, B.; Darcos, V.; Porsio, B.; Lemaire, L.; Franconi, F.; Garric, X.; Coudane, J., *Biomacromolecules* **2013**, *14* (10), 3626-3634.
46. Jazkewitsch, O.; Ritter, H., *Macromolecules* **2011**, *44* (2), 375-382.
47. Li, H.; Jérôme, R.; Lecomte, P., *Polymer* **2006**, *47* (26), 8406-8413.
48. Sinnwell, S.; Ritter, H., *Macromolecules* **2006**, *39* (8), 2804-2807.
49. Takeda, K.; Imaoka, I.; Yoshii, E., *Tetrahedron* **1994**, *50* (37), 10839-10848.
50. Lowe, J. R.; Tolman, W. B.; Hillmyer, M. A., *Biomacromolecules* **2009**, *10* (7), 2003-2008.
51. Lowe, J. R.; Martello, M. T.; Tolman, W. B.; Hillmyer, M. A., *Polym. Chem.* **2011**, *2* (3), 702-708.
52. Gao, Y.; Mori, T.; Manning, S.; Zhao, Y.; Nielsen, A. d.; Neshat, A.; Sharma, A.; Mahnen, C. J.; Everson, H. R.; Crotty, S.; Clements, R. J.; Malcuit, C.; Hegmann, E., *ACS Macro Lett.* **2016**, *5* (1), 4-9.
53. Detrembleur, C.; Mazza, M.; Halleux, O.; Lecomte, P.; Mecerreyes, D.; Hedrick, J. L.; Jérôme, R., *Macromolecules* **2000**, *33* (1), 14-18.
54. Detrembleur, C.; Mazza, M.; Lou, X.; Halleux, O.; Lecomte, P.; Mecerreyes, D.; Hedrick, J. L.; Jérôme, R., *Macromolecules* **2000**, *33* (21), 7751-7760.
55. Riva, R.; Lazzari, W.; Billiet, L.; Du Prez, F.; Jérôme, C.; Lecomte, P., *J. Polym. Sci., Part A: Polym. Chem.* **2011**, *49* (7), 1552-1563.
56. Latere, J.-P.; Lecomte, P.; Dubois, P.; Jérôme, R., *Macromolecules* **2002**, *35* (21), 7857-7859.
57. Prime, E. L.; Hamid, Z. A. A.; Cooper-White, J. J.; Qiao, G. G., *Biomacromolecules* **2007**, *8* (8), 2416-2421.
58. Dai, W.; Zhu, J.; Shanguan, A.; Lang, M., *Eur. Polym. J.* **2009**, *45* (6), 1659-1667.
59. Mecerreyes, D.; Humes, J.; Miller, R. D.; Hedrick, J. L.; Detrembleur, C.; Lecomte, P.; Jérôme, R.; San Roman, J., *Macromol. Rapid Commun.* **2000**, *21* (11), 779-784.
60. Vaida, C.; Mela, P.; Keul, H.; Möller, M., *J. Polym. Sci., Part A: Polym. Chem.* **2008**, *46* (20), 6789-6800.
61. Lou, X.; Jérôme, C.; Detrembleur, C.; Jérôme, R., *Langmuir* **2002**, *18* (7), 2785-2788.
62. Rieger, J.; Van Butsele, K.; Lecomte, P.; Detrembleur, C.; Jerome, R.; Jerome, C., *Chem. Commun.* **2005**, (2), 274-276.
63. Vaida, C.; Mela, P.; Kunna, K.; Sternberg, K.; Keul, H.; Möller, M., *Macromol. Biosci.* **2010**, *10* (8), 925-933.
64. Mecerreyes, D.; Atthoff, B.; Boduch, K. A.; Trollsås, M.; Hedrick, J. L., *Macromolecules* **1999**, *32* (16), 5175-5182.
65. Garle, A.; Kong, S.; Ojha, U.; Budhlall, B. M., *ACS Appl. Mater. Interfaces* **2012**, *4* (2), 645-657.
66. Chen, D.; Chang, C.-C.; Cooper, B.; Silvers, A.; Emrick, T.; Hayward, R. C., *Biomacromolecules* **2015**, *16* (10), 3329-3335.

67. Parrish, B.; Quansah, J. K.; Emrick, T., *J. Polym. Sci., Part A: Polym. Chem.* **2002**, *40* (12), 1983-1990.
68. Parrish, B.; Emrick, T., *Macromolecules* **2004**, *37* (16), 5863-5865.
69. Parrish, B.; Breitenkamp, R. B.; Emrick, T., *J. Am. Chem. Soc.* **2005**, *127* (20), 7404-7410.
70. Herrmann, J. L.; Schlessinger, R. H., *J. Chem. Soc., Chem. Commun.* **1973**, (19), 711-712.
71. Cooper, B. M.; Chan-Seng, D.; Samanta, D.; Zhang, X.; Parelkar, S.; Emrick, T., *Chem. Commun.* **2009**, (7), 815-817.
72. Ende, A. E. v. d.; Kravitz, E. J.; Harth, E., *J. Am. Chem. Soc.* **2008**, *130* (27), 8706-8713.
73. Stöhr, O.; Ritter, H., *Macromol. Chem. Phys.* **2014**, *215* (5), 426-430.
74. Upton, B. M.; Gipson, R. M.; Duhovic, S.; Lydon, B. R.; Matsumoto, N. M.; Maynard, H. D.; Diaconescu, P. L., *Inorg. Chem. Front.* **2014**, *1* (3), 271-277.
75. Houk, K. N.; Jabbari, A.; Hall, H. K.; Alemán, C., *J. Org. Chem.* **2008**, *73* (7), 2674-2678.
76. Nobes, G. A. R.; Kazlauskas, R. J.; Marchessault, R. H., *Macromolecules* **1996**, *29* (14), 4829-4833.
77. Tada, K.; Numata, Y.; Saegusa, T.; Furukawa, J., *Makromol. Chem.* **1964**, *77* (1), 220-228.
78. Hong, M.; Chen, E. Y. X., *Nat. Chem.* **2016**, *8* (1), 42-49.
79. Zhou, J.; Schmidt, A. M.; Ritter, H., *Macromolecules* **2010**, *43* (2), 939-942.
80. Tang, X.; Hong, M.; Falivene, L.; Caporaso, L.; Cavallo, L.; Chen, E. Y. X., *J. Am. Chem. Soc.* **2016**, *138* (43), 14326-14337.
81. Murray, A. W.; Reid, R. G., *Synthesis* **1985**, *1985* (01), 35-38.
82. Undin, J.; Olsén, P.; Godfrey, J.; Odelius, K.; Albertsson, A.-C., *Polymer* **2016**, *87*, 17-25.
83. Iida, M.; Araki, T.; Teranishi, K.; Tani, H., *Macromolecules* **1977**, *10* (2), 275-284.
84. Lavallée, C.; Leborgne, A.; Spassky, N.; Prud'homme, R. E., *J. Polym. Sci., Part A: Polym. Chem.* **1987**, *25* (5), 1315-1328.
85. Lavallee, C.; Lemay, G.; Leborgne, A.; Spassky, N.; Prud'homme, R. E., *Macromolecules* **1984**, *17* (12), 2457-2462.
86. Voyer, R.; Prud'Homme, R. E., *J. Polym. Sci., Part A: Polym. Chem.* **1986**, *24* (11), 2773-2787.
87. Liu, X.-Q.; Li, Z.-C.; Du, F.-S.; Li, F.-M., *Macromol. Rapid Commun.* **1999**, *20* (9), 470-474.
88. Liu, X.-Q.; Wang, M.-X.; Li, Z.-C.; Li, F.-M., *Macromol. Chem. Phys.* **1999**, *200* (2), 468-473.
89. Yamashita, Y.; Tsuda, T.; Ishida, H.; Uchikawa, A.; Kuriyama, Y., *Makromol. Chem.* **1968**, *113* (1), 139-146.
90. Ohse, V. H.; Cherdron, H., *Makromol. Chem.* **1966**, *95* (1), 283-295.
91. Lee, J. T.; Thomas, P. J.; Alper, H., *J. Org. Chem.* **2001**, *66* (16), 5424-5426.
92. Kramer, J. W.; Lobkovsky, E. B.; Coates, G. W., *Org. Lett.* **2006**, *8* (17), 3709-3712.
93. Guillaume, C.; Ajellal, N.; Carpentier, J.-F.; Guillaume, S. M., *J. Polym. Sci., Part A: Polym. Chem.* **2011**, *49* (4), 907-917.
94. Sinclair, F.; Chen, L.; Greenland, B. W.; Shaver, M. P., *Macromolecules* **2016**, *49* (18), 6826-6834.
95. Leboucher-Durand, M.-A.; Langlois, V.; Guérin, P., *React. Funct. Polym.* **1996**, *31* (1), 57-65.
96. Bizzarri, R.; Chiellini, F.; Solaro, R.; Chiellini, E.; Cammas-Marion, S.; Guerin, P., *Macromolecules* **2002**, *35* (4), 1215-1223.
97. Jeanbat-Mimaud, V.; Barbaud, C.; Caruelle, J.-P.; Barritault, D.; Cammas-Marion, S.; Langlois, V.; Guérin, P., *C. R. Acad. Sci., Ser. IIC: Chim.* **1999**, *2* (7), 393-401.
98. Caruelle, J.-P.; Barritault, D.; Jeanbat-Mimaud, V.; Cammas-Marion, S.; Langlois, V.; Guerin, P.; Barbaud, C., *Journal of Biomaterials Science, Polymer Edition* **2000**, *11* (9), 979-991.
99. Coulembier, O.; Degée, P.; Gerbaux, P.; Wantier, P.; Barbaud, C.; Flammang, R.; Guérin, P.; Dubois, P., *Macromolecules* **2005**, *38* (8), 3141-3150.
100. Xu, Y.-C.; Zhou, H.; Sun, X.-Y.; Ren, W.-M.; Lu, X.-B., *Macromolecules* **2016**, *49* (16), 5782-5787.
101. Xu, Y.-C.; Ren, W.-M.; Zhou, H.; Gu, G.-G.; Lu, X.-B., *Macromolecules* **2017**, *50* (8), 3131-3142.
102. Saiyasombat, W.; Molloy, R.; Nicholson, T. M.; Johnson, A. F.; Ward, I. M.; Poshyachinda, S., *Polymer* **1998**, *39* (23), 5581-5585.
103. Duda, A.; Kowalski, A., Thermodynamics and Kinetics of Ring-Opening Polymerization. In *Handbook of Ring-Opening Polymerization*, Wiley-VCH Verlag GmbH & Co. KGaA: 2009; pp 1-51.

104. Kobayashi, S., *Proc. Jpn. Acad., Ser. B* **2010**, *86* (4), 338-365.
105. Kobayashi, S., *Polym. Adv. Technol.* **2015**, *26* (7), 677-686.
106. Ates, Z.; Audouin, F.; Harrington, A.; O'Connor, B.; Heise, A., *Macromol. Biosci.* **2014**, *14* (11), 1600-1608.
107. Ates, Z.; Heise, A., *Polym. Chem.* **2014**, *5* (8), 2936-2941.
108. Claudino, M.; van der Meulen, I.; Trey, S.; Jonsson, M.; Heise, A.; Johansson, M., *J. Polym. Sci., Part A: Polym. Chem.* **2012**, *50* (1), 16-24.
109. Ates, Z.; Thornton, P. D.; Heise, A., *Polym. Chem.* **2011**, *2* (2), 309-312.
110. van der Meulen, I.; Li, Y.; Deumens, R.; Joosten, E. A. J.; Koning, C. E.; Heise, A., *Biomacromolecules* **2011**, *12* (3), 837-843.
111. van der Meulen, I.; de Geus, M.; Antheunis, H.; Deumens, R.; Joosten, E. A. J.; Koning, C. E.; Heise, A., *Biomacromolecules* **2008**, *9* (12), 3404-3410.
112. Vaida, C.; Keul, H.; Moeller, M., *Green Chem.* **2011**, *13* (4), 889-899.
113. Uyama, H.; Kobayashi, S.; Morita, M.; Habae, S.; Okamoto, Y., *Macromolecules* **2001**, *34* (19), 6554-6556.
114. Leemhuis, M.; Akeroyd, N.; Kruijtzter, J. A. W.; van Nostrum, C. F.; Hennink, W. E., *Eur. Polym. J.* **2008**, *44* (2), 308-317.
115. Coumes, F.; Darcos, V.; Domurado, D.; Li, S.; Coudane, J., *Polym. Chem.* **2013**, *4* (13), 3705-3713.
116. Yu, Y.; Zou, J.; Yu, L.; Ji, W.; Li, Y.; Law, W.-C.; Cheng, C., *Macromolecules* **2011**, *44* (12), 4793-4800.
117. Barker, I. A.; Hall, D. J.; Hansell, C. F.; Du Prez, F. E.; O'Reilly, R. K.; Dove, A. P., *Macromol. Rapid Commun.* **2011**, *32* (17), 1362-1366.
118. Jing, F.; Hillmyer, M. A., *J. Am. Chem. Soc.* **2008**, *130* (42), 13826-13827.
119. Martin Vaca, B.; Bourissou, D., *ACS Macro Lett.* **2015**, *4* (7), 792-798.
120. Zou, J.; Hew, C. C.; Themistou, E.; Li, Y.; Chen, C.-K.; Alexandridis, P.; Cheng, C., *Adv. Mater.* **2011**, *23* (37), 4274-4277.
121. Delle Chiaie, K. R.; Yablon, L. M.; Biernesser, A. B.; Michalowski, G. R.; Sudyn, A. W.; Byers, J. A., *Polym. Chem.* **2016**, *7* (28), 4675-4681.
122. Jones, C. H.; Chen, C.-K.; Chen, M.; Ravikrishnan, A.; Zhang, H.; Gollakota, A.; Chung, T.; Cheng, C.; Pfeifer, B. A., *Mol. Pharmaceutics* **2015**, *12* (3), 846-856.
123. Jiang, X.; Vogel, E. B.; Smith, M. R.; Baker, G. L., *Macromolecules* **2008**, *41* (6), 1937-1944.
124. Kalelkar, P. P.; Alas, G. R.; Collard, D. M., *Macromolecules* **2016**, *49* (7), 2609-2617.
125. Rubinshtein, M.; James, C. R.; Young, J. L.; Ma, Y. J.; Kobayashi, Y.; Gianneschi, N. C.; Yang, J., *Org. Lett.* **2010**, *12* (15), 3560-3563.
126. Borchmann, D. E.; Tarallo, R.; Avendano, S.; Falanga, A.; Carberry, T. P.; Galdiero, S.; Weck, M., *Macromolecules* **2015**, *48* (4), 942-949.
127. Borchmann, D. E.; ten Brummelhuis, N.; Weck, M., *Macromolecules* **2013**, *46* (11), 4426-4431.
128. Castillo, J. A.; Borchmann, D. E.; Cheng, A. Y.; Wang, Y.; Hu, C.; García, A. J.; Weck, M., *Macromolecules* **2012**, *45* (1), 62-69.
129. Fiore, G. L.; Jing, F.; Young, J. V. G.; Cramer, C. J.; Hillmyer, M. A., *Polym. Chem.* **2010**, *1* (6), 870-877.
130. Smith, I. J.; Tighe, B. J., *J. Polym. Sci., Polym. Chem. Ed.* **1976**, *14* (4), 949-960.
131. Pounder, R. J.; Dove, A. P., *Polym. Chem.* **2010**, *1* (3), 260-271.
132. Zhang, Z.; Yin, L.; Tu, C.; Song, Z.; Zhang, Y.; Xu, Y.; Tong, R.; Zhou, Q.; Ren, J.; Cheng, J., *ACS Macro Lett.* **2013**, *2* (1), 40-44.
133. Wang, R.; Zhang, J.; Yin, Q.; Xu, Y.; Cheng, J.; Tong, R., *Angew. Chem. Int. Ed.* **2016**, *55* (42), 13010-13014.
134. Wang, H.; Tang, L.; Tu, C.; Song, Z.; Yin, Q.; Yin, L.; Zhang, Z.; Cheng, J., *Biomacromolecules* **2013**, *14* (10), 3706-3712.
135. Li, Y.; Niu, Y.; Hu, D.; Song, Y.; He, J.; Liu, X.; Xia, X.; Lu, Y.; Xu, W., *Macromol. Chem. Phys.* **2015**, *216* (1), 77-84.
136. Zhang, Z.; Yin, L.; Xu, Y.; Tong, R.; Lu, Y.; Ren, J.; Cheng, J., *Biomacromolecules* **2012**, *13* (11), 3456-3462.

137. Li, J.; Zhang, Y.; Chen, J.; Wang, C.; Lang, M., *J. Macromol. Sci., Part A: Pure Appl. Chem.* **2009**, *46* (11), 1103-1113.
138. He, Y.; Zhang, Y.; Xiao, Y.; Lang, M., *Colloids Surf., B* **2010**, *80* (2), 145-154.
139. Tunc, D.; Le Coz, C.; Alexandre, M.; Desbois, P.; Lecomte, P.; Carlotti, S., *Macromolecules* **2014**, *47* (23), 8247-8254.
140. Russo, S.; Casazza, E., 4.14 - Ring-Opening Polymerization of Cyclic Amides (Lactams) A2 - Matyjaszewski, Krzysztof. In *Polymer Science: A Comprehensive Reference*, Möller, M., Ed. Elsevier: Amsterdam, 2012; pp 331-396.
141. Schmidt, V. E., *Angew. Makromol. Chem.* **1970**, *14* (1), 185-202.
142. Graf, R., *Angew. Chem.* **1968**, *80* (5), 179-189.
143. Lin, J.; Winkelman, C.; Worley, S. D.; Broughton, R. M.; Williams, J. F., *J. Appl. Polym. Sci.* **2001**, *81* (4), 943-947.
144. Jia, X.; Herrera-Alonso, M.; McCarthy, T. J., *Polymer* **2006**, *47* (14), 4916-4924.
145. Perry, E.; Savory, J., *J. Appl. Polym. Sci.* **1967**, *11* (12), 2473-2483.
146. Honda, N.; Kawai, T.; Higashi, F., *Makromol. Chem.* **1978**, *179* (6), 1643-1646.
147. Huesmann, D.; Klinker, K.; Barz, M., *Polym. Chem.* **2017**, *8* (6), 957-971.
148. Deming, T. J., *Chem. Rev.* **2016**, *116* (3), 786-808.
149. Hadjichristidis, N.; Iatrou, H.; Pitsikalis, M.; Sakellariou, G., *Chem. Rev.* **2009**, *109* (11), 5528-5578.
150. Gradišar, Š.; Žagar, E.; Pahovnik, D., *ACS Macro Lett.* **2017**, *6* (6), 637-640.
151. Van Heeswijk, W. A. R.; Eenink, M. J. D.; Feijen, J., *Synthesis* **1982**, *1982* (09), 744-747.
152. Kramer, J. R.; Deming, T. J., *Biomacromolecules* **2010**, *11* (12), 3668-3672.
153. Engler, A. C.; Lee, H.-i.; Hammond, P. T., *Angew. Chem. Int. Ed.* **2009**, *48* (49), 9334-9338.
154. Xiao, C.; Zhao, C.; He, P.; Tang, Z.; Chen, X.; Jing, X., *Macromol. Rapid Commun.* **2010**, *31* (11), 991-997.
155. Engler, A. C.; Shukla, A.; Puranam, S.; Buss, H. G.; Jreige, N.; Hammond, P. T., *Biomacromolecules* **2011**, *12* (5), 1666-1674.
156. Lin, Y.-C.; Wang, P.-I.; Kuo, S.-W., *Soft Matter* **2012**, *8* (37), 9676-9684.
157. Huang, Y.; Zeng, Y.; Yang, J.; Zeng, Z.; Zhu, F.; Chen, X., *Chem. Commun.* **2011**, *47* (26), 7509-7511.
158. Liu, W.; Zhu, M.; Xiao, J.; Ling, Y.; Tang, H., *J. Polym. Sci., Part A: Polym. Chem.* **2016**, *54* (21), 3425-3435.
159. Zhang, R.; Zheng, N.; Song, Z.; Yin, L.; Cheng, J., *Biomaterials* **2014**, *35* (10), 3443-3454.
160. Poché, D. S.; Thibodeaux, S. J.; Rucker, V. C.; Warner, I. M.; Daly, W. H., *Macromolecules* **1997**, *30* (25), 8081-8084.
161. Tang, H.; Zhang, D., *Polym. Chem.* **2011**, *2* (7), 1542-1551.
162. Zhang, Y.; Lu, H.; Lin, Y.; Cheng, J., *Macromolecules* **2011**, *44* (17), 6641-6644.
163. Luijten, J.; Groeneveld, D. Y.; Nijboer, G. W.; Vorenkamp, E. J.; Schouten, A. J., *Langmuir* **2007**, *23* (15), 8163-8169.
164. Lu, H.; Bai, Y.; Wang, J.; Gabrielson, N. P.; Wang, F.; Lin, Y.; Cheng, J., *Macromolecules* **2011**, *44* (16), 6237-6240.
165. Lu, H.; Wang, J.; Bai, Y.; Lang, J. W.; Liu, S.; Lin, Y.; Cheng, J., *Nat. Commun.* **2011**, *2*, 206.
166. Gabrielson, N. P.; Lu, H.; Yin, L.; Li, D.; Wang, F.; Cheng, J., *Angew. Chem. Int. Ed.* **2012**, *51* (5), 1143-1147.
167. Masato, N.; Hiroyoshi, K., *Bull. Chem. Soc. Jpn.* **1975**, *48* (9), 2588-2591.
168. Kadoma, Y.; Ueno, A.; Takeda, K.; Uno, K.; Iwakura, Y., *J. Polym. Sci., Part B: Polym. Lett.* **1974**, *12* (12), 715-718.
169. Yan, L.; Yang, L.; He, H.; Hu, X.; Xie, Z.; Huang, Y.; Jing, X., *Polym. Chem.* **2012**, *3* (5), 1300-1307.
170. Ueno, A.; Toda, F.; Iwakura, Y., *Chem. Lett.* **1974**, *3* (2), 97-100.
171. Ding, J.; Xiao, C.; Tang, Z.; Zhuang, X.; Chen, X., *Macromol. Biosci.* **2011**, *11* (2), 192-198.
172. Ding, J.; Xu, W.; Zhang, Y.; Sun, D.; Xiao, C.; Liu, D.; Zhu, X.; Chen, X., *J. Controlled Release* **2013**, *172* (2), 444-455.
173. Tang, H.; Zhang, D., *Biomacromolecules* **2010**, *11* (6), 1585-1592.
174. Tang, H.; Yin, L.; Kim, K. H.; Cheng, J., *Chem. Sci.* **2013**, *4* (10), 3839-3844.

175. Hu, Q.; Deng, Y.; Yuan, Q.; Ling, Y.; Tang, H., *J. Polym. Sci., Part A: Polym. Chem.* **2014**, *52* (2), 149-153.
176. Song, Z.; Zheng, N.; Ba, X.; Yin, L.; Zhang, R.; Ma, L.; Cheng, J., *Biomacromolecules* **2014**, *15* (4), 1491-1497.
177. Wu, Y.; Wang, X.; Ling, Y.; Tang, H., *RSC Advances* **2015**, *5* (51), 40772-40778.
178. Xiong, M.; Lee, M. W.; Mansbach, R. A.; Song, Z.; Bao, Y.; Peek, R. M.; Yao, C.; Chen, L.-F.; Ferguson, A. L.; Wong, G. C. L.; Cheng, J., *Proc. Natl. Acad. Sci. U. S. A.* **2015**, *112* (43), 13155-13160.
179. Deng, Y.; Xu, Y.; Wang, X.; Yuan, Q.; Ling, Y.; Tang, H., *Macromol. Rapid Commun.* **2015**, *36* (5), 453-458.
180. Ishikawa, K.; Endo, T., *J. Am. Chem. Soc.* **1988**, *110* (6), 2016-2017.
181. Dubruel, P.; Dekie, L.; Schacht, E., *Biomacromolecules* **2003**, *4* (5), 1168-1176.
182. Lu, D.; Wang, H.; Li, T. e.; Li, Y.; Dou, F.; Sun, S.; Guo, H.; Liao, S.; Yang, Z.; Wei, Q.; Lei, Z., *ACS Appl. Mater. Interfaces* **2017**, *9* (20), 16756-16766.
183. Xu, Q.; He, C.; Xiao, C.; Yu, S.; Chen, X., *Polym. Chem.* **2015**, *6* (10), 1758-1767.
184. Liu, Y.; Chen, P.; Li, Z., *Macromol. Rapid Commun.* **2012**, *33* (4), 287-295.
185. Rhodes, A. J.; Deming, T. J., *ACS Macro Lett.* **2013**, *2* (5), 351-354.
186. Tang, H.; Yin, L.; Lu, H.; Cheng, J., *Biomacromolecules* **2012**, *13* (9), 2609-2615.
187. Yakovlev, I.; Deming, T. J., *J. Am. Chem. Soc.* **2015**, *137* (12), 4078-4081.
188. Zhou, J.; Chen, P.; Deng, C.; Meng, F.; Cheng, R.; Zhong, Z., *Macromolecules* **2013**, *46* (17), 6723-6730.
189. Xiao, J.; Li, M.; Liu, W.; Li, Y.; Ling, Y.; Tang, H., *Eur. Polym. J.* **2017**, *88*, 340-348.
190. Schäfer, O.; Huesmann, D.; Muhl, C.; Barz, M., *Chem. - Eur. J.* **2016**, *22* (50), 18085-18091.
191. Schäfer, O.; Huesmann, D.; Barz, M., *Macromolecules* **2016**, *49* (21), 8146-8153.
192. Kramer, J. R.; Deming, T. J., *Biomacromolecules* **2012**, *13* (6), 1719-1723.
193. Gharakhanian, E. G.; Deming, T. J., *Biomacromolecules* **2015**, *16* (6), 1802-1806.
194. Kramer, J. R.; Deming, T. J., *Chem. Commun.* **2013**, *49* (45), 5144-5146.
195. Rodriguez, A. R.; Kramer, J. R.; Deming, T. J., *Biomacromolecules* **2013**, *14* (10), 3610-3614.
196. Yu, M.; Deming, T. J., *Macromolecules* **1998**, *31* (15), 4739-4745.
197. Fuller, W. D.; Verlander, M. S.; Goodman, M., *Biopolymers* **1978**, *17* (12), 2939-2943.
198. Sulistio, A.; Blencowe, A.; Wang, J.; Bryant, G.; Zhang, X.; Qiao, G. G., *Macromol. Biosci.* **2012**, *12* (9), 1220-1231.
199. Lu, D.; Wang, H.; Li, T. e.; Li, Y.; Wang, X.; Niu, P.; Guo, H.; Sun, S.; Wang, X.; Guan, X.; Ma, H.; Lei, Z., *Chem. Mater.* **2017**, *29* (13), 5493-5503.
200. Schlögl, K.; Fabitschowitz, H., *Monatsh. Chem. Verw. Teile Anderer Wiss.* **1954**, *85* (5), 1060-1076.
201. Sun, J.; Schlaad, H., *Macromolecules* **2010**, *43* (10), 4445-4448.
202. Krannig, K.-S.; Schlaad, H., *J. Am. Chem. Soc.* **2012**, *134* (45), 18542-18545.
203. Guinn, R. M.; Margot, A. O.; Taylor, J. R.; Schumacher, M.; Clark, D. S.; Blanch, H. W., *Biopolymers* **1995**, *35* (5), 503-512.
204. Schlögl, K.; Pelousek, H., *Monatsh. Chem. Verw. Teile Anderer Wiss.* **1960**, *91* (2), 227-237.
205. Huang, J.; Habraken, G.; Audouin, F.; Heise, A., *Macromolecules* **2010**, *43* (14), 6050-6057.
206. Huang, J.; Bonduelle, C.; Thévenot, J.; Lecommandoux, S.; Heise, A., *J. Am. Chem. Soc.* **2012**, *134* (1), 119-122.
207. Jacobs, J.; Gathergood, N.; Heuts, J. P. A.; Heise, A., *Polym. Chem.* **2015**, *6* (25), 4634-4640.
208. Robinson, J. W.; Schlaad, H., *Chem. Commun.* **2012**, *48* (63), 7835-7837.
209. Robinson, J. W.; Secker, C.; Weidner, S.; Schlaad, H., *Macromolecules* **2013**, *46* (3), 580-587.
210. Lahasky, S. H.; Serem, W. K.; Guo, L.; Garno, J. C.; Zhang, D., *Macromolecules* **2011**, *44* (23), 9063-9074.
211. Guo, L.; Lahasky, S. H.; Ghale, K.; Zhang, D., *J. Am. Chem. Soc.* **2012**, *134* (22), 9163-9171.
212. Secker, C.; Brosnan, S. M.; Limberg, F. R. P.; Braun, U.; Trunk, M.; Strauch, P.; Schlaad, H., *Macromol. Chem. Phys.* **2015**, *216* (21), 2080-2085.
213. Haberthür, U.; Elias, H.-G., *Makromol. Chem.* **1971**, *144* (1), 193-212.
214. Nadeau, V.; Leclair, G.; Sant, S.; Rabanel, J.-M.; Quesnel, R.; Hildgen, P., *Polymer* **2005**, *46* (25), 11263-11272.

215. Fonseca, A. C.; Gil, M. H.; Simões, P. N., *Prog. Polym. Sci.* **2014**, *39* (7), 1291-1311.
216. Franz, N.; Klok, H.-A., *Macromol. Chem. Phys.* **2010**, *211* (7), 809-820.
217. Taherimehr, M.; Pescarmona, P. P., *J. Appl. Polym. Sci.* **2014**, *131* (21), n/a-n/a.
218. Rokicki, G., *Prog. Polym. Sci.* **2000**, *25* (2), 259-342.
219. Ding, L.; Li, Y.; Li, Y.; Liang, Y.; Huang, J., *Eur. Polym. J.* **2001**, *37* (12), 2453-2459.
220. Webster, D. C.; Crain, A. L., Synthesis of Cyclic Carbonate Functional Polymers. In *Functional Polymers*, 1998; Vol. 704, pp 303-320.
221. Pratt, R. C.; Nederberg, F.; Waymouth, R. M.; Hedrick, J. L., *Chem. Commun.* **2008**, (1), 114-116.
222. Sanders, D. P.; Fukushima, K.; Coady, D. J.; Nelson, A.; Fujiwara, M.; Yasumoto, M.; Hedrick, J. L., *J. Am. Chem. Soc.* **2010**, *132* (42), 14724-14726.
223. Chan, J. M. W.; Sardon, H.; Engler, A. C.; García, J. M.; Hedrick, J. L., *ACS Macro Lett.* **2013**, *2* (10), 860-864.
224. Olsson, J. V.; Hult, D.; Cai, Y.; Garcia-Gallego, S.; Malkoch, M., *Polym. Chem.* **2014**, *5* (23), 6651-6655.
225. Liu, G.; He, F.; Wang, Y. P.; Feng, J.; Zhuo, R. X., *Chin. Chem. Lett.* **2006**, *17* (1), 137-139.
226. Venkataraman, S.; Veronica, N.; Voo, Z. X.; Hedrick, J. L.; Yang, Y. Y., *Polym. Chem.* **2013**, *4* (10), 2945-2948.
227. He, F.; Wang, Y.-P.; Liu, G.; Jia, H.-L.; Feng, J.; Zhuo, R.-X., *Polymer* **2008**, *49* (5), 1185-1190.
228. Jiang, T.; Li, Y.-M.; Lv, Y.; Cheng, Y.-J.; He, F.; Zhuo, R.-X., *Colloids Surf., B* **2013**, *111*, 542-548.
229. Parzuchowski, P. G.; Jaroch, M.; Tryznowski, M.; Rokicki, G., *Macromolecules* **2008**, *41* (11), 3859-3865.
230. Jiang, T.; Li, Y.; Lv, Y.; Cheng, Y.; He, F.; Zhuo, R., *J. Mater. Sci.: Mater. Med.* **2014**, *25* (1), 131-139.
231. Zhang, X.; Wang, H.; Dai, Y., *Mater. Lett.* **2017**, *198*, 144-147.
232. Lu, C.; Shi, Q.; Chen, X.; Lu, T.; Xie, Z.; Hu, X.; Ma, J.; Jing, X., *J. Polym. Sci., Part A: Polym. Chem.* **2007**, *45* (15), 3204-3217.
233. Shi, Q.; Chen, X.; Lu, T.; Jing, X., *Biomaterials* **2008**, *29* (8), 1118-1126.
234. Shi, Q.; Huang, Y.; Chen, X.; Wu, M.; Sun, J.; Jing, X., *Biomaterials* **2009**, *30* (28), 5077-5085.
235. Hu, D.; Peng, H.; Niu, Y.; Li, Y.; Xia, Y.; Li, L.; He, J.; Liu, X.; Xia, X.; Lu, Y.; Xu, W., *J. Polym. Sci., Part A: Polym. Chem.* **2015**, *53* (6), 750-760.
236. Tempelaar, S.; Barker, I. A.; Truong, V. X.; Hall, D. J.; Mespouille, L.; Dubois, P.; Dove, A. P., *Polym. Chem.* **2013**, *4* (1), 174-183.
237. Xiong, H.; Zhou, D.; Qi, Y.; Zhang, Z.; Xie, Z.; Chen, X.; Jing, X.; Meng, F.; Huang, Y., *Biomacromolecules* **2015**, *16* (12), 3980-3988.
238. Xiong, H.; Wei, X.; Zhou, D.; Qi, Y.; Xie, Z.; Chen, X.; Jing, X.; Huang, Y., *Bioconjugate Chem.* **2016**, *27* (9), 2214-2223.
239. Mullen, B. D.; Tang, C. N.; Storey, R. F., *J. Polym. Sci., Part A: Polym. Chem.* **2003**, *41* (13), 1978-1991.
240. Wang, C.-F.; Lin, Y.-X.; Jiang, T.; He, F.; Zhuo, R.-X., *Biomaterials* **2009**, *30* (27), 4824-4832.
241. Stevens, D. M.; Tempelaar, S.; Dove, A. P.; Harth, E., *ACS Macro Lett.* **2012**, *1* (7), 915-918.
242. Hu, X.; Chen, X.; Liu, S.; Shi, Q.; Jing, X., *J. Polym. Sci., Part A: Polym. Chem.* **2008**, *46* (5), 1852-1861.
243. Kuang, H.; Wu, S.; Xie, Z.; Meng, F.; Jing, X.; Huang, Y., *Biomacromolecules* **2012**, *13* (9), 3004-3012.
244. Kuang, H.; Wu, S.; Meng, F.; Xie, Z.; Jing, X.; Huang, Y., *J. Mater. Chem.* **2012**, *22* (47), 24832-24840.
245. Truong, V. X.; Barker, I. A.; Tan, M.; Mespouille, L.; Dubois, P.; Dove, A. P., *J. Mater. Chem. B* **2013**, *1* (2), 221-229.
246. Barker, I. A.; Ablett, M. P.; Gilbert, H. T. J.; Leigh, S. J.; Covington, J. A.; Hoyland, J. A.; Richardson, S. M.; Dove, A. P., *Biomater. Sci.* **2014**, *2* (4), 472-475.
247. Olofsson, K.; Malkoch, M.; Hult, A., *J. Polym. Sci., Part A: Polym. Chem.* **2016**, *54* (15), 2370-2378.
248. Heo, G. S.; Cho, S.; Wooley, K. L., *Polym. Chem.* **2014**, *5* (11), 3555-3558.

249. Chen, W.; Yang, H.; Wang, R.; Cheng, R.; Meng, F.; Wei, W.; Zhong, Z., *Macromolecules* **2010**, *43* (1), 201-207.
250. Xiong, J.; Meng, F.; Wang, C.; Cheng, R.; Liu, Z.; Zhong, Z., *J. Mater. Chem.* **2011**, *21* (15), 5786-5794.
251. Chen, F.; Hayami, J. W. S.; Amsden, B. G., *Biomacromolecules* **2014**, *15* (5), 1593-1601.
252. Sanders, D. P.; Coady, D. J.; Yasumoto, M.; Fujiwara, M.; Sardon, H.; Hedrick, J. L., *Polym. Chem.* **2014**, *5* (2), 327-329.
253. Hu, X.; Chen, X.; Cheng, H.; Jing, X., *J. Polym. Sci., Part A: Polym. Chem.* **2009**, *47* (1), 161-169.
254. Wang, R.; Chen, W.; Meng, F.; Cheng, R.; Deng, C.; Feijen, J.; Zhong, Z., *Macromolecules* **2011**, *44* (15), 6009-6016.
255. Mindemark, J.; Bowden, T., *Polymer* **2011**, *52* (25), 5716-5722.
256. Mindemark, J.; Bowden, T., *Polym. Chem.* **2012**, *3* (6), 1399-1401.
257. Ong, Z. Y.; Fukushima, K.; Coady, D. J.; Yang, Y.-Y.; Ee, P. L. R.; Hedrick, J. L., *J. Controlled Release* **2011**, *152* (1), 120-126.
258. Ding, X.; Yang, C.; Lim, T. P.; Hsu, L. Y.; Engler, A. C.; Hedrick, J. L.; Yang, Y.-Y., *Biomaterials* **2012**, *33* (28), 6593-6603.
259. Nederberg, F.; Zhang, Y.; Tan, J. P. K.; Xu, K.; Wang, H.; Yang, C.; Gao, S.; Guo, X. D.; Fukushima, K.; Li, L.; Hedrick, J. L.; Yang, Y.-Y., *Nat. Chem.* **2011**, *3* (5), 409-414.
260. Ong, Z. Y.; Yang, C.; Gao, S. J.; Ke, X.-Y.; Hedrick, J. L.; Yan Yang, Y., *Macromol. Rapid Commun.* **2013**, *34* (21), 1714-1720.
261. Ng, V. W. L.; Tan, J. P. K.; Leong, J.; Voo, Z. X.; Hedrick, J. L.; Yang, Y. Y., *Macromolecules* **2014**, *47* (4), 1285-1291.
262. Engler, A. C.; Tan, J. P. K.; Ong, Z. Y.; Coady, D. J.; Ng, V. W. L.; Yang, Y. Y.; Hedrick, J. L., *Biomacromolecules* **2013**, *14* (12), 4331-4339.
263. Ng, V. W. L.; Ke, X.; Lee, A. L. Z.; Hedrick, J. L.; Yang, Y. Y., *Adv. Mater.* **2013**, *25* (46), 6730-6736.
264. Chin, W.; Yang, C.; Ng, V. W. L.; Huang, Y.; Cheng, J.; Tong, Y. W.; Coady, D. J.; Fan, W.; Hedrick, J. L.; Yang, Y. Y., *Macromolecules* **2013**, *46* (22), 8797-8807.
265. Ono, R. J.; Liu, S. Q.; Venkataraman, S.; Chin, W.; Yang, Y. Y.; Hedrick, J. L., *Macromolecules* **2014**, *47* (22), 7725-7731.
266. Park, N. H.; Voo, Z. X.; Yang, Y. Y.; Hedrick, J. L., *ACS Macro Lett.* **2017**, *6* (3), 252-256.
267. Engler, A. C.; Chan, J. M. W.; Coady, D. J.; O'Brien, J. M.; Sardon, H.; Nelson, A.; Sanders, D. P.; Yang, Y. Y.; Hedrick, J. L., *Macromolecules* **2013**, *46* (4), 1283-1290.
268. Chan, J. M. W.; Ke, X.; Sardon, H.; Engler, A. C.; Yang, Y. Y.; Hedrick, J. L., *Chem. Sci.* **2014**, (5), 3294-3300.
269. Engler, A. C.; Ke, X.; Gao, S.; Chan, J. M. W.; Coady, D. J.; Ono, R. J.; Lubbers, R.; Nelson, A.; Yang, Y. Y.; Hedrick, J. L., *Macromolecules* **2015**, *48* (6), 1673-1678.
270. Chan, J. M. W.; Wojtecki, R. J.; Sardon, H.; Lee, A. L. Z.; Smith, C. E.; Shkumatov, A.; Gao, S.; Kong, H.; Yang, Y. Y.; Hedrick, J. L., *ACS Macro Lett.* **2017**, *6* (2), 176-180.
271. Zhou, Y.; Zhuo, R.-X.; Liu, Z.-L., *Macromol. Rapid Commun.* **2005**, *26* (16), 1309-1314.
272. Park, N. H.; Fevre, M.; Voo, Z. X.; Ono, R. J.; Yang, Y. Y.; Hedrick, J. L., *ACS Macro Lett.* **2016**, *5* (11), 1247-1252.
273. Chen, W.; Zou, Y.; Jia, J.; Meng, F.; Cheng, R.; Deng, C.; Feijen, J.; Zhong, Z., *Macromolecules* **2013**, *46* (3), 699-707.
274. Chen, W.; Zou, Y.; Meng, F.; Cheng, R.; Deng, C.; Feijen, J.; Zhong, Z., *Biomacromolecules* **2014**, *15* (3), 900-907.
275. Barcan, G. A.; Zhang, X.; Waymouth, R. M., *J. Am. Chem. Soc.* **2015**, *137* (17), 5650-5653.
276. Zhang, X.; Waymouth, R. M., *J. Am. Chem. Soc.* **2017**, *139* (10), 3822-3833.
277. Mespouille, L.; Nederberg, F.; Hedrick, J. L.; Dubois, P., *Macromolecules* **2009**, *42* (16), 6319-6321.
278. Williams, R. J.; O'Reilly, R. K.; Dove, A. P., *Polym. Chem.* **2012**, *3* (8), 2156-2164.
279. Dag, A.; Aydin, M.; Durmaz, H.; Hizal, G.; Tunca, U., *J. Polym. Sci., Part A: Polym. Chem.* **2012**, *50* (21), 4476-4483.
280. Thongsomboon, W.; Sherwood, M.; Arellano, N.; Nelson, A., *ACS Macro Lett.* **2013**, *2* (1), 19-22.

281. Williams, R. J.; Barker, I. A.; O'Reilly, R. K.; Dove, A. P., *ACS Macro Lett.* **2012**, *1* (11), 1285-1290.
282. Kühling, S.; Keul, H.; Höcker, H., *Makromol. Chem.* **1990**, *191* (7), 1611-1622.
283. Mindemark, J.; Imholt, L.; Montero, J.; Brandell, D., *J. Polym. Sci., Part A: Polym. Chem.* **2016**, *54* (14), 2128-2135.
284. Thomas, A. W.; Kuroishi, P. K.; Perez-Madriral, M. M.; Whittaker, A. K.; Dove, A. P., *Polym. Chem.* **2017**.
285. Kuroishi, P. K.; Bennison, M. J.; Dove, A. P., *Polym. Chem.* **2016**, *7* (46), 7108-7115.
286. Miyagawa, T.; Shimizu, M.; Sanda, F.; Endo, T., *Macromolecules* **2005**, *38* (19), 7944-7949.
287. Zhang, Q. J.; Zhu, W. P.; Shen, Z. Q., *Chin. Chem. Lett.* **2010**, *21* (10), 1255-1258.
288. Zhu, W.; Wang, Y.; Sun, S.; Zhang, Q.; Li, X.; Shen, Z., *J. Mater. Chem.* **2012**, *22* (23), 11785-11791.
289. Zhu, W.; Wang, Y.; Zhang, Q.; Shen, Z., *J. Polym. Sci., Part A: Polym. Chem.* **2011**, *49* (22), 4886-4893.
290. Zhu, W.; Wang, Y.; Cai, X.; Zha, G.; Luo, Q.; Sun, R.; Li, X.; Shen, Z., *J. Mater. Chem. B* **2015**, *3* (15), 3024-3031.
291. Zhang, X.; Zhong, Z.; Zhuo, R., *Macromolecules* **2011**, *44* (7), 1755-1759.
292. Zhang, X.; Dong, H.; Fu, S.; Zhong, Z.; Zhuo, R., *Macromol. Rapid Commun.* **2016**, *37* (12), 993-997.
293. Xu, J.; Filion, T. M.; Prifti, F.; Song, J., *Chem. - Asian J.* **2011**, *6* (10), 2730-2737.
294. Zou, Y.; Fang, Y.; Meng, H.; Meng, F.; Deng, C.; Zhang, J.; Zhong, Z., *J. Controlled Release* **2016**, *244*, 326-335.
295. Chen, X.; McCarthy, S. P.; Gross, R. A., *Macromolecules* **1997**, *30* (12), 3470-3476.
296. Chen, X.; McCarthy, S. P.; Gross, R. A., *Macromolecules* **1998**, *31* (3), 662-668.
297. Steinbach, T.; Wurm, F. R., *Angew. Chem. Int. Ed.* **2015**, *54* (21), 6098-6108.
298. Bauer, K. N.; Tee, H. T.; Velencoso, M. M.; Wurm, F. R., *Prog. Polym. Sci.* **2017**, *73*, 61-122.
299. Becker, G.; Wurm, F. R., *Tetrahedron* **2017**, *73* (25), 3536-3540.
300. Clément, B.; Grignard, B.; Koole, L.; Jérôme, C.; Lecomte, P., *Macromolecules* **2012**, *45* (11), 4476-4486.
301. Wang, Y.-C.; Yuan, Y.-Y.; Wang, F.; Wang, J., *J. Polym. Sci., Part A: Polym. Chem.* **2011**, *49* (2), 487-494.
302. Zhang, S.; Li, A.; Zou, J.; Lin, L. Y.; Wooley, K. L., *ACS Macro Lett.* **2012**, *1* (2), 328-333.
303. Zhang, S.; Zou, J.; Zhang, F.; Elsabahy, M.; Felder, S. E.; Zhu, J.; Pochan, D. J.; Wooley, K. L., *J. Am. Chem. Soc.* **2012**, *134* (44), 18467-18474.
304. Lim, Y. H.; Heo, G. S.; Cho, S.; Wooley, K. L., *ACS Macro Lett.* **2013**, *2* (9), 785-789.
305. Gustafson, T. P.; Lim, Y. H.; Flores, J. A.; Heo, G. S.; Zhang, F.; Zhang, S.; Samarajeewa, S.; Raymond, J. E.; Wooley, K. L., *Langmuir* **2014**, *30* (2), 631-641.
306. Zhang, F.; Zhang, S.; Pollack, S. F.; Li, R.; Gonzalez, A. M.; Fan, J.; Zou, J.; Leininger, S. E.; Pavía-Sanders, A.; Johnson, R.; Nelson, L. D.; Raymond, J. E.; Elsabahy, M.; Hughes, D. M. P.; Lenox, M. W.; Gustafson, T. P.; Wooley, K. L., *J. Am. Chem. Soc.* **2015**, *137* (5), 2056-2066.
307. Zhang, S.; Zou, J.; Elsabahy, M.; Karwa, A.; Li, A.; Moore, D. A.; Dorshow, R. B.; Wooley, K. L., *Chem. Sci.* **2013**, *4* (5), 2122-2126.
308. Lim, Y. H.; Tiemann, K. M.; Heo, G. S.; Wagers, P. O.; Rezenom, Y. H.; Zhang, S.; Zhang, F.; Youngs, W. J.; Hunstad, D. A.; Wooley, K. L., *ACS Nano* **2015**, *9* (2), 1995-2008.
309. Aweda, T. A.; Zhang, S.; Mupanomunda, C.; Burkemper, J.; Heo, G. S.; Bandara, N.; Lin, M.; Cutler, C. S.; Cannon, C. L.; Youngs, W. J.; Wooley, K. L.; Lapi, S. E., *J. Labelled Compd. Radiopharm.* **2015**, *58* (6), 234-241.
310. Zeynep, E. Y.; Antoine, D.; Brice, C.; Frank, B.; Christine, J., *J. Mater. Chem. B* **2015**, *3* (36), 7227-7236.
311. Ergul Yilmaz, Z.; Cordonnier, T.; Debuigne, A.; Calvignac, B.; Jerome, C.; Boury, F., *Int. J. Pharm.* **2016**, *513* (1), 130-137.
312. Du, J.-Z.; Du, X.-J.; Mao, C.-Q.; Wang, J., *J. Am. Chem. Soc.* **2011**, *133* (44), 17560-17563.
313. Yang, X.-Z.; Du, J.-Z.; Dou, S.; Mao, C.-Q.; Long, H.-Y.; Wang, J., *ACS Nano* **2012**, *6* (1), 771-781.
314. Clément, B.; Molin, D. G.; Jérôme, C.; Lecomte, P., *J. Polym. Sci., Part A: Polym. Chem.* **2015**, *53* (22), 2642-2648.

315. Zou, J.; Zhang, F.; Zhang, S.; Pollack, S. F.; Elsabahy, M.; Fan, J.; Wooley, K. L., *Adv. Healthcare Mater.* **2014**, *3* (3), 441-448.
316. Baeten, E.; Vanslambrouck, S.; Jérôme, C.; Lecomte, P.; Junkers, T., *Eur. Polym. J.* **2016**, *80*, 208-218.
317. Lim, Y. H.; Heo, G. S.; Rezenom, Y. H.; Pollack, S.; Raymond, J. E.; Elsabahy, M.; Wooley, K. L., *Macromolecules* **2014**, *47* (14), 4634-4644.
318. Shao, H.; Zhang, M.; He, J.; Ni, P., *Polymer* **2012**, *53* (14), 2854-2863.
319. Iwasaki, Y.; Komatsu, S.; Narita, T.; Akiyoshi, K.; Ishihara, K., *Macromol. Biosci.* **2003**, *3* (5), 238-242.
320. Iwasaki, Y.; Nakagawa, C.; Ohtomi, M.; Ishihara, K.; Akiyoshi, K., *Biomacromolecules* **2004**, *5* (3), 1110-1115.
321. Wachiralarpphaithoon, C.; Iwasaki, Y.; Akiyoshi, K., *Biomaterials* **2007**, *28* (6), 984-993.
322. Du, J.-Z.; Sun, T.-M.; Weng, S.-Q.; Chen, X.-S.; Wang, J., *Biomacromolecules* **2007**, *8* (11), 3375-3381.
323. Iwasaki, Y.; Akiyoshi, K., *Macromolecules* **2004**, *37* (20), 7637-7642.
324. Iwasaki, Y.; Akiyoshi, K., *Biomacromolecules* **2006**, *7* (5), 1433-1438.
325. Lapienis, G.; Penczek, S., *Macromolecules* **1977**, *10* (6), 1301-1306.
326. Biela, T.; Penczek, S.; Slomkowski, S.; Vogl, O., *Makromol. Chem., Rapid Commun.* **1982**, *3* (10), 667-671.
327. Brosse, J.-C.; Derouet, D.; Fontaine, L.; Chairatanathavorn, S., *Makromol. Chem.* **1989**, *190* (9), 2339-2345.
328. Wang, J.; Zhang, P.-C.; Lu, H.-F.; Ma, N.; Wang, S.; Mao, H.-Q.; Leong, K. W., *J. Controlled Release* **2002**, *83* (1), 157-168.
329. Wang, J.; Mao, H.-Q.; Leong, K. W., *J. Am. Chem. Soc.* **2001**, *123* (38), 9480-9481.
330. Huang, S.-W.; Wang, J.; Zhang, P.-C.; Mao, H.-Q.; Zhuo, R.-X.; Leong, K. W., *Biomacromolecules* **2004**, *5* (2), 306-311.
331. Wang, J.; P.-C., Z.; Mao, H.-Q.; Leong, K. W., *Gene Ther.* **2002**, *9* (18), 1254-1261.
332. Zhang, P.-C.; Wang, J.; Leong, K. W.; Mao, H.-Q., *Biomacromolecules* **2005**, *6* (1), 54-60.
333. Jiang, X.; Qu, W.; Pan, D.; Ren, Y.; Williford, J.-M.; Cui, H.; Luijten, E.; Mao, H.-Q., *Adv. Mater.* **2013**, *25* (2), 227-232.
334. Oswald, A. A., *Can. J. Chem.* **1959**, *37* (9), 1498-1504.
335. Kaluzynski, K.; Libisowski, J.; Penczek, S., *Macromolecules* **1976**, *9* (2), 365-367.
336. Pretula, J.; Kaluzynski, K.; Penczek, S., *Macromolecules* **1986**, *19* (7), 1797-1799.
337. Łapienis, G.; Penczek, S.; Aleksyuk, G. P.; Kropachev, V. A., *J. Polym. Sci., Part A: Polym. Chem.* **1987**, *25* (7), 1729-1736.
338. Łapienis, G.; Penczek, S., *J. Polym. Sci., Part A: Polym. Chem.* **1990**, *28* (6), 1519-1526.
339. Kuznetsova, O.; Kaluzynski, K.; Lapienis, G.; Pretula, J.; Penczek, S., *J. Bioact. Compat. Polym.* **1999**, 232-242.
340. Wolf, T.; Rheinberger, T.; Wurm, F. R., *Eur. Polym. J.* **2017**, <https://doi.org/10.1016/j.eurpolymj.2017.05.048>.
341. Wolf, T.; Steinbach, T.; Wurm, F. R., *Macromolecules* **2015**, *48* (12), 3853-3863.
342. Steinbach, T.; Ritz, S.; Wurm, F. R., *ACS Macro Lett.* **2014**, *3* (3), 244-248.
343. Teasdale, I.; Brüggemann, O., *Polymers* **2013**, *5* (1), 161-187.
344. Gleria, M.; De Jaeger, R., Polyphosphazenes: A Review. In *New Aspects in Phosphorus Chemistry*, Majoral, J.-P., Ed. Springer Berlin Heidelberg: Berlin, Heidelberg, 2005; pp 165-251.
345. Allcock, H. R.; Coley, S. M.; Manners, I.; Nuyken, O.; Renner, G., *Macromolecules* **1991**, *24* (8), 2024-2028.
346. Dodge, J. A.; Manners, I.; Allcock, H. R.; Renner, G.; Nuyken, O., *J. Am. Chem. Soc.* **1990**, *112* (3), 1268-1269.
347. Manners, I.; Allcock, H. R.; Renner, G.; Nuyken, O., *J. Am. Chem. Soc.* **1989**, *111* (14), 5478-5480.
348. Allcock, H. R.; Coley, S. M.; Morrissey, C. T., *Macromolecules* **1994**, *27* (11), 2904-2911.
349. Liang, M.; Manners, I., *J. Am. Chem. Soc.* **1991**, *113* (10), 4044-4045.

350. Ni, Y.; Stammer, A.; Liang, M.; Massey, J.; Vancso, G. J.; Manners, I., *Macromolecules* **1992**, *25* (26), 7119-7125.
351. Herzberger, J.; Niederer, K.; Pohlitz, H.; Seiwert, J.; Worm, M.; Wurm, F. R.; Frey, H., *Chem. Rev.* **2016**, *116* (4), 2170-2243.
352. Winnacker, M.; Rieger, B., *Polym. Chem.* **2016**, *7* (46), 7039-7046.
353. Maisonneuve, L.; Lamarzelle, O.; Rix, E.; Grau, E.; Cramail, H., *Chem. Rev.* **2015**, *115* (22), 12407-12439.
354. Espeel, P.; Du Prez, F. E., *Eur. Polym. J.* **2015**, *62*, 247-272.

## 2. Joining two natural motifs: Catechol-containing poly(phosphoester)s

Greta Becker,<sup>1,2</sup> Lisa-Maria Ackermann,<sup>1</sup> Eugen Schechtel,<sup>2,3</sup> Markus Klapper,<sup>1</sup> Wolfgang Tremel,<sup>3</sup> Frederik R. Wurm<sup>1</sup>

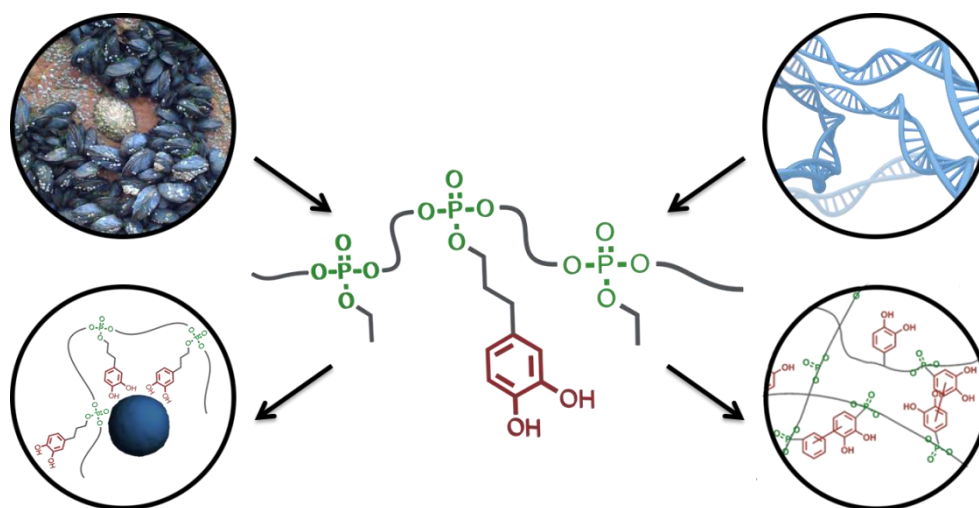
<sup>1</sup>Max Planck Institute for Polymer Research, Ackermannweg 10, 55128 Mainz, Germany

<sup>2</sup>Graduate School Materials Science in Mainz, Staudinger Weg 9, 55128 Mainz, Germany

<sup>3</sup>Johannes Gutenberg-University Mainz, Institute of Inorganic Chemistry and Analytical Chemistry, Duesbergweg 10-14, 55128 Mainz, Germany

Reproduced with permission from "Biomacromolecules, **2017**, 18 (3), 767-777". Copyright 2017 American Chemical Society.

Magnetite nanoparticles were synthesized and characterized by Eugen Schechtel. ITC measurements were performed and evaluated by Lisa-Maria Ackermann.



**Keywords:** poly(phosphoester), catechol, mussel-inspired, biodegradable, degradation, hydrogel, surface functionalization, adhesive groups.

## 2.1 Abstract

Numerous catechol-containing polymers, including biodegradable polymers, are currently heavily discussed for modern biomaterials. However, there is no report combining poly(phosphoester)s (PPEs) with catechols. Adhesive PPEs have been prepared via acyclic diene metathesis polymerization. A novel acetal-protected catechol phosphate monomer was homo- and copolymerized with phosphoester comonomers with molecular weights up to 42,000 g/mol. Quantitative release of the catechols was achieved by careful hydrolysis of the acetal groups without backbone degradation. Degradation of the PPEs under basic conditions revealed complete and statistical degradation of the phosphotri- to phosphodiester. In addition, a phosphodiester monomer with an adhesive P-OH group and no protective group chemistry was used to compare the binding to metal oxides with the multicatechol PPEs. All PPEs can stabilize magnetite particles in polar solvents, e.g. methanol, due to the binding of the phosphoester groups in the backbone to the particles (NPs). ITC measurements reveal that multicatechol PPEs exhibit a higher binding affinity to magnetite NPs compared to PPEs bearing phosphodi- or phosphotriesters as repeating units. In addition, the catechol-containing PPEs were used to generate organo- and hydrogels by oxidative cross-linking, due to cohesive properties of catechol groups. This unique combination of two natural adhesive motives, catechols and phosphates, will allow the design of novel future gels for tissue engineering applications or novel degradable adhesives.

## 2.2 Introduction

The catechol (1,2-dihydroxybenzene) motif<sup>1-2</sup> is a bioadhesive that is found in the mussel foot proteins of marine mussels.<sup>3-4</sup> The catechol group was used in many “mussel-inspired” synthetic materials to date, but never combined with the versatile class of also adhesive poly(phosphoester)s (PPEs).

Catechols can act as chelators or bind covalently to nearly all surfaces and are especially useful for gluing under humid conditions.<sup>4</sup> In biomimetic materials, catechols exhibit both adhesive and cohesive features; their adhesive properties are strong and reversible relying on the bidentate binding of the OH-groups to metal oxides or ions with a high binding affinity ( $k_s > 10^{40}$ ).<sup>5</sup> In alkaline solution, auto-oxidation or oxidants generate quinones which cross-link in the presence of many nucleophiles or with other catechols (Figure 2.1).<sup>6</sup> This is an attractive strategy for the preparation of catechol-containing synthetic polymers or hydrogels for tissue engineering.<sup>7-8</sup> While Messersmith and colleagues<sup>9</sup> introduced PEG star polymers, functionalized with DOPA for the formation of hydrogels, del Campo et al.<sup>10</sup> intensively studied cross-linking kinetics of these PEG-stars

end-functionalized with catecholamines with varying substituents. Frey and co-workers<sup>11</sup> prepared multicatechol containing PEGs by the copolymerization of ethylene oxide with catechol acetonide glycidyl ether. The catechol functionality can serve either as main chain, side chain, or end chain precursor in antifouling<sup>12</sup> or adhesive<sup>13</sup> surface coatings, for colloid stabilization (where a catechol unit serves as anchor group)<sup>14</sup> and as hydrogels for self-healing materials<sup>15</sup> or biomedical applications under physiological conditions as soft tissue adhesive.<sup>16</sup>

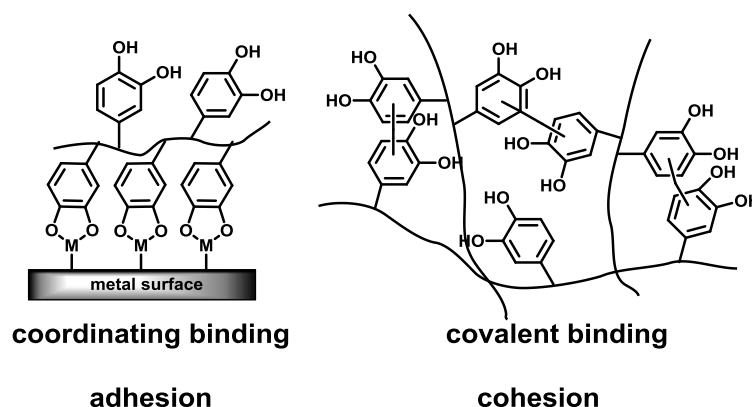


**Figure 2.1.** Catechols can bind by coordinative or covalent linkages and exhibit adhesion or cohesion.

The combination of the catechol motif with biodegradable synthetic polymers is an attractive strategy for the generation of degradable hydrogels or for biomedical imaging based on metal oxide nanoparticles. To date, catechol-containing biodegradable hydrogels based on poly(diols citrate),<sup>17</sup> poly(ester urea)s,<sup>18</sup> poly(lactide),<sup>19</sup> and poly(amino ester)s<sup>20-21</sup> have been reported.

Inspired by natural poly(phosphoester)s like desoxyribose nucleic acid (DNA), synthetic PPEs are a versatile class of polymers. Initially designed in the middle of last century, they find currently an increased attention as potential materials for biomedical applications<sup>22-23</sup> or as flame retardant additives. Today, several research groups<sup>24-27</sup> focus on PPEs mainly as materials in biomedical applications. PPEs are a unique class of polymers: (i) the number of methylene groups in the backbone can be varied in a way that the obtained polymers range from hydrophobic to hydrophilic materials; (ii) the pentavalency of phosphorus in the backbone allows a high flexibility of the side chains in every repeat unit. Additionally, the phosphorus linkage itself can be varied leading to poly(phosphate)s, poly(phosphonate)s,<sup>28-29</sup> or poly(phosphoramidate)s<sup>30-31</sup> with various properties. Finally, established protocols for a high number of different polymerization techniques including traditional polycondensation<sup>32</sup> and -addition,<sup>33</sup> ring-opening polymerization,<sup>34-35</sup> as well as ring-opening metathesis (ROMP)<sup>36</sup> and acyclic diene metathesis polymerization (ADMET)<sup>37-38</sup> are available today.

Herein, we present the first PPEs carrying catechol functionalities in their pendant chains. In addition, we compare the adhesive properties of such catechol-modified PPEs with P-OH-functional poly(phosphodiester)s (Scheme 2.1). PPEs are typically biocompatible, nontoxic, and biodegradable.<sup>23</sup> PPEs with both adhesive groups can efficiently bind to magnetite nanoparticles and this functionalization enhances their stability in polar solvents, for example, ethanol or methanol (dispersions were colloidal stable over at least seven months). While PPEs with a pendant P-OH-group lack the ability of network formation, catechol-containing PPEs can be irreversibly and covalently cross-linked after addition of an oxidant.

## 2.3 Experimental Section

**Materials.** All reagents were used without further purification, unless otherwise stated. Solvents, dry solvents (over molecular sieves) and deuterated solvents were purchased from Acros Organics, Sigma-Aldrich, Deutero GmbH or Fluka. 3,4-Dihydroxyhydrocinnamic acid, 3-buten-1-ol, HCl (37%), tris(hydroxymethyl)phosphine (90%), sodium oleate (82%), trioctylamine (98%), oleic acid (90%), trifluoroacetic acid, Na<sub>2</sub>CO<sub>3</sub>, and MgSO<sub>4</sub> were purchased from Sigma-Aldrich. Iron(III) chloride hexahydrate (97%) was obtained from abcr GmbH. Calcium(II) chloride hexahydrate was purchased from Fisher Scientific. *p*-Toluenesulfonic acid monohydrate, 2,2-dimethoxypropane, LiAlH<sub>4</sub> (2.4 M in THF), POCl<sub>3</sub> (phosphoryl chloride, 99%), 1-chloronaphthalene and aluminum oxide (neutral, for chromatography) were purchased from Acros Organics. Triethylamine (Et<sub>3</sub>N, 99.5%) was purchased from Roth, dried with CaH<sub>2</sub>, distilled, and stored over molecular sieve.

**Instrumentation and Characterization Techniques.** For the poly(phosphoester)s, size exclusion chromatography (SEC) measurements were performed in THF with a PSS SecCurity system (Agilent Technologies 1260 Infinity). Sample injection was performed by a 1260-ALS autosampler (Waters) at 30 °C. SDV columns (PSS) with dimensions of 300 × 80 mm, 10 μm particle size, and pore sizes of 106, 104, and 500 Å were employed. The DRI Shodex RI-101 detector (ERC) and UV-vis 1260-VWD detector (Agilent) were used for detection. Calibration was achieved using PS or PMMA standards provided by Polymer Standards Service. For SEC measurements in DMF (containing 0.25 g/L of lithium bromide as an additive) an Agilent 1100 Series was used as an integrated instrument, including a PSS GRAM columns (1000/1000/100 g), a UV detector (270 nm), and a RI detector at a flow rate of 1 mL/min at 60 °C. Calibration was carried out using PS or PMMA standards provided by Polymer Standards Service. For nuclear magnetic resonance analysis <sup>1</sup>H, <sup>13</sup>C, and <sup>31</sup>P NMR spectra were recorded on a Bruker AVANCE III 300, 500, or 700 MHz spectrometer. All spectra were measured in either DMSO-*d*<sub>6</sub> or CDCl<sub>3</sub> at 298 K. The spectra were calibrated against the solvent signal and analyzed using MestReNova 8 from Mestrelab Research S.L. The thermal

properties of the synthesized polymers have been measured by differential scanning calorimetry (DSC) on a Mettler Toledo DSC 823 calorimeter. Three scanning cycles of heating-cooling were performed in a N<sub>2</sub> atmosphere (30 mL/min) with a heating and cooling rate of 10 °C/min. Samples for transmission electron microscopy (TEM) were prepared by placing one drop of a dilute solution in hexane or chloroform onto a carbon-coated copper grid, dried at room temperature. TEM images were acquired on a FEI Tecnai T12 microscope operating at 120 kV (LaB<sub>6</sub> filament) or a FEI Tecnai F20 microscope operating at 200 kV. The average size of the blank nanoparticles was measured by image analysis of TEM images for 50 particles. All nanoparticles were analyzed by means of dynamic light scattering (DLS) on an ALV spectrometer consisting of a ALV/CGS3 compact goniometer and an ALV/LSE-5004 multiple-tau full-digital correlator (320 channels), which allows measurements over an angular range from 20° to 150°. A He-Ne laser operating at a laser wavelength of 632.8 nm was used as light source. Diluted dispersions in chloroform were filtered through PTFE membrane filters with a pore size of 5 μm (Millex LS syringe filters). Measurements were performed at 20°C at nine angles ranging from 30° to 150° and analyzed with ALV5000 software program. FT-IR spectra were recorded using a Thermo Scientific iS10 FT-IR spectrometer, equipped with a diamond ATR unit. Isothermal Titration Calorimetry (ITC) measurements were performed using a Microcal VP-ITC titration microcalorimeter (MicroCal, Inc., Northhampton, MA) at 25°C. Magnetite (Fe<sub>3</sub>O<sub>4</sub>) nanoparticles were dispersed in chloroform (0.33 or 0.17 μM) and placed in the calorimeter cell (1.4 mL). This corresponds to weight concentrations of 1.2 or 0.6 g/L. The reference cell contained pure chloroform. Aliquots of 10 μL of a solution containing the polymers in chloroform (150 mM with respect to the phosphate group of the polymer backbone) were added sequentially in 28 steps from a syringe rotating at 307 rpm to the cell. Additionally, the same amount of polymer was titrated into pure chloroform to determine the heat of dilution for reference. The integrated reference heats were then subtracted from the integrated heats of the adsorption experiments.

**Syntheses.** *Di(but-3-en-1-yl) (3-(2,2-Dimethylbenzo[d][1,3]dioxol-5-yl)propyl) Phosphate (1):* To a stirred solution of POCl<sub>3</sub> (3.68 g, 24.01 mmol, 1 equiv.) in 200 mL of dry DCM a mixture of 2,2-dimethyl-1,3-benzodioxole-5-propanol<sup>39</sup> (5.0 g, 24.01 mmol, 1 equiv.) and Et<sub>3</sub>N (2.43 g, 24.01 mmol, 1 equiv.) in 100 mL of dry DCM at 0°C was added dropwise. After 18 h, a mixture of 3-buten-1-ol (4.33 g, 60.05 mmol, 2.5 equiv.) and Et<sub>3</sub>N (6.08 g, 60.05 mmol, 2.5 equiv.) in 50 mL of dry DCM was added dropwise at 0°C. After 24 h, the solvent was concentrated, diethyl ether added and Et<sub>3</sub>N·HCl as a white solid removed by filtration. The organic phase was dried with MgSO<sub>4</sub>. Column chromatography (silica gel, DCM/ethyl acetate = 10:1) gave the pure product (*R*<sub>f</sub>=0.54). Yield: 35% (3.25 g). <sup>1</sup>H NMR (300 MHz, CDCl<sub>3</sub>): δ 6.64-6.55 (m, 3H, H<sub>arom</sub>), 5.86-5.72 (m, 2H, CH<sub>2</sub>=CH-CH<sub>2</sub>-CH<sub>2</sub>-O-P), 5.17-5.07 (m, 4H, CH<sub>2</sub>=CH-CH<sub>2</sub>-CH<sub>2</sub>-O-P), 4.11-4.00 (m, 6H, -CH<sub>2</sub>-O-P), 2.64-2.59 (t, 2H, Ar-CH<sub>2</sub>-), 2.47-2.40 (dd, 4H, CH<sub>2</sub>=CH-CH<sub>2</sub>-CH<sub>2</sub>-O-P), 1.96-1.91 (t, 2H, Ar-CH<sub>2</sub>-CH<sub>2</sub>-), 1.66 (s, 6H, CH<sub>3</sub>-). <sup>13</sup>C {H}

NMR (76 MHz, CDCl<sub>3</sub>):  $\delta$  147.61 (O-C-CH-C), 145.80 (O-C-CH-CH-C), 134.16 (CH<sub>2</sub>=CH-CH<sub>2</sub>-CH<sub>2</sub>-O-P), 133.50 (-CH-C(CH)-CH<sub>2</sub>-), 120.69 (O-C-CH-CH-C), 117.86 (CH<sub>2</sub>=CH-CH<sub>2</sub>-CH<sub>2</sub>-O-P), 117.75 (O-C(CH<sub>3</sub>)<sub>2</sub>-O), 108.79 (O-C-CH-C), 108.11 (O-C-CH-CH-C), 67.02 (CH<sub>2</sub>=CH-CH<sub>2</sub>-CH<sub>2</sub>-O-P), 66.87 (-CH<sub>2</sub>-O-P), 34.78 (CH<sub>2</sub>=CH-CH<sub>2</sub>-CH<sub>2</sub>-O-P), 32.23 (Ar-CH<sub>2</sub>-CH<sub>2</sub>-), 31.49 (Ar-CH<sub>2</sub>-CH<sub>2</sub>-), 25.97 (-CH<sub>3</sub>). <sup>31</sup>P{H}NMR (202 MHz, CDCl<sub>3</sub>):  $\delta$  -0.94. ESI-MS:  $m/z$  435.15 [M + K]<sup>+</sup>, 815.35 [2 M + Na]<sup>+</sup> (calcd. for C<sub>20</sub>H<sub>29</sub>O<sub>6</sub>P: 396.17). FTIR (cm<sup>-1</sup>): 3078, 2984, 2960, 2901, 2860, 1642, 1609, 1496, 1444, 1385, 1377, 1252 (P=O), 1232 (P=O), 1156, 1121, 1012 (P-O-C), 979 (P-O-C), 916, 835, 807, 787, 732, 657.

*Di(but-3-en-1-yl) Ethyl Phosphate (2)*: To a stirred solution of POCl<sub>3</sub> (10.00 g, 65.22 mmol, 1 equiv.) in 100 mL of dry DCM a mixture of 3-buten-1-ol (9.41 g, 130.44 mmol, 2 equiv.) and Et<sub>3</sub>N (13.20 g, 130.44 mmol, 2 equiv.) in 20 mL of dry DCM at 0°C was added dropwise. After 18 h, a mixture of dry ethanol (6.01 g, 130.44 mmol, 2 equiv.) and Et<sub>3</sub>N (13.20 g, 130.44 mmol, 2 equiv.) in 20 mL of dry DCM was added dropwise at 0°C. After 24 h, the solvent was concentrated, diethyl ether added and Et<sub>3</sub>N·HCl as a white solid removed by filtration. Remaining di(but-3-en-1-yl) phosphorochloridate was removed by flushing the crude product over neutral Al<sub>2</sub>O<sub>3</sub> with DCM to give the pure product (DCM/ethyl acetate = 10:1,  $R_f$ =0.53). Yield: 73% (11.15 g). <sup>1</sup>H NMR (300 MHz, CDCl<sub>3</sub>):  $\delta$  5.83-5.70 (m, 2H, CH<sub>2</sub>=CH-CH<sub>2</sub>-CH<sub>2</sub>-O-P), 5.14-5.04 (m, 4H, CH<sub>2</sub>=CH-CH<sub>2</sub>-CH<sub>2</sub>-O-P), 4.13-4.01 (m, 6H, -CH<sub>2</sub>-O-P), 2.45-2.37 (dd, 4H, CH<sub>2</sub>=CH-CH<sub>2</sub>-CH<sub>2</sub>-O-P), 1.30 (t, 3H, CH<sub>3</sub>-). <sup>13</sup>C {H} NMR (76 MHz, CDCl<sub>3</sub>):  $\delta$  133.51 (CH<sub>2</sub>=CH-CH<sub>2</sub>-CH<sub>2</sub>-O-P), 117.81 (CH<sub>2</sub>=CH-CH<sub>2</sub>-CH<sub>2</sub>-O-P), 66.83 (CH<sub>2</sub>=CH-CH<sub>2</sub>-CH<sub>2</sub>-O-P), 63.97 (-CH<sub>2</sub>-O-P), 34.77 (CH<sub>2</sub>=CH-CH<sub>2</sub>-CH<sub>2</sub>-O-P), 16.22 (-CH<sub>3</sub>). <sup>31</sup>P{H} NMR (202 MHz, CDCl<sub>3</sub>):  $\delta$  -1.03. ESI-MS:  $m/z$  257.07 [M + Na]<sup>+</sup>, 491.17 [2 M + Na]<sup>+</sup> (calcd for C<sub>10</sub>H<sub>19</sub>O<sub>4</sub>P: 234.10). FTIR (cm<sup>-1</sup>): 3080, 2981, 2933, 2904, 1642, 1473, 1432, 1391, 1369, 1264 (P=O), 1165, 1013 (P-O-C), 988 (P-O-C), 914, 860, 799, 734, 701.

*Di(but-3-en-1-yl) Hydrogen Phosphate (3)*: To a stirred solution of POCl<sub>3</sub> (26.73 g, 174.32 mmol, 1 equiv.) in 100 mL of dry DCM a mixture of 3-buten-1-ol (25.14 g, 348.65 mmol, 2 equiv.) and Et<sub>3</sub>N (35.28 g, 348.65 mmol, 2 equiv.) in 40 mL of dry DCM at 0°C was added dropwise. After 18 h, the solvent was concentrated, diethyl ether added and Et<sub>3</sub>N·HCl as a white solid removed by filtration. The organic phase was washed with Na<sub>2</sub>CO<sub>3</sub> solution (10 wt %). The aqueous phase was acidified with HCl solution (37%) and extracted with diethyl ether. The combined organic phases were dried over MgSO<sub>4</sub> and the solvent removed to give the pure product. Yield: 51% (13.75 g). <sup>1</sup>H NMR (300 MHz, CDCl<sub>3</sub>):  $\delta$  8.08 (s, 1H, P-OH), 5.86-5.72 (m, 2H, CH<sub>2</sub>=CH-CH<sub>2</sub>-CH<sub>2</sub>-O-P), 5.17-5.07 (m, 4H, CH<sub>2</sub>=CH-CH<sub>2</sub>-CH<sub>2</sub>-O-P), 4.11-4.02 (m, 6H, -CH<sub>2</sub>-O-P), 2.48-2.40 (dd, 4H, CH<sub>2</sub>=CH-CH<sub>2</sub>-CH<sub>2</sub>-O-P). <sup>13</sup>C {H} NMR (76 MHz, CDCl<sub>3</sub>):  $\delta$  133.45 (CH<sub>2</sub>=CH-CH<sub>2</sub>-CH<sub>2</sub>-O-P), 117.83 (CH<sub>2</sub>=CH-CH<sub>2</sub>-CH<sub>2</sub>-O-P), 66.83 (CH<sub>2</sub>=CH-CH<sub>2</sub>-CH<sub>2</sub>-O-P), 66.86 (-CH<sub>2</sub>-O-P), 34.68 (CH<sub>2</sub>=CH-CH<sub>2</sub>-CH<sub>2</sub>-O-P). <sup>31</sup>P{H} NMR (202 MHz, CDCl<sub>3</sub>):  $\delta$  -1.03. ESI-MS:  $m/z$  847.21 [4 M + Na]<sup>+</sup>, 901.29 [4 M + 2K]<sup>+</sup>, 1076.22 [5 M + 2Na]<sup>+</sup> (calcd for

C<sub>8</sub>H<sub>15</sub>O<sub>4</sub>P: 206.07). FTIR (cm<sup>-1</sup>): 3080, 2963, 2903, 1642, 1473, 1431, 1391, 1225 (P=O), 1008 (P-O-C), 986 (P-O-C), 912, 855, 799, 756.

*General Procedure for ADMET Polymerization:* The respective monomer or comonomer mixture and catalyst Grubbs first, second or Hoveyda-Grubbs first generation 3 mol% were mixed under an argon atmosphere. For the solution polymerization, about 50 wt % 1-chloronaphthalene was additionally added. Polymerization was carried out at reduced pressure to remove the evolving ethylene at 60-80°C for up to 72 h until reaction was completed. Reaction progress was monitored with <sup>1</sup>H NMR spectroscopy and a spatula tip of additional catalyst added after measurement if necessary until reaction was completed. The reaction was cooled down, 7 mL of DCM, about 10 mg of tris(hydroxymethyl)phosphine and 3 drops of Et<sub>3</sub>N were added to deactivate the catalyst. After 1 h, 5 mL of distilled water were added and stirred overnight. The organic phase was extracted with aqueous HCl (5 wt%) and brine. The mixture was concentrated at reduced pressure and the polymer precipitated into hexane twice. Yields 50-90%.

**Poly1:** <sup>1</sup>H NMR (300 MHz, CDCl<sub>3</sub>): δ 6.63-6.55 (m, H<sub>arom</sub>), 5.52-5.50 (m, -CH<sub>2</sub>-CH=CH-CH<sub>2</sub>-), 4.03-4.01 (m, -CH<sub>2</sub>-O-P), 2.60 (t, Ar-CH<sub>2</sub>-), 2.60-2.36 (m, -CH=CH-CH<sub>2</sub>-CH<sub>2</sub>-O), 1.92 (t, Ar-CH<sub>2</sub>-CH<sub>2</sub>-), 1.64 (s, CH<sub>3</sub>-). <sup>13</sup>C {H} NMR (76 MHz, CDCl<sub>3</sub>): δ 147.59, 145.79, 134.08, 128.20, 127.25, 120.67, 117.73, 108.75, 108.10, 67.09, 33.75, 33.25, 31.47, 25.96. <sup>31</sup>P {H} NMR (202 MHz, CDCl<sub>3</sub>): δ -0.89.

**Poly2:** <sup>1</sup>H NMR (300 MHz, CDCl<sub>3</sub>): δ 5.86-5.73 (m, CH<sub>2</sub>=CH-CH<sub>2</sub>-CH<sub>2</sub>-O-P), 5.63-5.46 (m, -CH<sub>2</sub>-CH=CH-CH<sub>2</sub>-), 5.18-5.07 (m, CH<sub>2</sub>=CH-CH<sub>2</sub>-CH<sub>2</sub>-O-P), 4.15-3.98 (m, -CH<sub>2</sub>-O-P), 2.48-2.37 (m, CH<sub>2</sub>=CH-CH<sub>2</sub>-CH<sub>2</sub>-O-P), 1.33 (t, CH<sub>3</sub>-). <sup>13</sup>C {H} NMR (76 MHz, CDCl<sub>3</sub>): δ 128.28, 127.31, 122.02, 67.07, 33.71, 16.34. <sup>31</sup>P {H} NMR (202 MHz, CDCl<sub>3</sub>): δ -0.98.

**Poly3:** <sup>1</sup>H NMR (300 MHz, DMSO-*d*<sub>6</sub>): δ 5.83-5.72 (m, CH<sub>2</sub>=CH-CH<sub>2</sub>-CH<sub>2</sub>-O-P), 5.52-5.47 (m, -CH<sub>2</sub>-CH=CH-CH<sub>2</sub>-), 5.16-5.04 (m, CH<sub>2</sub>=CH-CH<sub>2</sub>-CH<sub>2</sub>-O-P), 4.02-3.69 (m, -CH<sub>2</sub>-O-P), 2.40-2.26 (m, CH<sub>2</sub>=CH-CH<sub>2</sub>-CH<sub>2</sub>-O-P).

**Poly4:** <sup>1</sup>H NMR (300 MHz, CDCl<sub>3</sub>): δ 6.64-6.55 (m, H<sub>arom</sub>), 5.59-5.48 (m, -CH<sub>2</sub>-CH=CH-CH<sub>2</sub>-), 4.15-3.98 (m, -CH<sub>2</sub>-O-P), 2.61 (t, Ar-CH<sub>2</sub>-), 2.48-2.36 (m, -CH=CH-CH<sub>2</sub>-CH<sub>2</sub>-O), 1.93 (t, Ar-CH<sub>2</sub>-CH<sub>2</sub>-), 1.65 (s, CH<sub>3</sub>-O-), 1.33 (s, CH<sub>3</sub>-CH<sub>2</sub>). <sup>13</sup>C {H} NMR (76 MHz, CDCl<sub>3</sub>): δ 128.25, 127.30, 67.06, 63.98, 59.94, 33.71, 28.77, 25.95, 25.42, 16.27. <sup>31</sup>P {H} NMR (202 MHz, CDCl<sub>3</sub>): δ -0.99.

**Poly5:** <sup>1</sup>H NMR (300 MHz, CDCl<sub>3</sub>): δ 5.69-5.45 (m, -CH<sub>2</sub>-CH=CH-CH<sub>2</sub>-), 5.17-5.08 (m, CH<sub>2</sub>=CH-CH<sub>2</sub>-CH<sub>2</sub>-O-P), 4.15-3.98 (m, -CH<sub>2</sub>-O-P), 2.48-2.36 (m, -CH=CH-CH<sub>2</sub>-CH<sub>2</sub>-O), 1.34 (s, CH<sub>3</sub>-CH<sub>2</sub>). <sup>13</sup>C {H} NMR (76 MHz, CDCl<sub>3</sub>): δ 128.25, 127.31, 67.11, 64.04, 33.75, 16.43. <sup>31</sup>P {H} NMR (202 MHz, CDCl<sub>3</sub>): δ -2.93.

*Catechol-Containing PPEs: General Procedure for Removal of Ketal Protecting Group.* The respective polymer (**poly1** or **poly4**) was dissolved in a mixture of TFA/DCM 50:50 with a concentration of about 100 mg/mL and stirred for 30 min. The polymer was precipitated into hexane once, dissolved in DCM and extracted with distilled water (3x). The organic phase was dried with NaSO<sub>4</sub> and filtered. The product was obtained after removal of the solvent. Yield: quantitative.

**Poly4-dep:** <sup>1</sup>H NMR (300 MHz, CDCl<sub>3</sub>): δ 6.81-6.51 (m, H<sub>arom</sub>), 5.55-5.51 (m, -CH<sub>2</sub>-CH=CH-CH<sub>2</sub>-), 4.15-3.99 (m, -CH<sub>2</sub>-O-P), 2.58 (t, Ar-CH<sub>2</sub>-), 2.48-2.37 (m, -CH=CH-CH<sub>2</sub>-CH<sub>2</sub>-O), 1.94 (t, Ar-CH<sub>2</sub>-CH<sub>2</sub>-), 1.33 (t, CH<sub>3</sub>-CH<sub>2</sub>). <sup>13</sup>C {H} NMR (176 MHz, CDCl<sub>3</sub>): δ 145.16, 143.42, 131.68, 129.50, 128.33, 127.32, 118.85, 115.65, 115.45, 66.33, 63.23, 33.12, 31.61, 30.32, 15.98. <sup>31</sup>P {H} NMR (202 MHz, CDCl<sub>3</sub>): δ -2.94.

*General Procedure for Covalent Network Formation.* A total of 40 mg poly4-1-dep was dissolved in 200 μL of ethanol to provide a concentration of 200 mg/mL, with a catechol content of ~0.09 mol/L. To achieve gelation, an aqueous mixture of 40 μL 0.5 M NaOH solution and 30 μL 0.15 M NaIO<sub>4</sub> solution was added and well mixed, to give a final polymer concentration of 150 mg/mL and catechol/NaIO<sub>4</sub> ratio of 4:1. The mixture turns immediately dark red-brown and gels within 3 h.

*Swelling of PPE Gels.* Polymer gels were extensively dried at reduced pressure. Dry polymer (W<sub>d</sub>) gel was soaked in 10 mL of ethanol or distilled water for 24 h to obtain a swelling equilibrium. After removal of the surface solvent, the gels were weighted (W<sub>s</sub>). The swelling ratio was calculated by (W<sub>s</sub>-W<sub>d</sub>)/W<sub>d</sub>·100%.

*Degradation Studies.* The polymers (ca. 13 mg) were dissolved in an alkaline EtOD/D<sub>2</sub>O/NaOH mixture (1.5 M), 5.9 M NaOH-D<sub>2</sub>O solution, EtOD/D<sub>2</sub>O 3:1 (0.5 : 0.17 mL)). The NMR tubes were incubated at 37 °C. <sup>1</sup>H and <sup>31</sup>P {H} NMR spectra were measured at room temperature.

*Preparation of Iron Oxide Nanoparticles.* The particles were prepared through thermal decomposition of iron oleate in a high-boiling solvent, following a well-established procedure with slight modifications.<sup>40, 41</sup> To produce the iron oleate precursor, a solution of iron chloride (FeCl<sub>3</sub>·6H<sub>2</sub>O, 21.6 g, 80 mmol) in distilled water (120 mL) was added to a solution of sodium oleate (73.0 g, 240 mmol) in a mixture of ethanol (160 mL) and *n*-hexane (280 mL). The resulting biphasic mixture was refluxed at 70°C for 4 h under vigorous magnetic stirring. After cooling down to room temperature, the brown organic phase was separated from the yellowish aqueous phase, washed with mixtures of distilled water and ethanol (5 x 100/20 mL) and then dried over MgSO<sub>4</sub>. Eventually, the organic solvents were removed using a rotary evaporator, leaving an oily brown residue that was further vacuum-dried on a Schlenk line (10<sup>-2</sup> mbar, 100°C) for several hours. The

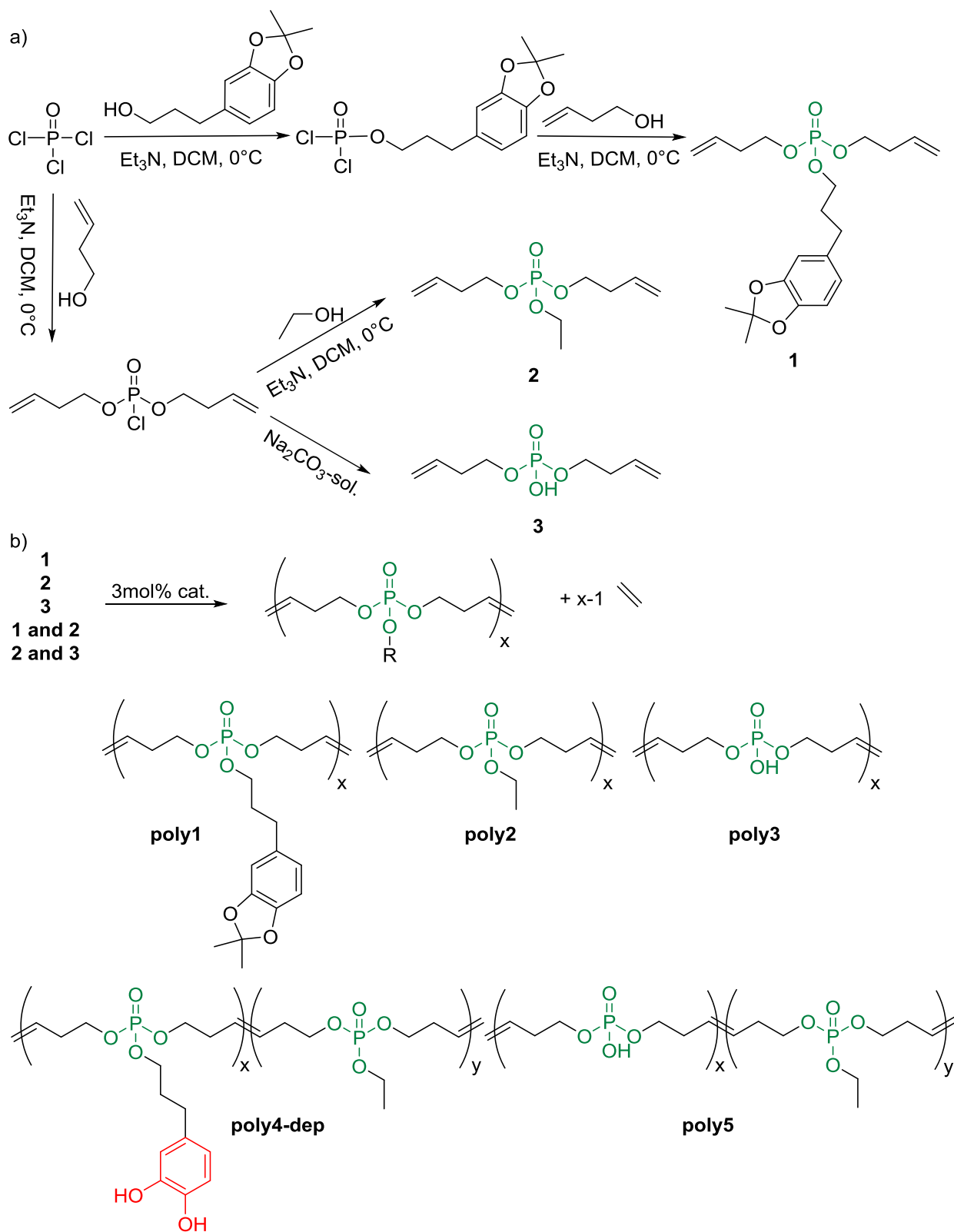
obtained iron oleate complex was a waxy brown solid. In a typical synthesis of iron oxide nanoparticles with an average diameter of 13 nm, iron oleate precursor (1.8 g, 2.0 mmol) and oleic acid (0.44 g, 0.50 mL, 1.6 mmol) were dissolved in trioctylamine (10 mL) and vacuum-dried on a Schlenk line ( $10^{-2}$  mbar,  $100^{\circ}\text{C}$ ) for 30 min. Afterward, the reaction mixture was heated to  $350^{\circ}\text{C}$  with a constant heating rate of  $3.3^{\circ}\text{C min}^{-1}$  and kept at that temperature for 30 min. After cooling down to room temperature, the nanoparticles were precipitated by addition of ethanol (30 mL), separated by centrifugation (9000 rpm, 10 min), and the nanoparticle residue was redissolved in chloroform.

*Surface Functionalization of Iron Oxide Nanoparticles.* For the functionalization of the iron oxide nanoparticles with PPEs, 250  $\mu\text{L}$  of polymer solutions in chloroform were added dropwise to 1.4 mL of a nanoparticle suspension of 0.12 wt % in chloroform under stirring. The concentrations of poly4-1 and poly4-1-dep were adjusted to give a catechol concentration of 15 mmol/L sample and overall phosphate (or side chain) concentration of 155 mmol/L. The polymer solutions of poly2-2 and poly5-2 also exhibited a phosphate (or side chain) concentration of 155 mmol/L. The functionalized particles were precipitated twice by addition of hexane to the chloroform solution. The particles were collected with a magnet at the wall of the glass vial. The supernatant was decanted and the particles were resuspended in chloroform. After a second precipitation, the particles were suspended in ethanol or methanol.

## 2.4 Results and Discussion

**Monomer Syntheses.** Three novel phosphate monomers suitable for the ADMET polymerization to PPEs<sup>29, 37-38</sup> were prepared. Different pendant groups were attached to compare their adhesion properties: a novel catechol containing monomer (**1**), a phosphodiester monomer (**3**; carrying an adhesive P-OH-group), and a phosphate monomer with an ethyl side chain (**2**), with expected low adhesive properties. (2,2-dimethyl-benzo[d][1,3]dioxole)-5-propanol<sup>39</sup> was reacted with phosphoryl chloride, followed by esterification with 2 equiv. 3-buten-1-ol to produce di(but-3-en-1-yl) (3-(2,2-dimethylbenzo[d][1,3]dioxol-5-yl)propyl) phosphate (**1**; Scheme 2.1). Di(but-3-en-1-yl) ethyl phosphate (**2**) was obtained in a similar way: in this case, two chlorides of phosphoryl chloride were substituted with 3-buten-1-ol, followed by esterification with ethanol. It has to be mentioned, that the order of esterification is exchangeable, but the reactivity of phosphoryl chloride for nucleophilic substitution decreases during the progress of substitution. For the ethyl containing monomer, a reaction set up *vice versa* compared to the synthesis of catechol monomer is rational due to easy removal of ethanol, which can be used in excess. Di(but-3-en-1-yl) hydrogen phosphate (**3**) was obtained by the reaction of phosphoryl chloride

with 3-buten-1-ol, followed by careful hydrolysis of di(but-3-en-1-yl) chloro phosphate in alkaline sodium bicarbonate solution to yield the final monomer.



**Scheme 2.1.** (a) Syntheses of ADMET phosphate monomers and (b) homo- or copolycondensation of monomers 1-3.

Monomers **1** and **2** were purified by column chromatography and obtained as colorless or off-white liquids, monomer **3** was purified by extraction. Purity of the monomers was verified by  $^1\text{H}$  and  $^{31}\text{P}$  {H} NMR spectroscopy (Figure 2.2 and Supporting Information, Figure S2.1-S2.9).  $^1\text{H}$  NMR spectra of all monomers show the characteristic resonances for protons of terminal double bonds as multiplets at 5.04-5.17 and 5.70-5.86 ppm, neighboring methylene groups at 2.37-2.48 ppm and methylene groups neighboring O-P at 4.00-4.13 ppm.  $^{31}\text{P}$  {H} NMR spectra show a single resonance in the range of -0.96 and -1.03 ppm. All monomers can be stored at room temperature, without decomposition or unwanted polymerization at least for several months.

**ADMET Polycondensation.** All phosphate monomers were investigated with respect to their polymerization behavior in the ADMET polycondensation according to the conditions developed in our group for the polycondensation of phosphates<sup>37</sup> and phosphonates.<sup>29</sup> In general, successful polycondensation can be detected from the  $^1\text{H}$  NMR spectra by the decrease of signals for terminal double bonds at 5.10 and 5.80 ppm. At the same time, a new signal at about 5.50 ppm arises for the internal double bonds, which are formed during the metathesis reaction. Molecular weights were determined by end-group analysis, namely, the ratio between signals for terminal and internal double bonds. Additionally, the molecular weights were obtained by gel permeation chromatography in DMF, THF, or DMSO (depending on the solubility of each polymer). Polycondensation was carried out either in bulk or in solution (50 wt %) at reduced pressure to guarantee continuous mixing and the removal of ethylene. 1-Chloronaphthalene was a convenient solvent due to its high boiling point. Furthermore, different robust catalysts for metathesis, in particular, Grubbs first (G1) and second (G2) generation and Hoveyda-Grubbs first generation (H1), were examined. A total of 3 mol% compared to monomer feed were applied. Additionally, different temperatures ranging from 60 to 80°C were applied; the latter did not have a pronounced impact on the degree of polymerization. The obtained polymers are viscous oils with molecular weights up to  $4.3 \times 10^5$  g/mol (Table 2.1) and molecular weight dispersities of  $\mathcal{D} \approx 2$ , which are in good agreement with the theoretically predicted distribution by the Carothers equation. Progress of all polycondensations was monitored by  $^1\text{H}$  NMR spectroscopy after changing of the color of the catalyst from violet (metathesis active species) to brown (inactive species). When reaction was not completed, an additional spatula tip (about 2-5 mg) of catalyst was added to the reaction. After ceasing of ethylene evolution, all reactions were terminated with tris(hydroxymethyl)phosphine and few drops (about 30  $\mu\text{L}$ ) of triethylamine in dichloromethane to deactivate the remaining catalyst. After acidic extraction, the polymers were precipitated into hexane twice. All polymers, including deprotected polymers, were soluble in organic solvents such as dichloromethane, or polar solvents such as THF, ethanol, methanol, but insoluble in hexane. Protected, as well as deprotected, catechol-containing polymers were soluble in a mixture of ethanol/water (80:20), ethyl, and hydrogen-containing PPEs in mixtures up to 50:50 (ethanol/water).

Polymerization of catechol monomer **1** with Grubbs first generation catalyst showed a higher degree of polymerization for reaction in solution (**poly1-2**) than in bulk (**poly1-1**) with up to 35,400 g/mol. Reaction in bulk with Grubbs second gen. (**poly1-3**) or Hoveyda-Grubbs first gen. (**poly1-4**) formed only oligomers (around 1,700 g/mol) or moderate degrees of polymerization (12,400 g/mol), respectively. All degrees of polymerization were obtained by analysis of the proton ratio of terminal to internal double bonds in  $^1\text{H}$  NMR spectra. Polymerization conditions need to be optimized for each monomer. While polymerization of catechol monomer **1** with Hoveyda-Grubbs first gen. in bulk shows only moderate molecular weights (**poly1-4**), the polymerization of **2** under these conditions resulted in higher molecular weights (up to 29,000 g/mol (**poly2-4**)). In contrast, the polymerization with Grubbs second gen. (**poly2-3**) only produced oligomers. Grubbs second gen. is known to show generally higher reactivity in metathesis reaction than Grubbs first gen. Reaction with Grubbs first gen. either in bulk (**poly2-1**) or solution (**poly2-2**) showed similar results, 7,300 and 10,900 g/mol, respectively, yet lower than for the catechol monomer. Monomer **3** carries the unprotected adhesive P-OH-group and produced oligomers with resulting molecular weights below 1,000 g/mol for all different catalysts and in bulk as well as in solution (**poly3-1** to **poly3-4**). It is known that Grubbs catalysts are slowed down or can be poisoned by acids. Tew and co-workers reported successful polymerization of an unprotected carboxylate-functionalized norbornene monomer for ROMP polymerization. However, they only found polymerization occurring, when the carboxylate function was fully protonated, since otherwise the carboxylate anion would act as ligand to the ruthenium catalyst and quench or retard the polymerization.<sup>42-43</sup> Therefore, protection is usually applied for acidic functionalities in the monomers.<sup>44</sup> To the best of our knowledge, phosphonic acid containing ROMP or ADMET monomers are also always polymerized in the protected state (as esters),<sup>45-48</sup> due to the same reason that they might act as a ligand. Although homopolymerization of monomer **3** was not possible, copolymerization with monomer **2** in a ratio of 10 or 20 mol% succeeded. Molecular weights of 19,300 g/mol (**poly5-1**) and 10,300 g/mol (**poly5-2**) were obtained. In this case, dilution of the acidic monomer **3** with monomer **2** allows polymerization.

The copolymerization of catechol **1** and ethyl monomer **2** in different ratios, 10, 20 and 40 mol% catechol monomer content (**poly4-1** to **poly4-3**) also provided copolymers with an adjustable amount of catechol units in the PPE and molecular weights between 25,100 and 42,500 g/mol. The monomer feed ratio was proven to be incorporated in the final copolymer by integration of the respective resonances in the  $^1\text{H}$  NMR spectra. The molecular weights did not show any trend for different monomer ratios. A representative  $^1\text{H}$  NMR spectrum is shown in Figure 2.2 (all other spectra are summarized in the Supporting Information). All GPC measurements either in THF, DMF, or DMSO exhibit  $\bar{M}_w$  between 1.32 and 2.74 (Figure S2.29-S2.33).

**Table 2.1.** Polymerization conditions and resulting molecular weight of the PPEs prepared in this study.

entry	monomer	catalyst	condition	$M_n^a$ (g mol <sup>-1</sup> )	$M_w/M_n^b$	DP <sup>a</sup>
<b>poly1-1</b>	1	G1	bulk	35,400	1.77 <sup>c</sup>	96
<b>poly1-2</b>	1	G1	solution	n.c.	2.06 <sup>c</sup>	n.c.
<b>poly1-3</b>	1	G2	bulk	1,700	-	5
<b>poly1-4</b>	1	H1	bulk	12,400	2.28 <sup>c</sup>	34
<b>poly2-1</b>	2	G1	bulk	7,300	n.d.	36
<b>poly2-2</b>	2	G1	solution	10,900	1.93 <sup>d</sup>	53
<b>poly2-3</b>	2	G2	bulk	600	-	3
<b>poly2-4</b>	2	H1	bulk	28,900	2.38 <sup>d</sup>	140
<b>poly3-1</b>	3	G1	bulk	500	n.d.	3
<b>poly3-2</b>	3	G1	solution	800	n.d.	5
<b>poly3-3</b>	3	G2	solution	900	n.d.	5
<b>poly3-4</b>	3	H1	bulk	600	n.d.	3
<b>poly4-1</b>	1- <i>co</i> -2 (1:9)	G1	solution	27,500	1.32 <sup>c</sup>	124
<b>poly4-1-dep</b>	1- <i>co</i> -2 (1:9)	-	-	n.c.	1.47 <sup>c</sup>	124
<b>poly4-2</b>	1- <i>co</i> -2 (2:8)	G1	solution	42,500	1.54 <sup>c</sup>	178
<b>poly4-3</b>	1- <i>co</i> -2 (4:6)	G1	solution	25,100	1.54 <sup>c</sup>	93
<b>poly5-1</b>	3- <i>co</i> -2 (2:8)	G1	solution	19,300	2.74 <sup>e</sup>	96
<b>poly5-2</b>	3- <i>co</i> -2 (1:9)	G1	solution	10,300	n.d.	56

<sup>a</sup> DP= degree of polymerization, determined by <sup>1</sup>H NMR. <sup>b</sup>Determined by GPC. <sup>c</sup> In THF. <sup>d</sup> In DMF. <sup>e</sup> In DMSO. n.c.: not calculable; n.d.: not determined.

**Release of Catechols.** The release of the catechol function from their acetal-protected precursor is typically achieved under acidic conditions.<sup>49</sup> As all protected homo- as well as copolymers **poly1** and **poly4** are insoluble in water or organic mixtures with aqueous content over 20%, several attempts in THF, THF/water, ethanol/water, or dioxane/water mixtures with different concentrations of acetic acid, hydrochloric acid or Amberlite IR120 (cation exchange resins in protonated form) at room temperature or under reflux or at reduced pressure (to remove the acetone side-product) were conducted. These protocols, however, showed only partial deprotection or degradation of the polyphosphate backbone. Quantitative hydrolysis of the pendant acetals without backbone degradation or transesterification was achieved when the polymers were dissolved in dichloromethane/concd TFA (50:50, with approximately 10 wt% polymer) within 15-30 min at room temperature. The deprotection was proven by <sup>1</sup>H NMR spectroscopy from the disappearance of the methyl resonances of the acetal group at 1.65 ppm (Figure 2.2). GPC (Figure S2.32) and <sup>1</sup>H NMR data (Figures 2.2 and S2.26) support the fact that no transesterification or degradation occurred during the hydrolysis step of the acetal. The ratio of the side chains of the initial monomer feed can be still retrieved in the <sup>1</sup>H NMR spectra of the deprotected **poly4-1-dep**. GPC data show a slight shift of elution volume to smaller values for the deprotected polymer. This observation can be reasoned by change of the hydrophilicity of **poly4-1-dep** compared to **poly4-1**, and therefore, different behavior in GPC measurement. However, the shape of GPC curve remains unchanged (Figure S2.32). To further prove the stability of the PPEs under the deprotection

conditions, **poly2-2** was treated with concd TFA. In the absence of water, **poly2-2** remains stable over a period of 3 h. After longer incubation (6 and 24 h), a slight shift of the molecular weight distribution can be observed, indicating backbone hydrolysis. However, since the deprotection of **poly4-1** was completed after 15-30 min, no degradation during the catechol release is expected.

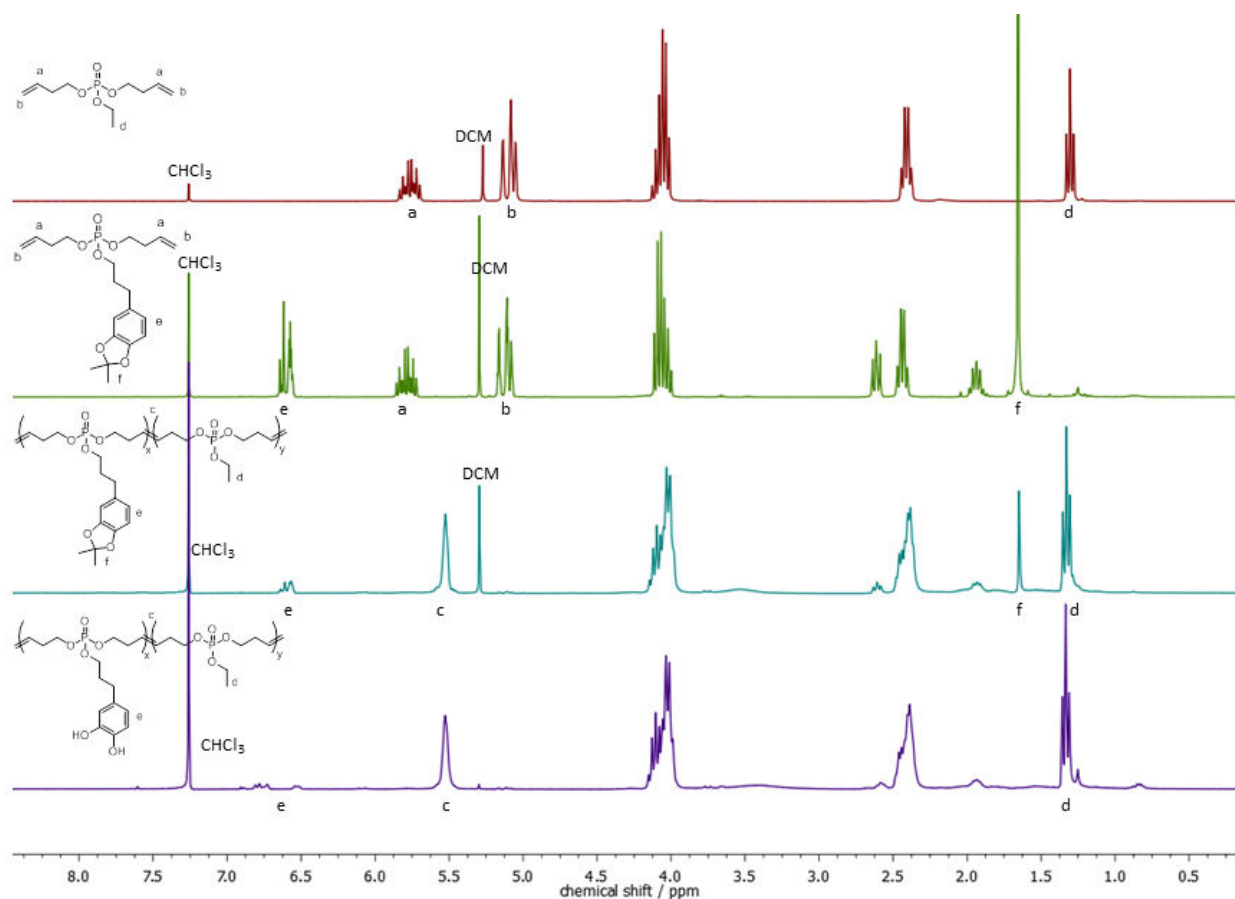


**Figure 2.2.** <sup>1</sup>H NMR spectra of monomers **1** and **2** and the corresponding copolymer in protected, as well as deprotected, forms **poly4-1** and **poly4-1-dep**.

**Degradation Studies.** In general PPEs undergo backbone and side-chain hydrolysis under acidic and alkaline conditions<sup>50</sup> and/or by enzymatic degradation.<sup>25, 51</sup> The ethyl homopolymer (**poly2-2**), protected catechol homopolymer (**poly1-4**) and a protected ethyl/catechol copolymer (**poly4-2**) were examined in <sup>1</sup>H and <sup>31</sup>P{H} NMR kinetics under accelerated hydrolysis conditions at alkaline pH (ca. 1.5 M NaOH in EtOD/D<sub>2</sub>O at 37 °C). Under these conditions the degradation is accelerated to a moderate time scale. The deprotected catechol polymers were not considered here, due to additional reactions of the catechol functionalities under basic conditions. For all polymers, <sup>31</sup>P{H} NMR spectra show that full degradation from phosphotriesters to phosphodiester takes place within 3 days (Figure 2.3b). Herein, **poly2-2** will be discussed in detail, the data for the other polymers are summarized in the Supporting Information. Under basic conditions, the cleavage of the triesters to diesters is expected, resulting in different degradation products: either the pendant chain is released or the polymer backbone is cleaved (Scheme S2.1; note: for copolymers two

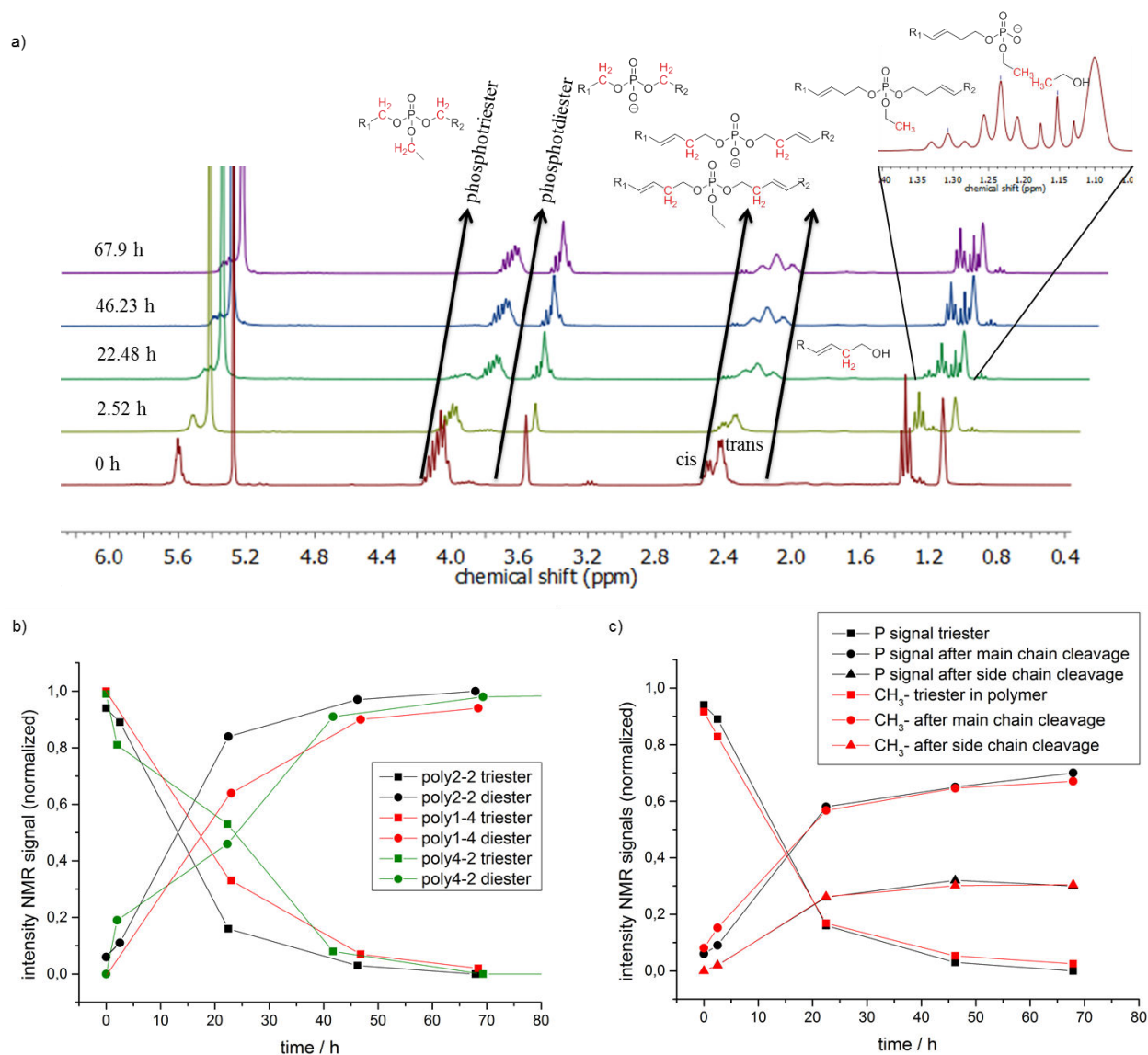


**Figure 2.3.** Degradation studies: (a) Overlay of the  $^1\text{H}$  NMR spectra of **poly2-2** after different incubation times (300 MHz, EtOD/ $\text{D}_2\text{O}$ , 298 K); (b) Integral of the NMR signals (normalized) vs degradation time: degradation of **poly2-2**, **poly1-4** and **poly4-2** from phosphotriesters to phosphodiester in  $^1\text{H}$  NMR spectra from signals at 4.06 and 3.84 ppm; (c) Integrals from  $^1\text{H}$  and  $^{31}\text{P}$  NMR spectra showing the cleavage (**poly2-2**) of the side and main chains.

different diesters can be obtained either containing an ethyl or a catechol side chain and a main chain residue.) Due to limited spectra resolution, the signals of  $^{31}\text{P}\{\text{H}\}$  NMR spectra for the different degradation products can hardly be examined separately. However, signal of the phosphotriester at -1.35 ppm fully disappears, while two signals for phosphodiester at 0.31-0.54 ppm arise (Figure S2.35). At the same time, a signal for a phosphomonoester cannot be observed. After cleavage of one ester bond a phosphodiester anion is formed under alkaline conditions. A second cleavage of an ester bond is unlikely due to the negative charge, however in the presence of enzymes further degradation may occur. Penczek et al.<sup>50</sup> mentioned earlier that the first cleavage is

up to  $10^5$  times faster as a second cleavage at pH 12.0 and 125 °C. The degradation rates can be determined from both  $^{31}\text{P}$  {H} and  $^1\text{H}$  NMR spectra (Figures 2.3a and S2.36). The  $^1\text{H}$  NMR spectra allow to follow the hydrolysis precisely: the signal at 4.06 ppm from the methylene group neighboring the phosphotriester group decreases over time, and the resonance of the methylene group neighboring the phosphodiester group increases (3.84 ppm). The  $^1\text{H}$  NMR spectra also allow calculating the ratio between backbone and side-chain cleavage (Figures 2.3b and c). The resonances of the pendant methyl group of the side chain in **poly2-2** are detected as a triplet at 1.31 ppm. This signal decreases during hydrolysis, while two new triplet signals are detectable, corresponding to ethanol (at 1.15 ppm) or the resulting phosphodiester after main chain hydrolysis (at 1.23 ppm, Figure 2.3a). An expected statistical cleavage of the three ester bonds under alkaline conditions<sup>50</sup> can be confirmed in the fully degraded polymer **poly2-2** after 72 h, where 31% of side chain and 69% of the main chain ester bonds were cleaved. The ratio of degradation of the different ester bonds is in agreement with the two signals in the  $^{31}\text{P}$  NMR spectra (Figures 2.3c and S2.35). A similar degradation ratio of 30% and 70% for side and main chain cleavage respectively was observed for the protected catechol homopolymer (**poly1-4**) after full degradation (Figures S2.37-S2.39), as well as for the copolymer **poly4-2** (Figures S2.40-S2.42).

**Formation of Gels.** Polymer networks and gels from catechol-containing polymers<sup>8</sup> can be prepared by pH-dependent complexation of metal oxides or ions with high binding constants.<sup>52, 11</sup> Under alkaline and oxidizing conditions quinones are generated from the catechols which undergo Michael(-type) reactions with thiols and amines or other catechols to form networks. PEG-based<sup>53</sup> and chitosan/pluronic hydrogels<sup>16</sup> were produced by this strategy.

The catechol-containing PPEs (**poly4-1-dep**) were dissolved in ethanol and cross-linked by the addition of aqueous base in the presence of  $\text{NaIO}_4$  as an oxidant. At a concentration of 200 mg/mL polymer with a catechol concentration of about 0.09 M gelation was observed, while lower polymer concentrations did only produce incomplete gelation. After the addition of a mixture of NaOH solution (0.5 M) and  $\text{NaIO}_4$  solution (0.15 M) (60:40, 30v% compared to polymer solution), the mixture (exhibiting a final concentration of 150 mg/mL) turned to dark red-brown within 3 h (known as “quinone tanning”,<sup>54</sup> Figure S2.43). The catechol/ $\text{NaIO}_4$  ratio in the sample was adjusted to be 4:1. Faster gelation (within seconds) was achieved by either increasing the ratio to 2:1 or by addition of NaOH solution first, followed by consecutive addition of the oxidant. However, homogeneous mixing cannot be achieved in these cases.

The swelling behavior of the gel was explored in ethanol and water. To determine the degree of swelling, the gel was first extensively dried at reduced pressure. The obtained stiff gel was immersed in either 10 mL ethanol or water for 24h, yielding a solvent uptake of 600% in water and 1000% in ethanol in the swollen state (Figure S2.43).

Gelation was also analyzed by DSC: the polymers (**poly4-1** and **poly4-1-dep**) exhibit glass transition temperatures of  $-69^{\circ}\text{C}$  for the protected PPE and  $-59^{\circ}\text{C}$  for the PPE with free catechols. After gelation, the  $T_g$  increased to  $-51^{\circ}\text{C}$  with a much broader transition, typical for gels (Figure 2.4).

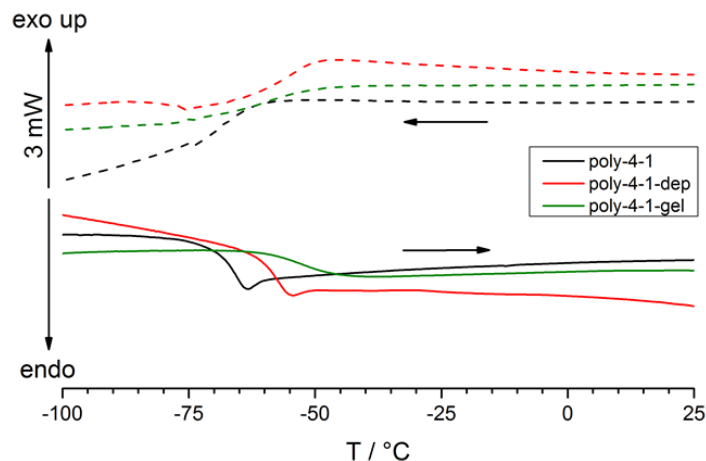


**Figure 2.4.** DSC thermograms of **poly4-1**, **poly4-1-dep** and poly4-1-gel (heating and cooling rate  $10\text{ K min}^{-1}$ , first run).

**Surface Functionalization of Magnetite Nanoparticles with Catechol-PPEs.** Magnetic nanoparticles are attractive candidates in nanomedicine for multimodal tracking and as MRI contrast agents. However, due to their low colloidal stability in polar solvents and lack of biocompatibility, modification is necessary to increase their hydrophilicity and biocompatibility. Besides PEG, also biodegradable polymers like poly(lactic acid) or poly(glycolic acid), although hydrophobic, and their copolymers were applied.<sup>55, 14</sup> The surface of iron oxide particles can be addressed with ligands such as carboxylates, phosphates, sulfates, or catechols. Additionally, stronger binding of “multidentate” polymers (with more than one anchor group) is expected.

The magnetite nanoparticles (NPs) were synthesized by an established protocol,<sup>40, 41</sup> resulting in particles with diameters of about 13.3 nm stabilized with oleic acid ( $\pm 0.9\text{ nm}$ , Figure 2.5). The particles then were coated with different PPEs varying in their adhesion profile. PPEs containing 90% ethyl side-chains and 10% catechol side-chains were compared to PPEs with no catechols (i.e., 100% ethyl side chains (**poly2-2**)), the protected catechols (**poly4-1**), or with 10% P-OH side-chains (**poly5-2**).

For this purpose, to 1.4 mL of a magnetite nanoparticle dispersion (0.12 wt% in chloroform) 250  $\mu\text{L}$  of polymer solutions in chloroform were added dropwise. The concentrations of **poly4-1** and **poly4-1-dep** was adjusted to give a catechol concentration of 15 mmol/L in the sample and overall phosphoester (or side chain) concentration of 150 mmol/L. The polymer solutions of **poly2-2** and **poly5-2** were adjusted to the same phosphoester concentration of 150 mol/L to keep them equal for later comparison. The unmodified NPs formed stable dispersions in hexane,

chloroform, or THF, but precipitated after adding polar solvents like methanol. After polymer-coating, dispersions of the nanoparticles in ethanol, methanol, and chloroform or THF were stable (for at least 7 months), but precipitated in hexane, which is a precipitant for the PPEs. Figure S2.44 (middle) shows that all coated NP dispersions (vials 1-4) are selectively dispersible in methanol when overlaid with hexane. After mixing and resettlement of the biphasic system, the coated particles remained stable in the polar phase (Figure S2.44, right), while uncoated particles agglomerated (Figure S2.44, left). Dynamic light scattering revealed an  $R_h$  of 11 nm for the “as prepared” NPs, while the particles functionalized with **poly2-2** and **poly4-1** showed increased radii of 21 and 16 nm, respectively. In contrast, particles functionalized with **poly4-1-dep** exhibited a radius of 73 nm and with **poly5-2**, a bimodal distribution with 18 and 113 nm, assuming the formation of small conglomerates. TEM images (Figure 2.5D) underline this assumption for NPs with **poly5-2**. DLS measurements of the functionalized nanoparticles after 7 months remain unchanged and prove the long-term stability of the dispersion.

While NPs stabilized with oleic acid are monodisperse and order in a close-packed fashion (Figure 2.5A), polymer-functionalized NPs normally lack this property. Therefore, the ordering arrangement of the functionalized NPs with **poly2-2** shown in Figure 2.5B is unusual. However, small darker domains in the background indicate that the binding affinity of the polymer to the particles is low, which leads to an inefficient functionalization of the particles (also compared with the ITC data below). NPs functionalized with **poly4-1** showed a similar behavior (Figure S2.45), but TEM images of particles with **poly4-1-dep** and **poly5-2** (Figures 2.5C and D) remained isolated and did not pack, and a closed polymer film was observed as background. Based on the findings from DLS measurements and TEM images, all PPEs bind to the NPs, but the adhesive polymers carrying P-OH or catechol groups have a higher binding affinity to the iron oxide nanoparticles.

From these findings, we assume also strong binding of the phosphate groups in the backbone of polymers to the particles and probably even a displacement of the catechol groups. The assumption can be supported by several observations from the literature. Generally, phosphates show high affinity to iron and iron oxides which is utilized in phosphatation of steel for corrosion resistance. Bawendi et al.<sup>56</sup> reported  $\text{Fe}_2\text{O}_3$  nanoparticles, among other metal particles which were well dispersible in water after functionalization with a phosphonate-functionalized PEG. Furthermore, McQuillan et al. reported a binding constant of phosphate ions onto  $\text{TiO}_2$  films ( $k_s=3.8 \times 10^4$  L/mol, pH=2.3)<sup>57</sup> similar to the one for the catechol species ( $k_s=8 \times 10^4$  L/mol, pH=3.6).<sup>58</sup> Wang et al. recently reported a displacement of catechols by phosphate ions from phosphate buffer on magnetite NPs at pH 4.5 and 6.5.<sup>59</sup>

The binding between the PPEs and magnetite particles was further analyzed by IR spectroscopy (Figure 2.6): in all polymer-coated NP dispersions, the P=O stretch is detected at 1265-1257  $\text{cm}^{-1}$ .

This is in good agreement with literature values for triethyl phosphate.<sup>60</sup> Strong signals for the P-O-C stretches of polymer samples were measured at 969-966 and 1001  $\text{cm}^{-1}$ . For the functionalized NPs the band intensity at 969-966  $\text{cm}^{-1}$  decreases and shifts to higher wave numbers of 975-973  $\text{cm}^{-1}$ . The second band at 1001  $\text{cm}^{-1}$  remains its intensity and shows clear shift to higher wavenumbers as well (1015-1013  $\text{cm}^{-1}$ ). These shifts indicate a binding of the phosphoester groups of all polymers to the NPs and are thus responsible for the stabilization of the NPs in polar solvents. However, for functionalized NPs with **poly4-1-dep**, an additional observation can be made: While in the IR spectrum of the polymer a small signal at 1520  $\text{cm}^{-1}$  can be observed, it disappears in the spectrum for functionalized NPs. The signal refers to a C-C ring stretch vibration of free catechol, according to Wesselink et al.<sup>61</sup> In their studies, the signal also disappeared upon complexation of alumina as well as upon adsorption of free catechol groups. It indicates an additional binding of the catechol groups to the nanoparticles.

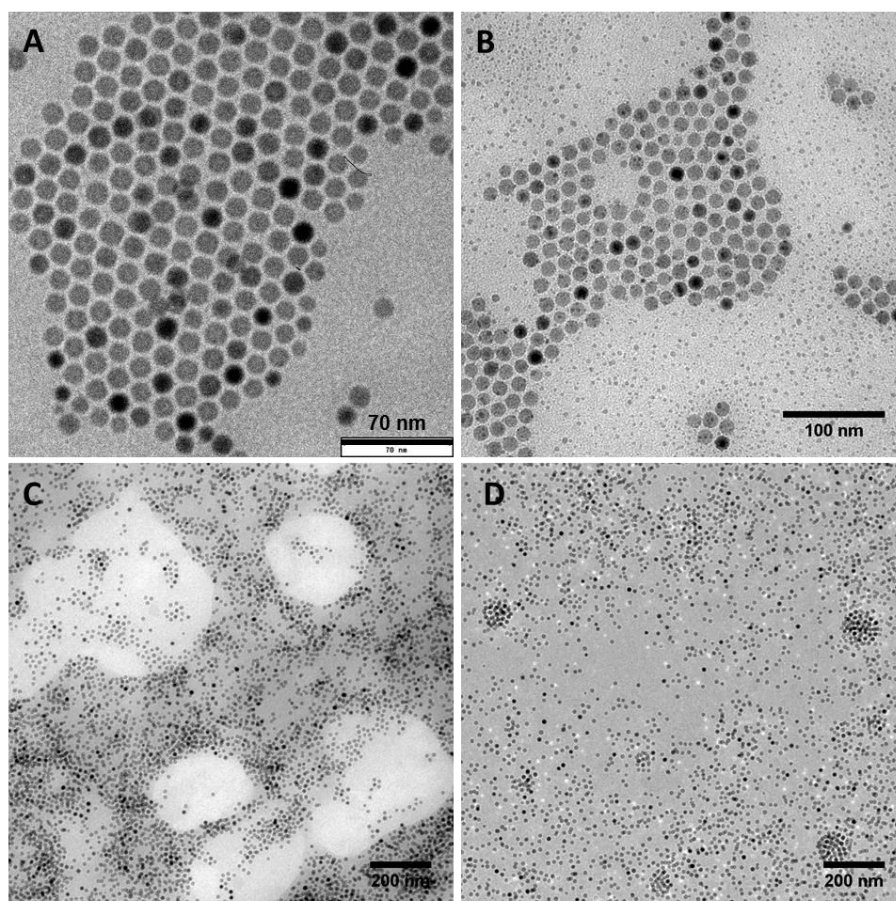


**Figure 2.5.** TEM image of magnetite nanoparticles (NPs): (A) NPs stabilized with oleic acid; (B) functionalized NPs with **poly2-2**; (C) functionalized NPs with **poly4-1-dep**; (D) functionalized NPs with **poly5-2**.

Isothermal titration calorimetry (ITC), a useful technique for quantification of interactions in polymer hybrid systems,<sup>62</sup> revealed the binding of all polymers to the NPs due to an exothermic interaction (negative  $\Delta H$  values) when titrated to the NP dispersion in chloroform (Table 2.2; Figure 2.6 shows a representative titration diagram for **poly4-1-dep**, all other diagrams are shown in the Supporting Information, Figure S2.48). For all polymers about 900-3,800 chains bind to each NP (binding stoichiometry  $N$ ). The binding affinities (association constant  $k_A$ ) significantly differ for the polymers carrying different adhesive groups. **Poly2-2** (pure ethyl) and **poly4-1** (with protected catechols) carry only phosphotriester units that can act as adhesive functionalities to the NPs; ITC determines similar values of 6,500 and 5,700 L/mol for both polymers. After hydrolysis, **poly4-1-dep** carries free catechol groups and a much stronger binding affinity ( $k_A = 15,300$  L/mol) is detected. For **Poly5-2**, a binding affinity of about 4,000 L/mol was detected, however, this last value should only be taken as an estimate, as the integrated heat data does not show a lower plateau which is needed for exact calculation. In summary, all polymers bind to the NPs with their phosphoester groups in the backbone and can stabilize them in polar organic solvents. The free catechol groups of **poly4-1** contribute to binding and therefore a higher binding affinity can be observed.

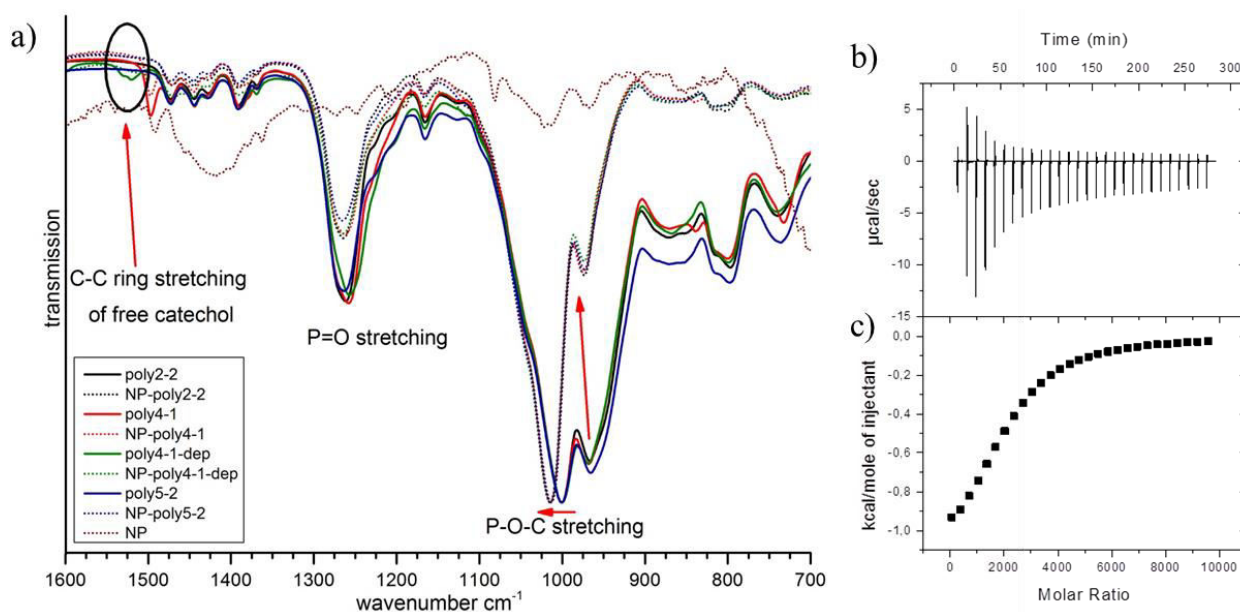


**Figure 2.6.** Analysis of binding of polymers to NPs: (a) IR spectra of polymers, oleic acid-functionalized nanoparticles (NPs), and functionalized NPs (the P=O and P-O-C stretching vibrations for polymers and shift for functionalized particles, as well as C-C ring stretching of free catechol in **poly4-1-dep** and disappearance in **NP-poly4-1-dep** are highlighted); (b) ITC: titration diagram for the interaction of polymer **poly4-1-dep** with magnetite nanoparticles: raw heat rate; (c) integrated heat of each peak (titration isotherms).

**Table 2.2.** Isothermal titration calorimetry (ITC) data of iron oxide nanoparticles and PPEs.

sample	$N^a$	$K_A^b$ (L mol <sup>-1</sup> )	$\Delta H$ (kcal mol <sup>-1</sup> )	$\Delta G$ (kcal mol <sup>-1</sup> )	$T\Delta S$ (kcal mol <sup>-1</sup> )
<b>poly4-1-dep</b>	1,700	15,300	-1.0	-4.9	4.5
<b>poly4-1</b>	3,800	5,700	-0.5	-5.1	4.6
<b>poly2-2</b>	1,600	6,500	-1.0	-5.1	4.1
<b>poly5-2</b>	900	(4,000)*	-3.1	-4.9	1.8

<sup>a</sup>Binding stoichiometry. <sup>b</sup>Association constant. \*See main text for details.

## 2.5 Conclusions

The joining of two natural adhesives: the catechol motif was combined with phosphate units in degradable poly(phosphoester)s for the first time. Since poly(phosphoester)s (PPEs) are biocompatible and biodegradable, catechol-containing PPEs are interesting materials for biomedical applications, that is, as adhesive gels for soft tissue engineering or for nanocarrier functionalization.

Two adhesive motifs were compared: PPEs with adhesive catechols and P-OH groups were synthesized by ADMET polymerization. While the P-OH-groups can be incorporated to a certain extent by polymerization of the unprotected monomer, the catechol needs to be protected. A novel catechol-containing phosphate monomer was designed, protected as ketal, and homo- as well as copolymerized with molecular weights up to 42,000 g/mol. Deprotection of the catechol units was achieved without any backbone degradation under carefully selected acidic conditions in several minutes. The P-OH-containing monomer was successfully copolymerized with a phosphotriester comonomer with up to 20 mol% P-OH (higher amounts of P-OH showed catalyst deactivation).

All polymers, either carrying phosphotriesters only, catechols, or phosphodiester (i.e., with P-OH groups) adhere onto the surface of magnetite nanoparticles and stabilize them in polar solvents due to binding of phosphoester groups. In addition, polymers with catechol groups proved higher binding affinity to the magnetite NPs because of additional binding of the adhesive group to the NPs. Besides binding to metal oxides, catechol-containing PPEs can form cross-linked gels under oxidizing conditions to PPE-hydro- and organogels which show a swelling of up to 1000%. This is the first step toward PPE-catechol hydrogels for drug delivery or tissue engineering, however, higher swelling ratios are necessary, which is currently under investigation in our group.

## 2.6 Acknowledgments

The authors thank Prof. Dr. Katharina Landfester (MPIP) for her support. G.B. and E.S. are recipients of a fellowship through funding of the Excellence Initiative (DFG/GSC 266) in the context of the graduate school of excellence "MAINZ" (Material Sciences in Mainz). E.S. and F.R.W. are grateful to the Max Planck Graduate School (MPGC) for support. F.R.W. thanks the Deutsche Forschungsgemeinschaft (DFG, WU750/5-1) for support.

## 2.7 Supporting Information

The Supporting Information contains additional synthetic procedures, characterization data for monomers, polymers, nanoparticle interactions, degradation studies, and further images.

### Content

- 2.7.1 Synthetic procedures
- 2.7.2 Monomers:
  - a. NMR spectra
  - b. IR spectra
- 2.7.3 Polymers:
  - a. NMR spectra
  - b. GPC diagrams
- 2.7.4 Degradation studies
- 2.7.5 Gels
- 2.7.6 Magnetite particles:
  - a. Biphasic system
  - b. TEM images
  - c. IR spectra
  - d. ITC data

### 2.7.1 Synthetic procedures

*2,2-Dimethyl-1,3-benzodioxole-5-propanol*: The alcohol was synthesized according to literature<sup>39</sup>. Briefly, a three-neck round-bottom flask was equipped with a Soxhlet extractor with a reflux condenser. The Soxhlet thimble was filled with CaCl<sub>2</sub>. 3,4-dihydroxyhydrocinnamic acid

(20.0 g, 109.8 mmol, 1 eq.) and p-toluenesulfonic acid monohydrate (756.19 mg, 4.39 mmol, 0.04 eq.) were dissolved in 750 mL benzene. 2,2-Dimethoxypropane (17.15 g, 164.68 mmol, 1.5 eq.) was added and the reaction mixture was refluxed overnight. The solution was filtered and the solvent concentrated under reduced pressure. The crude product was not further purified (TLC, petroleum ether/ethyl acetate 7:3). A three-neck round-bottom flask was equipped with a reflux condenser and a dropping funnel. LiAlH<sub>4</sub> in THF (2.4M, 100.65 mL, 241.5 mmol, 2.2 eq.) was dissolved in 700 mL of dry diethyl ether. The crude product (24.40 g, 109.8 mmol, 1 eq.), dissolved in 100 mL of dry diethyl ether, was added dropwise in order to keep the diethyl ether refluxing and the reaction mixture was stirred overnight. Excess of LiAlH<sub>4</sub> was decomposed by addition of ice water. Precipitated aluminum hydroxide was filtered off and washed with diethyl ether. After drying over magensia sulfate, the solvent was concentrated under reduced pressure. Column chromatography (silica gel, petroleum ether/ethyl acetate 7:3) gave the pure product. Yield: 65%. <sup>1</sup>H NMR (300 MHz, CDCl<sub>3</sub>): δ [ppm] 6.66–6.57 (m, 3 H, H<sub>arom</sub>), 3.66 (t, 2 H, CH<sub>2</sub>OH), 2.60 (t, 2 H, Ar-CH<sub>2</sub>CH<sub>2</sub>CH<sub>2</sub>-OH), 1.90– 1.78 (m, 2 H, Ar-CH<sub>2</sub>CH<sub>2</sub>CH<sub>2</sub>-OH), 1.65 (s, 6 H, CH<sub>3</sub>). <sup>13</sup>C {H} NMR (76 MHz, CDCl<sub>3</sub>): δ [ppm] 147.37 (O-C-CH-C), 145.45 (O-C-CH=CH), 134.90 (C-CH<sub>2</sub>), 120.40 (O-C-CH=CH), 117.49 (C(CH<sub>3</sub>)<sub>2</sub>), 108.62 (O-C-CH=C), 107.89 (O-C-CH=CH), 62.13 (C-CH<sub>2</sub>-CH<sub>2</sub>-CH<sub>2</sub>-OH), 34.41 (C-CH<sub>2</sub>-CH<sub>2</sub>-CH<sub>2</sub>-OH), 31.78 (C-CH<sub>2</sub>-CH<sub>2</sub>-CH<sub>2</sub>-OH), 25.78 (CH<sub>3</sub>).

## 2.7.2 Monomer

### a. NMR spectra

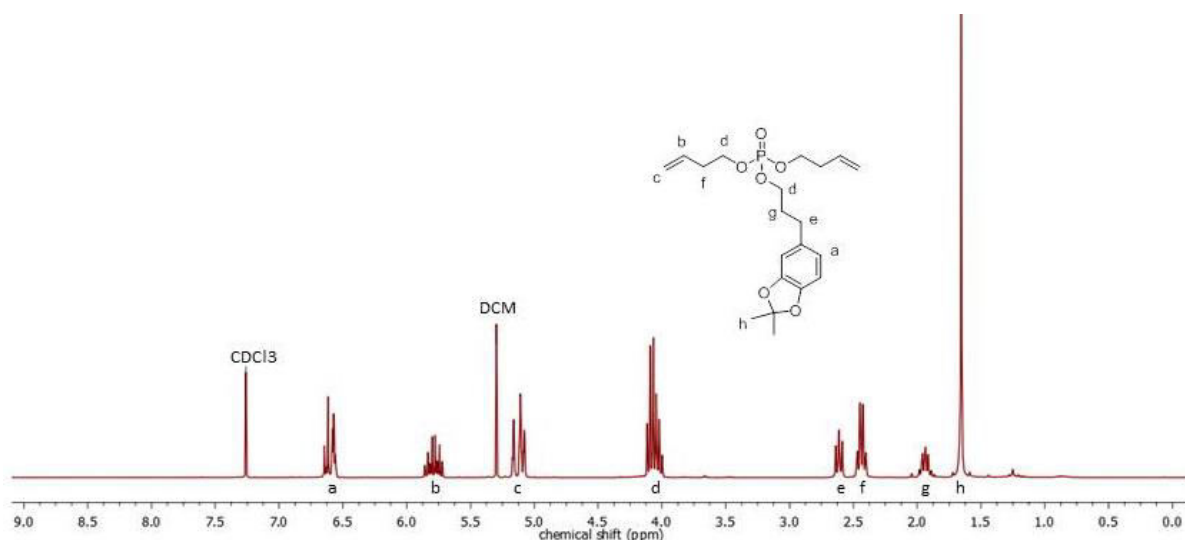


**Figure S2.1.** <sup>1</sup>H NMR (300 MHz, CDCl<sub>3</sub>) of monomer di-butenyl-(3-(2,2-dimethylbenzo[d][1,3]dioxol-5-yl) propyl) phosphate (**1**).

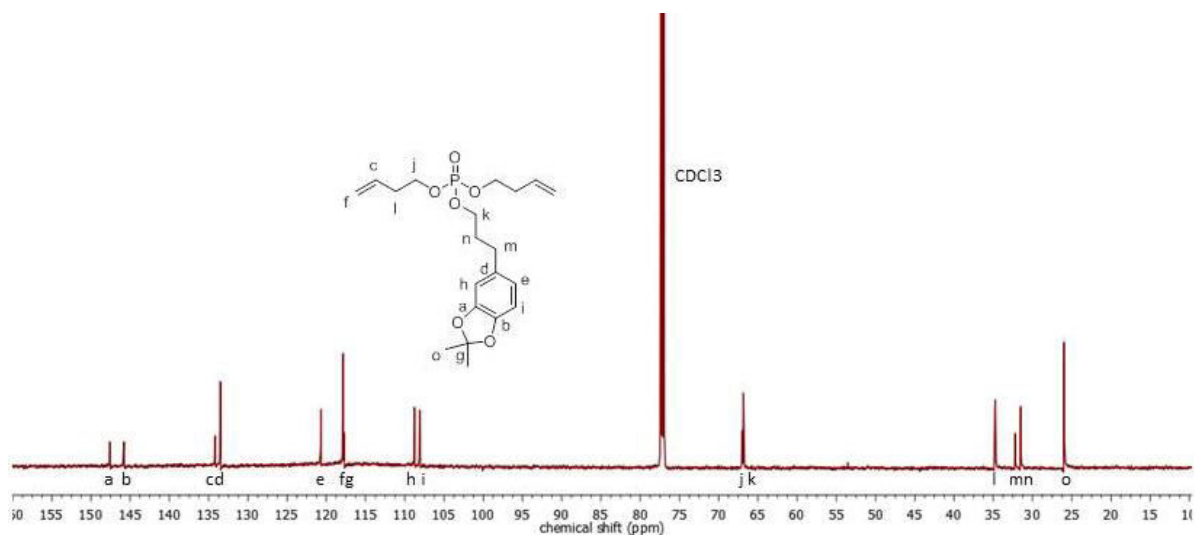


**Figure S2.2.**  $^{13}\text{C}$  {H} NMR (76 MHz,  $\text{CDCl}_3$ ) of monomer di-butenyl-(3-(2,2-dimethylbenzo[d][1,3]dioxol-5-yl) propyl) phosphate (**1**).

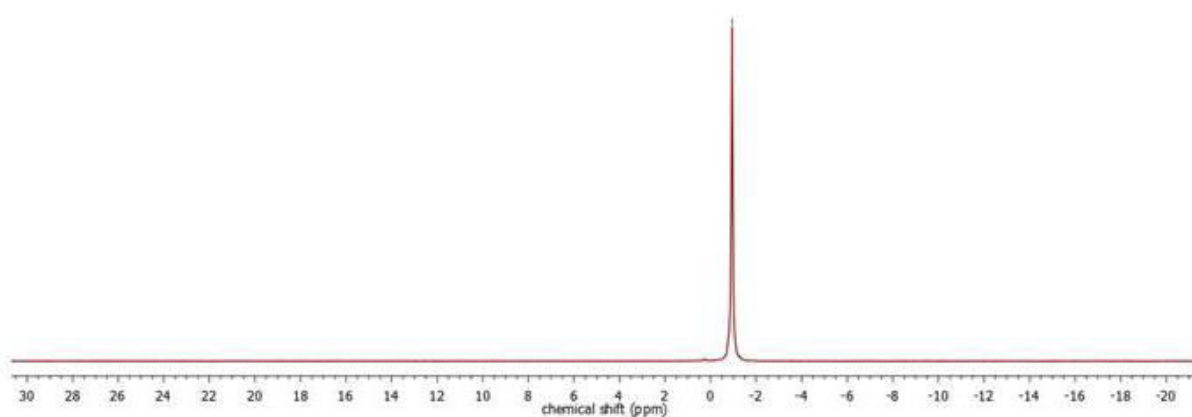


**Figure S2.3.**  $^{31}\text{P}$  {H} NMR (202 MHz,  $\text{CDCl}_3$ ) of monomer di-butenyl-(3-(2,2-dimethylbenzo[d][1,3]dioxol-5-yl) propyl) phosphate (**1**).

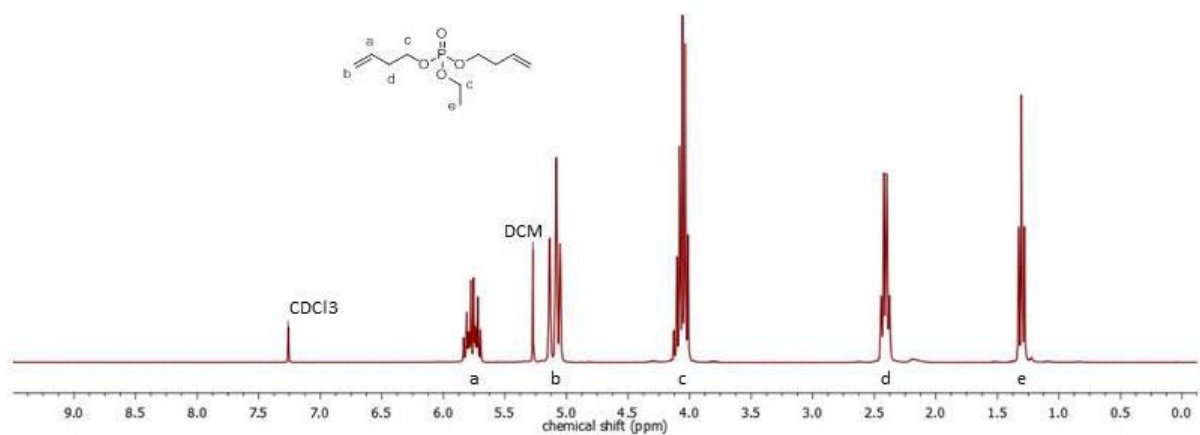


**Figure S2.4.**  $^1\text{H}$  NMR (300 MHz,  $\text{CDCl}_3$ ) of monomer di-butenyl-ethyl phosphate (**2**).

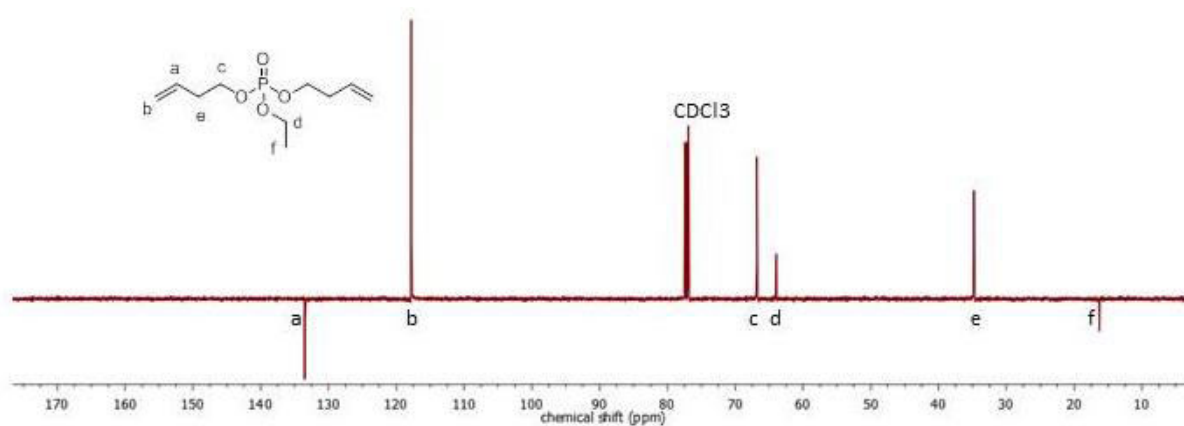


**Figure S2.5.**  $^{13}\text{C}$  {H} NMR (76 MHz,  $\text{CDCl}_3$ ) of monomer di-butenyl-ethyl phosphate (2).

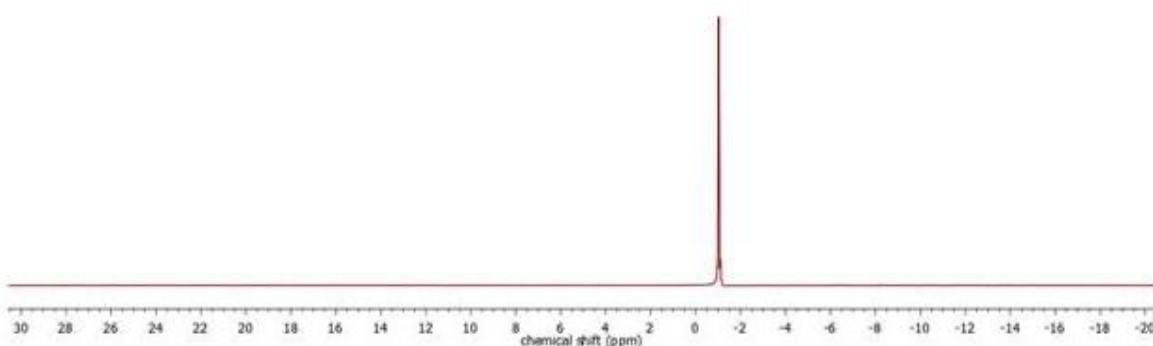


**Figure S2.6.**  $^{31}\text{P}$  {H} NMR (202 MHz,  $\text{CDCl}_3$ ) of monomer di-butenyl-ethyl phosphate (2).

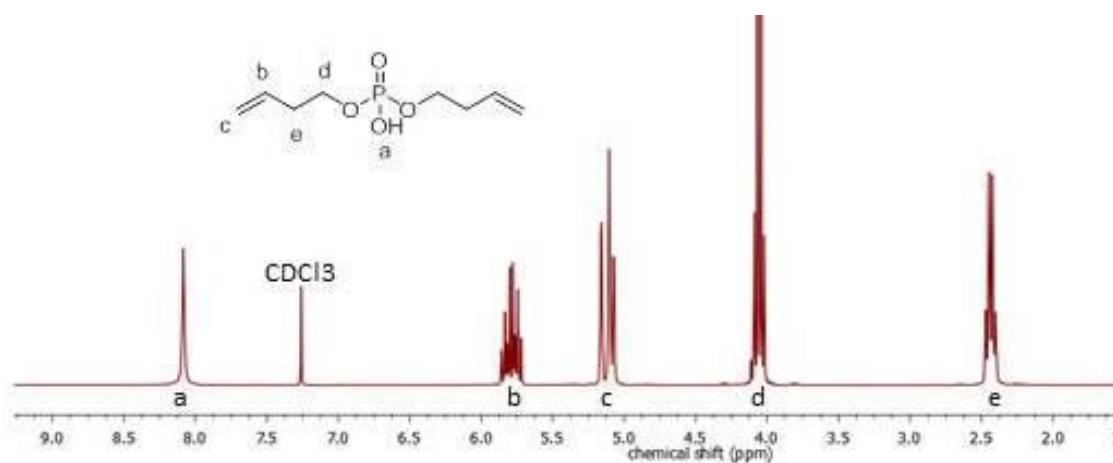


**Figure S2.7.**  $^1\text{H}$  NMR (300 MHz,  $\text{CDCl}_3$ ) of monomer di-butenyl-hydrogen phosphate (3).

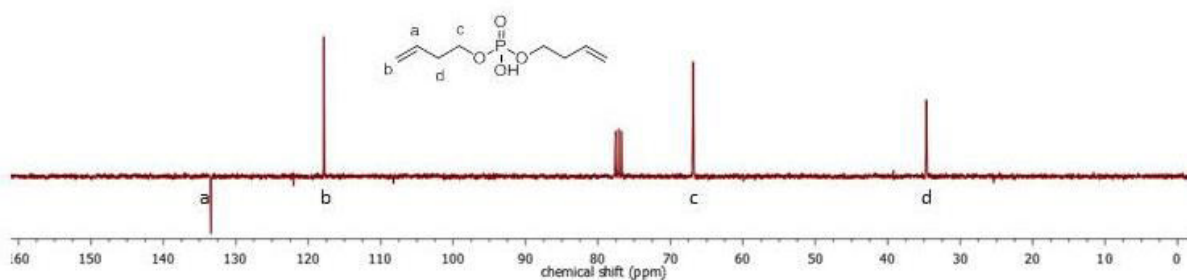


**Figure S2.8.**  $^{13}\text{C}$  {H} NMR (76 MHz,  $\text{CDCl}_3$ ) of monomer di-butenyl-hydrogen phosphate (3).

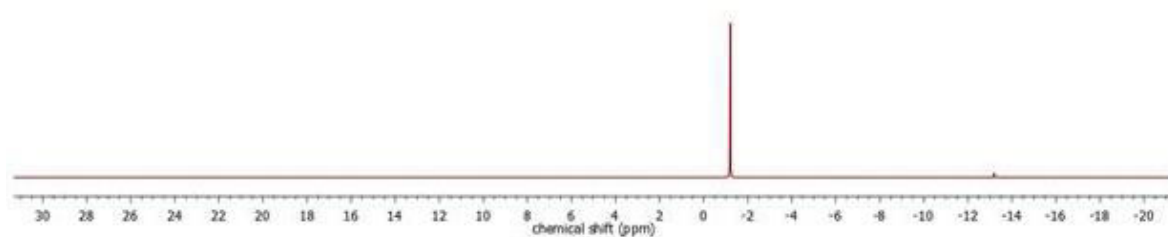


Figure S2.9.  $^{31}\text{P}$  {H} NMR (202 MHz,  $\text{CDCl}_3$ ) of monomer di-butenyl-hydrogen phosphate (3).

b. IR spectra

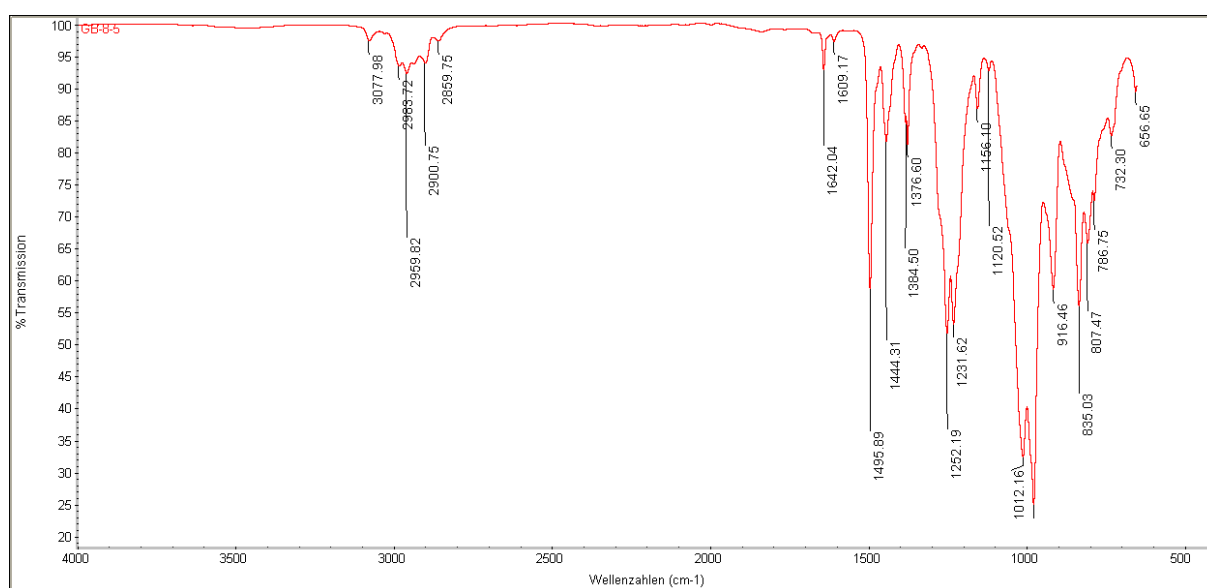


Figure S2.10. FTIR spectrum of (1) at 298 K.

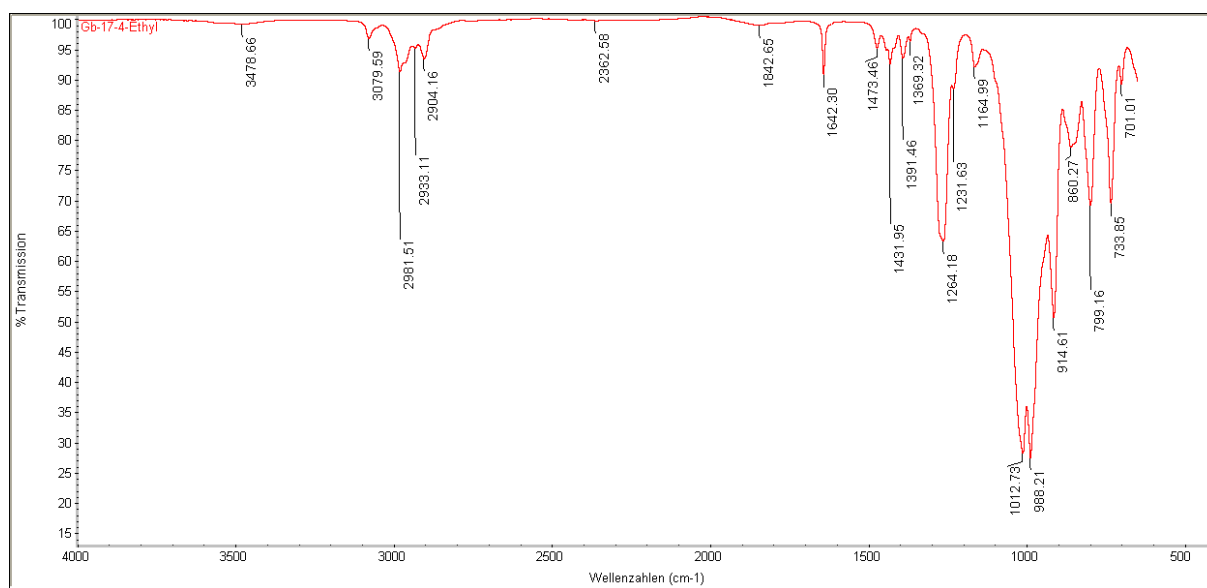


Figure S2.11. FTIR spectrum of (2) at 298 K.

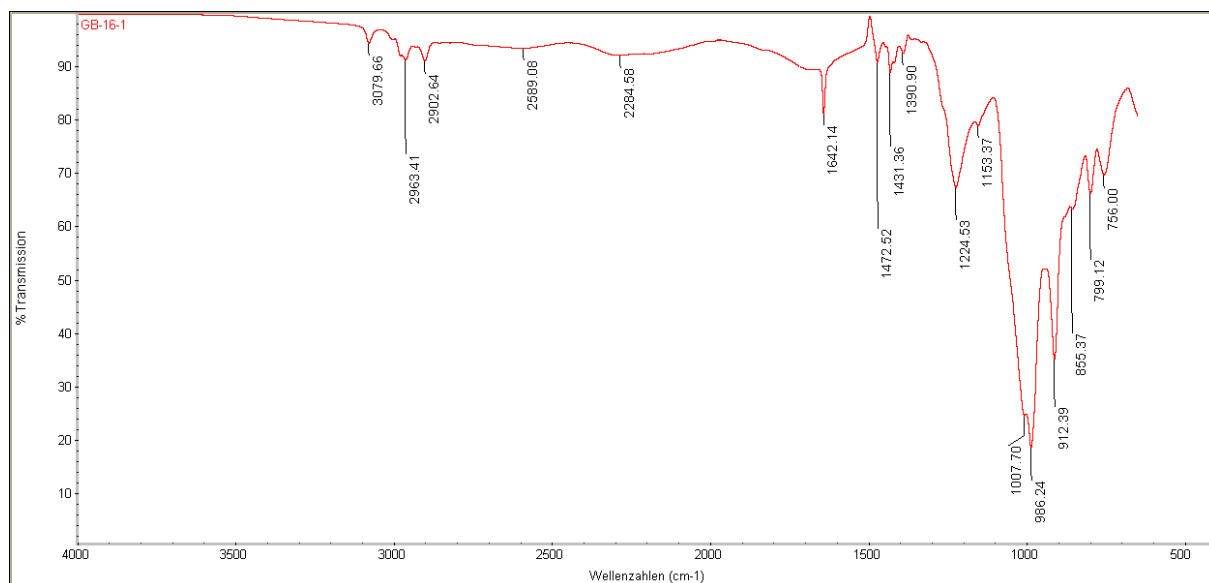


Figure S2.12. FTIR spectrum of (3) at 298 K.

### 2.7.3 Polymers

#### a. NMR spectra

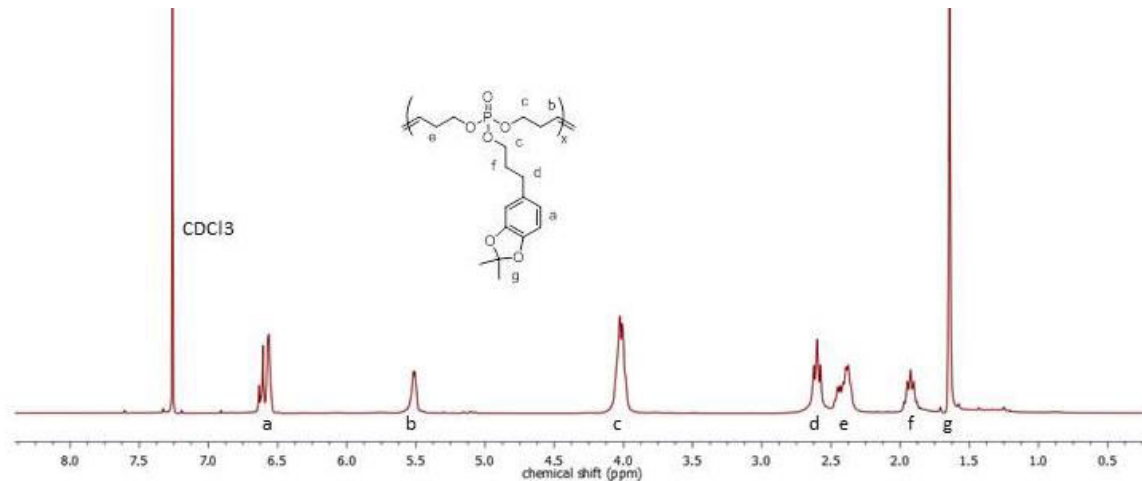


Figure S2.13. <sup>1</sup>H NMR (300 MHz, CDCl<sub>3</sub>) of (poly1).

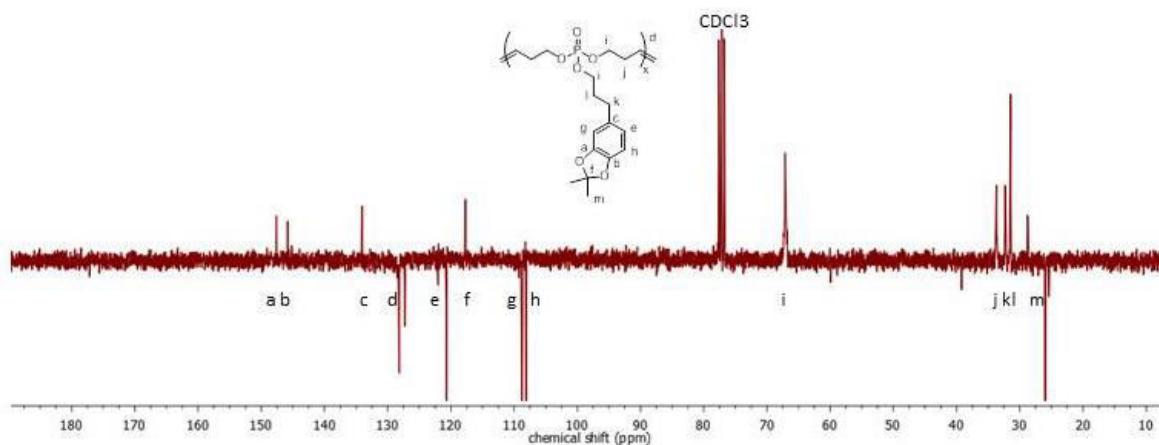


Figure S2.14.  $^{13}\text{C}$  {H} NMR (76 MHz,  $\text{CDCl}_3$ ) of (poly1).

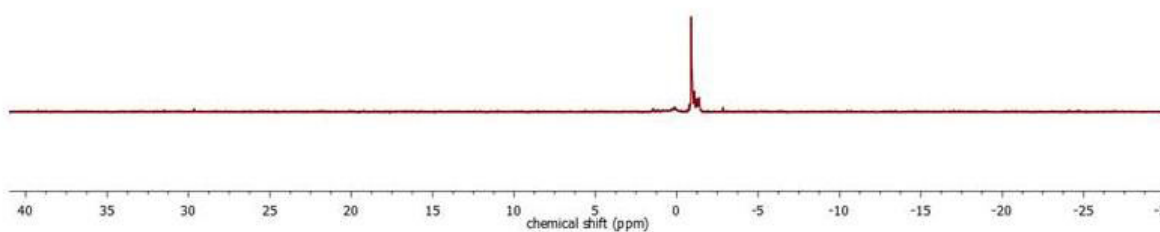


Figure S2.15.  $^{31}\text{P}$  {H} NMR (202 MHz,  $\text{CDCl}_3$ ) of (poly1).

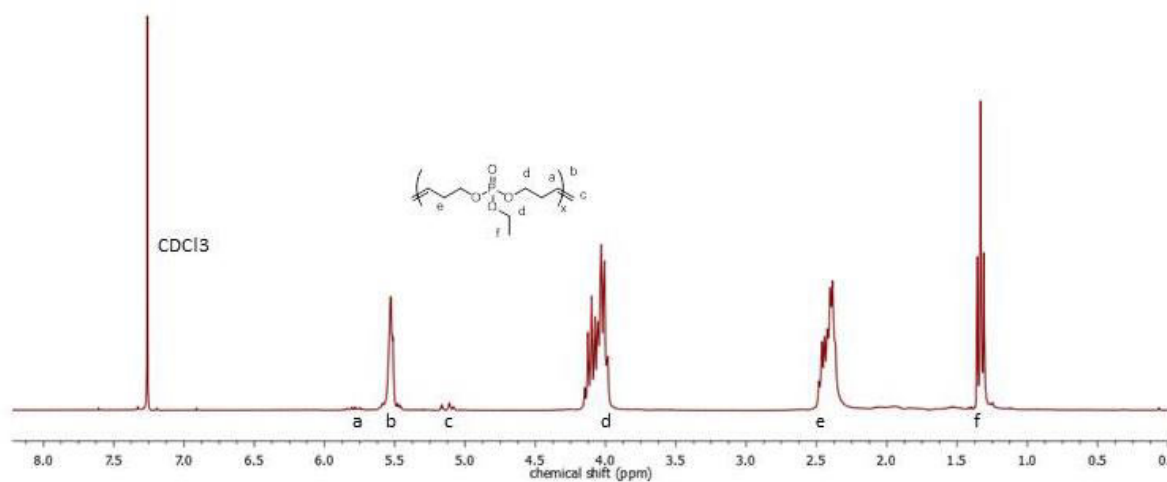


Figure S2.16.  $^1\text{H}$  NMR (300 MHz,  $\text{CDCl}_3$ ) of (poly2).

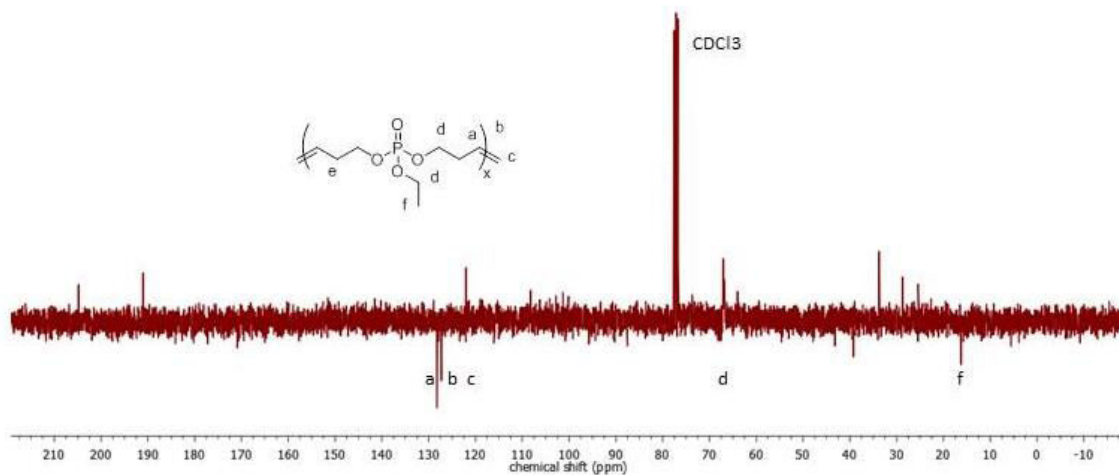


Figure S2.17.  $^{13}\text{C}$  {H} NMR (76 MHz,  $\text{CDCl}_3$ ) of (poly2).

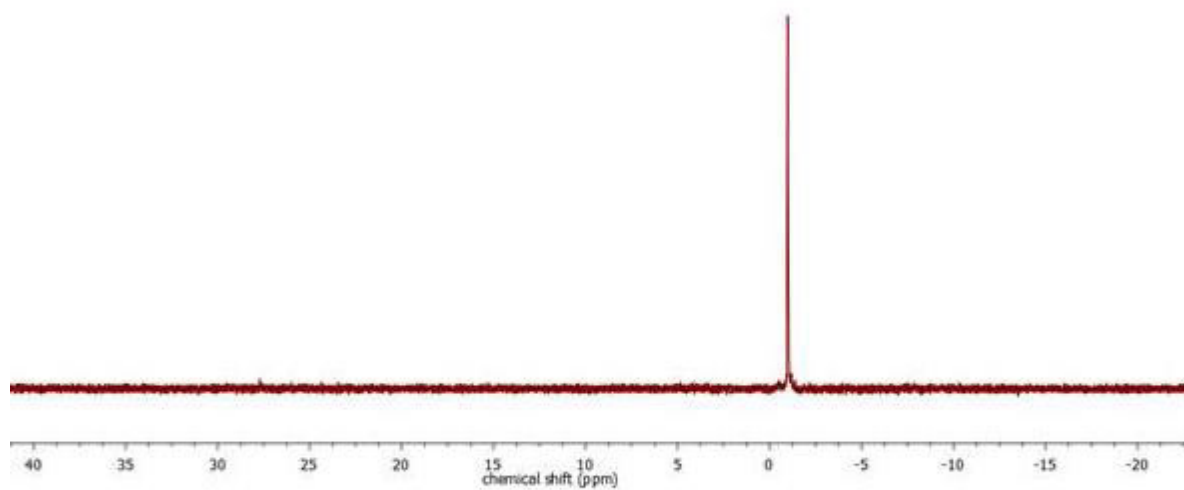


Figure S2.18.  $^{31}\text{P}$  {H} NMR (202 MHz,  $\text{CDCl}_3$ ) of (poly2).

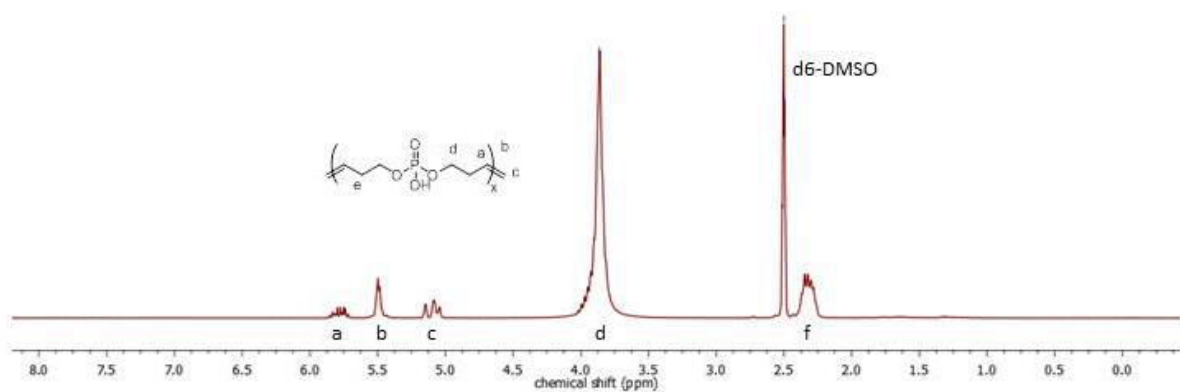


Figure S2.19.  $^1\text{H}$  NMR (300 MHz,  $\text{d}_6\text{-DMSO}$ ) of (poly3).

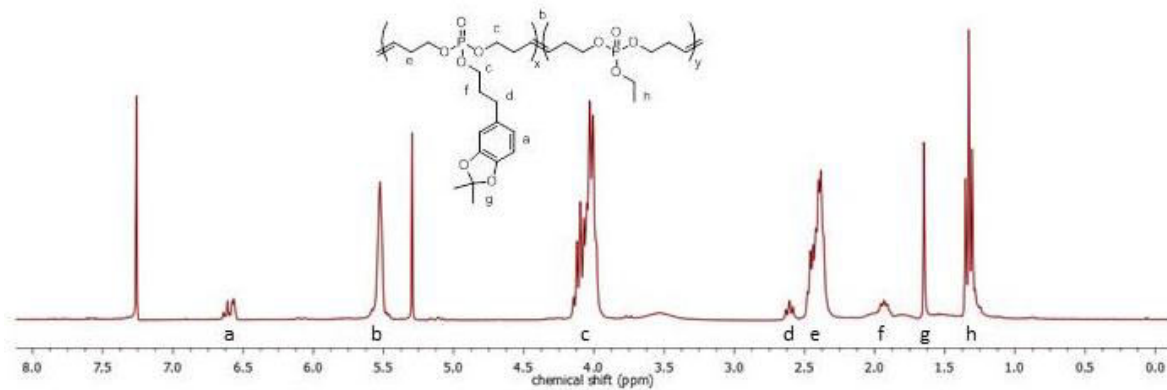


Figure S2.20. <sup>1</sup>H NMR (300 MHz, CDCl<sub>3</sub>) of (poly4).

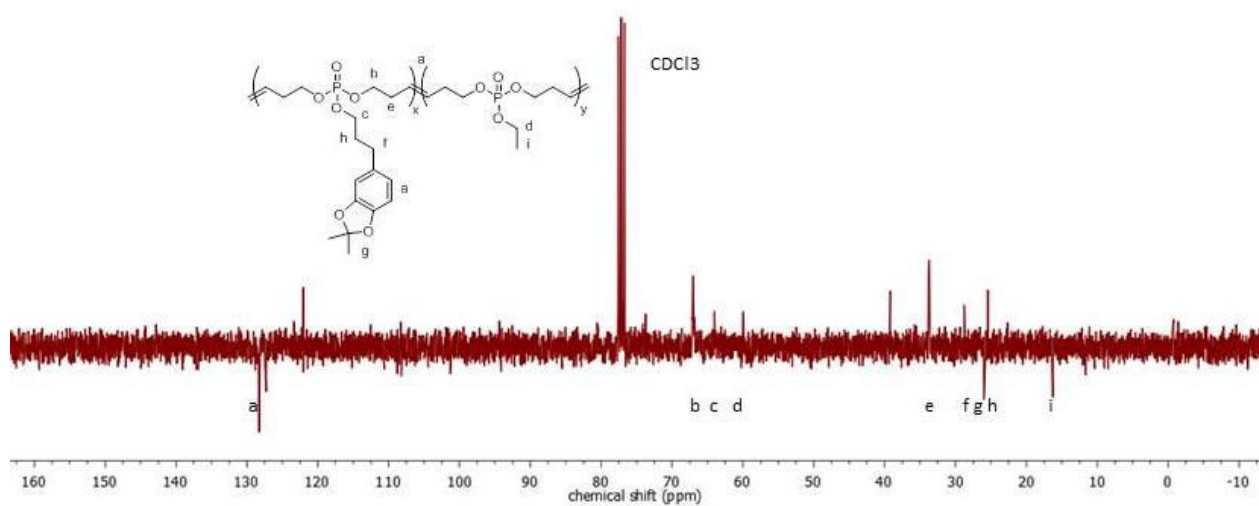


Figure S2.21. <sup>13</sup>C {<sup>1</sup>H} NMR (76 MHz, CDCl<sub>3</sub>) of (poly4).

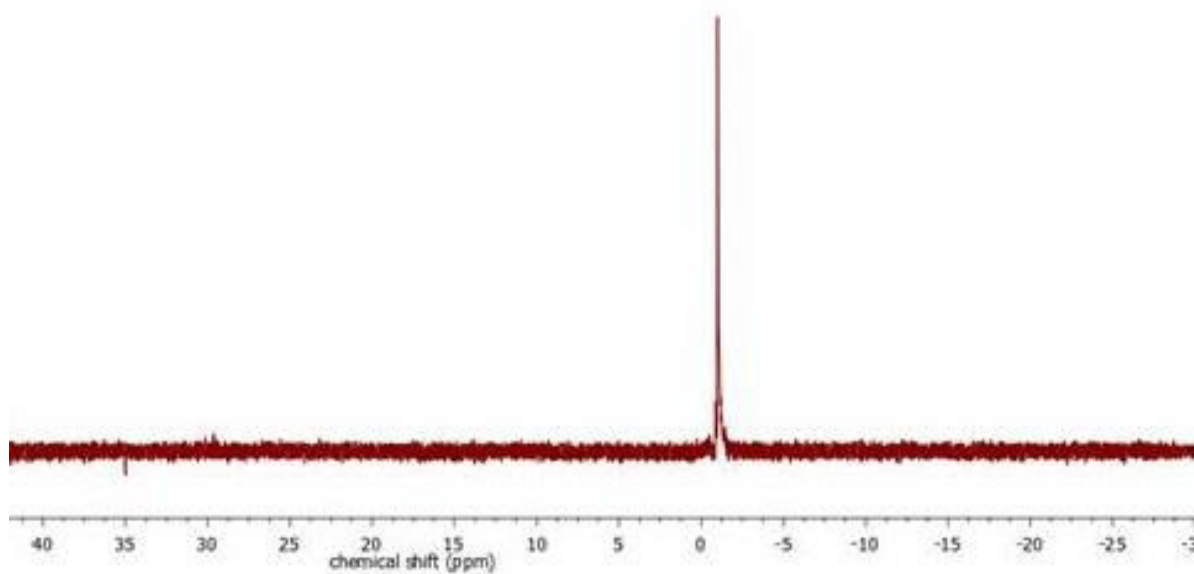


Figure S2.22. <sup>31</sup>P {<sup>1</sup>H} NMR (202 MHz, CDCl<sub>3</sub>) of (poly4).

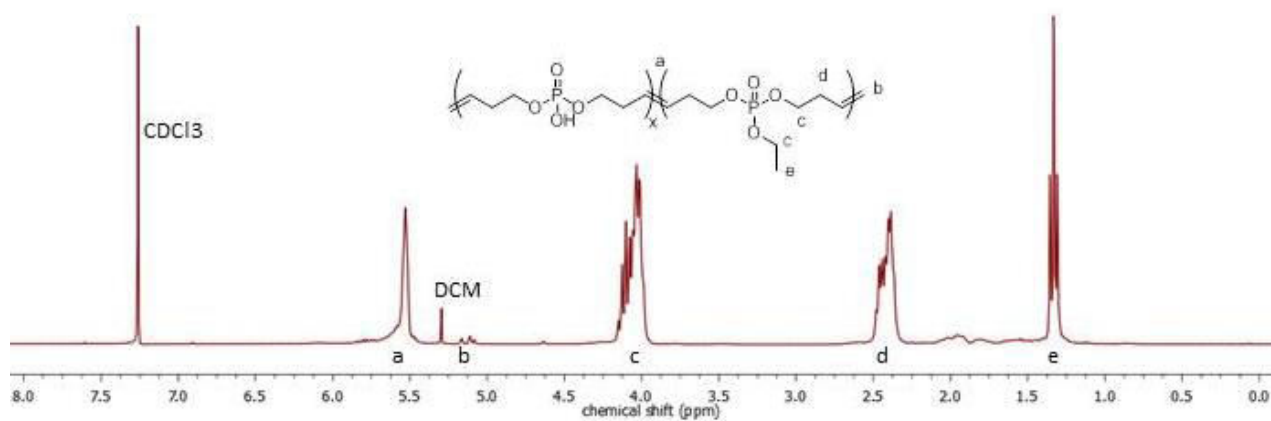


Figure S2.23.  $^1\text{H}$  NMR (300 MHz,  $\text{CDCl}_3$ ) of (poly5).

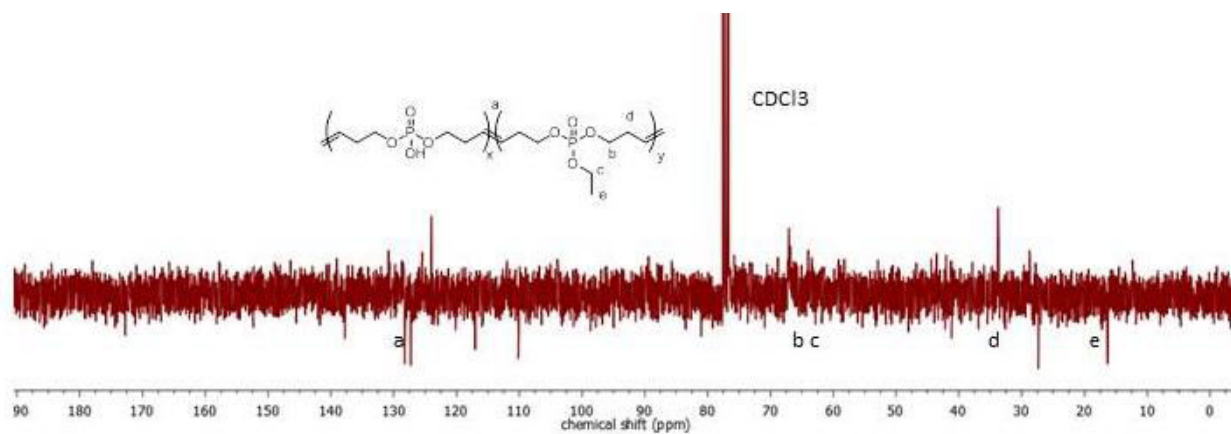


Figure S2.24.  $^{13}\text{C}$   $\{^1\text{H}\}$  NMR (76 MHz,  $\text{CDCl}_3$ ) of (poly5).

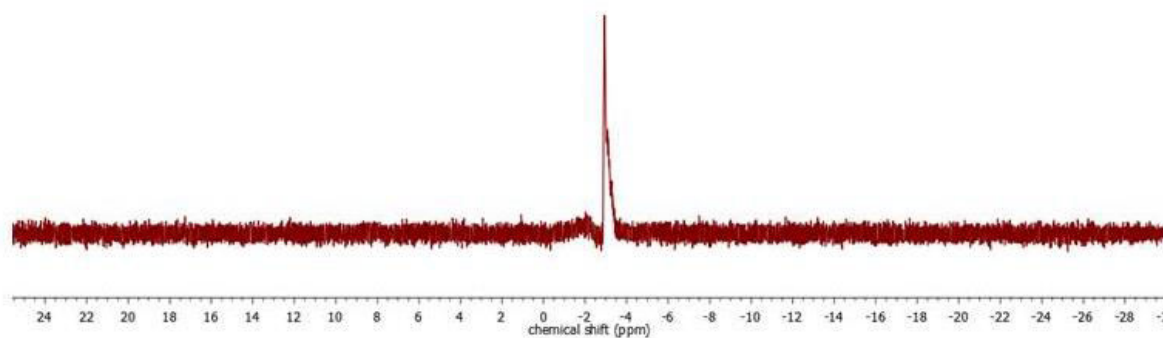


Figure S2.25.  $^{31}\text{P}$   $\{^1\text{H}\}$  NMR (202 MHz,  $\text{CDCl}_3$ ) of (poly5).

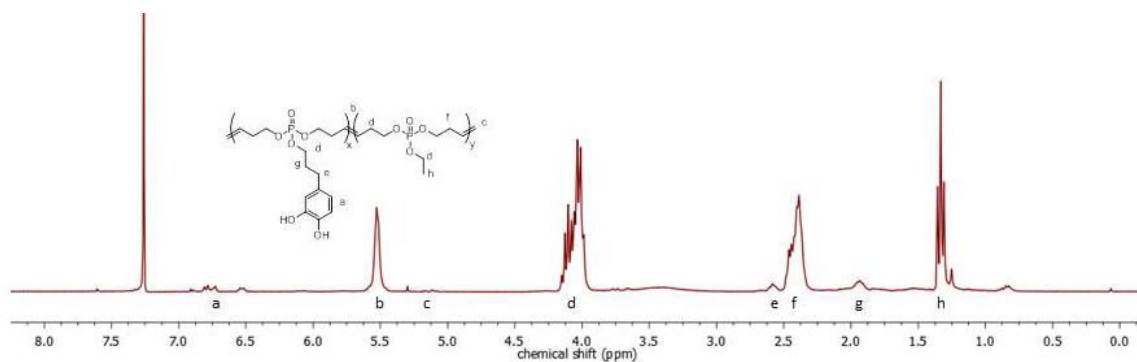


Figure S2.26.  $^1\text{H}$  NMR (300 MHz,  $\text{CDCl}_3$ ) of (poly4-1dep).

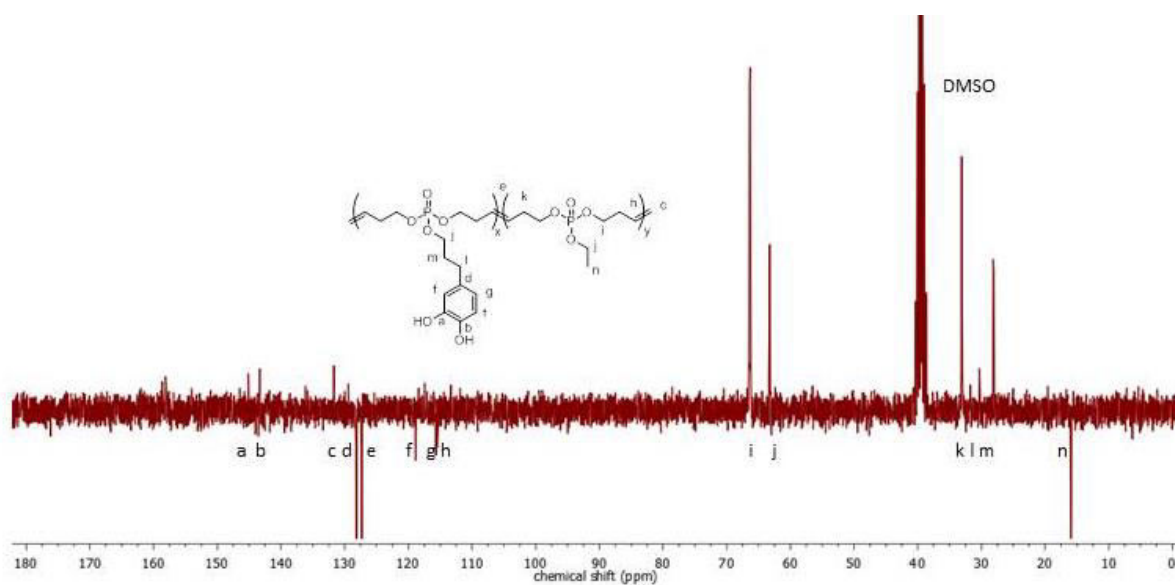


Figure S2.27.  $^{13}\text{C}$  { $^1\text{H}$ } NMR (76 MHz,  $\text{CDCl}_3$ ) of (poly4-1dep).

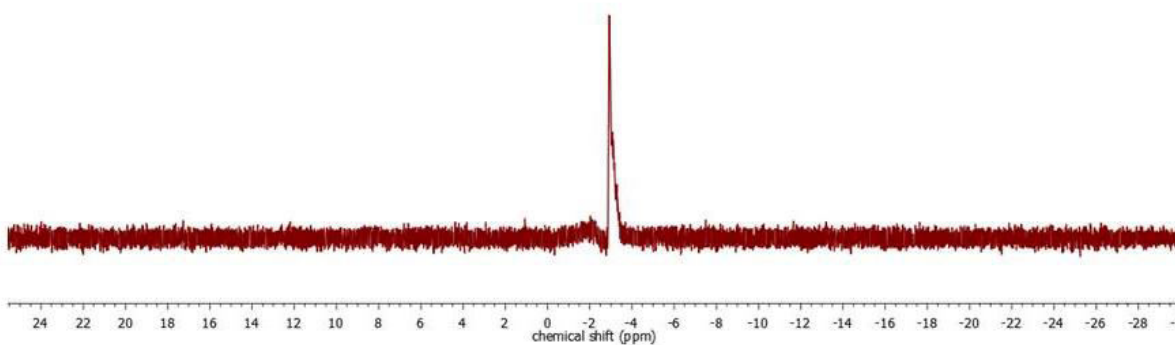
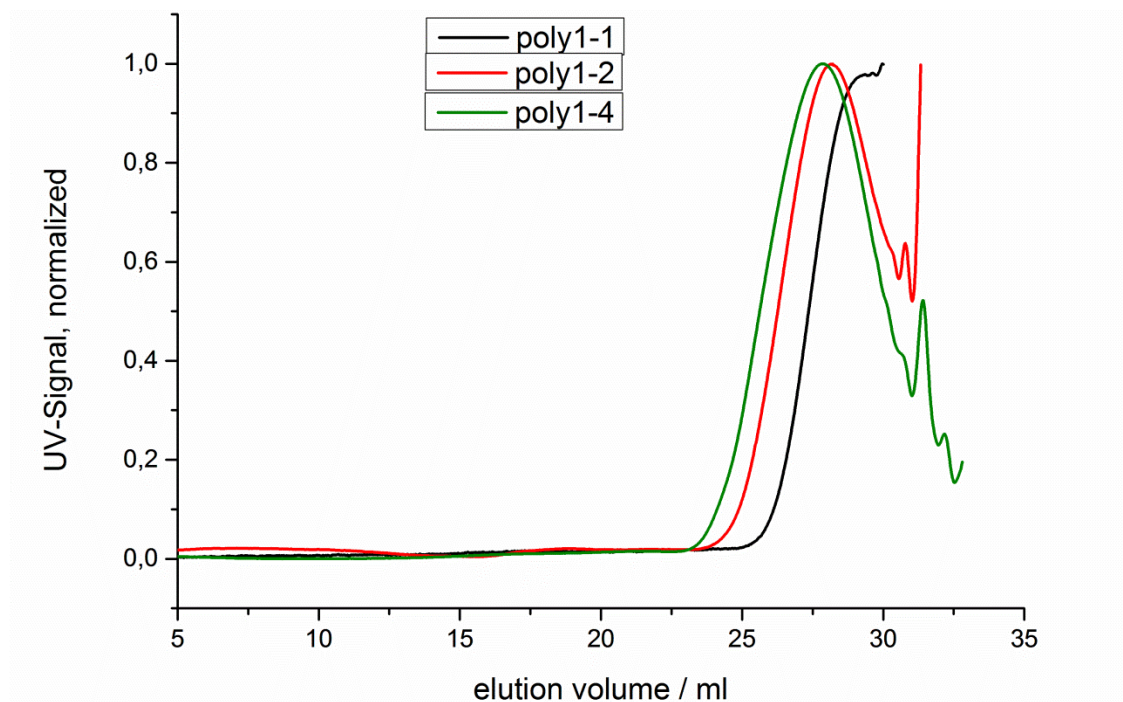
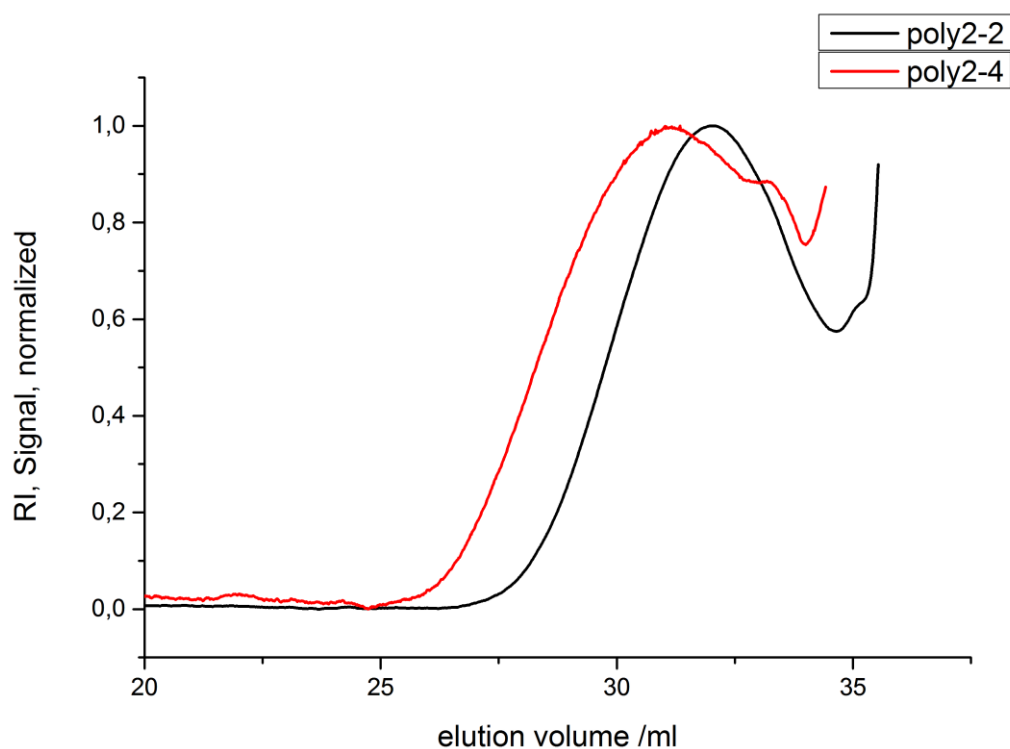


Figure S2.28.  $^{31}\text{P}$  { $^1\text{H}$ } NMR (202 MHz,  $\text{CDCl}_3$ ) of (poly4-1dep).

b. GPC diagrams



**Figure S2.29.** GPC elugrams of **poly1s** in THF, UV-Signal. Samples elute at the lower limit of GPC standard PS, increasing signal at 31 mL belongs to internal standard. Note, Elugram of poly1-3 not included.



**Figure S2.30.** GPC elugrams of **poly2s** in DMF, RI-Signal. Samples elute at the lower limit of GPC standard PS, increasing signal at 35 mL belongs to internal standard. Note, elugrams of poly2-1 and poly2-3 not included.

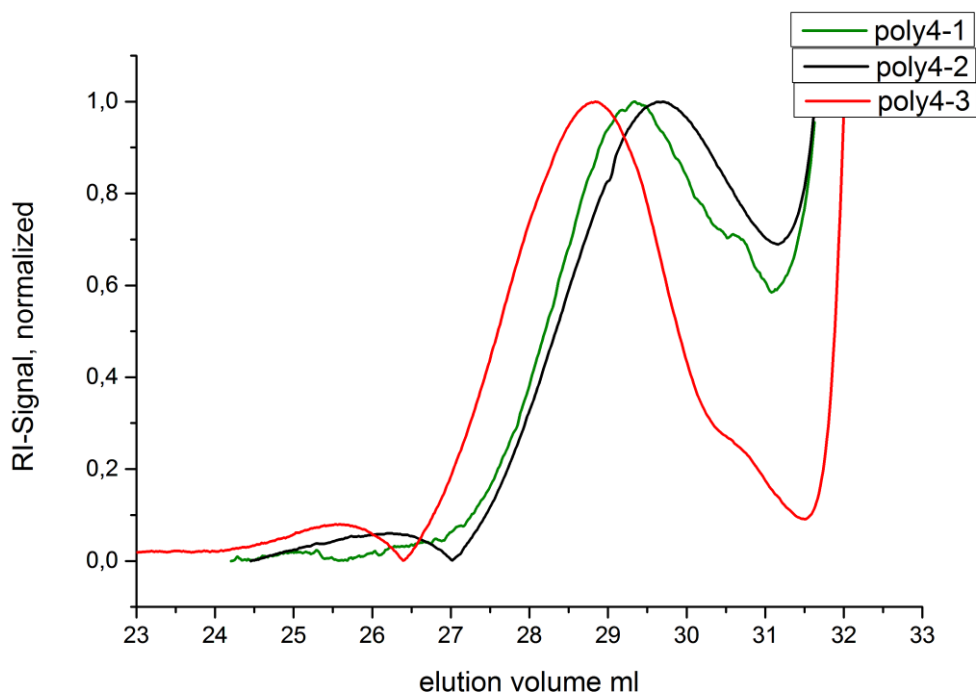


**Figure S2.31.** GPC elugrams of **poly4** in THF, RI-Signal. Samples elute at the lower limit of GPC standard PS, increasing signal at 32 mL belongs to internal standard.

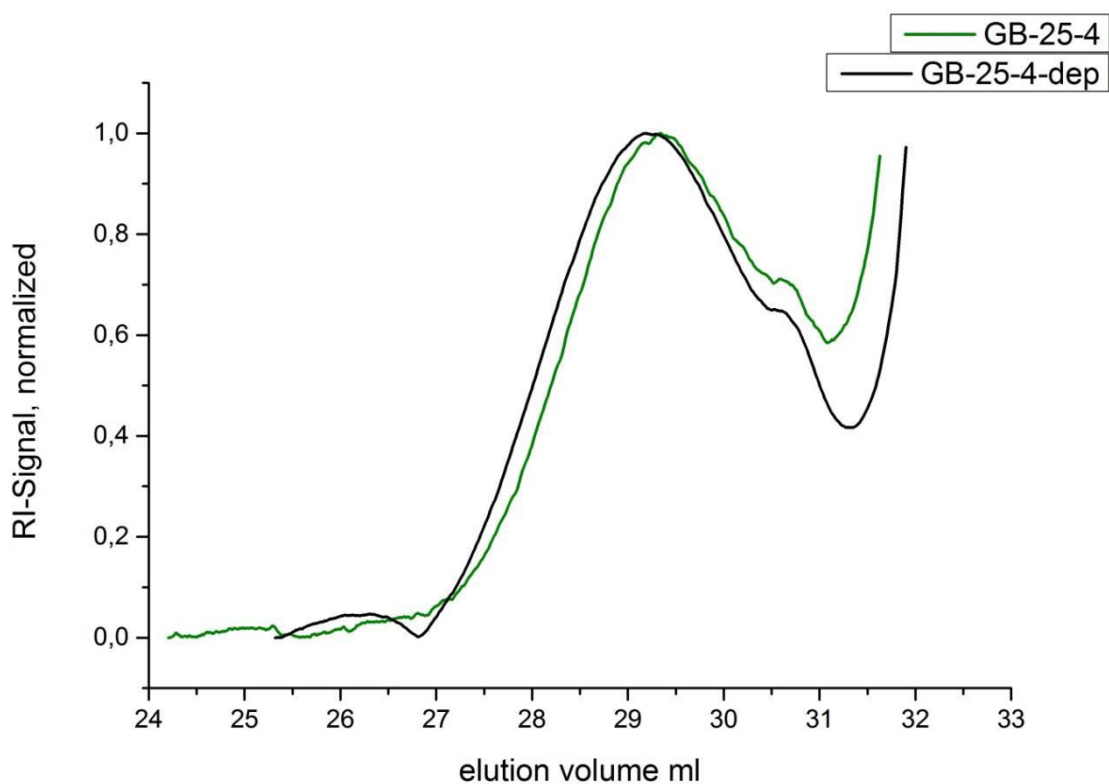


**Figure S2.32.** GPC elugrams of **poly4-1** and **poly4-1-dep** in THF, RI-Signal. Samples elute at the lower limit of GPC standard PS, increasing signal at 32 mL belongs to internal standard.

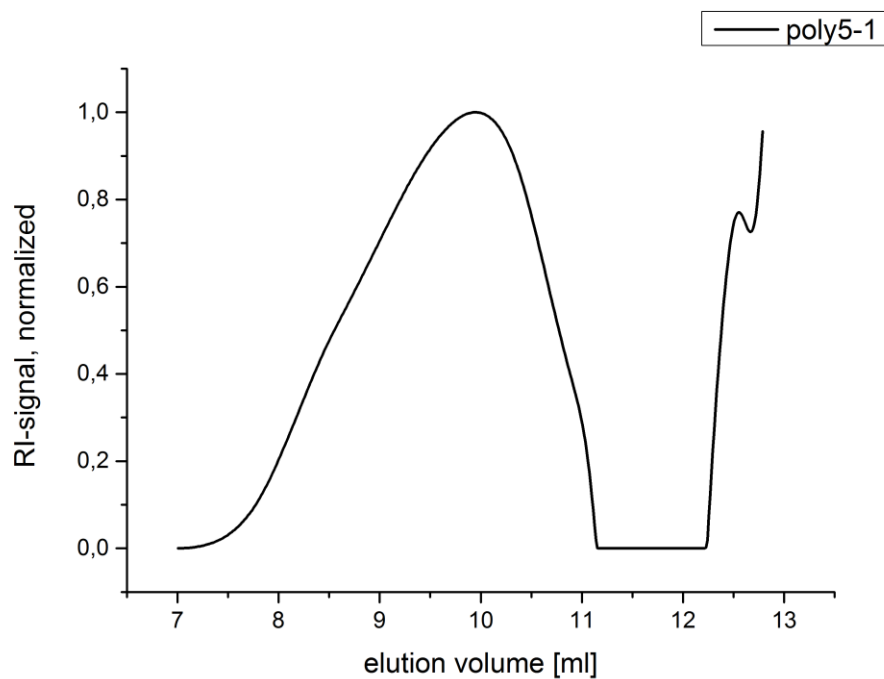


**Figure S2.33.** GPC elugram of **poly5-1** in DMSO, RI-signal. Signal at 12-13 mL belongs to internal standard.

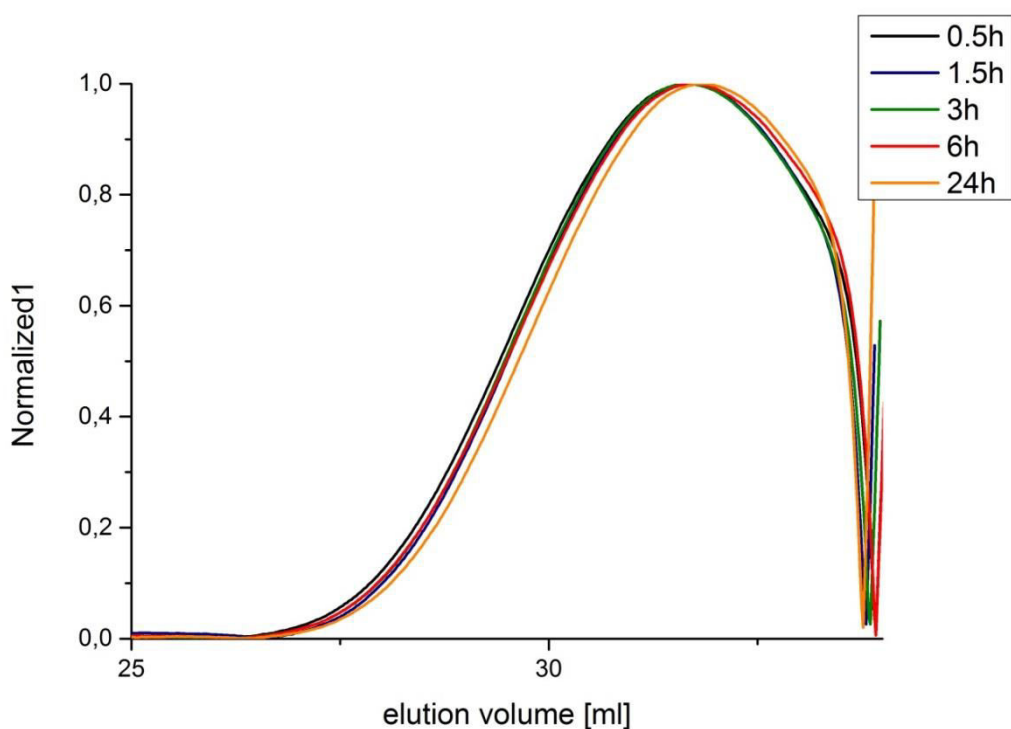
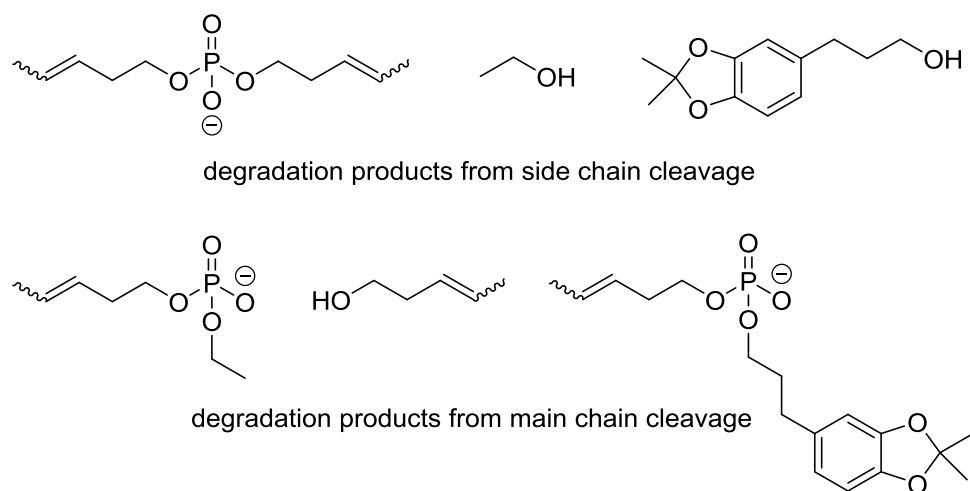


**Figure S2.34.** GPC elugrams of degradation of **poly2-2** in conc. TFA, in DMF, RI-signal. Samples elute at the lower limit of GPC standard PS, increasing signal at 35 mL belongs to internal standard.

### 2.7.4 Degradation studies



**Scheme S2.1.** Degradation products from main chain or side chain cleavage.

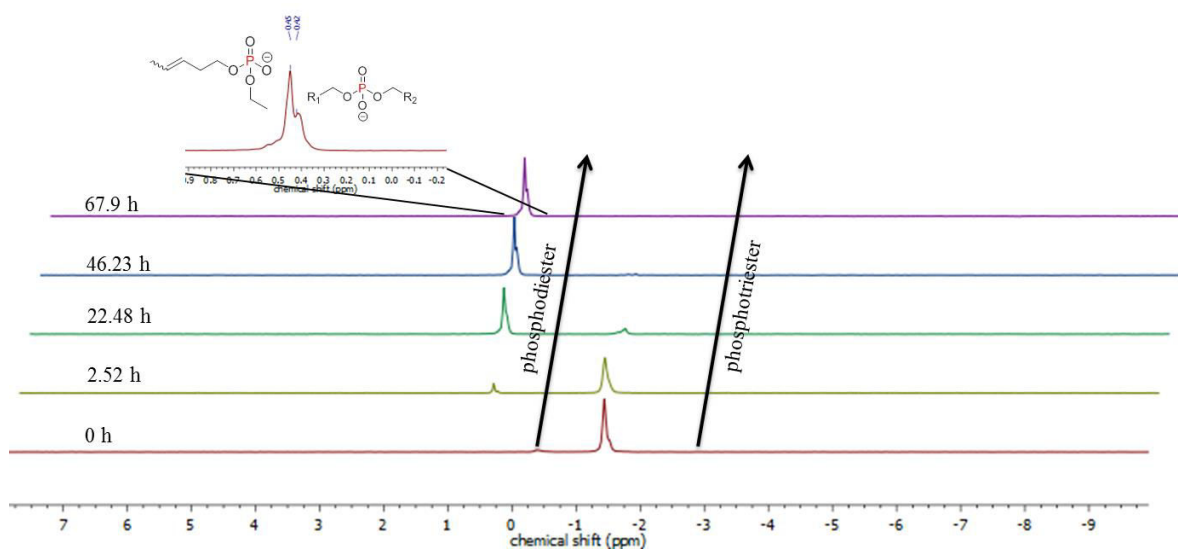


**Figure S2.35.** <sup>31</sup>P {H} NMR spectra (121 MHz, EtOD/D<sub>2</sub>O, 298K) of the degradation of **poly2-2**.

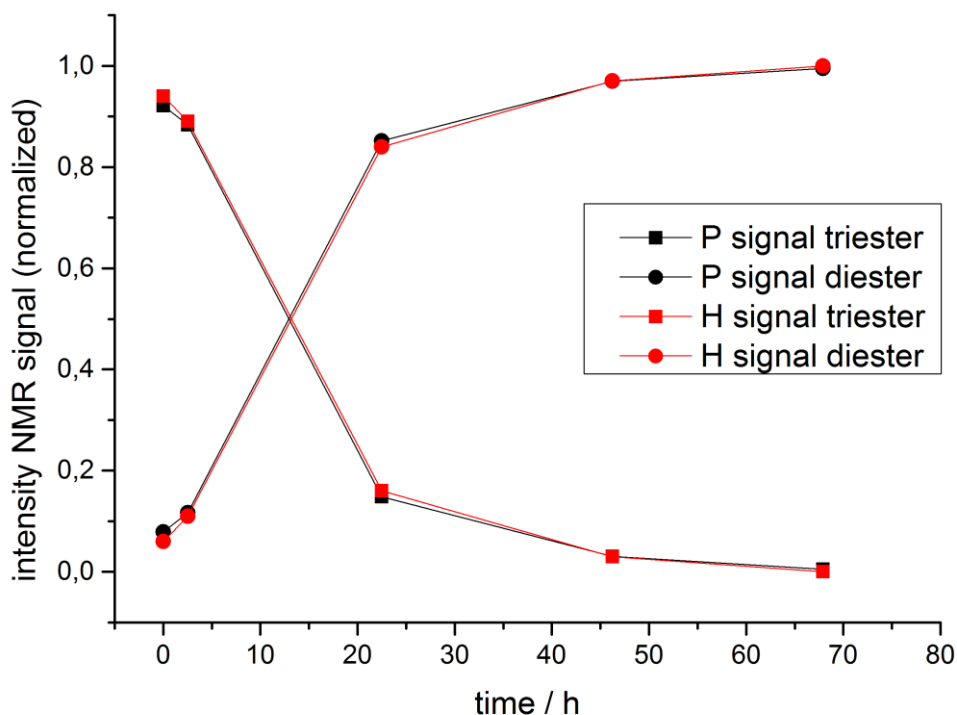


**Figure S2.36.** plotted intensity NMR signals (normalized) vs. degradation time: degradation of **poly2-2** from phosphotriesters to phosphodiester in  $^1\text{H}$  NMR and  $^{31}\text{P}$   $\{^1\text{H}\}$  NMR spectra.

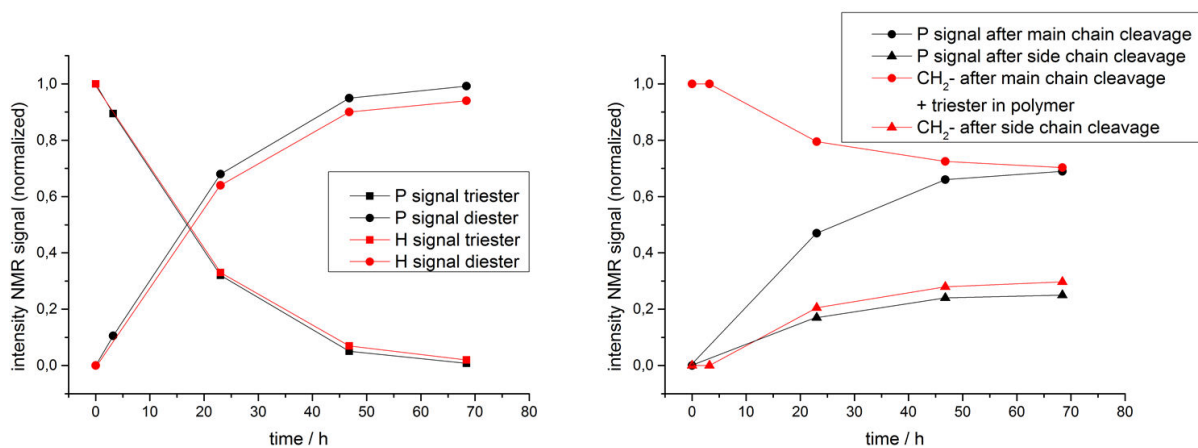


**Figure S2.37.** degradation studies, intensity NMR signals (normalized) vs. degradation time: left) degradation of **poly1-4** from phosphotriesters to phosphodiester in  $^1\text{H}$  NMR and  $^{31}\text{P}$   $\{^1\text{H}\}$  NMR spectra; right) cleavage from **poly1-4** at side chain and main chain ester bonds in  $^1\text{H}$  NMR and  $^{31}\text{P}$   $\{^1\text{H}\}$  NMR spectra.

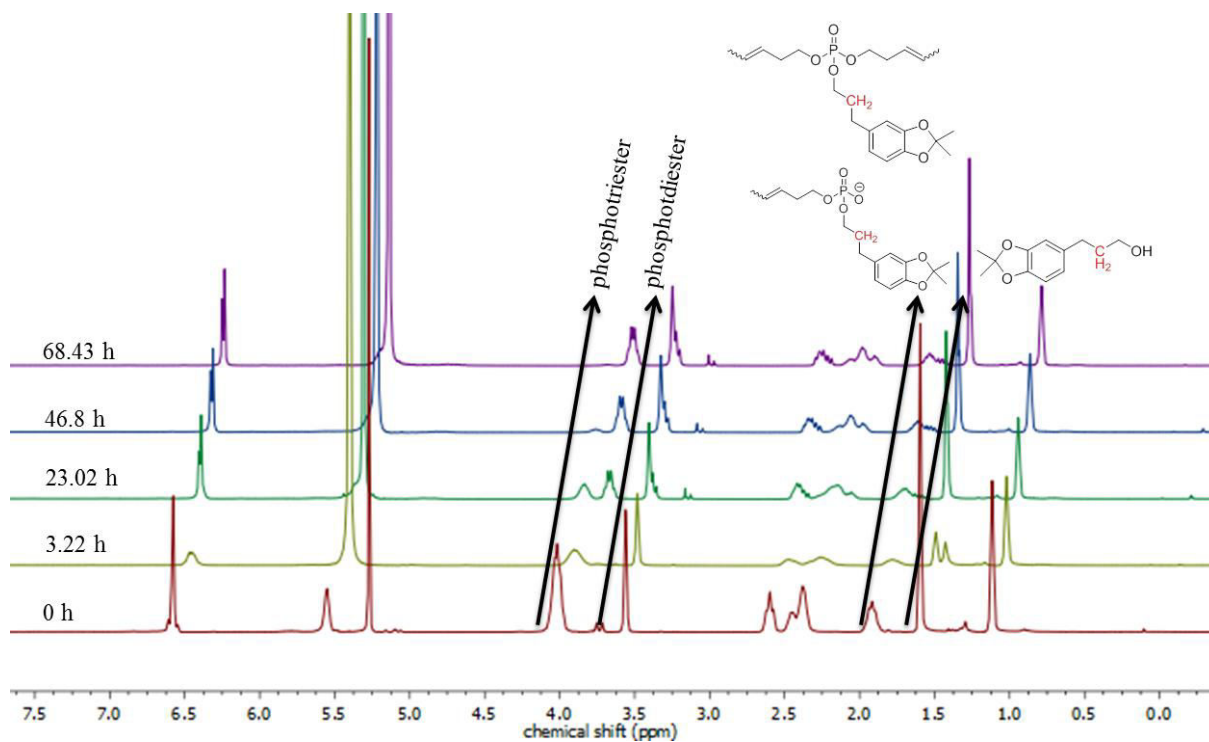


**Figure S2.38.**  $^1\text{H}$  NMR spectra (300 MHz, EtOD/D<sub>2</sub>O, 298 K) of the degradation of **poly1-4**.

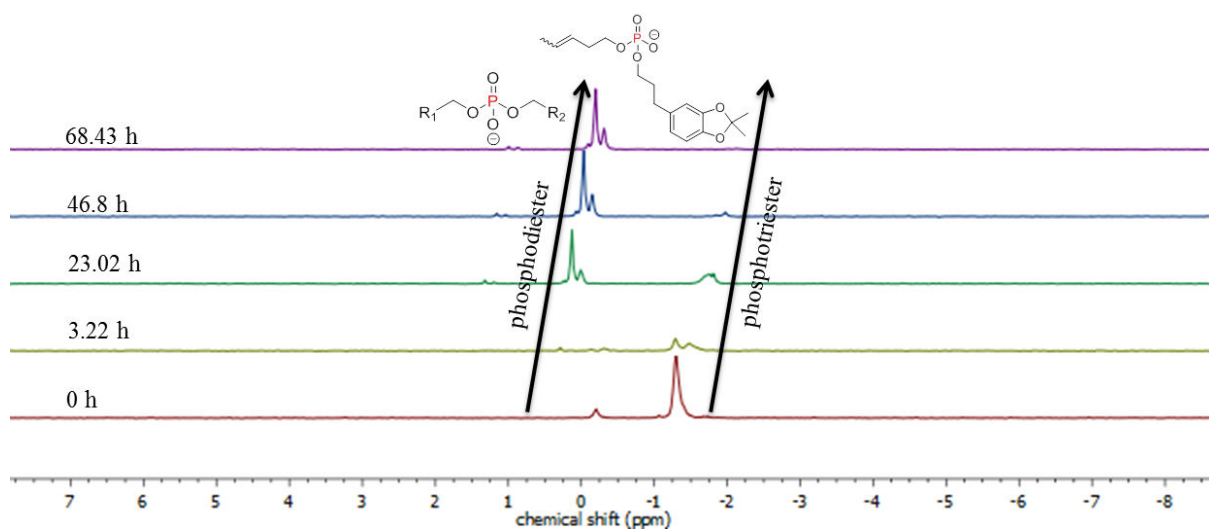


**Figure S2.39.**  $^{31}\text{P}$  {H} NMR spectra (121 MHz, EtOD/D<sub>2</sub>O, 298 K) of the degradation of **poly1-4**.

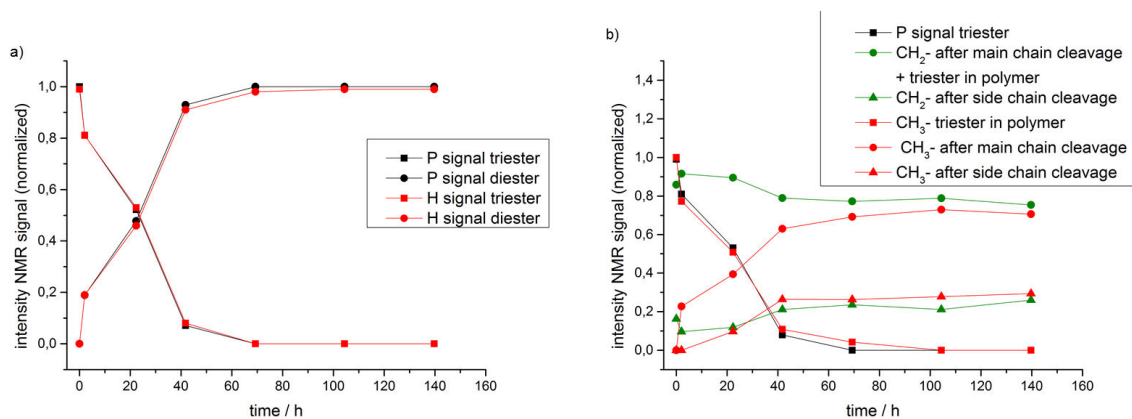


**Figure S2.40.** degradation studies, intensity NMR signals (normalized) vs. degradation time: left) degradation of **poly4-2** from phosphotriesters to phosphodiester in <sup>1</sup>H NMR and <sup>31</sup>P {H} NMR spectra; right) cleavage from **poly4-2** at side chain and main chain ester bonds in <sup>1</sup>H NMR and <sup>31</sup>P {H} NMR spectra.

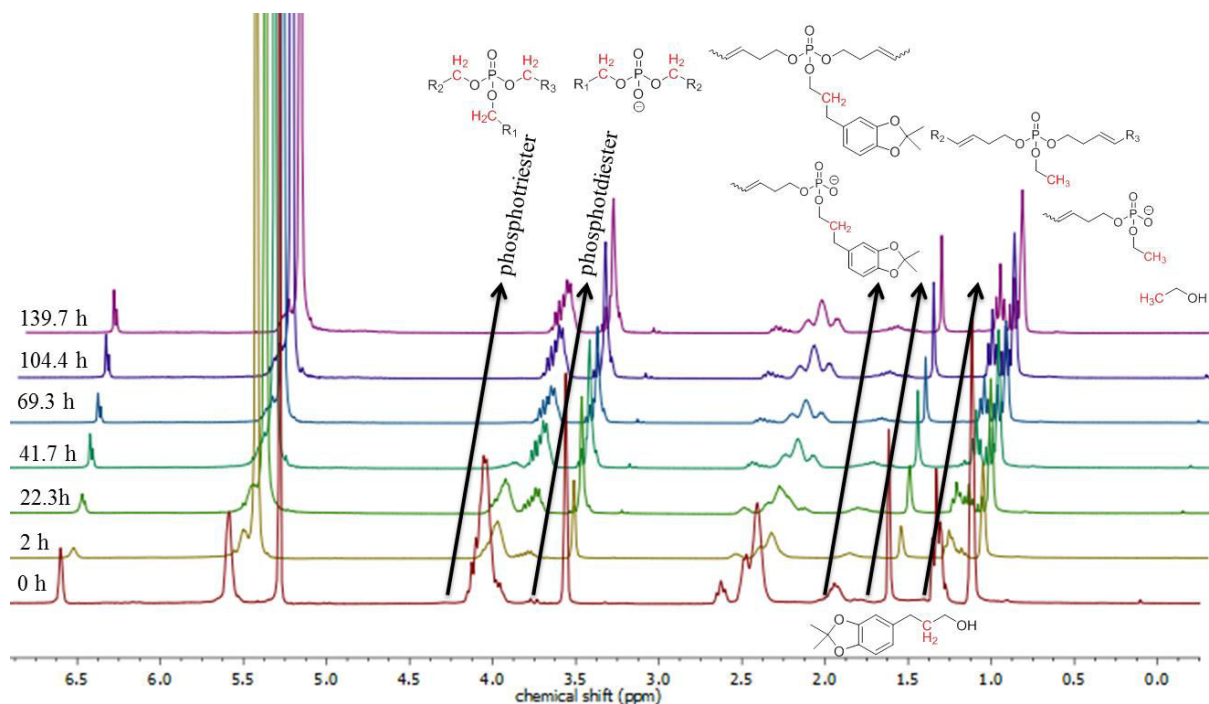


**Figure S2.41.** <sup>1</sup>H NMR spectra (300MHz, EtOD/D<sub>2</sub>O, 298K) of the degradation of **poly4-2**.

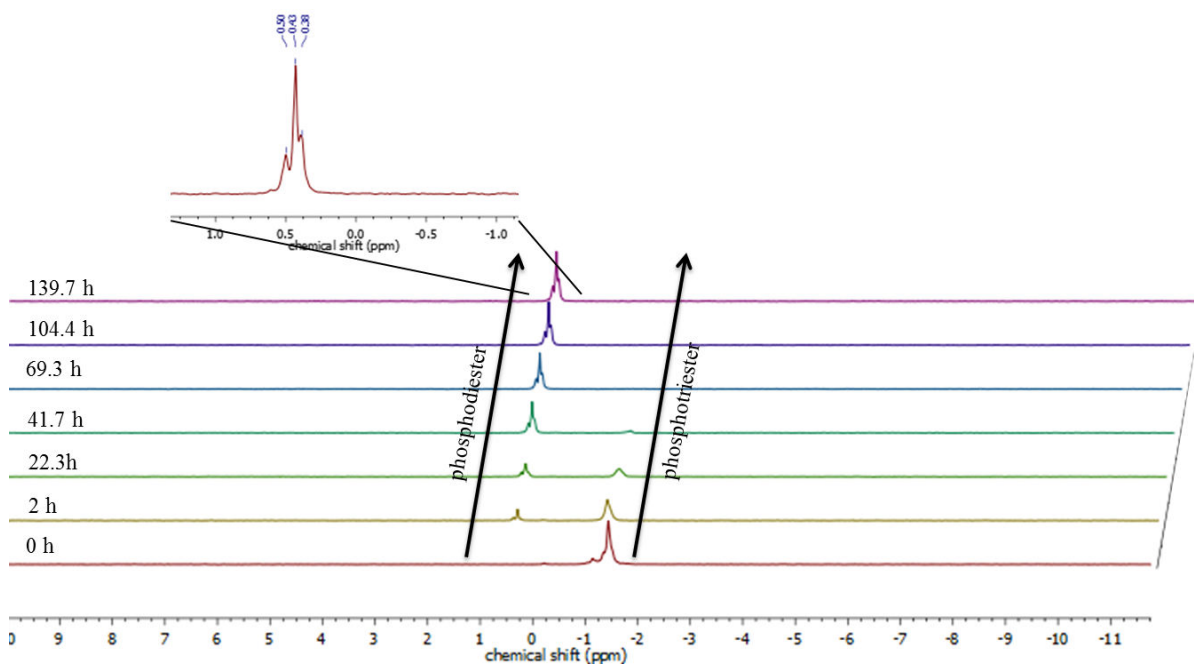


**Figure S2.42.**  $^{31}\text{P}$  {H} NMR spectra (121MHz, EtOD/ $\text{D}_2\text{O}$ , 298K) of the degradation of **poly4-2**.

### 2.7.5 Gels

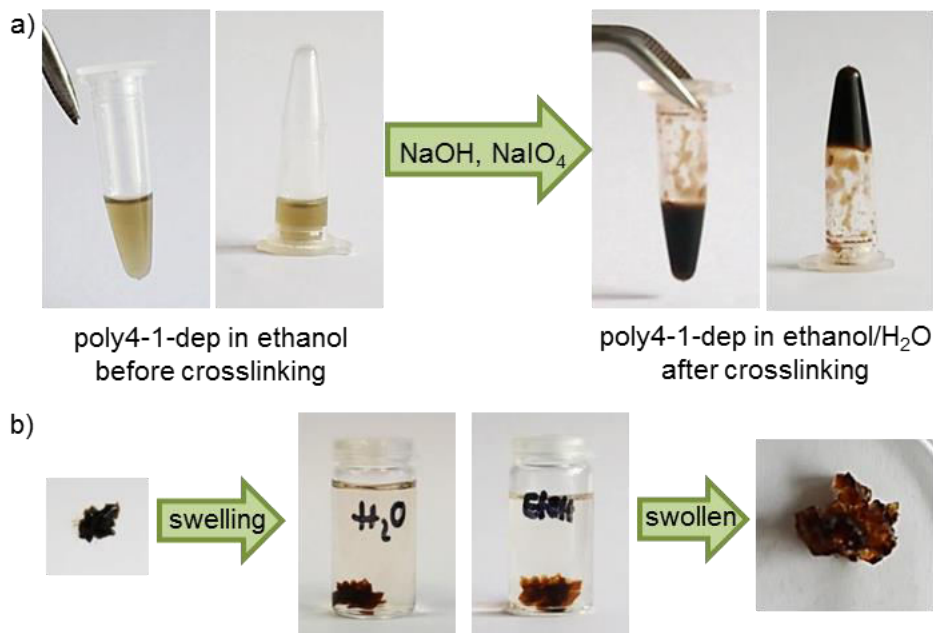


**Figure S2.43.** a) Oxidative gelation of **poly4-1-dep**: *left*: polymer solution before crosslinking, *right*: gel after crosslinking; b) swelling of networks: *left*: dried gel, *middle*: swelling of gel in distilled water or ethanol, *right*: swollen gel in ethanol.

### 2.7.6 Magnetite particles

#### a. Biphasic system



**Figure S2.44.** unmodified (0) and modified (1-4) magnetite nanoparticles in a biphasic hexane/methanol system. Upper phase: hexane, lower phase: methanol. 0: unmodified particles; particles modified with 1: **poly4-1-dep**, 2: **poly4-1**, 3: **poly2-2**, 4: **poly5-2**. Middle image: all biphasic systems before shaking. Left image: unmodified particles (0) after shaking. Right image: modified particles with poly4-1-dep: before shaking (1a), 10 seconds after shaking (1b), 1 min after shaking (1c).

#### b. TEM image

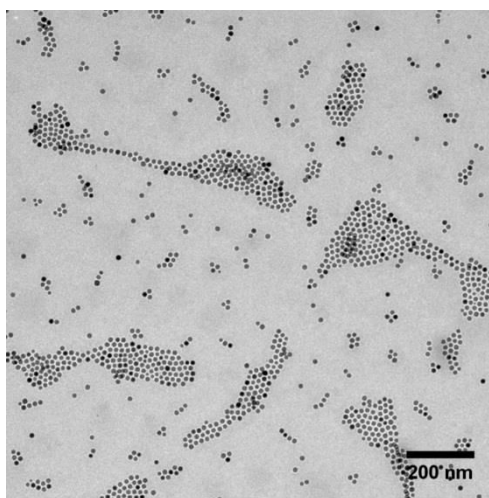


**Figure S2.45.** TEM image of functionalized magnetite NPs with **poly4-1**.

c. IR spectra

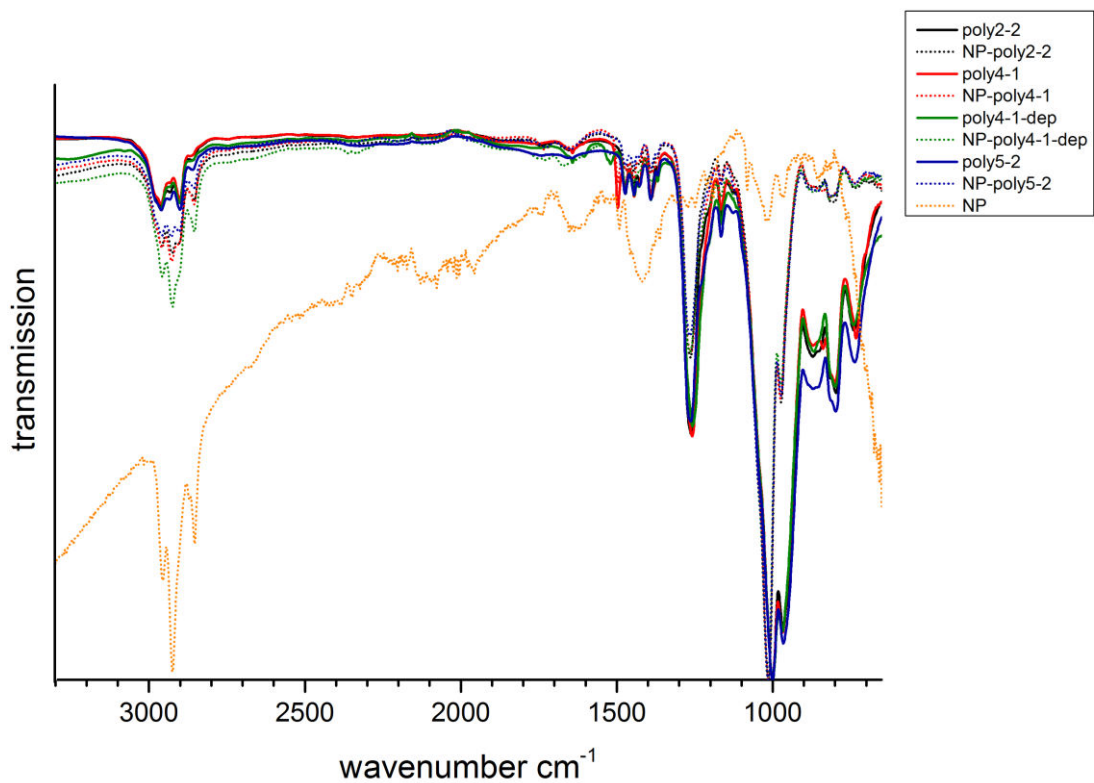


**Figure S2.46.** IR spectra of polymers, oleic acid-functionalized nanoparticles (NPs) and functionalized NPs.

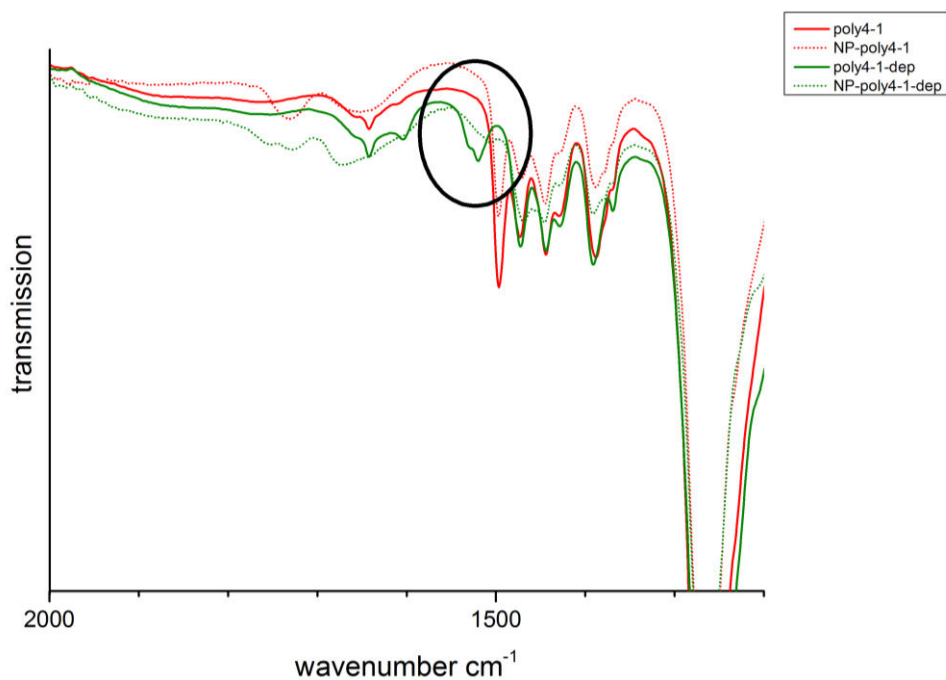


**Figure S2.47.** Zoom in of IR spectra: C-C stretching signal of free catechol in **poly4-1-dep** and vanished in **NP-poly4-1-dep**.

#### d. ITC data

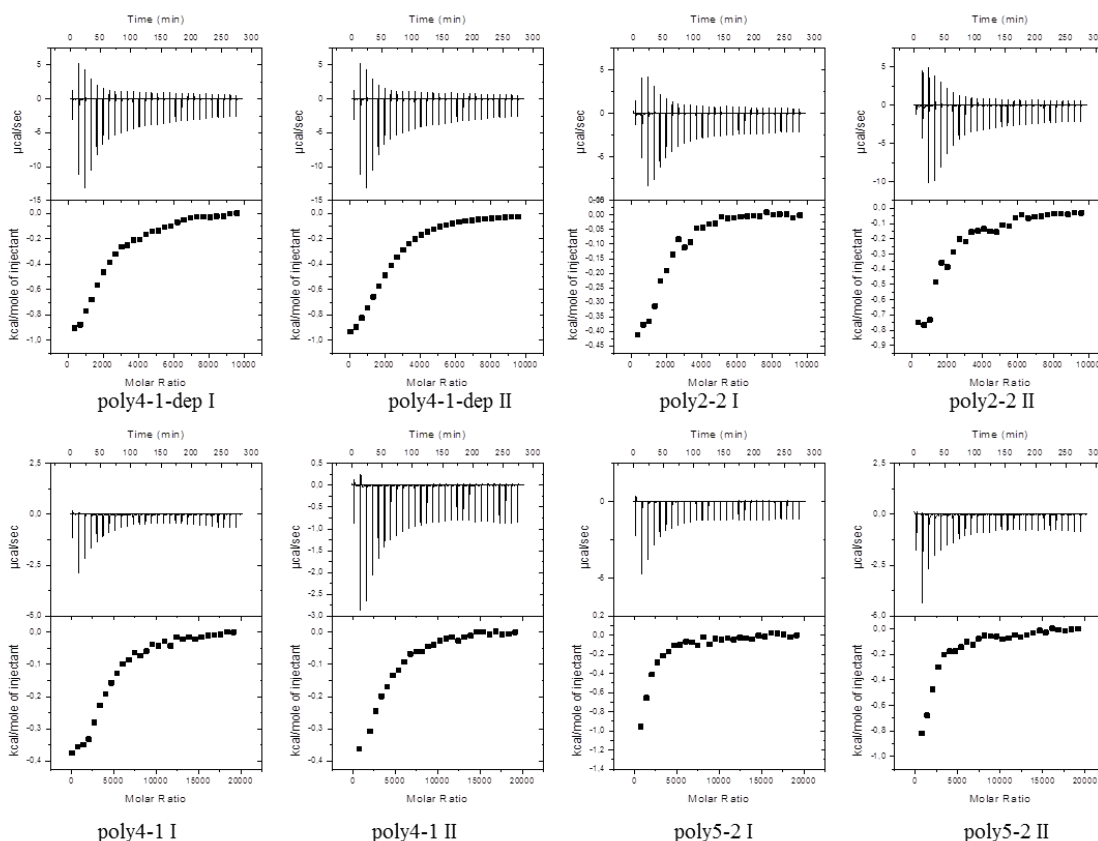


**Figure S2.48.** ITC: titration diagrams upper diagram: raw heat rate; lower diagram: integrated heat of each peak (titration isotherms).

## 2.8 References

1. Molinoff, P. B.; Axelrod, J., *Annu. Rev. Biochem.* **1971**, *40* (1), 465-500.
2. Penczek, S.; Pretula, J.; Kaluzynski, K., *Biomacromolecules* **2005**, *6* (2), 547-551.
3. Waite, J. H.; Tanzer, M. L., *Science* **1981**, *212* (4498), 1038-1040.
4. Lee, B. P.; Messersmith, P. B.; Israelachvili, J. N.; Waite, J. H., *Annu. Rev. Mater. Res.* **2011**, *41* (1), 99-132.
5. Avdeef, A.; Sofen, S. R.; Bregante, T. L.; Raymond, K. N., *J. Am. Chem. Soc.* **1978**, *100* (17), 5362-5370.
6. Yu, M.; Hwang, J.; Deming, T. J., *J. Am. Chem. Soc.* **1999**, *121* (24), 5825-5826.
7. Faure, E.; Falentin-Daudré, C.; Jérôme, C.; Lyskawa, J.; Fournier, D.; Woisel, P.; Detrembleur, C., *Prog. Polym. Sci.* **2013**, *38* (1), 236-270.
8. Sedó, J.; Saiz-Poseu, J.; Busqué, F.; Ruiz-Molina, D., *Adv. Mater.* **2013**, *25* (5), 653-701.
9. Lee, B. P.; Dalsin, J. L.; Messersmith, P. B., *Biomacromolecules* **2002**, *3* (5), 1038-1047.
10. Paez, J. I.; Ustahüseyin, O.; Serrano, C.; Ton, X.-A.; Shafiq, Z.; Auernhammer, G. K.; d'Ischia, M.; del Campo, A., *Biomacromolecules* **2015**, *16* (12), 3811-3818.
11. Niederer, K.; Schüll, C.; Leibig, D.; Johann, T.; Frey, H., *Macromolecules* **2016**, *49* (5), 1655-1665.
12. Statz, A. R.; Meagher, R. J.; Barron, A. E.; Messersmith, P. B., *J. Am. Chem. Soc.* **2005**, *127* (22), 7972-7973.
13. Lee, H.; Dellatore, S. M.; Miller, W. M.; Messersmith, P. B., *Science* **2007**, *318* (5849), 426-430.

14. Yuen, A. K. L.; Hutton, G. A.; Masters, A. F.; Maschmeyer, T., *Dalton Trans.* **2012**, 41 (9), 2545-2559.
15. Krogsgaard, M.; Nue, V.; Birkedal, H., *Chem. - Eur. J.* **2016**, 22 (3), 844-857.
16. Ryu, J. H.; Lee, Y.; Kong, W. H.; Kim, T. G.; Park, T. G.; Lee, H., *Biomacromolecules* **2011**, 12 (7), 2653-2659.
17. Mehdizadeh, M.; Weng, H.; Gyawali, D.; Tang, L.; Yang, J., *Biomaterials* **2012**, 33 (32), 7972-7983.
18. Zhou, J.; Defante, A. P.; Lin, F.; Xu, Y.; Yu, J.; Gao, Y.; Childers, E.; Dhinojwala, A.; Becker, M. L., *Biomacromolecules* **2015**, 16 (1), 266-274.
19. Shi, D.; Shen, J.; Zhao, Z.; Shi, C.; Chen, M., *Polymers* **2016**, 8 (3), 92.
20. Zhang, H.; Bré, L. P.; Zhao, T.; Zheng, Y.; Newland, B.; Wang, W., *Biomaterials* **2014**, 35 (2), 711-719.
21. Yu, M.; Deming, T. J., *Macromolecules* **1998**, 31 (15), 4739-4745.
22. Zhao, Z.; Wang, J.; Mao, H.-Q.; Leong, K. W., *Adv. Drug Delivery Rev.* **2003**, 55 (4), 483-499.
23. Steinbach, T.; Wurm, F. R., *Angew. Chem. Int. Ed.* **2015**, 54 (21), 6098-6108.
24. Li, Q.; Wang, J.; Shahani, S.; Sun, D. D. N.; Sharma, B.; Elisseeff, J. H.; Leong, K. W., *Biomaterials* **2006**, 27 (7), 1027-1034.
25. Wang, Y.-C.; Yuan, Y.-Y.; Du, J.-Z.; Yang, X.-Z.; Wang, J., *Macromol. Biosci.* **2009**, 9 (12), 1154-1164.
26. Iwasaki, Y.; Yamaguchi, E., *Macromolecules* **2010**, 43 (6), 2664-2666.
27. Lim, Y. H.; Tiemann, K. M.; Heo, G. S.; Wagers, P. O.; Rezenom, Y. H.; Zhang, S.; Zhang, F.; Youngs, W. J.; Hunstad, D. A.; Wooley, K. L., *ACS Nano* **2015**, 9 (2), 1995-2008.
28. Steinbach, T.; Ritz, S.; Wurm, F. R., *ACS Macro Lett.* **2014**, 3 (3), 244-248.
29. Bauer, K. N.; Tee, H. T.; Lieberwirth, I.; Wurm, F. R., *Macromolecules* **2016**, 49 (10), 3761-3768.
30. Zhang, S.; Wang, H.; Shen, Y.; Zhang, F.; Seetho, K.; Zou, J.; Taylor, J.-S. A.; Dove, A. P.; Wooley, K. L., *Macromolecules* **2013**, 46 (13), 5141-5149.
31. Cankaya, A.; Steinmann, M.; Bulbul, Y.; Lieberwirth, I.; Wurm, F. R., *Polym. Chem.* **2016**, 7 (31), 5004-5010.
32. Baran, J.; Klosinski, P.; Penczek, S., *Makromol. Chem.* **1989**, 190 (8), 1903-1917.
33. Klosinski, P.; Penczek, S., *Makromol. Chem., Rapid Commun.* **1988**, 9 (3), 159-164.
34. Libiszowski, J.; Kałużynski, K.; Penczek, S., *J. Polym. Sci., Polym. Chem. Ed.* **1978**, 16 (6), 1275-1283.
35. Clément, B.; Grignard, B.; Koole, L.; Jérôme, C.; Lecomte, P., *Macromolecules* **2012**, 45 (11), 4476-4486.
36. Steinbach, T.; Alexandrino, E. M.; Wurm, F. R., *Polym. Chem.* **2013**, 4 (13), 3800-3806.
37. Marsico, F.; Wagner, M.; Landfester, K.; Wurm, F. R., *Macromolecules* **2012**, 45 (21), 8511-8518.
38. Steinmann, M.; Markwart, J.; Wurm, F. R., *Macromolecules* **2014**, 47 (24), 8506-8513.
39. Wilms, V. S.; Bauer, H.; Tonhauser, C.; Schilman, A.-M.; Müller, M.-C.; Tremel, W.; Frey, H., *Biomacromolecules* **2013**, 14 (1), 193-199.
40. Ahniyaz, A.; Sakamoto, Y.; Bergström, L., *Proceedings of the National Academy of Sciences* **2007**, 104 (45), 17570-17574.
41. Park, J.; An, K.; Hwang, Y.; Park, J.-G.; Noh, H.-J.; Kim, J.-Y.; Park, J.-H.; Hwang, N.-M.; Hyeon, T., *Nat. Mater.* **2004**, 3 (12), 891-895.
42. Lienkamp, K.; Kins, C. F.; Alfred, S. F.; Madkour, A. E.; Tew, G. N., *J. Polym. Sci., Part A: Polym. Chem.* **2009**, 47 (5), 1266-1273.
43. Slugovc, C., *Macromol. Rapid Commun.* **2004**, 25 (14), 1283-1297.
44. Colak, S.; Tew, G. N., *Macromolecules* **2008**, 41 (22), 8436-8440.
45. Eren, T.; Tew, G. N., *J. Polym. Sci., Part A: Polym. Chem.* **2009**, 47 (15), 3949-3956.
46. Oppen, K. L.; Markova, D.; Klapper, M.; Müllen, K.; Wagener, K. B., *Macromolecules* **2010**, 43 (8), 3690-3698.
47. Markova, D.; Oppen, K. L.; Wagner, M.; Klapper, M.; Wagener, K. B.; Müllen, K., *Polym. Chem.* **2013**, 4 (5), 1351-1363.
48. Bingöl, B.; Kroeger, A.; Jannasch, P., *Polymer* **2013**, 54 (25), 6676-6688.

49. Wuts, P. G. M.; Greene, T. W., *Greene's Protective Groups in Organic Synthesis*. 4th ed. ed.; Wiley-Interscience: 2007.
50. Baran, J.; Penczek, S., *Macromolecules* **1995**, *28* (15), 5167-5176.
51. Wang, D.; Williams, C. G.; Yang, F.; Cher, N.; Lee, H.; Elisseff, J. H., *Tissue Eng.* **2005**, ( 11), 201-213.
52. Holten-Andersen, N.; Harrington, M. J.; Birkedal, H.; Lee, B. P.; Messersmith, P. B.; Lee, K. Y. C.; Waite, J. H., *Proceedings of the National Academy of Sciences* **2011**, *108* (7), 2651-2655.
53. Brubaker, C. E.; Kissler, H.; Wang, L.-J.; Kaufman, D. B.; Messersmith, P. B., *Biomaterials* **2010**, *31* (3), 420-427.
54. Waite, J. H., *Comp. Biochem. Physiol., Part B: Biochem. Mol. Biol.* **1990**, *97* (1), 19-29.
55. Schladt, T. D.; Schneider, K.; Schild, H.; Tremel, W., *Dalton Trans.* **2011**, *40* (24), 6315-6343.
56. Kim, S.-W.; Kim, S.; Tracy, J. B.; Jasanoff, A.; Bawendi, M. G., *J. Am. Chem. Soc.* **2005**, *127* (13), 4556-4557.
57. Connor, P. A.; McQuillan, A. J., *Langmuir* **1999**, *15* (8), 2916-2921.
58. Moser, J.; Punchihewa, S.; Infelta, P. P.; Graetzel, M., *Langmuir* **1991**, *7* (12), 3012-3018.
59. Yang, X.; He, J.; Sun, Z.; Holmgren, A.; Wang, D., *J. Environ. Sci.* **2016**, *39*, 69-72.
60. National Institute of Advanced Industrial Science and Technology (AIST). Spectral Database for Organic Compounds (SDBS). [http://sdfs.db.aist.go.jp/sdfs/cgi-bin/direct\\_frame\\_disp.cgi?sdfsno=2164](http://sdfs.db.aist.go.jp/sdfs/cgi-bin/direct_frame_disp.cgi?sdfsno=2164) (accessed Sep 16, 2016).
61. McBride, M. B.; Wesselink, L. G., *Environ. Sci. Technol.* **1988**, *22* (6), 703-708.
62. Chiad, K.; Stelzig, S. H.; Gropeanu, R.; Weil, T.; Klapper, M.; Müllen, K., *Macromolecules* **2009**, *42* (19), 7545-7552.



### 3. Investigation on catechol-containing poly(phosphoester)-hydrogels

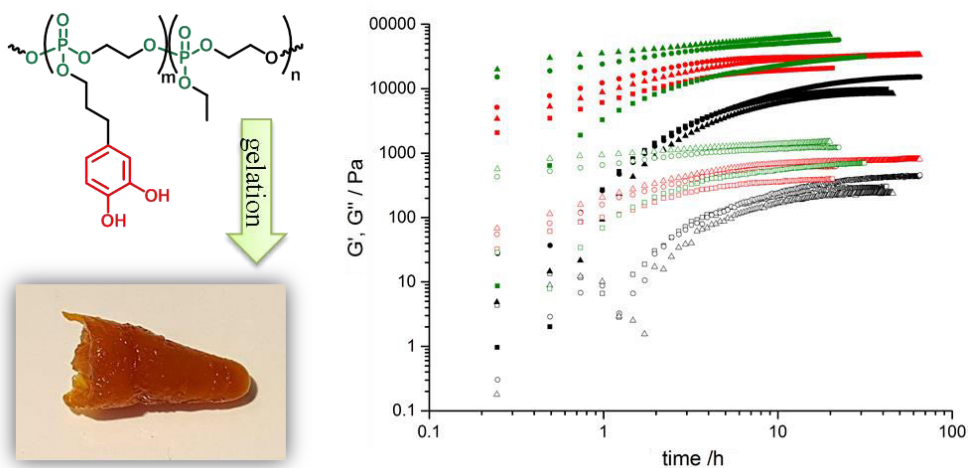
Greta Becker,<sup>1,2</sup> Oya Ustahüseyin,<sup>3</sup> Aránzazu del Campo,<sup>3</sup> Frederik R. Wurm<sup>1</sup>

<sup>1</sup>Max Planck Institute for Polymer Research, Ackermannweg 10, 55128 Mainz, Germany

<sup>2</sup>Graduate School Materials Science in Mainz, Staudinger Weg 9, 55128 Mainz, Germany

<sup>3</sup>INM-Leibniz Institute for New Materials, Campus D2 2, 66123 Saarbrücken, Germany

Unpublished results.



### 3.1 Abstract

Catechol-containing polymers are currently discussed as bioadhesives for soft and hard tissue engineering. The recently reported combination of the catechol motif with phosphate units in degradable poly(phosphoester)s from ADMET polycondensation was extended to more hydrophilic PPEs, obtained by ROP. A cyclic phosphate carrying a protected catechol functionality was developed, and successfully copolymerized. Copolymers exhibit a catechol content of up to 20 mol% and molecular weights up to 36,000 g/mol. Quantitative deprotection of the catechol functionalities was succeeded under acidic conditions without backbone degradation. Cross-linked PPE-gels were formed under oxidative conditions, exhibiting curing times of 10-15 h and storage moduli of up to 68,300 Pa, measured by piezorheology. The cross-linked polymers are promising candidates to be further developed as bone adhesive materials.

### 3.2 Introduction

An increasing market share demands the development of novel wound sealants for soft tissue as well as bioadhesives for hard bone tissue. These materials should overcome and replace traditional methods as surgical sutures, staples, joints, or pins. Applications for soft or hard tissue demand very different requirements to the functional materials. While for soft tissue the materials have to exhibit softness and elastomeric features, bone adhesives require very high mechanical strength.<sup>1-3</sup>

Commercial products for soft tissue are based on synthetic polymers such as cyanoacrylates (Dermabond®, Histoacryl®), biodegradable PEG (CoSeal®) and urethanes (TissuGlu™), or naturally derived biopolymers such as gelatin- (FloSeal™), chitosan- (Celox™) or fibrin-based sealants (Tisseel™). Cyanoacrylates show high mechanical strengths, but biocompatibility and –degradation, often discussed in the literature, are critical.<sup>4</sup> The other products exhibit a high level of biocompatibility and –degradation, but may lack mechanical strength.<sup>1-2</sup>

Products for hard tissue engineering are mainly limited to void fillers and bone cement or substitute scaffolds. To date, there is no “true” bone-glue available. An ideal bone-glue might replace plates and screws, which is favorable to avoid a second surgical intervention to remove the fixation. Drilling holes may weaken the bone and cause additional fracture, as well as the load is transferred onto the site of the screws, causing punctual stress overload and possible fixation failure.<sup>5</sup> Requirements for a bone-glue are versatile: besides high adhesive strength to bone material, cohesive strength within the material is crucial. An adhesive strength to bone higher than

0.2 MPa is claimed.<sup>6</sup> The material needs to adhere and cure to moist surfaces, be chemical stable and non-toxic. Additionally, bioresorption on a decent time-scale (above three months) is necessary, exhibiting also non-toxic degradation products. It has to support the natural process of bone healing, cell-migration, osteointegration, and angiogenesis. Finally, adequate curing time, easy handling for the surgeons, and economical feasibility are demanded.<sup>5, 7</sup> The ability to deliver drugs and growth factors at the same time is highly desirable.

Commercialized bone cements are the void fillers OsteoCrete™ (key components: MgO<sub>2</sub>, KH<sub>2</sub>PO<sub>4</sub>, NaH<sub>2</sub>PO<sub>4</sub>, Ca<sub>3</sub>(PO<sub>4</sub>)<sub>2</sub>)<sup>8</sup> or Kryptonite™ (prepolymer isocyanate, liquid polyester polyol, CaCO<sub>3</sub>)<sup>9</sup>. PMMA is today the mostly applied polymeric bone cement (i.e. CemFix 3®, OsteoPal®, Mendec® Spine, Spineplex™), applied for fixation of prosthetic implants to bone.<sup>2, 7</sup> However, for vertebral compression fractures (i.e. in the spine), the exhibited elastic modulus of 2000-2700 MPa is too high (compressive elastic modulus of a normal human vertebral body is 50-800 MPa). The high stiffness causes stress concentration and therefore secondary fractures. Bioinertness of PMMA hampers interfacial interaction with bone tissue and osteointegration. Improvements include addition of bioactive hydroxyapatite (HA, Ca<sub>5</sub>(PO<sub>4</sub>)<sub>3</sub>OH) powder, calcium and magnesium phosphate or mineralized collagen (MC).<sup>10</sup>

Most ceramics and metals are too stiff as substitute, may cause mechanical mismatch, and finally resorption of bone tissue.<sup>11</sup> Investigated polymeric systems include polyurethane foams, epoxy resins, lactide-methacrylate-based systems or bisphenol-A glycidyl dimethacrylate/ethylene glycol dimethacrylate (Bis-GMA/EGDMA). They are all critical to a certain point of strength and stiffness.<sup>3</sup> A promising n-butyl cyanoacrylate formulation showed higher shear bond strength than resorbable plates,<sup>5</sup> but cyanoacrylates are known to be cytotoxic and induce adverse biological reactions.<sup>2</sup> Composites are investigated including demineralized bone matrix (DBM), collagen, hydroxyapatite (HA) or β-tricalcium phosphate (β-TCP).<sup>11-12</sup> Inorganic calcium and magnesium phosphate-based cements,<sup>13</sup> or composites as zinc polycarboxylate,<sup>2</sup> and glass ionomer cements<sup>14</sup> are alternatively discussed.<sup>7</sup>

Recent promising investigations use biopolymers such as chitosan<sup>15-16</sup> and study the improvement of adhesion under wet conditions. Groll and coworkers<sup>17</sup> recently improved a photocurable PEGDMA matrix by addition of a six-armed isocyanate functional star-shaped prepolymer (NCO-star-P(EO-stat-PO)) and biodegradable ceramic fillers, exhibiting adhesive strength over 0.2 MPa in wet environment. Polymers functionalized with a biomimicking approach inspired by marine mussels<sup>18</sup> are heavily studied (for hard as well as soft tissue), and described in many reviews.<sup>1, 19-21</sup> Functional catechol groups<sup>22-23</sup> are found in the mussel foot proteins.<sup>19, 24</sup> They provide adhesive as well as cohesive features to biomaterials. The bidentate coordinative binding to metal oxides or ions is strong, reversible and pH-dependent ( $k_s > 10^{40}$ ).<sup>25</sup> Quinone intermediates

are formed by auto-oxidation or generated by oxidants in alkaline solution, which subsequently cross-link with other catechols or nucleophiles (amines or thiols, i.e. from biomaterial or proteins).<sup>26</sup> Catechols bind to a wide range of surfaces, even under humid conditions.<sup>19</sup> Their versatile chemistry and strong adhesion to biomaterial, including hydroxyapatite (HA),<sup>27</sup> are attractive for the preparation of polymeric hydrogels or scaffolds for tissue engineering.<sup>28-29</sup>

Herein, we extend our recently reported combination of the catechol motif with phosphate units in degradable poly(phosphoester)s (PPEs) from ADMET polycondensation<sup>30</sup> to more hydrophilic PPEs prepared by ring-opening polymerization (ROP). PPEs are known to be biocompatible and biodegradable.<sup>31</sup> Phosphates show high binding affinity to hydroxyapatite (HA), a main component of bones. Our group recently showed the adhesion and efficient binding of PPEs to commercially available bone substitute (MBCP+™ from Biomatlante) due to the phosphate groups in the backbone.<sup>32</sup> A cross-linked matrix of PPEs from polycondensation of (1,2-propyleneglycol) fumarate and ethyl dichlorophosphate exhibited mechanical properties close to natural trabecular bone and good operation properties for injectable application as tissue scaffold.<sup>33</sup> Phosphorus-containing polymers (phosphonated polymers and polyphosphazene-type polymers) proved to be promising materials for tissue and organ regeneration and showed osteoblast-like cell adhesion and proliferation, or calcium phosphate mineral growth with a typical HA morphology.<sup>34</sup>

Catechol-PPEs obtained from ROP were covalently crosslinked in the presence of an oxidant to form hydrogels. The curing time and mechanical properties of these materials were examined by piezorheology. The cross-linked polymers are promising candidates to be further developed as bone adhesive materials (see Outlook).

### 3.3 Experimental Section

**Materials.** Solvents, dry solvents (over molecular sieves) and deuterated solvents were purchased from Acros Organics, Sigma-Aldrich, Deutero GmbH or Fluka. 3,4-dihydroxyhydrocinnamic acid, 2-chloro-2-oxo-1,3,2-dioxaphospholane, pyridine, trifluoroacetic acid, 1,8-diazabicyclo[5.4.0]undec-7-ene, and hexamethyldisiloxane (HDMSO) were purchased from Sigma-Aldrich. MgSO<sub>4</sub> and calcium(II) chloride hexahydrate were purchased from Fisher Scientific. *P*-Toluenesulfonic acid monohydrate, 2,2-dimethoxypropane, and LiAlH<sub>4</sub> (2.4M in THF) were purchased from Acros Organics. 3,5-bis(trifluoromethyl)phenylisothiocyanat was purchased from Alfa Aesar GmbH & Co KG. All reagents were used without further purification, unless otherwise stated. 2-(benzyloxy)ethanol and triethylamine were dried with CaH<sub>2</sub> prior to use, distilled, and

stored over molecular sieve. 1,8-diazabicyclo[5.4.0]undec-7-ene was distilled prior to use and stored over molecular sieve at 4 °C.

**Instrumentation and Characterization Techniques.** Size exclusion chromatography (SEC) measurements were performed in DMF (containing 0.25 g/L of lithium bromide as an additive) on an Agilent 1100 Series as an integrated instrument, including a PSS GRAM columns (1000/1000/100 g), a UV detector (270 nm), and a RI detector at a flow rate of 1 mL/min at 60 °C. Calibration was carried out using PEO standards provided by Polymer Standards Service. For nuclear magnetic resonance analysis <sup>1</sup>H, <sup>13</sup>C, and <sup>31</sup>P NMR spectra were recorded on a Bruker AVANCE III 300, 500, 700 or 850 MHz spectrometer. All spectra were measured in either *d*<sub>6</sub>-DMSO or CDCl<sub>3</sub> at 298 K. The spectra were calibrated against the solvent signal and analyzed using MestReNova 8 from Mestrelab Research S.L. DOSY spectra were analyzed with TOPSPIN 3.2 software. The thermal properties of the synthesized polymers have been measured by differential scanning calorimetry (DSC) on a Mettler Toledo DSC 823 calorimeter. Three scanning cycles of heating-cooling were performed in a N<sub>2</sub> atmosphere (30 mL/min) with a heating and cooling rate of 10 °C/min. For rheological measurements of shear moduli (*G'* and *G''*) and cross-linking kinetics of catechol-PPEs a homemade oscillating mikro-piezorheometer<sup>35</sup> was used. The samples were placed between two glass substrates (1 x 20 x 2 mm<sup>3</sup>), which were connected to two piezoactuators. The lower piezoactuator applies the shear deformation to the sample, the upper one detects the stress transmitted through the sample. The gap between the glass slides was adjusted to 100 μm. For accurate placement of the samples, the 12 μL of the fluid sample was placed on the lower glass slide of the rheometer directly after mixing, surrounded with a low viscous PDMS oil, the upper glass slide attached and adjusted. The residual gap was sealed with additional PDMS oil. The measurements were directly started. The experiments were performed at room temperature in the time sweep modus at a frequency of 4.64 Hz, 9.5 V and 0.32% strain. The noise level of rheological measurements is ca. 10 Pa.

**Syntheses.** *2-(3-(2,2-dimethylbenzo[d][1,3]dioxol-5-yl)propoxy)-2-oxo-1,3,2-dioxaphospholane (CEP,1):* 2,2-Dimethyl-1,3-benzodioxole-5-propanol (8.03 g, 38.6 mmol, 1 eq.) was dissolved in 150 mL dry THF in a flame-dried 3-necked round-bottom flask. Dry pyridine (3.05 g, 38.6 mmol, 1 eq.) was added and the mixture was cooled to 0°C. 2-chloro-2-oxo-1,3,2-dioxaphospholane (8.24 g, 57.8 mmol, 1.5 eq.) in 50 mL dry THF was added over a period of 1 h, the reaction mixture was stirred for an additional 4 h and stored at -20°C overnight. During the addition of COP, hydrogen chloride was formed and precipitated as pyridinium hydrochloride. The reaction was filtered with a Schlenk-frit and concentrated. Column chromatography with a RP-1 column (silica gel deactivated with 5v% hexamethyldisiloxane, dichloromethane/ethyl acetate 10:1, *R*<sub>f</sub>=0.32) gave the pure product CEP as a colorless solid. Yield: 6.90 g, 57%. <sup>1</sup>H NMR (300 MHz, CDCl<sub>3</sub>): δ [ppm]

6.65–6.56 (m, 3H,  $H_{\text{arom}}$ ), 4.50–4.31 (m, 4H,  $-\text{CH}_2\text{-O-P(=O)-O-CH}_2\text{-CH}_2\text{-}$ ), 4.18–4.11 (dt, 2H,  $\text{Ar-CH}_2\text{-CH}_2\text{-CH}_2\text{-O-P(=O)-}$ ), 2.62 (t, 2H,  $\text{Ar-CH}_2\text{-CH}_2\text{-CH}_2\text{-O-P(=O)-}$ ), 2.02–1.92 (quin, 2H,  $\text{Ar-CH}_2\text{-CH}_2\text{-CH}_2\text{-O-P(=O)-}$ ), 1.66 (s, 6H,  $-\text{CH}_3$ ).  $^{13}\text{C}$  {H} NMR (76 MHz,  $\text{CDCl}_3$ ):  $\delta$  [ppm] 147.61 (O-C-CH-C), 145.81 (O-C-CH-CH-C), 133.95 ( $-\text{CH-C}(\text{CH})\text{-CH}_2\text{-}$ ), 120.68 (O-C-CH-CH-C), 117.72 (O-C( $\text{CH}_3$ ) $_2$ -O), 108.73 (O-C-CH-C), 108.09 (O-C-CH-CH-C), 68.30 ( $\text{Ar-CH}_2\text{-CH}_2\text{-CH}_2\text{-O-P}$ ), 66.05 ( $-\text{O-CH}_2\text{-CH}_2\text{-O-P}$ ), 32.26 ( $\text{Ar-CH}_2\text{-CH}_2\text{-}$ ), 31.39 ( $\text{Ar-CH}_2\text{-CH}_2\text{-}$ ), 25.93 ( $-\text{CH}_3$ ).  $^{31}\text{P}$  {H} NMR (121 MHz,  $\text{CDCl}_3$ ):  $\delta$  [ppm] 17.59. FTIR ( $\text{cm}^{-1}$ ): 3069–2861 ( $-\text{CH}_2\text{-}$ ,  $-\text{CH=}$ , and  $-\text{CH}_3$  stretching), 1672 (C=C stretching), 1608 (aromatic ring), 1495, 1444 (O- $\text{CH}_2\text{-}$  deformation), 1377 ( $-\text{CH}_3$  deformation), 1288 (P=O stretching), 1252 (aryl-O-alkyl), 1231 (aryl-O-alkyl), 1157, 1120, 1019 (P-O-C stretching), 979 (P-O-C stretching), 927, 833 (P-O-C stretching), 787, 767, 724, 681.

*General procedure for the copolymerization of EEP (or MEP) and CEP:* The polymerization was conducted according to literature procedures reported for other monomers.<sup>36</sup> Exemplarily for **P1a**, EEP (540 mg, 3.55 mmol, 135 eq.), CEP (124 mg, 394  $\mu\text{mol}$ , 15 eq.) and TU (78 mg, 210  $\mu\text{mol}$ , 5.3 mol% to monomer) were introduced into a Schlenk tube under an argon atmosphere. A stock solution of DBU in dry DCM (32 mg/0.2mL, 210  $\mu\text{mol}$ , 5.3 mol% to monomer) and a stock solution of the initiator (2-(benzyloxy)ethanol) in dry DCM (4 mg/0.4 mL, 26  $\mu\text{mol}$ ) were prepared and 0.4 mL dry DCM was added to EEP, CEP and TU to give a total concentration of 4 mol/L. All solutions were cooled down to 0 °C. 0.4 mL of the stock solution of the initiator was added to the stirred solution of EEP, CEP and TU. The polymerization was started by rapid addition of 0.2 mL stock solution of DBU to the reaction mixture by a syringe. The polymerization was terminated after 90 min by the addition of 10 drops glacial acetic acid in 1 mL DCM). 20 mL DCM were added and the organic layer was washed with 0.1M HCl-solution once. The organic phase was then extracted with water (3 times) until the aqueous solution exhibited a neutral pH. The organic phase was concentrated to 5 mL residual solvent and the polymer precipitated in 40 mL ice-cold diethyl ether. The ether was decanted after centrifugation (15 min, 4000 rpm, 4 °C). The residual polymer was dried *in vacuo* to give the final product.

*Workup for P3:* After terminating the polymerization, the polymer was dialysed in DCM (benzoylated dialysis tubing, MWCO: 2000Da) for three days and then dried *in vacuo* to give the final product.

**P1a:** Yield: 595 mg, 89%.  $M_n$ (NMR): 24,600 g/mol.  $^1\text{H}$  NMR (500 MHz,  $\text{DMSO-d}_6$ ):  $\delta$  [ppm] 7.37–7.26 (m, 5H *Ar-*, initiator), 6.76–6.54 (m, 37H, *Ar-*, catechol), 4.87 (t, 1H,  $-\text{CH}_2\text{-CH}_2\text{-OH}$ ), 4.52 (s, 2H,  $\text{Ar-CH}_2\text{-O-}$ ), 4.27–3.93 (m, 875H, catechol- $\text{CH}_2\text{-CH}_2\text{-CH}_2\text{-O-P-}$ ,  $-\text{P-O-CH}_2\text{-CH}_3$ ,  $-\text{O-CH}_2\text{-CH}_2\text{-O-}$ , backbone), 3.63 (t, 2H,  $-\text{CH}_2\text{-CH}_2\text{-OH}$ ), 2.58–2.52 (m, 24H, catechol- $\text{CH}_2\text{-CH}_2\text{-CH}_2\text{-O-P-}$ ), 1.91–1.81 (m, 24H, catechol- $\text{CH}_2\text{-CH}_2\text{-CH}_2\text{-O-P-}$ ), 1.61 (s, 77H,  $-\text{CH}_3$ , protecting group), 1.25 (t, 408H,  $-\text{CH}_3$ ).  $^{31}\text{P}$  {H}

NMR (202 MHz, DMSO- $d_6$ ):  $\delta$  [ppm] -1.23 (EEP repeat unit), -1.13 (catechol repeat unit), -0.98 (ending repeat unit).

**P1b:** EEP (1.08 g, 7.10 mmol, 135 eq.), CEP (248 mg, 788  $\mu$ mol, 15 eq.), DBU (64 mg, 421  $\mu$ mol, 8 eq.), TU (156 mg, 421  $\mu$ mol, 8 eq.), initiator (8 mg, 53  $\mu$ mol, 1 eq.). Yield: 1.18 g, 86%.  $M_n$ (NMR): 31,700 g/mol.  $^1\text{H}$  NMR (300 MHz, DMSO- $d_6$ ):  $\delta$  [ppm] 7.38-7.28 (m, 5H  $Ar$ -, initiator), 6.77-6.55 (m, 57H,  $Ar$ -, catechol), 4.89 (t, 1H,  $-CH_2-CH_2-OH$ ), 4.52 (s, 2H,  $Ar-CH_2-O$ -), 4.37-3.89 (m, 1215H, catechol- $CH_2-CH_2-CH_2-O-P$ -,  $-P-O-CH_2-CH_3$ -,  $-O-CH_2-CH_2-O$ -, backbone), 3.63 (t, 2H,  $-CH_2-CH_2-OH$ ), 2.58-2.52 (m, 33H, catechol- $CH_2-CH_2-CH_2-O-P$ -), 1.96-1.79 (m, 38H, catechol- $CH_2-CH_2-CH_2-O-P$ -), 1.60 (s, 119H,  $-CH_3$ , protecting group), 1.26 (t, 561H,  $-CH_3$ ).  $^{31}\text{P}$  {H} NMR (121 MHz, DMSO- $d_6$ ):  $\delta$  [ppm] -1.24 (EEP repeat unit), -1.13 (catechol repeat unit), -0.98 (ending repeat unit).

**P2:** EEP (1.08 g, 7.10 mmol, 120 eq.), CEP (558 mg, 1.77 mmol, 30 eq.), DBU (72 mg, 473  $\mu$ mol, 8 eq.), TU (175 mg, 473  $\mu$ mol, 8 eq.), initiator (9 mg, 59  $\mu$ mol, 1 eq.). Yield: 1.34 g, 81%.  $M_n$ (NMR): 36,000 g/mol.  $^1\text{H}$  NMR (300 MHz, DMSO- $d_6$ ):  $\delta$  [ppm] 7.38-7.24 (m, 5H  $Ar$ -, initiator), 6.77-6.54 (m, 10H,  $Ar$ -, catechol), 4.90 (t, 1H,  $-CH_2-CH_2-OH$ ), 4.51 (s, 2H,  $Ar-CH_2-O$ -), 4.30-3.88 (m, 1158H, catechol- $CH_2-CH_2-CH_2-O-P$ -,  $-P-O-CH_2-CH_3$ -,  $-O-CH_2-CH_2-O$ -, backbone), 3.63 (t, 2H,  $-CH_2-CH_2-OH$ ), 2.59-2.52 (m, 44H, catechol- $CH_2-CH_2-CH_2-O-P$ -), 1.93-1.77 (m, 72H, catechol- $CH_2-CH_2-CH_2-O-P$ -), 1.59 (s, 224H,  $-CH_3$ , protecting group), 1.25 (m, 476H,  $-CH_3$ ).  $^{31}\text{P}$  {H} NMR (121 MHz, DMSO- $d_6$ ):  $\delta$  [ppm] -1.24 (EEP repeat unit), -1.13 (catechol repeat unit), -0.98 (ending repeat unit).

**P3:** MEP (857 mg, 6.21 mmol, 135 eq.), CEP (217 mg, 690  $\mu$ mol, 15 eq.), DBU (56 mg, 368  $\mu$ mol, 8 eq.), TU (136 mg, 368  $\mu$ mol, 8 eq.), initiator (7 mg, 46  $\mu$ mol, 1 eq.). Yield: 1.02 g, 97%.  $M_n$ (NMR): 28,400 g/mol.  $^1\text{H}$  NMR (300 MHz, DMSO- $d_6$ ):  $\delta$  [ppm] 7.39-7.27 (m, 5H  $Ar$ -, initiator), 6.76-6.54 (m, 48H,  $Ar$ -, catechol), 4.90 (t, 1H,  $-CH_2-CH_2-OH$ ), 4.52 (s, 2H,  $Ar-CH_2-O$ -), 4.36-3.90 (m, 755H, catechol- $CH_2-CH_2-CH_2-O-P$ -,  $-O-CH_2-CH_2-O$ -, backbone), 3.83-3.62 (d, 503H,  $CH_3-O-P$ -), 3.50 (t, 2H,  $-CH_2-CH_2-OH$ ), 2.59-2.53 (m, 17H, catechol- $CH_2-CH_2-CH_2-O-P$ -), 1.94-1.77 (m, 32H, catechol- $CH_2-CH_2-CH_2-O-P$ -), 1.60 (s, 112H,  $-CH_3$ , protecting group).  $^{31}\text{P}$ {H} NMR (121 MHz, DMSO- $d_6$ ):  $\delta$  [ppm] -1.15 (catechol repeat unit), -0.12 (MEP repeat unit).

*General procedure for removal of the ketal protecting group.* The respective polymer was dissolved in a mixture of TFA/DCM 1:1 with a concentration of 100 mg/mL and stirred for 30 min at room temperature. The deprotected polymer was precipitated into hexane and centrifuged (4000 rpm, 15min, room temperature), dissolved in 20 mL DCM, and extracted with distilled water (3x20 mL), until the aqueous phase was neutral. The organic phase was dried with  $\text{NaSO}_4$ , filtered and evaporated till dryness. Yield: quantitative.

**P1a-dep:**  $^1\text{H}$  NMR (500 MHz, DMSO- $d_6$ ):  $\delta$  [ppm] 8.68 (Ar-OH), 8.62 (Ar-OH), 7.33 (m, Ar-, initiator), 6.65-6.53 (m, -O-C-CH-CH-C, -O-C-CH-C- ), 6.44 (m, -O-CH-CH-C), 4.88 (t, -CH<sub>2</sub>-CH<sub>2</sub>-OH), 4.52 (s, Ar-CH<sub>2</sub>-O-), 4.24-3.92 (m, catechol-CH<sub>2</sub>-CH<sub>2</sub>-CH<sub>2</sub>-O-P-, -P-O-CH<sub>2</sub>-CH<sub>3</sub>, -O-CH<sub>2</sub>-CH<sub>2</sub>-O-, backbone), 3.64 (t, -CH<sub>2</sub>-CH<sub>2</sub>-OH), 2.46 (t, catechol-CH<sub>2</sub>-CH<sub>2</sub>-CH<sub>2</sub>-O-P-), 1.84 (m, catechol-CH<sub>2</sub>-CH<sub>2</sub>-CH<sub>2</sub>-O-P-), 1.26 (t, -CH<sub>3</sub>).  $^{31}\text{P}$  {H} NMR (202 MHz, DMSO- $d_6$ ):  $\delta$  [ppm] -1.23 (EEP repeat unit), -1.13 (catechol repeat unit), -0.98 (ending repeat unit).

**P3-dep:**  $^1\text{H}$  NMR (300 MHz, DMSO- $d_6$ ):  $\delta$  [ppm] 8.70 (Ar-OH), 8.64 (Ar-OH), 7.34 (m, Ar-, initiator), 6.67-6.55 (m, -O-C-CH-CH-C, -O-C-CH-C- ), 6.43 (m, -O-CH-CH-C), 4.90 (t, -CH<sub>2</sub>-CH<sub>2</sub>-OH), 4.52 (s, Ar-CH<sub>2</sub>-O-), 4.28-3.91 (m, catechol-CH<sub>2</sub>-CH<sub>2</sub>-CH<sub>2</sub>-O-P-, -O-CH<sub>2</sub>-CH<sub>2</sub>-O-, backbone), 3.70 (d, CH<sub>3</sub>-O-P-), 3.57 (t, 2H, -CH<sub>2</sub>-CH<sub>2</sub>-OH), 2.46 (t, catechol-CH<sub>2</sub>-CH<sub>2</sub>-CH<sub>2</sub>-O-P-), 1.83 (m, catechol-CH<sub>2</sub>-CH<sub>2</sub>-CH<sub>2</sub>-O-P-).  $^{31}\text{P}$  {H} NMR (121 MHz, DMSO- $d_6$ ):  $\delta$  [ppm] -1.16 (catechol repeat unit), -0.12 (MEP repeat unit).

*General Procedure for Covalent Network Formation as a proof of concept.* 79.28 mg **P1b-dep** were dissolved in 99  $\mu\text{L}$  of ethanol (25 v% of total sample volume). An aqueous mixture of 135  $\mu\text{L}$  0.05 M NaOH solution (34 v% of total sample volume) was added and mixed by micropipette suction. 163  $\mu\text{L}$  0.15 M NaIO<sub>4</sub> solution (41 v%) were added and well mixed by micropipette suction, to give a final polymer concentration of 200 mg/mL and catechol/NaIO<sub>4</sub> ratio of 2:1. The mixture turned immediately dark red-brown and formed a gel within 5 min.

*Swelling of PPE Gels.* The polymer gel was soaked in 200 mL water for 24h to obtain equilibrium swelling. During this time the water was exchanged three times to remove residual ethanol, NaOH and NaIO<sub>4</sub>. After removal of the surface water with a KIMTECH precision wipe, the gel was weighted ( $W_s$ ). The polymer was extensively freeze-dried at 0.001 mbar for 72 h and the dry polymer weighted again ( $W_d$ ). The swelling ratio was calculated by  $(W_s - W_d)/W_d \cdot 100\%$ .

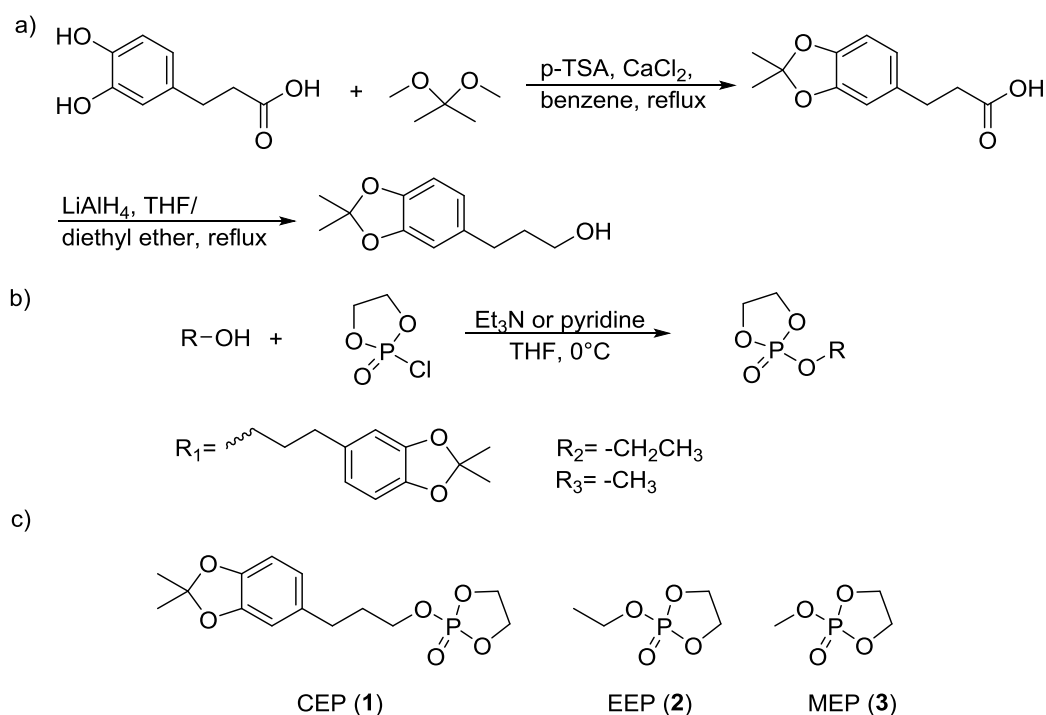
*General procedure for preparation of samples for rheological measurements:* All samples exhibited a final polymer concentration of 200 or 400 mg/mL. Detailed composition of the different samples for rheological measurements are listed in Table 3.2. **P1a-dep** or **P1b-dep** were dissolved in 25, 30 or 50 v% EtOH, 26.1, 50.6 or 57.8 v% phosphate buffer (pH 8.5, 100mM) or 9 or 34 v% water were added and mixed well by micropipette suction. 12.2-48.9 v% NaIO<sub>4</sub>-solution (0.2-0.4 M) was added. The molar ratio of catechol/NaIO<sub>4</sub> in the samples was adjusted to 4:1, 2:1 or 1:1. The sample was mixed fast by micropipette suction, and 12  $\mu\text{L}$  of the fluid sample loaded into the rheometer. The measurements were immediately started. In the following is the procedure for the preparation of sample **C3** described as an distinct example (**C3**: polymer concentration 400 mg/mL, catechol/NaIO<sub>4</sub> 2:1, 25 v% EtOH, 50.6 v% PBS buffer, 24.4 v% 0.4M NaIO<sub>4</sub>-solution ): 8 mg of **P1a-dep** were dissolved in 5  $\mu\text{L}$  EtOH, 10.12  $\mu\text{L}$  PBS buffer added and mixed well by micropipette

suction. 4.88  $\mu\text{L}$   $\text{NaIO}_4$ -solution (0.4 M) were added and the sample was mixed fast by micropipette suction. 12  $\mu\text{L}$  of the mixture was immediately used for the measurement.

### 3.4 Results and Discussion

**Monomer Syntheses.** A cyclic phosphate monomer, containing a catechol group as pendant group, suitable for the ring-opening polymerization (ROP) to PPEs was prepared (Scheme 3.1). Since the ROP does not tolerate hydroxyl groups (they serve as initiator for the polymerization), the pendant catechol group was protected as a ketal, which is removed after polymerization to release the free catechol functionality.

The cyclic monomer 2-(3-(2,2-dimethylbenzo[d][1,3]dioxol-5-yl)propoxy)-2-oxo-1,3,2-dioxaphospholane (**CEP**, **1**) was prepared in three steps, starting from 3,4-dihydroxyhydrocinnamic acid. The catechol was ketal-protected with 2,2-dimethoxypropane under acidic conditions. Subsequently, the carboxyl group was reduced by  $\text{LiAlH}_4$  to the alcohol (Scheme 3.1a).<sup>37</sup> The resulting alcohol serves as pendant group for the cyclic monomer (**1**), which was obtained after esterification with 2-chloro-1,3,2-dioxaphospholane oxide (COP) (Scheme 3.1b). **1** was purified by column chromatography to yield the pure monomer as colorless solid. The monomer can be stored at  $-28^\circ\text{C}$  under dry inert gas for at least one year; elevated temperatures or humidity should be at



**Schem 3.1.** a) Synthesis of 2,2-dimethyl-1,3-benzodioxole-5-propanol; b) synthesis of cyclic phosphate monomers; c) cyclic phosphate monomers used in the study.

-28 °C under dry inert gas for at least one year; elevated temperatures or humidity should be avoided. The monomer was characterized by  $^1\text{H}$  and  $^{31}\text{P}\{\text{H}\}$  NMR spectroscopy (Figure 3.1a and S3.1-S3.3). While the aromatic ring of the catechol group showed resonances at 6.56-6.65 ppm (a) and the protecting group a singlet at 1.66 ppm (f), signals for the dioxaphospholane ring were observed at 4.31-4.50 ppm (b) as multiplet. The  $^{31}\text{P}\{\text{H}\}$  NMR spectrum showed a singlet at 17.59 ppm, typical for cyclic phosphate monomers.<sup>36</sup>

To ensure water-solubility of the polymer, the comonomer 2-ethoxy-2-oxo-1,3,2-dioxaphospholane **EEP** (**2**) was synthesized according to literature protocols (Scheme 3.1b and c).<sup>38</sup> EEP forms water-soluble PEEP, which is used as hydrophilic building block in PPE-based drug delivery systems,<sup>39-40</sup> and it was also used as comonomer for the catechol-PPEs synthesized in this study. A further cyclic monomer, 2-methoxy-2-oxo-1,3,2-dioxaphospholane **MEP** (**3**), was alternatively used as comonomer. MEP is known to form more hydrophilic polymers compared to EEP.

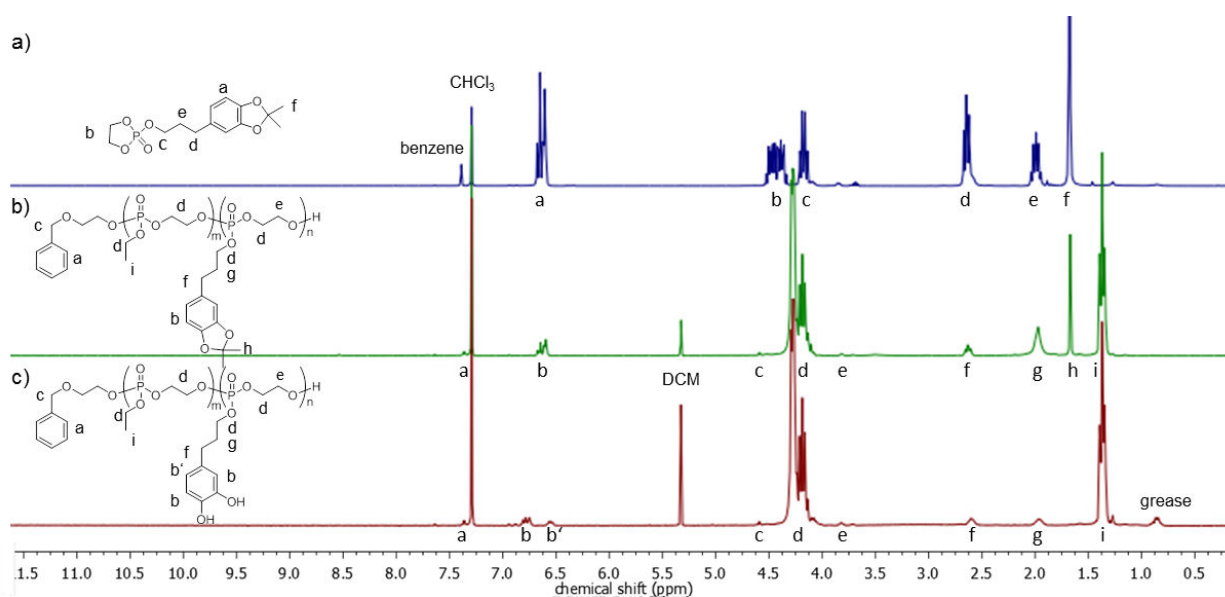


**Figure 3.1.**  $^1\text{H}$  NMR spectra (300 MHz,  $\text{CDCl}_3$ ) of a) CEP monomer (**1**), b) copolymer **P1b** and c) deprotected copolymer **P1a-dep**.

**Polymerization.** A series of copolymers, containing the cyclic phosphate monomers **CEP** and **EEP** or **MEP**, was prepared by the anionic ROP (Scheme 3.1a) with 1,8-diazabicyclo[5.4.0]undec-7-ene (DBU) and *N*-cyclohexyl-*N'*-(3,5-bis(trifluoromethyl)phenyl) thiourea (TU) as the catalyst mixture according to a literature protocol<sup>36</sup> at 0 °C in dry DCM with a total monomer concentration of 4 mol/L.

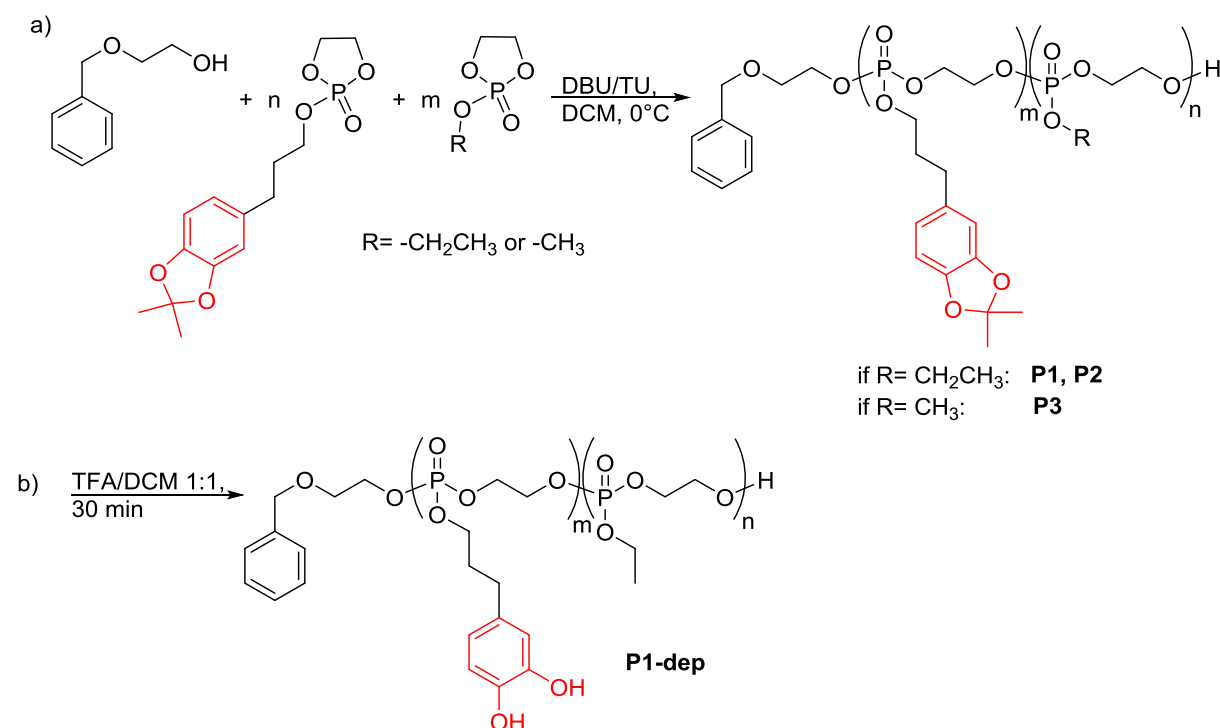
Successful copolymerization was proven by SEC and  $^{31}\text{P}\{\text{H}\}$  NMR measurements (Table 3.1). The ROP produced PPEs with narrow molecular weight distributions of  $\mathcal{D}$ = 1.14-1.37 (Figure 3.2a),

indicating the controlled nature of the DBU/TU catalyst system for the mixture of **EEP** and **CEP**, and high monomer conversions (86-97%). **P3** showed a, broader, bimodal distribution than **P1** and **P2**, probably due to additional initiation by residual water traces. The copolymers will be cross-linked to form hydrogels (*see below*), therefore the broader distribution is assumed to not have a strong or negative influence for the following experiments. The phosphorus signals in  $^{31}\text{P}\{\text{H}\}$  NMR spectra shifted from 16.83, 17.59 and 17.89 ppm for the monomers **EEP**, **CEP**, and **MEP**, respectively, to -0.98, -1.13 and -1.24 ppm for the polymers (endgroup, **CEP** and **EEP** units, respectively; or -0.12 and -1.15 ppm for **P3**) and confirmed polymerization (Figures S3.5 and S3.7). A  $^1\text{H}$  DOSY spectrum of **P1b** confirmed the formation of copolymers (Figure S3.12). The aromatic protons of the initiator 2-(benzyloxy)ethanol from  $^1\text{H}$  NMR spectra were used for molecular weight calculation by end

**Table 3.1.** Overview on polymerizations and results.

entry	[I]/[1]/ [2]	$DP_{th}$ a	1 / DP <sup>a</sup>	1 / %	2 / DP <sup>a</sup>	2 / %	$DP^a$	yield	$M_n^b$ / g/mol	$M_w$ / $M_n^c$	$T_g^d$ / °C
<b>P1a</b>	1/15/135	150	12	8	136	92	148	0.89	24,600	1.18	-
<b>P1b</b>	1/15/135	150	19	10	168	90	187	0.86	31,700	1.15	-49
<b>P1b-dep</b>	-	-	-	-	-	-	-	quant.	30,900 <sup>d</sup>	1.18	-39
<b>P2</b>	1/30/120	150	37	19	159	81	196	0.81	36,000	1.14	-50
<b>P3</b>	1/15/135	150	16	9	168 <sup>e</sup>	91 <sup>e</sup>	184	0.97	28,400	1.37	-53
<b>P3-dep</b>	-	-	-	-	-	-	-	quant.	27,900	1.39	-

<sup>a</sup>DP= degree of polymerization. <sup>b</sup>Determined by  $^1\text{H}$  NMR spectra. <sup>c</sup>Determined by SEC in DMF, RI-signal. <sup>d</sup>Determined by DSC. <sup>e</sup>MEP.



**Scheme 3.1.** a) copolymerization of cyclic monomers **CEP** and **EEP** or **MEP** by ROP forming **P1**, **P2** or **P3** b) deprotection of **P1**.

group analysis. The calculated degree of polymerization ranged from 148-196 for the polymers and molecular weights of 24,600-36,000 g/mol were obtained under these conditions. A  $^1\text{H}$  NMR spectrum of **P1b** is exemplarily shown in Figure 3.1b (other spectra in the supporting information, Figures S3.4 and S3.6). The resonances of the aromatic protons of the initiator at 7.33 ppm (a) were compared with distinct resonances for the two different repeat units in the polymer (note: for endgroup analysis spectra in  $\text{DMSO-d}_6$  were used, Figure 3.1 shows spectra in  $\text{CDCl}_3$  for better comparison with **CEP** monomer): the aromatic signal at 6.54-6.65 ppm (b) for the **CEP** repeat unit and the triplet signal at 1.36 ppm (i) which belongs to the **EEP** repeat unit (or a doublet signal at 3.62-3.83 ppm for **MEP** repeat unit). The signal of the backbone and methylene groups of side chains neighboring the P-O bond at 4.04-4.36 ppm (d) gives the degree of polymerization and coincided with the total number of monomer repeat units. The ratios of comonomers from initial feed were retrieved in all copolymers.

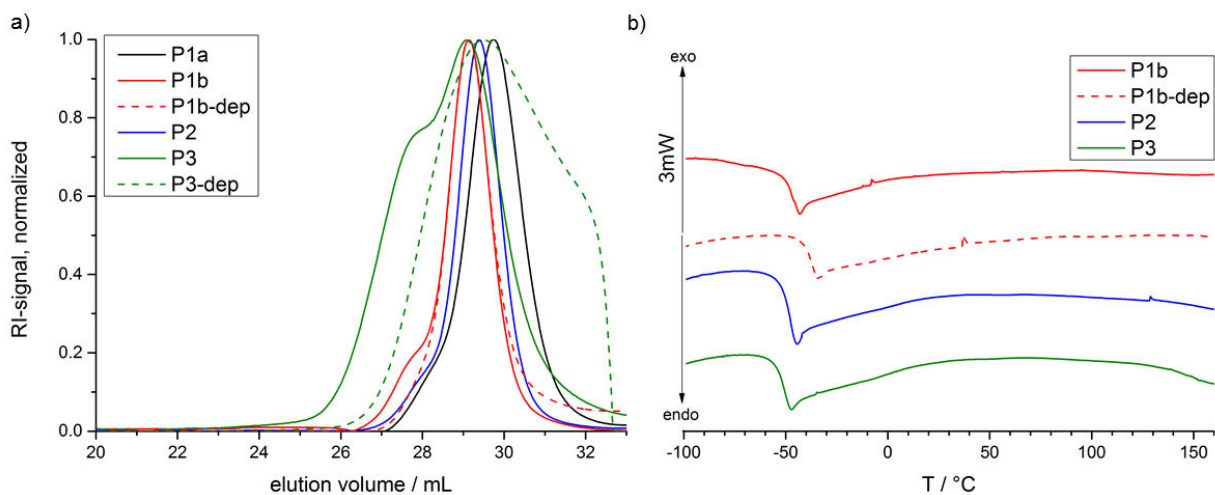


**Figure 3.2.** a) SEC elugrams of all protected copolymers and deprotected **P1b** in DMF, PEO standard, RI-signal; b) DSC thermograms of polymers (heating and cooling rate  $10\text{ K min}^{-1}$ , 1<sup>st</sup> run).

**Release of Catechols.** The release of the catechol function from their ketal-protected precursor is typically realized under acidic conditions.<sup>41</sup> We recently established a protocol for quantitative deprotection of catechol-containing PPEs from ADMET polymerization,<sup>30</sup> where the degradable backbone remained unaffected. This protocol was also applied for the catechol-PPEs from ROP polymerization. Quantitative hydrolysis of the pendant ketals without backbone degradation or transesterification was achieved when the polymers were dissolved in dichloromethane/TFA (50:50, with approx. 10 wt% polymer) within 30 min at room temperature. Deprotection was proven by  $^1\text{H}$  NMR spectroscopy (Figure 3.1c and S3.8): the methyl resonances of the ketal group at 1.65 ppm disappeared and the multiplet in the aromatic region at 6.54-6.65 ppm split into two distinct signals at 6.52 and 6.68-6.82 ppm (measured in  $\text{CDCl}_3$ ).  $^1\text{H}$  NMR spectra from  $\text{DMSO-d}_6$  showed two additional singlets at 8.62 and 8.68 ppm, belonging to the released hydroxyl groups

(Figure S3.8)  $^{31}\text{P}$  NMR spectra showed, that the resonance of the **CEP** unit at -1.13 ppm was not affected by deprotection (Figure S3.9). SEC (Figure 3.2a) and  $^1\text{H}$  NMR data (Figure 3.1c and S3.8) supported the fact that no transesterification or degradation occurred during the hydrolysis step of the ketal in the case of **P1b-dep**. The ratio of the side chains of the initial monomer feed were retrieved in the  $^1\text{H}$  NMR spectra of **P1a-dep** and **P1b-dep**. SEC data of **P1b-dep** showed a slight broadening of the molecular weight distribution from  $\bar{M}_w/\bar{M}_n=1.15$  to 1.18, but the maximum elution volume remained unchanged. The molecular weights distribution for **P3-dep** broadens also only slightly, but the maximum elution volume and shape of curve changes. This is probably due to transesterification during deprotection. The methyl side chain of MEP units known to be more labile for transesterification compared to the EEP side chain. Nevertheless, since the polymers will be crosslinked, this is not expected to influence the further application. All protected copolymers are fully amorphous and exhibited  $T_g$ 's between -53 and -49 °C (Figure 3.2b), typical for PPEs from ROP.<sup>42</sup> Deprotection of the catechol group increased the  $T_g$  of ca. 10 °C (for **P1b-dep**). The polymers were soluble in organic solvents such as dichloromethane and chloroform, or polar solvents as THF, ethanol, methanol and DMSO, but insoluble in hexane or diethyl ether. **P1b**, **P1b-dep** and **P2** were soluble in aqueous solutions with 24, 20 or 38 v% ethanol, respectively; hydrophilicity decreased with increasing amount of catechols, and slightly increased after deprotection. **P3** as well as **P3-dep** exhibited higher hydrophilicity, as expected, and were soluble in water (for 20 mg/mL).

**Formation of Gels.** Catechol-containing polymers<sup>29</sup> can form gels and networks upon cross-linking of the catechol functionalities. Cross-linking can be realized (a) by pH-dependent coordinative and reversible complexation of metal oxides or ions with high binding constants,<sup>43, 44</sup> or (b) covalently and irreversibly under alkaline and oxidative conditions. Quinones are generated as intermediates, undergoing Michael(-type) reactions with thiols and amines or other catechols to form covalent crosslinked gels.<sup>45 46</sup>

Cross-linking and gelation of **P1b-dep** was achieved in an alkaline water (0.05M NaOH solution)/ethanol mixture by addition of  $\text{NaIO}_4$  as an oxidant (0.15M). The final solution exhibited a polymer concentration of 200 mg/mL, a water/ethanol volume ratio of 3:1, a catechol concentration of 0.12 M and a catechol/ $\text{NaIO}_4$  ratio of 2:1. The solution turned to dark red-brown immediately after mixing, known as “quinone tanning”,<sup>47</sup> and gelation was achieved within 5 min. The swelling behavior of the gel was explored in water, yielding a solvent uptake of 900% in the swollen state (Figure 3.3).

**Cross-Linking Kinetics.** Del Campo and coworkers<sup>48</sup> extensively investigated the cross-linking kinetics of four-arm PEG-star polymers modified with catecholamines. They were able to

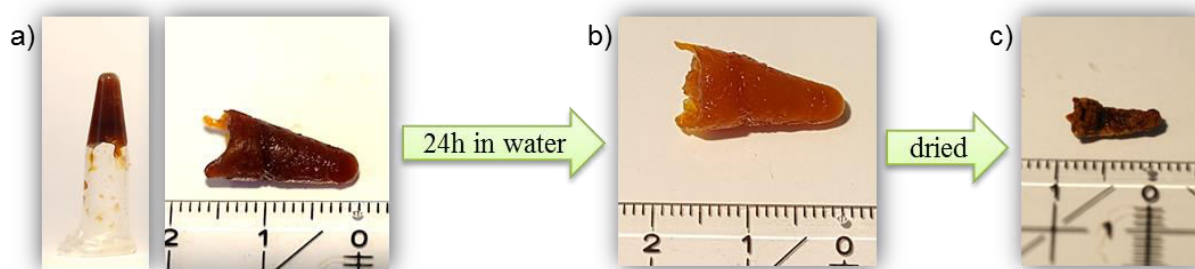


**Figure 3.3.** PPE-gel a) after synthesis, b) after swelling in water for 24h and c) in the dried state.

gauge and tune the polymerization kinetics and final mechanical properties of the tissue-adhesive PEG-gels by varying the substituents in the catecholamines, which may find application as tissue glue or for cell encapsulation. We recently presented PPE-networks based on catechol-containing PPEs from ADMET polycondensation.<sup>30</sup> The ADMET-PPEs lacked enough hydrophilicity to be water-soluble. In this study, PPEs, obtained by ROP, are more hydrophilic and their cross-linking kinetics and mechanical properties in aqueous solution were investigated.

The mechanical properties during curing were measured by oscillating piezorheology, which can determine the shear moduli (dynamic storage modulus  $G'$  and loss modulus  $G''$ ) of soft gels ( $10^1$ - $10^5$  Pa) in small samples with a volume of 12-15  $\mu$ L. A mixture of catechol-PPE (200 or 400 mg/mL, in different solvents (EtOH/PBS buffer pH 8.5, 0.1M or EtOH/water) was mixed with different amounts of  $\text{NaIO}_4$ -solutions (as oxidant) and immediately loaded between the two plates of the piezorheometer in the fluid state. The shear moduli were recorded over time until the periodate-induced cross-linking was completed (i.e. until the rheological curves reached a stable plateau). The catechol/ $\text{NaIO}_4$  ratios were adjusted to 4:1, 2:1 or 1:1. Data are shown in Figure 3.4 and Figures S3.15-S3.22, and compositions of sample solutions in Table 3.2.

Preliminary experiments using a polymer concentration of 200 mg/mL and catechol/ $\text{NaIO}_4$  ratio of 4:1 (in 30 v% EtOH and 70 v% PBS buffer pH 8.5, sample **A**) showed values of the shear moduli at the lower sensitivity limit of the device (Figures S3.15 and S3.16) and therefore polymer concentrations of 400 mg/mL were applied for further measurements. Samples **B1-B3** with polymer concentration of 400 mg/mL showed measurable storage moduli  $G'$  of 8,300-15,200 Pa (Figure 3.4) and curing times of ca. 20-40 h. The curing time was shortened by decreasing the molar ratio of catechol/ $\text{NaIO}_4$ . Lee and coworkers<sup>49-50</sup> reported the fastest curing times for four-arm dopamine functionalized PEG-stars for molar ratios of catechol/ $\text{NaIO}_4$  between 2:1 and 1:1. For catechol-PPEs, the curing time shortened to about 10-20 h for a catechol/ $\text{NaIO}_4$  ratio of 2:1 (samples **C1-C3**, Figure 3.4), and the storage modulus after curing additionally increased to 20,800-30,300 Pa. Increasing the amount of oxidant results in a faster and higher cross-linking of the gel, implicating a higher storage modulus. For a molar ratio of 1:1, the curing time did not

further improve; the storage modulus was 16,400 Pa (samples **D1-D2**, Figure S3.17 and S3.18). A second sample did not result any reliable data, but exhibited several jumps of collected data points. Both samples showed crystals after the curing procedure under an optical microscope. Presumably, periodate precipitated during the curing process from mixture (containing 25 v% EtOH) due to high amounts of the oxidant in the sample, not tolerating the amount of EtOH. It also reasons the observation, that the curing time could not be improved, since the amount of oxidant was actually lower than targeted, and that the second sample showed spread data points.

All identical samples measured under the same conditions showed significant deviations in their results above 10%. This can either be attributed to varying sample preparation or inhomogeneities in the samples. Although the catechol-PPEs are generally water soluble, the polymers were not completely soluble at concentration of 400 mg/mL. Buffer and periodate ions additionally lowered the solubility of the polymer in the mixture, which is known as salting-out for polymers and was also observed for PPEs.<sup>51-52</sup> Therefore ethanol was added as cosolvent to increase the polymer solubility in the sample. On the other hand, higher ethanol content influences and decreases the solubility of buffer and periodate ions in the solution, which may precipitate in the sample. Compared to sample **C1-C3**, the ethanol content was increased from 25 to 50 v% and water instead of PBS buffer was used, to keep the salt concentration in the sample low (samples **E1-E2**). The samples did not show any improvement in the curing time (again around 15-20 h) or storage moduli (26,900-31,700 Pa, Figures S3.19 and S3.20). Also crystal needles were observed again in the samples after curing. Lowering the ethanol content again to 25 v% and the salt concentration using water instead of PBS buffer, the curing time was lowered to 10-15 h and storage moduli increased from 31,100 up to 68,300 Pa (samples **F1-F3**). However, measurements remained not reproducible. Also improving sample preparation by use of stock solutions (samples **G1-G2**) did not further improve the reproducibility of measurements (Figures S3.21 and S3.22).

Summarizing the results, the slope of rheology curves reflects the gelation kinetics, which increases with increasing oxidant concentration. The final value of shear modulus reflects the mechanical stability of the cured gels, indicates the final cross-linking degree of networks and depends on the catechol/ $\text{NaIO}_4$ , the pH of sample, and ethanol and salt concentration in the sample. Increasing oxidant concentration leads to increased oxidized catechols and therefore increased cross-linking density and higher mechanical stability. Samples **F1-F3** with a molar ratio of catechol/ $\text{NaIO}_4$  2:1 in 25 v% EtOH and 75 v% water gave the fastest curing times (10-15 h) and highest storage modulus (31,100-68,300 Pa).

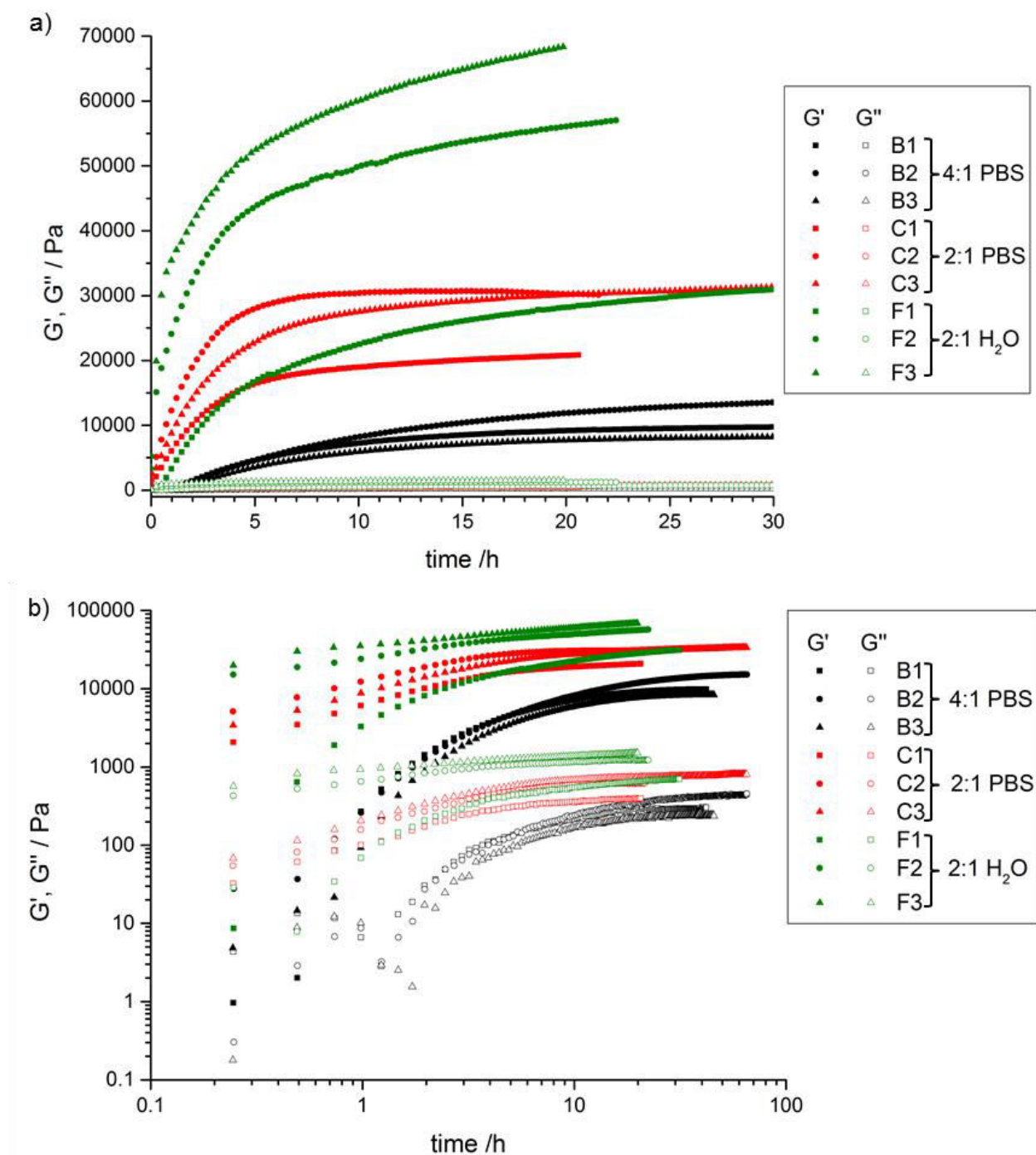


**Figure 3.4.** Rheological measurements of **P1a-dep** or **P1b-dep**: Shear moduli ( $G'$ ,  $G''$ ) of catechol-PPEs in EtOH/PBS buffer (black and red) or EtOH/water (green) as a function of cross-linking time, polymer concentration 400 mg/mL, with different oxidant ratios of catechol/ $\text{NaIO}_4$  of 4:1 (black) or 2:1 (red and green),  $G'$  data points are filled,  $G''$  unfilled. a) linear scaling; b) double logarithmic scaling.

**Table 3.2.** Overview on sample composition for rheological measurements and results.

entry	polymer	polymer conc. / mg/mL	Cat/NaIO <sub>4</sub> ratio	EtOH / v%	PBS buffer / v%	NaIO <sub>4</sub> sol. / v%	NaIO <sub>4</sub> sol. / M	time / h	G' / Pa	G'' / Pa	comment
A	P1a-dep	200	4:1	30	57.8	12.2	0.2	20	300	-	lower sensitivity limit
B1	P1a-dep	400	4:1	25	50.6	24.4	0.2	30	9,900	300	-
B2	P1a-dep	400	4:1	25	50.6	24.4	0.2	30	15,200	450	-
B3	P1a-dep	400	4:1	25	50.6	24.4	0.2	50	8,300	240	-
C1	P1a-dep	400	2:1	25	50.6	24.4	0.4	20	20,800	400	-
C2	P1a-dep	400	2:1	25	50.6	24.4	0.4	10	30,400	600	-
C3	P1a-dep	400	2:1	25	50.6	24.4	0.4	21	30,300	700	-
D1	P1a-dep	400	1:1	25	26.1	48.9	0.4	20	16,400	400	crystal formation
D2	P1a-dep	400	1:1	25	26.1	48.9	0.4	-	-	-	crystal formation
E1	P1b-dep	400	2:1	50	9 <sup>a</sup>	41	0.3	20	31,700	700	crystal formation
E2	P1b-dep	400	2:1	50	9 <sup>a</sup>	41	0.3	17	26,900	500	crystal formation
F1	P1b-dep	400	2:1	25	34 <sup>a</sup>	41	0.3	15	31,100	700	-
F2	P1b-dep	400	2:1	25	34 <sup>a</sup>	41	0.3	10	57,000	1,200	-
F3	P1b-dep	400	2:1	25	34 <sup>a</sup>	41	0.3	15	68,300	1,500	-
G1	P1b-dep	400	2:1	25	34 <sup>a</sup>	41	0.3	25	34,600	800	-
G2	P1b-dep	400	2:1	25	34 <sup>a</sup>	41	0.3	25	27,600	700	-

<sup>a</sup>H<sub>2</sub>O

### 3.5 Conclusions

Water-soluble, catechol-containing poly(phosphoester)s (PPEs) were prepared by the anionic copolymerization of cyclic phosphates and crosslinked to form hydrogels. These might be interesting materials for biomedical applications, e.g. as adhesive gels for (soft) tissue engineering.

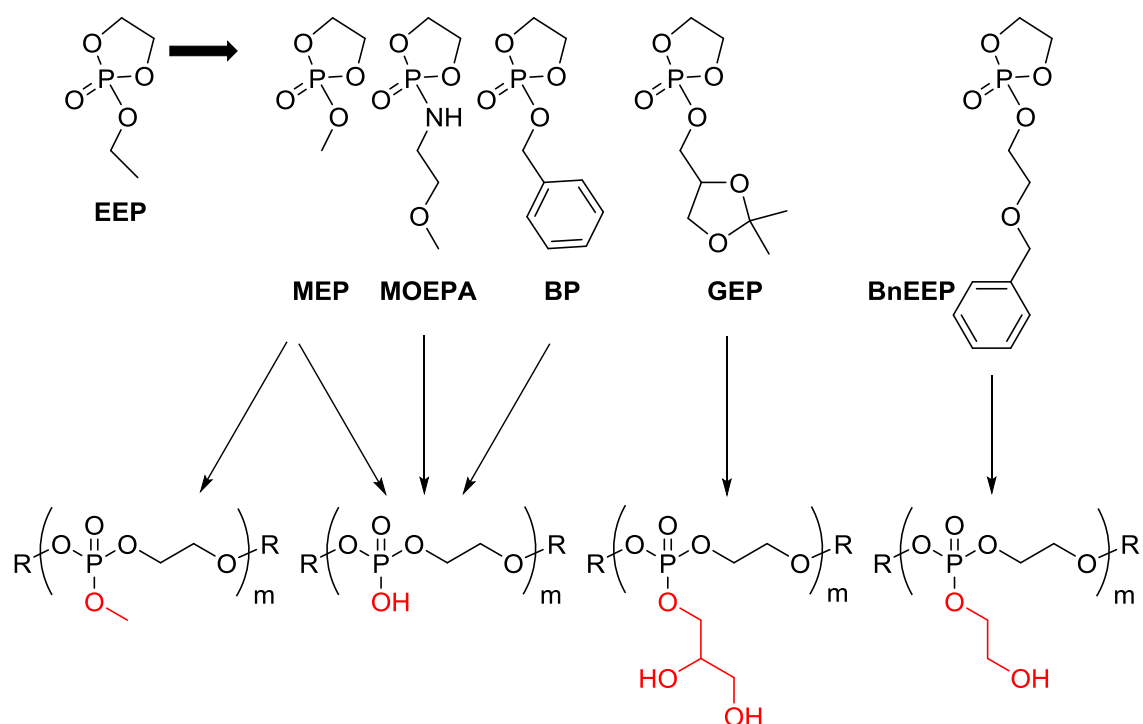
The recently reported combination of the catechol motif with phosphate units in degradable poly(phosphoester)s from ADMET polycondensation<sup>30</sup> was extended to more hydrophilic PPEs, obtained by ROP. For this purpose, a novel cyclic phosphate monomer carrying a protected catechol functionality was developed, and successfully copolymerized in ROP with an ethyl (EEP) or methyl (MEP) comonomer. The obtained copolymers exhibited up to 20 mol% catechol functionalities, molecular weights up to 36,000 g/mol and molecular weight distributions as low as 1.18 (1.37 for MEP copolymers). Quantitative deprotection of the catechol functionalities from the copolymers was succeeded under acidic conditions by release of the ketal group, at the same time the phosphate backbone remained unaffected. Cross-linked PPE-gels were formed under oxidative conditions, exhibiting curing times of 10-15 h and storage moduli of up to 68,300 Pa, measured by piezorheology.

### 3.6 Outlook

Catechol-PPE gels presented in this chapter are interesting materials as bone adhesive or glue for tissue engineering applications. Therefore, their mechanical properties, cross-linking kinetics and homogeneity of samples need to be further improved: shorter curing times of 15-30 min would be favorable for more convenient handling, and higher cohesiveness would increase the mechanical strength of the gels.

So far, the rheological measurements of identical samples (same conditions) exhibit deviations above 10 % and lack enough reproducibility. This might be further improved by increasing the solubility of the samples, which would lead to more homogeneous hydrogels. Investigation on the copolymerization reaction could be interesting to determine the composition of the polymers. <sup>31</sup>P NMR spectra to measure real-time kinetics during the polymerization might give deep insight into the copolymerization kinetics and copolymer composition, as it was conducted for the copolymers in the sections X and X. A statistical distribution of the catechols in the polymers would be favorable to minimize inhomogeneity in the polarity of the polymer itself and avoid “catechol-patches”, which lead to inhomogeneous distribution of cross-linking density in the gels. Furthermore, the system would benefit from increased hydrophilicity of the polymers, ensuring better and more

homogeneous mixing of the samples. A good strategy is altering the comonomer and using a more hydrophilic monomer than EEP (Scheme 3.3). MEP can be an alternative, exhibiting a methyl instead of ethyl side chain and therefore more hydrophilicity. However, this approach involves the danger of formation methanol as toxic byproduct after biodegradation in the body. Copolymerization with MEP was realized in the polymer entry **P3**, which was already successfully deprotected. **P3** exhibits a broader molecular weight distribution ( $\mathcal{D}=1.37$ ), compared to copolymers with EEP, which might be explained by increased transesterification during polymerization. However, a narrow distribution is believed to be less important for the formation of cross-linked gels. The MEP-copolymers can be transformed to even more hydrophilic polymers by cleavage of the methyl side chains releasing P-OH groups, as reported from Iwasaki and coworkers.<sup>53</sup> Besides, two more cyclic phosphate or phosphoramidate monomers are reported, where the side chain can selectively be cleaved after polymerization to release free P-OH.<sup>54-55</sup> Our group recently reported two further monomers GEP and BnEEP,<sup>56</sup> exhibiting free hydroxyl groups in the side chains after deprotection, which can also be from interest to increase the hydrophilicity of the polymers. Another point can be the improvement of sample preparation, to enhance the uniformity of the samples by use of stock solutions.



**Scheme 3.3.** Possible monomer alternatives to EEP, increasing the hydrophilicity of catechol-PPEs.

The cross-linking ability and kinetic of the gels are influenced by several parameters, i.e. hydrophilicity of the polymers, catechol content, oxidant concentration, pH of the solution, and additional cross-linkers. Increased hydrophilicity of the polymers ensures more homogenous mixing of the samples, which might influence the cross-linking efficiency. Higher catechol amounts

would increase the cross-linking density and probably fastens the curing time. It might additionally influence the general hydrophilicity of the polymers, and also the adhesiveness of the gels to substrates. A polymer with 20 mol% catechol groups was realized in entry **P2**, but not further investigated so far. From four-arm PEG-stars with DOPA groups it is known, that increasing the oxidants concentration strongly influences the curing time.<sup>49-50</sup> In our studies, the oxidant concentration was limited to a certain point by the ethanol content in the samples. High periodate concentrations do not tolerate high ethanol amounts, but instead precipitated in the samples during cross-linking. Applying more hydrophilic polymers allow the reduction of ethanol content and at the same time higher periodate concentration would be possible to realize. Finally, the pH strongly influences the ability of oxidizing catechols to quinone intermediates. In our studies, we either used PBS buffer at pH 8.5 or just water at neutral pH. Increasing the pH by using another buffer system and probably decreasing the molarity of the buffer, to minimize the salt concentration in the sample (which influences the salting-out of polymer and periodate solubility) would clearly fasten the cross-linking kinetics. Avoiding buffer systems with high salt concentration, a further consideration can be the use of NaOH solution to increase the pH in the sample and speed up curing time. For sure, when copolymers with free P-OH groups are used, the pH need to be adjusted due to an acidic character of these polymers. In this case, using just water as solvent would end up in an acidic pH, where oxidation of the catechols is strongly reduced or hindered. Applying additional crosslinkers as HSA, BSA or ethylene diamine will also influence the cross-linking kinetic.

The highest storage modulus measured so far was ca. 69,000 Pa. The mechanical strength of the gels can be approved by several factors: higher cross-linking density, additional crosslinkers, or addition of inorganic nanoparticles can increase the cohesiveness of the material. The cross-linking density can be increased simply enhancing the catechol content in the sample (*see above*), or using additional cross-linkers as i.e. HSA with multibinding sites. A further interesting approach is the addition of inorganic nanoparticles, i.e. from hydroxy apatite. Hydroxyapatite is a main component of bones (around 40 %) and therefore seems to be a good additive. Our group recently showed, that PPE-nanoparticles showed good adhesion to MBCP+™ (Biomatlante), a popular bone substituent consisting of calcium phosphate.<sup>32</sup> Probably beneficial for the cohesion of this composite is the additional adhesion of the phosphate groups to the apatite particles. Another alternative can be the mixing with DOPA functionalized PEG-stars.

Besides, the curing time and cohesive strength of the material and its improvement, the adhesive strength to meaningful substrates is from great importance. While in piezorheology the shear moduli can be determined, tensile testing gives insight into the tensile stress (yield, ultimate and rupture strength). Depending on the application purpose, two different biomaterials are convenient and established as substrates: porcine skin as soft tissue substrate or bone discs from

porcine femur bones as hard tissue substrate. In both cases, the gel can be cured between two pieces of skin or bone, fixed in a tensile testing device and pulled apart (Figure 3.5). Data are usually interpreted in a stress-strain-relationship. Besides stress values, the samples provide insight into the failure behavior concerning adhesive or cohesive failing. For applications as tissue adhesive, the mechanical properties of the PPE-networks need to be counterbalanced between adhesive and cohesive strength, to provide a suitable material.

A further improvement of the system can be the introduction of growth factors or proteins, which induce cell migration, mitogenesis and differentiation of mesenchymal stem cells (MSCs) to osteochondroprogenitor cells and finally osteoblasts, being responsible for osteoinduction and -genesis.<sup>12</sup> Bone morphogenetic proteins (BMPP-2, BMP-7) and several growth factors (GF: including fibroblast GF, vascular endothelial GF, platelet-derived GF, insulin-like GF-1, transforming GF, and others), are known to promote migration, proliferation and differentiation of bone cells.<sup>12, 57</sup>

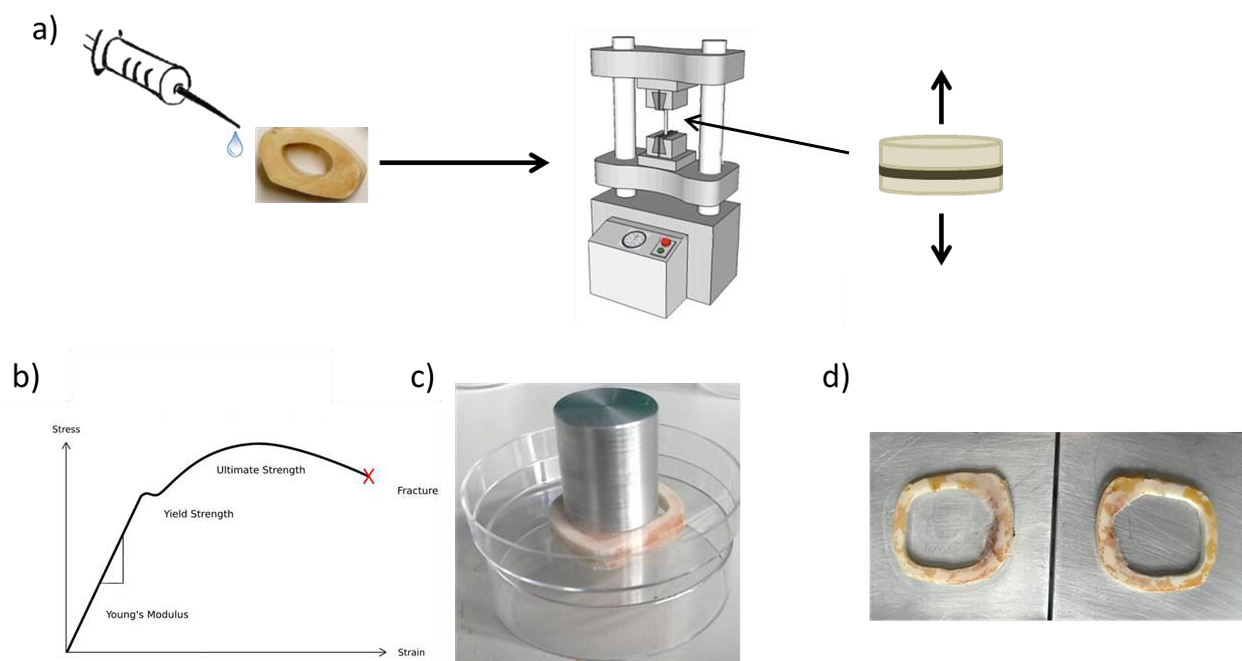


**Figure 3.5.** Exemplary set-up for adhesion tests of catechol-PPEs: a) sample preparation and tensile testing, b) stress-strain curve obtained from tensile tests, c) curing of a catechol-PPE sample between two porcine femur bone discs, d) two bone discs after rupture in a tensile test showing the PPE-adhesive as brownish material.

### 3.7 Supporting Information

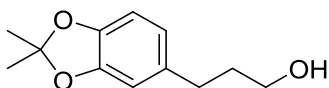
The Supporting Information contains additional synthetic procedures, characterization data for monomers and polymers and rheology data.

#### Content

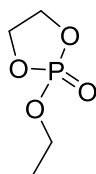
- 3.7.1 Synthetic procedures
- 3.7.2 NMR spectra
- 3.7.3 IR spectra
- 3.7.4 Rheological measurements

#### 3.7.1 Synthetic procedures

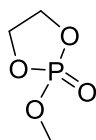
*2,2-Dimethyl-1,3-benzodioxole-5-propanol*: The alcohol was synthesized according to literature<sup>37</sup>. Briefly, a three-neck round-bottom flask was equipped with a Soxhlet extractor with a reflux condenser. The extraction thimble was filled with CaCl<sub>2</sub>. 3,4-dihydroxyhydrocinnamic acid (20.0 g, 109.8 mmol, 1 eq.) and p-toluenesulfonic acid monohydrate (756.19 mg, 4.39 mmol, 0.04 eq.) were dissolved in 750 mL benzene. 2,2-Dimethoxypropane (17.15 g, 164.68 mmol, 1.5 eq.) was added and the reaction mixture was refluxed overnight. The solution was filtered and the solvent concentrated under reduced pressure. The crude product was not further purified (TLC, petroleum ether/ethyl acetate 7:3). A three-neck round-bottom flask was equipped with a reflux condenser and a dropping funnel. LiAlH<sub>4</sub> in THF (2.4M, 100.65 mL, 241.5 mmol, 2.2 eq.) was dissolved in 700 mL of dry diethyl ether. The crude product (24.40 g, 109.8 mmol, 1 eq.), dissolved in 100 mL of dry diethyl ether, was added dropwise in order to keep the diethyl ether refluxing and the reaction mixture was stirred overnight. Excess of LiAlH<sub>4</sub> was decomposed by addition of ice water. Precipitated aluminum hydroxide was filtered off and washed with diethyl ether. After drying over magnesium sulfate, the solvent was concentrated under reduced pressure. Column chromatography (silica gel, petroleum ether/ethyl acetate 7:3, *R<sub>f</sub>*=0.45) gave the pure product. Yield: 5.94 g, 49%. <sup>1</sup>H NMR (300 MHz, CDCl<sub>3</sub>): δ [ppm] 6.66–6.57 (m, 3 H, H<sub>arom</sub>), 3.66 (t, 2 H, CH<sub>2</sub>OH), 2.60 (t, 2 H, Ar-CH<sub>2</sub>CH<sub>2</sub>CH<sub>2</sub>-OH), 1.90–1.78 (m, 2 H, Ar-CH<sub>2</sub>CH<sub>2</sub>CH<sub>2</sub>-OH), 1.65 (s, 6 H, CH<sub>3</sub>). <sup>13</sup>C{H} NMR (76 MHz, CDCl<sub>3</sub>): δ [ppm] 147.37 (O-C-CH-C), 145.45 (O-C-CH=CH), 134.90 (C-CH<sub>2</sub>), 120.40 (O-C-CH=CH), 117.49 (C(CH<sub>3</sub>)<sub>2</sub>), 108.62 (O-C-CH=C), 107.89 (O-C-CH=CH), 62.13 (C-CH<sub>2</sub>-CH<sub>2</sub>-CH<sub>2</sub>-OH), 34.41 (C-CH<sub>2</sub>-CH<sub>2</sub>-CH<sub>2</sub>-OH), 31.78 (C-CH<sub>2</sub>-CH<sub>2</sub>-CH<sub>2</sub>-OH), 25.78 (CH<sub>3</sub>).



*2-ethoxy-2-oxo-1,3,2-dioxaphospholane (EEP, 2)*: The monomer was synthesized according to literature.<sup>38</sup> Briefly, a flame-dried 500mL three-neck flask, equipped with a dropping funnel, was charged with 2-chloro-2-oxo-1,3,2-dioxaphospholane (50.00 g, 0.35 mol) dissolved in dry THF (100 mL). A solution of dry ethanol (16.17 g, 0.35 mol) and dry triethylamine (35.51 g, 0.35 mol) in dry THF (70 mL) was added dropwise to the stirring solution of COP at -20 °C under argon atmosphere. During reaction, hydrogen chloride was formed and precipitated as pyridinium hydrochloride. The reaction was stirred at 4 °C overnight. The salt was removed by filtration and the filtrate concentrated in vacuo. The residue was purified by distillation under reduced pressure to give a fraction at 105-110 °C/0.095 mbar, obtaining the clear, colorless, liquid product EEP. Yield: 34.60 g (0.23 mol), 65%. <sup>1</sup>H NMR (300 MHz, DMSO- d<sub>6</sub>): δ [ppm] 4.47-4.34 (m, 4H, O-CH<sub>2</sub>-CH<sub>2</sub>-O), 4.11-4.04 (m, 2H, O-CH<sub>2</sub>-CH<sub>3</sub>), 1.25 (t, 3H, O-CH<sub>2</sub>-CH<sub>3</sub>). <sup>13</sup>C{H} NMR (76 MHz, DMSO- d<sub>6</sub>): δ [ppm] 66.35 (-O-CH<sub>2</sub>-CH<sub>2</sub>-O-), 64.18 (-O-CH<sub>2</sub>-CH<sub>3</sub>), 15.96 (-O-CH<sub>2</sub>-CH<sub>3</sub>). <sup>31</sup>P{H} NMR (202 MHz, DMSO-d<sub>6</sub>): δ [ppm] 16.83.

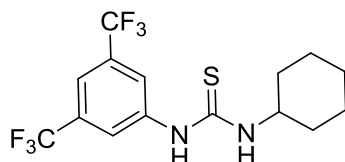


*2-Methoxy-2-oxo-1,3,2-dioxaphospholane (MEP, 3)*: A flame-dried 1000mL three-neck flask, equipped with a dropping funnel, was charged with 2-chloro-2-oxo-1,3,2-dioxaphospholane (50 g, 0.35 mol) dissolved in dry THF (300 mL). A solution of dry methanol (11.24 g, 0.35 mol) and dry pyridine (27.72 g, 0.35 mol) in dry THF (45 mL) was added dropwise to the stirring solution of COP at -20 °C under argon atmosphere. During reaction, hydrogen chloride was formed and precipitated as pyridinium hydrochloride. The reaction was stirred at 4 °C overnight. The salt was removed by filtration and the filtrate concentrated *in vacuo*. The residue was purified by distillation under reduced pressure to give a fraction at 89-97 °C/0.001 mbar, obtaining the clear, colorless, liquid product. Yield: 25.54 g, 53%. <sup>1</sup>H NMR (500 MHz, DMSO-d<sub>6</sub>): δ [ppm] 4.43 (m, 4H, O-CH<sub>2</sub>-CH<sub>2</sub>-O), 3.71 (d, 3H, O-CH<sub>3</sub>). <sup>13</sup>C{H} NMR (121 MHz, DMSO-d<sub>6</sub>): δ [ppm] 66.57 (s, 2C, O-CH<sub>2</sub>-CH<sub>2</sub>-O), 54.72 (s, 1C, O-CH<sub>3</sub>). <sup>31</sup>P {H}NMR (202 MHz, DMSO-d<sub>6</sub>): δ [ppm] 17.89.



*N-cyclohexyl-N'-(3,5-bis(trifluoromethyl)phenyl)thiourea (TU)*: TU was synthesized according to the method described previously<sup>58</sup>. Briefly, in a flame-dried 50 mL flask 3,5-bis(trifluoromethyl)phenylisothiocyanat (2.00 g, 7.4\*10<sup>-3</sup>mol) was dissolved in 10 mL dry THF under argon atmosphere. Cyclohexylamine (0.73 g, 7.2\*10<sup>-3</sup>mol) was added dropwise at room

temperature to the stirring solution. After the reaction mixture was stirred for 5 h, the solvent was removed *in vacuo*. The colourless residue was recrystallized from boiling chloroform. It was filtered hot and cooled down. Colourless needles precipitated in a yellowish solution. The product, TU, was collected by filtration, washed with cold chloroform and dried *in vacuo*. Yield: 1.77g, 370.36 g/mol, 4.8 mmol, 67%.  $^1\text{H NMR}$  (300 MHz, DMSO- $d_6$ ):  $\delta$  [ppm] 9.84 (s, 1H, Ar-NH-C(=S)-NH-Cy), 8.23 (s, 1H, *p*-Ar-NH), 8.17 (s, 2H, *o*-Ar-NH), 7.72 (s, 1H, Ar-NH-C(=S)-NH-Cy), 4.11 (s, 1H, Ar-NH-C(=S)-NH-(*H*)Cy), 1.94-1.15 (m, 10H, Ar-NH-C(=S)-NH-Cy).



### 3.7.2 NMR spectra

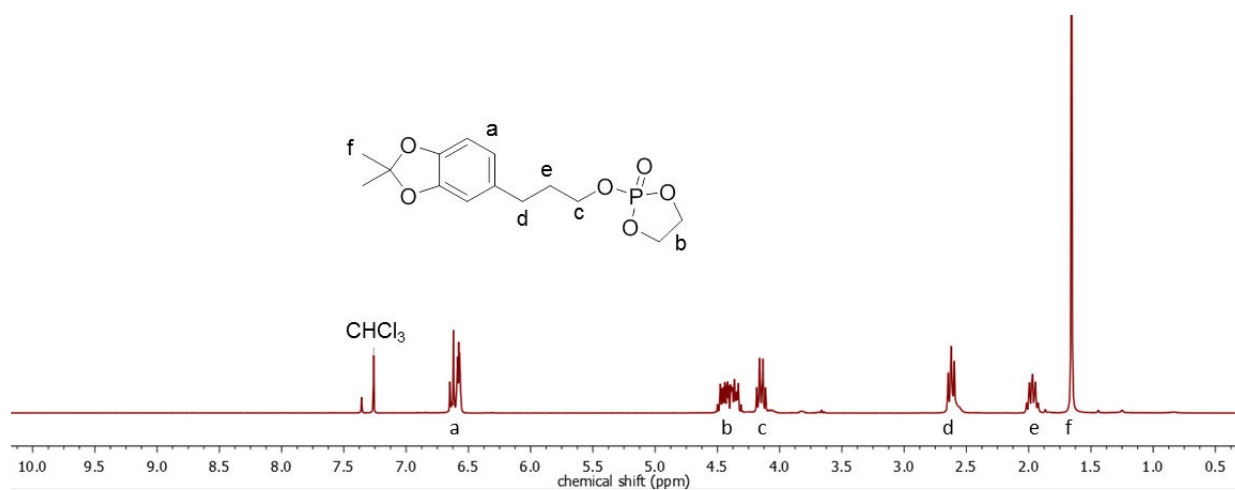


**Figure S3.1.**  $^1\text{H NMR}$  (300 MHz,  $\text{CDCl}_3$ ) of 2-(3-(2,2-dimethylbenzo[d][1,3]dioxol-5-yl)propoxy)-2-oxo-1,3,2-dioxaphospholane (**CEP, 1**) at 298 K.

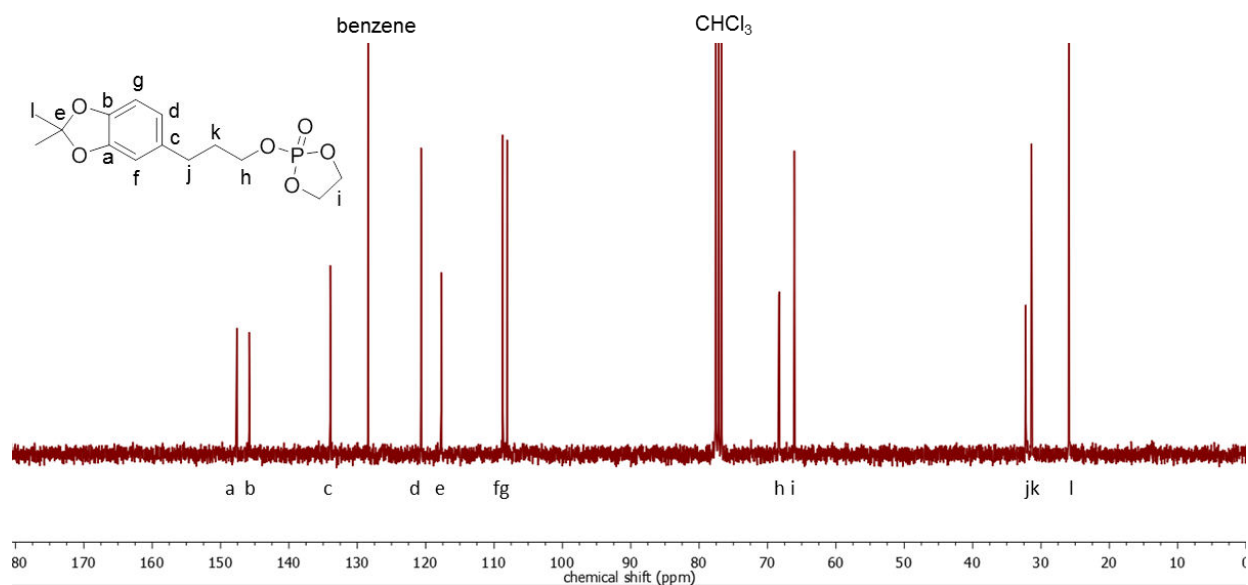


Figure S3.2.  $^{13}\text{C}\{\text{H}\}$  NMR (76 MHz,  $\text{CDCl}_3$ ) of CEP (1) at 298 K.

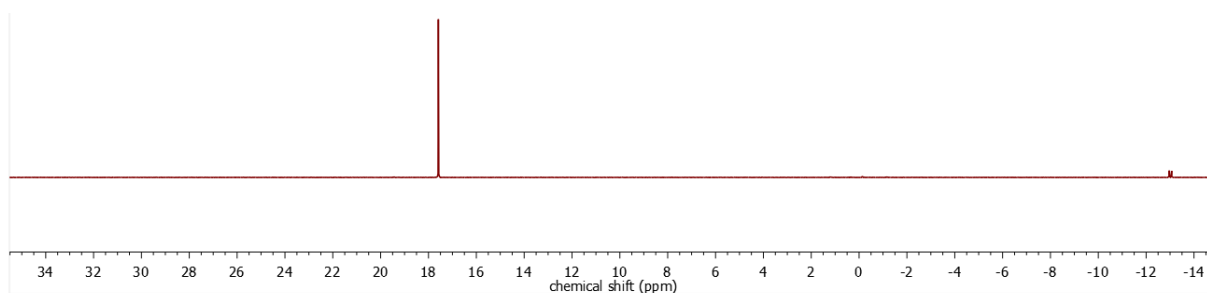


Figure S3.3.  $^{31}\text{P}\{\text{H}\}$  NMR (121 MHz,  $\text{CDCl}_3$ ) of CEP (1) at 298 K.

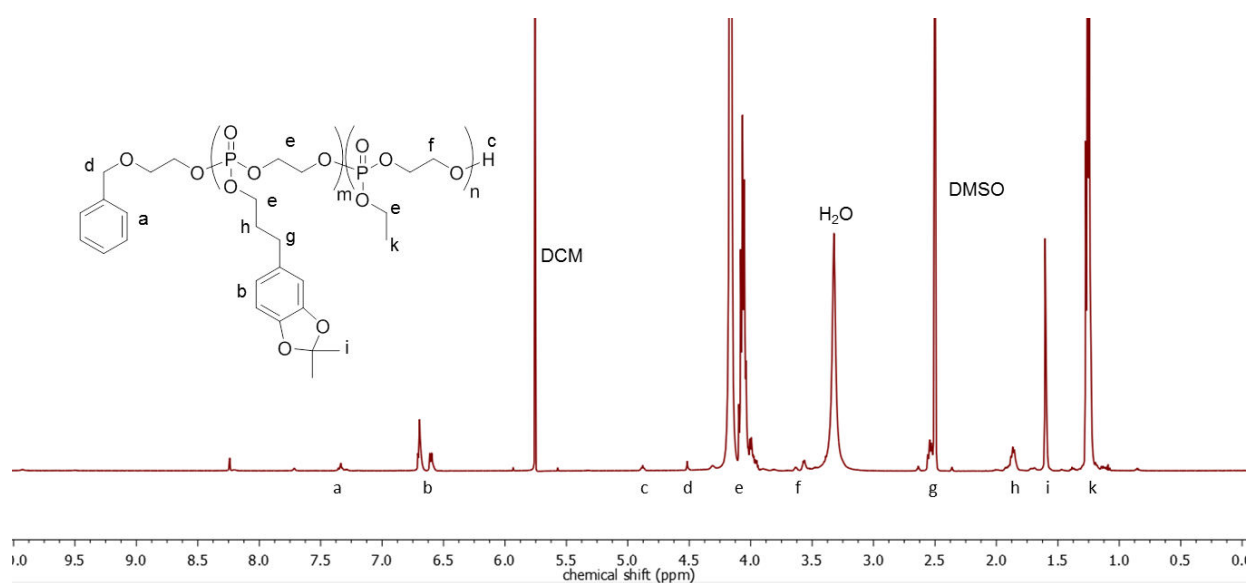
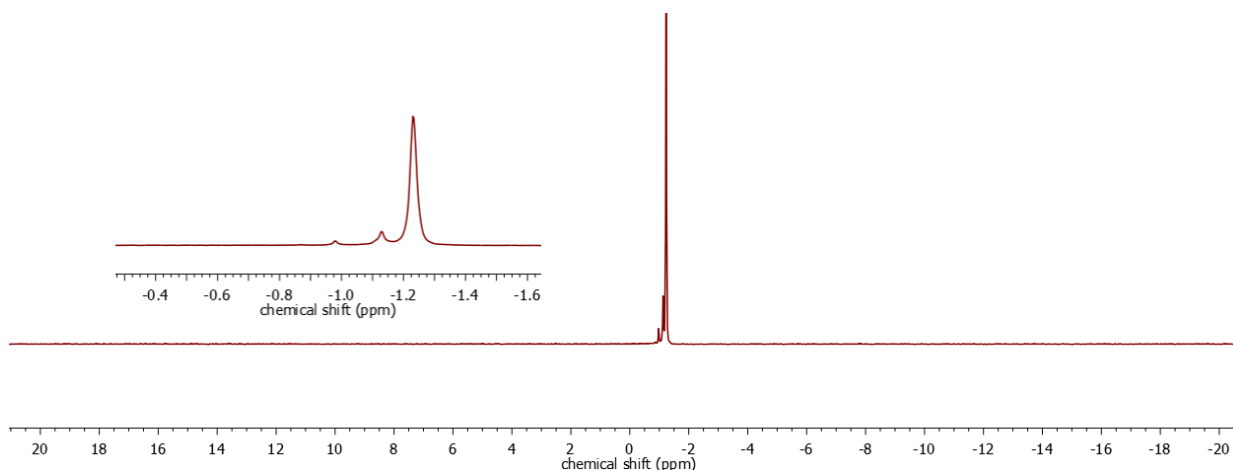
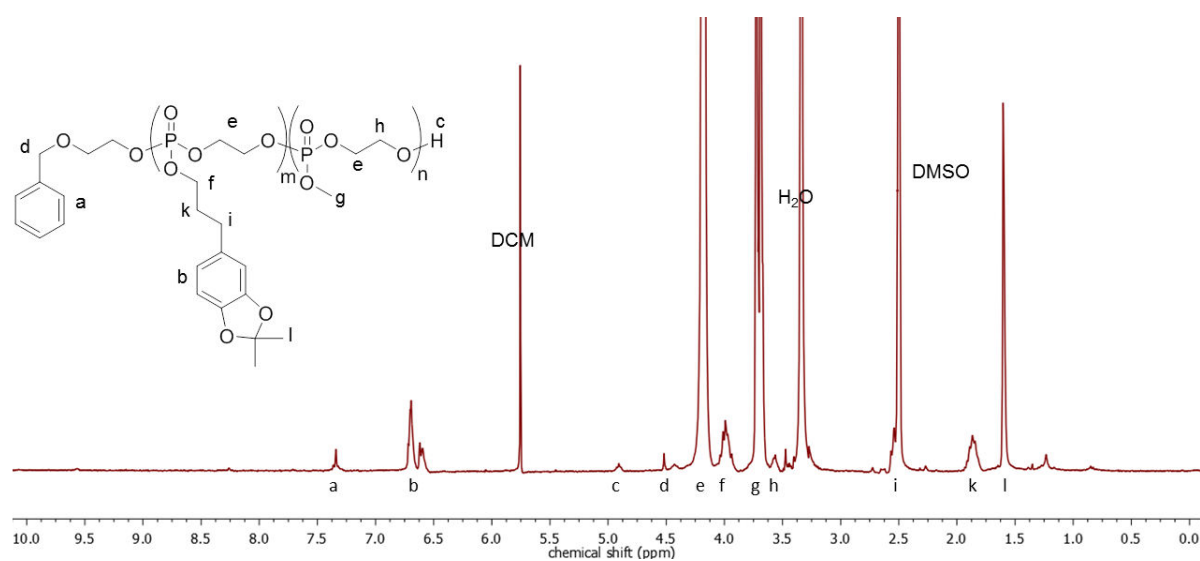


Figure S3.4.  $^1\text{H}$  NMR (500 MHz,  $\text{DMSO-d}_6$ ) of P1a at 298 K.



**Figure S3.5.**  $^{31}\text{P}\{\text{H}\}$  NMR (202 MHz, DMSO- $d_6$ ) of P1a at 298 K.



**Figure S3.6.**  $^1\text{H}$  NMR (300 MHz, DMSO- $d_6$ ) of P3 at 298 K.

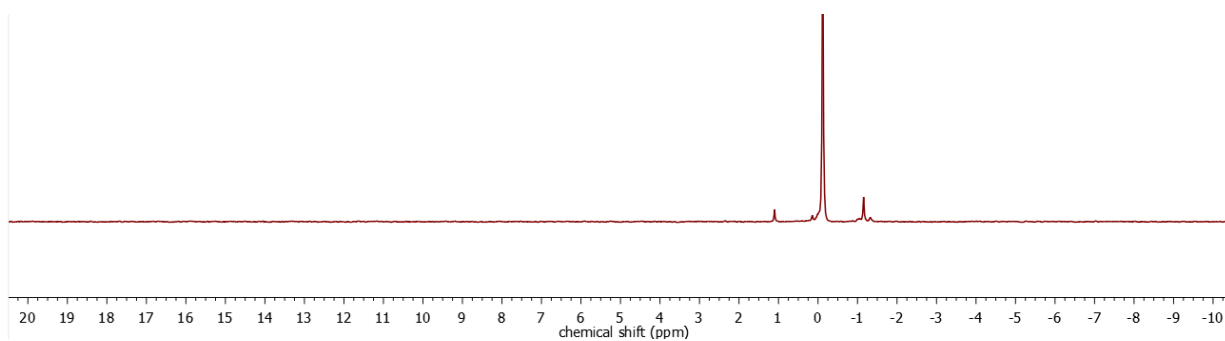


**Figure S3.7.**  $^{31}\text{P}\{\text{H}\}$  NMR (121 MHz, DMSO- $d_6$ ) of P3 at 298 K.

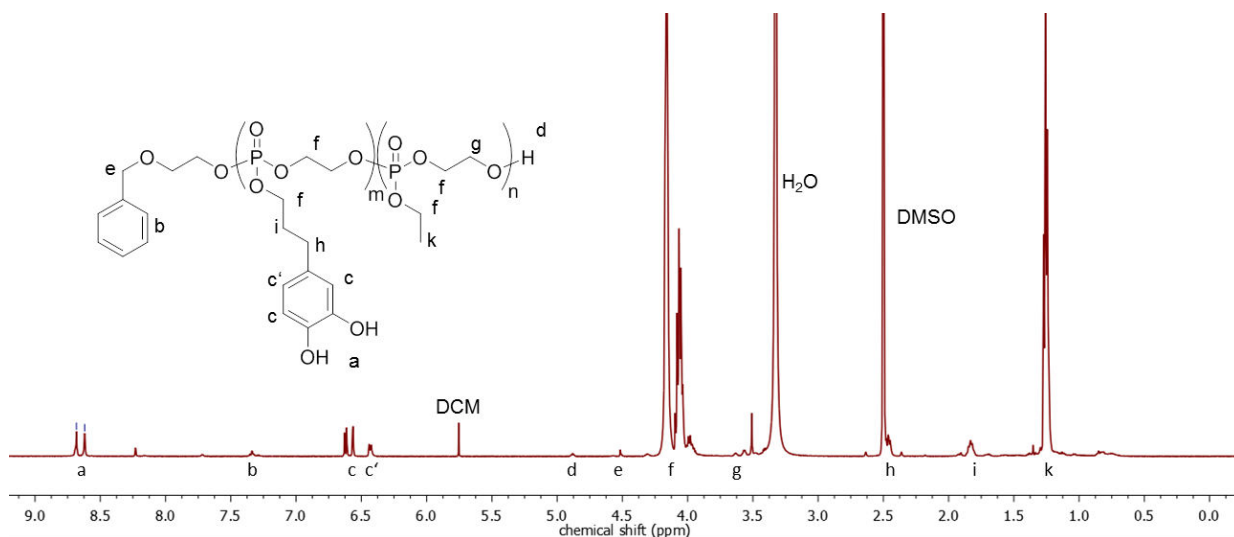


**Figure S3.8.**  $^1\text{H}$  NMR (500 MHz,  $\text{DMSO-d}_6$ ) of **P1a-dep** at 298 K.

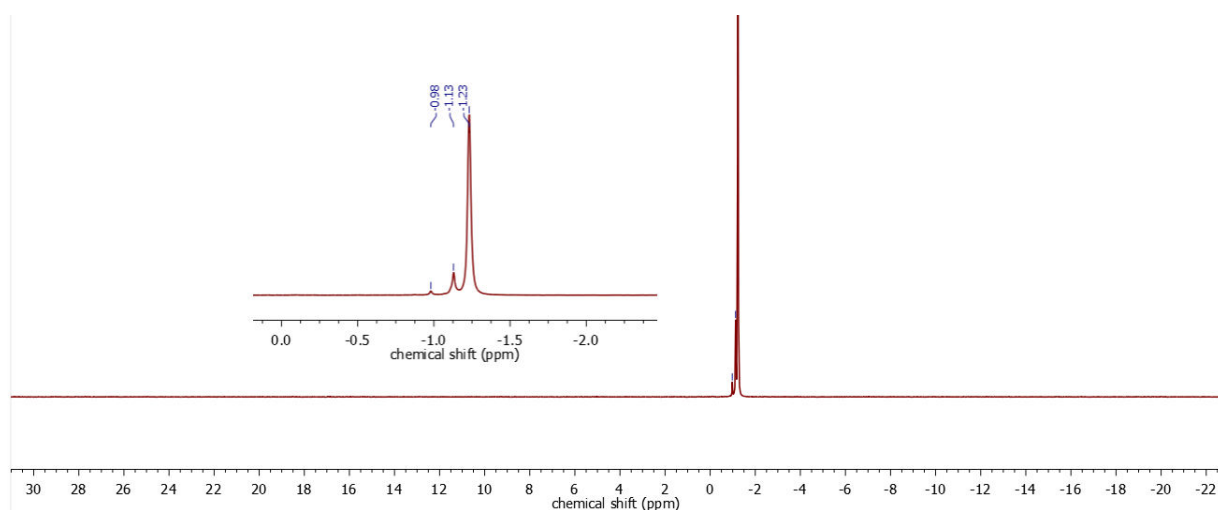


**Figure S3.9.**  $^{31}\text{P}\{\text{H}\}$  NMR (202 MHz,  $\text{DMSO-d}_6$ ) of **P1a-dep** at 298 K.

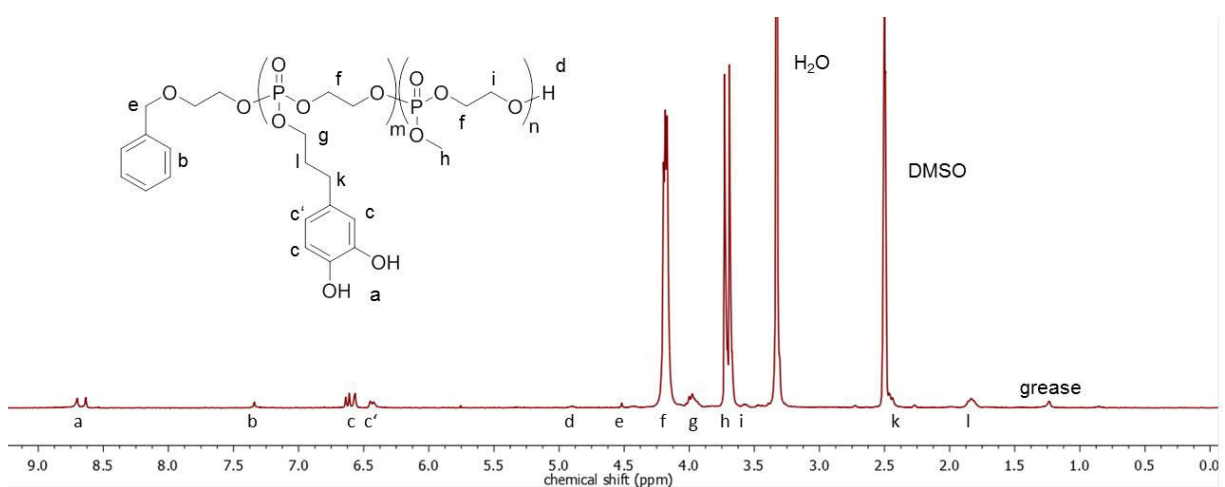


**Figure S3.10.**  $^1\text{H}$  NMR (300 MHz,  $\text{DMSO-d}_6$ ) of **P3-dep** at 298 K.

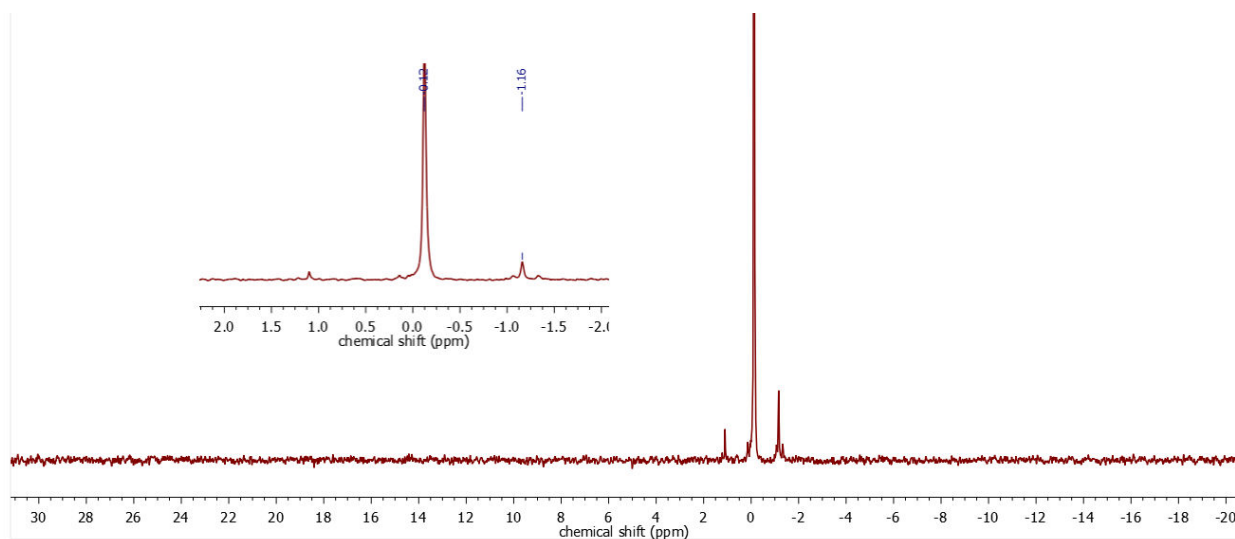


**Figure S3.11.**  $^{31}\text{P}$  NMR (121 MHz,  $\text{DMSO-d}_6$ ) of **P3-dep** at 298 K.

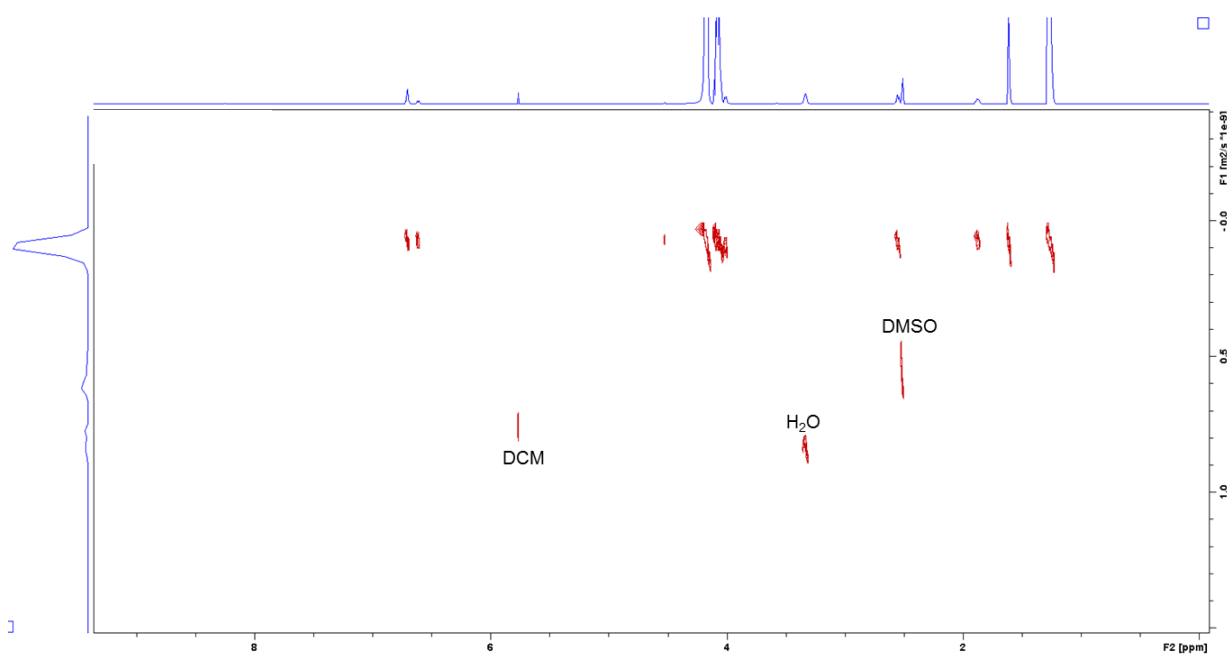


**Figure S3.12.**  $^1\text{H}$ -DOSY (500 MHz,  $\text{CDCl}_3$ ) of **P1** at 298 K.

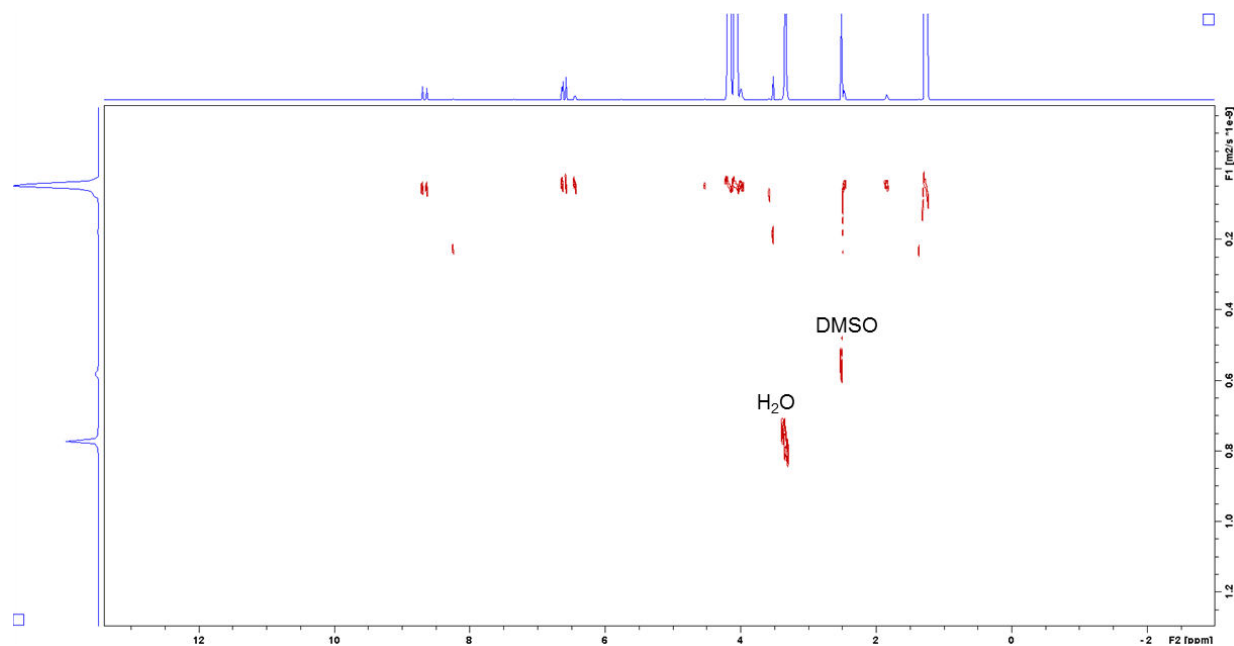


Figure S3.13. <sup>1</sup>H-DOSY (500 MHz, CDCl<sub>3</sub>) of **P1-dep** at 298 K.

### 3.7.3 IR spectra

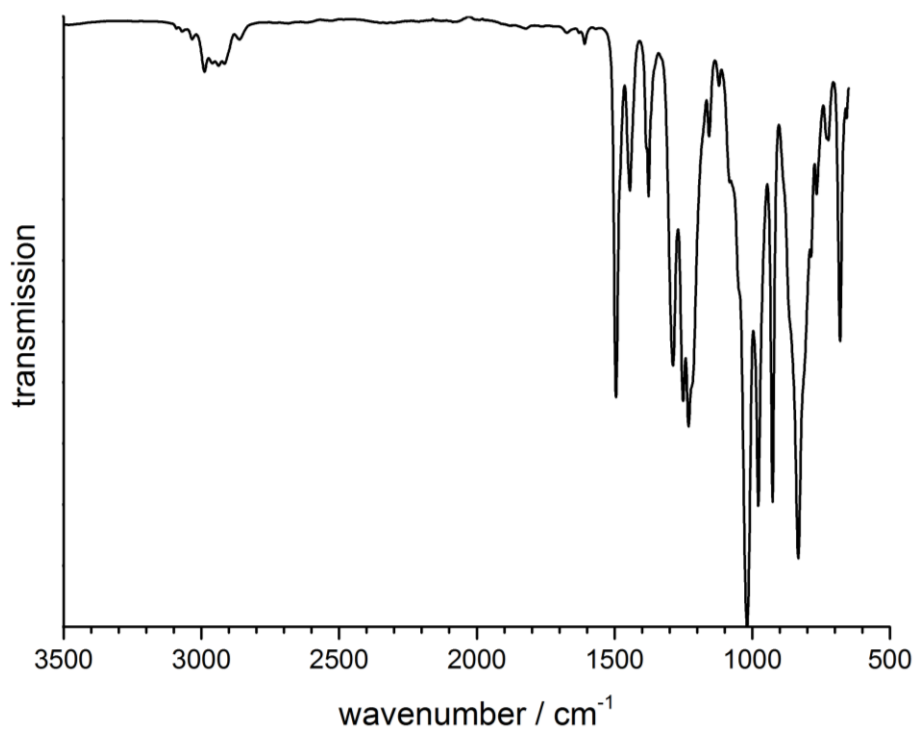
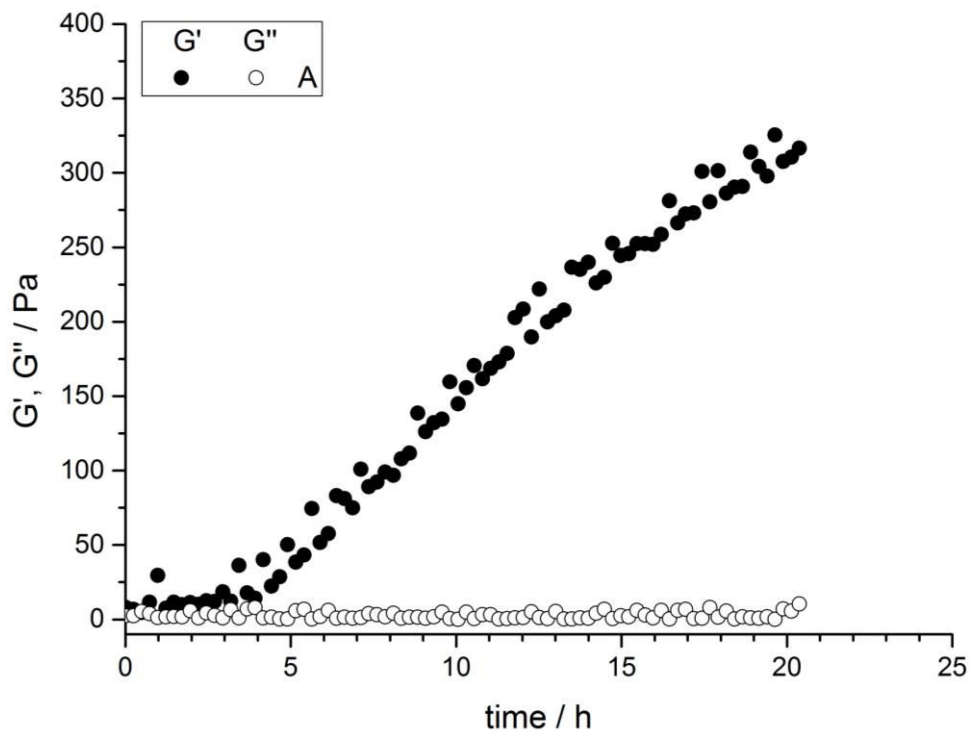
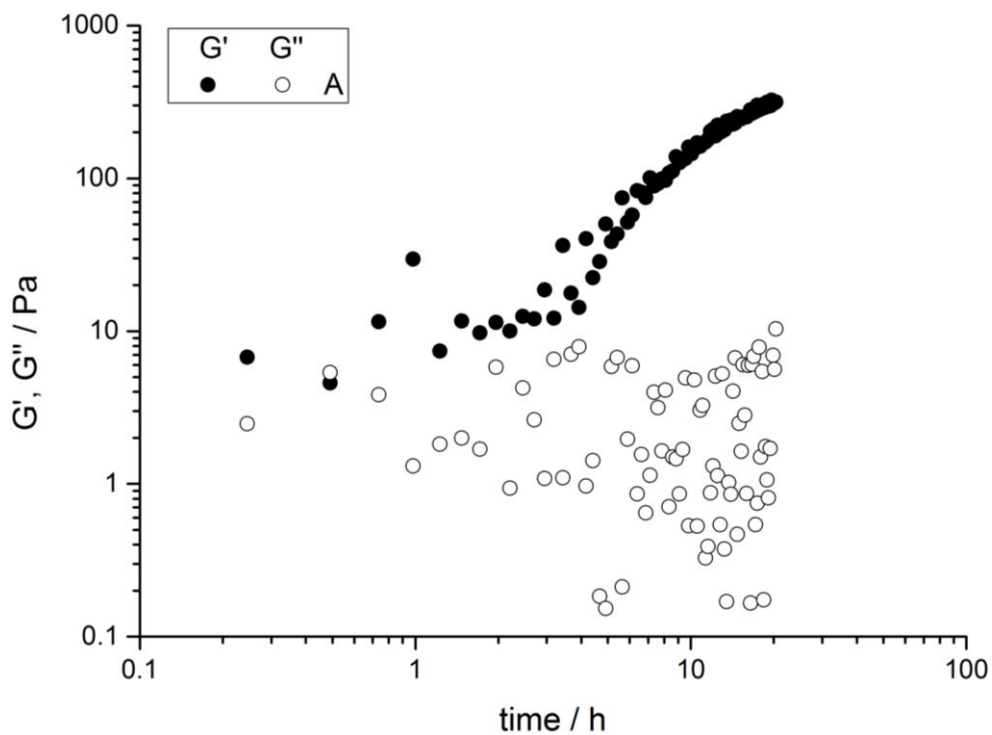


Figure S3.14. FTIR spectrum of **CEP** at 298 K.

### 3.7.4 Rheological measurements



**Figure S3.15.** Shear moduli ( $G'$ ,  $G''$ ), of catechol-PPE in EtOH/PBS buffer as a function of cross-linking time, sample A. Note: linear scaling.



**Figure S3.16.** Shear moduli ( $G'$ ,  $G''$ ), of catechol-PPE in EtOH/PBS buffer as a function of cross-linking time, sample A. Note: double logarithmic scaling.

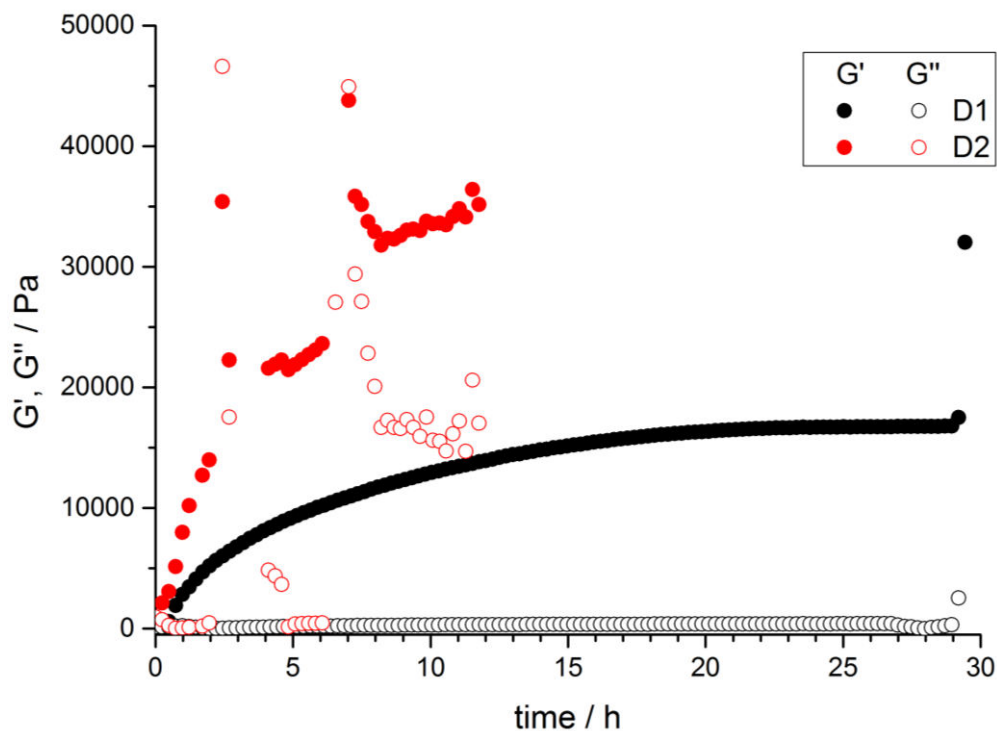


**Figure S3.17.** Shear moduli ( $G'$ ,  $G''$ ), of catechol-PPE in EtOH/PBS buffer as a function of cross-linking time, sample **D1** and **D2**. Note: linear scaling.

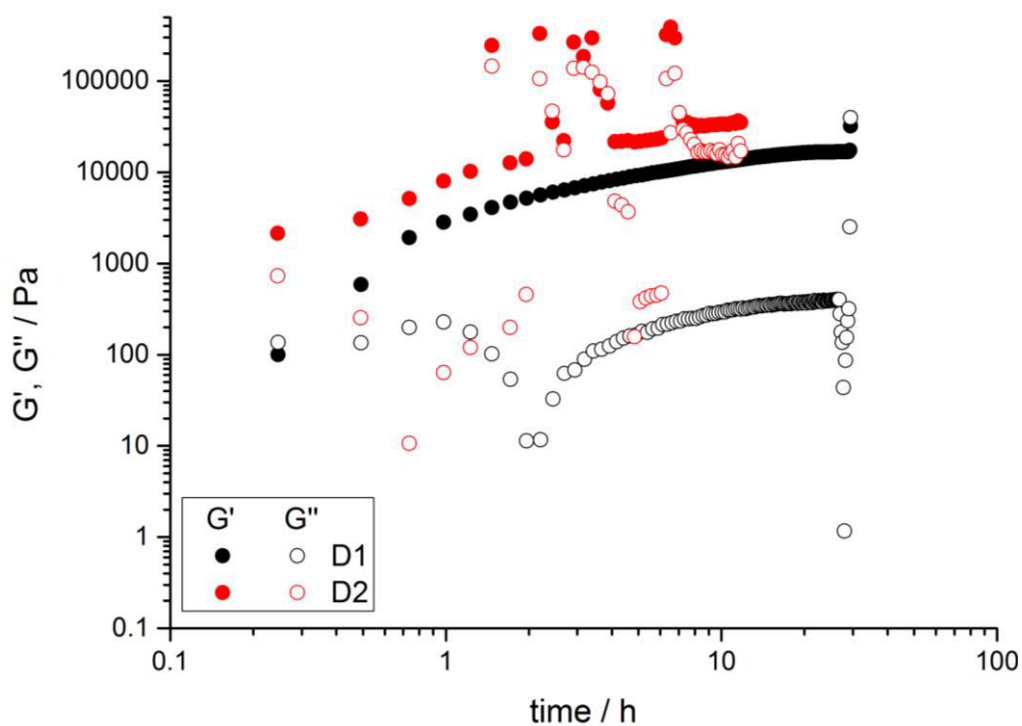


**Figure S3.18.** Shear moduli ( $G'$ ,  $G''$ ), of catechol-PPE in EtOH/PBS buffer as a function of cross-linking time, sample **D1** and **D2**. Note: double logarithmic scaling.

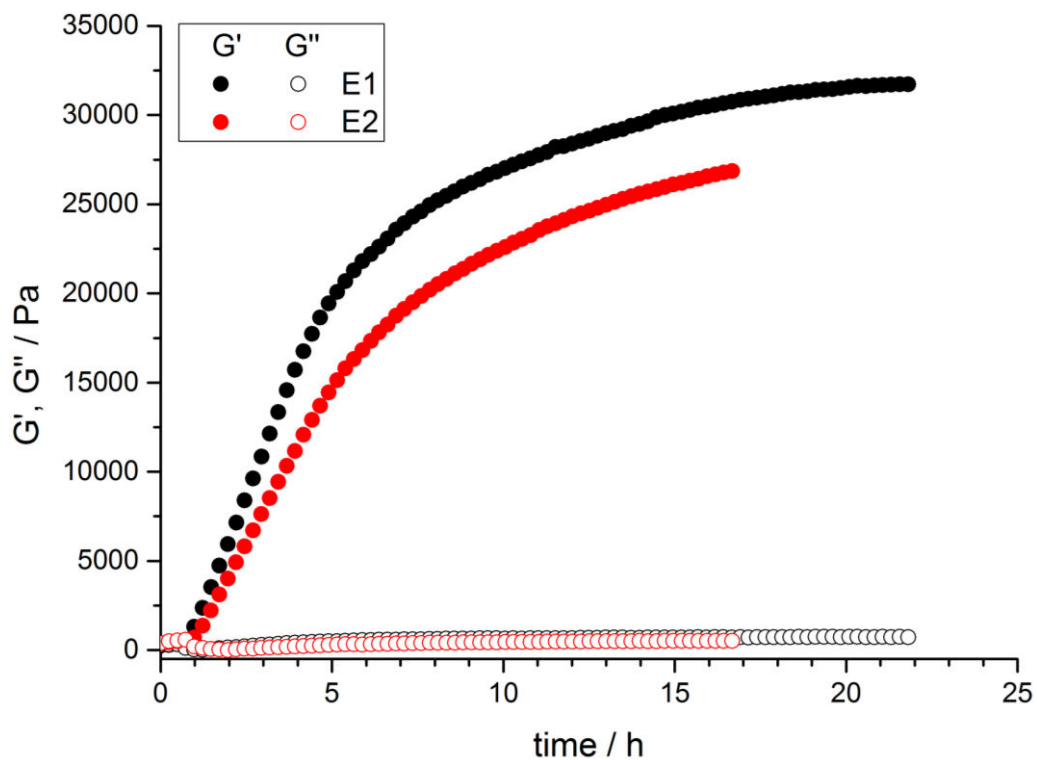


**Figure S3.19.** Shear moduli ( $G'$ ,  $G''$ ), of catechol-PPE in EtOH/water as a function of cross-linking time, sample **E1** and **E2**. Note: linear scaling.

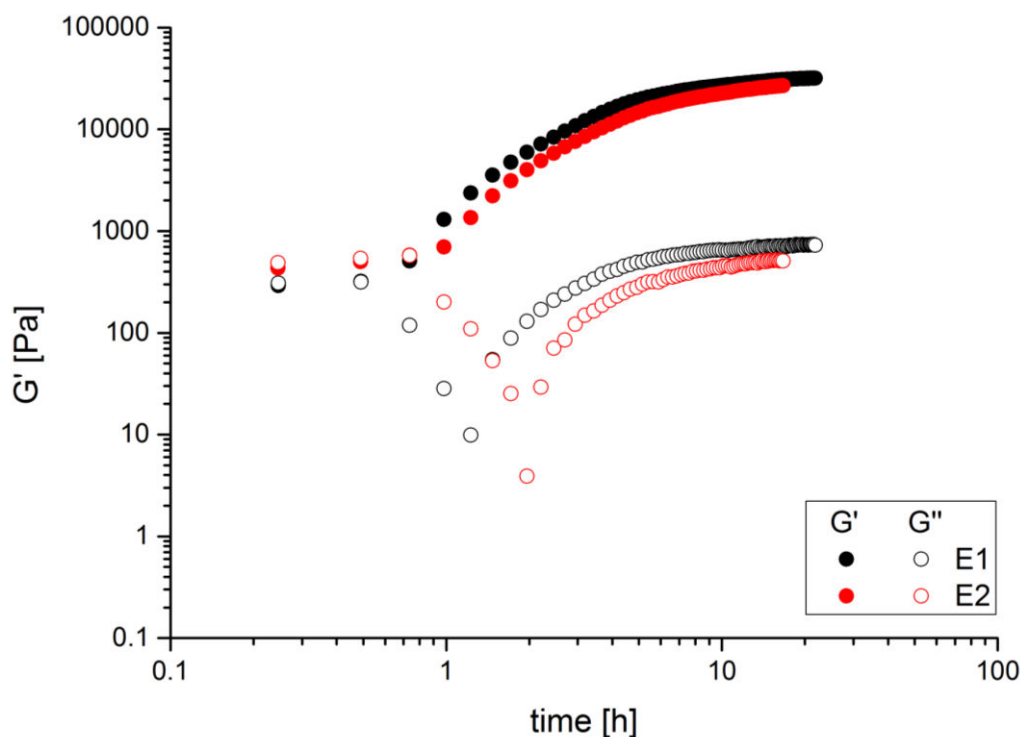


**Figure S3.20.** Shear moduli ( $G'$ ,  $G''$ ), of catechol-PPE in EtOH/water as a function of cross-linking time, sample **E1** and **E2**. Note: double logarithmic scaling.

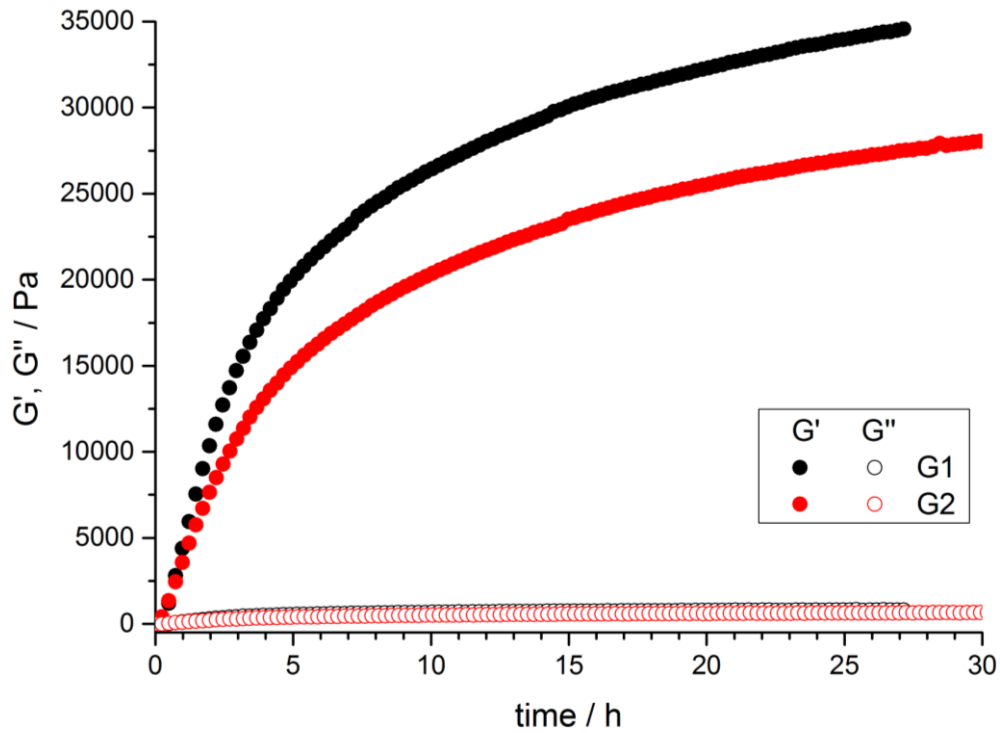


**Figure S3.21.** Shear moduli ( $G'$ ,  $G''$ ), of catechol-PPE in EtOH/water as a function of cross-linking time, sample **G1** and **G2**. Note: linear scaling.

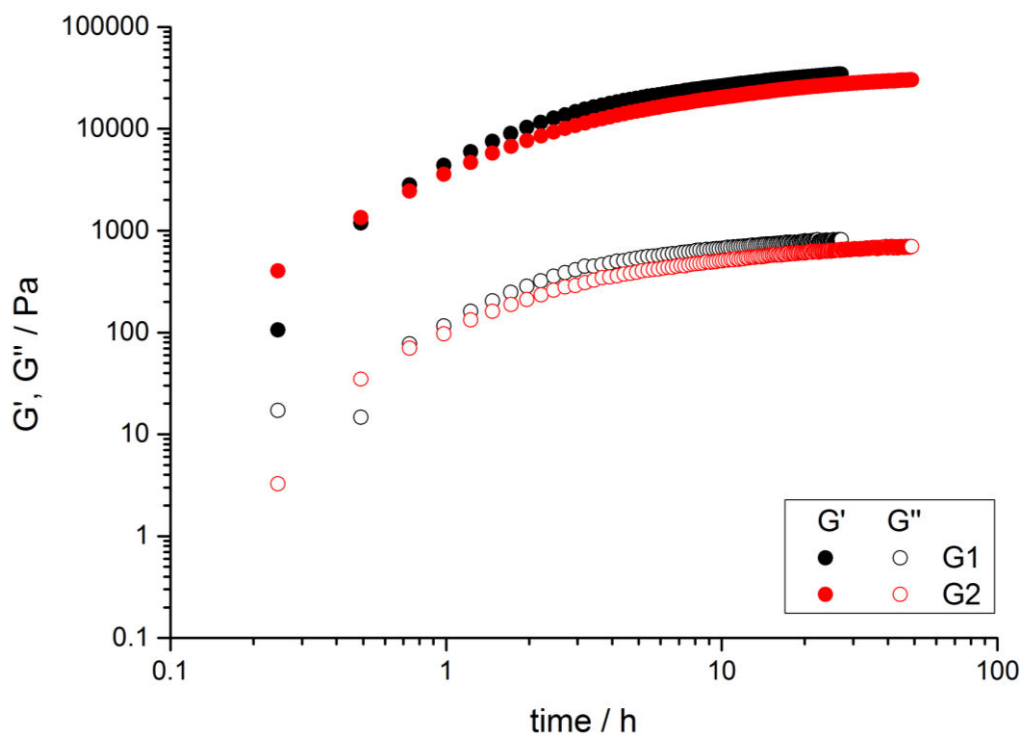


**Figure S3.22.** Shear moduli ( $G'$ ,  $G''$ ), of catechol-PPE in EtOH/water as a function of cross-linking time, sample **G1** and **G2**. Note: double logarithmic scaling.

### 3.8 References

1. Khanlari, S.; Dubé, M. A., *Macromol. React. Eng.* **2013**, *7* (11), 573-587.
2. Farrar, D. F., *Int. J. Adhes. Adhes.* **2012**, *33* (0), 89-97.
3. Heiss, C.; Kraus, R.; Schluckebier, D.; Stiller, A.-C.; Wensch, S.; Schnettler, R., *Eur J Trauma* **2006**, *32* (2), 141-148.
4. Vauthier, C.; Dubernet, C.; Fattal, E.; Pinto-Alphandary, H.; Couvreur, P., *Adv. Drug Delivery Rev.* **2003**, *55* (4), 519-548.
5. Kandalam, U.; Bouvier, A. J.; Casas, S. B.; Smith, R. L.; Gallego, A. M.; Rothrock, J. K.; Thompson, J. Y.; Huang, C. Y. C.; Stelnicki, E. J., *Int. J. Oral Surg.* **2013**, *42* (9), 1054-1059.
6. Weber, S.; Chapman, M., *Clinical Orthopedics and Related Research* **1984**, *191*, 249-261.
7. Shah, N.; Meislin, R., *Orthopedics* **2013**, *36* (12), 945-956.
8. <http://www.orthopaediclist.com/product/6392-OsteoCrete.html> [29th may, 2017; 15:56h].
9. [https://www.accessdata.fda.gov/cdrh\\_docs/pdf9/K091382.pdf](https://www.accessdata.fda.gov/cdrh_docs/pdf9/K091382.pdf) [29th may, 2017; 16:02h].
10. Jiang, H.-J.; Xu, J.; Qiu, Z.-Y.; Ma, X.-L.; Zhang, Z.-Q.; Tan, X.-X.; Cui, Y.; Cui, F.-Z., *Materials* **2015**, *8* (5), 2616.
11. Roeder, R. K.; Converse, G. L.; Kane, R. J.; Yue, W., *JOM* **2008**, *60* (3), 38-45.
12. Dimitriou, R.; Jones, E.; McGonagle, D.; Giannoudis, P. V., *BMC Medicine* **2011**, *9*, 66-66.
13. Waselau, M.; Samii, V. F.; Weisbrode, S. E.; Litsky, A. S.; Bertone, A. L., *Am. J. Vet. Res.* **2007**, *68* (4), 370-378.
14. Rüdell, C.; W., Z., *Eye, Ear, Nose Throat Mon.* **1994**, *73* (3), 189-191.
15. Cedano Serrano, F. J.; Pinzón, L. M.; Narváez, D. M.; Castro Paéz, C. I.; Moreno-Serrano, C. L.; Tabima, D. M.; Salcedo, F.; Briceno, J. C.; J.P., C. R., *J. Adhes. Sci. Technol.* **2017**, *31* (13), 1480-1495.
16. Ryu, J. H.; Hong, S.; Lee, H., *Acta Biomater.* **2015**, *27*, 101-115.
17. Wistlich, L.; Rücker, A.; Schamel, M.; Kübler, A. C.; Gbureck, U.; Groll, J., *Adv. Healthcare Mater.* **2017**, *6* (3), 1600902-n/a.
18. Madhurakkat Perikamana, S. K.; Lee, J.; Lee, Y. B.; Shin, Y. M.; Lee, E. J.; Mikos, A. G.; Shin, H., *Biomacromolecules* **2015**, *16* (9), 2541-2555.
19. Lee, B. P.; Messersmith, P. B.; Israelachvili, J. N.; Waite, J. H., *Annu. Rev. Mater. Res.* **2011**, *41* (1), 99-132.
20. Duarte, A. P.; Coelho, J. F.; Bordado, J. C.; Cidade, M. T.; Gil, M. H., *Prog. Polym. Sci.* **2012**, *37* (8), 1031-1050.
21. Bre, L. P.; Zheng, Y.; Pego, A. P.; Wang, W., *Biomater. Sci.* **2013**, *1* (3), 239-253.
22. Molinoff, P. B.; Axelrod, J., *Annu. Rev. Biochem.* **1971**, *40* (1), 465-500.
23. Penczek, S.; Pretula, J.; Kaluzynski, K., *Biomacromolecules* **2005**, *6* (2), 547-551.
24. Waite, J. H.; Tanzer, M. L., *Science* **1981**, *212* (4498), 1038-1040.
25. Avdeef, A.; Sofen, S. R.; Bregante, T. L.; Raymond, K. N., *J. Am. Chem. Soc.* **1978**, *100* (17), 5362-5370.
26. Yu, M.; Hwang, J.; Deming, T. J., *J. Am. Chem. Soc.* **1999**, *121* (24), 5825-5826.
27. Chirdon, W. M.; O'Brien, W. J.; Robertson, R. E., *J. Biomed. Mater. Res., Part B* **2003**, *66B* (2), 532-538.
28. Faure, E.; Falentin-Daudré, C.; Jérôme, C.; Lyskawa, J.; Fournier, D.; Woisel, P.; Detrembleur, C., *Prog. Polym. Sci.* **2013**, *38* (1), 236-270.
29. Sedó, J.; Saiz-Poseu, J.; Busqué, F.; Ruiz-Molina, D., *Adv. Mater.* **2013**, *25* (5), 653-701.
30. Becker, G.; Ackermann, L.-M.; Schechtel, E.; Klapper, M.; Tremel, W.; Wurm, F. R., *Biomacromolecules* **2017**, *18* (3), 767-777.
31. Steinbach, T.; Wurm, F. R., *Angew. Chem. Int. Ed.* **2015**, *54* (21), 6098-6108.
32. Alexandrino, E. M.; Ritz, S.; Marsico, F.; Baier, G.; Mailander, V.; Landfester, K.; Wurm, F. R., *J. Mater. Chem. B* **2014**, *2* (10), 1298-1306.
33. Qiu, J.-J.; Liu, C.-M.; Hu, F.; Guo, X.-D.; Zheng, Q.-X., *J. Appl. Polym. Sci.* **2006**, *102* (4), 3095-3101.
34. Monge, S.; Cannicconi, B.; Graillet, A.; Robin, J.-J., *Biomacromolecules* **2011**, *12* (6), 1973-1982.

35. Roth, M.; D'Acunzi, M.; Vollmer, D.; Auernhammer, G. K., *J. Chem. Phys.* **2010**, *132* (12), 124702.
36. Clément, B.; Grignard, B.; Koole, L.; Jérôme, C.; Lecomte, P., *Macromolecules* **2012**, *45* (11), 4476-4486.
37. Wilms, V. S.; Bauer, H.; Tonhauser, C.; Schilman, A.-M.; Müller, M.-C.; Tremel, W.; Frey, H., *Biomacromolecules* **2013**, *14* (1), 193-199.
38. Schöttler, S.; Becker, G.; Winzen, S.; Steinbach, T.; Mohr, K.; Landfester, K.; Mailänder, V.; Wurm, F. R., *Nat. Nano.* **2016**, *11* (4), 372-377.
39. Lim, Y. H.; Tiemann, K. M.; Heo, G. S.; Wagers, P. O.; Rezenom, Y. H.; Zhang, S.; Zhang, F.; Youngs, W. J.; Hunstad, D. A.; Wooley, K. L., *ACS Nano* **2015**, *9* (2), 1995-2008.
40. Zhao, Z.; Wang, J.; Mao, H.-Q.; Leong, K. W., *Adv. Drug Delivery Rev.* **2003**, *55* (4), 483-499.
41. Wuts, P. G. M.; Greene, T. W., *Greene's Protective Groups in Organic Synthesis*. 4th ed. ed.; Wiley-Interscience: 2007.
42. Steinbach, T.; Schroder, R.; Ritz, S.; Wurm, F. R., *Polym. Chem.* **4** (16), 4469-4479.
43. Holten-Andersen, N.; Harrington, M. J.; Birkedal, H.; Lee, B. P.; Messersmith, P. B.; Lee, K. Y. C.; Waite, J. H., *Proceedings of the National Academy of Sciences* **2011**, *108* (7), 2651-2655.
44. Niederer, K.; Schüll, C.; Leibig, D.; Johann, T.; Frey, H., *Macromolecules* **2016**, *49* (5), 1655-1665.
45. Brubaker, C. E.; Kissler, H.; Wang, L.-J.; Kaufman, D. B.; Messersmith, P. B., *Biomaterials* **2010**, *31* (3), 420-427.
46. Ryu, J. H.; Lee, Y.; Kong, W. H.; Kim, T. G.; Park, T. G.; Lee, H., *Biomacromolecules* **2011**, *12* (7), 2653-2659.
47. Waite, J. H., *Comp. Biochem. Physiol., B: Biochem. Mol. Biol.* **1990**, *97* (1), 19-29.
48. Paez, J. I.; Ustahüseyin, O.; Serrano, C.; Ton, X.-A.; Shafiq, Z.; Auernhammer, G. K.; d'Ischia, M.; del Campo, A., *Biomacromolecules* **2015**, *16* (12), 3811-3818.
49. Lee, B. P.; Dalsin, J. L.; Messersmith, P. B., *Biomacromolecules* **2002**, *3* (5), 1038-1047.
50. Cencer, M.; Liu, Y.; Winter, A.; Murley, M.; Meng, H.; Lee, B. P., *Biomacromolecules* **2014**, *15* (8), 2861-2869.
51. Sadeghi, R.; Jahani, F., *J. Phys. Chem. B* **2012**, *116* (17), 5234-5241.
52. Iwasaki, Y., *Modern Synthesis and Thermoresponsivity of Polyphosphoesters, in Biomedical Engineering - Frontiers and Challenges*. [www.intechopen.com](http://www.intechopen.com): 2011; Vol. n.a.
53. Kootala, S.; Tokunaga, M.; Hilborn, J.; Iwasaki, Y., *Macromol. Biosci.* **2015**, *15*, 1634-1640.
54. Zhang, S.; Wang, H.; Shen, Y.; Zhang, F.; Seetho, K.; Zou, J.; Taylor, J.-S. A.; Dove, A. P.; Wooley, K. L., *Macromolecules* **2013**, *46* (13), 5141-5149.
55. Iwasaki, Y.; Kawakita, T.; Yusa, S.-i., *Chem. Lett.* **2009**, *38* (11), 1054-1055.
56. Müller, L. K.; Steinbach, T.; Wurm, F. R., *RSC Advances* **2015**, *5* (53), 42881-42888.
57. Bragdon, B.; Moseychuk, O.; Saldanha, S.; King, D.; Julian, J.; Nohe, A., *Cell. Signalling* **2011**, *23* (4), 609-620.
58. Pratt, R. C.; Lohmeijer, B. G. G.; Long, D. A.; Lundberg, P. N. P.; Dove, A. P.; Li, H.; Wade, C. G.; Waymouth, R. M.; Hedrick, J. L., *Macromolecules* **2006**, *39* (23), 7863-7871.



## 4. Multifunctional poly(phosphoester)s for reversible Diels-Alder postmodification to tune the LCST in water

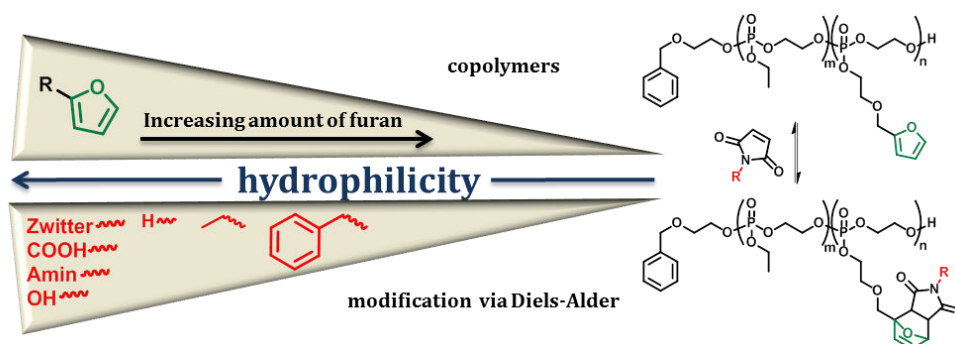
Greta Becker,<sup>1,2</sup> Tristan Alexei Marquetant,<sup>1</sup> Manfred Wagner,<sup>1</sup> Frederik R. Wurm<sup>1</sup>

<sup>1</sup>Max Planck Institute for Polymer Research, Ackermannweg 10, 55128 Mainz, Germany

<sup>2</sup>Graduate School Materials Science in Mainz, Staudinger Weg 9, 55128 Mainz, Germany

Reproduced with permission from “*Macromolecules*”, submitted for publication. Unpublished work; copyright 2017 American Chemical Society. All data of the degradation studies are unpublished results.

Polymer syntheses and parts of the post-modification reactions were conducted and characterized by Tristan A. Marquetant. NMR kinetic measurements were performed in collaboration with Manfred Wagner.



**Keywords:** poly(phosphoester), ring-opening polymerization, furan, maleimide, Diels-Alder reaction, LCST.

## 4.1 Abstract

Thermoresponsive materials are currently discussed for applications, e.g. in drug delivery or sensor systems. While homopolymers exhibit a certain LCST, copolymers allow adjusting the cloud points depending on the comonomer ratio. We report on degradable poly(phosphoester) (PPE) copolymers exhibiting LCSTs, which can be further tuned by reversible postmodification. A library of copolymers with different cloud points is obtained from a single “precursor polymer”. A novel furfuryl-carrying cyclic phosphate was designed and different PPE-copolymers were prepared via ring-opening polymerization with adjustable furan contents (up to 25 mol% were targeted and achieved) and molecular weights up to 40,000 g/mol ( $\bar{D} < 1.25$ ). Modification was achieved by a Diels-Alder reaction with maleimides of different hydrophilicity to further alter the solubility profile of the polymers. While the postmodification is thermally reversible, the biodegradable PPE backbone remains unaffected. This first report on the Diels-Alder postmodification of PPEs to adjust LCST-behavior further underlines the versatility of this polymer class and might be used in future drug delivery and temperature-responsive devices.

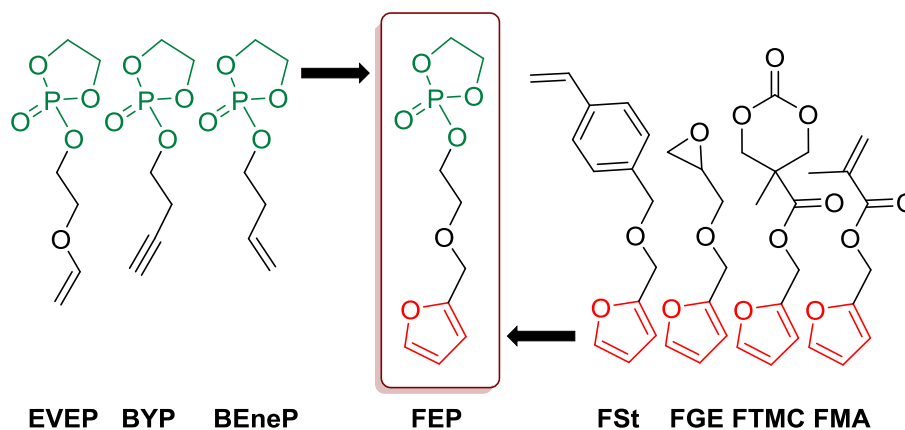
## 4.2 Introduction

Thermoresponsive polymers are currently under intensive investigation for applications in nanotechnology and as biomaterials, e.g. as tissue engineering scaffolds, in sensors, in separation and chromatography, as self-healing materials or in drug and gene delivery.<sup>1-3</sup> They exhibit a lower or upper critical solution temperature (LCST or UCST), where phase transition from coil-to-globule structure or *vice versa* occurs. Thermoresponsivity in aqueous solution is of particular interest, with several LCST-type polymers, such as polypeptides, poly(oxazoline)s, poly(ether)s, poly(vinylether)s and poly(acrylic acid) derivatives.<sup>2, 4-6</sup> Poly(*N*-isopropylacrylamide) (PNiPAAm) is probably the most considered material, due to a LCST of ~32 °C near the body temperature.<sup>1</sup> Thermoresponsive homopolymers exhibit a single LCST temperature, whereas copolymerization allows tuning of the cloud point by different comonomer ratios, e.g. via the OEGMA-platform (oligo(ethylene glycol) methacrylates).<sup>7</sup> Iwasaki et al. reported several poly(phosphoester) (PPE) copolymers of poly(isopropyl-*co*-ethyl ethylene phosphate) with LCSTs between 5-38 °C.<sup>8</sup> However, in these cases, adjustment of the cloud point occurs during the polymerization process by the comonomer feed and cannot be altered afterwards, i.e. each LCST needs a separate synthesis.

Herein, we present a series of PPE copolymers with thermoresponsive behavior that is i) determined by the comonomer ratio (hydrophilic: hydrophobic), and ii) that can be further fine-tuned by a convenient post-modification via Diels-Alder cycloaddition with several maleimides.

PPEs are a versatile class of synthetic biodegradable polymers.<sup>9</sup> Because of their biocompatibility and -degradability, they exhibit desirable features for potential materials in biomedical applications or as flame retardant additives.<sup>10-15</sup> Aliphatic PPEs range from hydrophobic to hydrophilic materials, depending on (I) the number of methylene groups in the backbone, (II) the binding motif around the phosphorus atom (that is poly(phosphate)s,<sup>16-19</sup> -(phosphite)s,<sup>20-21</sup> -(phosphonate)s,<sup>22-23</sup> or -(phosphoramidate)s<sup>24-25</sup>) and (III) the pendant group on each phosphoester repeat unit. Several cyclic phosphate monomers for the ring-opening polymerization (ROP) have been reported, mainly with aliphatic side chains or protected hydroxyl,<sup>26-27</sup> amino,<sup>28</sup> or guanidyl<sup>29</sup> groups. Other monomers carrying alkynes,<sup>30</sup> alkenes,<sup>31</sup> or vinyl ethers<sup>32</sup> can be installed into PPEs without the use of protective groups (Scheme 4.1). However, their modifications are typically irreversible.

The reversible Diels-Alder (DA) cycloaddition is attractive to modify polymer structures, due to high yields, mild reaction conditions, and a broad range of reagents. However, only few DA-reactive monomers for chain-growth polymerizations have been reported: FSt (4-furfuryloxymethylstyrene),<sup>33</sup> FMA (furfuryl methacrylate)<sup>34</sup>, FGE (furfuryl glycidyl ether)<sup>35</sup> and FTMC (furfuryl trimethylene carbonate)<sup>36</sup> (Scheme 4.1). The current manuscript is the first combination of a furan-functionalized cyclic ester monomer to prepare fully degradable multifunctional PPEs. In addition, retro-DA reaction occurs at elevated temperatures (ca. 110 °C), while -if carefully conducted- the biodegradable backbone of PPEs remains unaffected. The new furfuryl phosphate monomer (FEP) allows access to functional PPEs with pendant groups that would not sustain an anionic ROP, e.g. PPE-polyelectrolytes.



**Scheme 4.1.** *Left:* Functional cyclic phosphate monomers without protective group chemistry. *Right:* furan-containing monomers for chain-growth polymerization. *Middle:* the new furan-functionalized cyclic phosphate monomer **FEP**.

### 4.3 Experimental Section

**Materials.** Solvents, dry solvents (over molecular sieves) and deuterated solvents were purchased from Acros Organics, Sigma-Aldrich, Deutero GmbH or Fluka. All reagents were used without further purification, unless otherwise stated. Furfuryl alcohol, *N*-methoxycarbonylmaleimide, *N*-(2-carboxylethyl)maleimide, maleimide, 2-chloro-2-oxo-1,3,2-dioxaphospholane, pyridine, furan, sodium hydride, bromoacetate, hexamethyldisiloxane (HDMSO), *N*-ethylmaleimide, *N*-benzylmaleimide, maleic anhydride, *N*-*boc*-lysine, 2-(benzyloxy)ethanol, triphenylphosphine oxide, 1,8-diazabicyclo[5.4.0]undec-7-ene, and 4 M HCl-solution in dioxane, NaOH solution (1M), and HCl (37%) were purchased from Sigma-Aldrich. NaHCO<sub>3</sub> and MgSO<sub>4</sub> were purchased from Fisher Scientific. *N*-(2-aminoethyl)maleimide hydrochloride was purchased from TCI chemicals (Deutschland GmbH). 3,5-bis(trifluoromethyl)phenylisothiocyanate was purchased from Alfa Aesar GmbH & Co KG. Lithium aluminumhydride (2.4 M in THF), cyclohexylamine, and ethanolamine were purchased from Acros Organics. 3-(benzyloxy)ethanol was dried with CaH<sub>2</sub> prior to use, distilled, and stored over molecular sieve at 4 °C. 1,8-diazabicyclo[5.4.0]undec-7-ene was distilled prior to use, and stored over molecular sieve at 4 °C.

**Instrumentation and Characterization Techniques.** Size exclusion chromatography (SEC) measurements were performed in DMF (containing 0.25 g/L of lithium bromide as an additive) on an Agilent 1100 Series as an integrated instrument, including a PSS GRAM columns (1000/1000/100 g), a UV detector (270 nm), and a RI detector at a flow rate of 1 mL/min at 60 °C. Calibration was carried out using PEO standards provided by Polymer Standards Service. For nuclear magnetic resonance analysis <sup>1</sup>H, <sup>13</sup>C{H}, and <sup>31</sup>P{H} NMR spectra were recorded on a Bruker AVANCE III 300, 500, 700 or 850 MHz spectrometer. All spectra were measured in either *d*<sub>6</sub>-DMSO or CDCl<sub>3</sub> at 298 K, unless otherwise stated. The spectra were calibrated against the solvent signal and analyzed using MestReNova 8 from Mestrelab Research S.L. DOSY and NOESY spectra were analyzed with TOPSPIN 3.2 software. The quantitative kinetic <sup>1</sup>H-NMR experiments for the retro-Diels-Alder reaction were recorded on the 500 MHz Bruker AVANCE III system (TOPSPIN 3.2 software version) with a 5 mm BBFO z-gradient probe. The spectra were obtained with  $\pi/2$ -pulse lengths of 14,8  $\mu$ s for proton (32 number of scans, spectra width 8000 Hz) with a relaxation delay of 10s at 353K. The spectra were referenced with the residual C<sub>2</sub>DHCl<sub>4</sub> at 5.95 ppm ( $\delta$ (<sup>1</sup>H)). The temperature was kept at 353K and calibrated with a standard <sup>1</sup>H-NMR ethylene glycol NMR sample from the Bruker company. The control of the temperature was realized with a VTU (variable temperature unit) and an accuracy of +/- 0,1K, which was checked with the standard Bruker Topspin 3.2 software. The spectra were calibrated against the solvent signal and analyzed using MestReNova 8 from Mestrelab Research S.L. For the quantitative <sup>31</sup>P-NMR experiments for copolymerization studies a 5 mm triple resonance TXI <sup>1</sup>H/<sup>13</sup>C/<sup>15</sup>N probe equipped with a z-gradient

on the 850 MHz Bruker AVANCE III system was used. The  $^{31}\text{P}$  NMR (334 MHz) measurements were obtained with invers gated decoupling,<sup>37</sup> which allows the integration of the  $^{31}\text{P}$ -NMR signals. The used relaxation delay was fixed at 10s with a scan number of 32 and a  $90^\circ$  flip angle of  $27\ \mu\text{s}$  and a spectral width of 34000Hz (100ppm). For the control  $^1\text{H}$  NMR measurements one transients were used with a  $90^\circ$  pulse of  $10,8\ \mu\text{s}$ , a spectral width of 17000 Hz (20 ppm) and a recycling delay of 5s. The temperature was kept at 253.3 K and regulated by a standard  $^1\text{H}$  methanol NMR sample using the topspin 3.1 software (Bruker). The control of the temperature was realized with a VTU (variable temperature unit) and an accuracy of  $\pm 0,1\text{K}$ .  $^1\text{H}$  and  $^{31}\text{P}$  {H} NMR spectra for degradation studies were recorded on a Bruker AVANCE III 300 MHz spectrometer.  $^1\text{H}$  NMR spectra were measured with water suppression (64 scans). All spectra were measured in  $\text{H}_2\text{O}/\text{D}_2\text{O}$  (90:10) at 298 K, calibrated against the solvent signal and analyzed with MestReNova 8. The thermal properties of the synthesized polymers have been measured by differential scanning calorimetry (DSC) on a Mettler Toledo DSC 823 calorimeter. Three scanning cycles of heating-cooling were performed in a  $\text{N}_2$  atmosphere (30 mL/min) with a heating and cooling rate of  $10\ ^\circ\text{C}/\text{min}$ . Measurements of the cloud point were performed in a Jasco V-630 photo spectrometer with a Jasco ETC-717 Peltier element. They were determined in distilled water at a concentration of 3 g/L and detected by optical transmittance of a light beam ( $\lambda = 500\ \text{nm}$ ) through a 1 cm sample cell. The intensity of the transmitted light was recorded versus the temperature of the sample cell. The heating / cooling rate was  $1\ ^\circ\text{C}/\text{min}$  and values were recorded every  $0.1\ ^\circ\text{C}$ . FT-IR spectra were recorded using a Thermo Scientific iS10 FT-IR spectrometer, equipped with a diamond ATR unit.

**Syntheses.** *2-(2-(furan-2-ylmethoxy)ethoxy)-2-oxo-1,3,2-dioxaphospholane (FEP, 1)*: 2-(furan-2-ylmethoxy)ethan-1-ol (5.00 g, 35.3 mmol, 1 eq.) was dissolved in 100 mL dry THF in a flame-dried 3-necked round-bottom flask. Dry pyridine (2.78 g, 35.2 mmol, 1 eq.) was added and the mixture was cooled to  $0^\circ\text{C}$ . 2-chloro-2-oxo-1,3,2-dioxaphospholane (7.52 g, 52.8 mmol, 1.5 eq.) in 35 mL dry THF was added over a period of 1h, stirred for 4 h and kept at  $-20^\circ\text{C}$  for additional 8h.. During reaction, hydrogen chloride was formed and precipitated as pyridinium hydrochloride. The ice-cold reaction mixture was then filtered under inert-gas atmosphere and concentrated at reduced pressure. Column chromatography with a RP-1 column (silica gel deactivated with 5v% hexamethyldisiloxane, dichloromethane/ethyl acetate 1:3,  $R_f=0.77$ ) afforded 4.09 g (47%) of the pure product FEP as a yellow oil.  $^1\text{H}$  NMR (500 MHz,  $\text{CDCl}_3$ ):  $\delta$  [ppm] 7.37 (s, 1H, -O-CH=CH-), 6.35 (m, 2H, -O-CH=CH-CH=), 4.52 (s, 2H, O-C(=CH)-CH<sub>2</sub>-O-), 4.43-4.23 (m, 6H, -O-CH<sub>2</sub>-CH<sub>2</sub>-O-P(-O-)-O-CH<sub>2</sub>-CH<sub>2</sub>-), 3.72-3.68 (s, 2H, -O-CH<sub>2</sub>-CH<sub>2</sub>-O-P(-O-)-O-).  $^{13}\text{C}\{\text{H}\}$  NMR (126 MHz,  $\text{CDCl}_3$ ):  $\delta$  [ppm] 151.36 (O-C(=CH)-CH<sub>2</sub>-O-), 143.21 (-O-CH=CH-), 110.46 (-O-CH=CH-CH=), 109.67 (-O-CH=CH-CH=), 68.18 (O-C(=CH)-CH<sub>2</sub>-O-), 67.02 (-O-CH<sub>2</sub>-CH<sub>2</sub>-O-P(-O-)-O-), 66.40 (-O-P(-O-)-O-CH<sub>2</sub>-CH<sub>2</sub>-), 63.88 (-O-CH<sub>2</sub>-CH<sub>2</sub>-O-P(-O-)-O-).  $^{31}\text{P}\{\text{H}\}$  NMR (202 MHz,  $\text{CDCl}_3$ ):  $\delta$  [ppm] 17.75. FTIR ( $\text{cm}^{-1}$ ): 3119 (-CH= stretching), 3034 (-CH= stretching), 2956 (-CH<sub>2</sub>- stretching), 2914 (-CH<sub>2</sub>- stretching), 2868 (-CH<sub>2</sub>-

stretching), 1503 (C=C stretching), 1479 (O-CH<sub>2</sub>- deformation), 1356, 1285 (P=O stretching), 1225, 1150 (=CH- stretching), 1103, 1063, 1023 (P-O-C stretching), 987 (P-O-C stretching), 927, 884, 866, 838 (O-CH<sub>2</sub>- stretching), 749 (-CH<sub>2</sub>- rocking), 684 (C-H deformation).

*General procedure for the (co)polymerization of cyclic phosphates:* The polymerization was conducted according to literature procedures for other cyclic phosphate monomers.<sup>19</sup> EEP (1.84 g, 12.13 mmol), FEP (170 mg, 0.683 mmol) and TU (253 mg, 0.683 mmol, 5.3 mol% to monomer) were introduced into a tube. A stock solution of DBU in dry DCM (104 mg/0.2mL, 0.683 mmol, 5.3 mol% to monomer) and a stock solution of the initiator in dry DCM (13 mg/0.2 mL, 0.085 mmol) were prepared and 2.8 mL dry DCM was added to EEP, FEP and TU to give a total concentration of ca. 4 mol/L. All solutions were cooled down to 0 °C. 0.2 mL of the stock solution of the initiator was added to the stirred solution of EEP, FEP and TU. The polymerization was started by rapid addition of 0.2 mL from the stock solution of DBU to the reaction mixture. The polymerization was terminated after 90 min by the addition of an excess of acetic acid in DCM. 2 mL DCM were added and precipitated in ice-cold diethyl ether. The suspension was centrifuged for 15 min (4000rpm, 4 °C), after that the supernatant was decanted and the residue dissolved in water. The polymer was dialyzed exhaustively against water (MWCO 3500Da). The polymer filtered to remove any solids and freeze-dried to give the final product (yields typically 80-90%).

**PEEP:** EEP (500.00 mg, 3.29 mmol, 90.00 eq), DBU (85.8 mg, 558.34 μmol), TU (60.88 mg, 164.38 μmol, 4.50 eq), initiator (31.7 mg, 203.69 μmol). Yield: 0.48 g, 90%. M<sub>n</sub>(NMR): 16,700 g/mol. <sup>1</sup>H NMR (300 MHz, DMSO-d<sub>6</sub>): δ [ppm] 7.34 (m, 5H, Ar-, initiator), 4.89 (t, 1H, OH-CH<sub>2</sub>-), 4.52 (s, 2H, Ar-CH<sub>2</sub>-O-), 4.26-3.98 (m, 644H, -O-P(-O-CH<sub>2</sub>-)-O-CH<sub>2</sub>-CH<sub>2</sub>-, backbone), 3.63(m, 2H, Ar-CH<sub>2</sub>-O-CH<sub>2</sub>-CH<sub>2</sub>-O-P-O-), 3.57 (m,2H, -O-P-O-CH<sub>2</sub>-CH<sub>2</sub>-OH), 1.26 (t, 328H, CH<sub>3</sub>-). <sup>31</sup>P{H} NMR (121 MHz, DMSO-d<sub>6</sub>): δ [ppm] -1.24, -0.98 (end groups).

**PEF5:** EEP (1.84 g, 12.13 mmol, 142 eq), FEP (169.59 mg, 683.35 μmol, 8.00 eq), DBU (104.03 mg, 683.35 μmol, 8 eq), initiator (13.00 mg, 85.42 μmol, 1.00 eq), TU (253.08 mg, 683.35 μmol, 8.00 eq). Yield: 1.74 g, 86%, M<sub>n</sub>(NMR): 23,100 g/mol, 6 % FEP, 94 % EEP. <sup>1</sup>H NMR (300 MHz, DMSO-d<sub>6</sub>): δ [ppm] 7.64 (s, 8H, -O-CH=CH-), 7.34 (m, 5H, Ar-, initiator), 6.43 (s, 17H, -O-CH=CH-CH=), 4.89 (t, 1H, OH-CH<sub>2</sub>-), 4.52 (s, 2H, Ar-CH<sub>2</sub>-O-), 4.45 (s, 18H, O-C(=CH)-CH<sub>2</sub>-O-), 4.26-3.98 (m, 874H, -O-P(-O-CH<sub>2</sub>-)-O-CH<sub>2</sub>-CH<sub>2</sub>-, backbone), 3.60 (s, 24H, -O-CH<sub>2</sub>-CH<sub>2</sub>-O-P(-O-)-O-, side chain), 1.26 (t, 413H, CH<sub>3</sub>-). <sup>31</sup>P{H} NMR (121 MHz, DMSO-d<sub>6</sub>): δ [ppm] -1.24, -0.98 (endgroups).

**PEF10:** EEP (1.75 g, 11.53 mmol, 135 eq), FEP (317.98 mg, 1.28 mmol, 15.00 eq), DBU (104.03 mg, 683.35 μmol, 8 eq), initiator (13.00 mg, 85.42 μmol, 1.00 eq), TU (253.08 mg, 683.35 μmol, 8.00 eq). Yield: 1.79 g, 85%, M<sub>n</sub>(NMR): 35,400 g/mol, 6 % FEP, 94 % EEP. <sup>1</sup>H NMR (300 MHz, DMSO-d<sub>6</sub>): δ [ppm] 7.64 (s, 20H, -O-CH=CH-), 7.34 (m, 5H, Ar-, initiator), 6.43 (s, 42H, -O-

CH=CH-CH=), 4.89 (t, 1H, OH-CH<sub>2</sub>-), 4.51 (s, 2H, Ar-CH<sub>2</sub>-O-), 4.45 (s, 50H, O-C(=CH)-CH<sub>2</sub>-O-), 4.35-3.98 (m, 1330H, -O-P(-O-CH<sub>2</sub>-)-O-CH<sub>2</sub>-CH<sub>2</sub>-, backbone), 3.60 (s, 52H, -O-CH<sub>2</sub>-CH<sub>2</sub>-O-P(-O-)-O-, side chain), 1.26 (t, 599H, CH<sub>3</sub>-). <sup>31</sup>P{H} NMR (121 MHz, DMSO-d<sub>6</sub>): δ [ppm] -1.24, -0.98 (endgroups).

**PEF25:** EEP (1.46 g, 9.61 mmol, 112.5 eq), FEP (794.94 mg, 3.20 mmol, 37.50 eq), DBU (104.03 mg, 683.35 μmol, 8 eq), initiator (13.00 mg, 85.42 μmol, 1.00 eq), TU (253.08 mg, 683.35 μmol, 8.00 eq). Yield: 1.97 g, 87%, M<sub>n</sub>(NMR): 40,000 g/mol, 25% FEP, 75% EEP. <sup>1</sup>H NMR (300 MHz, DMSO-d<sub>6</sub>): δ [ppm] 7.63 (s, 56H, -O-CH=CH-), 7.33 (m, 5H, Ar-, initiator), 6.43 (s, 115H, -O-CH=CH-CH=), 4.89 (t, 1H, OH-CH<sub>2</sub>-), 4.51 (s, 2H, Ar-CH<sub>2</sub>-O-), 4.44 (s, 117H, O-C(=CH)-CH<sub>2</sub>-O-), 4.35-3.98 (m, 1350H, -O-P(-O-CH<sub>2</sub>-)-O-CH<sub>2</sub>-CH<sub>2</sub>-, backbone), 3.60 (s, 125H, -O-CH<sub>2</sub>-CH<sub>2</sub>-O-P(-O-)-O-, side chain), 1.26 (t, 513H, CH<sub>3</sub>-). <sup>31</sup>P{H} NMR (121 MHz, DMSO-d<sub>6</sub>): δ [ppm] -1.24, -0.98 (endgroups).

**PMF10:** MEP (1.40 g, 10.13 mmol, 135 eq), FEP (279.40 mg, 1.13 mmol, 15.00 eq), DBU (91.41 mg, 600.45 μmol, 8 eq), initiator (11.42 mg, 75.06 μmol, 1.00 eq), TU (222.38 mg, 600.45 μmol, 8.00 eq). Yield: 1.28 g, 76%, M<sub>n</sub>(NMR): 36,100 g/mol, 9% FEP, 91% MEP. <sup>1</sup>H NMR (300 MHz, DMSO-d<sub>6</sub>): δ [ppm] 7.63 (s, 22H, -O-CH=CH-), 7.34 (m, 5H, Ar-, initiator), 6.44 (s, 46H, -O-CH=CH-CH=), 4.91 (t, 1H, OH-CH<sub>2</sub>-), 4.52 (s, 2H, Ar-CH<sub>2</sub>-O-), 4.45 (s, 58H, O-C(=CH)-CH<sub>2</sub>-O-), 4.31-4.05 (m, 1021H, -O-P(-O-CH<sub>2</sub>-)-O-CH<sub>2</sub>-CH<sub>2</sub>-, backbone), 3.71 (d, 663H, -O-P(-O-CH<sub>3</sub>)-O-), 3.60 (s, 52H, -O-CH<sub>2</sub>-CH<sub>2</sub>-O-P(-O-)-O-, side chain). <sup>31</sup>P{H} NMR (121 MHz, DMSO-d<sub>6</sub>): δ [ppm] -1.23 (furfuryl side chain), -0.12 (methyl side chain).

*Real-time Copolymerization Kinetics.* The copolymerization was conducted in the NMR tube with a total volume of 0.6 mL in d<sub>2</sub>-DCM, at -20 °C and a degree of polymerization of 120 was targeted. Triphenylphosphine oxide was used as internal standard for calibration of the obtained NMR spectra. The reaction was initiated by the addition of the initiator after cooling down to -20°C and shimming of the NMR device. Used amounts: EEP (32.38 mg, 212,9 μmol, 108 eq.), FEP (5.87 mg, 23,65 μmol, 12 eq.), DBU (1.80 mg, 11.83 μmol, 6 eq.), TU (4.38 mg, 11.83 μmol, 6 eq.), triphenylphosphine oxide (32.91 mg, 118.27 μmol, 60 eq.), initiator (300μg, 1.97 μmol, 1eq.).

*General procedure for post-polymerization functionalization of PPEs by Diels-Alder Reaction:* 150 mg of the respective polymer and 5 eq. of the respective maleimide were dissolved in 1 mL toluene/DCM-mixture (8:2) (for *N*-ethylmaleimide, *N*-benzylmaleimide, *N*-(2-hydroxyethyl)maleimide, maleimide) or in 1 mL DMF (for *N*-(2-carboxylethyl)maleimide, maleimide, *N*-(2-aminoethyl)maleimide hydrochloride, *N*-ε-maleimido-l-lysine hydrochlorid). It was heated to 65 °C for 18 h. Dialysis in DCM (benzoylated dialysis tubing, MWCO: 2000Da) or water (MWCO 3500Da) give the pure polymers. Yields: quantitative.

**PEF25-Bn:**  $^1\text{H}$  NMR (300 MHz,  $\text{CDCl}_3$ ):  $\delta$  [ppm] 7.30 (m, *Ar*-, initiator, *Ar-CH*<sub>2</sub>-N-), 6.55 (m, -*CH=CH*-, exo), 6.14-5.98 (dd, -*CH=CH*-, endo), 5.30 (d, =*CH-CH*(-O-)-*CH*-, endo), 5.25 (s, =*CH-CH*(-O-)-*CH*-, exo), 4.62 (s, DA adduct-*CH*<sub>2</sub>-O), 4.44 (s, *Ar-CH*<sub>2</sub>-O-), 4.37-4.04 (m, -O-P(-O-*CH*<sub>2</sub>-)-O-*CH*<sub>2</sub>-*CH*<sub>2</sub>-, backbone ), 3.89-3.67 (m, DA adduct-*CH*<sub>2</sub>-O-*CH*<sub>2</sub>-*CH*<sub>2</sub>-O-P(-O-)-O-, side chain, -CO-(C)*CH*-(*CH*)*CH*-CO- endo, -CO-(C)*CH*-(*CH*)*CH*-CO- endo), 2.97-2.89 (-CO-(C)*CH*-(*CH*)*CH*-CO- exo , -CO-(C)*CH*-(*CH*)*CH*-CO-, exo), 1.35 (t, -O *CH*<sub>2</sub>-*CH*<sub>3</sub>).

**PEF10-Et:**  $^1\text{H}$  NMR (300 MHz,  $\text{CDCl}_3$ ):  $\delta$  [ppm] 7.39 (s, -O-*CH=CH*-), 7.30 (m, *Ar*-, initiator), 6.51 (m, -*CH=CH*-, exo), 6.40-6.24 (dd, -*CH=CH*-, endo), 6.31 (s, -O-*CH=CH-CH=*), 5.25 (d, =*CH-CH*(-O-)-*CH*-, endo), 5.20 (d, =*CH-CH*(-O-)-*CH*-, exo), 4.53 (s, *Ar-CH*<sub>2</sub>-O-), 4.46 (s, furan-*CH*<sub>2</sub>-O- ), 4.35-3.98 (m, -O-P(-O-*CH*<sub>2</sub>-)-O-*CH*<sub>2</sub>-*CH*<sub>2</sub>-, backbone ), 3.78 (m, DA adduct-*CH*<sub>2</sub>-O-*CH*<sub>2</sub>-*CH*<sub>2</sub>-O-P(-O-)-O-, side chain), 3.61-3.28 (m, DA adduct-*CH*<sub>2</sub>-O-, -CO-(C)*CH*-(*CH*)*CH*-CO- endo, -CO-(C)*CH*-(*CH*)*CH*-CO- endo, -N-*CH*<sub>2</sub>-*CH*<sub>3</sub>), 2.93-2.82 (-CO-(C)*CH*-(*CH*)*CH*-CO- exo, -CO-(C)*CH*-(*CH*)*CH*-CO- exo), 1.32 (t, -O *CH*<sub>2</sub>-*CH*<sub>3</sub>), 1.11 (-N-*CH*<sub>2</sub>-*CH*<sub>3</sub>, exo), 0.99 (-N-*CH*<sub>2</sub>-*CH*<sub>3</sub>, endo).

**PEF10-H:**  $^1\text{H}$  NMR (300 MHz,  $\text{CDCl}_3$ ):  $\delta$  [ppm] 7.33 (m, *Ar*-, initiator), 6.51 (m, -*CH=CH*-, exo), 6.40 (d, -*CH=CH*-, endo), , 5.30 (d, =*CH-CH*(-O-)-*CH*-, endo), 5.23 (s, =*CH-CH*(-O-)-*CH*-, exo), 4.56 (s, *Ar-CH*<sub>2</sub>-O-), 4.43-4.04 (m, -O-P(-O-*CH*<sub>2</sub>-)-O-*CH*<sub>2</sub>-*CH*<sub>2</sub>-, backbone ), 3.99-3.95 (m, DA adduct-*CH*<sub>2</sub>-O, -CO-(C)*CH*-(*CH*)*CH*-CO- endo, -CO-(C)*CH*-(*CH*)*CH*-CO- endo), 3.81 (m, DA adduct-*CH*<sub>2</sub>-O-*CH*<sub>2</sub>-*CH*<sub>2</sub>-O-P(-O-)-O-, side chain), 2.98-2.82 (-CO-(C)*CH*-(*CH*)*CH*-CO- exo, -CO-(C)*CH*-(*CH*)*CH*-CO- exo), 1.35 (t, -O-*CH*<sub>2</sub>-*CH*<sub>3</sub>).

**PEF10-OH:**  $^1\text{H}$  NMR (300 MHz,  $\text{CDCl}_3$ ):  $\delta$  [ppm] 7.33 (m, *Ar*-, initiator), 6.55 (m, -*CH=CH*-, exo), 6.45-6.28 (dd, -*CH=CH*-, endo), 5.27 (d, =*CH-CH*(-O-)-*CH*-, endo), 5.23 (d, =*CH-CH*(-O-)-*CH*-, exo), 4.56 (s, *Ar-CH*<sub>2</sub>-O-), 4.42-4.06 (m, -O-P(-O-*CH*<sub>2</sub>-)-O-*CH*<sub>2</sub>-*CH*<sub>2</sub>-, backbone), 3.93-3.90 (m, DA adduct-*CH*<sub>2</sub>-O-, -CO-(C)*CH*-(*CH*)*CH*-CO- endo, -CO-(C)*CH*-(*CH*)*CH*-CO- endo), 3.81 (m, DA adduct-*CH*<sub>2</sub>-O-*CH*<sub>2</sub>-*CH*<sub>2</sub>-O-P(-O-)-O-, side chain), 3.69-3.65 (m, -N-*CH*<sub>2</sub>-*CH*<sub>2</sub>-OH), 3.48 (m, -N-*CH*<sub>2</sub>-*CH*<sub>2</sub>-OH), 3.01-2.89 (-CO-(C)*CH*-(*CH*)*CH*-CO- exo, -CO-(C)*CH*-(*CH*)*CH*-CO- exo), 1.35 (t, -O *CH*<sub>2</sub>-*CH*<sub>3</sub>).

**PEF10-COOH:**  $^1\text{H}$  NMR (300 MHz,  $\text{CDCl}_3$ ):  $\delta$  [ppm] 7.42 (s, -O-*CH=CH*-), 7.33 (m, *Ar*-, initiator), 6.52 (m, -*CH=CH*-, exo), 6.43-6.28 (dd, -*CH=CH*-, endo), 6.33 (s, -O-*CH=CH-CH=*), 5.27 (d, =*CH-CH*(-O-)-*CH*-, endo), 5.21 (d, =*CH-CH*(-O-)-*CH*-, exo), 4.56 (s, *Ar-CH*<sub>2</sub>-O-), 4.49 (s, furan-*CH*<sub>2</sub>-O-), 4.38-4.04 (m, -O-P(-O-*CH*<sub>2</sub>-)-O-*CH*<sub>2</sub>-*CH*<sub>2</sub>-, backbone ), 3.95-3.91 (m, DA adduct-*CH*<sub>2</sub>-O), 3.80 (m, DA adduct-*CH*<sub>2</sub>-O-*CH*<sub>2</sub>-*CH*<sub>2</sub>-O-P(-O-)-O-, side chain), 3.69-3.60 (m, -CO-(C)*CH*-(*CH*)*CH*-CO- endo, -CO-(C)*CH*-(*CH*)*CH*-CO- endo, -N-*CH*<sub>2</sub>-*CH*<sub>2</sub>-COOH), 2.96-2.82 (-CO-(C)*CH*-(*CH*)*CH*-CO- exo, -CO-(C)*CH*-(*CH*)*CH*-CO- exo), 2.58 (t, -N-*CH*<sub>2</sub>-*CH*<sub>2</sub>-COOH, exo), 2.47 (t, -N-*CH*<sub>2</sub>-*CH*<sub>2</sub>-COOH, endo), 1.35 (t, -O *CH*<sub>2</sub>-*CH*<sub>3</sub>).

**PEF25-NH<sub>3</sub>Cl**: <sup>1</sup>H NMR (300 MHz, CDCl<sub>3</sub>): δ [ppm] 7.42 (s, -O-CH=CH-), 7.33 (m, Ar-, initiator), 6.53 (m, -CH=CH-, exo), 6.43-6.29 (dd, -CH=CH-, endo), 6.34 (s, -O-CH=CH-CH=), 5.27 (d, =CH-CH(-O)-CH-, endo), 5.22 (d, =CH-CH(-O)-CH-, exo), 4.56 (s, Ar-CH<sub>2</sub>-O-), 4.49 (s, furan-CH<sub>2</sub>-O-), 4.42-4.07 (m, -O-P(-O-CH<sub>2</sub>-)-O-CH<sub>2</sub>-CH<sub>2</sub>-, backbone), 3.95-3.91 (m, DA adduct-CH<sub>2</sub>-O), 3.81 (m, DA adduct-CH<sub>2</sub>-O-CH<sub>2</sub>-CH<sub>2</sub>-O-P(-O)-O-, side chain), 3.70-3.45 (m, -CO-(C)CH-(CH)CH-CO- endo, -CO-(C)CH-(CH)CH-CO- endo, -N-CH<sub>2</sub>-CH<sub>2</sub>-NH<sub>2</sub>), 2.97-2.85 (-CO-(C)CH-(CH)CH-CO- exo, -CO-(C)CH-(CH)CH-CO- exo), 2.59 (m, (-N-CH<sub>2</sub>-CH<sub>2</sub>-NH<sub>2</sub>, exo), 2.49 (t, (-N-CH<sub>2</sub>-CH<sub>2</sub>-NH<sub>2</sub>, endo), 1.35 (t, -O CH<sub>2</sub>-CH<sub>3</sub>).

**PEF25-Zwitter**: <sup>1</sup>H NMR (300 MHz, CD<sub>2</sub>Cl<sub>2</sub>): δ [ppm] 7.45 (s, -O-CH=CH-), 7.34 (m, Ar-, initiator), 6.53 (m, -CH=CH-, exo), 6.36 (s, -O-CH=CH-CH=), 5.27 (d, =CH-CH(-O)-CH-, exo), 5.19 (s, =CH-CH(-O)-CH-, exo), 4.48 (s, furan-CH<sub>2</sub>-O-), 4.35-4.07 (m, -O-P(-O-CH<sub>2</sub>-)-O-CH<sub>2</sub>-CH<sub>2</sub>-, backbone), 4.00 (m, DA adduct-CH<sub>2</sub>-O), 3.79 (m, DA adduct-CH<sub>2</sub>-O-CH<sub>2</sub>-CH<sub>2</sub>-O-P(-O)-O-, side chain), 3.66-3.45 (m, -N-CH<sub>2</sub>-CH<sub>2</sub>-), 2.97-2.88 (-CO-(C)CH-(CH)CH-CO- exo, -CO-(C)CH-(CH)CH-CO- exo), 1.88 (m, CH<sub>2</sub>-CH(-NH<sub>3</sub>Cl)-COOH), 1.53 (m, N-CH<sub>2</sub>-CH<sub>2</sub>-CH<sub>2</sub>-CH<sub>2</sub>-CH(NH<sub>3</sub>Cl)-COOH), 1.35-1.26 (t, -O CH<sub>2</sub>-CH<sub>3</sub>).

**PMF10-Bn**: <sup>1</sup>H NMR (300 MHz, CDCl<sub>3</sub>): δ [ppm] 7.41 (s, -O-CH=CH-), 7.33 (m, Ar-, initiator), 7.29 (s, Ar-CH<sub>2</sub>-N-), 6.55 (m, -CH=CH-, exo), 6.33 (s, -O-CH=CH-CH=), 6.14-5.98 (dd, -CH=CH-, endo), 5.25 (d, =CH-CH(-O)-CH-), 4.62 (s, DA adduct-CH<sub>2</sub>-O), 4.56 (s, Ar-CH<sub>2</sub>-O-), 4.48 (s, Ar-CH<sub>2</sub>-N-), 4.44 (s, furan-CH<sub>2</sub>-O-), 4.38-4.12 (m, -O-P(-O-CH<sub>2</sub>-)-O-CH<sub>2</sub>-CH<sub>2</sub>-, backbone), 3.88-3.71 (m, DA adduct-CH<sub>2</sub>-O-CH<sub>2</sub>-CH<sub>2</sub>-O-P(-O)-O- side chain, -O-CH<sub>3</sub>), 3.64-3.37 (m, -CO-(C)CH-(CH)CH-CO- endo, -CO-(C)CH-(CH)CH-CO- endo), 3.00-2.88 (-CO-(C)CH-(CH)CH-CO- exo, -CO-(C)CH-(CH)CH-CO-, exo).

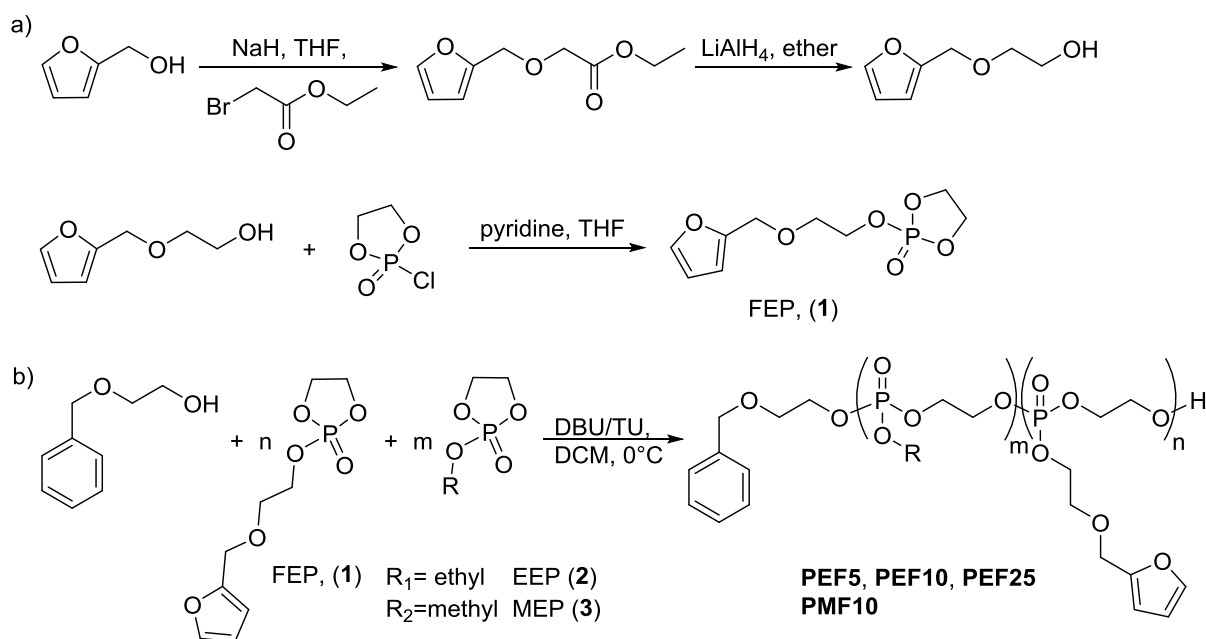
*Retro-Diels Alder Studies.* The polymer **PEF10-Et-b** (ca. 5 mg) was dissolved in 0.5 mL d<sub>4</sub>-tetrachlorethane in a NMR tube. <sup>1</sup>H NMR spectra were recorded at 110°C every 6.5 min. The reaction is also applicable on larger scale in tetrachloroethane at 110°C within 1h.

*Degradation Studies.* 5 mg of each polymer were dissolved in 0.6 mL of a partially deuterated NaHCO<sub>3</sub>-NaOH-buffer; the buffer stock was prepared from 5 mL 0.4M NaHCO<sub>3</sub> solution, 1.84 mL 1M NaOH solution, 1 mL D<sub>2</sub>O and 2.16 mL H<sub>2</sub>O (i.e. 0.2M, pH 11.1 and 10 v% D<sub>2</sub>O). For the degradation of **PEEP** at pH 4, the pH of a mixture of H<sub>2</sub>O/D<sub>2</sub>O 9:1 was adjusted with conc. HCl. For **PEEP** at pH 7, the pH of a mixture of H<sub>2</sub>O/D<sub>2</sub>O 9:1 was adjusted with NaOH-solution. The NMR tubes were incubated at room temperature and <sup>1</sup>H and <sup>31</sup>P {H} NMR spectra were measured at 298 K.

## 4.4 Results and Discussion

**Monomer Synthesis.** 2-(2-(furan-2-ylmethoxy) ethoxy)-1,3,2-dioxaphospholane 2-oxide (**FEP**, **1**), a functional, unprotected monomer for the ring-opening polymerization (ROP) was prepared in three steps (Scheme 4.2). Its pendant ester contains a furfuryl group, which is inert to ring-opening of the phosphate, but can undergo a reversible DA postpolymerization modification.<sup>38</sup> No toxic byproducts are obtained, which makes the reaction interesting for biomedical applications. Also, furan derivatives can be obtained from renewable resources, making the DA reaction to an important contribution to the growing role of sustainable and green chemistry.<sup>39</sup> In recent years, the step-growth polyaddition of furfuryl and maleimide monomers,<sup>40</sup> or furan (or maleimide)-terminated poly(urethane)s<sup>41</sup>, poly(lactic acid)<sup>42</sup> or poly( $\epsilon$ -caprolactone)<sup>43</sup> were used to prepare networks upon reaction with multi-functional maleimide (or furan) cross-linkers. 2-Substituted furan-based monomers (e.g. FDCA, 2,5-furandicarboxylic acid) gave access to the biobased PET analogue poly(ethylene 2,5-furandicarboxylate).<sup>44</sup>

**1** was prepared starting from furan-2-yl-methanol, which was reacted with bromoacetate to ethyl-2-(furan-2-ylmethoxy)acetate,<sup>45</sup> followed by reduction with lithium aluminium hydride to 2-(furan-2-yl-methoxy)-ethanol. **1** was then prepared by reacting 2-(furan-2-yl-methoxy)-ethanol in the presence of pyridine with 2-chloro-1,3,2-dioxaphospholane oxide (COP). **1** was purified by column chromatography to yield the pure monomer as slightly yellow oil. The monomer can be stored at -28 °C under dry inert gas for at least several months (decomposition of the monomer is



**Scheme 4.2.** a) Synthesis of FEP monomer 2-(2-(furan-2-ylmethoxy)ethoxy)-2-oxo-1,3,2-dioxaphospholane (**1**), b) copolymerization of **FEP** (**1**) and **EFP** (**2**) or **MEP** (**3**) to **PEF5**, **PEF10**, **PEF25** and **PMF10**.

indicated by color change to black and the formation of insoluble residue<sup>46</sup>). The monomer was characterized by <sup>1</sup>H and <sup>31</sup>P{H} NMR spectroscopy (Figures 4.1a and S4.1-S4.3): the resonances of the furfuryl group are detected as singlets at 7.37 and 6.35 ppm (a+b), the dioxaphospholane ring can be observed between 4.43-4.23 ppm (d). Further signals of the pendant group show resonances at 4.52 (c) and 3.70 ppm (e). The <sup>31</sup>P {H}NMR spectrum shows a singlet at 17.75 ppm, typical for 5-membered cyclic phosphates.<sup>19</sup>

**Polymerization.** The cyclic phosphate monomer **1** was used in the organocatalytic anionic ROP with 1,8-diazabicyclo[5.4.0]undec-7-ene (DBU) and *N*-cyclohexyl-*N'*-(3,5-bis(trifluoromethyl)-phenyl) thiourea (TU) as the catalyst mixture.<sup>19</sup> When the polymerizations were carried out at 0 °C in dry DCM (4 mol/L), PPEs with narrow molecular weight distributions and high monomer conversion (typically up to 90%) were accessible. EEP (**2**) or MEP (**3**) were used as comonomers to

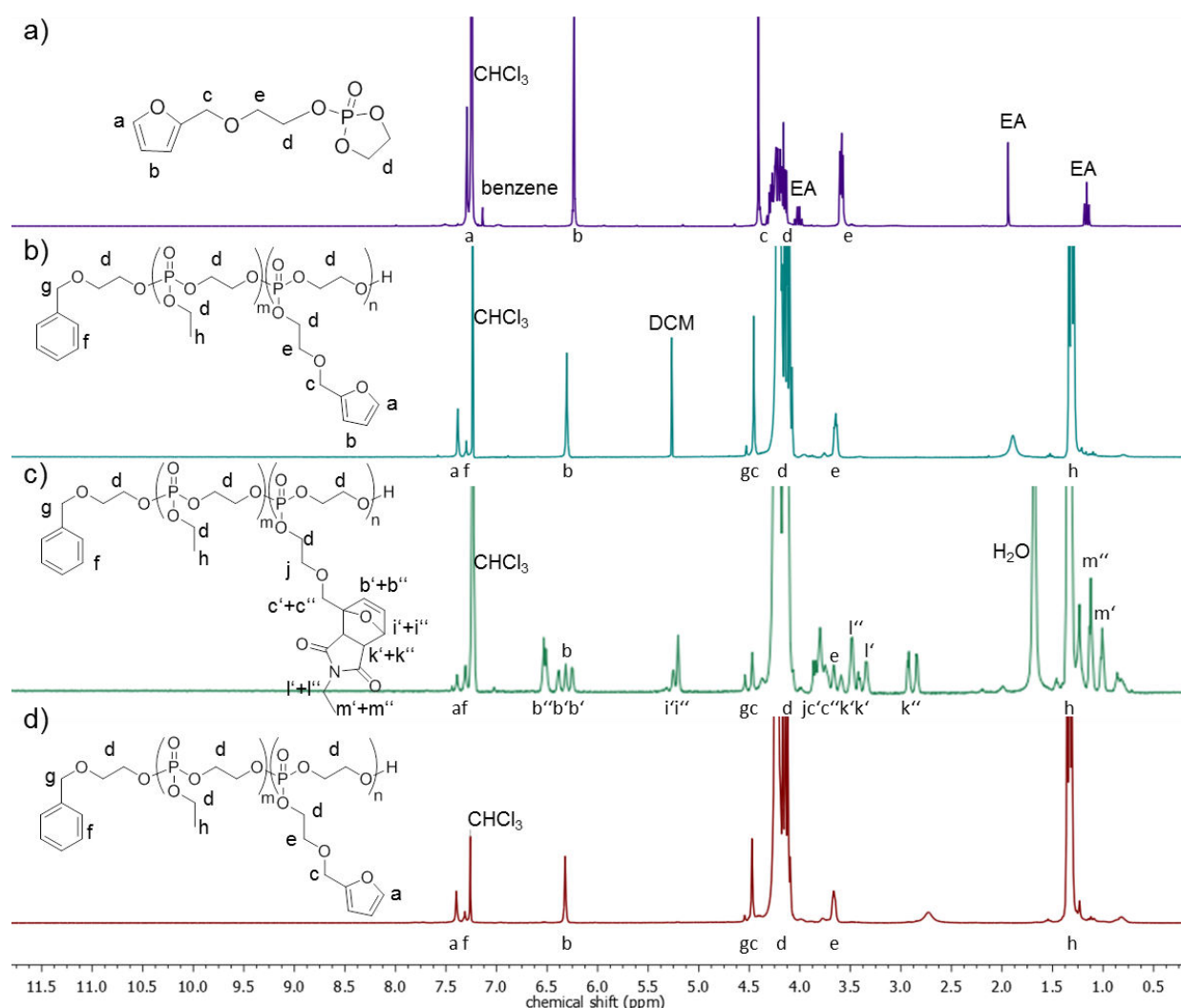


**Figure 4.1.** <sup>1</sup>H NMR spectra (300 MHz, CDCl<sub>3</sub>, 298K) of a) FEP monomer (**1**), b) copolymer **PEF10**, c) modified copolymer **PEF10-Et** after Diels-Alder reaction, d) copolymer **PEF10** after retro-Diels-Alder reaction. *Note:* characters with ' denotes signals of the *endo* Diels-Alder product, with '' denotes signals of the *exo* Diels-Alder product.

**1** to adjust the hydrophilicity of the copolymers by the comonomer feed ratio. Copolymers of **FEP** (**1**) and **EFP** (**2**) with furan contents of 5, 10, and 25 mol% and a targeted degree of polymerization of 150 were synthesized (Table 4.1). SEC measurements (Figure S4.14) showed narrow molecular weight distributions of  $D=1.08-1.19$  indicating minimal transesterification under these conditions. Only **PMF10** exhibited a broader molecular weight distribution of 1.24, which could be attributed to a certain degree of transesterification during the polymerization, which is known for **MEP**. The

Table 4.1. Overview of polymerizations and results.

entry	[I]/[FEP]/ [EEP]	$DP_{th}^a$	FEP $DP^a$	FEP / %	EEP $DP^a$	EEP / %	$DP^a$	con- vers.	$M_n^b$ g/mol	$M_w/M_n^c$	$T_g^d$ /°C	$T_{CP, inf.}^e$ /°C
PEEP	1/0/90	90	-	-	109	100	109	0.90	16,700	1.10	-53	no CP
PEF5	1/8/142	150	8	5.5	138	94.5	146	0.86	23,100	1.08	-51	44.0
PEF10	1/15/135	150	20	9.1	199	90.9	219	0.85	35,400	1.15	-49	17.4
PEF25	1/38/112	150	56	24.7	171	75.3	227	0.87	40,000	1.19	-45	insoluble
PMF10	1/15/135	150	22	9	221 <sup>f</sup>	91 <sup>f</sup>	243	0.76	36,100	1.24	-43	no CP

<sup>a</sup>DP= degree of polymerization (th: theoretical). <sup>b</sup>Determined from the <sup>1</sup>H-NMR spectra. <sup>c</sup>Determined by SEC in DMF, RI-signal. <sup>d</sup>Determined by DSC. <sup>e</sup>CP= inflection cloud point, determined by turbidity measurement in water, 3g/L, <sup>f</sup>MEP

$^{31}\text{P}\{\text{H}\}$  NMR signals of the monomer shifted from 17.75 ppm (for **FEP**) and 16.83 ppm (for **EFP**) to ca. -1.24 ppm for the polymers (r.t., 121 MHz,  $\text{CDCl}_3$ ).  $^1\text{H}$  DOSY spectra confirmed the formation of copolymers (Figure S4.6). End group analysis from the  $^1\text{H}$  NMR spectra (from **PEF10** in Figures 4.1b and S4.4) revealed that molecular weights of 16,700-40,000 g/mol were obtained under these conditions. The resonances of the aromatic protons of the initiator (2-benzyloxy ethanol) at 7.34 ppm (f) were compared with distinct resonances for the two different repeat units: the signal at 7.64 ppm (a) for the **FEP** repeat unit and the triplet signal at 1.26 ppm (h) which belongs to the **EFP** repeat unit (or a doublet for the pendant methoxy group (due to coupling with P) at 3.71 ppm in the case of **MEP** repeat units, see also Figure S4.9). The signal of the backbone at 4.26-3.98 ppm (d) gave the degree of polymerization and coincided with the total number of **FEP** and **EFP** (or **MEP**) repeat units. The ratios of comonomers from initial feed could be retrieved in all copolymers.

All polymers were soluble in organic solvents such as dichloromethane and chloroform, or polar solvents as THF, ethanol, methanol and DMF, but insoluble in hexane or diethyl ether. The water-solubility strongly depends on the content of furfuryl moieties: while **PEEP**, **PEF5**, **PEF10** and **PMF10** were water-soluble, **PEF25** could not be solubilized in water (cf. Table 4.1).

**Copolymerization behavior.** The copolymerization behavior of **FEP** and **EFP** was investigated via real-time  $^{31}\text{P}\{\text{H}\}$  NMR kinetics. Starting with an initial monomer feed of **FEP/EFP** of 0.1/0.9 and a targeted degree of polymerization of 120 in  $d_2$ -DCM at  $-20\text{ }^\circ\text{C}$ , monomer consumption was monitored at every time point during the copolymerization (Figure 4.2a). From the recorded real-time  $^{31}\text{P}\{\text{H}\}$  NMR spectra, a faster incorporation of the **FEP** monomer was observed, which might be attributed to coordination of the ethoxy-side chain to the propagating species (similar findings have been reported in the anionic polymerization of glycidyl ethers under certain conditions<sup>47</sup>). Due to increasing viscosity in the NMR-polymerization, the reaction was stopped at 42 % of total conversion, revealing ca. 50 % of **FEP** was consumed at this conversion, while 65 % of **EFP** monomer remained unreacted (Figure 4.2c). Fitting of the curves provided the full copolymerization plot. This gradual comonomer incorporation might influence the solubility profile of copolymers with higher ratios of **1**, however, was not further considered in the current study, but might be used in order to design sequence-controlled aggregation phenomena.

**Diels-Alder Post-Polymerization Modification of Polymers.** **PEF5**, **PEF10**, and **PEF25** were functionalized with a series of maleimide derivatives via DA cycloaddition. Different maleimide derivatives were used for functionalization, either unsubstituted (I), substituted with aliphatic (II) or aromatic (III) residues, with a polar (IV) or charged group (VI and VII) and a zwitterionic substituent (V). Scheme 4.3 exemplarily shows a post-modification reaction of a copolymer and all maleimide derivatives used in this study.

DA postmodification was carried out at 70 °C either in toluene/DCM-mixture (8:2) (for I-IV) or in DMF (for V-VII) with a polymer concentration of ca. 100 mg/mL and 5 eq. of maleimide. All functionalized polymers were characterized by  $^1\text{H}$  and  $^{31}\text{P}$  {H} NMR spectroscopy. In the  $^1\text{H}$  NMR spectrum of **PEF10-Et** (Figure 4.1c) the aromatic resonances of the furane groups at 7.41 and 6.33 ppm (a+b) disappeared – partially or completely (depending on the degree of functionalization) and new signals from the DA product at 6.54-6.26 (b'+b''), 5.27-5.22 (i'+i''), 3.55-3.30 (c', c'', k', l', l''), 2.98-2.81 (k'') and 1.14-1.01 ppm (m'+m'') were detected. The DA reaction can

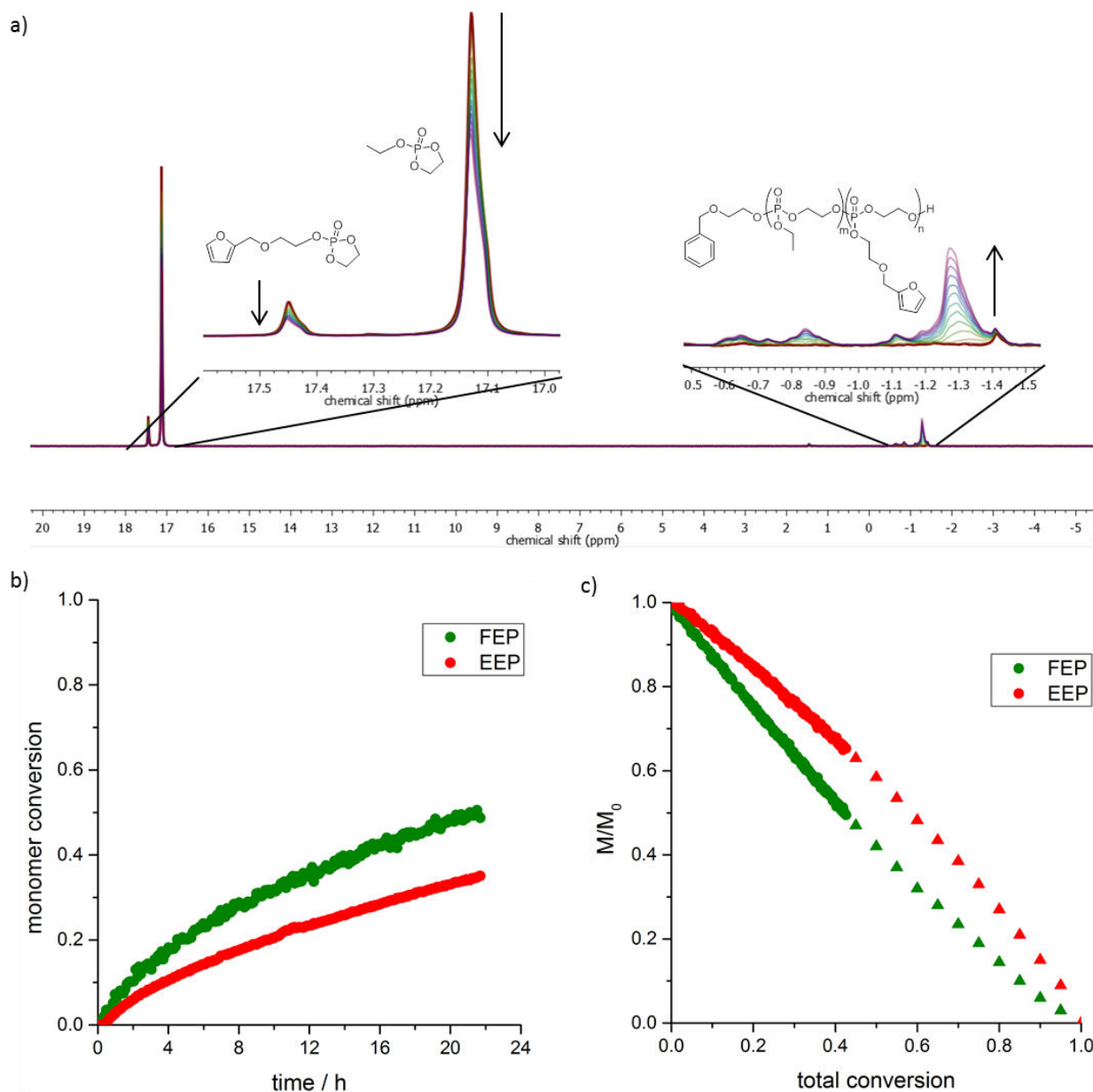


**Figure 4.2.** Simultaneous copolymerization of EEP and FEP: a) overlay and zoom-in into real-time  $^{31}\text{P}$ {H} NMR measurements, b) monomer conversion vs. time, b) normalized monomer concentrations in the reaction versus total conversion (note: triangles represent extrapolated data points).

produce two diastereomers;<sup>48-49</sup> while the *endo* compound is the kinetically favored product, the *exo* compound is the thermodynamically more stable product (Scheme 4.3c), which can be distinguished from the <sup>1</sup>H NMR and <sup>1</sup>H NOESY spectra (Figures 4.1c and S4.8). The *endo/exo* ratio is listed in Table 4.2, but was not further considered. The <sup>31</sup>P {H} NMR spectra of the DA-modified PPEs remained unchanged (-1.24 ppm) compared to the starting materials, indicating the stability of the phosphotriester under these conditions. From <sup>1</sup>H NMR spectra of modified polymers, the degree of functionalization was also calculated (exemplarily shown in Figure 4.1c). The signals of the *endo* and *exo* products, b' and b'' respectively, were compared to remaining signal of furan (b), yielding the conversion:

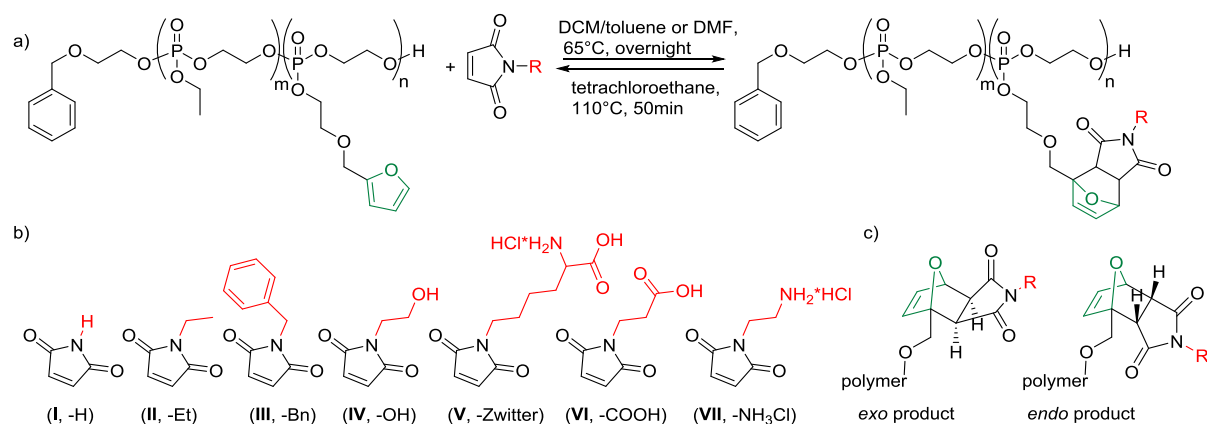
$$\frac{b' + b''}{b + b' + b''} \cdot 100 = x \% \text{ conversion}$$

While compounds I-IV resulted in high degrees of functionalization between 72% to full conversion (see Table 4.2 for all results), the reaction with ionic maleimides resulted in moderate degrees of functionalization (23-61% for compound V, 48-89% for VI and VII). The results correlated with the choice of solvent for the reaction.

SEC curves for the DA-modified polymers with maleimides I-IV showed slight changes in dispersities and hydrodynamic radii compared to the starting materials (Figures S4.15-S4.17, dispersities change from 1.08-1.19, for **PEF5** and **PEF25**, respectively; to 1.08-1.21 for **PEF5-H** and **PEF25-Et**, Table 4.2 and exemplarily shown in Figure 4.5). Shifting and broadening of the MWDs were more dominant for modification with the COOH maleimide (VI). This is probably attributed to interactions with the column material under these conditions. Polymers with amine (VII) and zwitterionic functionalization (V) could not be measured on our SEC setup, due to strong interaction with the column material.

Copolymers showed low  $T_g$ 's between -53 and -43 °C and no crystallization, typical for PPEs obtained by ring-opening polymerization (Figures S4.18 and S4.19).<sup>48</sup> With increasing amount of the aromatic FEP units, the  $T_g$  increased. Postmodification of the copolymers increased their  $T_g$ 's (between -21 to -11 °C, exemplarily listed for modified **PEF25** in Table 4.3).

**Control of Hydrophilicity.** Thermoresponsivity of the herein prepared PPE-copolymers were adjusted by the comonomer ratio as well as the nature of the pendant group after DA-reaction. We determined the cloud points of an aqueous solution of the respective polymer by turbidity measurements on a UV-VIS spectrometer (polymer concentration: 3 g/L in water, heating rate: 1 °C/min). As recently proposed by Iván et al.,<sup>1</sup> we used the inflection point of the transmittance-temperature curves as the cloud point temperature ( $T_{CP}$ ), determined by the minimum of the first derivative of the curve, which allow an accurate comparison between different materials (Figures 4.3 and S4.20-4.29 (for cooling curves)).



**Scheme 4.3.** a) DA reaction of a furfuryl-containing PPE with a maleimide, b) maleimide derivatives used in this study, c) the two possible endo or exo diastereomers obtained by DA reaction.

**Table 4.2.** Overview of post-polymerization modifications and cloud points.

entry	conversion <sup>a</sup>	exo/endo <sup>a</sup> / %	$M_n^b$ / g/mol	$M_w/M_n^c$	$T_{CP, infl.}^d$ / °C
PEEP	-	-	16,700	1.10	-
PEF5	-	-/-	23,100 <sup>a</sup>	1.08	44.0
PEF5-Bn	0.94	58/42	24,500	1.11	15.5
PEF5-Et	0.72	63/37	23,800	1.10	64.6
PEF5-H	0.98	95/5	23,900	1.08	-
PEF5-OH	0.90	75/25	24,100	1.10	-
PEF5-COOH	0.50	66/34	23,800	1.12	-
PEF5-NH <sub>3</sub> Cl	0.48	100/0	23,800	n.d.	-
PEF5-Zwitter	0.23	100/0	23,500	n.d.	-
PEF10	-	-/-	35,400 <sup>a</sup>	1.15	17.4
PEF10-Bn	0.97	70/30	39,000	1.17	insoluble
PEF10-Et	0.74	63/37	37,200	1.15	29.2
PEF10-Et-b <sup>e</sup>	0.84	64/36	37,500	1.20	n.d.
PEF10-H	1	96/4	37,300	1.15	43.5
PEF10-OH	1	83/17	38,200	1.17	-
PEF10-COOH	0.70	72/28	37,700	1.24	-
PEF10-NH <sub>3</sub> Cl	0.60	100/0	37,500	n.d.	-
PEF10-Zwitter	0.39	100/0	37,200	n.d.	-
PEF25	-	-	40,000 <sup>a</sup>	1.19	insoluble
PEF25-Bn	1	82/18	50,500	1.21	insoluble
PEF25-Et	0.90	62/38	46,400	1.21	23.9
PEF25-H	0.99	97/3	45,400	1.20	28.7 <sup>f</sup>
PEF25-OH	0.98	85/15	47,800	1.17	-
PEF25-COOH	0.59	75/25	45,600	1.29	32.4, >70
PEF25-NH <sub>3</sub> Cl	0.89	62/38	48,900	n.d.	-
PEF25-Zwitter	0.61	100/0	47,700	n.d.	-
PMF10	-	-	36,100	1.23	-
PMF10-Bn	0.98	84/16	40,200 <sup>t</sup>	1.53	insoluble

<sup>a</sup>Determined from the <sup>1</sup>H-NMR spectra. <sup>b</sup>Theoretically calculated. <sup>c</sup>Determined by SEC in DMF, PEO standard, RI-signal. <sup>d</sup>CP= inflection cloud point, determined by turbidity measurement in water, 3g/L., 2-80 °C. <sup>e</sup>For retro-DA reaction. <sup>f</sup>Miscibility gap. n.d. = not determined.

**PEEP** is a water-soluble polymer with no cloud point temperature in pure water. With increasing amount of **FEP** in the copolymer structure, the hydrophilicity was reduced and a phase separation upon heating of the aqueous solution of the polymers was observed (Table 4.1, Figures 4.3 and S4.20): **PEF5**, with 5% FEP, phase-separated at 44.0 °C, **PEF10**, with 10% FEP, was only water-soluble below 17.4 °C; **PEF25** was not soluble in the measured range anymore. In contrast, **PMF10** did not show any thermal response in water, due to the more hydrophilic methyl ester side chains of **MEP** units compared to ethyl esters in **EEP**.

The solubility profile of those copolymers was then systematically adjusted by DA-postmodification with different maleimide derivatives (Figure 4.3). Functionalization with benzyl maleimide (**III**) decreased the hydrophilicity and thus the cloud point temperatures could be shifted to lower temperatures precisely by the choice of the comonomer ratio and degree of functionalization. While **PEF5-Bn** remained water-soluble up to 15.5 °C, **PEF10-Bn** and **PEF25-Bn** were changed into water-insoluble polymers after DA with **III**. Also the **PMF10** derivative could be turned from a fully water-soluble (without cloud point) into a hydrophobic material after modification with **III** (**PMF10-Bn**). In contrast, functionalization with ethyl maleimide (**II**) produced copolymers with increased cloud points compared to the unmodified copolymers: **PEF5-Et** and **PEF10-Et** were soluble until 64.6 and 29.2 °C, respectively. Also the copolymer with 25% FEP units could be turned into a thermoresponsive polymer by functionalization with **II** as hydrophilic imide groups were attached to the PPE-copolymer (**PEF25-Et**,  $T_{CP} = 23.9$  °C). For benzyl functionalized copolymers, the hydrophobicity of the aromatic groups predominated the hydrophilicity of imide groups, for the ethyl functionalized one, this could not be observed. For maleimide (**I**) (-hydrogen) functionalized copolymers, a further increase of the hydrophilicity resulted in an increase of the phase separation temperatures: **PEF5-H** did not exhibit any cloud point in the measured range, **PEF10-H** at 43.5 °C. Since the transmittance for **PEF10-H** decreased only down to 27%, we assume a miscibility gap and for higher temperatures an increase in solubility and a clearing point again (not measured here). The decrease of solubility can be explained by hydrogen bond formation between the imide groups. The assumption of a miscibility gap and a clearing point could be confirmed by the temperature dependent behavior of **PEF25-H**: while it showed a cloud point at 28.7 °C (with the transmittance reduced to 82%) and a clearing point at 53.6 °C, e.g. a UCST-like phase separation, could be observed. The polymer solubilized again, due to breakage of hydrogen bonds from imide groups at high temperatures. In addition, the functionalization with hydroxyethyl maleimide (**IV**) introduced additional OH-groups to the copolymers and further increased the hydrophilicity in the polymers, that all modified copolymers (**PEF5-OH**, **PEF10-OH**, and **PEF25-OH**) were turned into non-thermoresponsive, but still functional polymers.

Besides tuning of the thermoresponsivity of the furfuryl-PPEs, a further pH-stimulus can be introduced by DA reaction with acidic or basic maleimides. The resulting polyelectrolytes were investigated at different pH-values (pH 1-2, pH 11-12, and in water without additives (pH's of samples in water are listed in Table S4.1) to ensure complete protonation or deprotonation of the charged groups. All amine- and zwitterionic-modified copolymers showed complete solubility at basic or acidic conditions and in water (Figures S4.21-S4.29). In contrast, **PEF5-COOH** and **PEF10-COOH** were fully water-soluble when deprotonated, but showed a thermal response when protonated (at 51.9 and 28.7 °C, respectively). The protonated carboxyl groups undergo intramolecular hydrogen bonding, causing the decrease of solubility of the polymers compared to samples at higher pH values. **PEF5-COOH** showed minimal solubility at 59.4 °C (61% transmittance). At higher temperatures the hydrogen bonds between the COOH-groups fracture and solubilize the polymer (UCST-like behavior). The effect of the miscibility gap was more dominant for **PEF10-COOH** due to enhanced number of carboxyl groups (cloud point at 28.7 °C and minimal solubility at 37.0 °C / 25% transmittance). At higher temperatures, the polymer could be

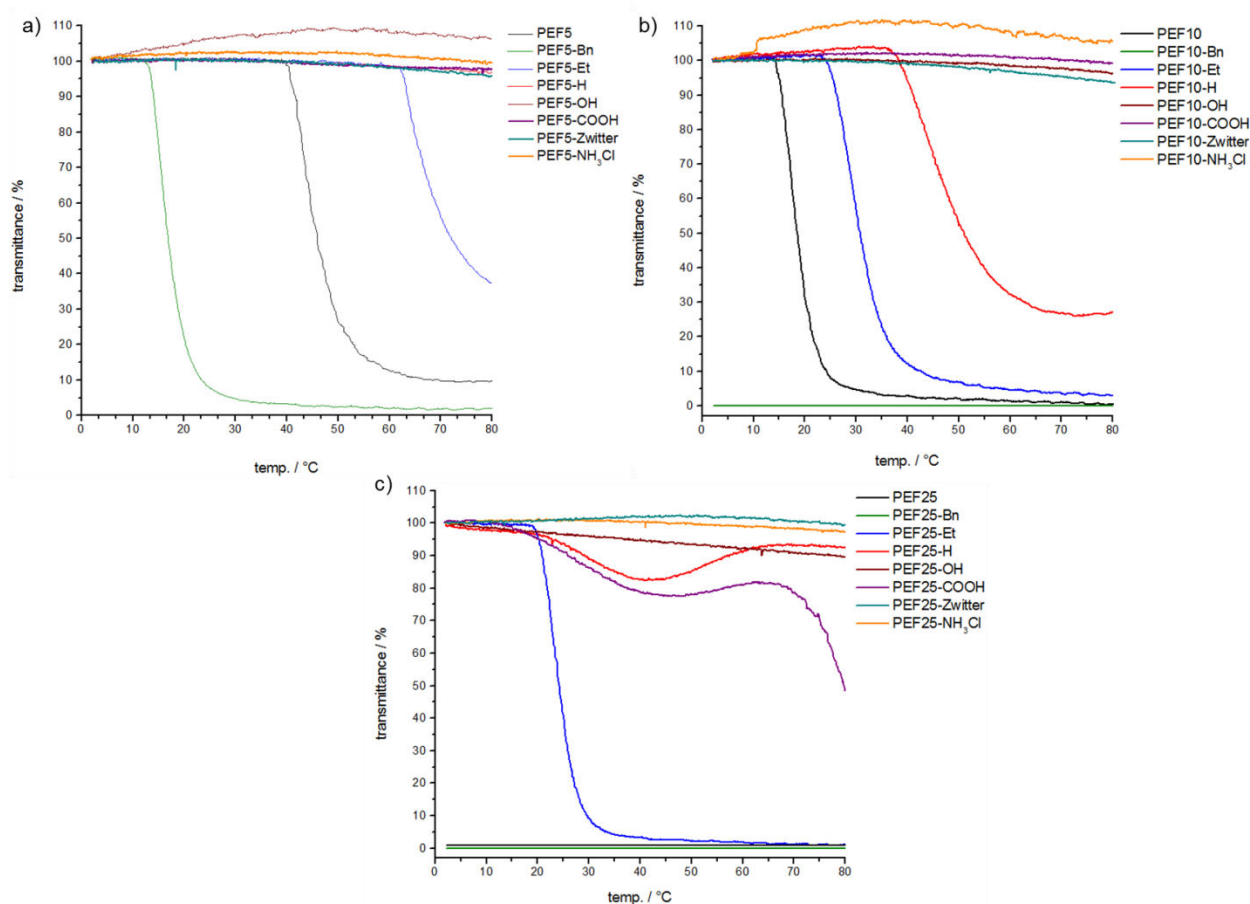


**Figure 4.3.** Solubility profiles of PPE-copolymers based on furan-functionalized PPEs modified with different maleimides: turbidity measurements of a) unmodified and modified **PEF5**, b) unmodified and modified **PEF10** and c) unmodified and modified **PEF25** (measurements were conducted in water with  $c=3$  g/L and measured in a temperature range of 2-80 °C, heating rate 1 °C/min).

solubilized again and also lacked a miscibility gap during cooling. To exclude that polymer degradation took place under such conditions, a second heating/cooling cycle was run and confirmed the thermal behavior in all cases. Finally, **PEF25-COOH** was also completely soluble at pH 11.1, but insoluble at pH 1.2. In water, the polymer exhibited decreased solubility due to dimerization of carboxyl groups, resulting in a first cloud point at 32.4 °C. At higher temperatures, dimerization broke, causing a stable transmittance behavior between 40-70 °C. The polymer became insoluble over 70 °C due to the hydrophobic effect.

Summarizing the results, the hydrophilicity and solubility for unmodified copolymers decreased with increasing amount of FEP monomer. **PMF10** did not show any thermal response compared to **PEF10**. Functionalization with ethyl (**II**), hydrogen (**I**) and hydroxyethyl maleimides (**VI**) increased the hydrophilicity of the copolymers, while modification with benzyl maleimide (**III**) decreased the hydrophilicity significantly. **PEF25-H** exhibited a miscibility gap between 29-52 °C, resultant from H-bonding between the maleimides. All amine- and zwitterion-modified copolymers did not exhibit any thermal response, while COOH- modified copolymers showed pH-dependent solubility profiles (Figure 4.4).

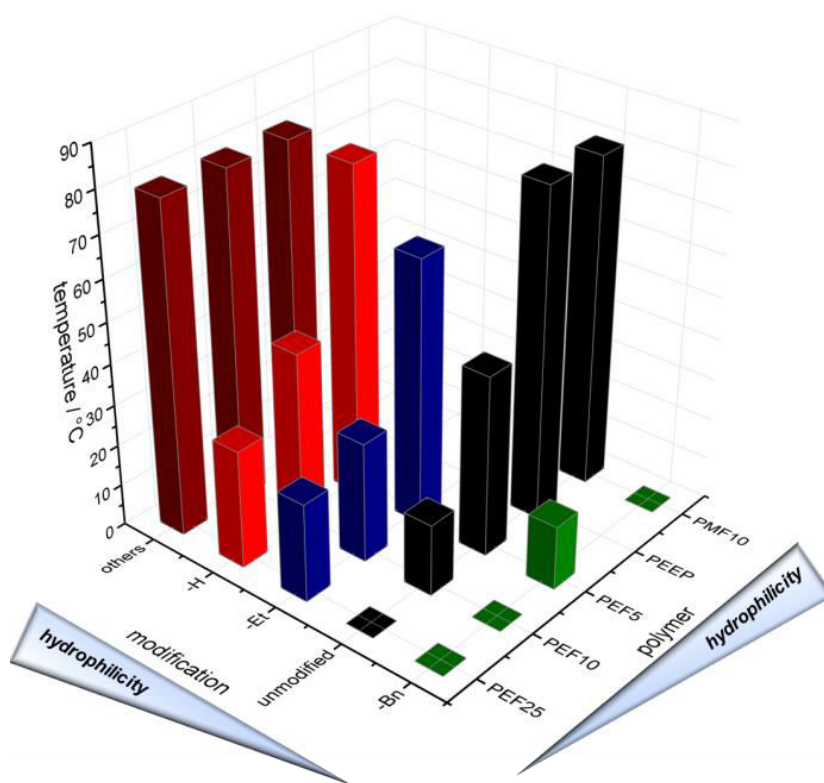


**Figure 4.4.** Overview of hydrophilicity trends of unmodified and modified copolymers. X-axis represents the polymers, y-axis the modification, z-axis the temperature. Columns express the solubility of polymers, the highest point depicts the cloud point or 80°C in case of complete solubility. The hydrophilicity trends are shown by the triangles. *Note:* “others” include modification with -OH, -COOH, -NH<sub>3</sub>Cl and -Zwitter, which are all fully soluble under these conditions.

**Retro-Diels-Alder Reaction.** The Diels-Alder cycloaddition of furans with maleimides is a reversible reaction. While the DA-product is formed between ca. 60-80 °C, the reverse reaction takes place at higher temperatures of ca. 100-120 °C. Under these conditions, a non-degradable polymer can undergo the retro-DA reaction easily.<sup>49</sup> In contrast, heating PPEs might lead to unwanted transesterification or backbone degradation. As a proof-of-concept, **PEF10-Et-b** was heated up to 110 °C and monitored by <sup>1</sup>H NMR kinetics to follow the release of the furan units (Figures 4.5a and S4.30). Resonances for the furan group, the DA-adduct and *N*-ethylmaleimide, which was formed during unblocking, were evaluated. The retro-DA reaction showed complete conversion after ca. 50min. From the initially 84% functionalized furan groups, a quantitative release of *N*-ethylmaleimide was achieved under these conditions (<sup>1</sup>H NMR spectrum after complete reaction is depicted in Figure 4.1d). All resonances belonging to the DA-adduct vanished and only signals of the furan moiety could be observed. Importantly, the molecular weight distribution and shape of elugram remained unchanged compared to **PEF10**, with  $\bar{D}$ = 1.16 and 1.15 respectively. This clearly indicated that the polymer backbone was not affected by transesterification or degradation reactions under the chosen (especially dry!) reaction conditions (Figure 4.5b and Table S4.2). Longer reaction times or aqueous impurities resulted in partial or complete backbone hydrolysis (data not shown).

DSC was additionally used to study the retro-DA reaction on the PPE-copolymers.<sup>50-51</sup> In the case of mixed *exo/endo* isomers, two endotherms during the DSC experiment can be observed: the thermodynamically favored *exo* product is more stable than the *endo* product and therefore undergoes a retro-DA reaction at higher temperatures. All post-modified PPEs contained a mixture of *exo/endo* DA-products as observed via the <sup>1</sup>H NMR spectra and therefore also two endothermic maxima in DSC measurements were expected. The temperatures at the inflection points are listed

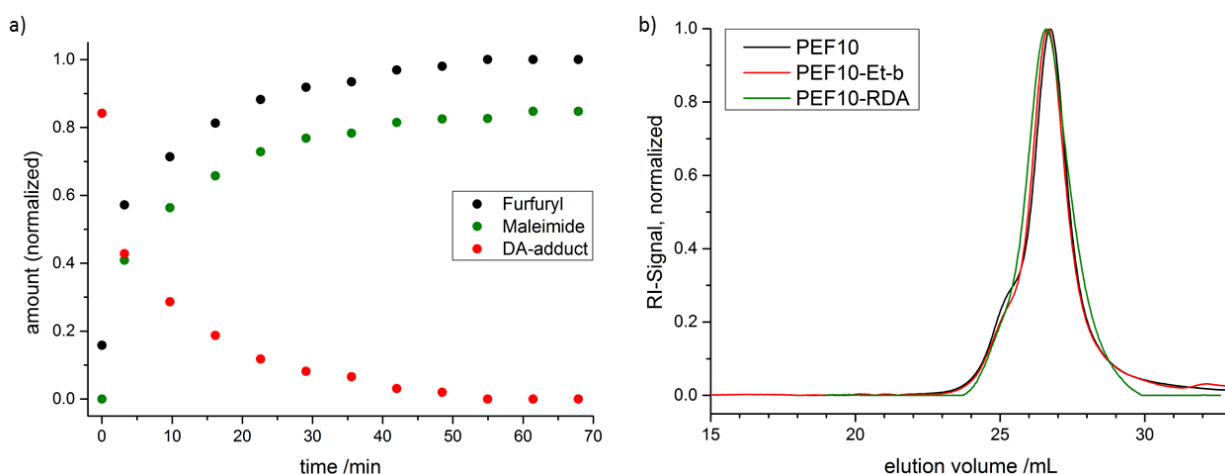


**Figure 4.5.** Retro-Diels Alder reaction on PPEs: a) Integral values of the resonances for furan, DA-adduct, and maleimide vs. reaction time (measured by <sup>1</sup>H NMR spectroscopy); b) SEC elugrams of **PEF10** before DA reaction, **PEF10-Et-b** after DA reaction and **PEF10-RDA** after RDA reaction.

in Table 4.3 for all modified polymers of **PEF25** (minimum of the endotherms could not be obtained due to overlay of both endotherms). While the *endo* product was cleaved between 100-107 °C, the *exo* product underwent the RDA at ca. 30 °C higher temperatures (129-137 °C) (Figure S4.19). Only **PEF25-H** showed a single endothermic maximum at 124 °C. The observation correlated with the evaluation of the <sup>1</sup>H NMR spectrum, that nearly only *endo* product was formed (97%).

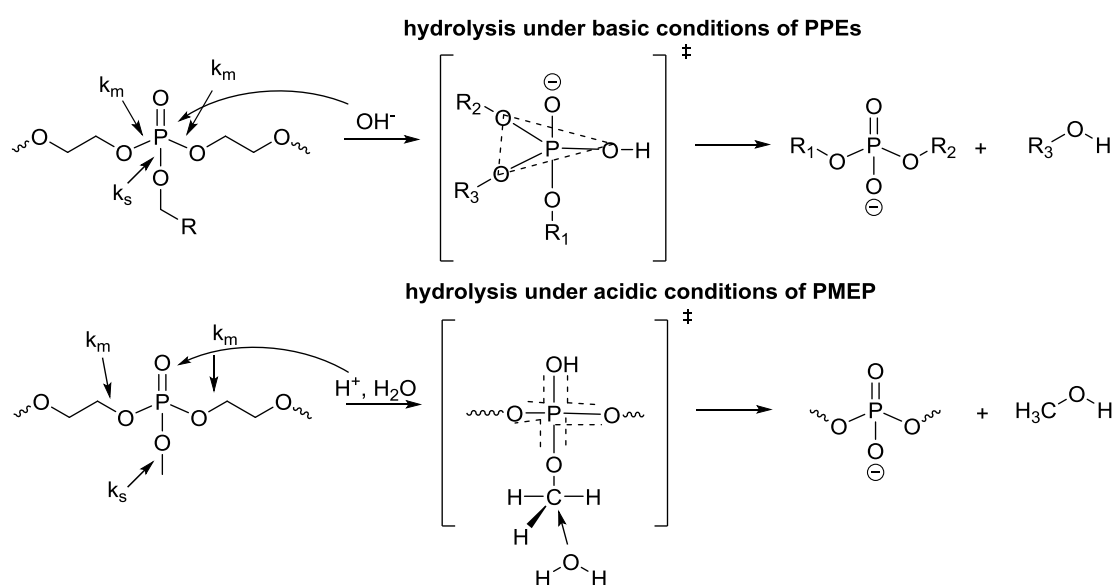
**Table 4.3.** Overview of thermal data of post-modified polymers **PEF25** determined by DSC measurements.

entry	$T_g / ^\circ\text{C}$	$T_{\text{RDA}} / ^\circ\text{C}$	
		endo	exo
<b>PEF25</b>	-45	-	-
<b>PEF25-Bn</b>	-11	103	131
<b>PEF25-Et</b>	-21	105	137
<b>PEF25-H</b>	-18	124	
<b>PEF25-OH</b>	-14	107	129
<b>PEF25-COOH</b>	-16	100	134
<b>PEF25-NH<sub>3</sub>Cl</b>	-17	105	133
<b>PEF25-Zwitter</b>	-8	101	134

**Degradation Studies.** PPEs are biodegradable and undergo backbone and side-chain hydrolysis under acidic or alkaline conditions<sup>52</sup> and by enzymatic degradation.<sup>13, 53</sup> Penczek and coworkers extensively investigated the degradation behavior of poly(methyl ethylene phosphate) (**PMEP**) at different pH-values at 45 °C.<sup>52</sup> They found that **PMEP** was relatively stable under acidic and neutral conditions with rather slow degradation times, but degraded faster under basic conditions: from the determination of rate constants of hydrolysis from the phosphotri- to diesters, they calculated the time for 50% cleavage of the ester bonds in the side chain or main chain at pH 3.78 to be  $t_{1/2}=157$  days for the side chain and  $t_{1/2}=704$  days for the main chain, at pH 7.30 to be  $t_{1/2}=213$  days for the side chain and  $t_{1/2}=632$  days for the main chain and at pH 11.7 to be  $t_{1/2}=14$  hours for the side chain and  $t_{1/2}=15$  hours for the main chain. Moreover, while in acidic and neutral media cleavage of the side chain dominates degradation ( $k_s/k_m= 4.46$  at pH 3.78 and  $k_s/k_m=2.95$  at pH 7.30), a statistical cleavage of ester bonds in the side and main chain occurs ( $k_s/k_m= 1.06$  at pH 11.7). The authors explained the observation by different mechanisms of hydrolysis, which was already described by Welch and coworkers for trimethyl and triphenyl phosphate:<sup>54</sup> basic degradation occurs by nucleophilic attack of the phosphorus atom by a hydroxide anion and cleavage of an ester bond in apical position (Scheme 4.4). They claimed the probability of side or main chain being in apical position to be comparable, resulting in a statistical cleavage of the ester bonds. In contrast, during the neutral and acidic hydrolysis, (after protonation of the P=O-bond,) the  $\alpha$ -carbon atom in the alkyl ester is attacked by water. While the hydrogen substituents of the methyl group in the side chain do not hamper this attack, the polymer chain of the backbone sterically impedes the attack.<sup>52</sup>

Herein, we studied the degradation of the analogous polymer with an ethyl side chain, i.e. **PEEP**. **PEEP** is the most prominent PPE for biomedical applications, due to its water-solubility and better control during the polymerization of **EPE** compared to **MEP** (less transesterification). However, most papers only claim the degradability of **PEEP**. We studied the degradation profiles of **PEEP** at different pH values and were able to prove a significant backbone cleavage which degrades the polymer chain under basic conditions, while neutral and acidic conditions did not result in any degradation during our experiments. Compared to **PMEP**, with a methoxy group as side chain, we expected a different behavior for **PEEP** and other PPEs with more bulky side chains during acidic hydrolysis, due to an increased steric hindrance of attack of  $\alpha$ -carbon atom. Also the comparison with poly(phosphonate)s with a hydrolytically stable P-C bond in the side chain showed similar degradation profiles under neutral and basic conditions for the backbone. While they did not show any degradation after 42 days at pH 6.1, complete degradation was observed after 1 hour at pH 12.<sup>55</sup> In contrast, poly(phosphoramidate)s undergo hydrolysis in acidic and basic media.<sup>24-25, 56-58</sup> Penczek and coworkers studied the cleavage of side-chain poly(phosphoramidate)s at different pH's of 1.5, 6.5 and 8.5. While hydrolysis almost exclusively proceeded at the P-N bond under acidic and nearly neutral conditions, P-O as well as P-N bond cleavage was observed for basic conditions, still with a higher probability for P-N cleavage ( $k_{P-N}=1.9 \cdot 10^{-8} \text{ s}^{-1}$  and  $k_{P-O}=1.0 \cdot 10^{-9} \text{ s}^{-1}$ ).<sup>57</sup> Wooley and coworkers showed accelerated and selective cleavage at the P-N bonds of side-chain poly(phosphoramidate)s at pH 1.0 within 10 h.<sup>24</sup> Cleavage of main-chain poly(phosphoramidate)s has been shown at pH 3.0, where 94% of triesters was cleaved within 12.5 days to diesters.<sup>56</sup>

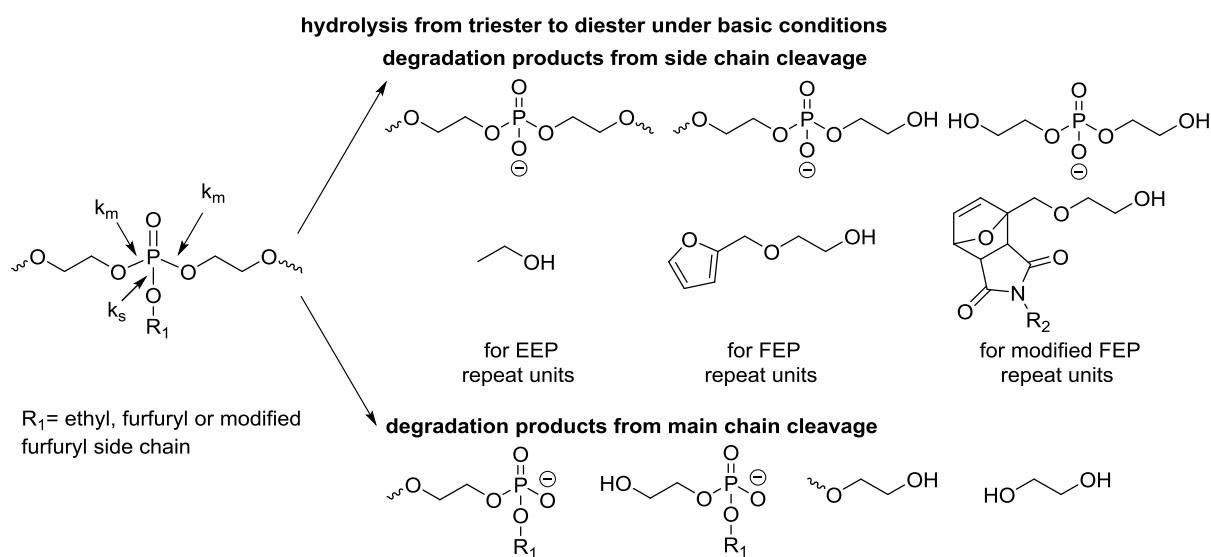
The degradation of **PEEP** was examined via  $^1\text{H}$  and  $^{31}\text{P}\{\text{H}\}$  NMR kinetics at different pH-values of 4.0, 7.0, and 11.1. The copolymers **PEF5** and several DA-modified copolymers were examined at



**Scheme 4.4.** Hydrolysis of poly(phosphate) under basic conditions and PMEP s under acidic conditions from phosphotri- to -diesters.

pH 11.1 In contrast to PMEPE studied by Penczek, no degradation of **PEEP** (<1% formation of phosphodiester, determined from the  $^{31}\text{P}\{\text{H}\}$  NMR spectra) was observed within 4 months (131 days) for pH's 4.0 and 7.0 under our conditions (Figures S4.31 and S4.32). The observation might be attributed to the facts, that methoxy side chains of **PMEPE** are hydrolytically less stable under acidic conditions than ethoxy side chains of **PEEP**, due to less steric hindrance of the attack of  $\alpha$ -carbon or because the hydrolysis experiments of Penczek's lab were conducted at higher temperature (45°C) and different conditions (the pH was kept constant by automatic addition of NaOH-solution, which changed the polymer concentration in the experiment continuously). **PMEPE** degradation with the conditions used for **PEEP** should be conducted in the future.

For the degradation of **PEEP** at pH 11.1 a 0.2 M bicarbonate-NaOH-buffer was chosen. The buffer capacity was high enough for a possible full degradation of the polymer to phosphoric acid, ethylene glycol, and ethanol, but keeping the pH constant. Under basic conditions, the cleavage of the phosphotriesters to the respective diesters can occur, resulting in different degradation products, as either the pendant chain or the polymer backbone can be hydrolyzed. The expected degradation products are shown in Scheme 4.5. A further hydrolysis of the phosphodiester to the monoesters or phosphate is unlikely under basic conditions, but eventually may occur over prolonged exposition to basic conditions.<sup>52</sup> The resulting phosphodiester anion, i.e. with a negative charge, is unlikely to be attacked by additional nucleophiles and happens only very slowly. In previous studies of trimethyl phosphate as model compound, the first hydrolysis step was up to several magnitudes times faster than the second hydrolysis to the monoester, both at basic pH.<sup>54, 59</sup> The combination of  $^1\text{H}$  and  $^{31}\text{P}$  NMR is a sensitive tool to study the different degradation pathways and products in detail. For that, a partially deuterated buffer was prepared and the degradation was conducted directly in the NMR tube over a period of several weeks.  $^{31}\text{P}$  NMR spectra detected the degradation from the phosphotriesters with a chemical shift of -1.25 ppm to the phosphodiester



**Scheme 4.5.** Possible degradation products after hydrolysis of the phosphotri- to -diester.

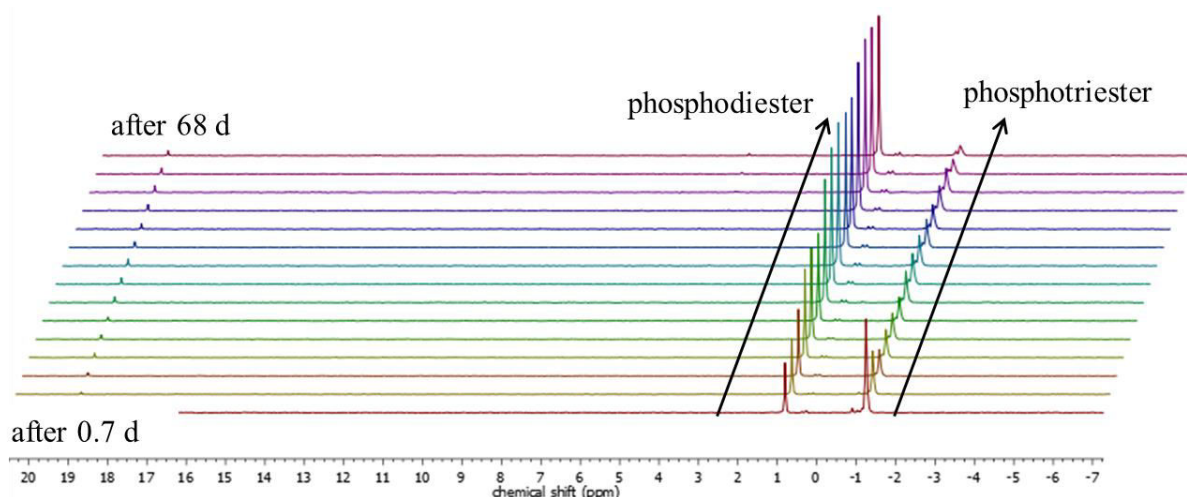


**Figure 4.6.**  $^{31}\text{P}\{\text{H}\}$  NMR spectra (121MHz,  $\text{H}_2\text{O}/\text{D}_2\text{O}$ , 298K) of the degradation of PEEP at pH 11.1.

with a resonance at 0.80 ppm (Figure 4.6). Under these conditions, no signals for the phosphomonoester (4-5 ppm)<sup>60-61</sup> or phosphate (ca. 6 ppm)<sup>60-61</sup> were observed over a period of up to 68 days. 50% of triesters had been degraded after 65.6 h and 20% remained after 68 days (Figures 4.6 and 4.7a, and Table 4.4).  $^{31}\text{P}\{\text{H}\}$  NMR spectra did not allow further examination of hydrolysis by side or main chain cleavage due to overlapping resonances for both possible diester structures. From the  $^1\text{H}$  NMR spectra, however, the backbone and side-chain hydrolysis can be distinguished (Figure 4.8). The resonance of the methyl group of the ethoxy side chain of the starting **PEEP** was detected as a triplet at 1.34 ppm. This signal decreased during the hydrolysis process and two new triplet signals were detectable, corresponding to the methyl group of the resulting phosphodiester after main chain cleavage (at 1.23 ppm) and to the methyl group of ethanol (at 1.15 ppm) after side chain cleavage of **PEEP**. 79 % phosphodiesters were detected in  $^1\text{H}$  NMR spectra after 68 days, which is in good agreement with the results obtained from  $^{31}\text{P}\{\text{H}\}$  NMR spectra. Penczek and coworkers reported a statistical cleavage of the three phosphoester bonds under alkaline conditions for **PMEP** under similar, but not identical conditions,<sup>52</sup> however, under these conditions from the **PEEP** degradation, 94% of the hydrolysis occurred in the main chain, while only 6 % in the side chain ester bonds after 68 days ( $n_{\text{side}}/n_{\text{main}}=0.068$ , Table 4.4). The degradation of triesters followed an exponential function with two reaction rate constants, i.e. no statistical cleavage, for the degradation of the main or the side chain respectively (exemplarily shown for the phosphorus signals of **PEEP** in Figure 4.7b). The degradation rates are currently under further investigation (*see outlook*). However, hydrolysis of the ester bonds in the main chain is favorable for polymer degradation, as it reduces molecular weight and does not produce polyanions, as a major side chain hydrolysis would, which might alter further degradation in applications.

**PEF5** showed a similar degradation profile at pH 11.1 under the same conditions as **PEEP** (Figures 4.7c and S4.33a).  $^{31}\text{P}\{\text{H}\}$  NMR spectra revealed the cleavage of 50% triesters after 90.3 h

and 79% after 68 days. Analysis of  $^1\text{H}$  NMR spectra resulted in a hydrolysis ratio between side and main chains of  $n_{\text{side}}/n_{\text{main}}=0.055$ . The results only consider the cleavage of ester bonds in **EEP** repeat units. Distinct signals of the **FEP** repeat unit, which might be useful to follow their degradation, overlaid with resonances of the backbone and of degradation products.

The degradation profiles of post-modified polymers were analyzed by the same method and samples of modifications with the different maleimide derivatives were considered (**PEF5-H**, **PEF5-OH**, **PEF10-COOH**, **PEF5-NH<sub>3</sub>Cl**; for all results see Table 4.4). Samples modified with **Mal-Bn** and **Mal-Et** were not considered due to low solubility under the conditions of the degradation experiment, samples modified with **Mal-Zwitter** due to arising of undefined phosphorus signals. All modified polymers showed a similar degradation profile, following an exponential decrease of phosphotriesters (Figures 4.7c and S4.33b-e). The ratios between side chain and main chain cleavage ( $n_{\text{side}}/n_{\text{main}}$ ) of the modified polymers were between 0.072 and 0.087, similar to **PEEP**. The hydrolysis kinetics significantly differed for modified: **PEF5-H** and **PEF5-OH** showed 50% degradation of triesters within 5-6 days, **PEF10-COOH** and **PEF5-NH<sub>3</sub>Cl** after 18-46 days, all

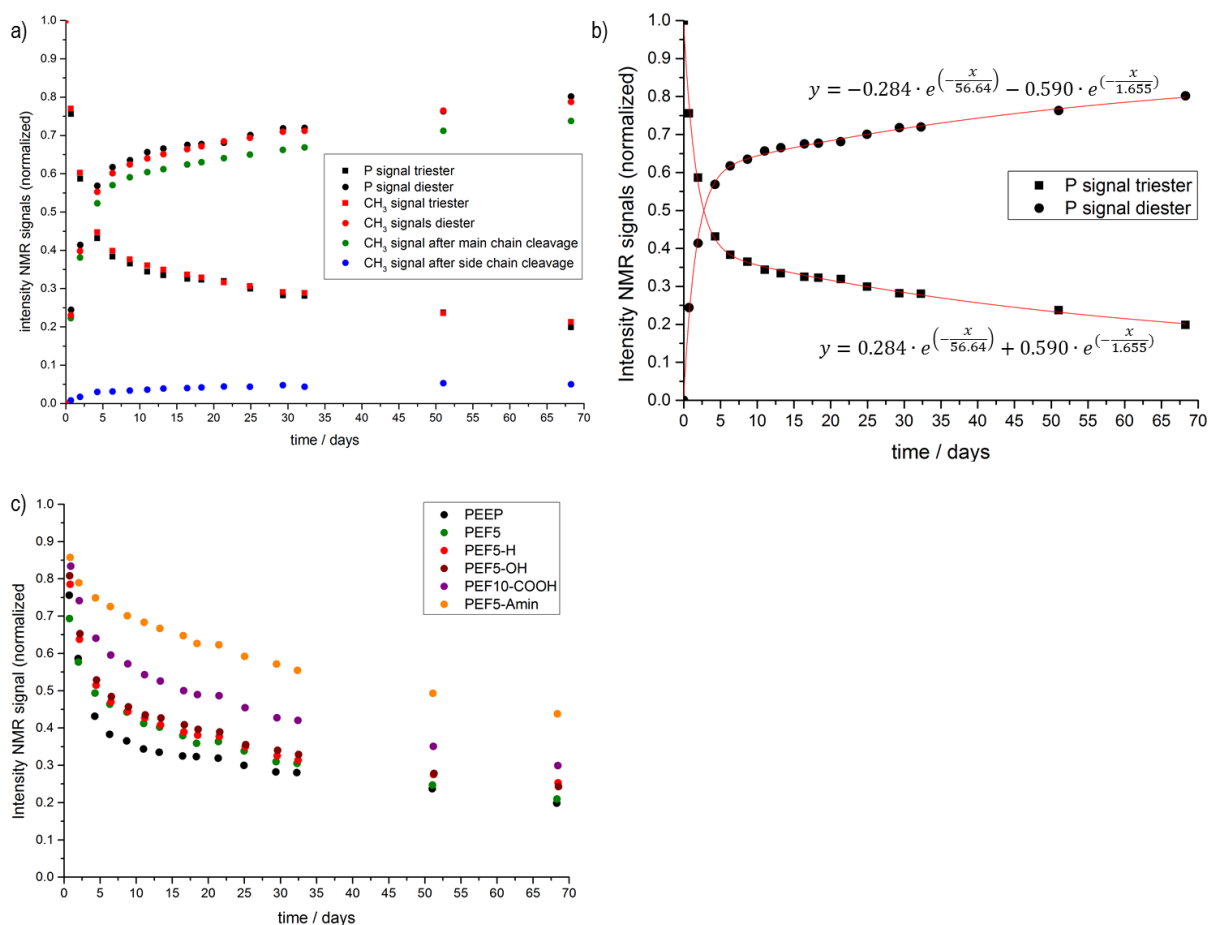


**Figure 4.7.** Degradation studies: a) intensity of the  $^1\text{H}$  and  $^{31}\text{P}\{\text{H}\}$  NMR signals (normalized) vs degradation time, showing the decrease of phosphotriester and increase of -diester in **PEEP** at pH11.1 and the cleavage of the side and main chains; b) intensity of phosphotriester signals from  $^{31}\text{P}\{\text{H}\}$  NMR spectra of all analyzed polymers.

significantly slower than for **PEEP**. Slower degradation rates might be associated to different solubility and in the case of **PEF10-COOH** and **PEF5-NH<sub>3</sub>Cl** due to charged groups in the side chains, which need to be further investigated.

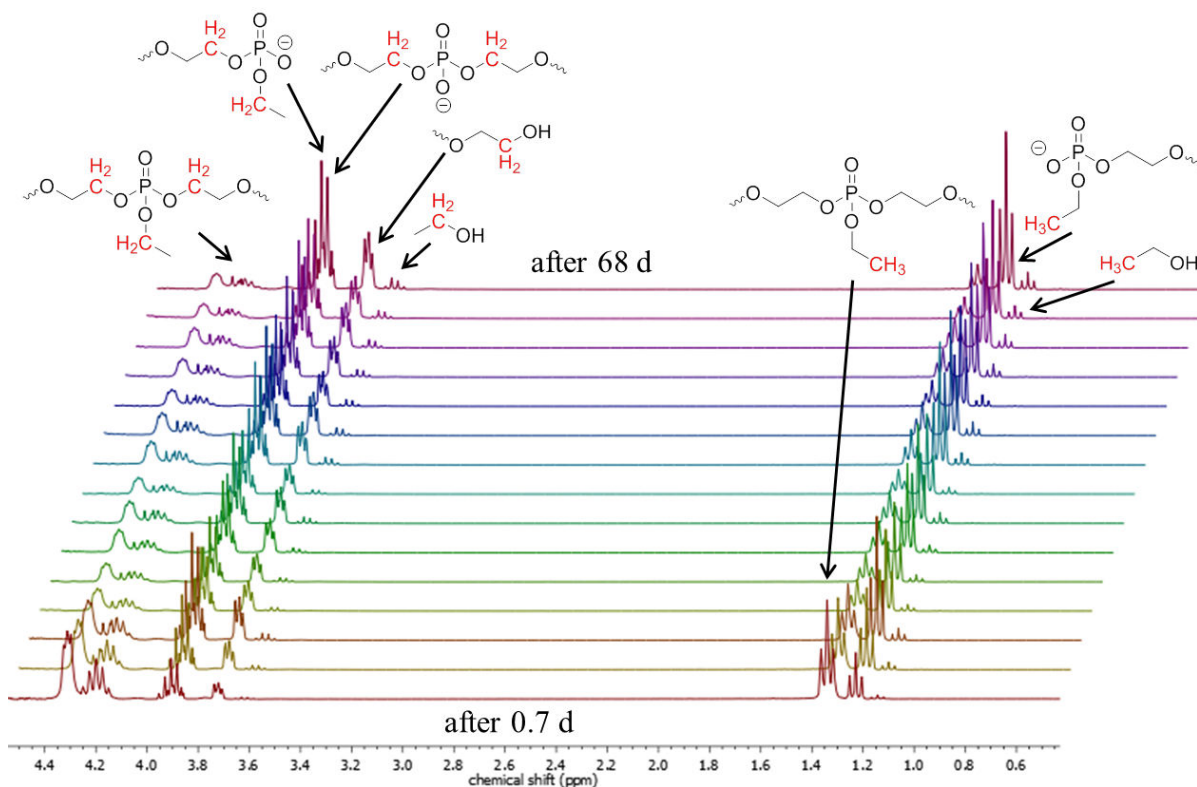


**Figure 4.8.** <sup>1</sup>H NMR spectra (300MHz, H<sub>2</sub>O/D<sub>2</sub>O, 298K) of the degradation of **PEEP** at pH 11.1.

**Table 4.4.** Overview of results from degradation studies at pH 11.1.

sample	intensity of <sup>31</sup> P signals after 68 d / %		intensity of <sup>1</sup> H signals after 68 d / %				ratio side chain / main chain cleavage (n <sub>side</sub> /n <sub>main</sub> )	t <sub>1/2</sub> / h <sup>a</sup>	k <sub>1</sub> / s <sup>-1 b</sup>	k <sub>2</sub> / s <sup>-1 b</sup>
	triester / -1.25 ppm	diester / 0.80 ppm	triester / 1.34 ppm	diester / 1.15 & 1.23 ppm	main chain cleavage / 1.23 ppm	side chain cleavage / 1.15 ppm				
PEEP	20	80	21	79	74	5	0.068	65.6	2.04·10 <sup>-7</sup>	6.99·10 <sup>-6</sup>
PEF5	21	79	23	77	73	4	0.055	90.3	4.25·10 <sup>-7</sup>	1.52·10 <sup>-5</sup>
PEF5-H	25	75	25	75	69	6	0.087	118.4	4.31·10 <sup>-7</sup>	7.27·10 <sup>-6</sup>
PEF5-OH	24	76	26	74	69	5	0.072	136.6	4.29·10 <sup>-7</sup>	1.52·10 <sup>-5</sup>
PEF10-COOH	30	70	31	69	64	5	0.078	422.5	2.76·10 <sup>-7</sup>	6.34·10 <sup>-6</sup>
PEF5-NH <sub>3</sub> Cl	44	56	43	57	52	4	0.077	1115.2	2.74·10 <sup>-7</sup>	1.28·10 <sup>-5</sup>

<sup>a</sup> Determined from exponential fits from <sup>31</sup>P NMR signals of triesters at 50% degradation. <sup>b</sup> Determined from exponential fits from <sup>31</sup>P NMR signals

## 4.5 Conclusions

The versatile furan functionality was combined with poly(phosphoester)s (PPEs) for the first time. Furan derivatives undergo thermoreversible Diels-Alder reaction with maleimides. While PPEs are biocompatible and biodegradable and DA adducts are thermodegradable, furfuryl-containing PPEs are interesting materials for thermoresponsive applications.

Copolymers of EEP/MEP and FEP (up to 25mol%) were synthesized by anionic co-ROP with molecular weights up to 40,000 g/mol and a gradient like copolymer structure, confirmed by real-time NMR kinetic measurements. Functionalization of furan groups with aliphatic, aromatic, polar or charged maleimide derivatives by DA reaction changes the solubility and thermal behavior of copolymers and allows adjustment of cloud point temperatures of the “precursor polymers”. Cationic, anionic, and zwitterionic PPE-polyelectrolytes were obtained, which pH-dependently differ their solubility in water. Kinetic studies confirmed thermodegradation of the DA adduct at higher temperatures, while the biodegradable backbone remained unaffected.

This combination of synthetic platforms (PPE and Diels-Alder-chemistry) may allow the development of reversible gels and novel drug carriers.

Furthermore, the degradation behavior of PEEP, furfuryl-containing copolymers, and DA-modified copolymers was investigated at different pH's and compared. PEEP was stable at neutral and acidic conditions (pH 4 and pH 7) over the measured range of time (68 days); degradation of all polymers under basic conditions at pH 11.1 occurred from phosphotri- to -diesters. The formation of phosphomonoesters or phosphate was not observed under the chosen conditions. 50% degradation of triesters occurred between 66 h and 46 days. Contrary to Penzcek and coworkers<sup>52</sup>, a statistical cleavage of ester bonds in the side and main chain was not observed under basic conditions and degradation took predominantly place in the backbone of the polymer.

This finding is important and favorable for the use of PPEs for biomedical applications, when degradation of the material is desired.

## 4.6 Outlook

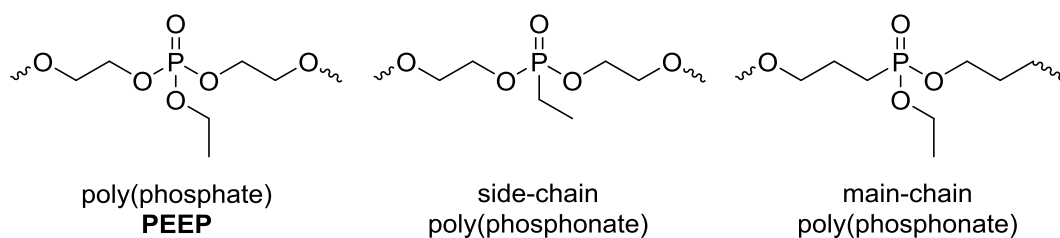
The degradation studies give insight into the hydrolysis of PPEs under alkaline conditions and need further investigations. So far it remains unclear why cleavage of the triesters is not statistical under the chosen conditions.

The degradation of triesters follows an exponential function with two different rate constants, which might be the constants for main or side chain cleavage ( $k_s$  and  $k_m$ ). However, appearance of the proton signals of  $\text{CH}_3$  groups corresponding to ethanol or the degradation product in the case of main chain cleavage follows an exponential function with two rate constants in both cases as well. We expected just one rate constant for each fit equal to the constants from the triester decrease. So far it remains unclear, if the formation of the signals also involves two different simultaneous reactions. Transesterification reactions of the degradation products might need to be taken into account. Furthermore, the formed ethanol might be involved in the hydrolysis of the triester bonds as an ethoxide.

For copolymers, investigation on the influence of different side chains on the probability of side chain or main chain cleavage has not been reported so far and is a further interesting aspect to consider.

The degradation profile of copolymers modified with charged groups is significantly lower and a reasonable explanation has not been found so far, which needs further investigation. Furthermore, the degradation profile of zwitterionic modified copolymers would be attractive. The  $^{31}\text{P}\{\text{H}\}$  NMR spectrum of the polymer shows two further signals at 0.07 and -0.16 ppm (ca. 30% intensity). The nature of these phosphorus species is not clarified yet:  $^{31}\text{P}\{\text{H}\}$  DOSY indicates the presence of them within the polymer,  $^1\text{H}$ - $^{31}\text{P}$ -HMBC the association to DA modified repeat units. They are also observed in spectra of the amino modified polymer with a much lower intensity of ca. 5%, but are not present in the other DA modified polymers. The issue needs to be elucidated.

The comparison of the degradation profile from **PEEP** to profiles of corresponding side-chain and main-chain poly(phosphonates) (Scheme 4.6) will give insight in the possibility to alter degradation times and is under current investigation in the research group.



**Scheme 4.6.** Chemical structures of poly(phosphate) PEEP, side- and main-chain poly(phosphonate)s.

## 4.7 Acknowledgements

The authors thank Prof. Dr. Katharina Landfester (MPIP) for her support. G.B. is recipient of a fellowship through funding of the Excellence Initiative (DFG/GSC 266) in the context of the graduate school of excellence "MAINZ" (Material Sciences in Mainz). F.R.W. thanks the Deutsche Forschungsgemeinschaft (DFG, WU750/6-1) for support.

## 4.8 Supporting Information

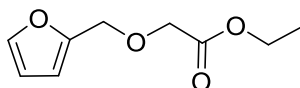
The Supporting Information contains additional synthetic procedures, characterization data for monomers, unmodified, and modified polymers, turbidity measurements and retro-Diels Alder.

### Content

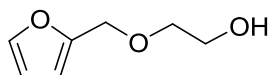
- 4.8.1 Synthetic procedures
- 4.8.2 NMR spectra
- 4.8.3 IR spectra
- 4.8.4 SEC curves
- 4.8.5 DSC thermograms
- 4.8.6 Turbidity measurements
- 4.8.7 Retro Diels-Alder reaction
- 4.8.8 Degradation studies

### 4.8.1 Synthetic procedures

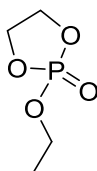
*Ethyl-2-(furan-2-ylmethoxy)acetate*: The acetate was synthesized according to literature.<sup>45</sup> Briefly, furfuryl alcohol (25.00 g, 254.8 mmol, 1 eq.) was dissolved in 200 mL dry THF in a flame-dried round-bottom flask under argon-atmosphere. Sodium hydride (7.34 g, 305.8 mmol, 1.2 eq.) were added and the reaction was refluxed for 1 h. Bromoacetate (46.81 g, 280.3 mmol, 1.1 eq.) was added and refluxed overnight. Then, water was slowly added. The aqueous phase was extracted with ethyl acetate twice and the organic phase with brine once. The organic phase was dried with  $\text{MgSO}_4$  and concentrated. Column chromatography (silica gel, dichloromethane/ethyl acetate 98:2,  $R_f=0.94$ ) gave the pure product. Yield: 75%.  $^1\text{H}$  NMR (300 MHz,  $\text{CDCl}_3$ ):  $\delta$  [ppm] 7.42 (s, 1H, -O-CH=CH-), 6.36 (m, 2H, -O-CH=CH-CH=), 4.54 (s, 2H, O-C(=CH)-CH<sub>2</sub>-O-), 4.21 (q, 2H, -O-CH<sub>2</sub>-CH<sub>3</sub>), 4.08 (t, 2H, -O-CH<sub>2</sub>-C(=O)-O-), 1.28 (t, 3H, -CH<sub>3</sub>).



*2-(furan-2-ylmethoxy)ethan-1-ol*: The alcohol was synthesized according to literature.<sup>45</sup> Briefly, lithium aluminium hydride (2.4 M in THF, 47.79 mL, 114.7 mmol, 0.6 eq.) was dissolved in 100L dry diethyl ether in a flame-dried 3-necked round-bottom flask. Ethyl 2-(furan-2-ylmethoxy)acetate (35.21 g, 191.2 mmol, 1 eq.) in 50 mL dry diethyl ether was added dropwisely in the way that the reaction gently refluxed. It was stirred overnight at room temperature and then water was slowly added. The aqueous phase was extracted with diethyl ether twice and the organic phase with brine once. The organic phase was dried with MgSO<sub>4</sub> and concentrated. Column chromatography (silica gel, dichloromethane/acetone 19:1, R<sub>f</sub>=0.42) gave the pure product. Yield: 36%. <sup>1</sup>H NMR (300 MHz, CDCl<sub>3</sub>): δ [ppm] 7.40 (s, 1H, -O-CH=CH-), 6.32 (m, 2H, -O-CH=CH-CH=), 4.49 (s, 2H, O-C(=CH)-CH<sub>2</sub>-O-), 3.73 (m, 2H, .O-CH<sub>2</sub>-CH<sub>2</sub>-OH ), 3.59 (m, 2H, .O-CH<sub>2</sub>-CH<sub>2</sub>-OH ), 2.31 (s, 1H, -OH).

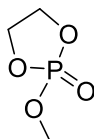


*2-ethoxy-2-oxo-1,3,2-dioxaphospholane (EEP, 2)*: The monomer was synthesized according to literature.<sup>62</sup> Briefly, a flame-dried 500mL three-neck flask, equipped with a dropping funnel, was charged with 2-chloro-2-oxo-1,3,2-dioxaphospholane (50.00 g, 0.35 mol) dissolved in dry THF (100 mL). A solution of dry ethanol (16.17 g, 0.35 mol) and dry triethylamine (35.51 g, 0.35 mol) in dry THF (70 mL) was added dropwise to the stirring solution of COP at -20 °C under argon atmosphere. During reaction, hydrogen chloride was formed and precipitated as pyridinium hydrochloride. The reaction was stirred at 4 °C overnight. The salt was removed by filtration and the filtrate concentrated in vacuo. The residue was purified by distillation under reduced pressure to give a fraction at 105-110 °C/0.095 mbar, obtaining the clear, colorless, liquid product EEP. Yield: 34.60 g (0.23 mol), 65%. <sup>1</sup>H-NMR (300 MHz, DMSO-d<sub>6</sub>): δ [ppm] 4.47-4.34 (m, 4H, O-CH<sub>2</sub>-CH<sub>2</sub>-O), 4.11-4.04 (m, 2H, O-CH<sub>2</sub>-CH<sub>3</sub>), 1.25 (t, 3H, O-CH<sub>2</sub>-CH<sub>3</sub>). <sup>13</sup>C{H}-NMR (76 MHz, DMSO-d<sub>6</sub>): δ [ppm] 66.35 (-O-CH<sub>2</sub>-CH<sub>2</sub>-O-), 64.18 (-O-CH<sub>2</sub>-CH<sub>3</sub>), 15.96 (-O-CH<sub>2</sub>-CH<sub>3</sub>). <sup>31</sup>P{H}NMR (202 MHz, DMSO-d<sub>6</sub>): δ [ppm] 16.83.

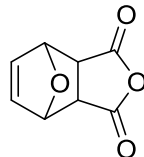


*2-Methoxy-2-oxo-1,3,2-dioxaphospholane (MEP, 3)*: A flame-dried 1000mL three-neck flask, equipped with a dropping funnel, was charged with 2-chloro-2-oxo-1,3,2-dioxaphospholane (50 g, 0.35 mol) dissolved in dry THF (300 mL). A solution of dry methanol (11.24 g, 0.35 mol) and dry pyridine (27.72 g, 0.35 mol) in dry THF (45 mL) was added dropwise to the stirring solution of COP

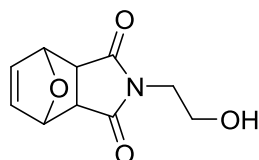
at -20 °C under argon atmosphere. During reaction, hydrogen chloride was formed and precipitated as pyridinium hydrochloride. The reaction was stirred at 4 °C overnight. The salt was removed by filtration and the filtrate concentrated *in vacuo*. The residue was purified by distillation under reduced pressure to give a fraction at 89-97 °C/0.001 mbar, obtaining the clear, colorless, liquid product. Yield: 25.54 g, 53%. <sup>1</sup>H-NMR (500 MHz, DMSO-d<sub>6</sub>): δ [ppm] 4.43 (m, 4H, O-CH<sub>2</sub>-CH<sub>2</sub>-O), 3.71 (d, 3H, O-CH<sub>3</sub>). <sup>13</sup>C-NMR (126 MHz, DMSO-d<sub>6</sub>): δ [ppm] 66.57 (s, 2C, O-CH<sub>2</sub>-CH<sub>2</sub>-O), 54.72 (s, 1C, O-CH<sub>3</sub>). <sup>31</sup>P-NMR (202 MHz, DMSO-d<sub>6</sub>): δ [ppm] 17.89.



*7-Oxabicyclo[2.2.1]hept-2-ene-5,6-dicarboxylic acid anhydride*: The compound was synthesized according to literature<sup>63</sup>. Maleic anhydride (20.00 g, 104 mmol, 1 eq.) and furan (20.83 g, 306 mmol, 1.5 eq.) were suspended in 250 mL toluene, heated to 80 °C and stirred overnight. The reaction was cooled down, and stored in the fridge, where the product precipitates from solution. The reaction was filtered and dried *in vacuo* to give the pure product, colourless crystals. Yield: 17.90 g 53%. <sup>1</sup>H NMR (300 MHz, CDCl<sub>3</sub>): δ [ppm] 6.58 (s, 2H, -CH=CH-), 5.46 (s, 2H, =CH-CH(-O)-CH-), 3.18. (s, 2H, -CH-CH(-C-)-C=O).

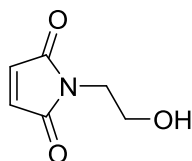


*N-(2-Hydroxyethyl)-7-oxabicyclo[2.2.1]hept-2-ene-5,6-dicarboimide*<sup>63</sup>: 7-Oxabicyclo[2.2.1]hept-2-ene-5,6-dicarboxylic acid anhydride (17.90 g, 108 mmol, 1 eq.) was suspended in 300 mL methanol and cooled to 0 °C. Ethanolamine was dissolved in 60 mL methanol and added dropwisely. It was stirred for 1h and room temperature and under reflux overnight. The solvent was removed and the crude residue recrystallized from ethanol to give the pure product, colourless crystals. Yield: 9.86 g, 44%. <sup>1</sup>H NMR (300 MHz, DMSO-d<sub>6</sub>): δ [ppm] 6.55 (s, 2H, -CH=CH-), 5.12 (s, 2H, =CH-CH(-O)-CH-), 4.79 (s, 1H, -OH), 3.41 (m, 4H, -N-CH<sub>2</sub>-CH<sub>2</sub>-OH), 2.92 (s, 2H, -CH-CH(-C-)-C=O).

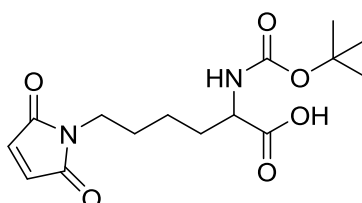


*N-(2-hydroxyethyl)maleimide*<sup>63</sup> (**IV**, -OH): *N*-(2-Hydroxyethyl)-7-oxabicyclo[2.2.1]hept-2-ene-5,6-dicarboimide was suspended in 200 mL toluene and refluxed overnight. The solvent was removed and the crude product recrystallized from hot toluene to give the pure product, colourless

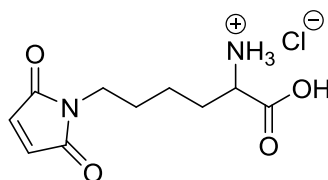
crystals. Yield: 4.40 g, 45%.  $^1\text{H NMR}$  (300 MHz,  $\text{CDCl}_3$ ):  $\delta$  [ppm] 6.74 (s, 2H,  $-\text{CH}=\text{CH}-$ ), 3.81-3.71 (m, 4H,  $-\text{N}-\text{CH}_2-\text{CH}_2-\text{OH}$ ), 1.94 (s, 1H,  $-\text{OH}$ ).



*N- $\epsilon$ -maleimido- $\alpha$ -boc-L-lysine*: The compound synthesized according to literature<sup>64</sup>. N-Boc-lysine (3.18 g, 12.9 mmol, 1 eq.) was dissolved in 90 mL saturated  $\text{NaHCO}_3$ -solution. N-methoxycarbonylmaleimide (2.00 g, 12.9 mmol, 1 eq.) was added at 0 °C and stirred overnight at room temperature. The reaction was acidified with conc.  $\text{H}_2\text{SO}_4$  to pH 3. The aqueous phase was extracted with ethyl acetate three times and the organic phase washed with brine once. The organic phase was concentrated. Column chromatography (silica gel, DCM/methanol 10:1,  $R_f=0.73$ ) gave the pure product. Yield: 3.53 g, 84%.  $^1\text{H NMR}$  (300 MHz,  $\text{CDCl}_3$ ):  $\delta$  [ppm] 6.35 (q, 2H,  $-\text{CH}=\text{CH}-$ ), 5.28 (s, 1H,  $-\text{CH}-\text{NH}-\text{C}(=\text{O})-\text{O}-$ ), 4.28 (s, 1H,  $-\text{CH}_2-\text{CH}(\text{NH})-\text{C}(=\text{O})$ ), 3.53-3.43 (m, 2H,  $\text{N}-\text{CH}_2-(\text{CH}_2)_3-$ ), 2.17-1.62 (m, 6H,  $\text{N}-\text{CH}_2-(\text{CH}_2)_3-$ ), 1.44 (s, 9H,  $\text{C}-(\text{CH}_3)_3$ ).

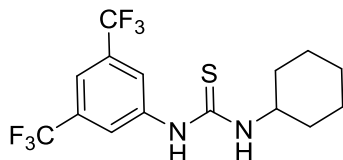


*N- $\epsilon$ -Maleimido-L-Lysine hydrochlorid*<sup>64</sup>: N- $\epsilon$ -Maleimido- $\alpha$ -Boc-L-Lysine (3.53 g, 10.8 mmol) was dissolved in 10 mL DCM and 5 mL 4M HCl-solution in dioxane added. It was stirred at room temperature. The product started to precipitate after ca. 30 min. After 2 h, the supernatant was decanted. The residue was dissolved in ethanol and precipitated from hexane, to give the product. Yield: 1.66 g, 68%.  $^1\text{H NMR}$  (300 MHz,  $\text{DMSO}-d_6$ ):  $\delta$  [ppm] 9.46 (s, 1H,  $-\text{COOH}$ ), 8.41 (s, 3H,  $-\text{NH}_3\text{Cl}$ ), 6.53-6.23 (dd, 2H,  $-\text{CH}=\text{CH}-$ ), 3.86 (s, 1H,  $-\text{CH}_2-\text{CH}(\text{NH}_3\text{Cl})-\text{COOH}$ ), 3.18 (m, 2H,  $\text{N}-\text{CH}_2-(\text{CH}_2)_3-$ ), 1.80 (t, 2H,  $\text{CH}_2-\text{CH}(\text{NH}_3\text{Cl})-\text{COOH}$ ), 1.50 (m, 4H,  $\text{N}-\text{CH}_2-\text{CH}_2-\text{CH}_2-\text{CH}_2-\text{CH}(\text{NH}_3\text{Cl})-\text{COOH}$ ).



*N-cyclohexyl-N'-(3,5-bis(trifluoromethyl)phenyl)thiourea (TU)*: TU was synthesized according to the method described previously<sup>65</sup>. Briefly, in a flame-dried 50 mL flask 3,5-bis(trifluoromethyl)phenylisothiocyanat (2.00 g,  $7.4 \cdot 10^{-3}$  mol) was dissolved in 10 mL dry THF under argon atmosphere. Cyclohexylamine (0.73 g,  $7.2 \cdot 10^{-3}$  mol) was added dropwisely at room temperature to the stirring solution. After the reaction mixture was stirred for 5 h, the solvent was

removed *in vacuo*. The colourless residue was recrystallized from boiling chloroform. It was filtered hot and cooled down. Colourless needles precipitated in a yellowish solution. The product, TU, was collected by filtration, washed with cold chloroform and dried *in vacuo*. Yield: 1.77g, 370.36 g/mol, 4.8 mmol, 67%.  $^1\text{H-NMR}$  (300 MHz,  $\text{DMSO-d}_6$ ):  $\delta$  [ppm] 9.84 (s, 1H, Ar-NH-C(=S)-NH-Cy), 8.23 (s, 1H, *p*-Ar-NH), 8.17 (s, 2H, *o*-Ar-NH), 7.72 (s, 1H, Ar-NH-C(=S)-NH-Cy), 4.11 (s, 1H, Ar-NH-C(=S)-NH-(*H*)Cy), 1.94-1.15 (m, 10H, Ar-NH-C(=S)-NH-Cy).



#### 4.8.2 NMR spectra

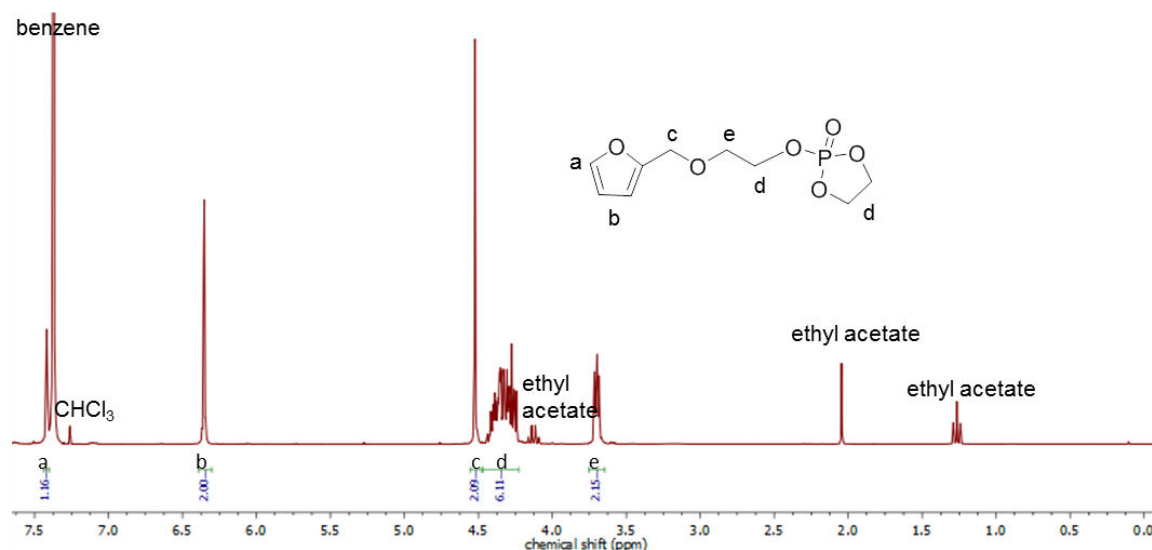


**Figure S4.1.**  $^1\text{H-NMR}$  (500 MHz,  $\text{CDCl}_3$ ) of 2-(2-(furan-2-ylmethoxy)ethoxy)-2-oxo-1,3,2-dioxaphospholane at 298K.

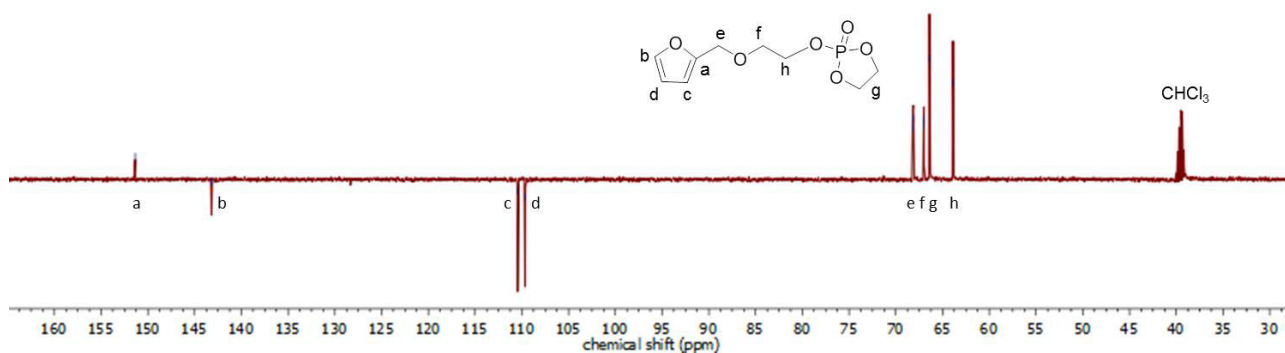


**Figure S4.2.**  $^{13}\text{C-NMR}$  (126 MHz,  $\text{CDCl}_3$ ) of 2-(2-(furan-2-ylmethoxy)ethoxy)-2-oxo-1,3,2-dioxaphospholane at 298K.

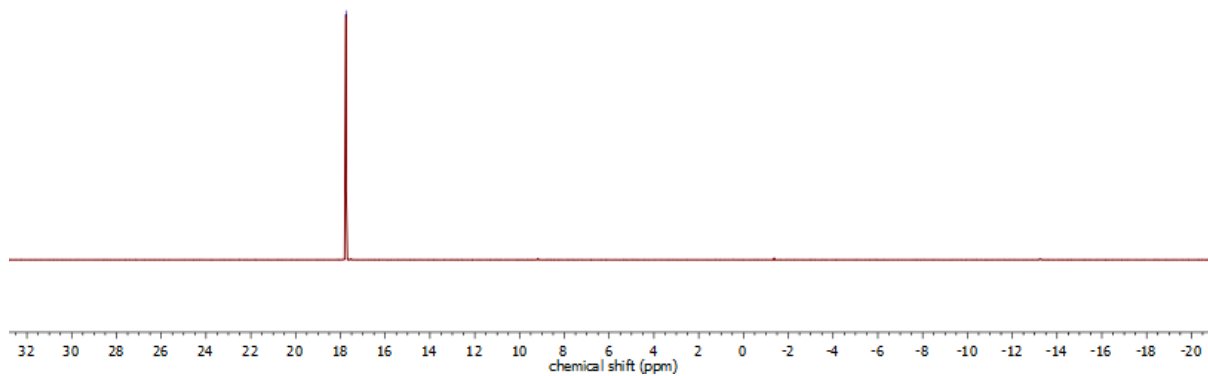


**Figure S4.3.**  $^{31}\text{P}$  {H}NMR (202 MHz,  $\text{CDCl}_3$ ) of 2-(2-(furan-2-ylmethoxy)ethoxy)-2-oxo-1,3,2-dioxaphospholane at 298K.

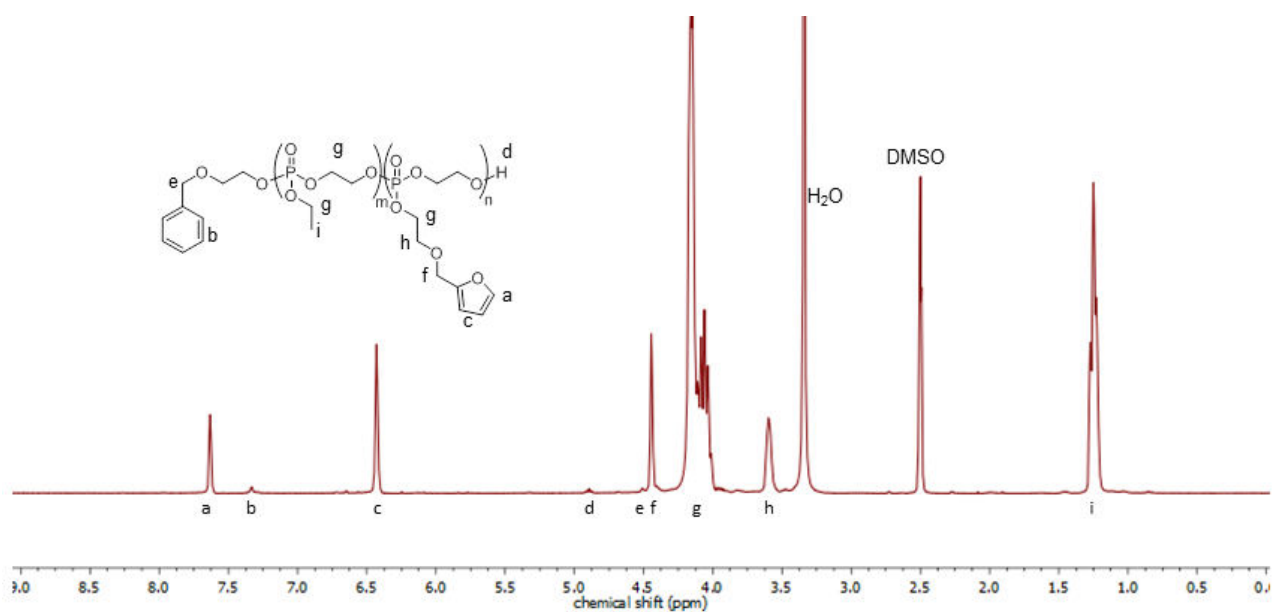


**Figure S4.4.**  $^1\text{H}$  NMR (300 MHz,  $\text{DMSO-d}_6$ ) of PEF25 at 298K.

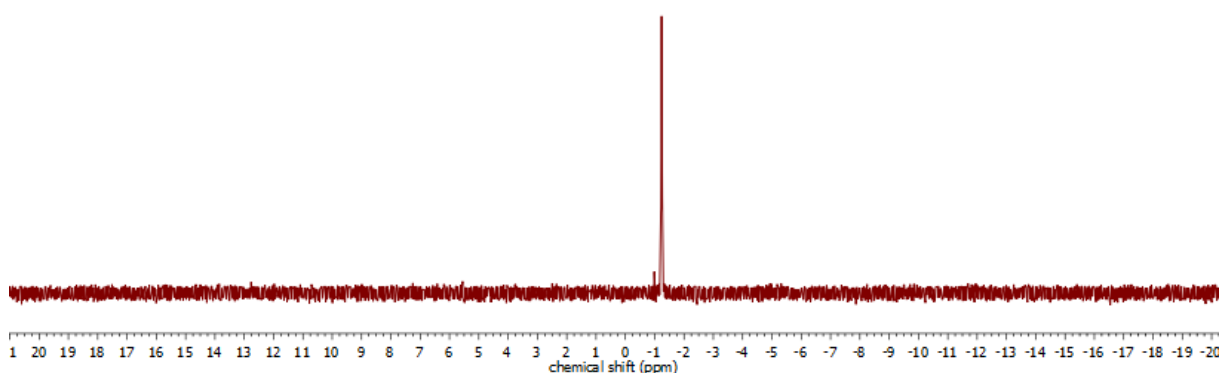


**Figure S4.5.**  $^{31}\text{P}$  {H}NMR (121 MHz,  $\text{DMSO-d}_6$ ) of PEF25 at 298K.

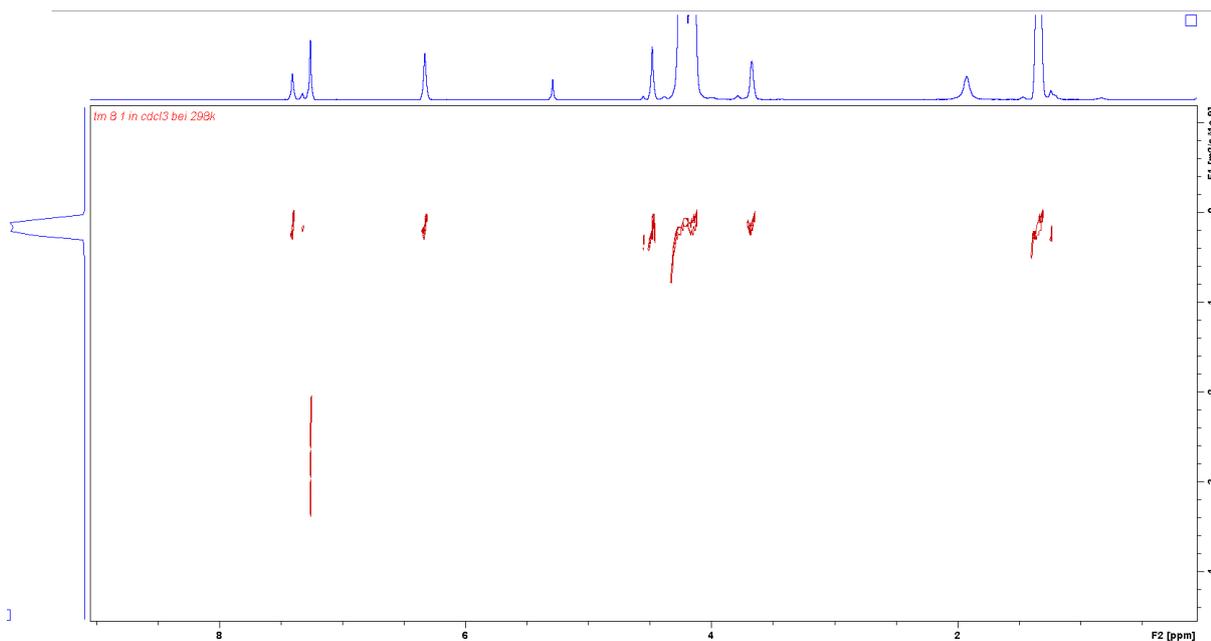


**Figure S4.6.** <sup>1</sup>H-DOSY (500 MHz, CDCl<sub>3</sub>) of PEF10 at 298K.

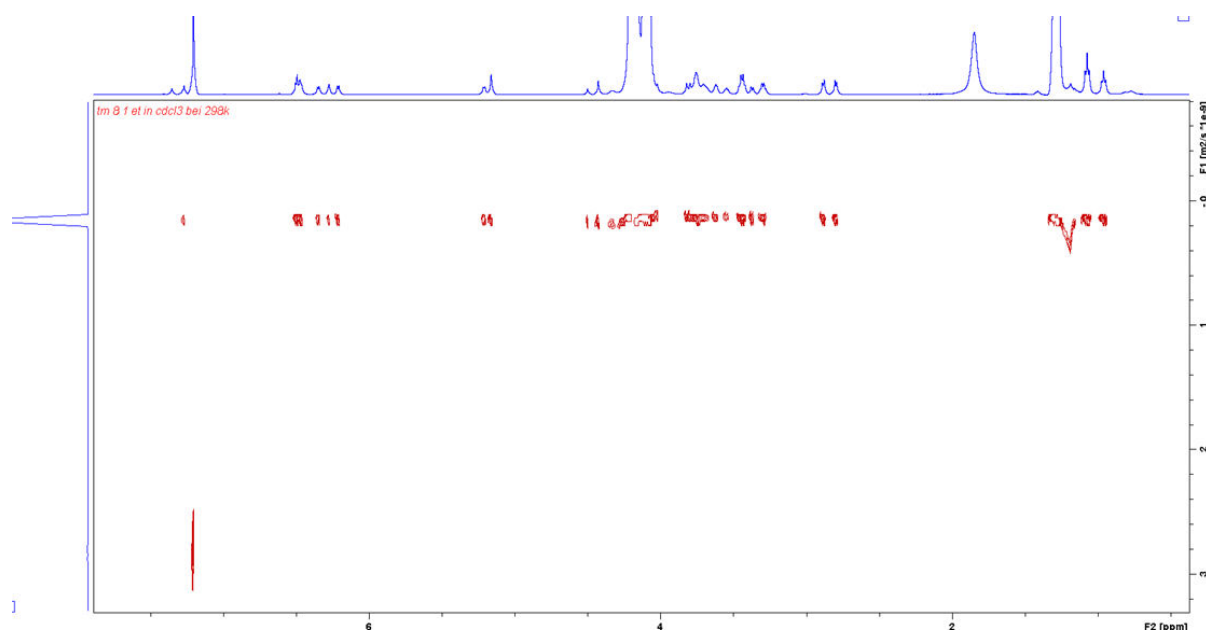


**Figure S4.7.** <sup>1</sup>H-DOSY (500 MHz, CDCl<sub>3</sub>) of PEF10-Et at 298K.

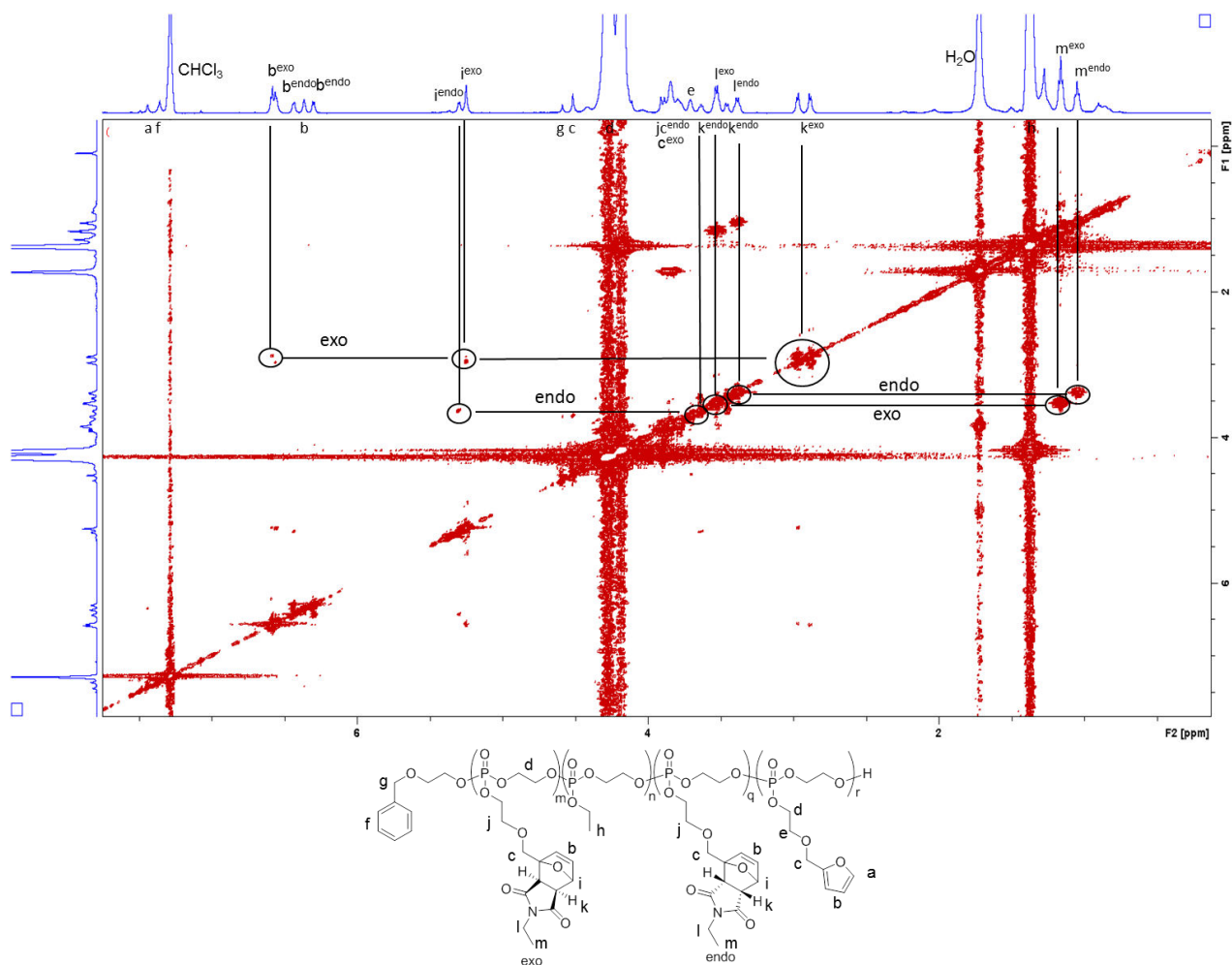


**Figure S4.8.**  $^1\text{H}$ -NOESY (500 MHz,  $\text{CDCl}_3$ ) of PEF10-Et at 298K.

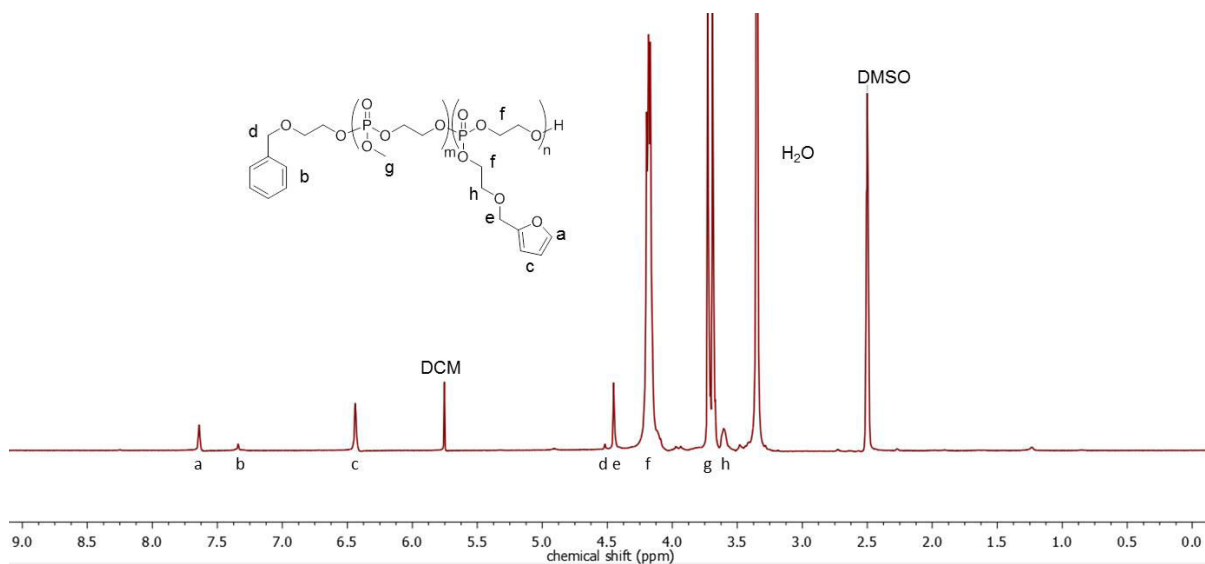


**Figure S4.9.**  $^1\text{H}$  NMR (300 MHz,  $\text{DMSO-d}_6$ ) of PMF10 at 298K.

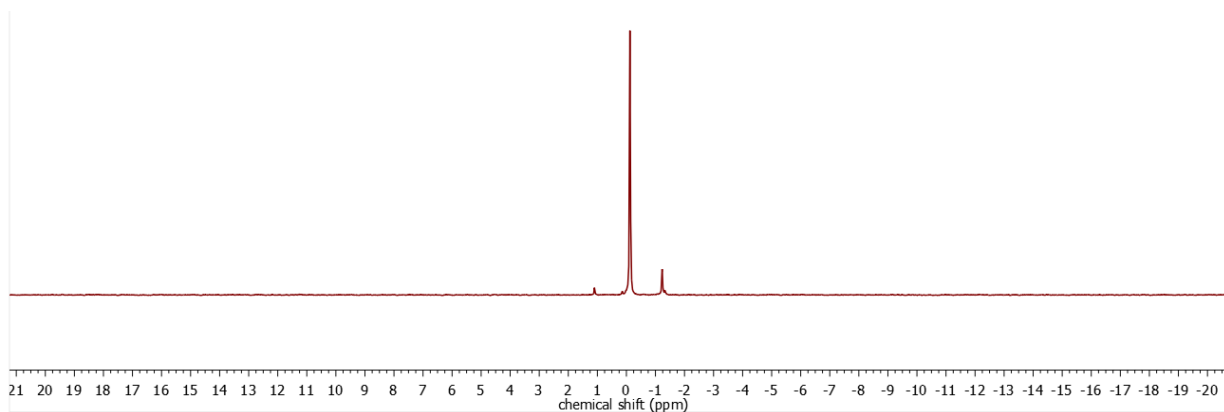


**Figure S4.10.**  $^{31}\text{P}$  { $^1\text{H}$ }NMR (121 MHz, DMSO- $d_6$ ) of PMF10 at 298K.

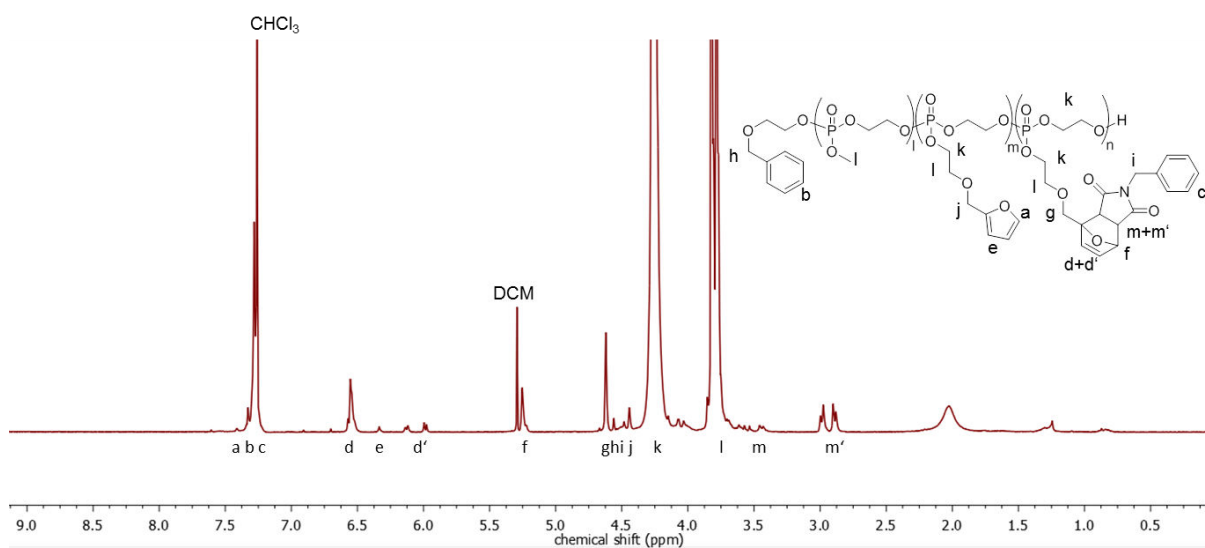


**Figure S4.11:**  $^1\text{H}$  NMR (300 MHz, CDCl<sub>3</sub>) of PMF10-Bn at 298K.

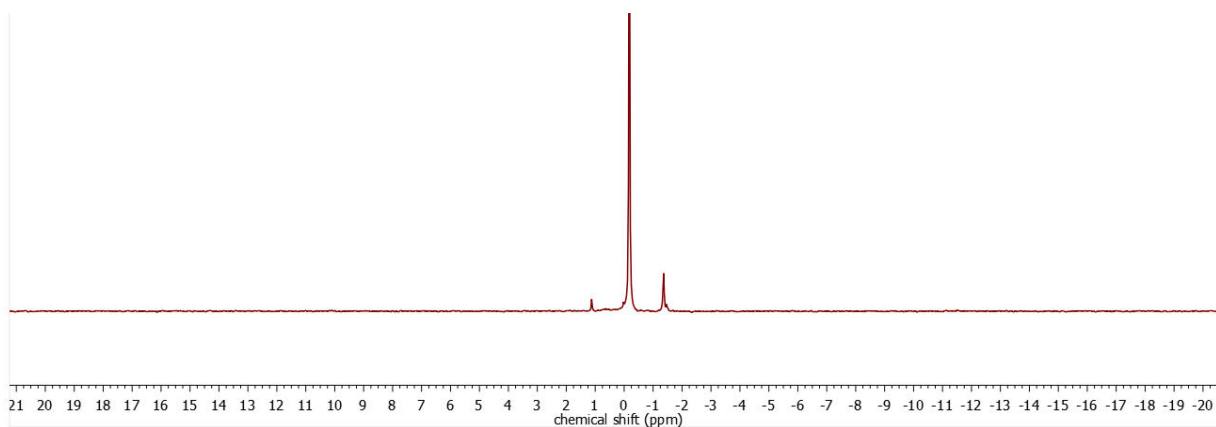


**Figure S4.12.**  $^{31}\text{P}$  NMR (121 MHz, CDCl<sub>3</sub>) of PMF10-Bn at 298K.

### 4.8.3 IR spectra

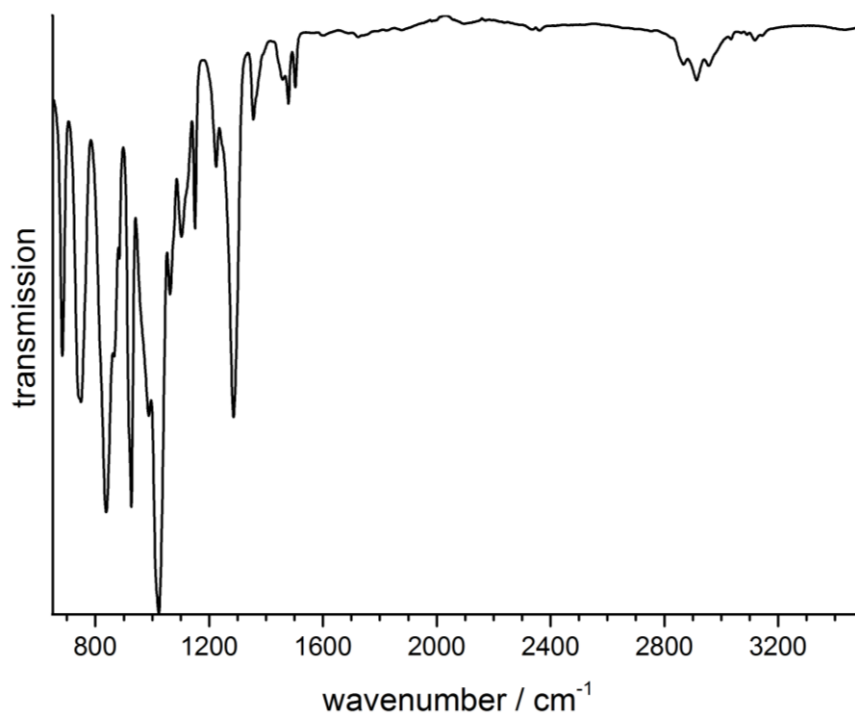


**Figure S4.13.** FTIR spectrum of FEP (2-(2-(furan-2-ylmethoxy)ethoxy)-2-oxo-1,3,2-dioxaphospholane) at 298 K.

### 4.8.4 SEC curves

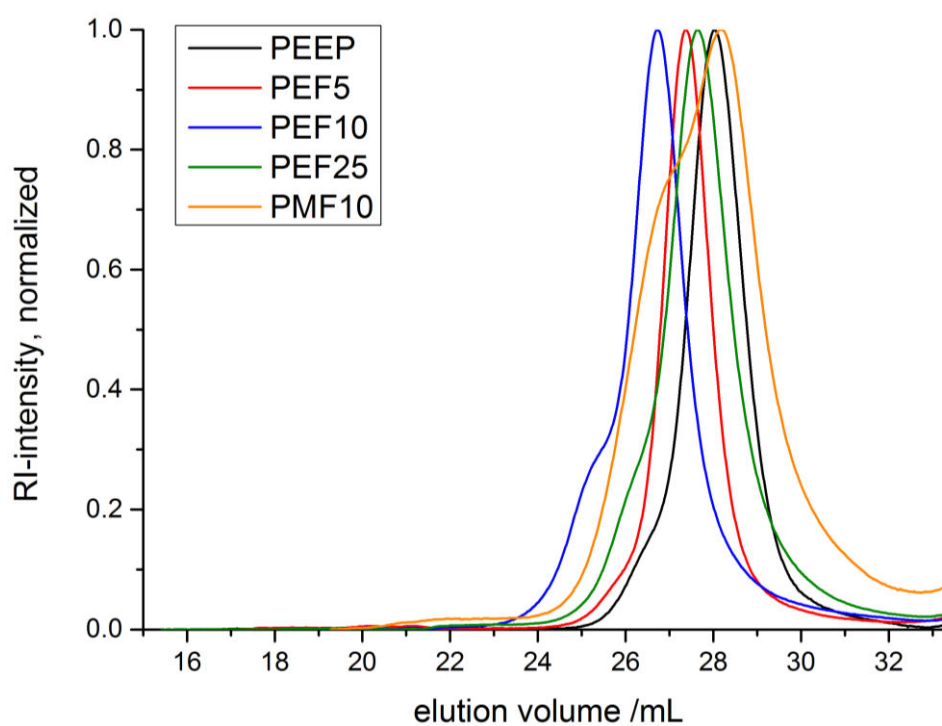


**Figure S4.14.** SEC elugrams of **polymers** in DMF, RI-Signal, PEO standard.

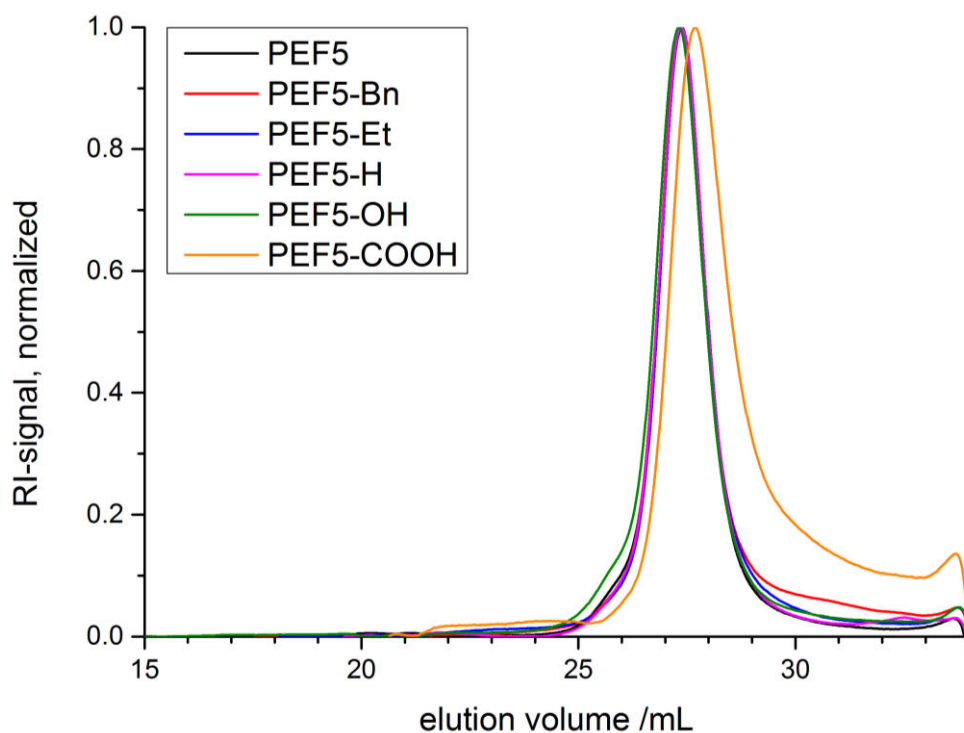


**Figure S4.15.** SEC elugrams of modified **PEF5** in DMF, RI-Signal, PEO standard.

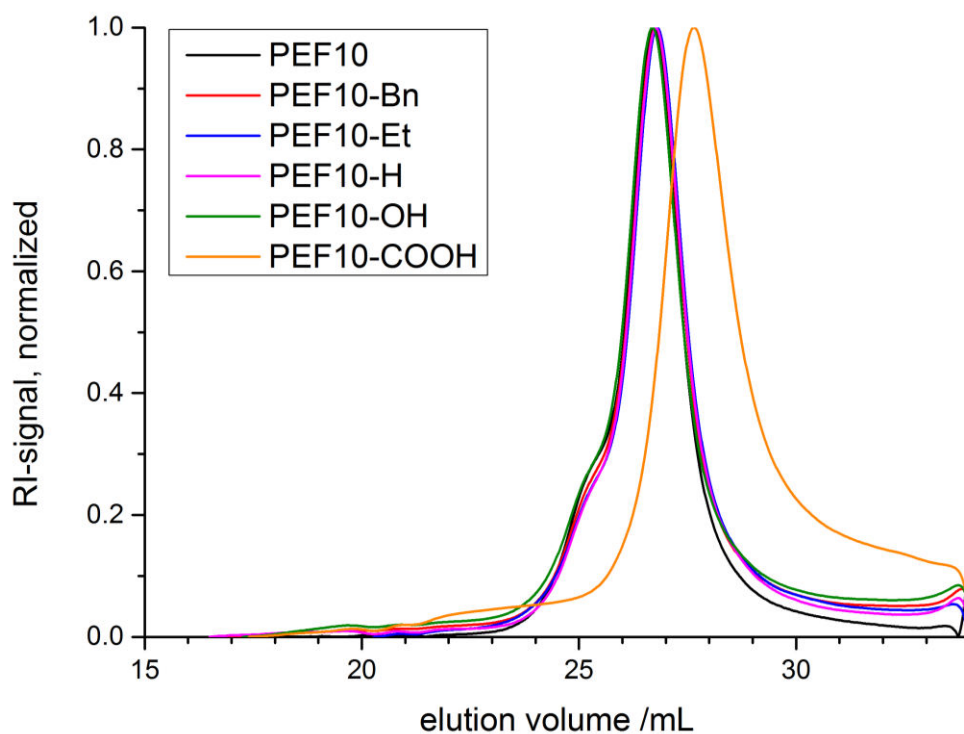


**Figure S4.16.** SEC elugrams of modified **PEF10** in DMF, RI-Signal, PEO standard.

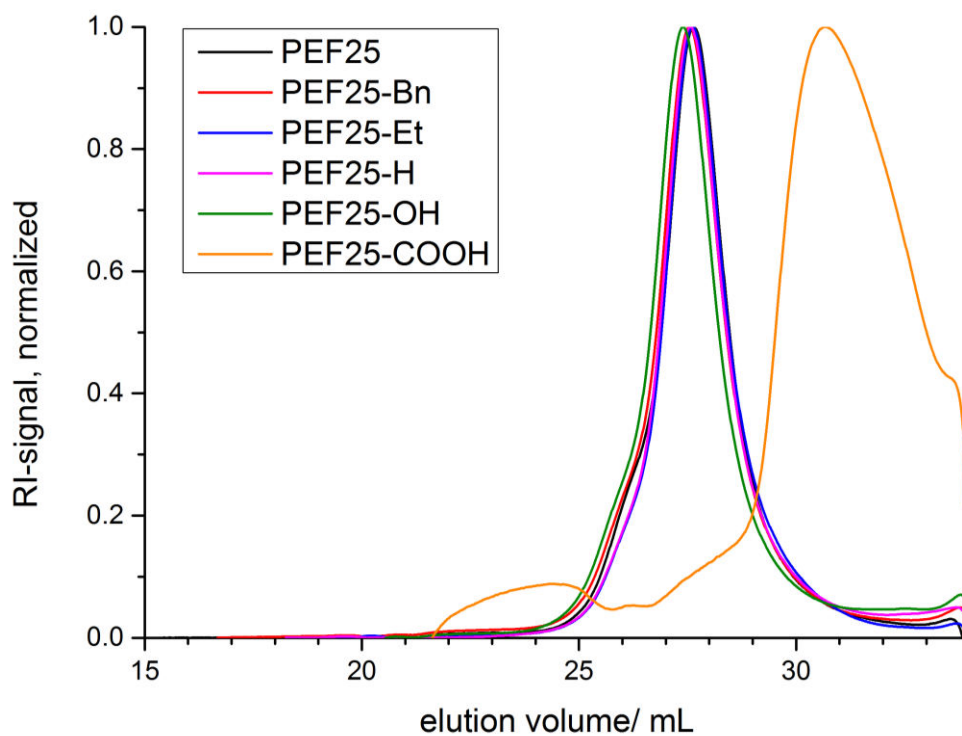


Figure S4.17. SEC elugrams of modified **PEF25** in DMF, RI-Signal, PEO standard.

#### 4.8.5 DSC thermograms

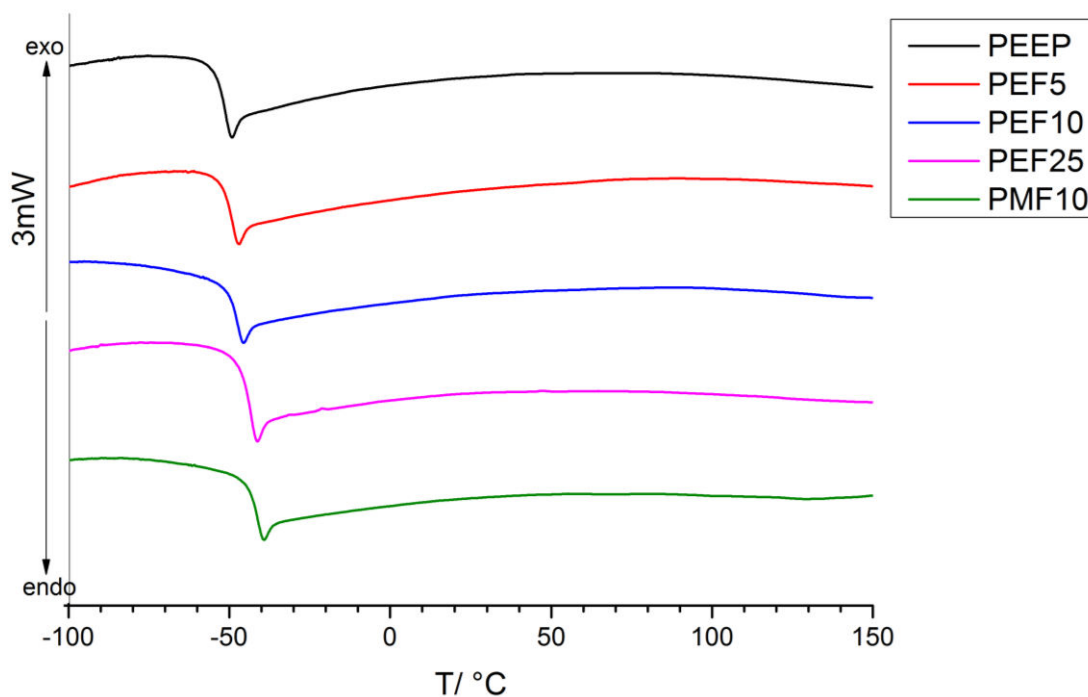
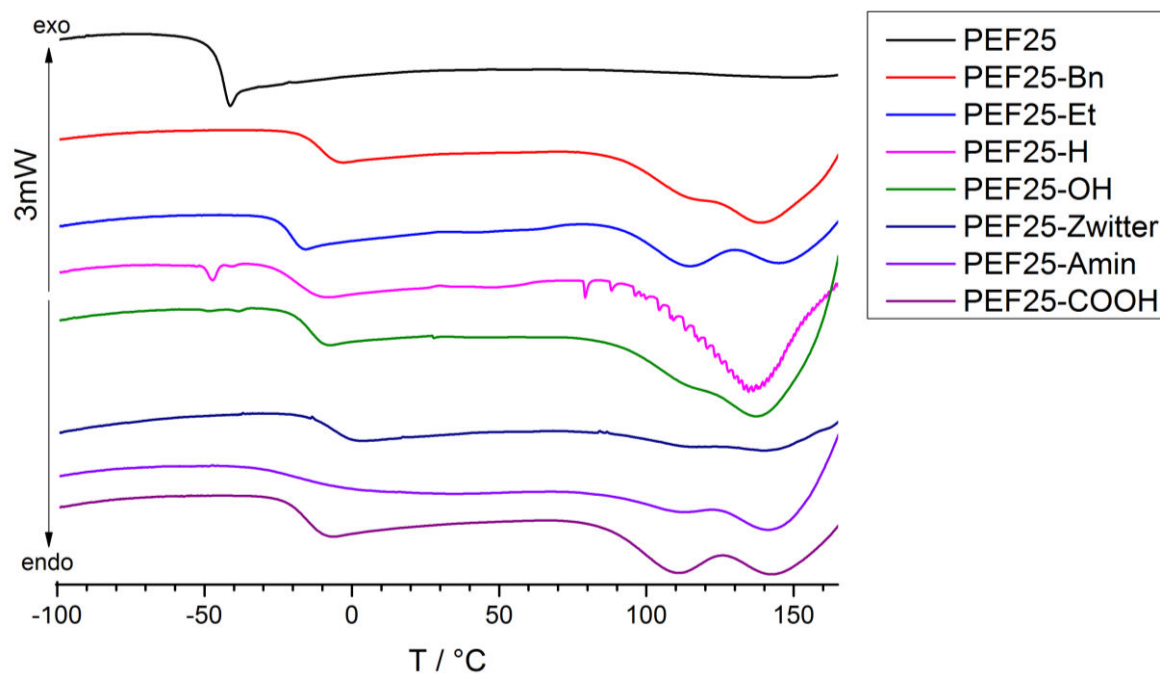


Figure S4.18. DSC thermograms of **polymers** (heating and cooling rate 10 K min<sup>-1</sup>, 1<sup>st</sup> run).



**Figure S4.19.** DSC thermograms of modified **PEF25** (heating and cooling rate 10 K min<sup>-1</sup>, 1<sup>st</sup> run).

#### 4.8.6 Turbidity measurements

**Table S4.1.** pH values of polymer solutions for turbidity measurements.

sample	acidic pH	alkaline pH	pH in water
<b>PEF5-COOH</b>	1.1	11.2	4.5
<b>PEF10-COOH</b>	1.2	11.6	4.6
<b>PEF25-COOH</b>	-	11.1	4.0
<b>PEF5-NH<sub>3</sub>Cl</b>	1.7	11.5	6.2
<b>PEF10-NH<sub>3</sub>Cl</b>	1.8	11.7	5.8
<b>PEF25-NH<sub>3</sub>Cl</b>	1.1	11.9	6.1
<b>PEF5-Zwitter</b>	1.4	11.2	5.5
<b>PEF10-Zwitter</b>	1.4	11.6	4.4
<b>PEF25-Zwitter</b>	1.5	11.6	4.3

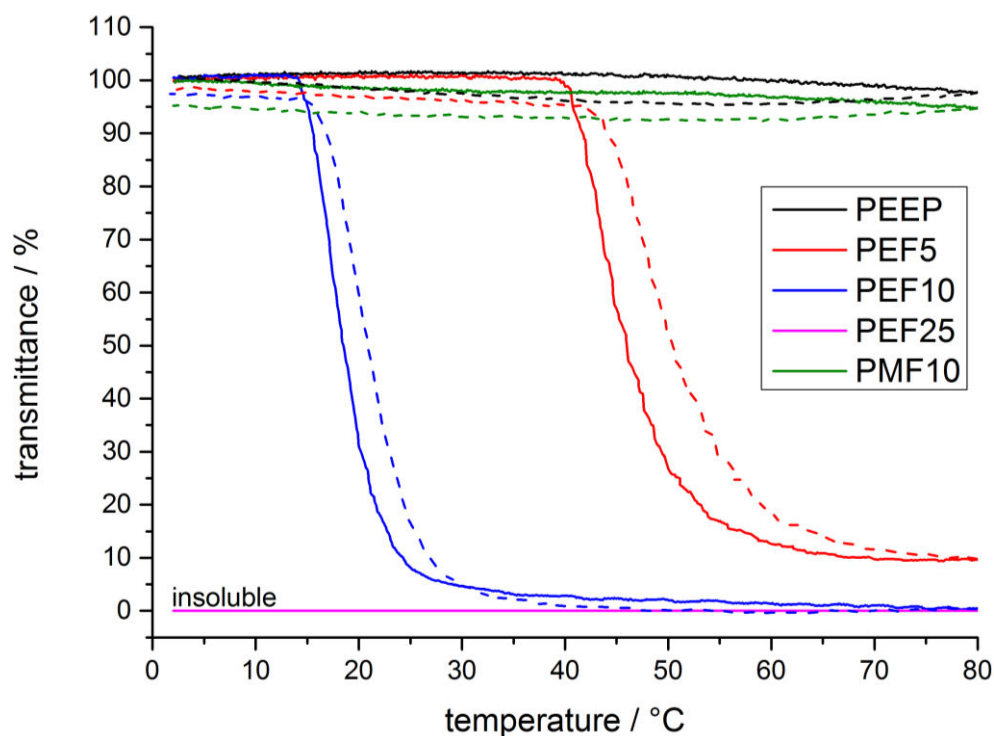


**Figure S4.20.** Turbidity measurements of unmodified **polymers**. Compact lines depict heating curves, dashed lines cooling curves. Line for PEF25 is fitted.

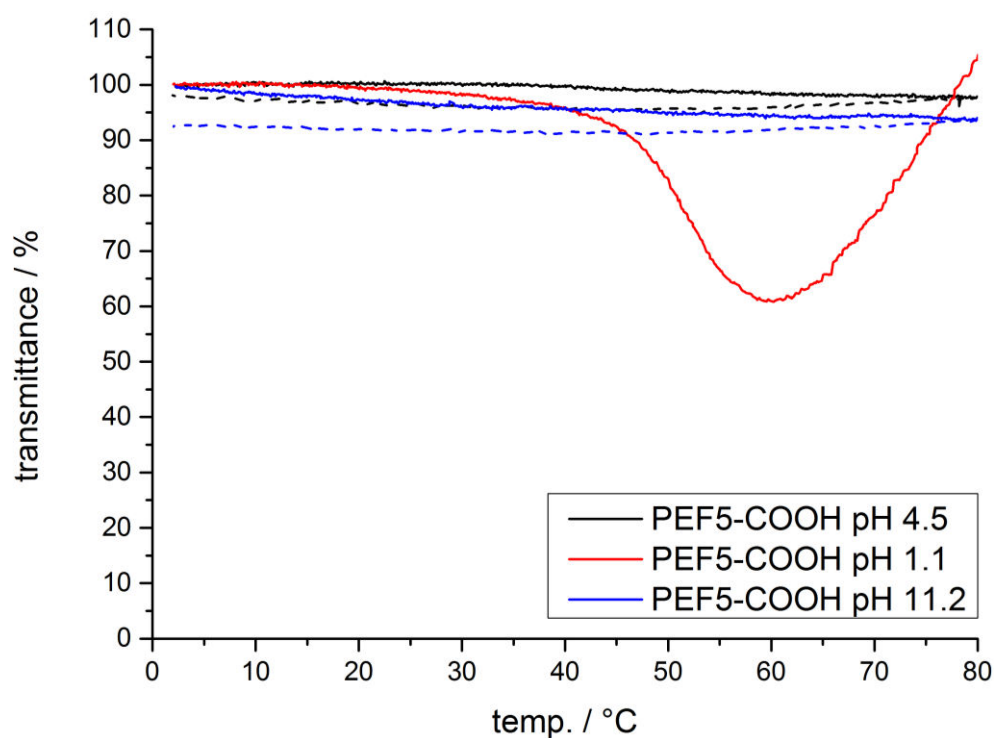


**Figure S4.21.** Turbidity measurements of **PEF5-COOH** at pH 1.1, 4.5 and 11.2. Compact lines depict heating curves, dashed lines cooling curves.

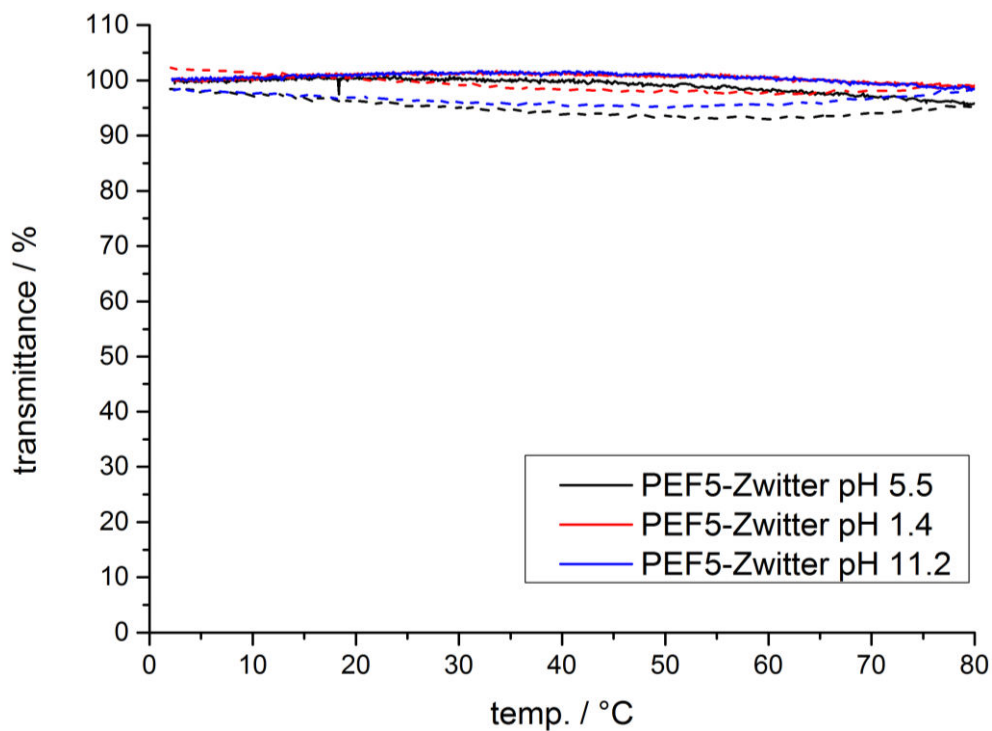


**Figure S4.22:** Turbidity measurements of **PE5-Zwitter** at pH 1.4, 5.5 and 11.2. Compact lines depict heating curves, dashed lines cooling curves.

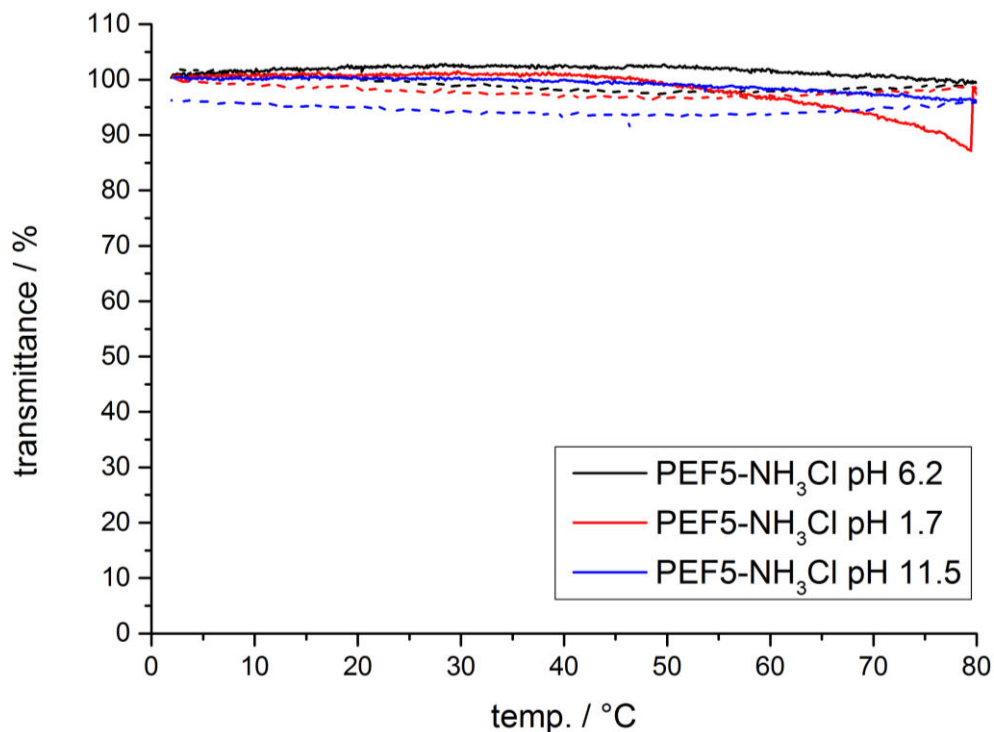


**Figure S4.23.** Turbidity measurements of **PEF5-NH<sub>3</sub>Cl** at pH 1.7, 6.2 and 11.5. Compact lines depict heating curves, dashed lines cooling curves.

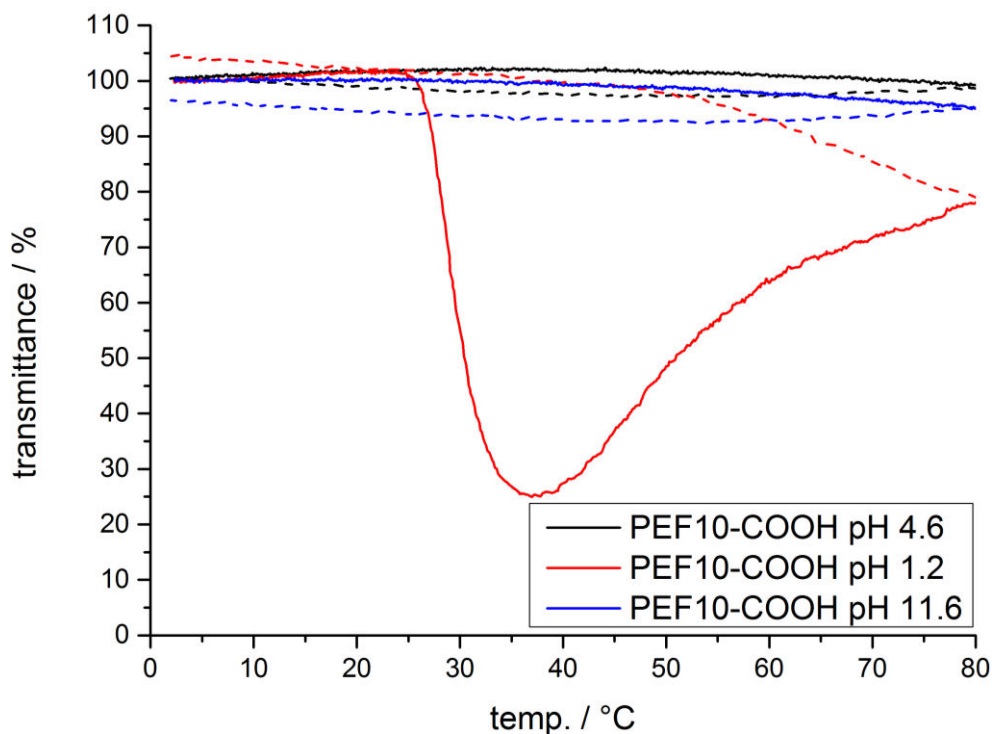


**Figure S4.24.** Turbidity measurements of **PEF10-COOH** at pH 1.2, 4.6 and 11.6. Compact lines depict heating curves, dashed lines cooling curves.

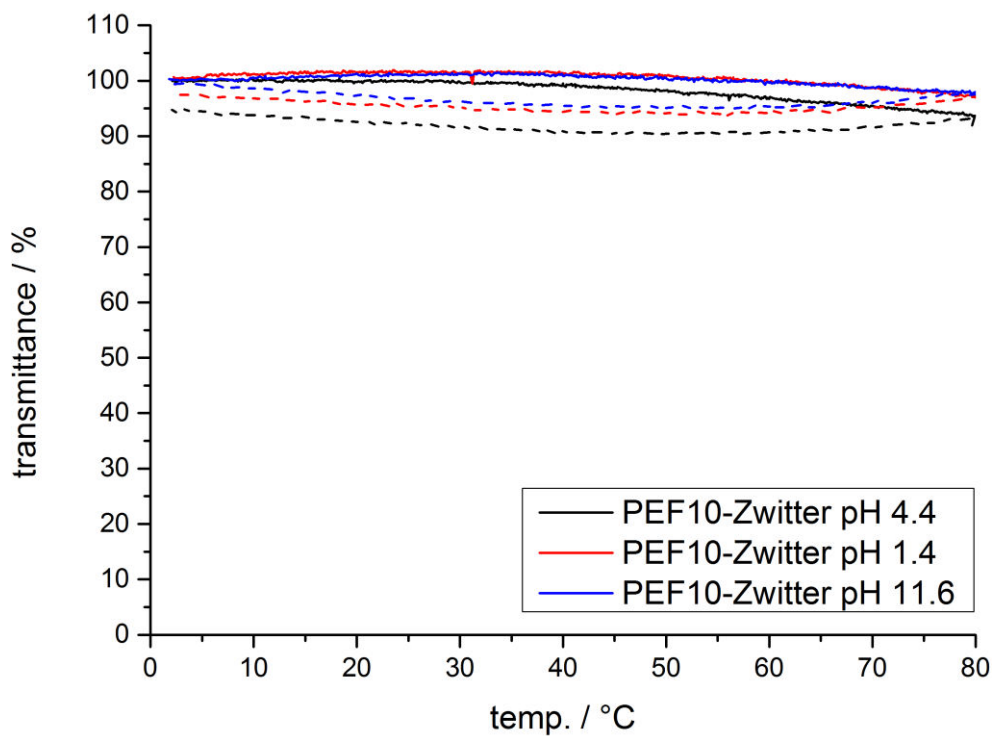


**Figure S4.25.** Turbidity measurements of **PEF10-Zwitter** at pH 1.4, 4.4 and 11.6. Compact lines depict heating curves, dashed lines cooling curves.

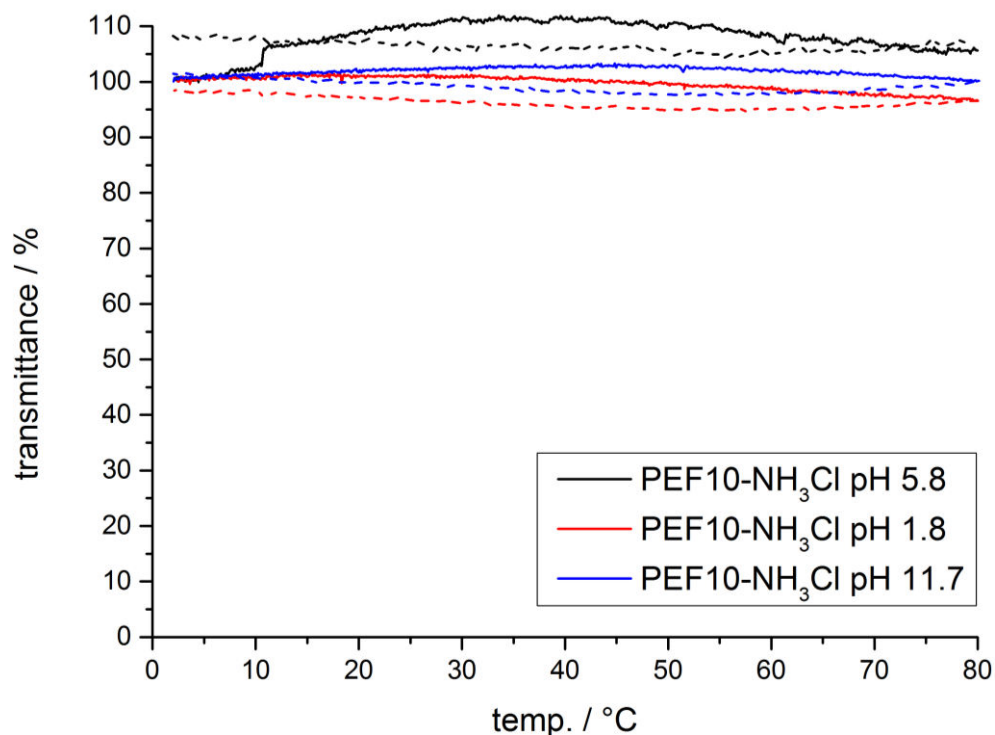


**Figure S4.26.** Turbidity measurements of **PEF10-NH<sub>3</sub>Cl** at pH 1.8, 5.8 and 11.7. Compact lines depict heating curves, dashed lines cooling curves.

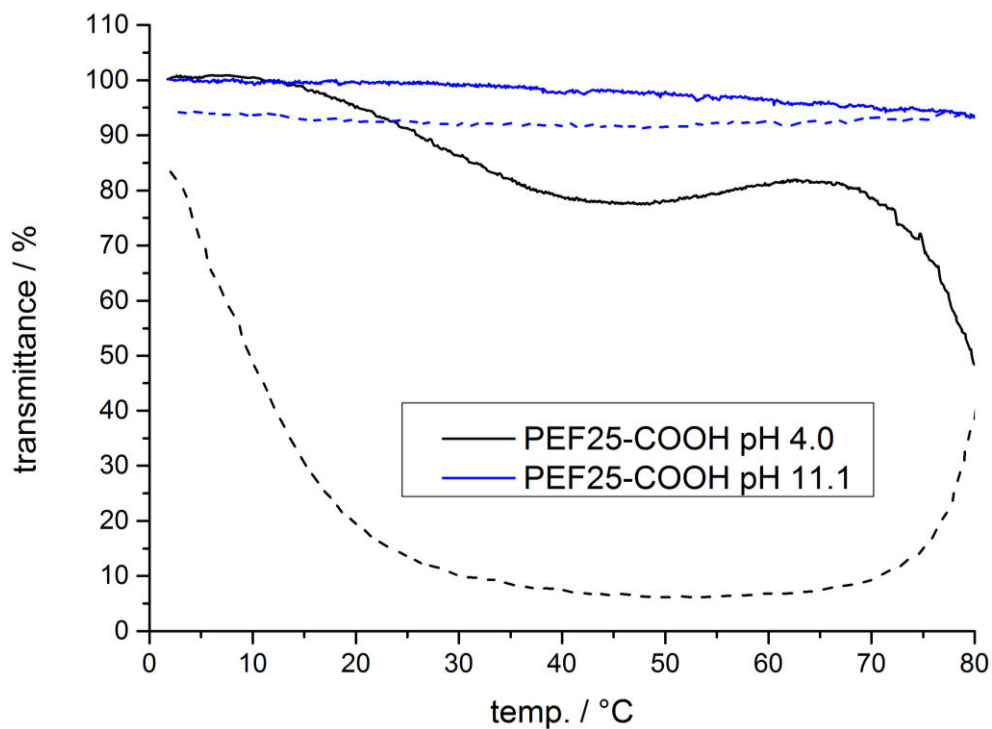


**Figure S4.27.** Turbidity measurements of **PEF25-COOH** at pH 4.0 and 11.1. Compact lines depict heating curves, dashed lines cooling curves. Note: PEF25-COOH is not soluble at pH 1-2.

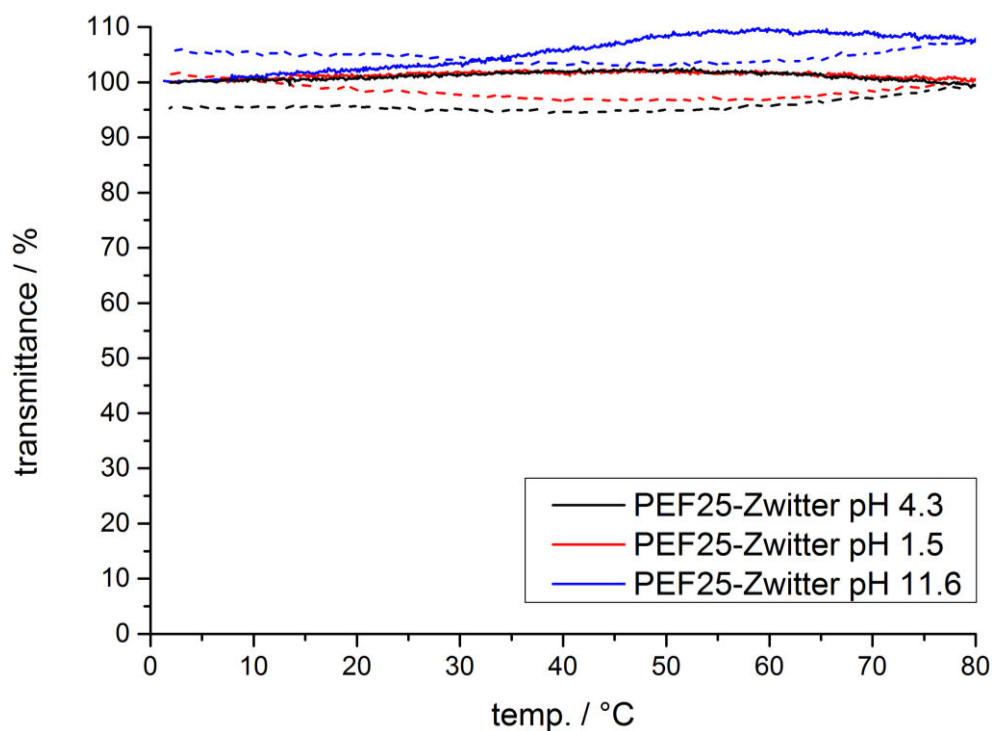


**Figure S4.28.** Turbidity measurements of **PEF25-Zwitter** at pH 1.5, 4.3 and 11.6. Compact lines depict heating curves, dashed lines cooling curves.

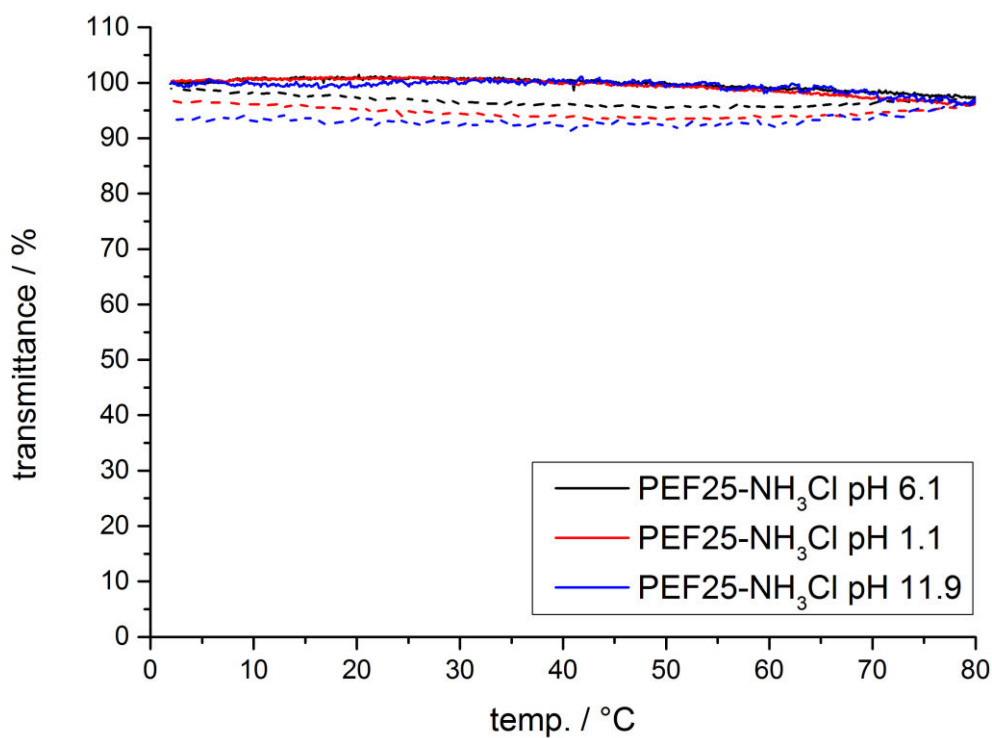


**Figure S4.29.** Turbidity measurements of **PEF25-NH<sub>3</sub>Cl** at pH 1.1, 6.1 and 11.9. Compact lines depict heating curves, dashed lines cooling curves.

### 4.8.7 Retro Diels-Alder reaction

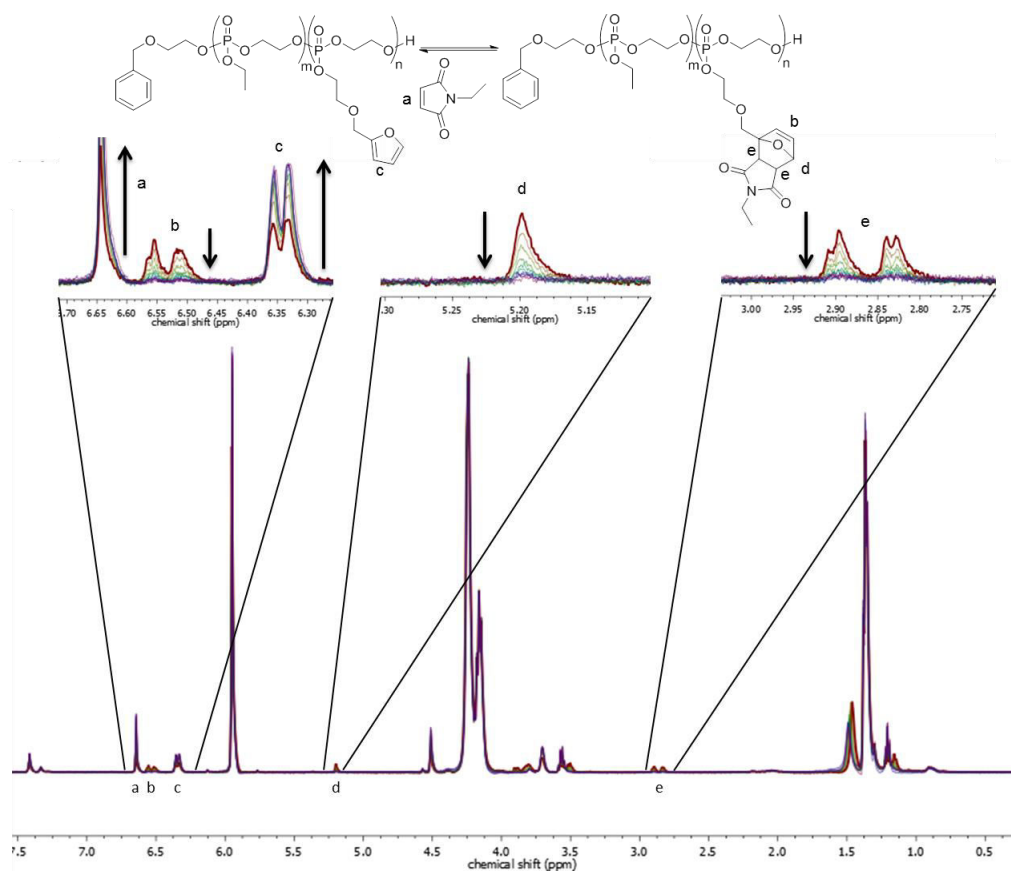


**Figure S4.30.**  $^1\text{H}$  NMR real-time kinetics of Retro Diels-Alder reaction of **PEF10-Et**, 500MHz, in  $d_2$ -tetrachlorethane at 110 °C.

**Table S4.2.** Overview of Diels-Alder and retro-Diels-Alder reaction of **PEF10** with *N*-ethylmaleimide.

entry	Conversion <sup>a</sup>	$M_w/M_n$ <sup>b</sup>	$T_g$ <sup>c</sup> / °C
<b>PEF10</b>	-	1.15	-49
<b>PEF10-Et-b</b>	0.85	1.20	-49
<b>PEF10-RDA</b>	1	1.16	-52

<sup>a</sup>Determined from the  $^1\text{H}$ -NMR spectra.  
<sup>b</sup>Determined by SEC in DMF. <sup>c</sup> Determined by DSC.

### 4.8.8 Degradation studies

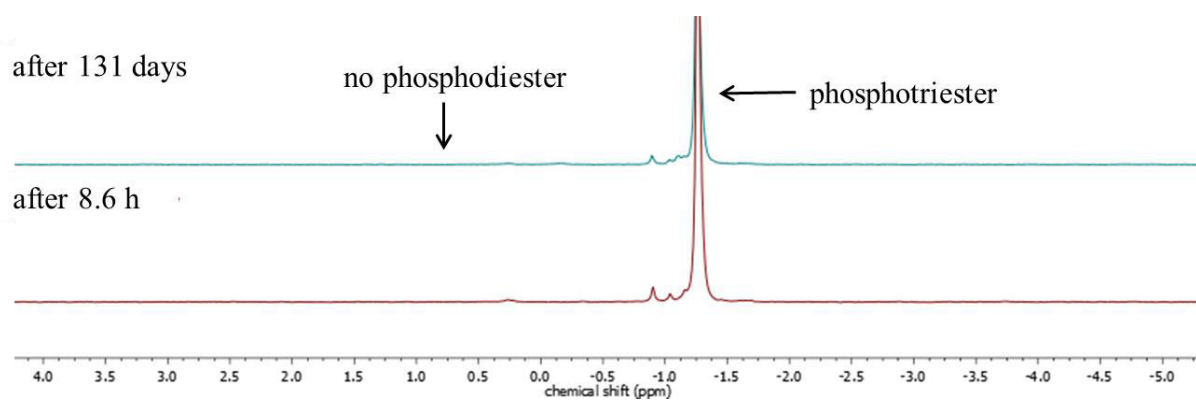


**Figure S4.31.**  $^{31}\text{P}\{\text{H}\}$  NMR spectra (121MHz,  $\text{H}_2\text{O}/\text{D}_2\text{O}$ , 298K) of the degradation of PEEP at pH 4.0.

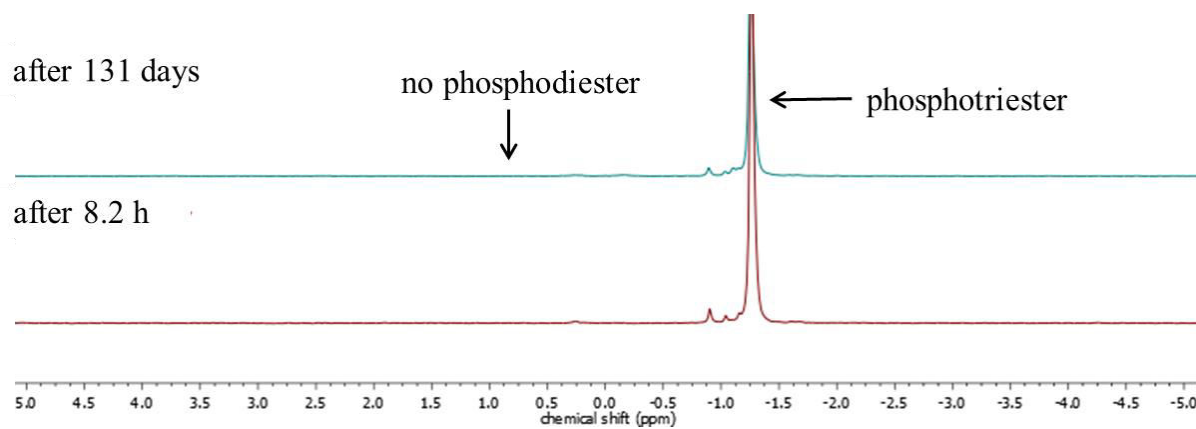


**Figure S4.32.**  $^{31}\text{P}\{\text{H}\}$  NMR spectra (121MHz,  $\text{H}_2\text{O}/\text{D}_2\text{O}$ , 298K) of the degradation of PEEP at pH 7.0.

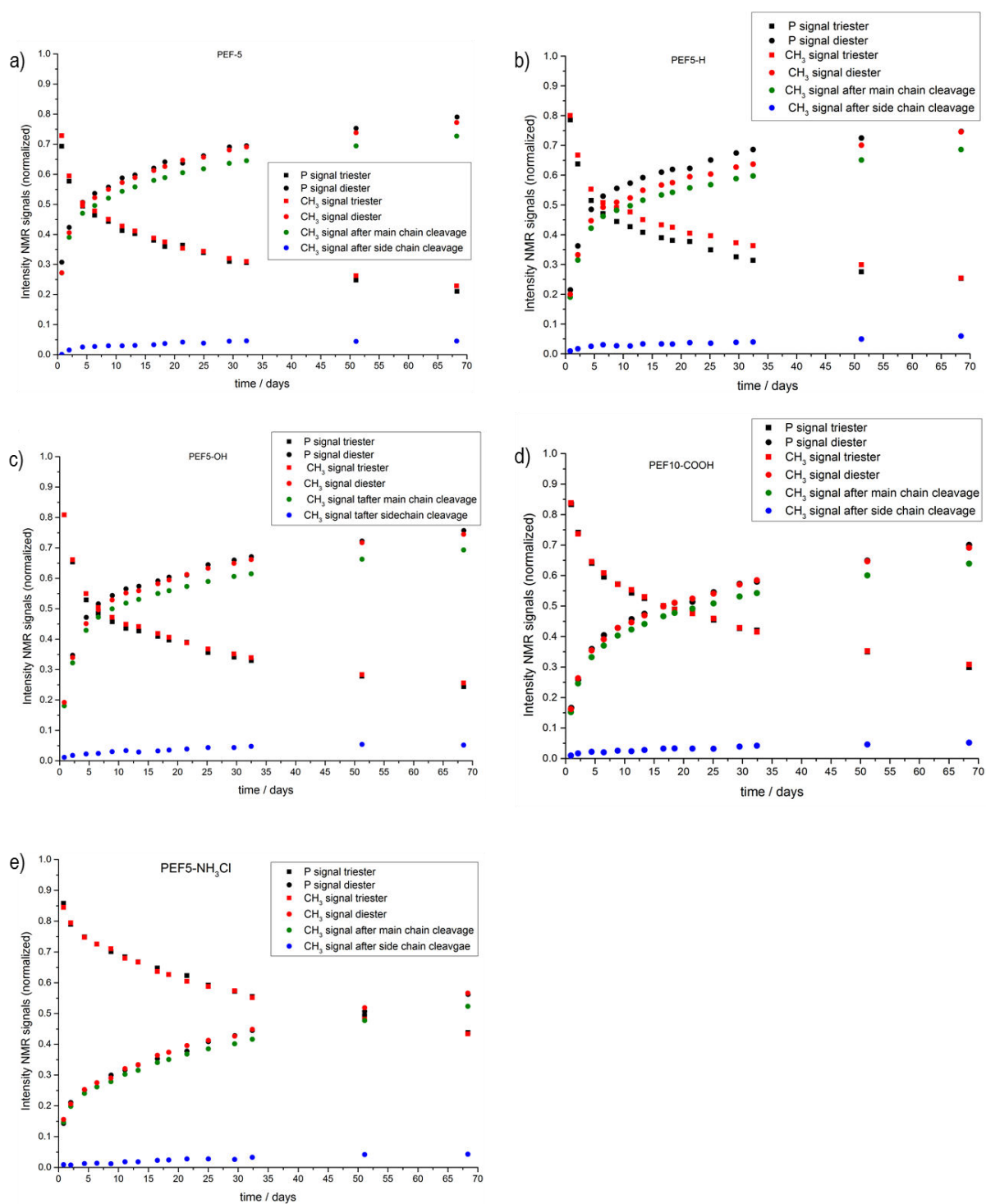


**Figure S4.33.** Degradation studies. Intensity of the <sup>1</sup>H and <sup>31</sup>P{H} NMR signals (normalized) vs degradation time of PEF5 and modified copolymers at pH 11.1, showing the decrease of phosphotriester and increase of -diester and the cleavage of the side and main chains of EEP repeat units: a) PEF5, b) PEF5-H, c) PEF5-OH, d) PEF10-COOH, e) PEF5-CH<sub>3</sub>Cl.

## 4.8 References

1. Osváth, Z.; Iván, B., *Macromol. Chem. Phys.* **2017**, *218* (4), 1600470-n/a.
2. Gandhi, A.; Paul, A.; Sen, S. O.; Sen, K. K., *Asian J. Pharm. Sci* **2015**, *10* (2), 99-107.
3. Nagase, K.; Okano, T., *J. Mater. Chem. B* **2016**, *4* (39), 6381-6397.
4. Roy, D.; Brooks, W. L. A.; Sumerlin, B. S., *Chem. Soc. Rev.* **2013**, *42* (17), 7214-7243.
5. Aseyev, V.; Tenhu, H.; Winnik, F. M., Non-ionic Thermoresponsive Polymers in Water. In *Self Organized Nanostructures of Amphiphilic Block Copolymers II*, Müller, A. H. E.; Borisov, O., Eds. Springer Berlin Heidelberg: Berlin, Heidelberg, 2011; pp 29-89.
6. Mangold, C.; Obermeier, B.; Wurm, F.; Frey, H., *Macromol. Rapid Commun.* **2011**, *32* (23), 1930-1934.
7. Lutz, J.-F., *Adv. Mater.* **2011**, *23* (19), 2237-2243.
8. Iwasaki, Y.; Wachiralarpphaithoon, C.; Akiyoshi, K., *Macromolecules* **2007**, *40* (23), 8136-8138.
9. Bauer, K. N.; Tee, H. T.; Velencoso, M. M.; Wurm, F. R., *Prog. Polym. Sci.* **2017**.
10. Zhao, Z.; Wang, J.; Mao, H.-Q.; Leong, K. W., *Adv. Drug Delivery Rev.* **2003**, *55* (4), 483-499.
11. Steinbach, T.; Wurm, F. R., *Angew. Chem. Int. Ed.* **2015**, *54* (21), 6098-6108.
12. Li, Q.; Wang, J.; Shahani, S.; Sun, D. D. N.; Sharma, B.; Elisseeff, J. H.; Leong, K. W., *Biomaterials* **2006**, *27* (7), 1027-1034.
13. Wang, Y.-C.; Yuan, Y.-Y.; Du, J.-Z.; Yang, X.-Z.; Wang, J., *Macromol. Biosci.* **2009**, *9* (12), 1154-1164.
14. Iwasaki, Y.; Yamaguchi, E., *Macromolecules* **2010**, *43* (6), 2664-2666.
15. Lim, Y. H.; Tiemann, K. M.; Heo, G. S.; Wagers, P. O.; Rezenom, Y. H.; Zhang, S.; Zhang, F.; Youngs, W. J.; Hunstad, D. A.; Wooley, K. L., *ACS Nano* **2015**, *9* (2), 1995-2008.
16. Steinbach, T.; Alexandrino, E. M.; Wurm, F. R., *Polym. Chem.* **2013**, *4* (13), 3800-3806.
17. Becker, G.; Ackermann, L.-M.; Schechtel, E.; Klapper, M.; Tremel, W.; Wurm, F. R., *Biomacromolecules* **2017**, *18* (3), 767-777.
18. Libiszowski, J.; Kałużynski, K.; Penczek, S., *J. Polym. Sci., Polym. Chem. Ed.* **1978**, *16* (6), 1275-1283.
19. Clément, B.; Grignard, B.; Koole, L.; Jérôme, C.; Lecomte, P., *Macromolecules* **2012**, *45* (11), 4476-4486.
20. Baran, J.; Klosinski, P.; Penczek, S., *Makromol. Chem.* **1989**, *190* (8), 1903-1917.
21. Klosinski, P.; Penczek, S., *Makromol. Chem., Rapid Commun.* **1988**, *9* (3), 159-164.
22. Steinbach, T.; Ritz, S.; Wurm, F. R., *ACS Macro Lett.* **2014**, *3* (3), 244-248.
23. Bauer, K. N.; Tee, H. T.; Lieberwirth, I.; Wurm, F. R., *Macromolecules* **2016**, *49* (10), 3761-3768.
24. Zhang, S.; Wang, H.; Shen, Y.; Zhang, F.; Seetho, K.; Zou, J.; Taylor, J.-S. A.; Dove, A. P.; Wooley, K. L., *Macromolecules* **2013**, *46* (13), 5141-5149.
25. Cankaya, A.; Steinmann, M.; Bulbul, Y.; Lieberwirth, I.; Wurm, F. R., *Polym. Chem.* **2016**, *7* (31), 5004-5010.
26. Müller, L. K.; Steinbach, T.; Wurm, F. R., *RSC Advances* **2015**, *5* (53), 42881-42888.
27. Song, W.-J.; Du, J.-Z.; Liu, N.-J.; Dou, S.; Cheng, J.; Wang, J., *Macromolecules* **2008**, *41* (19), 6935-6941.
28. Sun, T.-M.; Du, J.-Z.; Yan, L.-F.; Mao, H.-Q.; Wang, J., *Biomaterials* **2008**, *29* (32), 4348-4355.
29. McKinlay, C. J.; Waymouth, R. M.; Wender, P. A., *J. Am. Chem. Soc.* **2016**, *138* (10), 3510-3517.
30. Zhang, S.; Li, A.; Zou, J.; Lin, L. Y.; Wooley, K. L., *ACS Macro Lett.* **2012**, *1* (2), 328-333.
31. Baeten, E.; Vanslambrouck, S.; Jérôme, C.; Lecomte, P.; Junkers, T., *Eur. Polym. J.* **2016**, *80*, 208-218.
32. Lim, Y. H.; Heo, G. S.; Rezenom, Y. H.; Pollack, S.; Raymond, J. E.; Elsabahy, M.; Wooley, K. L., *Macromolecules* **2014**, *47* (14), 4634-4644.
33. Goussé, C.; Gandini, A.; Hodge, P., *Macromolecules* **1998**, *31* (2), 314-321.
34. Ito, T.; Aoshima, K.; Toda, F.; Uno, K.; Iwakura, Y., *Polym. J.* **1970**, *1* (3), 278-287.
35. Hu, Y.; Qiao, L.; Qin, Y.; Zhao, X.; Chen, X.; Wang, X.; Wang, F., *Macromolecules* **2009**, *42* (23), 9251-9254.

36. Thongsomboon, W.; Sherwood, M.; Arellano, N.; Nelson, A., *ACS Macro Lett.* **2013**, *2* (1), 19-22.
37. Freeman, R.; Hill, H. D. W.; Kaptein, R., *J. Magn. Reson.* **1972**, *7* (3), 327-329.
38. Kwart, H.; King, K., *Chem. Rev.* **1968**, *68* (4), 415-447.
39. Gandini, A.; Lacerda, T. M.; Carvalho, A. J. F.; Trovatti, E., *Chem. Rev.* **2016**, *116* (3), 1637-1669.
40. Gandini, A., *Prog. Polym. Sci.* **2013**, *38* (1), 1-29.
41. Du, P.; Wu, M.; Liu, X.; Zheng, Z.; Wang, X.; Joncheray, T.; Zhang, Y., *J. Appl. Polym. Sci.* **2014**, *131* (9), 40234-40240.
42. Yamashiro, M.; Inoue, K.; Iji, M., *Polym. J.* **2008**, *40* (7), 657-662.
43. Defize, T.; Riva, R.; Jérôme, C.; Alexandre, M., *Macromol. Chem. Phys.* **2012**, *213* (2), 187-197.
44. Gandini, A.; Silvestre, A. J. D.; Neto, C. P.; Sousa, A. F.; Gomes, M., *J. Polym. Sci., Part A: Polym. Chem.* **2009**, *47* (1), 295-298.
45. Burkholder, T. P.; Bratton, L. D.; Kudlacz, E. M.; Maynard, G. P.; Kane, J. M.; Santiago, B. US6329392 B1, 2001.
46. Gandini, A., *Polym. Chem.* **1977**, *25*, 47-96.
47. Lee, B. F.; Wolffs, M.; Delaney, K. T.; Sprafke, J. K.; Leibfarth, F. A.; Hawker, C. J.; Lynd, N. A., *Macromolecules* **2012**, *45* (9), 3722-3731.
48. Steinbach, T.; Schroder, R.; Ritz, S.; Wurm, F. R., *Polym. Chem.* **4** (16), 4469-4479.
49. Hilf, J.; Scharfenberg, M.; Poon, J.; Moers, C.; Frey, H., *Macromol. Rapid Commun.* **2015**, *36* (2), 174-179.
50. Canadell, J.; Fischer, H.; De With, G.; van Benthem, R. A. T. M., *J. Polym. Sci., Part A: Polym. Chem.* **2010**, *48* (15), 3456-3467.
51. Roos, K.; Dolci, E.; Carlotti, S.; Caillol, S., *Polym. Chem.* **2016**, *7* (8), 1612-1622.
52. Baran, J.; Penczek, S., *Macromolecules* **1995**, *28* (15), 5167-5176.
53. Wang, D.; Williams, C. G.; Yang, F.; Cher, N.; Lee, H.; Elisseeff, J. H., *Tissue Eng.* **2005**, (11), 201-213.
54. Barnard, P. W. C.; Bunton, C. A.; Llewellyn, D. R.; Vernon, C. A.; Welch, V. A., *J. Chem. Soc.* **1961**, (0), 2670-2676.
55. Wolf, T.; Rheinberger, T.; Simon, J.; Wurm, F. R., *J. Am. Chem. Soc.* **2017**, *139* (32), 11064-11072.
56. Wang, H.; Su, L.; Li, R.; Zhang, S.; Fan, J.; Zhang, F.; Nguyen, T. P.; Wooley, K. L., *ACS Macro Lett.* **2017**, *6* (3), 219-223.
57. Baran, J.; Kaluzynski, K.; Szymanski, R.; Penczek, S., *Biomacromolecules* **2004**, *5* (5), 1841-1848.
58. Steinmann, M.; Wagner, M.; Wurm, F. R., *Chem. - Eur. J.* **2016**, *22* (48), 17329-17338.
59. Kumamoto, J.; Cox, J. R.; Westheimer, F. H., *J. Am. Chem. Soc.* **1956**, *78* (19), 4858-4860.
60. Pretula, J.; Kaluzynski, K.; Wisniewski, B.; Szymanski, R.; Loontjens, T.; Penczek, S., *J. Polym. Sci., Part A: Polym. Chem.* **2006**, *44* (7), 2358-2362.
61. Liu, J.; Yang, J.; Liang, X.; Zhao, Y.; Cade-Menun, B. J.; Hu, Y., *Soil Sci. Soc. Am. J.* **2014**, *79*, 47-53.
62. Schöttler, S.; Becker, G.; Winzen, S.; Steinbach, T.; Mohr, K.; Landfester, K.; Mailänder, V.; Wurm, F. R., *Nat. Nano.* **2016**, *11* (4), 372-377.
63. Salewska, N.; Milewska, M. J., *J. Heterocycl. Chem.* **2014**, *51* (4), 999-1003.
64. Cheng, W.; Satyanarayananajois, S.; Lim, L.-Y., *Pharm. Res.* **2007**, *24* (1), 99-110.
65. Pratt, R. C.; Lohmeijer, B. G. G.; Long, D. A.; Lundberg, P. N. P.; Dove, A. P.; Li, H.; Wade, C. G.; Waymouth, R. M.; Hedrick, J. L., *Macromolecules* **2006**, *39* (23), 7863-7871.



## 5.1 Abstract

Photo-reactive PPEs have been studied with respect to their formation of surface-attached PPE-networks. PPEs are biocompatible and might be potential anti-fouling coatings for biomedical devices as implants or catheters. Benzophenones can photochemically cure polymer films by a C,H-insertion cross-linking reaction. Multibenzophenone-PPEs were formed, partially additionally including furfuryl or alkene groups as platform for post-polymerization modification reactions by thiol-ene or Diels Alder reaction. The incorporation kinetics of different comonomers into the PPE-terpolymers have been studied, indicating a gradient-like structure of the polymers. Film formation of covalently surface-attached and cross-linked PPE-networks was achieved, exhibiting smooth and hydrophilic networks (contact angles of 20-26°). Furfuryl-containing PPE-networks indicated a successful post-functionalization by decrease of hydrophilicity (contact angle of 38°). The additional furan functions present an addressable platform to further tune the properties of PPE-films.

## 5.2 Introduction

Surfaces of biomedical devices (such as implants, biosensors, catheters or carrier systems for drug delivery) often fail because of undesired adsorption of bacteria, proteins and other biomolecules. Even the adsorption of only few such molecules can trigger the formation of biofilms, which can cause severe systemic infections. Functional polymeric coatings exhibiting antifouling and/or antimicrobial properties are therefore currently intensively investigated.<sup>1-3</sup>

Examples for substance classes that resist biofilm formation are hydrophobic poly(dimethylsiloxane) (PDMS)-based<sup>4</sup> or fluorinated<sup>5</sup> polymers, which might be used for coating of ship hulls or pipelines. They are classified as “fouling release” coatings: while they have a high interfacial energy with water, which enables amphiphilic proteins to easily attach to them, these biofoulants can also be easily removed by shear stress, e.g. generated by hydrodynamic flow.<sup>6</sup>

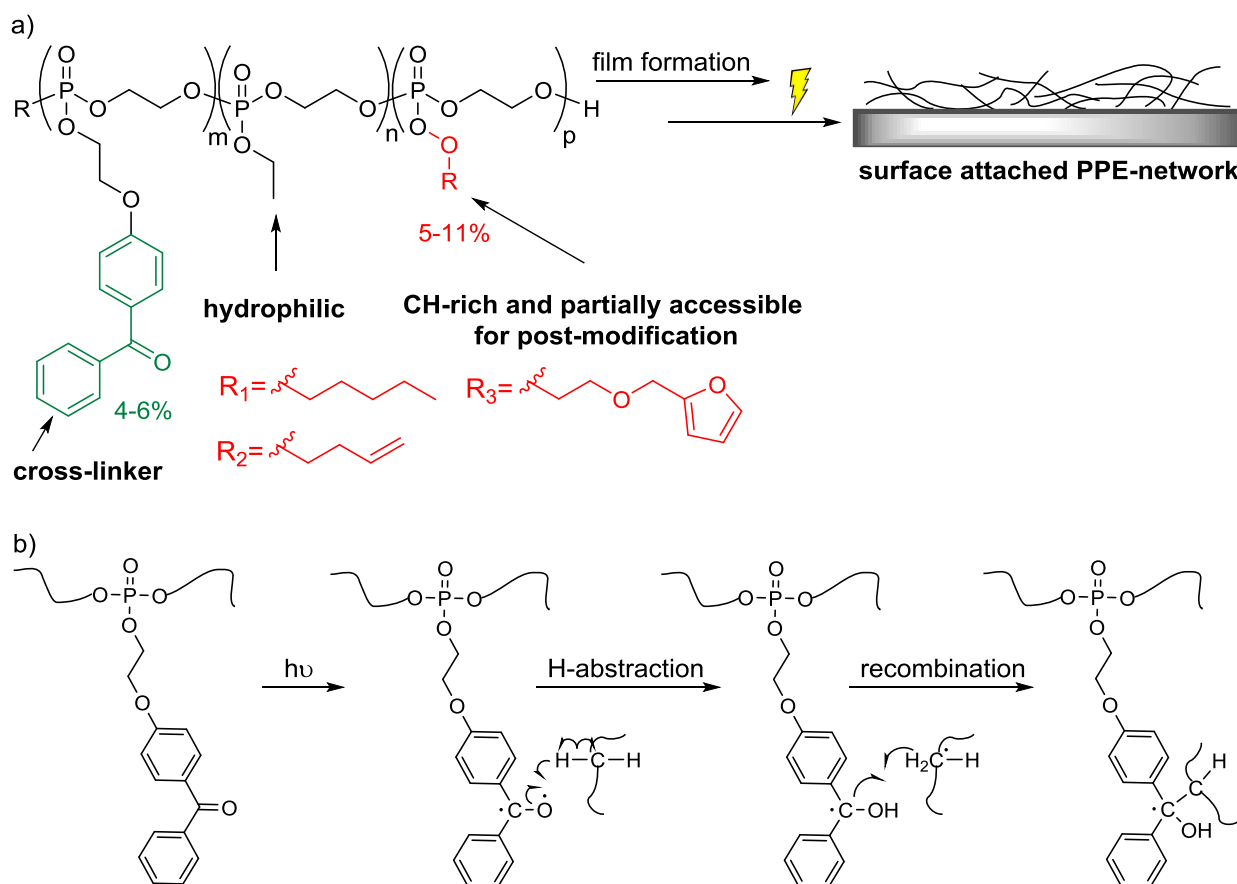
“Non-fouling” coatings, on the other hand, consist of hydrophilic polymeric systems and have a low interfacial energy with water.<sup>6</sup> Thus, adsorption of proteins is energetically not favored on these surfaces. Prominent protein-repellent examples include poly(ethylene glycol) (PEG)-based polymers, amphiphilic polymer coatings, including those with heterogeneities on the nanoscale, oligosaccharide-containing polymers mimicking the glycocalyx of blood vessels, and zwitterionic polymers.<sup>3, 6</sup> PEG is particularly well-known to suppress protein adhesion (“stealth effect”). Lienkamp and coworkers<sup>7</sup> recently reported polyzwitterionic surface-attached networks which

were simultaneously protein-repellent, strongly antimicrobial and highly compatibility with human cells.

The aim of this study was to explore the potential of poly(phosphoester) (PPE)-based surface-attached networks as protein-repellent coatings. PPEs have been reported to be biocompatible and have low cytotoxicity in many cases. Poly(ethyl ethylene phosphate) (PEEP) is hydrophilic and, the most prominent PPE in biomedical applications.<sup>8</sup> We recently showed that PEEP-functionalization of nanoparticles (using a grafting onto method) reduced protein adsorption on these particles, and also altered the interaction with immune cells in a similar way as PEG on nanocarriers.<sup>9</sup>

To study PPEs on macroscopic, planar surfaces, we designed PPE-(co)polymers that can form surface-attached polymer networks by a photoinduced crosslinking/ attaching to a surface (Scheme 5.1a). In contrast to grafting to methods, surface-attached polymer networks show a higher surface coverage and the coating thickness is independent of the molecular weight of the polymer used.

We designed a novel monomer for the ring-opening polymerization of cyclic phosphates, containing a benzophenone side chain. As this monomer would produce only hydrophobic



**Scheme 5.1.** a) Terpolymers used in this study, and formation of surface-attached PPE-networks; b) CHic process for cross-linking and surface-attachment of PPEs by UV-irradiation.

homopolymers, we copolymerized it with an ethyl monomer (EEP) (Scheme 5.1a), to obtain hydrophilic copolymers, which can be cross-linked by a UV-activated C,H-insertion cross-linking reaction (so called CHic process, Scheme 5.1b). The benzophenone groups in the polymers can react with CH groups of other parts of the polymer. The benzophenone groups act as a crosslinker when it forms a reactive intermediate (a triplet biradical at the carbonyl group (-C·-O·)) upon UV-activation, abstracts a proton from a nearby aliphatic group, and forms a covalent C-C bond to the thus created C radical on that group. Advantageously, the benzophenone group does not need a specific reaction partner, but reacts with any CH group from the backbone or other pendant side chains so that a polymeric network is formed.<sup>10-13</sup> This concept has been pioneered by R uhe and coworkers, who used copolymers containing covalently attached benzophenone to prepare surface-attached polymer hydrogels, e.g. made from dimethylacrylamide and methacryloyloxybenzophenone.<sup>13</sup>

We present the synthesis, copolymerization kinetics, and characterization of several PPE-copolymers with various pendant groups and the new benzophenone monomer, altering their hydrophilicity and abstractable C-H-bonds. Films of these polymers on silicon surfaces were prepared and crosslinked by irradiation. Contact angles were determined and further post-modification by thiol-ene or Diels-Alder reaction was studied.

### 5.3 Experimental Section

**Materials.** All reagents were used without further purification, unless otherwise stated. Solvents, dry solvents (over molecular sieves) and deuterated solvents were purchased from Acros Organics, Sigma-Aldrich, Deutero GmbH or Fluka. Furfuryl alcohol, 2-chloro-2-oxo-1,3,2-dioxaphospholane, pyridine, 1-pentanol, 4-hydroxybenzophenone, triethylamine, 3-buten-1-ol, potassium carbonate, 2-bromoethanol, 2-(benzyloxy)ethanol, 2-ethyl-1-butanol, sodium hydride, 1,8-diazabicyclo[5.4.0]undec-7-ene, bromoacetate, hexamethyldisiloxane (HDMSO), triethoxysilane, platinum on activated charcoal (10wt%), trimethox(propyl)silane, (3-aminopropyl)triethoxysilane, allylbromide, 1-propanethiol, cysteamine, pentaerythritoltetrakis(3-mercaptopropionate), dodecylmercaptane, dodecylamine, maleic anhydride, sodium acetate, and 2,2'-azobis(2-methylpropionitrile) were purchased from Sigma-Aldrich. MgSO<sub>4</sub> was purchased from Fisher Scientific. 3,5-bis(trifluoromethyl)phenylisothiocyanat was purchased from Alfa Aesar GmbH & Co KG. Lithium aluminumhydride (2.4 M in THF) and cyclohexylamine were purchased from Acros Organics. 3-Butenyltriethoxysilane was purchased from Gelest Inc., USA. 3-(benzyloxy)ethanol, 1-pentanol, 2-ethyl-1-butanol, triethylamine and 3-buten-1-ol was dried with NaH prior to use, distilled, and stored over molecular sieve.

1,8-diazabicyclo[5.4.0]undec-7-ene was distilled prior to use, and stored over molecular sieve at 4 °C. The silicon wafer substrates used were single or double side polished (for FT-IR measurements), with [100] orientation, 1.5x1.5 cm in size, and about 700 µm thickness, purchased from Si-Mat, Kaufering, Germany.

**Instrumentation and Characterization Techniques.** Size exclusion chromatography (SEC) measurements were performed in DMF (containing 0.25 g/L of lithium bromide as an additive) on an Agilent 1100 Series as an integrated instrument, including a PSS GRAM columns (1000/1000/100 g), a UV detector (270 nm), and a RI detector at a flow rate of 1 mL/min at 60 °C. Calibration was carried out using PEO standards provided by Polymer Standards Service. For nuclear magnetic resonance analysis <sup>1</sup>H, <sup>13</sup>C, and <sup>31</sup>P NMR spectra were recorded on a Bruker AVANCE III 300, 500, 700 or 850 MHz spectrometer. All spectra were measured in either *d*<sub>6</sub>-DMSO, CDCl<sub>3</sub> or *d*<sub>2</sub>-DCM at 298 K. The spectra were calibrated against the solvent signal and analyzed using MestReNova 8 from Mestrelab Research S.L. DOSY spectra were analyzed with TOPSPIN 3.2 software. For the quantitative <sup>31</sup>P-NMR experiments for copolymerization studies a 5 mm triple resonance TXI <sup>1</sup>H/<sup>13</sup>C/<sup>15</sup>N probe equipped with a z-gradient on the 850 MHz Bruker AVANCE III system was used. The <sup>31</sup>P NMR (334 MHz) measurements were obtained with invers gated decoupling,<sup>14</sup> which allows the integration of the <sup>31</sup>P-NMR signals. The used relaxation delay was fixed at 10 s with a scan number of 32 and a 90° flip angle of 27 µs and a spectral width of 34000Hz (100ppm). For the control <sup>1</sup>H NMR measurements one transients were used with a 90° pulse of 10.8 µs, a spectral width of 17000 Hz (20 ppm) and a recycling delay of 5 s. The temperature was kept at 253, 263 or 273 K and regulated by a standard <sup>1</sup>H methanol NMR sample using the topspin 3.1 software (Bruker). The control of the temperature was realized with a VTU (variable temperature unit) and an accuracy of +/- 0.1 K. The thermal properties of the synthesized polymers have been measured by differential scanning calorimetry (DSC) on a Mettler Toledo DSC 823 calorimeter. Three scanning cycles of heating–cooling were performed in a N<sub>2</sub> atmosphere (30 mL/min) with a heating and cooling rate of 10 °C/min. The used spin-coater was a SPIN150-NPP (SPS-Europe, Netherlands) or a Delta 80 BM Lackschleuder (Süss MicroTech, Germany) The UV irradiation unit was a BIO-LINK-Box (Vilber Lourmat GmbH, Germany) or a UV-Stratalinker 2400 (Stratagene®, California), each with 254 nm light bulbs. The thickness of the dry PPE layers on silicon wafers was measured by ellipsometry with an “auto-nulling imaging” ellipsometer Nanofilm EP<sup>3</sup> (Nanofilm Technologie GmbH, Göttingen, Germany), equipped with a 532 nm solid-state laser. A refractive index of 1.4734 for **P2** and 1.4805 for **P4** was used, for other samples the refractive index was set to 1.5. The angle of incidence was varied from 70-80° for silicon and from 64-74° for gold substrates. The average value from 2-3 different positions was taken, and the EP4-model used to fit the data. Static, advancing and receding contact angles of PPE-networks (CA) were measured with the CA system OCA 20 (Dataphysics GmbH, Filderstadt,

Germany). The average value was determined from three measurements on three different samples. The water droplet to determine the static CA had a volume of 5  $\mu\text{L}$ ; for the dynamic CA measurement, a volume reduction speed of 2  $\mu\text{L/s}$  was used. The static CAs were calculated with the Laplace–Young method, the advancing and receding CAs with the elliptical and the tangent method, respectively. FT-IR spectra of monomers and polymers were recorded using a Thermo Scientific iS10 FT-IR spectrometer equipped with a diamond ATR unit. ATR-FT-IR spectra of PPE-networks were measured on a Bio-Rad Excalibur spectrometer (Bio-Rad, Munich, Germany). PPE-networks on double-sided polished silicon wafers, immobilized on one side, were measured under nitrogen atmosphere. A non-coated silicon wafer was used as background sample. 64 scans were taken for each measurement. The spectra were recorded from 4000 to 400  $\text{cm}^{-1}$ . The topography of the surfaces was imaged by atomic force microscopy (AFM) with a Dimension Icon from Bruker. Commercially available ScanAsyst Air cantilevers (length: 115  $\mu\text{m}$ ; width: 25  $\mu\text{m}$ ; spring constant: 0.4 N/m; resonance frequency: 70 kHz) were used. All AFM images were recorded in ScanAsyst Mode in air. The obtained images were analyzed and processed with the software ‘Nanoscope Analysis 1.5’. For each sample, the root-mean-square (RMS) average roughness from three images of an area of 5  $\times$  5  $\mu\text{m}^2$  at different positions was taken.

**Syntheses.** *2-(2-(benzophenone-4-oxy)ethoxy)-2-oxo-1,3,2-dioxaphospholane (BeEP, 1):* 4-(2-Hydroxyethoxy)benzophenone (8.64 g, 35.7 mmol, 1 eq.) was dissolved in 60 mL dry THF in a flame-dried 3-necked round-bottom flask. Dry triethylamine (3.97 g, 39.2 mmol, 1.1 eq.) was added and cooled to 0°C. 2-chloro-2-oxo-1,3,2-dioxaphospholane (7.62 g, 53.5 mmol, 1.5 eq.) in 40 mL dry THF was added dropwisely, stirred for 4 h and stored at -20°C overnight. During reaction, hydrogen chloride was formed and precipitated as triethylammonium hydrochloride. The reaction was filtered with a Schlenk-frit and concentrated. Column chromatography with a RP-1 column (silica gel deactivated with 5v% hexamethyldisiloxane, dichloromethane/ethyl acetate 4:1,  $R_f=0.71$ ) gave the pure product BeEP, colourless crystals. Yield: 9.32 g, 78%.  $^1\text{H}$  NMR (300 MHz,  $\text{CDCl}_3$ ):  $\delta$  [ppm] 7.85-7.82 (d, 2H, =CH-CH=C(CH=)-C(=O)-Ar-O-CH<sub>2</sub>-), 7.77-7.74 (d, 2H, Ar-C(=O)-C(-CH=)-CH-CH=C-O-CH<sub>2</sub>-), 7.61-7.55 (t, 1H, -CH=CH-CH=C(CH=)-C(=O)-Ar-O-CH<sub>2</sub>-), 7.51-7.45 (t, 2H, -CH=CH-CH=C(CH=)-C(=O)-Ar-O-CH<sub>2</sub>-), 6.99 (d, 2H, Ar-C(=O)-C(-CH=)-CH-CH=C-O-CH<sub>2</sub>-), 4.57-4.50 (m, 2H, Ar-O-CH<sub>2</sub>-CH<sub>2</sub>-O-P(=O)-), 4.49-4.35 (m, 4H, -O-CH<sub>2</sub>-CH<sub>2</sub>-O-P(=O)-O-CH<sub>2</sub>-CH<sub>2</sub>-), 4.28 (t, 2H, Ar-O-CH<sub>2</sub>-CH<sub>2</sub>-O-P(=O)-).  $^{13}\text{C}\{\text{H}\}$  NMR (76 MHz,  $\text{CDCl}_3$ ):  $\delta$  [ppm] 132.54 (Ar-C(=O)-Ar-O-), 132.00 (Ar-C(=O)-Ar-O-), 129.74 (Ar-C(=O)-Ar-O-), 128.22 (Ar-C(=O)-Ar-O-), 114.16 (Ar-C(=O)-Ar-O-), 67.00 (d, -Ar-O-CH<sub>2</sub>-), 66.72 (d, -Ar-O-CH<sub>2</sub>-CH<sub>2</sub>-O-P-), 66.005 (d, -O-CH<sub>2</sub>-CH<sub>2</sub>-O-P).  $^{31}\text{P}\{\text{H}\}$  NMR (121 MHz,  $\text{CDCl}_3$ ):  $\delta$  [ppm] 17.90. FTIR ( $\text{cm}^{-1}$ ): 3068-2919 (-CH<sub>2</sub>- and -CH= stretching), 1643 (C=C stretching), 1601 (diaryl-C=O), 1576 (=CH- stretching), 1505 (=CH- stretching), 1457 (-CH<sub>2</sub>- deformation), 1444 (O-CH<sub>2</sub>- deformation), 1418, 1363, 1308, 1284 (P=O stretching), 1249, 1174, 1148, 1115, 1085,

1058, 1025 (P-O-C stretching), 998 (P-O-C stretching), 930, 920, 868, 844 (P-O-C stretching), 794, 774, 739 (monosubst. aryl), 703, 694 (-CH<sub>2</sub>- rocking).

*2-pentyloxy-2-oxo-1,3,2-dioxaphospholane (PEP, 3)*: The monomer was synthesized according to a modified literature protocol for EEP<sup>9</sup>. Briefly, a flame-dried 500 mL three-neck flask, equipped with a dropping funnel, was charged with a solution of dry 1-pentanol (12.37 g, 0.14 mol, 1eq.) and dry triethylamine (14.21 g, 0.14 mol, 1eq.) in dry THF (100 mL). 2-chloro-2-oxo-1,3,2-dioxaphospholane (20.00 g, 0.14 mol, 1eq.) dissolved in dry THF (50 mL) was added dropwisely to the stirring solution at 0 °C under argon atmosphere. During reaction, hydrogen chloride was formed and precipitated as triethylammonium hydrochloride. The reaction was stirred at 0 °C for 4h and stored at -20 °C overnight. The salt was removed by filtration with a Schlenk-frit and the filtrate concentrated *in vacuo*. The residue was purified by distillation under reduced pressure to give a fraction at 110-117 °C/0.13-0.17 mbar, obtaining the clear, colorless, liquid product PEP. Yield: 20.39 g, 75%. <sup>1</sup>H-NMR (300 MHz, CDCl<sub>3</sub>): δ [ppm] 4.48-4.29 (m, 4H, O-CH<sub>2</sub>-CH<sub>2</sub>-O), 4.19-4.08 (m, 2H, CH<sub>3</sub>-CH<sub>2</sub>-CH<sub>2</sub>-CH<sub>2</sub>-CH<sub>2</sub>-O-), 1.68 (m, 2H, CH<sub>3</sub>-CH<sub>2</sub>-CH<sub>2</sub>-CH<sub>2</sub>-CH<sub>2</sub>-O-), 1.43-1.27 (m, 4H, CH<sub>3</sub>-CH<sub>2</sub>-CH<sub>2</sub>-CH<sub>2</sub>-CH<sub>2</sub>-O-), 0.89 (t, 3H, CH<sub>3</sub>-CH<sub>2</sub>-CH<sub>2</sub>-CH<sub>2</sub>-CH<sub>2</sub>-O-). <sup>13</sup>C{H}-NMR (76 MHz, CDCl<sub>3</sub>): δ [ppm] 69.14 (d, -P-O-CH<sub>2</sub>-CH<sub>2</sub>-CH<sub>2</sub>-CH<sub>2</sub>-CH<sub>3</sub>), 65.93 (d, -O-CH<sub>2</sub>-CH<sub>2</sub>-O-P-), 29.98 (d, -P-O-CH<sub>2</sub>-CH<sub>2</sub>-CH<sub>2</sub>-CH<sub>2</sub>-CH<sub>3</sub>), 27.44 (-P-O-CH<sub>2</sub>-CH<sub>2</sub>-CH<sub>2</sub>-CH<sub>2</sub>-CH<sub>3</sub>), 22.14 (-P-O-CH<sub>2</sub>-CH<sub>2</sub>-CH<sub>2</sub>-CH<sub>2</sub>-CH<sub>3</sub>), 13.89 (-P-O-CH<sub>2</sub>-CH<sub>2</sub>-CH<sub>2</sub>-CH<sub>2</sub>-CH<sub>3</sub>). <sup>31</sup>P{H}-NMR (121 MHz, CDCl<sub>3</sub>): δ [ppm] 17.59. FTIR (cm<sup>-1</sup>): 2958 (-CH<sub>2</sub>- and -CH<sub>3</sub> stretching), 2932 (-CH<sub>2</sub>- and -CH<sub>3</sub> stretching), 2873 (-CH<sub>2</sub>- and -CH<sub>3</sub> stretching), 1469 (O-CH<sub>2</sub>-deformation), 1367 (-CH<sub>3</sub> deformation), 1285 (P=O stretching), 1222, 1151 (-CH<sub>3</sub> rocking), 1121, 1019 (P-O-C stretching), 1005 (P-O-C stretching), 927, 834 (P-O-C stretching), 754 (-CH<sub>2</sub>- rocking), 725.

*General procedure for copolymerizations*: The polymerization was conducted according to literature procedures for other cyclic phosphate monomers.<sup>15</sup> Exemplarily for **P1**: EEP (993 mg, 6.53 mmol), BeEP (128 mg, 368 μmol) and TU (136 mg, 368 μmol, 5.3 mol% to monomer) were introduced into a tube. A stock solution of DBU in dry DCM (56 mg/0.2mL, 368 μmol, 5.3 mol% to monomer) and a stock solution of the initiator (2-(benzyloxy)ethanol) in dry DCM (7 mg/0.5 mL, 46 μmol) were prepared and 1 mL dry DCM was added to EEP, BeEP and TU to give a total concentration of ca. 4 mol/L. All solutions were cooled down to 0 °C. 0.5 mL of the stock solution of the initiator was added to the stirred solution of EEP, BeEP and TU. The polymerization was started by rapid addition of 0.2 mL stock solution of DBU to the reaction mixture. The polymerization was terminated after 120 min by the addition of an excess of acetic acid in DCM. DCM were added and washed with acidic HCl-solution once. The organic phase was then extracted with water (3 times) until the aqueous solution exhibited a neutral pH. The organic phase was concentrated, 2 mL DCM added and the polymer precipitated into 40 mL ice-cold diethyl ether once. The suspension was

centrifuged for 15 min (4000rpm, 4 °C) and after that the supernatant was decanted. The polymer was dried *in vacuo* to give the final product.

**P1:** EEP (993 mg, 6.53 mmol, 142 eq.), BeEP (128 mg, 368  $\mu$ mol, 8 eq.), DBU (56 mg, 368  $\mu$ mol, 8 eq.), TU (136 mg, 368  $\mu$ mol, 8 eq.), initiator (7 mg, 46  $\mu$ mol, 1 eq.). Yield: 921 mg, 80%.  $M_n$ (NMR): 38,600 g/mol.  $^1\text{H-NMR}$  (300 MHz, DMSO- $d_6$ ):  $\delta$  [ppm] 7.76-7.53 (m, 86H Ar-C(=O)-Ar-O-CH<sub>2</sub>-CH<sub>2</sub>-O-P-), 7.33 (m, 5H, Ar-, initiator), 7.14-7.08 (m, 22H, Ar-C(=O)-Ar-O-CH<sub>2</sub>-CH<sub>2</sub>-O-P-), 4.47-3.84 (m, 1450H, Ar-C(=O)-Ar-O-CH<sub>2</sub>-CH<sub>2</sub>-O-P-, -P-O-CH<sub>2</sub>-CH<sub>3</sub>), -O-CH<sub>2</sub>-CH<sub>2</sub>-O-, backbone), 1.26 (t, 676, -CH<sub>3</sub>).  $^{31}\text{P}\{\text{H}\}$ NMR (121 MHz, DMSO- $d_6$ ):  $\delta$  [ppm] -1.24, -0.99.

**P2:** EEP (881 mg, 5.80 mmol, 126 eq.), BeEP (128 mg, 368  $\mu$ mol, 8 eq.), PEP (143 mg, 736  $\mu$ mol, 16 eq.), DBU (56 mg, 368  $\mu$ mol, 8 eq.), TU (136 mg, 368  $\mu$ mol, 8 eq.), initiator (7 mg, 46  $\mu$ mol, 1 eq.). Yield: 1002 mg, 83%.  $M_n$ (NMR): 21,000 g/mol.  $^1\text{H-NMR}$  (300 MHz, DMSO- $d_6$ ):  $\delta$  [ppm] 7.76-7.52 (m, 58H Ar-C(=O)-Ar-O-CH<sub>2</sub>-CH<sub>2</sub>-O-P-), 7.33 (m, 5H, Ar-, initiator), 7.14-7.05 (m, 16H, Ar-C(=O)-Ar-O-CH<sub>2</sub>-CH<sub>2</sub>-O-P-), 4.47-3.87 (m, 847H, Ar-C(=O)-Ar-O-CH<sub>2</sub>-CH<sub>2</sub>-O-P-, -P-O-CH<sub>2</sub>-CH<sub>3</sub>, -P-O-CH<sub>2</sub>-CH<sub>2</sub>-CH<sub>2</sub>-CH<sub>2</sub>-CH<sub>3</sub>, -O-CH<sub>2</sub>-CH<sub>2</sub>-O-, backbone), 1.70-1.51 (m, 30H, -P-O-CH<sub>2</sub>-CH<sub>2</sub>-CH<sub>2</sub>-CH<sub>2</sub>-CH<sub>3</sub>), 1.35-1.16 (m, 404H, -P-O-CH<sub>2</sub>-CH<sub>2</sub>-CH<sub>2</sub>-CH<sub>2</sub>-CH<sub>3</sub>, -P-O-CH<sub>2</sub>-CH<sub>3</sub>), 0.87 (t, 42H, -P-O-CH<sub>2</sub>-CH<sub>2</sub>-CH<sub>2</sub>-CH<sub>2</sub>-CH<sub>3</sub>).  $^{31}\text{P}\{\text{H}\}$ NMR (121 MHz, DMSO- $d_6$ ):  $\delta$  [ppm] -1.24, -1.14, -0.98, -0.89.

**P3:** EEP (268 mg, 1.76 mmol, 134 eq.), BeEP (37 mg, 105  $\mu$ mol, 8 eq.), EBP (22 mg, 105  $\mu$ mol, 8 eq.), DBU (16 mg, 105  $\mu$ mol, 8 eq.), TU (39 mg, 105  $\mu$ mol, 8 eq.), initiator (2 mg, 13  $\mu$ mol, 1 eq.). Yield: 269 mg, 82%.  $M_n$ (NMR): 28,600 g/mol.  $^1\text{H-NMR}$  (500 MHz, DMSO- $d_6$ ):  $\delta$  [ppm] 7.78-7.51 (m, 48H Ar-C(=O)-Ar-O-CH<sub>2</sub>-CH<sub>2</sub>-O-P-), 7.33 (m, 5H, Ar-, initiator), 7.16-7.06 (m, 13H, Ar-C(=O)-Ar-O-CH<sub>2</sub>-CH<sub>2</sub>-O-P-), 4.42-3.99 (m, 1051H, Ar-C(=O)-Ar-O-CH<sub>2</sub>-CH<sub>2</sub>-O-P-, -P-O-CH<sub>2</sub>-CH<sub>3</sub>, -O-CH<sub>2</sub>-CH<sub>2</sub>-O-, backbone), 3.99-3.87 (m, 34H, -P-O-CH<sub>2</sub>-CH-(CH<sub>2</sub>-CH<sub>3</sub>)<sub>2</sub>), 1.36-1.29 (m, 17H, -P-O-CH<sub>2</sub>-CH-(CH<sub>2</sub>-CH<sub>3</sub>)<sub>2</sub>), 1.26 (m, 479H, -P-O-CH<sub>2</sub>-CH-(CH<sub>2</sub>-CH<sub>3</sub>)<sub>2</sub>, -P-O-CH<sub>2</sub>-CH<sub>3</sub>), 0.86 (t, 72H, -P-O-CH<sub>2</sub>-CH-(CH<sub>2</sub>-CH<sub>3</sub>)).  $^{31}\text{P}\{\text{H}\}$ NMR (202 MHz, DMSO- $d_6$ ):  $\delta$  [ppm] -1.25, -1.01, -0.99.

**P4:** EEP (881 mg, 5.80 mmol, 126 eq.), BeEP (128 mg, 368  $\mu$ mol, 8 eq.), FEP (183 mg, 736  $\mu$ mol, 16 eq.), DBU (56 mg, 368  $\mu$ mol, 8 eq.), TU (136 mg, 368  $\mu$ mol, 8 eq.), initiator (7 mg, 46  $\mu$ mol, 1 eq.). Yield: 907 mg, 76%.  $M_n$ (NMR): 34,500 g/mol.  $^1\text{H-NMR}$  (300 MHz, DMSO- $d_6$ ):  $\delta$  [ppm] 7.76-7.52 (m, 108H Ar-C(=O)-Ar-O-CH<sub>2</sub>-CH<sub>2</sub>-O-P-, -P-CH<sub>2</sub>-CH<sub>2</sub>-O-CH<sub>2</sub>-C-O-CH=CH-CH=), 7.33 (m, 5H, Ar-, initiator), 7.14-7.05 (m, 22H, Ar-C(=O)-Ar-O-CH<sub>2</sub>-CH<sub>2</sub>-O-P-), 6.43 (s, 44H, -P-CH<sub>2</sub>-CH<sub>2</sub>-O-CH<sub>2</sub>-C-O-CH=CH-CH=), 4.45 (s, 53H, -P-CH<sub>2</sub>-CH<sub>2</sub>-O-CH<sub>2</sub>-C-O-CH=CH-CH=), 4.27-3.88 (m, 1167H, Ar-C(=O)-Ar-O-CH<sub>2</sub>-CH<sub>2</sub>-O-P-, -P-O-CH<sub>2</sub>-CH<sub>3</sub>, -P-CH<sub>2</sub>-CH<sub>2</sub>-O-CH<sub>2</sub>-C-O-CH=CH-CH=, -O-CH<sub>2</sub>-CH<sub>2</sub>-O-, backbone), 3.59 (s, 107H, -P-CH<sub>2</sub>-CH<sub>2</sub>-O-CH<sub>2</sub>-C-O-CH=CH-CH=), 1.26 (t, 494H, -P-O-CH<sub>2</sub>-CH<sub>3</sub>).  $^{31}\text{P}\{\text{H}\}$ NMR (121 MHz, DMSO- $d_6$ ):  $\delta$  [ppm] -1.29- -1.18, -0.98, -0.89.

**P5:** EEP (881 mg, 5.80 mmol, 126 eq.), BeEP (128 mg, 368  $\mu$ mol, 8 eq.), BuEP (131 mg, 736  $\mu$ mol, 16 eq.), DBU (56 mg, 368  $\mu$ mol, 8 eq.), TU (136 mg, 368  $\mu$ mol, 8 eq.), initiator (7 mg, 46  $\mu$ mol,

1 eq.). Yield: 1048 mg, 84%.  $M_n$ (NMR): 46,300 g/mol.  $^1\text{H-NMR}$  (300 MHz,  $\text{DMSO-}d_6$ ):  $\delta$  [ppm] 7.79-7.49 (m, 95H  $\text{Ar-C(=O)-Ar-O-CH}_2\text{-CH}_2\text{-O-P-}$ ), 7.33 (m, 5H,  $\text{Ar-}$ , initiator), 7.16-7.05 (m, 25H,  $\text{Ar-C(=O)-Ar-O-CH}_2\text{-CH}_2\text{-O-P-}$ ), 5.87-5.72 (m, 20H,  $\text{-P-O-CH}_2\text{-CH}_2\text{-CH=CH}_2$ ), 5.17-5.06 (m, 51H,  $\text{-P-O-CH}_2\text{-CH}_2\text{-CH=CH}_2$ ), 4.46-3.88 (m, 1720H,  $\text{Ar-C(=O)-Ar-O-CH}_2\text{-CH}_2\text{-O-P-}$ ,  $\text{-P-O-CH}_2\text{-CH}_3$ ,  $\text{-P-O-CH}_2\text{-CH}_2\text{-CH=CH}_2$ ,  $\text{-O-CH}_2\text{-CH}_2\text{-O-}$ , backbone), 2.44-2.32 (m, 61H,  $\text{-P-O-CH}_2\text{-CH}_2\text{-CH=CH}_2$ ), 1.26 (t, 729H,  $\text{-P-O-CH}_2\text{-CH}_3$ ).  $^{31}\text{P}\{\text{H}\}\text{NMR}$  (121 MHz,  $\text{DMSO-}d_6$ ):  $\delta$  [ppm] -1.28, -1.24, -0.99.

**P6:** EEP (937 mg, 6.16 mmol, 134 eq.), BuEP (131 mg, 736  $\mu\text{mol}$ , 16 eq.), DBU (56 mg, 368  $\mu\text{mol}$ , 8 eq.), TU (136 mg, 368  $\mu\text{mol}$ , 8 eq.), initiator (7 mg, 46  $\mu\text{mol}$ , 1 eq.). Yield: 942 mg, 85%.  $M_n$ (NMR): 28,100 g/mol.  $^1\text{H-NMR}$  (300 MHz,  $\text{DMSO-}d_6$ ):  $\delta$  [ppm] 7.34 (m, 5H,  $\text{Ar-}$ , initiator), 5.87-5.72 (m, 24H,  $\text{-P-O-CH}_2\text{-CH}_2\text{-CH=CH}_2$ ), 5.20-5.05 (m, 43H,  $\text{-P-O-CH}_2\text{-CH}_2\text{-CH=CH}_2$ ), 4.51 (s, 2H,  $\text{Ar-CH}_2\text{-O-}$ , initiator), 4.26-3.98 (m, 1058H,  $\text{-P-O-CH}_2\text{-CH}_3$ ,  $\text{-P-O-CH}_2\text{-CH}_2\text{-CH=CH}_2$ ,  $\text{-O-CH}_2\text{-CH}_2\text{-O-}$ , backbone), 2.42-2.38 (q, 46H,  $\text{-P-O-CH}_2\text{-CH}_2\text{-CH=CH}_2$ ), 1.26 (t, 468H,  $\text{-P-O-CH}_2\text{-CH}_3$ ).  $^{31}\text{P}\{\text{H}\}\text{NMR}$  (121 MHz,  $\text{DMSO-}d_6$ ):  $\delta$  [ppm] -1.27, -1.24, -0.98.

**P1, P2, P4, P5:** FTIR ( $\text{cm}^{-1}$ ): 3660-3358 (O-H stretching), 2983 ( $\text{-CH}_2\text{-}$  and  $\text{-CH}_3$  stretching), 2957 ( $\text{-CH}_2\text{-}$  and  $\text{-CH}_3$  stretching), 2911 ( $\text{-CH}_2\text{-}$  and  $\text{-CH}_3$  stretching), 1652 (diaryl-C=O), 1601 (C=C stretching), 1508 (C=C stretching), 1454 ( $\text{-CH}_2\text{-}$  deformation), 1394 (O- $\text{CH}_2\text{-}$  deformation), 1372 ( $\text{-CH}_3$  deformation), 1267 (P=O stretching), 1167 ( $\text{-CH}_3$  rocking), 1123 ( $\text{-CH}_3$  rocking), 1015 (P-O-C stretching), 958 (P-O-C stretching), 797 (O- $\text{CH}_2\text{-}$  stretching), 742 ( $\text{-CH}_2\text{-}$  rocking), 704, 683.

**P6:** FTIR ( $\text{cm}^{-1}$ ): 3660-3358 (O-H stretching), 2983 ( $\text{-CH}_2\text{-}$  and  $\text{-CH}_3$  stretching), 2957 ( $\text{-CH}_2\text{-}$  and  $\text{-CH}_3$  stretching), 2911 ( $\text{-CH}_2\text{-}$  and  $\text{-CH}_3$  stretching), 1642 (C=C stretching), 1454 ( $\text{-CH}_2\text{-}$  deformation), 1394 (O- $\text{CH}_2\text{-}$  deformation), 1372 ( $\text{-CH}_3$  deformation), 1267 (P=O stretching), 1167 ( $\text{-CH}_3$  rocking), 1123 ( $\text{-CH}_3$  rocking), 1015 (P-O-C stretching), 958 (P-O-C stretching), 797 (O- $\text{CH}_2\text{-}$  stretching), 738 ( $\text{-CH}_2\text{-}$  rocking), 704, 683.

*Pre-functionalization of Si Surfaces.* To obtain wafers which were exclusively benzophenone-functionalized, a solution of 4-(3-triethoxysilyl)propyloxybenzophenone (50 mM) in toluene was spin coated on a Si wafer at 1000 rpm, 1000 rpm/sec for 120 s. The wafer was cured for 45 min at 120 °C on a hot plate, washed with toluene, and dried under a continuous nitrogen flow. It was cut into 1.5x1.5 cm sized substrates with a diamond cutter. Pre-functionalized Si wafer with a benzophenone/amine ratio of 1:1 were obtained in a similar way: 33.4 mg of (3-aminopropyl)triethoxysilane were added to 3mL of a solution of 4-(3-triethoxysilyl)propyloxybenzophenone (50 mM) in toluene. The solution was spin-coated on the Si wafer at 3000 rpm, 1000 rpm/sec for 120 s and the wafer treated as described above.

For pre-functionalization with trimethox(propyl)silane and (3-aminopropyl)triethoxysilane, ethanol solutions with a total concentration of 50 mM were prepared: (a) propyl/amine ratio of 5:1, 20.5 mg (0.125 mmol, 5 eq.) trimethox(propyl)silane and 5.5 mg (0.0249 mmol, 1 eq.)

(3-aminopropyl)triethoxysilane in 3 mL ethanol; (b) propyl/amine ratio of 2:1, 16.4 mg (0.099 mmol, 2 eq.) trimethox(propyl)silane and 11.1 mg (0.050 mmol, 1 eq.) (3-aminopropyl)triethoxysilane in 3 mL ethanol; (c) propyl/amine ratio of 1:1, 12.3 mg (0.075 mmol, 1 eq.) trimethox(propyl)silane and 16.6 mg (0.075 mmol, 1 eq.) (3-aminopropyl)triethoxysilane in 3 mL ethanol. The Si wafer was cut in 1.5x1.5 cm sized substrates and a solution of (a), (b) or (c) was spin coated on the substrates at 1000 rpm, 1000 rpm/sec for 30 sec. The substrates were cured for 45 min at 120 °C on a hot plate, washed with DCM, and dried under a continuous nitrogen flow.

Pre-functionalization with 3-butenyltriethoxysilane and (3-aminopropyl)triethoxysilane was achieved in the same way with a total concentration of 50 mM in ethanol with different butenyl/amine ratios of 5:1, 2:1, and 1:1.

*Immobilization of PPE-Networks on Silicon Substrates:* The polymers were dissolved in chloroform with a concentration of 50 mg/mL (30, 20 or 10 mg/mL) and filtered with a syringe filter (Chromafil® Xtra H-PTFE-20/0.2 µm, Ø 25 mm from Macherey-Nagel, or Millex-LCR filter, hydrophilic PTFE, 0.45 µm, 13 mm from Merck). A polymer film was spin-coated from this solution onto the prefunctionalized silicon substrates at 3000 rpm, 1000 rpm/sec for 30 s. The PPE-films were directly crosslinked at 254 nm for 30 min in a UV-box. They were washed with DCM to remove unattached polymer chains (for at least 30 min or overnight) and dried under a continuous nitrogen flow. Polymer **P6** was dissolved in chloroform with a concentration of 50 mg/mL and the tetrathiol crosslinker (1 eq. thiol groups to 1 eq. alkene groups in the polymer) added. The films were coated and treated as described above.

*Post-Modification of P4-Network:* A silicon substrate with a **P4**-network was deposited in 1.5 mL solution of 125 mg 1-dodecyl-1H-pyrrole-2,5-dione in chloroform for 4 h at 60 °C. The substrate was washed with DCM for 18 h to remove unattached 1-dodecyl-1H-pyrrole-2,5-dione and dried under a continuous nitrogen flow.

*Post-Modification of P5-Network:* A silicon substrate with a **P5**-network was dipped in a solution of dodecylmercaptane in chloroform (1:9) and irradiated for 30 min in a UV-box. The substrate was washed with DCM for 1 h to remove unattached dodecylmercaptane and dried under a continuous nitrogen flow.

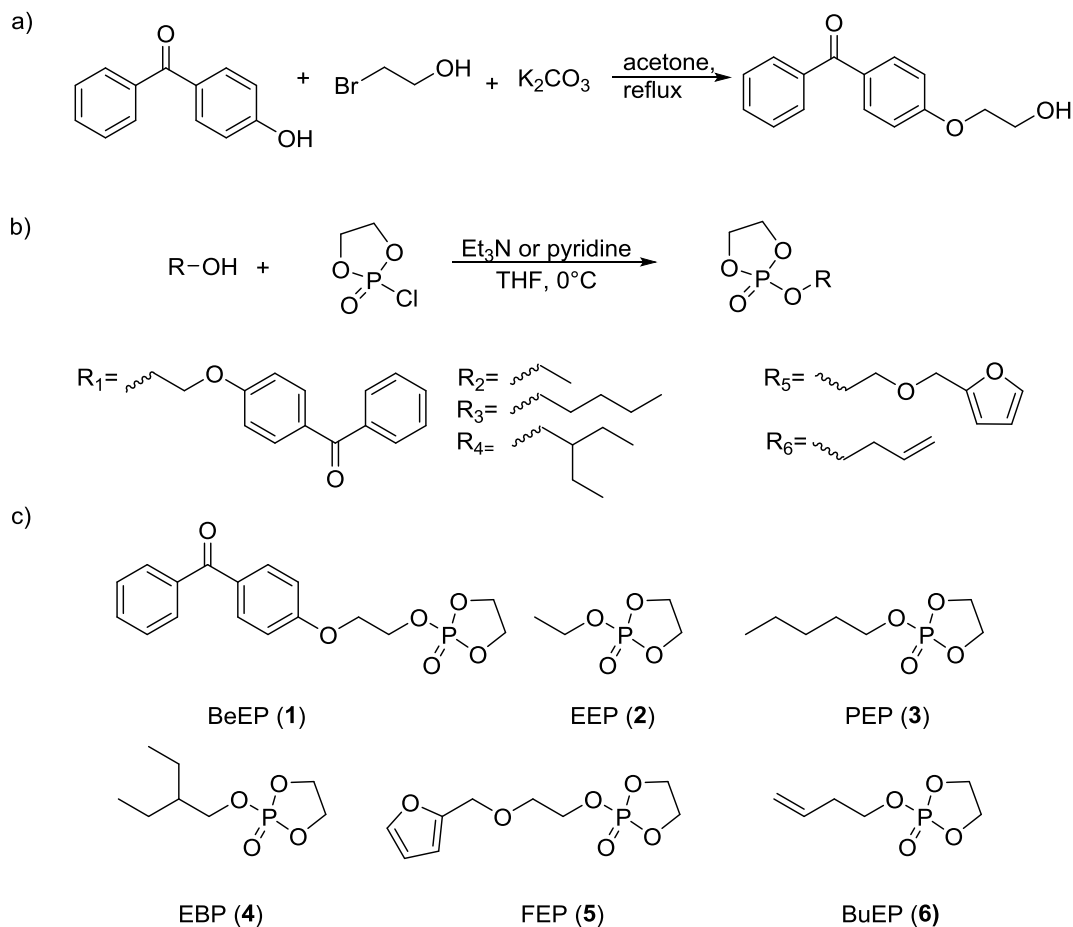
*Pre-crosslinking of P5:* 50 mg ( $1.08 \cdot 10^{-6}$  mol) polymer were dissolved in 1 mL toluene/DCM (8:2). AIBN and tetrathiol stock solutions in toluene were prepared and 0.02 mL of each added to the solution. The ratios of alkene/thiol/AIBN were adjusted to 100:1:1 and 10:1:1. The mixture was stirred for 18 h at 100 °C. It was dissolved in about 2 mL DCM, precipitated into diethyl ether and centrifuged (4000 rpm, 15 min, 4 °C). The supernatant was decanted and the polymer dried *in vacuo*. Yield: 29-34 mg, 58-68%. For the ratio of alkene/thiol/AIBN 1:1:1, 150 mg **P5** was dissolved

in 0.5 mL DMF, tetrathiol and AIBN added and stirred at 90 °C for 18 h. The reaction was worked up as described above. Yield: 110 mg, 73%.

## 5.4 Results and Discussion

**Monomer Syntheses.** The synthesis of the phosphate monomer carrying a benzophenone group is presented Scheme 5.2. This bifunctional molecule contains a cyclic phosphate group that can undergo ring-opening polymerization (ROP), and the UV-reactive benzophenone residue which can act as a crosslinker, but is inert during the ROP. The cyclic monomer 2-(2-(benzophenone-4-oxo)ethoxy)-2-oxo-1,3,2-dioxaphospholane (**BeEP**, **1**) was prepared in two steps, starting from 4-hydroxybenzophenone. This phenol was transformed to the aliphatic alcohol 4-(2-hydroxyethoxy)benzophenone by reaction with 2-bromoethanol and potassium carbonate (Scheme 5.2a).<sup>16</sup> The resulting alcohol was reacted with 2-chloro-2-oxo-1,3,2-dioxaphospholane (COP) to give the cyclic monomer **1** by esterification (Scheme 5.2b). The aliphatic ethylene linker was needed because 4-hydroxybenzophenone itself did not form a stable product in the esterification step. **1** was purified by column chromatography over deactivated silica to yield the pure monomer as a off-white solid. The monomer can be stored at -28 °C under dry conditions and inert gas for at least one year. The monomer was characterized by <sup>1</sup>H and <sup>31</sup>P{H} NMR spectroscopy (Figure 5.1a and S5.1-5.3). While the benzophenone group showed resonances in the aromatic region at 6.99-7.85 ppm, signals for the dioxaphospholane ring were observed at 4.35-4.49 ppm as multiplet. The <sup>31</sup>P{H}NMR spectrum showed a singlet at 17.90 ppm, typical for cyclic phosphate monomers.<sup>15</sup>

A second monomer, 2-ethoxy-2-oxo-1,3,2-dioxaphospholane **EEP** (**2**), was synthesized according to a literature procedure (Scheme 5.2).<sup>9</sup> **EEP** forms the water-soluble polymer PEEP, which is usually used as hydrophilic building block in PPE-based drug delivery systems,<sup>17-18</sup> and was the major comonomer in the polymers synthesized in this study. Further cyclic comonomers used in this study were 2-pentyloxy-2-oxo-1,3,2-dioxaphospholane (**PEP**, **3**), 2-(2-ethylbutoxy)-2-oxo-1,3,2-dioxaphospholane (**EBP**, **4**)<sup>19</sup>, 2-(2-(furan-2-ylmethoxy)ethoxy)-2-oxo-1,3,2-dioxaphospholane (**FEP**, **5**) and 2-(but-3-en-1-yloxy)-2-oxo-1,3,2-dioxaphospholane (**BuEP**, **6**)<sup>15</sup>, and are shown in Scheme 5.2c. Monomers **3-6** were used because they contained aliphatic CH-groups and thus served as reaction partner for the benzophenone moieties. **FEP** and **BuEP** additionally carry groups that are inert under ROP conditions and therefore can be used for the post-polymerization functionalization of the polymer or polymer networks by Diels-Alder or thiolene reactions.



**Scheme 5.2.** a) Synthesis of 4-(2-hydroxyethoxy)benzophenone; b) synthesis of cyclic phosphate monomers; c) cyclic phosphate monomers used in this study.

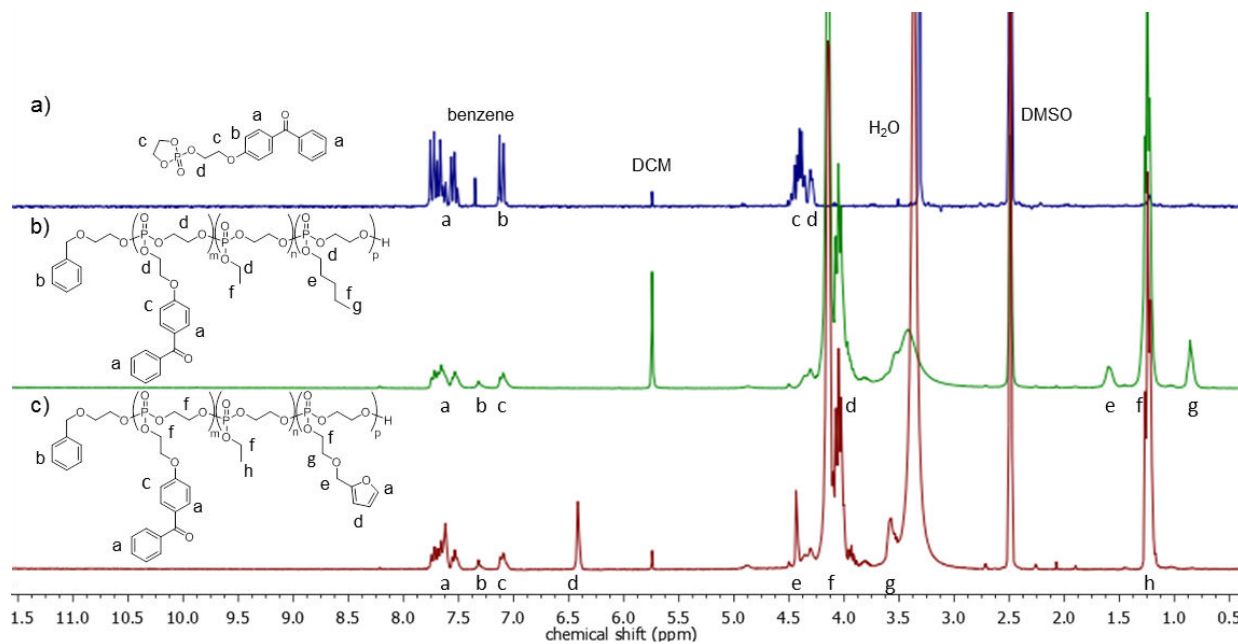
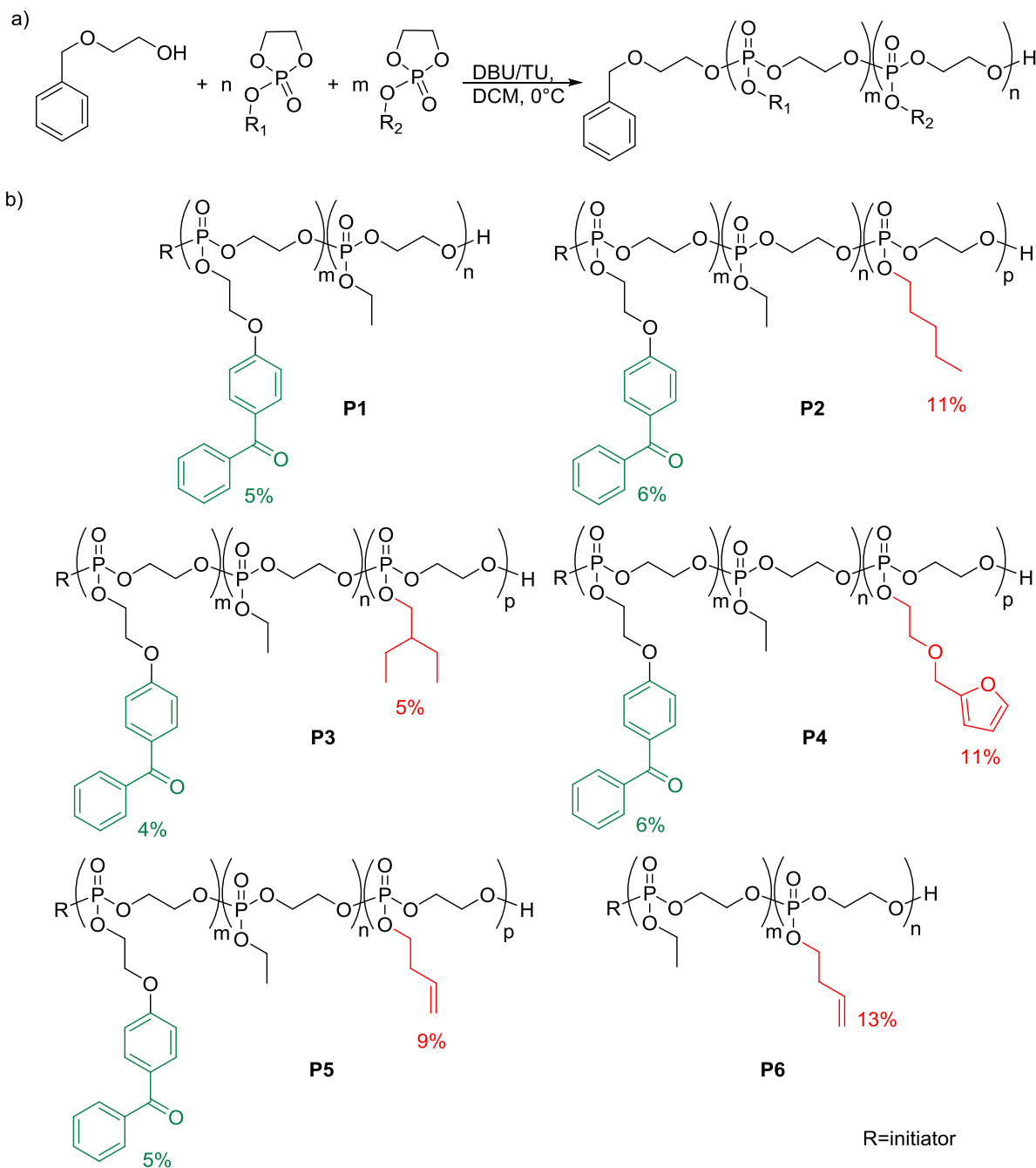


**Figure 5.1.** <sup>1</sup>H NMR spectra (300 MHz, DMSO-*d*<sub>6</sub>) of a) BeEP monomer (1), b) terpolymer **P2** and c) terpolymer **P4**.

**Polymerization.** A series of copolymers containing the cyclic phosphate monomers **BeEP** and **EEP** was investigated with respect to their polymerization behavior in the anionic ROP (Scheme 5.3a). **EEP** (**2**) was used as main comonomer due to its hydrophilic character. PPEs with a molecular weight above 20,000 g/mol and 5% benzophenone content were targeted. Higher amounts of **BeEP** tend to form hydrophobic patches within the polymer and thus decrease the hydrophilicity and potentially the protein-repellency of the PPEs. Besides the BeEP-EEP copolymer (**P1**), several terpolymers containing 5% **EBP**, 11% **PEP**, 11% **FEP** or 9% **BuEP** in addition to 5% **BeEP** and **EEP** were synthesized. These terpolymers had additional methylene groups for cross-linking and/or additional functional groups for post-polymerization functionalization (Scheme 5.3b). A copolymer (**P6**) without benzophenone was also produced, which contained 13% butenyl side chains. This functional group can be used in a similar way to the benzophenone residue: its double bonds can photo-chemically or radically be activated to react with a tetrathiol crosslinker, thereby forming networks. This could also be used to realize the surface attachment of the PPE polymers to alkenyl-functionalized surfaces. All polymerizations were carried out with 1,8-diazabicyclo[5.4.0]undec-7-ene (DBU) and *N*-cyclohexyl-*N'*-(3,5-bis(trifluoromethyl)phenyl) thiourea (TU) as catalyst system according to literature procedures<sup>15</sup> at 0 °C in dry DCM with a total monomer concentration of 4 mol/L. Successful copolymerization and formation of random copolymers was proven by SEC and <sup>31</sup>P{H} NMR measurements. An overview of all polymers obtained is given in Table 5.1. The ROP produced PPEs with narrow molecular weight distributions of  $\bar{D}$  = 1.10-1.19 (Figure 5.2a) and relatively high monomer conversions (76-84%), indicating the controlled nature of the DBU/TU catalyst system. The phosphorus signals in the <sup>31</sup>P{H} NMR spectra shifted from 16.83-17.90 ppm for the monomers to -0.89- -1.28 ppm for the polymers and confirmed polymerization (see supporting information). <sup>1</sup>H DOSY spectra confirmed the formation of copolymers (see supporting information). The aromatic protons of the initiator 2-(benzyloxy)ethanol were used for molecular weight calculations by end group analysis from <sup>1</sup>H NMR spectra. End group analysis revealed that the degree of polymerization varied from 138-282 for the polymers, i.e. molecular weights of 21,000 to 46,300 g/mol were obtained under these conditions. <sup>1</sup>H NMR spectra of **P2** and **P4** are shown in Figure 5.1b and 5.1c, all other spectra can be found in the supporting information,. The resonances of the aromatic protons of the initiator at 7.33 ppm (b) were compared with distinct resonances for the three different repeat units in the polymer: the doublet signal at 7.10 ppm (c) for the BeEP repeat unit, the signal at 1.60 ppm (e) for the PEP units in **P2** or the singlet at 6.43 ppm (d) for FEP units in **P4** and the triplet signal at 1.26 ppm (f or h) which belongs to the EEP repeat unit. The signal of the backbone and methylene groups of side chains neighboring the P-O bond at 4.50-3.80 ppm (d or f) gives the degree of polymerization and coincided with the total number of monomer repeat units. The ratios of comonomers from initial feed ratio could be retrieved in all copolymers. All copolymers exhibited  $T_g$ 's of -57 to -48 °C, typical for PPEs from ROP (Figure 5.2b).<sup>20</sup> The polymers were soluble in

organic solvents such as dichloromethane and chloroform, or polar solvents such as THF, ethanol, methanol and DMSO. They were insoluble in hexane or diethyl ether.



**Scheme 5.3.** a) Copolymerization of cyclic phosphates by ROP, b) obtained co- and terpolymers P1-P6.

**Table 5.1.** Overview of polymerizations and results.

entry	monomers	[1]/[1]/[2]/[3/4/5/6]	$DP_{th}^a$	1 /DP <sup>b</sup>	5 /%	2 /DP <sup>b</sup>	225 /%	2 /DP <sup>b</sup>	115 /%	3 /4/5/6 /DP <sup>b</sup>	15 /%	3 /4/5/6 /DP <sup>b</sup>	8 /%	5 /%	DP	yield	$M_n^b$ /g/mol	$M_w/M_n^c$	$T_g^d$ /°C
P1	1-co-2	1/8/142/-	150	12	5	225	95	-	-	-	-	237	0.80	38,600	1.16	-48			
P2	1-co-2-co-3	1/8/126/16	150	8	6	115	83	15	11	138	0.83	21,000	1.16	-58					
P3	1-co-2-co-4	1/8/134/8	150	7	4	160	91	8	5	175	0.82	28,600	1.19	-56					
P4	1-co-2-co-5	1/8/126/16	150	11	6	165	83	22	11	198	0.76	34,500	1.15	-51					
P5	1-co-2-co-6	1/8/126/16	150	13	5	243	86	26	9	282	0.84	46,300	1.16	-50					
P6	2-co-6	1/-/134/16	150	-	-	156	87	23	13	179	-	28,100	1.10	-57					

<sup>a</sup>DP= Degree of polymerization. <sup>b</sup>Determined from the <sup>1</sup>H-NMR spectra. <sup>c</sup>Determined by SEC in DMF, PEO standard, RI-signal. <sup>d</sup>Determined by DSC.

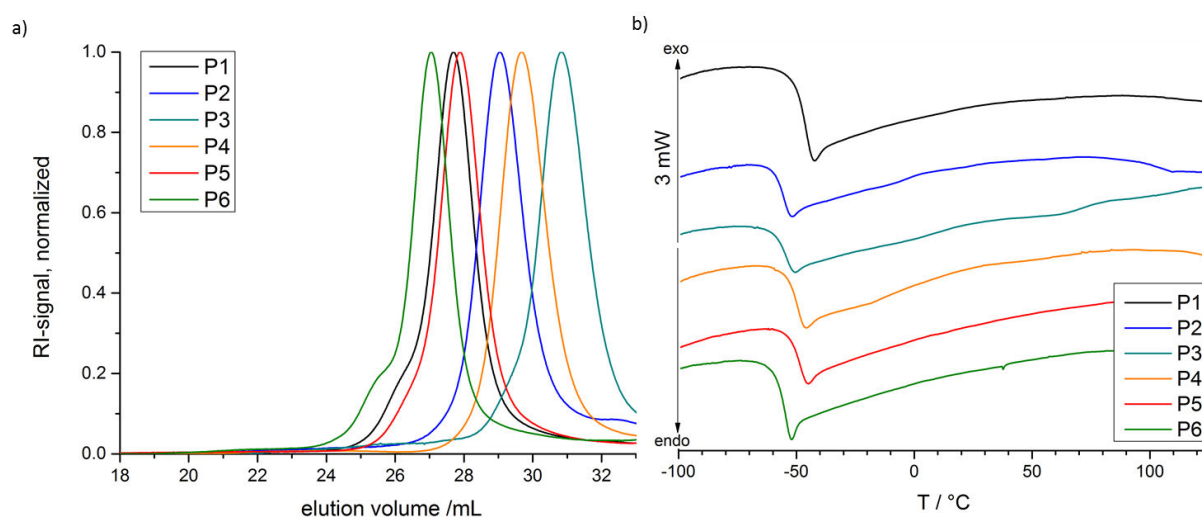


**Figure 5.2.** a) SEC elugrams of all co- and terpolymers (in DMF, PEO standard, RI-signal), b) DSC thermograms of all co- and terpolymers (heating and cooling rate 10 K min<sup>-1</sup>, 1<sup>st</sup> run).

**Copolymerization behavior.** Since an even distribution of the cross-linker groups in the polymer is important to obtain homogeneous polymer films, the copolymerization kinetics, i.e. consumption of the monomers, of **BeEP** with **EEP** and **FEP** or **PEP**, respectively, was investigated via <sup>31</sup>P{H} NMR. The initial monomer feeds for the kinetics experiments were the same as for the polymers **P1**, **P2** and **P4**: **BeEP/EEP** with a ratio of 0.05/0.95, and **BeEP/PEP/EEP** as well as **BeEP/FEP/EEP** each with ratios of 0.05/0.1/0.85. The targeted degree of polymerization was 120 for all samples. Reactions were conducted in *d*<sub>2</sub>-DCM at -20, 0 or -10 °C, respectively. All monomers had distinct signals in the <sup>31</sup>P{H} NMR spectra measured at 334 MHz (17.39 ppm for **BeEP** and 16.91 ppm for **EEP** at -20 °C for **P1** (Figure 5.3a); 17.52 ppm for **BeEP**, 17.20 ppm for **PEP** and 17.09 ppm for **EEP** at 0 °C for **P2**; 17.57 ppm for **BeEP**, 17.41 ppm for **FEP** and 17.11 ppm for **EEP** at -10 °C for **P4**). Thus, the consumption of each monomer was monitored over the course of the polymerization by determining the relative intensities of these signals (Figure S5.44-5.46). A faster incorporation of the **BeEP** and **FEP** monomer compared to **EEP** and **PEP** was observed (Figure 5.3b-d). For **P1** at 40% of total conversion, 60% of **BeEP** was consumed, while 80% of **EEP** monomer remained in the reaction mixture (Figure 5.3b). For **P2** a similar behavior was observed: after 40% conversion, 70% of **BeEP** was consumed, while 75% of **EEP** and **PEP**, respectively, remained in the reaction mixture. All **BeEP** monomer was incorporated into the polymers after about 70% of total conversion. In **P4**, again 62% of **BeEP** was consumed after 40% conversion, while 78% **EEP** remained. While **PEP** and **EEP** were incorporated in a similar ratio in **P2**, **FEP** was consumed faster in **P4** than **EEP**: 68% remained after 40% conversion. The reactions were terminated when no further consumption was detected in the NMR spectra, as increasing viscosity of the solution and lack of stirring in the NMR tube slowed down the polymerization at higher conversions. Fitting of the curves indicated the formation of copolymers with a gradient-like structure and the following reaction speeds of the monomers: **BeEP**>**FEP**>**PEP**≈**EEP**. A statistical

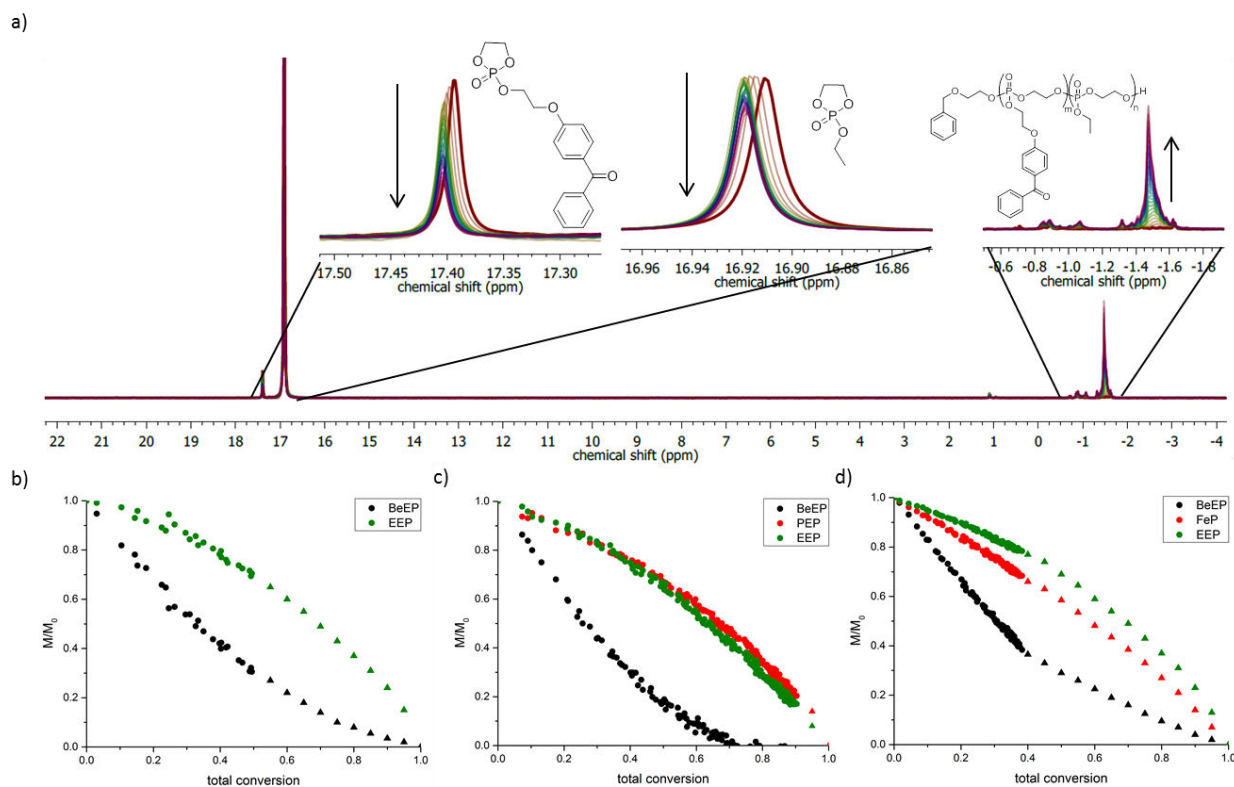


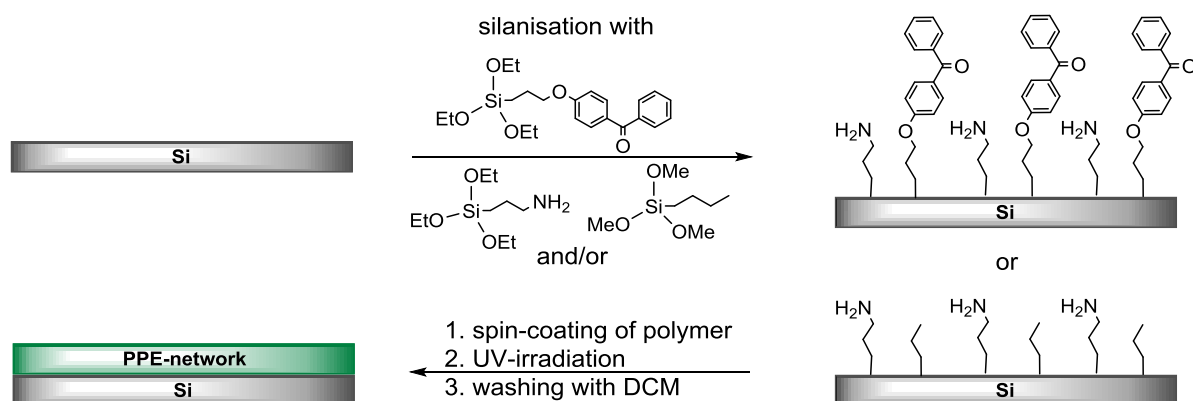
**Figure 5.3.** Simultaneous co- and terpolymerization. The monomer ratios are analog to polymers **P1**, **P2** and **P4**: a) overlay and zoom-in into real-time  $^{31}\text{P}\{\text{H}\}$  NMR measurements of copolymerization of **EEP** with **BeEP** (**P1**), b-d) normalized monomer concentrations in the reaction versus total conversion of b) **EEP** with **BeEP** (**P1**), c) **EEP** with **BeEP** and **PEP** (**P2**), d) **EEP** with **BeEP** and **FeP** (**P4**) (note: triangles are extrapolated).

incorporation of all comonomers would have been favorable for the formation of homogeneous polymer networks,

**Formation of surface-attached PPE-networks.** The formation of surface-attached PPE-networks was achieved by a C,H-insertion crosslinking reaction (CHic process).<sup>10-13</sup> First, standard silicon wafers were pre-functionalized by silanisation with benzophenone groups using 4-(3-triethoxysilyl)propoxybenzophenone (Scheme 5.4). However, these proved to be too hydrophobic for the here investigated polymers: after spin-coating of the polymer on these substrates, the initially smooth polymer films formed droplets on the surfaces immediately. Apparently, the polymers are highly hydrophilic and absorb moisture from air so fast that the viscosity of the polymer layer on the substrate decreases strongly, allowing it to adopt a thermodynamically more favorable state by avoiding contact with the hydrophobic benzophenone groups on the substrate. Therefore, the substrates were pre-functionalized differently to obtain more hydrophilic substrates: first, with a mixture of benzophenone and amino groups (3-aminopropyl chains) at a ratio of 1:1. On these substrates, films were formed, however, they were washed off after UV-irradiation, indicating insufficient network formation and surface-

attachment. Apparently, the methylene groups neighbouring phosphate groups do not seem to be accessible for the CHic reaction. To check this hypothesis, the film forming properties of the terpolymers **P2-P4** (with 5% 2-ethylbutyl, 10% pentyl or furfuryl side chains), which had significantly more aliphatic C-H groups, were tested. In line with the above hypothesis, **P2** and **P4** formed stable networks on substrates with benzophenone: amine ratio of 1:1 after UV-irradiation. After washing to remove unbound polymer, the layer thicknesses were  $164 \pm 1$  nm for **P4**, and  $78 \pm 1$  nm for **P2** (determined by ellipsometry).

**P3** (containing **EBP** units) formed a smooth layer on the pre-functionalized substrates, but after washing, the layer was removed completely. This was unexpected because the polymer contained many aliphatic CH groups; the reason for failed network formation might be insufficient surface attachment and cross-linking after UV-irradiation, due to formation of a stable tertiary radical in the side chains of **EBP** units after H-abstraction.



**Scheme 5.4.** Functionalization of silicon substrates by silanisation, spin-coating of polymer and formation of PPE-networks.

**Improvement of surface-attached PPE-networks.** Since the PPE-networks were intended as surface-coatings for biomedical devices, it would be advantageous if they could be used without a pre-functionalization step. Since polymeric materials (e.g. PMMA, poly(amide)s- or -(urethane)s) contain a high amount of aliphatic CH groups, they should be accessible for the CHic reaction, so that the PPE networks could be built directly onto these substrates. This has been shown for other polymers by R uhe and coworkers on PMMA substrates.<sup>21-22</sup> Since polymer substrates cannot be studied easily by many surface analytical techniques, this situation was modeled by pre-functionalizing standard silicon wafers via silanisation with propyl- (for the C-H groups) and 3-aminopropyl chains (to make the surface more hydrophilic) at different ratios (5:1, 2:1 and 1:1). Polymers **P2** and **P4** indeed formed surface attached networks on these substrates. With increasing hydrophilicity of the pre-functionalized substrates, the layer thickness of the coatings increased from  $132 \pm 2$  to  $199 \pm 2$  nm for **P4**, and from  $56 \pm 1$  to  $104 \pm 1$  nm for **P2** (see Table 5.2 and Figure 5.4a). This indicates that the hydrophilicity of the substrate strongly influences the thickness of

PPE-films. A layer thickness of  $263 \pm 1$  nm was observed for **P5**-networks. When multilayers of two or three films were prepared for **P2** and **P4** to obtain an overall higher film thickness on substrates pre-functionalized at a ratio of 1:1, an increase of thicknesses was observed (Table 5.2). However, the multilayers became visibly less homogeneous and were therefore not further considered in this study.

As is well known, the thickness obtained by spin-coating depends, among other parameters, on the concentration of polymer solution. The here used polymers complied with this rule, and the “master curve” for **P4** is shown in Figure 5.4b (and Table S5.1).

Besides the CHic mechanism, a thiol-ene reaction is another often used mechanism to form covalently crosslinked and surface attached polymer networks.<sup>7</sup> Alkene containing polymers can be

**Table 5.2.** Overview of layer thicknesses of PPE-networks of **P2**, **P4** and **P5** on silicon substrates and their functionalization ratios of propyl/amine groups. Films were coated from polymer solutions of 50 mg/mL in chloroform.

polymer	functionalization ratio propyl:amine	number of layers	layer thickness / nm
<b>P2</b>	5:1	1	$56 \pm 1$
<b>P2</b>	2:1	1	$86 \pm 1$
<b>P2</b>	1:1	1	$104 \pm 1$
<b>P2</b>	1:1	2	$233 \pm 20$
<b>P2</b>	1:1	3	$327 \pm 7$
<b>P4</b>	5:1	1	$132 \pm 2$
<b>P4</b>	2:1	1	$173 \pm 1$
<b>P4</b>	1:1	1	$199 \pm 2$
<b>P4</b>	1:1	2	$321 \pm 2$
<b>P4</b>	1:1	3	$434 \pm 3$
<b>P5</b>	1:1	1	$263 \pm 1$

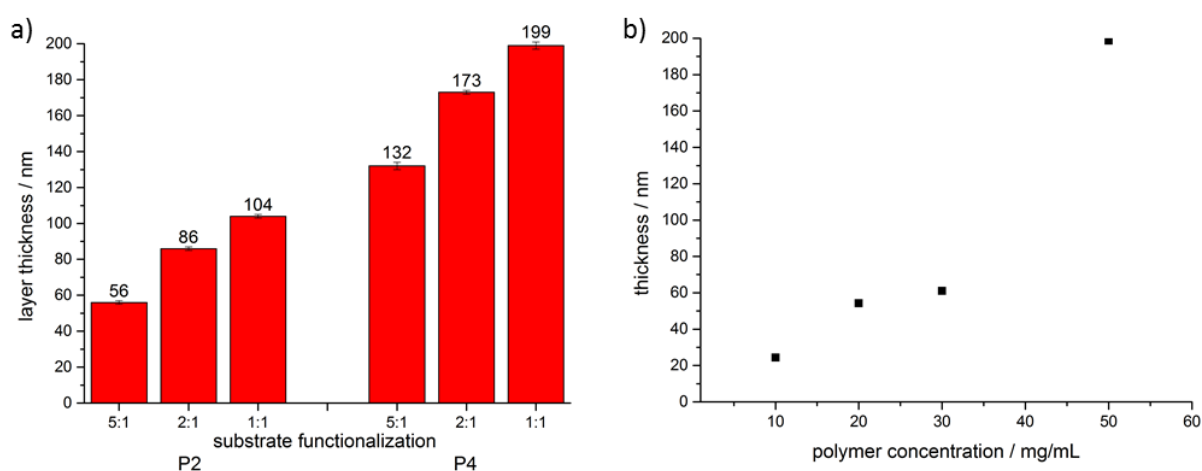
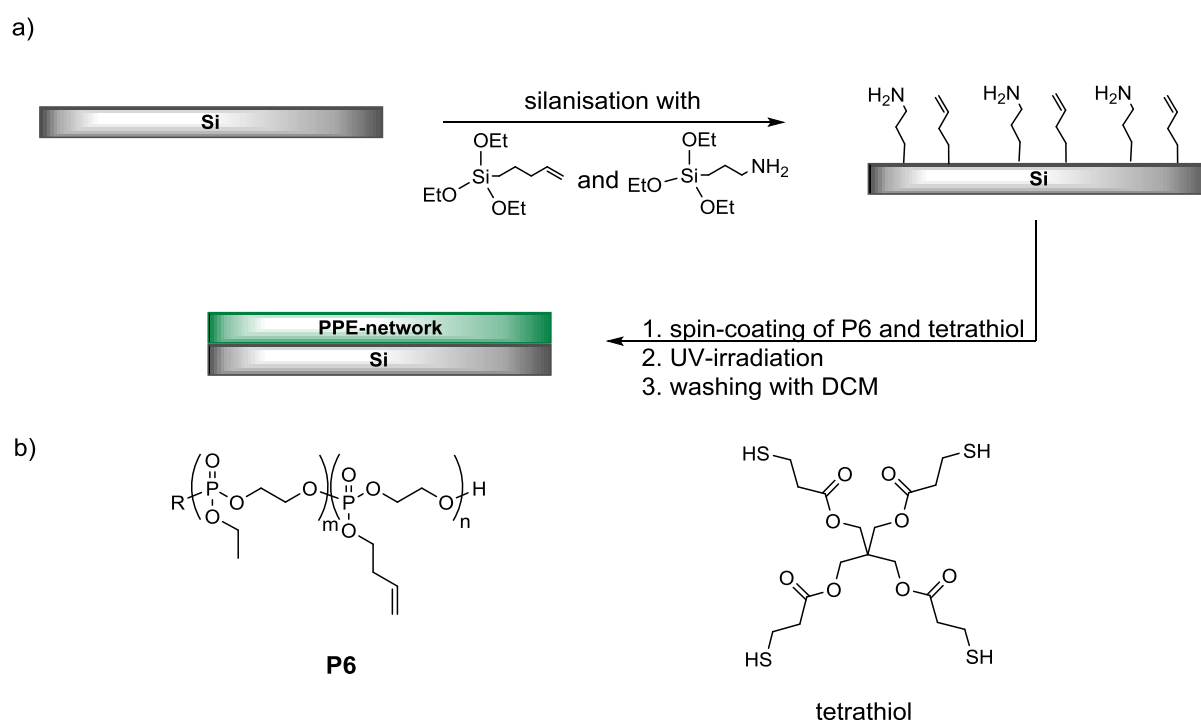


**Figure 5.4.** Overview of trends of layer thicknesses: a) from **P2** and **P4** on silicon substrates depending on the hydrophilicity of substrate; b): “master curve” layer thickness vs. concentration of polymer solution **P4** used for spin-coating.

cross-linked with a tetrathiol by adding a radical initiator or upon UV-irradiation, and can be covalently attached to surfaces pre-functionalized with alkenes by the same mechanism. It was investigated whether this approach would work for the here presented polymer **P6**, which contained 13 mol% of butenyl groups. Silicon substrates that had been pre-functionalized with 3-butenyltriethoxysilane and 3-aminopropyltriethoxysilane in different ratios (5:1, 2:1 and 1:1, Scheme 5.5a) were thus coated with a solution of **P6** and a tetrathiol (ratio alkene/thiol groups 1:1) (Scheme 5.5b). While polymer films were obtained on all substrates irrespective of the pre-functionalization ratios, they were washed off after UV-irradiation in all cases, indicating that a successful formation of the networks and sufficient surface-attachment did not take place. This approach to form PPE surface-attached networks was therefore not further considered.

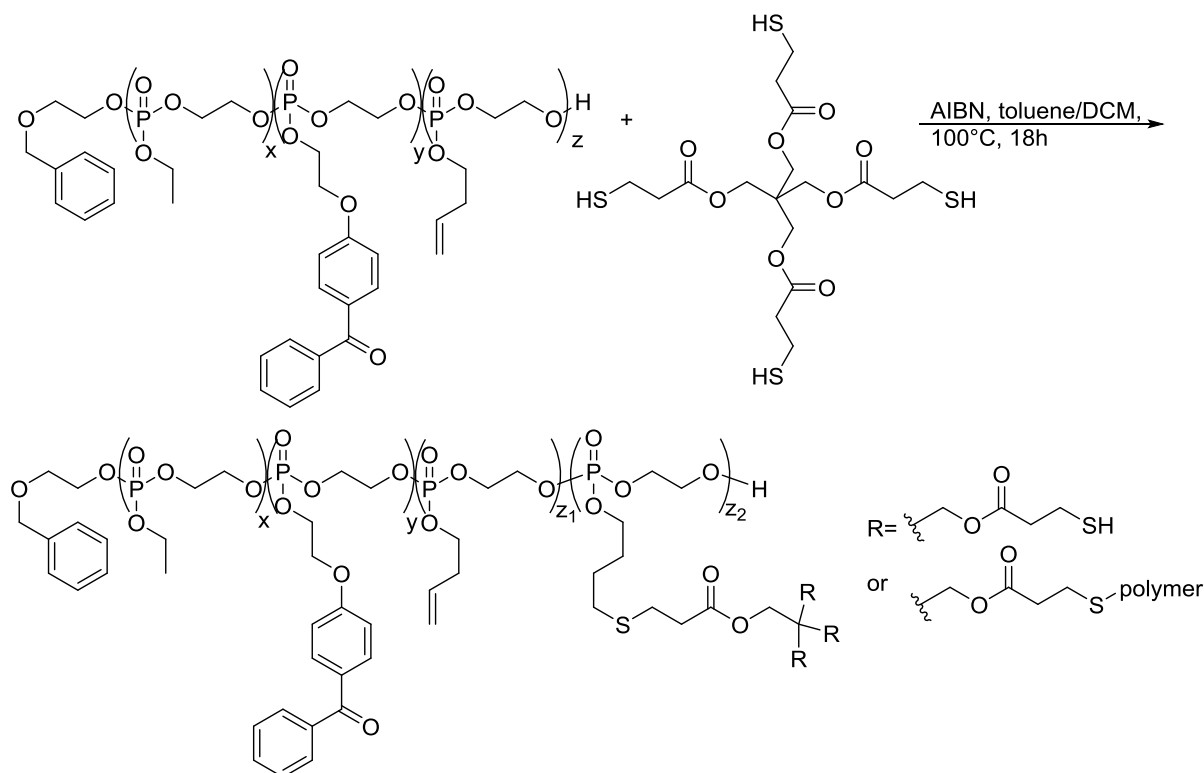


**Scheme 5.5.** a) functionalization of silicon substrates by silanisation, spin-coating of polymer and formation of PPE-networks, b) chemical structure of polymer **P6** and tetrathiol crosslinker.

As molecular weight influences the viscosity of the resulting spin coating solution, we also aimed to investigate the expected influences of molecular weight on the layer thickness of spin-coated polymer films: for higher molecular weights thicker layers are obtained when the concentration is kept constant.<sup>23</sup> Achieving increased layer thicknesses, **P5**, containing 5 mol% benzophenone and 9 mol% alkene groups, was precrosslinked with the previously used tetrathiol in a thiol-ene-reaction (Scheme 5.6). Different ratios of alkene/thiol 100:1, 10:1 and 1:1 were used and AIBN applied as initiator for the radical reaction in a ratio of 1:1 to thiol groups. <sup>1</sup>H NMR spectra and SEC measurements of **P5** and precrosslinking reactions **P5-1:1**, **P5-1:10** and **P5-1:100** are shown in the Supporting Information (Figures S5.50-5.51). The initial comonomer ratio of **BeEP**

and **BuEP** in  $^1\text{H}$  NMR spectra changed from 1:2.2 (in **P5**) only significantly for **P5-1:1** to 1:0.5 (NMR signals for **BeEP** at 6.98 ppm and for **BuEP** at 5.06-5.21 ppm were considered for calculation of comonomer ratio). Characteristic signals for the tetrathiol crosslinker overlapped with the backbone signal or appeared at 2.54-2.85 ppm, but were not integrable. For **P5-1:10** and **P5-1:100** comonomer ratios of 1:2 were observed in both cases. Findings from NMR spectra correlated with SEC measurements: in the cases of **P5-1:10** and **P5-1:100** a shift of elution volumes to higher molecular weights were not observed compared to **P5** (Figure S5.51). Polydispersity indices slightly broadened from  $D=1.16$  for **P5**, to 1.23 and 1.25 for **P5-1:10** and **P5-1:100**, respectively, presumably due to transesterification reactions under the chosen conditions. For **P5-1:1** instead, a significant broadening of the PDI was detected,  $D=1.86$ , as expected, with a shoulder to higher and tailoring to lower molecular weights. However, a shift of the elution maximum to higher molecular weights was not observed as expected. The shoulder indicates formation of some intermolecular precrosslinked polymers, tailoring indicates intramolecular reaction, rather than crosslinking. Both, the polymers and crosslinker, are flexible molecules, and therefore intramolecular reaction seems to occur under the chosen conditions. A further, less diluted reaction approach did not improve the results. The approach of precrosslinking the polymers to obtain higher molecular weights for spin-coating, was therefore not further considered in this study.

**Physical Characterization.** The physical properties of the surface-attached networks of **P2**, **P4** and **P5** on Si wafers (pre-functionalized with a propyl/amine ratio of 1:1, one layer) were



**Scheme 5.6.** Reaction scheme for precrosslinking of **P5** with a tetrathiol crosslinker.

thoroughly characterized. Besides the thickness, measured by ellipsometry (Figure 5.4 and Table 5.2) contact angle measurements were performed, and revealed that the materials were highly hydrophilic surfaces, with static contact angles of 21, 26 and 26 ° for **P2**, **P4** and **P5**, respectively (Figure 5.5, Table 5.3 and Table S5.2). The main comonomer **EEP** is known to produce hydrophilic PPEs. Atomic force microscopy was used to investigate the morphology of the **P2**- and **P4**-networks. Height images (Figure 5.5) showed a homogeneous morphology of the networks with an average roughness of 0.40 nm for **P2** and 0.68 nm for **P4**. Networks of **P4** showed nanosized pinholes, probably to minimize the contact area with the comparatively hydrophobic substrate surface. All AFM images were measured in the ScanAsyst mode, because the networks strongly interacted with the cantilever. This could be because they are strongly hydroscopic, and a thin water layer on the surface made them adhesive.

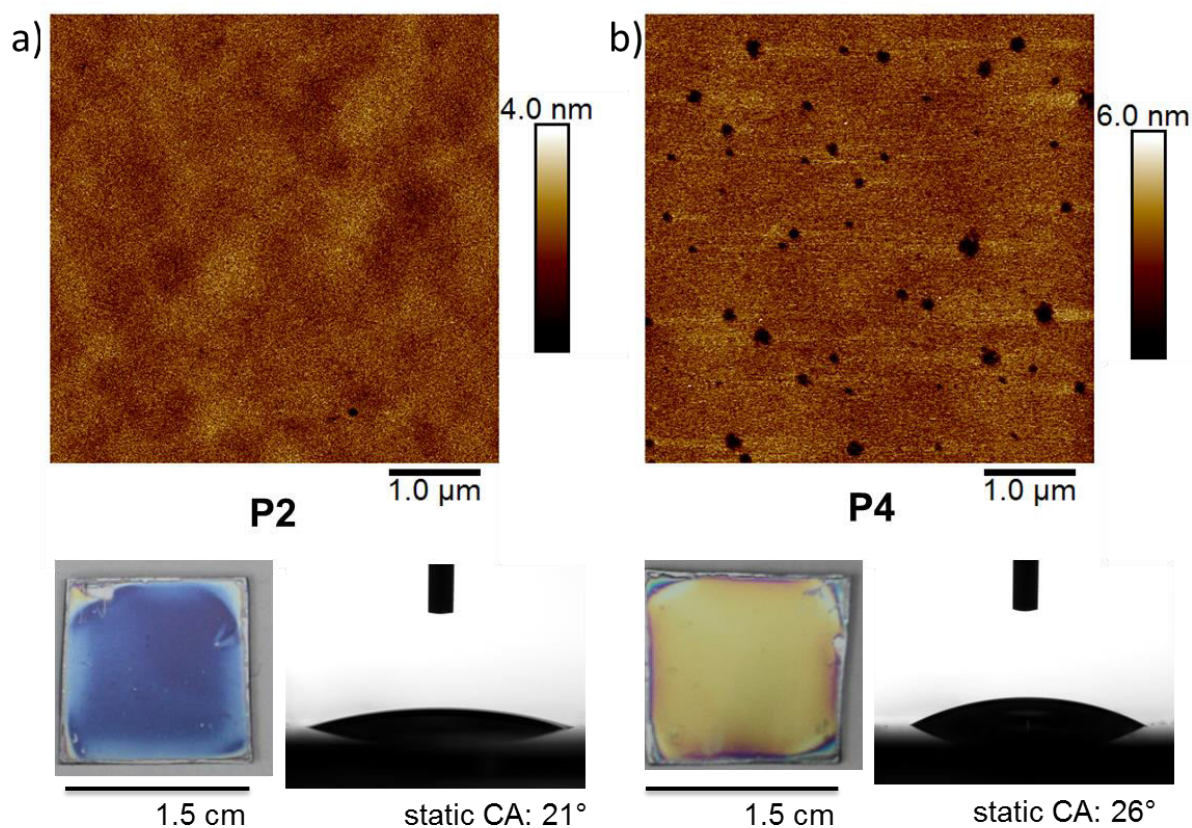


**Figure 5.5.** AFM height images of PPE-networks, photos of the coated silicon substrates and photos of a water droplet on the coatings to determine the static contact angles: a) **P2**-networks and b) **P4**-networks.

The PPE-networks of **P2**, **P4** and **P5** were further analyzed by FT-IR spectroscopy and compared with spectra of the monomers and polymers (all spectra are shown in Figures S5.37-5.43 and S5.47-5.49). The spectra confirmed that the expected IR bands were present. The dominant bands in the monomer spectra of P=O stretching at 1282-1285  $\text{cm}^{-1}$  and P-O-C stretching at 831-884, 980-1005 and 1016-1025  $\text{cm}^{-1}$  could be retrieved in the polymer spectra at 1267, 797, 958 and

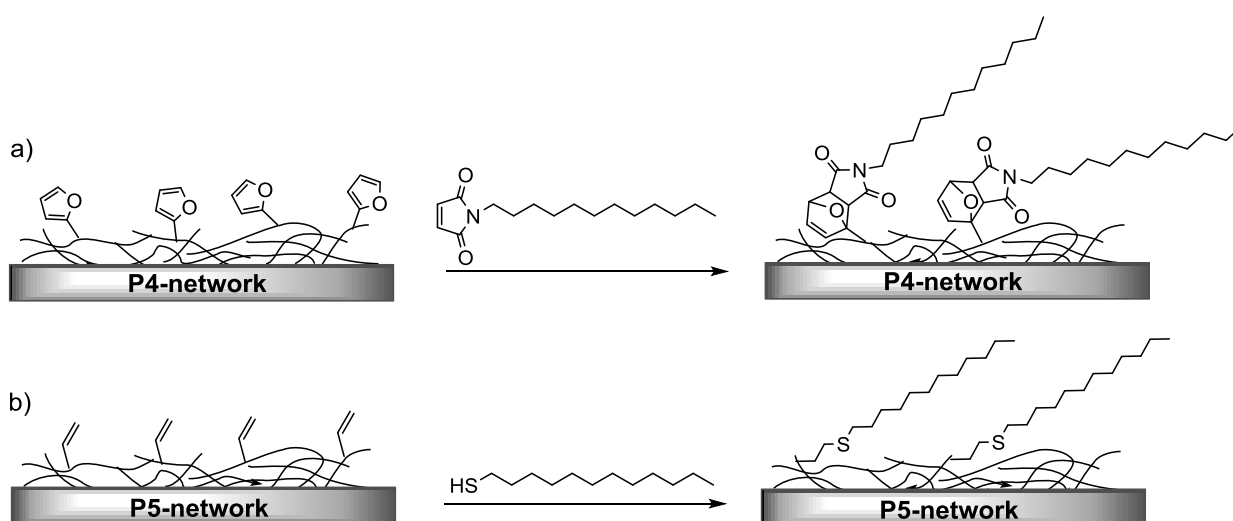
1015  $\text{cm}^{-1}$ .<sup>24-25</sup> They all exhibited a shift and broadening of the band because of the formation of a linear backbone containing the phosphate groups compared to the strained rings of monomers. Characteristic bands of  $-\text{CH}_2$ ,  $\text{O}-\text{CH}_2$  and  $-\text{CH}_3$  stretching and rocking of **EEP** monomer at 752, 1100, 1166, 1369, 1393, 1445, 2915 and 2985  $\text{cm}^{-1}$  were recovered in all polymer spectra with slight wavenumber shifts. Further characteristic bands for the pentyl, furfuryl or butenyl groups in the side chains from the comonomers **PEP**, **FEP** and **BuEP** in **P2**, **P4** and **P5** could not be observed, because the above mentioned signals were predominant and all polymers only contained the comonomers in small amounts. Characteristic aromatic bands of **FEP** or alkene bands of **BuEP** additionally may overlay with bands of **BeEP** or bands of **PEP** with bands of **EEP**. Characteristic bands of the **BeEP** monomer instead could be observed in all polymers (except **P6**, it does not contain **BeEP**): a carbonyl band at 1601  $\text{cm}^{-1}$  (at 1601  $\text{cm}^{-1}$  in the monomer spectrum of **BeEP**) and aromatic C=C stretching signals at 704, 1508 and 1652  $\text{cm}^{-1}$  (703, 1505 and 1643  $\text{cm}^{-1}$  in the monomer **BeEP**). In polymer **P6** (only containing **EEP** and **BuEP**) a C=C stretching band of an alkene group at 1641  $\text{cm}^{-1}$  could be retrieved, also being present in the **BuEP** monomer. In IR spectra of the PPE-networks of **P2**, **P4** and **P5** on Si substrates the dominant signals for P=O stretching at 1275  $\text{cm}^{-1}$  and P-O-C stretching at 822, 984 and 1026  $\text{cm}^{-1}$  could be retrieved again with a slight shift (around 10  $\text{cm}^{-1}$ ) to higher wavenumbers. Stretching bands of  $-\text{CH}_2-$ ,  $-\text{CH}_3$  and C=C were visible again at 741, 1398 and 1456  $\text{cm}^{-1}$  ( $-\text{CH}_2-$  stretching) or 1130, 1167, and 1371  $\text{cm}^{-1}$  ( $-\text{CH}_3$  stretching) as well as 2900-3000  $\text{cm}^{-1}$  or 1506 and 1653  $\text{cm}^{-1}$  again (C=C stretching), respectively. Most importantly, the C=O stretching band of the benzophenone residue at 1601  $\text{cm}^{-1}$  disappeared, because the carbonyl group reacted upon irradiation with UV-light, confirming successful covalent crosslinking of the networks.

**Table 5.3.** Overview of the physical characterization of PPE-networks of **P2**, **P4**, and **P5**.

polymer	dry layer thickness on silicon/ nm	static contact angle / °	roughness ( $R_q$ ) / nm
<b>P2</b>	104±1	21±1	0.40
<b>P4</b>	199±2	26±3	0.68
<b>P5</b>	263±1	26±1	-

**Post-Polymerization Modification of PPE-networks.** The PPE-networks **P4** and **P5** both contain furfuryl or alkene groups, respectively, which allow further post-polymerization modification of the PPE-networks on the surface of the films. Furans serve as electron-rich dienes in a [4+2] cycloaddition Diels-Alder reactions and can react with suitable maleimide derivatives as electron-deficient dienophiles. We recently presented furfuryl-containing PPEs and its successful post-modification in a separate article (see chapter 4).<sup>26</sup> Alkenes can be functionalized in a radical thiol-ene reaction with thiols. As proof of concept, PPE-networks of **P4** and **P5** were functionalized with  $\text{C}_{12}$ -alkyl chains (dodecyl-1-maleimide or dodecyl-1-mercaptane).

**P4-C<sub>12</sub>** showed an increased static contact angle of 38° (compared to 26°) and advancing angle of 64° (compared to 29°, all characterizations are shown in Table S5.3). The change of hydrophilicity of the surface after functionalization with hydrophobic alkyl chains indicated a successful post-modification. However, the thickness of layer decreased from 110 to 78 nm, which probably have several explanations. The polymer-networks are highly hydrophilic and might embed moisture from air. With decreasing hydrophilicity of the surface after functionalization less moisture is embedded and therefore the layer thickness decreases. Another explanation can be a mass loss of the networks. During washing the networks probably strongly swell, cross-links break and unbound polymer detaches. This is probably also the reason, why FT-IR measurements failed and did not show a distinct result (Figure S5.52). An increase of the intensity of CH<sub>2</sub>- and CH<sub>3</sub> bands was expected due to attachment of C<sub>12</sub>-alkyl chains. **P5-C<sub>12</sub>** did not show a significant increase of static contact angle (29° compared to 26° of **P5**). The layer thickness decreased as well from 263 nm to 213 nm, probably due to mass loss. FT-IR measurements did not show an increase of the intensity of CH<sub>2</sub>- and -CH<sub>3</sub> bands (Figure S5.53). The results indicated that post-modification of **P5**-networks did not occur.



**Scheme 5.7.** Post-modification reactions of PPE- networks: a) modification of **P4**-networks by Diels-Alder reaction; b) modification of **P5**-networks by thiol-ene reaction.

## 5.5 Conclusions

Surface-attached poly(phosphoester)-networks have been successfully prepared and physically characterized. They might be interesting coatings for biomedical devices.

For the formation of PPE-films, a photo-reactive cyclic phosphate monomer suitable for the ROP and containing a benzophenone group in the pendant chain (BeEP) has been designed and copolymerized with EEP as comonomer (ethyl side chains), to produce hydrophilic polymers.

Terpolymerization was achieved with additional comonomers, bearing pentyl (PEP), furfuryl (FEP) or butenyl (BuEP) pendant groups. The obtained polymers exhibited 5% benzophenone functionalities and additional 10% pentyl, furfuryl or butenyl functionalities in the case of terpolymers, molecular weights up to 46,300 g/mol and molecular weight distributions as low as 1.15-1.19. The incorporation behavior of the monomers for co- or terpolymerization has been studied by  $^{31}\text{P}\{\text{H}\}$  NMR kinetic measurements, indicating a gradient-like structure and reaction speed of the monomers  $\text{BeEP} > \text{FEP} > \text{EEP} \approx \text{PEP}$ .

Surface-attached PPE-networks has been obtained by spin-coating of polymer solutions onto silicon substrates and subsequent UV-irradiation, to cross-link the polymers and achieve covalent surface-binding. Layer thicknesses between 56 and 263 nm were received, depending on the applied polymer and hydrophilicity of the substrates. AFM images showed a homogeneous and smooth morphology of the P4- and P5-networks, contact angles between 21 and 26° revealed hydrophilic surfaces. While results of contact angle measurements of P4-networks after post-polymerization modification by Diels-Alder reaction indicated successful functionalization, functionalization of P5-networks by thiol-ene reaction was not confirmed. P4-networks offer an addressable platform to further tune the film properties.

## 5.6 Outlook

The PPE-films are promising coatings for biomedical devices. For the application non-fouling properties are required. The swellability and protein adsorption of P2- and P4-networks by surface plasmon resonance spectroscopy (SPR) is currently investigated. For the measurements, networks on gold substrates are needed and the coating process has been transferred to gold wafers. The swellability of networks can be measured by comparison of the dry and swollen layer thicknesses. Protein adsorption and potential protein-repellent properties will be measured by a well-established protocol<sup>7</sup> with a solution of fibrinogen under physiological conditions. Fibrinogen is a glycoprotein and involved in the process of blood clotting. It is a very “sticky” protein, making it an appropriate test substance for the examination of protein adhesion.<sup>1, 27</sup> After swelling of the network under physiological conditions, the kinetics of protein adsorption can be recorded online by changes of reflectivity in dependency on the time. The mass of absorbed proteins per area can quantitatively be determined from the reflectivity of the dry network before and after protein adhesion. The layer thickness of absorbed proteins and the adsorbed mass protein per unit area can be calculated. Alternatively, the kinetics of protein adsorption and mass of adsorbed proteins could be monitored and determined by measurements with a QCM-D (quartz crystal microbalance with dissipation monitoring).

Depending on the results of protein-repellency measurements, it is interesting to further fine-tune the properties of the PPE-networks by postmodification reaction, using the furfuryl functionalities in P4-networks as platforms. PPEs are known to be biocompatible and biodegradable.<sup>8</sup> Nevertheless, cell-compatibility tests of the PPE-coatings seem to be crucial for a potential later biomedical application. The stability or biodegradability of the networks on surfaces under physiological conditions could be gravimetrically examined.

Biomedical devices like wound dressing foams, catheters tubes or prostheses often consists of polymeric materials as poly(urethane)s, poly(amide)s or PMMA. It would be attractive to examine the film formation and attachment of PPE-networks on these materials.

## 5.7 Supporting Information

The Supporting Information contains additional synthetic procedures, characterization data for monomers, polymers, PPE-networks and post-modification of networks.

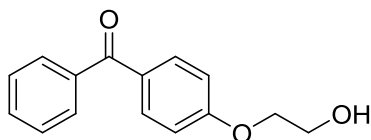
### Content

- 5.7.1 Synthetic procedures
- 5.7.2 Monomers and Polymers
  - a. NMR spectra
  - b. IR spectra
- 5.7.3 Kinetic measurements of copolymerizations
- 5.7.4 Network characterization
- 5.7.5 Alternative networks
- 5.7.6 Post-modification of networks

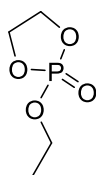
### 5.7.1 Synthetic procedures

*4-(2-hydroxyethoxy)benzophenone*: The alcohol was synthesized according to literature.<sup>16</sup> 4-Hydroxybenzophenone (15.00 g, 75.7 mmol, 1 eq.) and potassium carbonate (20.92 g, 151.4 mmol, 2 eq.) were suspended in 150 mL acetone and refluxed for 1 h under argon-atmosphere. Bromoethanol (18.91 g, 151.4 mmol, 2 eq.) was added via syringe and the reaction refluxed overnight. The reaction was cooled down to room temperature and water was added. The aqueous phase was extracted with diethyl ether three times and the combined organic

phases washed with brine once. The organic phase was concentrated. Column chromatography (silica gel, dichloromethane/ethyl acetate 4:1,  $R_f=0.67$ ) gave the pure product, colourless crystals. Yield: 7.76 g, 42%.  $^1\text{H NMR}$  (300 MHz,  $\text{DMSO-d}_6$ ):  $\delta$  [ppm] 7.78-7.50 (m, 7H, aromat. H), 7.10 (d, 2H, aromat. H), 4.94 (t, 1H, -OH), 4.10 (t, 2H, Ar-O- $\text{CH}_2$ - $\text{CH}_2$ -OH), 3.75 (q, 2H, Ar-O- $\text{CH}_2$ - $\text{CH}_2$ -OH).

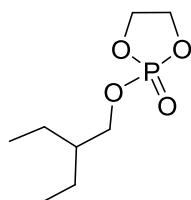


*2-ethoxy-2-oxo-1,3,2-dioxaphospholane (EEP, 2)*: The monomer was synthesized according to literature.<sup>9</sup> Briefly, a flame-dried 500mL three-neck flask, equipped with a dropping funnel, was charged with 2-chloro-2-oxo-1,3,2-dioxaphospholane (COP) (50.00 g, 0.35 mol) dissolved in dry THF (100 mL). A solution of dry ethanol (16.17 g, 0.35 mol) and dry triethylamine (35.51 g, 0.35 mol) in dry THF (70 mL) was added dropwise to the stirring solution of COP at  $-20\text{ }^\circ\text{C}$  under argon atmosphere. During reaction, hydrogen chloride was formed and precipitated as pyridinium hydrochloride. The reaction was stirred at  $4\text{ }^\circ\text{C}$  overnight. The salt was removed by filtration and the filtrate concentrated in vacuo. The residue was purified by distillation under reduced pressure to give a fraction at  $105\text{-}110\text{ }^\circ\text{C}/0.095\text{ mbar}$ , obtaining the clear, colorless, liquid product EEP. Yield: 34.60 g (0.23 mol), 65%.  $^1\text{H NMR}$  (500 MHz,  $\text{DMSO-d}_6$ ):  $\delta$  [ppm] 4.47-4.34 (m, 4H, O- $\text{CH}_2$ - $\text{CH}_2$ -O), 4.11-4.04 (m, 2H, O- $\text{CH}_2$ - $\text{CH}_3$ ), 1.25 (t, 3H, O- $\text{CH}_2$ - $\text{CH}_3$ ).  $^{13}\text{C}\{\text{H}\}$  NMR (126 MHz,  $\text{DMSO-d}_6$ ):  $\delta$  [ppm] 66.35 (-O- $\text{CH}_2$ - $\text{CH}_2$ -O-), 64.18 (-O- $\text{CH}_2$ - $\text{CH}_3$ ), 15.96 (-O- $\text{CH}_2$ - $\text{CH}_3$ ).  $^{31}\text{P}\{\text{H}\}$  NMR (202 MHz,  $\text{DMSO-d}_6$ ):  $\delta$  [ppm] 16.83. FTIR ( $\text{cm}^{-1}$ ): 2985 (- $\text{CH}_2$ - and - $\text{CH}_3$  stretching), 2915 (- $\text{CH}_2$ - and - $\text{CH}_3$  stretching), 1477 (O- $\text{CH}_2$ - deformation), 1445, 1393, 1369 (- $\text{CH}_3$  deformation), 1282 (P=O stretching), 1225, 1166 (- $\text{CH}_3$  rocking), 1101, 1056, 1016 (P-O-C stretching), 980 (P-O-C stretching), 926, 831 (P-O-C stretching), 752 (- $\text{CH}_2$ - rocking).

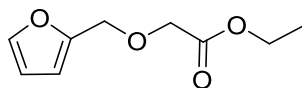


*2-(2-ethylbutoxy)-2-oxo-1,3,2-dioxaphospholane (EBP, 4)*: The monomer was synthesized according to a modified literature protocol<sup>19</sup>. Briefly, a flame-dried 500mL three-neck flask, equipped with a dropping funnel, was charged with a solution of dry 2-ethyl-1-butanol (11.60 g, 0.11 mol, 1.1eq.) and dry triethylamine (11.48 g, 0.11 mol, 1.1eq.) in dry THF (100 mL). 2-chloro-2-oxo-1,3,2-dioxaphospholane (14.70 g, 0.10 mol, 1eq.) dissolved in dry THF (50 mL) was added dropwisely to the stirring solution at  $0\text{ }^\circ\text{C}$  under argon atmosphere. During reaction, hydrogen chloride was formed and precipitated as triethylammonium hydrochloride. The reaction was stirred at  $0\text{ }^\circ\text{C}$  for 4h and stored in the freezer overnight. The salt was removed by filtration with a

Schlenk-frit and the filtrate concentrated in vacuo. The residue was purified by distillation under reduced pressure to give a fraction at 130 °C/1 mbar, obtaining the clear, colorless, liquid product EBP. Yield: 11.70 g, 54%.  $^1\text{H}$  NMR (300 MHz,  $\text{CDCl}_3$ ):  $\delta$  [ppm] 4.43-4.25 (m, 4H, O- $\text{CH}_2$ - $\text{CH}_2$ -O), 4.02-3.97 (m, 2H,  $(\text{CH}_3$ - $\text{CH}_2$ ) $_2$ -CH- $\text{CH}_2$ -O-), 1.52-1.41 (m, 1H,  $(\text{CH}_3$ - $\text{CH}_2$ ) $_2$ -CH- $\text{CH}_2$ -O-), 1.37-1.27 (quintett, 4H,  $(\text{CH}_3$ - $\text{CH}_2$ ) $_2$ -CH- $\text{CH}_2$ -O-), 0.84 (t, 6H,  $(\text{CH}_3$ - $\text{CH}_2$ ) $_2$ -CH- $\text{CH}_2$ -O-).  $^{13}\text{C}\{\text{H}\}$  NMR (76 MHz,  $\text{CDCl}_3$ ):  $\delta$  [ppm] 70.80 ( $(\text{CH}_3$ - $\text{CH}_2$ ) $_2$ -CH- $\text{CH}_2$ -O-), 65.99 (-O- $\text{CH}_2$ - $\text{CH}_2$ -O-), 41.60 ( $(\text{CH}_3$ - $\text{CH}_2$ ) $_2$ -CH- $\text{CH}_2$ -O-), 22.69 ( $(\text{CH}_3$ - $\text{CH}_2$ ) $_2$ -CH- $\text{CH}_2$ -O-), 10.86 ( $(\text{CH}_3$ - $\text{CH}_2$ ) $_2$ -CH- $\text{CH}_2$ -O-).  $^{31}\text{P}\{\text{H}\}$  NMR (202 MHz,  $\text{CDCl}_3$ ):  $\delta$  [ppm] 17.63. FTIR ( $\text{cm}^{-1}$ ): 2963 (- $\text{CH}_2$ - and - $\text{CH}_3$  stretching), 2934 (- $\text{CH}_2$ - and - $\text{CH}_3$  stretching), 2877 (- $\text{CH}_2$ - and - $\text{CH}_3$  stretching), 1463 (O- $\text{CH}_2$ - deformation), 1385, 1367 (- $\text{CH}_3$  deformation), 1285 (P=O stretching), 1225, 1151 (- $\text{CH}_3$  rocking), 1103, 1016 (P-O-C stretching), 975 (P-O-C stretching), 928, 836 (P-O-C stretching), 774 (- $\text{CH}_2$ - rocking).

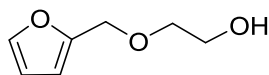


*Ethyl-2-(furan-2-ylmethoxy)acetate*: The acetate was synthesized according to literature.<sup>28</sup> Briefly, furfuryl alcohol (25.00 g, 254.8 mmol, 1 eq.) was dissolved in 200 mL dry THF in a flame-dried round-bottom flask under argon-atmosphere. Sodium hydride (7.34 g, 305.8 mmol, 1.2 eq.) were added and the reaction was refluxed for 1 h. Bromoacetate (46.81 g, 280.3 mmol, 1.1 eq.) was added and refluxed overnight. Then, water was slowly added. The aqueous phase was extracted with ethyl acetate twice and the organic phase with brine once. The organic phase was dried with  $\text{MgSO}_4$  and concentrated. Column chromatography (silica gel, dichloromethane/ethyl acetate 98:2,  $R_f=0.94$ ) gave the pure product. Yield: 75%.  $^1\text{H}$  NMR (300 MHz,  $\text{CDCl}_3$ ):  $\delta$  [ppm] 7.42 (s, 1H, -O- $\text{CH}=\text{CH}$ -), 6.36 (m, 2H, -O- $\text{CH}=\text{CH}$ -), 4.54 (s, 2H, O-C(=CH)- $\text{CH}_2$ -O-), 4.21 (q, 2H, -O- $\text{CH}_2$ - $\text{CH}_3$ ), 4.08 (t, 2H, -O- $\text{CH}_2$ -C(=O)-O-), 1.28 (t, 3H, - $\text{CH}_3$ ).

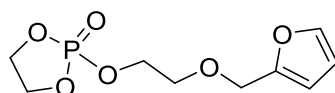


*2-(furan-2-ylmethoxy)ethan-1-ol*: The alcohol was synthesized according to literature.<sup>28</sup> Briefly, lithium aluminium hydride (2.4 M in THF, 47.79 mL, 114.7 mmol, 0.6 eq.) was dissolved in 100L dry diethyl ether in a flame-dried 3-necked round-bottom flask. Ethyl 2-(furan-2-ylmethoxy)acetate (35.21 g, 191.2 mmol, 1 eq.) in 50 mL dry diethyl ether was added dropwisely in the way that the reaction gently refluxed. It was stirred overnight at room temperature and then water was slowly added. The aqueous phase was extracted with diethyl ether twice and the organic phase with brine once. The organic phase was dried with  $\text{MgSO}_4$  and concentrated. Column chromatography (silica gel, dichloromethane/acetone 19:1,  $R_f=0.42$ ) gave the pure product. Yield: 36%.  $^1\text{H}$  NMR (300 MHz,

CDCl<sub>3</sub>): δ [ppm] 7.40 (s, 1H, -O-CH=CH-), 6.32 (m, 2H, -O-CH=CH-CH=), 4.49 (s, 2H, O-C(=CH)-CH<sub>2</sub>-O-), 3.73 (m, 2H, -O-CH<sub>2</sub>-CH<sub>2</sub>-OH), 3.59 (m, 2H, -O-CH<sub>2</sub>-CH<sub>2</sub>-OH), 2.31 (s, 1H, -OH).

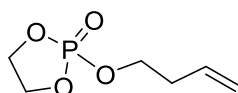


*2-(2-(furan-2-ylmethoxy)ethoxy)-2-oxo-1,3,2-dioxaphospholane (FEP, 5)*: 2-(furan-2-ylmethoxy)ethan-1-ol (5.00 g, 35.3 mmol, 1 eq.) was dissolved in 100 mL dry THF in a flame-dried 3-necked round-bottom flask. Dry pyridine (2.78 g, 35.2 mmol, 1 eq.) was added and the mixture was cooled to 0°C. 2-chloro-2-oxo-1,3,2-dioxaphospholane (7.52 g, 52.8 mmol, 1.5 eq.) in 35 mL dry THF was added over a period of 1h, stirred for 4 h and kept at -20°C for additional 8h.. During reaction, hydrogen chloride was formed and precipitated as pyridinium hydrochloride. The ice-cold reaction mixture was then filtered under inert-gas atmosphere and concentrated at reduced pressure. Column chromatography with a RP-1 column (silica gel deactivated with 5v% hexamethyldisiloxane, dichloromethane/ethyl acetate 1:3, *R<sub>f</sub>*=0.77) afforded 4.09 g (47%) of the pure product FEP as a yellow oil. <sup>1</sup>H NMR (500 MHz, CDCl<sub>3</sub>): δ [ppm] 7.37 (s, 1H, -O-CH=CH-), 6.35 (m, 2H, -O-CH=CH-CH=), 4.52 (s, 2H, O-C(=CH)-CH<sub>2</sub>-O-), 4.43-4.23 (m, 6H, -O-CH<sub>2</sub>-CH<sub>2</sub>-O-P(-O-)-O-CH<sub>2</sub>-CH<sub>2</sub>-), 3.72-3.68 (s, 2H, -O-CH<sub>2</sub>-CH<sub>2</sub>-O-P(-O-)-O-). <sup>13</sup>C{H} NMR (126 MHz, CDCl<sub>3</sub>): δ [ppm] 151.36 (O-C(=CH)-CH<sub>2</sub>-O-), 143.21 (-O-CH=CH-), 110.46 (-O-CH=CH-CH=), 109.67 (-O-CH=CH-CH=), 68.18 (O-C(=CH)-CH<sub>2</sub>-O-), 67.02 (-O-CH<sub>2</sub>-CH<sub>2</sub>-O-P(-O-)-O-), 66.40 (-O-P(-O-)-O-CH<sub>2</sub>-CH<sub>2</sub>-), 63.88 (-O-CH<sub>2</sub>-CH<sub>2</sub>-O-P(-O-)-O-). <sup>31</sup>P{H} NMR (202 MHz, CDCl<sub>3</sub>): δ [ppm] 17.75. FTIR (cm<sup>-1</sup>): 3119 (-CH= stretching), 3034 (-CH= stretching), 2956 (-CH<sub>2</sub>- stretching), 2914 (-CH<sub>2</sub>- stretching), 2868 (-CH<sub>2</sub>- stretching), 1503 (C=C stretching), 1479 (O-CH<sub>2</sub>- deformation), 1356, 1285 (P=O stretching), 1225, 1150 (=CH- stretching), 1103, 1063, 1023 (P-O-C stretching), 987 (P-O-C stretching), 927, 884, 866, 838 (O-CH<sub>2</sub>- stretching), 749 (-CH<sub>2</sub>- rocking), 684 (C-H deformation).

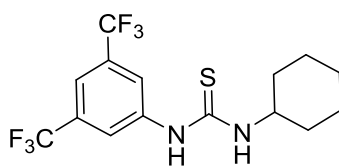


*2-(but-3-en-1-yloxy)-2-oxo-1,3,2-dioxaphospholane (BuEP, 6)*<sup>15</sup>: The monomer was synthesized according to a modified literature protocol for EEP<sup>9</sup>. Briefly, a flame-dried 500mL three-neck flask, equipped with a dropping funnel, was charged with a solution of dry 3-buten-1-ol (10.12 g, 0.14 mol, 1eq.) and dry triethylamine (14.21 g, 0.14 mol, 1eq.) in dry THF (100 mL). 2-chloro-2-oxo-1,3,2-dioxaphospholane (20.00 g, 0.14 mol, 1eq.) dissolved in dry THF (50 mL) was added dropwisely to the stirring solution at 0 °C under argon atmosphere. During reaction, hydrogen chloride was formed and precipitated as triethylammonium hydrochloride. The reaction was stirred at 0 °C for 4h and stored in the freezer overnight. The salt was removed by filtration with a Schlenk-frit and the filtrate concentrated in vacuo. The residue was purified by distillation under reduced pressure to give a fraction at 85-91 °C/0.048-0.071 mbar, obtaining the clear, colorless,

liquid product BuEP. Yield: 20.33 g, 81%.  $^1\text{H}$  NMR (300 MHz,  $\text{CDCl}_3$ ):  $\delta$  [ppm] 5.85-5.68 (m, 1H,  $\text{CH}_2=\text{CH}-\text{CH}_2-\text{CH}_2-\text{O}-$ ), 5.20-5.04 (m, 2H,  $\text{CH}_2=\text{CH}-\text{CH}_2-\text{CH}_2-\text{O}-$ ), 4.50-4.27 (m, 4H,  $\text{O}-\text{CH}_2-\text{CH}_2-\text{O}$ ), 4.22-4.09 (m, 2H,  $\text{CH}_2=\text{CH}-\text{CH}_2-\text{CH}_2-\text{O}-$ ), 2.50-2.36 (q, 2H,  $\text{CH}_2=\text{CH}-\text{CH}_2-\text{CH}_2-\text{O}-$ ).  $^{13}\text{C}\{\text{H}\}$  NMR (76 MHz,  $\text{CDCl}_3$ ):  $\delta$  [ppm] 132.99 (-P-O- $\text{CH}_2-\text{CH}_2-\text{CH}=\text{CH}_2$ ), 117.88 (-P-O- $\text{CH}_2-\text{CH}_2-\text{CH}=\text{CH}_2$ ), 67.84 (d, -P-O- $\text{CH}_2-\text{CH}_2-\text{CH}=\text{CH}_2$ ), 65.97 (d, -O- $\text{CH}_2-\text{CH}_2-\text{O}-\text{P}$ ), 34.59 (d, -P-O- $\text{CH}_2-\text{CH}_2-\text{CH}=\text{CH}_2$ ).  $^{31}\text{P}\{\text{H}\}$  NMR (121 MHz,  $\text{CDCl}_3$ ):  $\delta$  [ppm] 17.49. FTIR ( $\text{cm}^{-1}$ ): 3080 (-CH=CH<sub>2</sub> stretching), 2982 (-CH<sub>2</sub>- and =CH<sub>2</sub> stretching), 2913 (-CH= stretching), 1642 (C=C stretching), 1475 (O-CH<sub>2</sub>- deformation), 1433, 1368, 1285 (P=O stretching), 1228, 1154, 1067, 1015 (P-O-C stretching), 994 P-O-C stretching), 925, 832 (P-O-C stretching), 760 (-CH<sub>2</sub>- rocking).

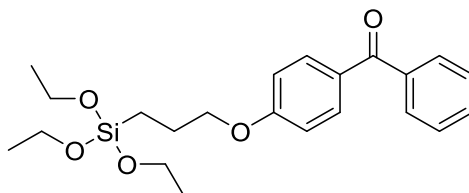


*N*-cyclohexyl-*N'*-(3,5-bis(trifluoromethyl)phenyl)thiourea (TU): TU was synthesized according to the method described previously<sup>29</sup>. Briefly, in a flame-dried 50 mL flask 3,5-bis(trifluoromethyl)phenylisothiocyanat (2.00 g,  $7.4 \cdot 10^{-3}$  mol) was dissolved in 10 mL dry THF under argon atmosphere. Cyclohexylamine (0.73 g,  $7.2 \cdot 10^{-3}$  mol) was added dropwisely at room temperature to the stirring solution. After the reaction mixture was stirred for 5 h, the solvent was removed *in vacuo*. The colourless residue was recrystallized from boiling chloroform. It was filtered hot and cooled down. Colourless needles precipitated in a yellowish solution. The product, TU, was collected by filtration, washed with cold chloroform and dried *in vacuo*. Yield: 1.77g, 370.36 g/mol, 4.8 mmol, 67%.  $^1\text{H}$  NMR (300 MHz,  $\text{DMSO}-d_6$ ):  $\delta$  [ppm] 9.84 (s, 1H, Ar-NH-C(=S)-NH-Cy), 8.23 (s, 1H, *p*-Ar-NH), 8.17 (s, 2H, *o*-Ar-NH), 7.72 (s, 1H, Ar-NH-C(=S)-NH-Cy), 4.11 (s, 1H, Ar-NH-C(=S)-NH-(*H*)Cy), 1.94-1.15 (m, 10H, Ar-NH-C(=S)-NH-Cy).

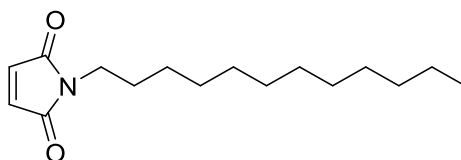


4-(3-triethoxysilyl)propyloxybenzophenone: The benzophenone silane was synthesized according to literature.<sup>30</sup> Briefly, 4-hydroxybenzophenone (5 g, 25.2 mmol, 1 eq.) and potassium carbonate (3.49 g, 25.2 mmol, 1 eq.) were dissolved in about 100 mL acetone and heated to reflux for 1 h. Allylbromid (3.36 g, 27.8 mmol, 1.1 eq.) was then added to the mixture and refluxed for 18 h. Water was added at room temperature, and extracted with diethyl ether three times. The combined organic phases were washed with 10 wt% NaOH solution, dried with  $\text{MgSO}_4$ , filtered, and concentrated. The product was recrystallized from boiling methanol to yield 4-allyloxybenzophenone as off-white crystals. Yield: 4.40 g, 238.29 g/mol, 18.5 mmol, 73%.

4-allyloxybenzophenone (0.5 g, 2.1 mmol, 1eq.) was dissolved in triethoxysilane (5 mL, 22.2 mmol) at room temperature under inert gas atmosphere. Platinum on activated charcoal (5 mg, 10%) was added to the mixture and stirred at room temperature for 2 d until the reaction was completed (petrol ether/acetone 5:1, product  $R_f=0.22$ ). The catalyst was removed by filtration and residual triethoxysilane under high vacuum to quantitatively yield the product as off-white solid. The product was used without further purification.



*1-dodecyl-1H-pyrrole-2,5-dione*: The maleimide derivative was synthesized according to literature.<sup>31</sup> Maleicanhydride (4.0 g, 40.79 mmol, 1 eq.) was dissolved in 20 mL toluene and dodecylamine (7.56 g, 40.79 mmol, 1. eq.) was added dropwisely. The reaction mixture was heated to 70 °C for 3 h. Sodium acetate (166 mg, 2.04 mmol, 0.05 eq.) and triethylamine (1.65 g, 16.32 mmol, 0.4 eq.) were added an the reaction heated to reflux for 16 h. After cooling the reaction mixture, the solcent was removed. Column chromatography (petrol ether/diethyl ether 4:1,  $R_f=0.42$ ) afforded 3.55 g (33%) of the pure product as a off-white powder.  $^1\text{H NMR}$  (300 MHz,  $\text{CDCl}_3$ ):  $\delta$  [ppm] 6.68 (s, 2H,  $-\text{C}(=\text{O})-\text{CH}=\text{CH}-\text{C}(=\text{O})-$ ), 3.50 (t, 2H,  $-\text{N}-\text{CH}_2-\text{CH}_2-(\text{CH}_2)_9-\text{CH}_3$ ), 1.57 (m, 2H,  $-\text{N}-\text{CH}_2-\text{CH}_2-(\text{CH}_2)_9-\text{CH}_3$ ), 1.27 (s, 18H,  $-\text{N}-\text{CH}_2-\text{CH}_2-(\text{CH}_2)_9-\text{CH}_3$ ), 0.87 (t, 3H,  $-\text{N}-\text{CH}_2-\text{CH}_2-(\text{CH}_2)_9-\text{CH}_3$ ).



## 5.7.2 Monomers and Polymers

### a. NMR spectra

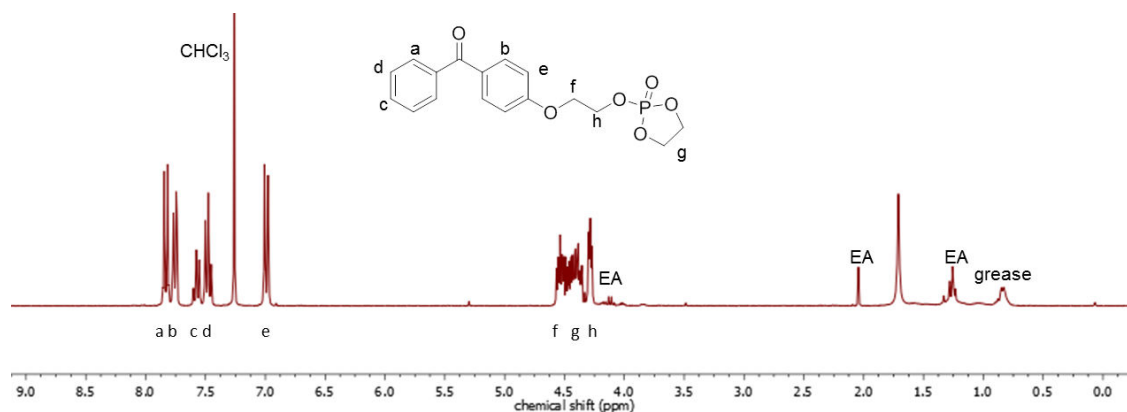


**Figure S5.1.**  $^1\text{H NMR}$  (300 MHz,  $\text{CDCl}_3$ ) of **BeEP (1)** at 298 K.

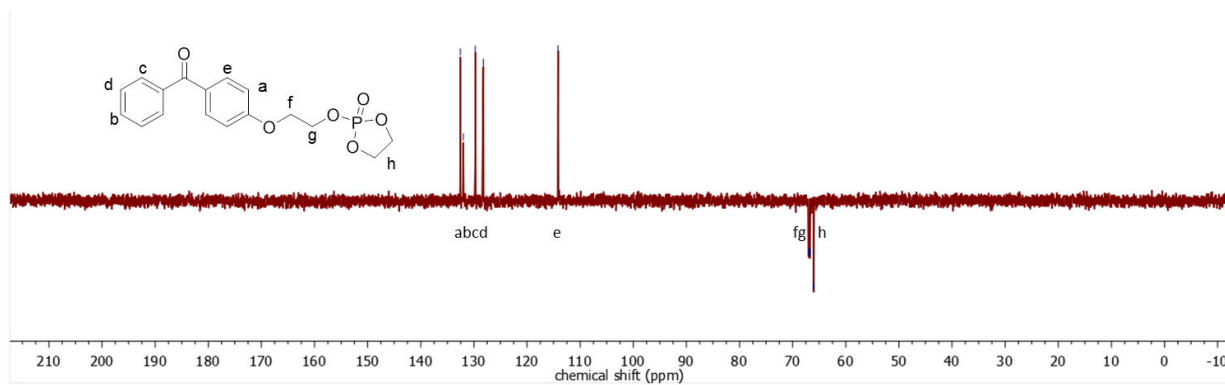


**Figure S5.2.**  $^{13}\text{C}\{\text{H}\}$ -DEPT NMR (76 MHz,  $\text{CDCl}_3$ ) of BeEP(1) at 298 K (Note: quaternary C-atoms are not depicted).

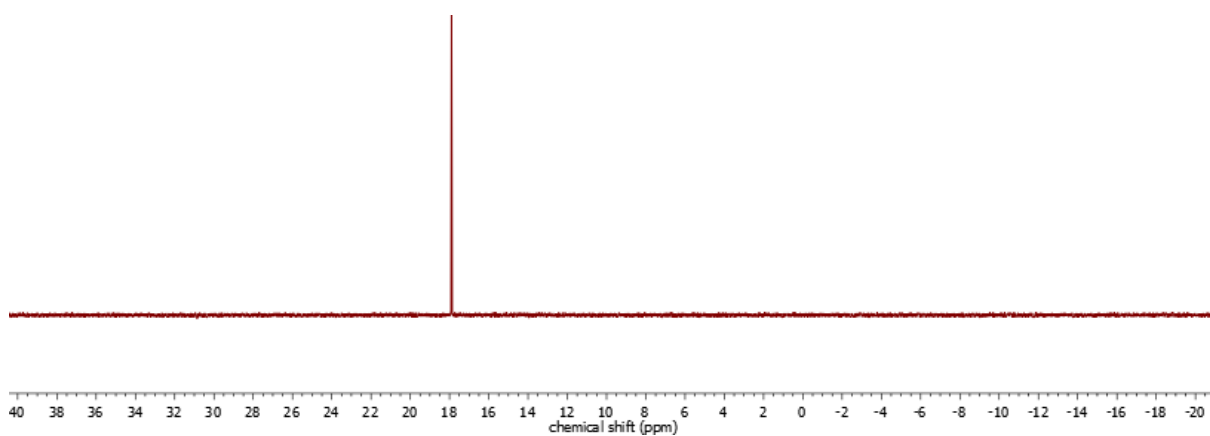


**Figure S5.3.**  $^{31}\text{P}\{\text{H}\}$  NMR (121 MHz,  $\text{CDCl}_3$ ) of BeEP (1) at 298 K.

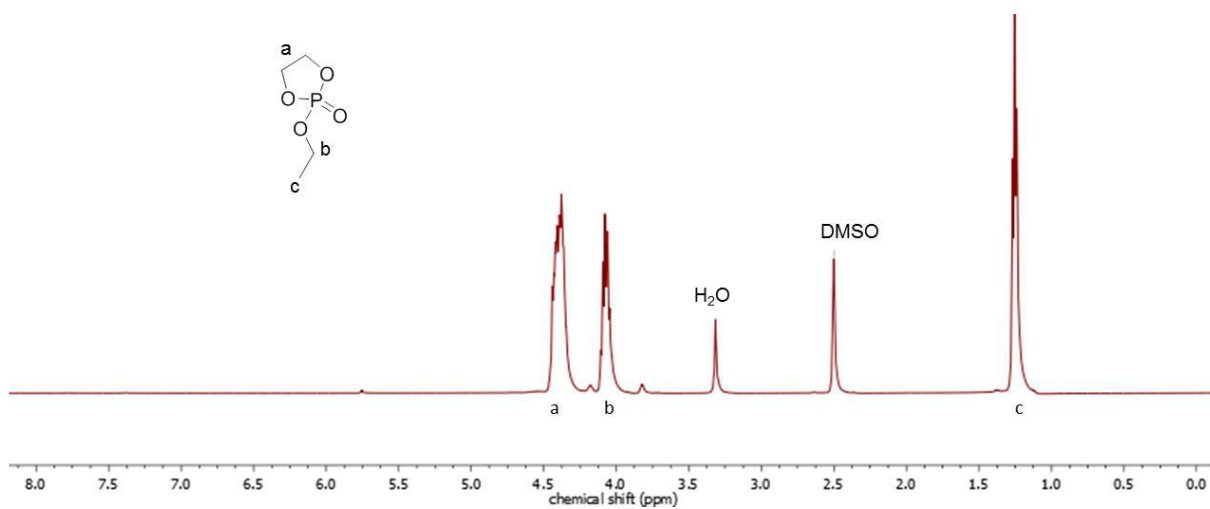


**Figure S5.4.**  $^1\text{H}$  NMR (500 MHz,  $\text{DMSO-d}_6$ ) of EEP (2) at 298 K.

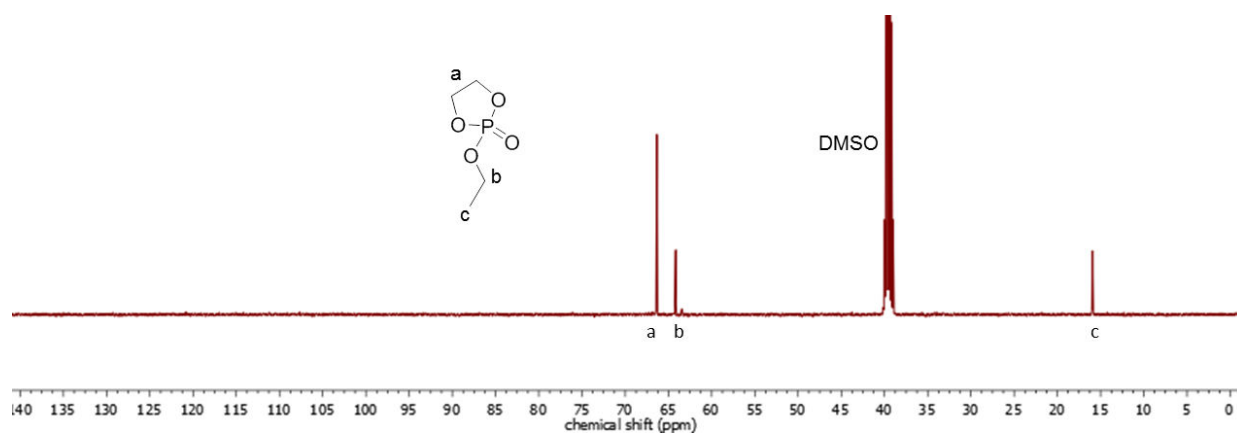


**Figure S5.5.**  $^{13}\text{C}\{\text{H}\}$  NMR (126 MHz,  $\text{DMSO-d}_6$ ) of EEP (2) at 298 K.

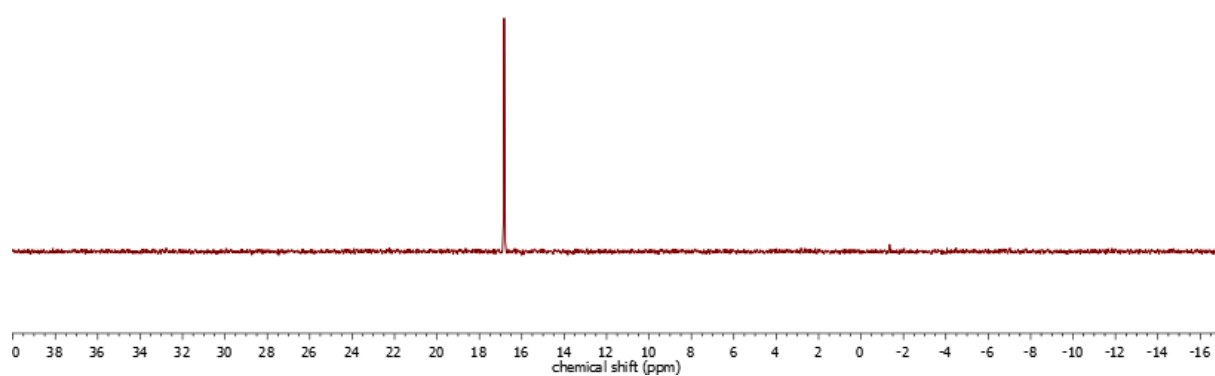


**Figure S5.6.**  $^{31}\text{P}\{\text{H}\}$  NMR (202 MHz,  $\text{DMSO-d}_6$ ) of EEP (2) at 298 K.

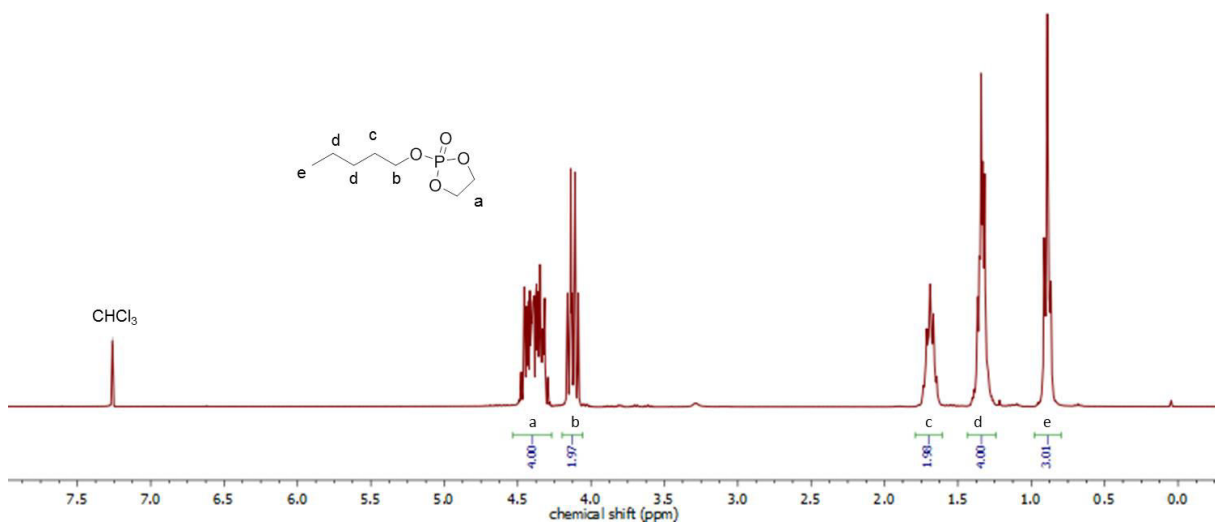


**Figure S5.7.**  $^1\text{H}$  NMR (300 MHz,  $\text{CDCl}_3$ ) of PEP (3) at 298 K.

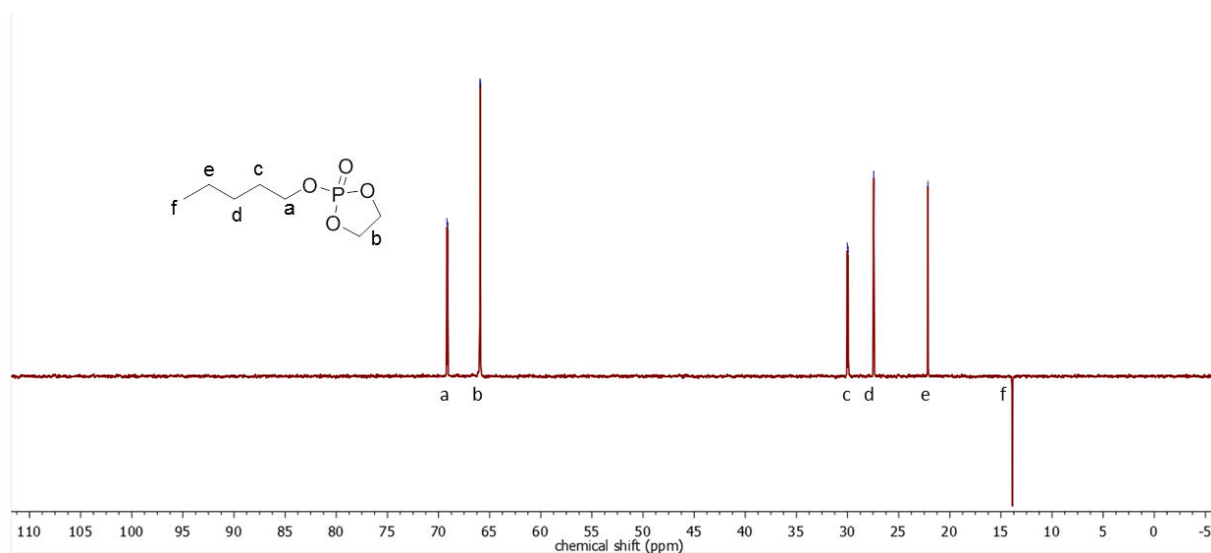


**Figure S5.8.**  $^{13}\text{C}\{\text{H}\}$ -DEPT NMR (76 MHz,  $\text{CDCl}_3$ ) of **PEP (3)** at 298 K.

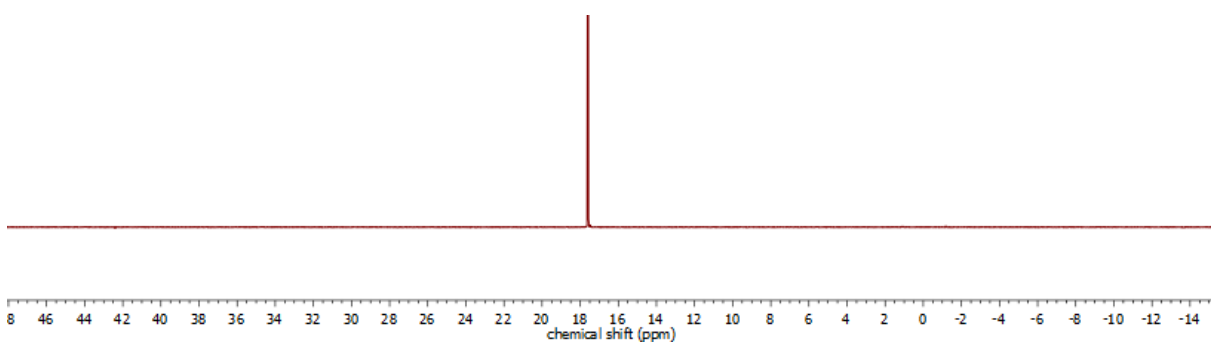


**Figure S5.9.**  $^{31}\text{P}\{\text{H}\}$  NMR (121 MHz,  $\text{CDCl}_3$ ) of **PEP (3)** at 298 K.

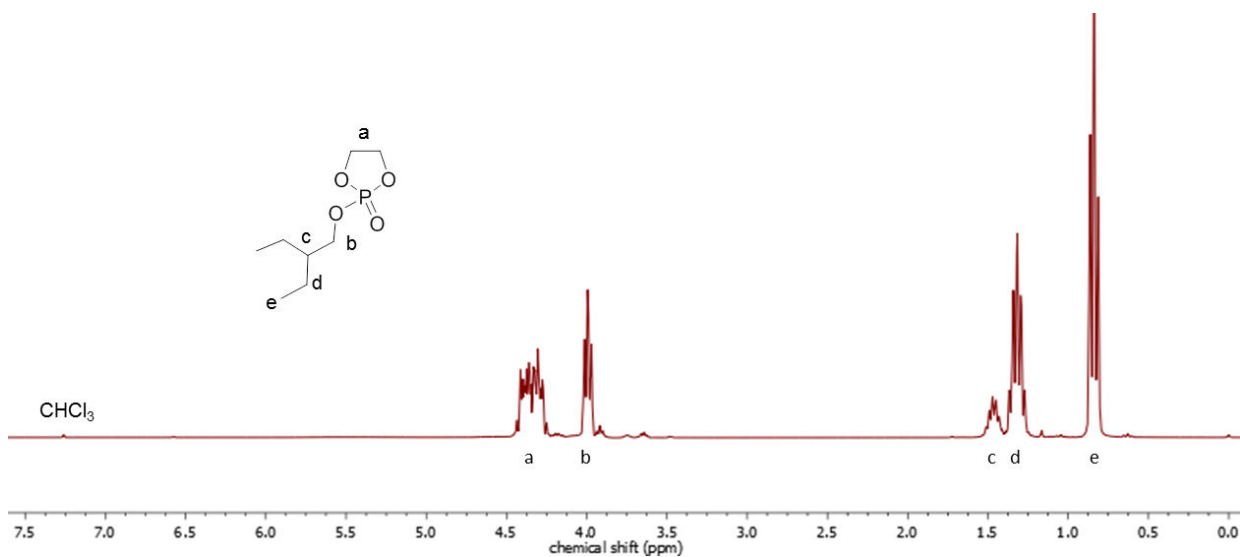


**Figure S5.10.**  $^1\text{H}$  NMR (300 MHz,  $\text{CDCl}_3$ ) of **EBP (4)** at 298 K.

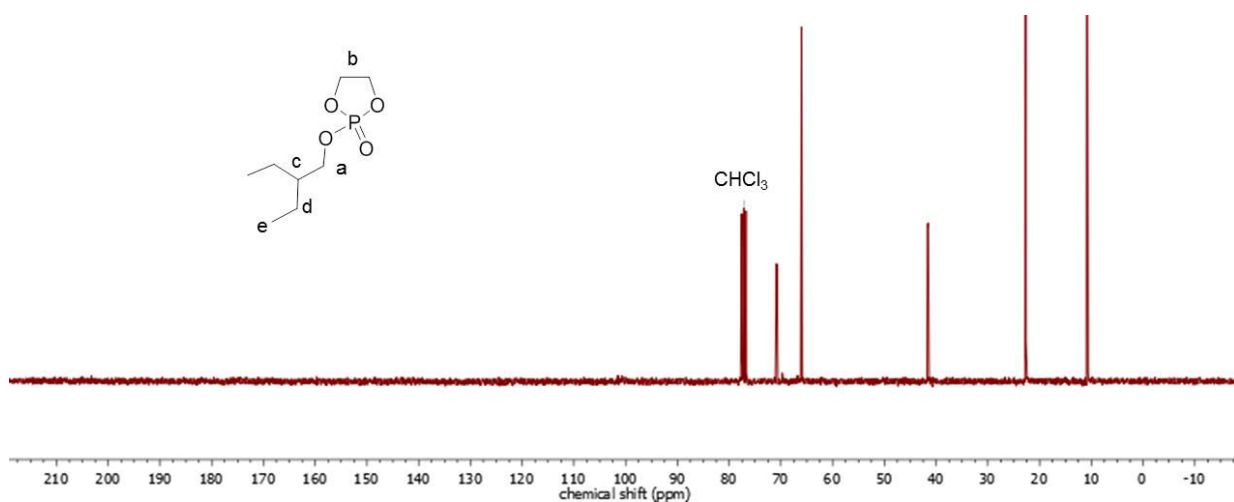


Figure S5.11. <sup>13</sup>C{<sup>1</sup>H} NMR (76 MHz, CDCl<sub>3</sub>) of EBP (4) at 298 K.

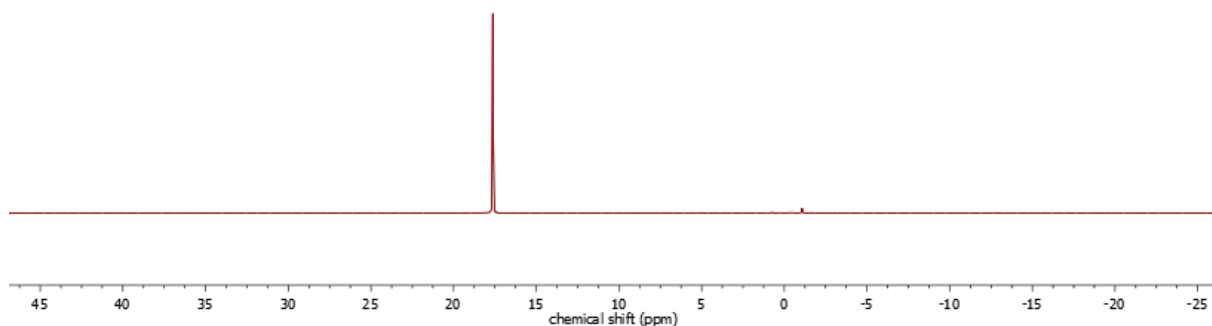


Figure S5.12. <sup>31</sup>P{<sup>1</sup>H} NMR (121 MHz, CDCl<sub>3</sub>) of EBP (4) at 298 K.

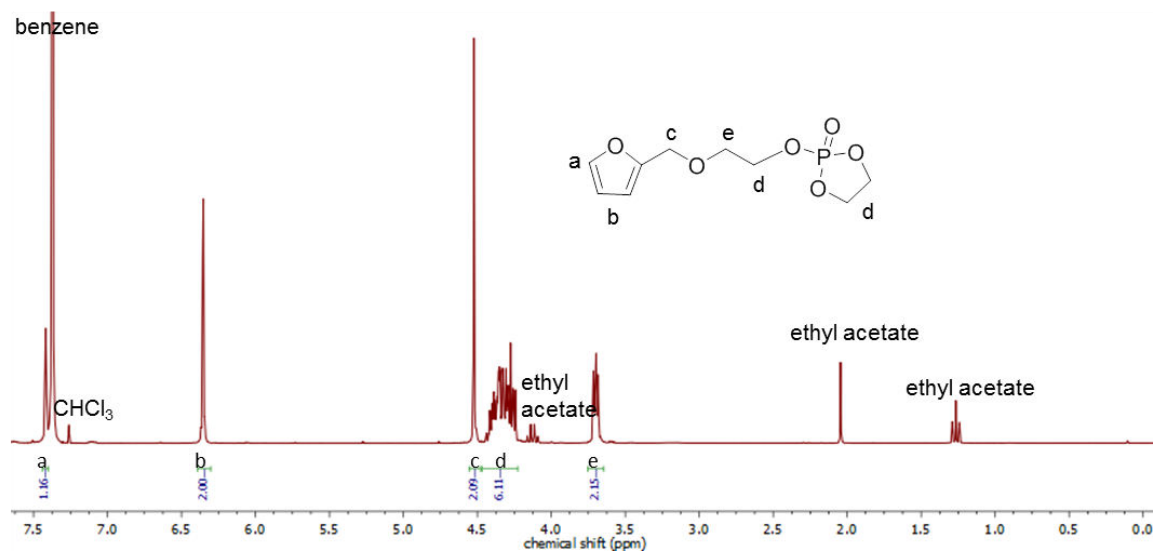
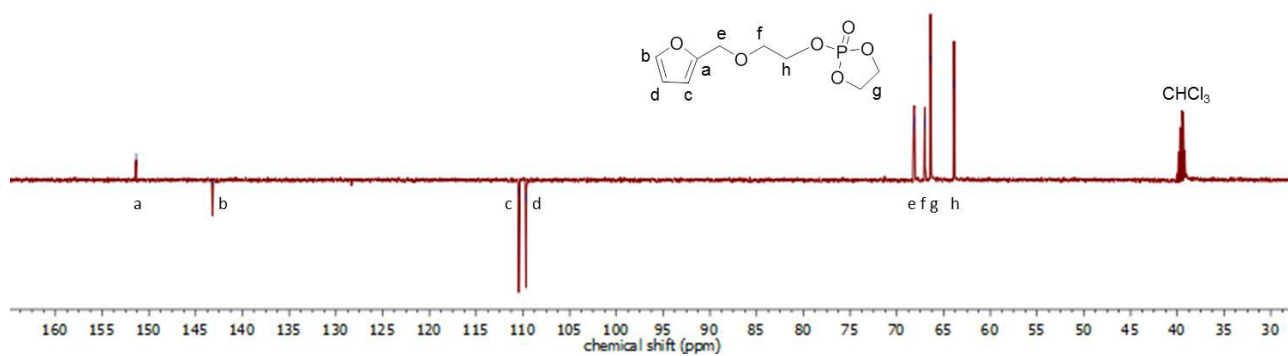
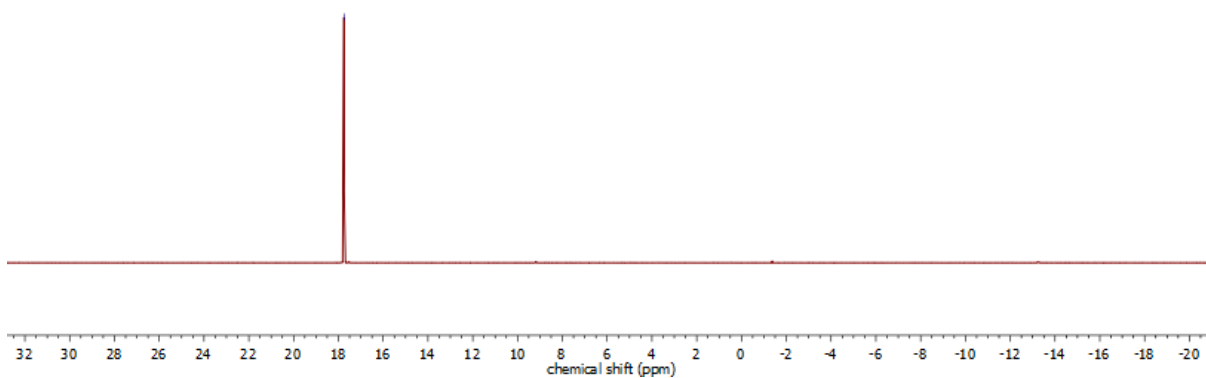


Figure S5.13. <sup>1</sup>H NMR (500 MHz, CDCl<sub>3</sub>) of FEP (5) at 298 K.



**Figure S5.14.**  $^{13}\text{C}\{\text{H}\}$ -DEPT NMR (126 MHz,  $\text{CDCl}_3$ ) of **FEP (5)** at 298 K.



**Figure S5.15.**  $^{31}\text{P}\{\text{H}\}$  NMR (202 MHz,  $\text{CDCl}_3$ ) of **FEP (5)** at 298 K.

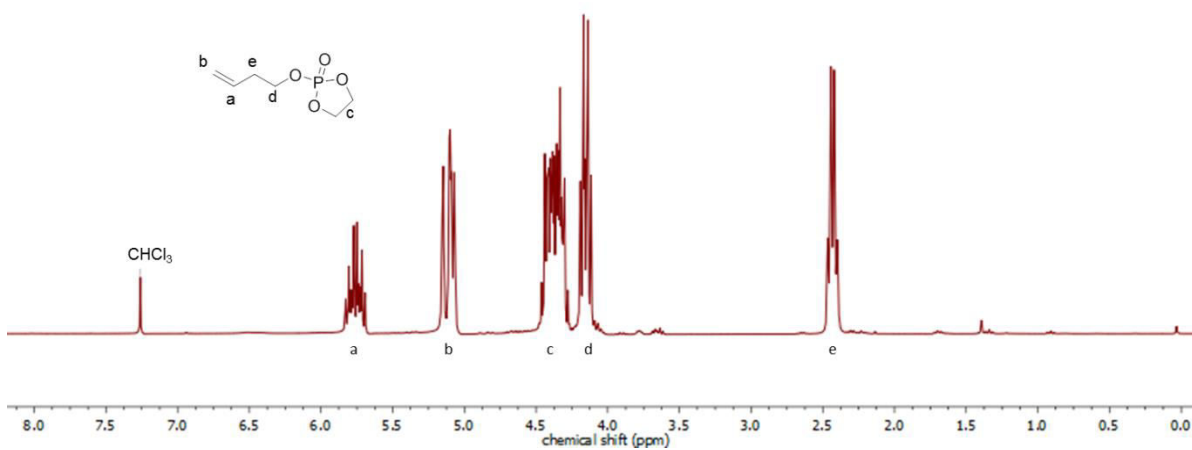


**Figure S5.16.**  $^1\text{H}$  NMR (300 MHz,  $\text{CDCl}_3$ ) of **BuEP (6)** at 298 K.

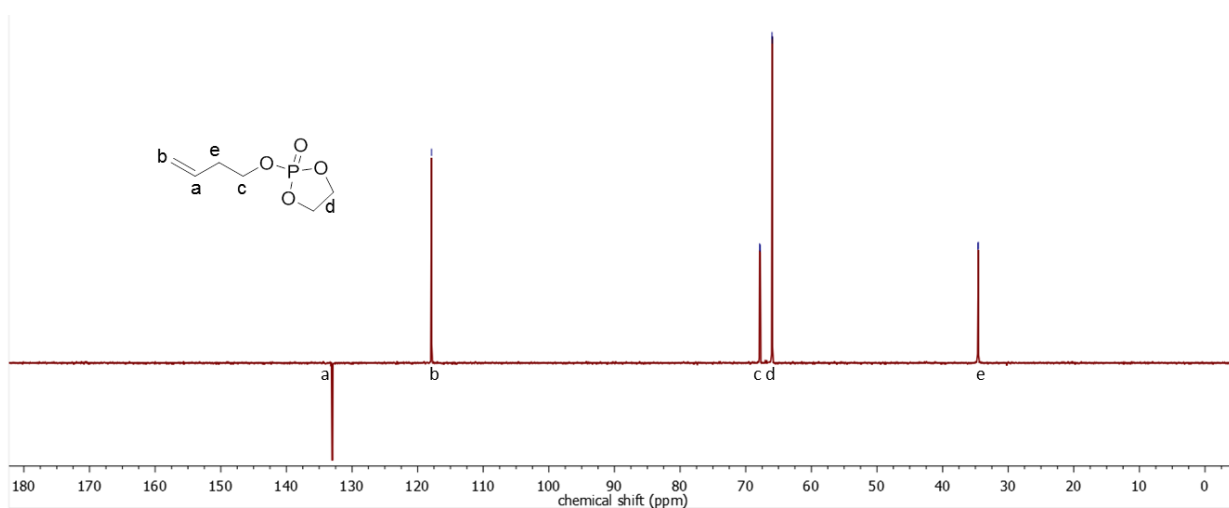


Figure S5.17.  $^{13}\text{C}\{\text{H}\}$ -DEPT NMR (76 MHz,  $\text{CDCl}_3$ ) of BuEP (6) at 298 K.

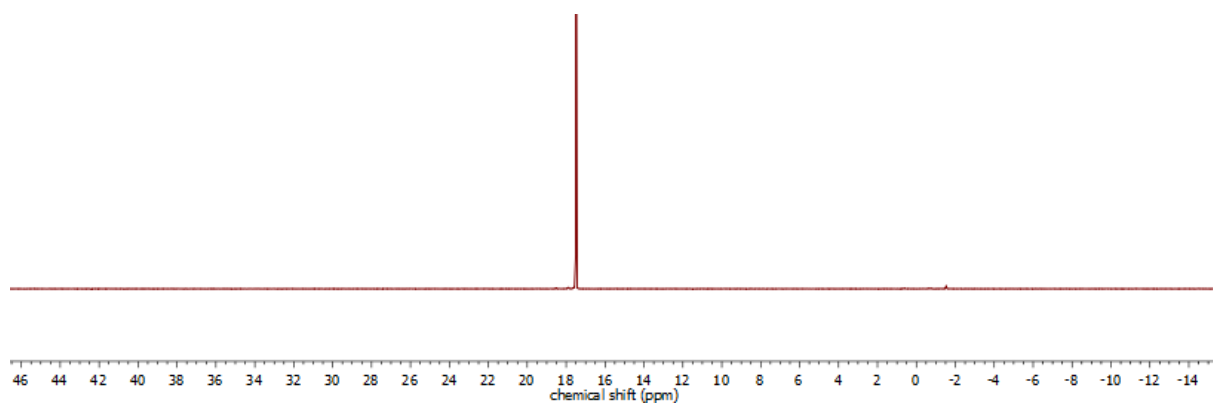


Figure S5.18.  $^{31}\text{P}\{\text{H}\}$  NMR (121 MHz,  $\text{CDCl}_3$ ) of BuEP (6) at 298 K.

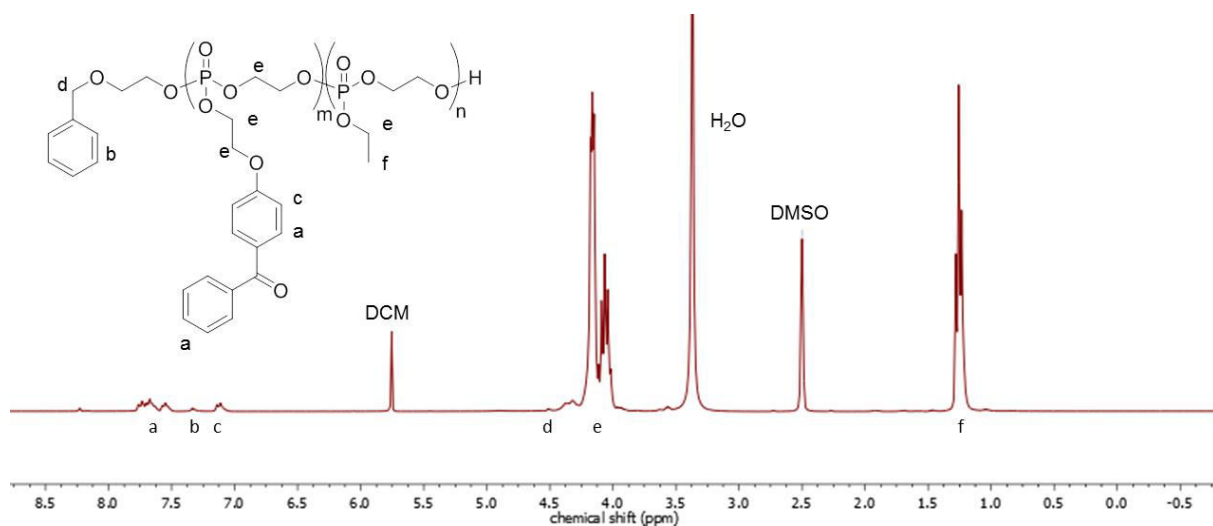


Figure S5.19.  $^1\text{H}$  NMR (300 MHz,  $\text{DMSO-d}_6$ ) of P1 at 298K.

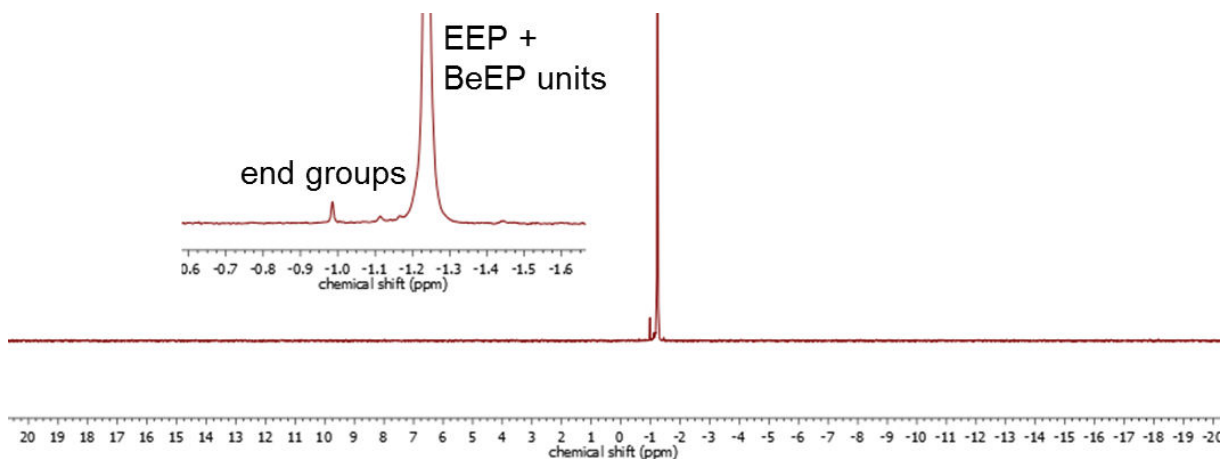


Figure S5.20.  $^{31}\text{P}\{\text{H}\}$  NMR (121 MHz,  $\text{DMSO-d}_6$ ) of P1 at 298K.

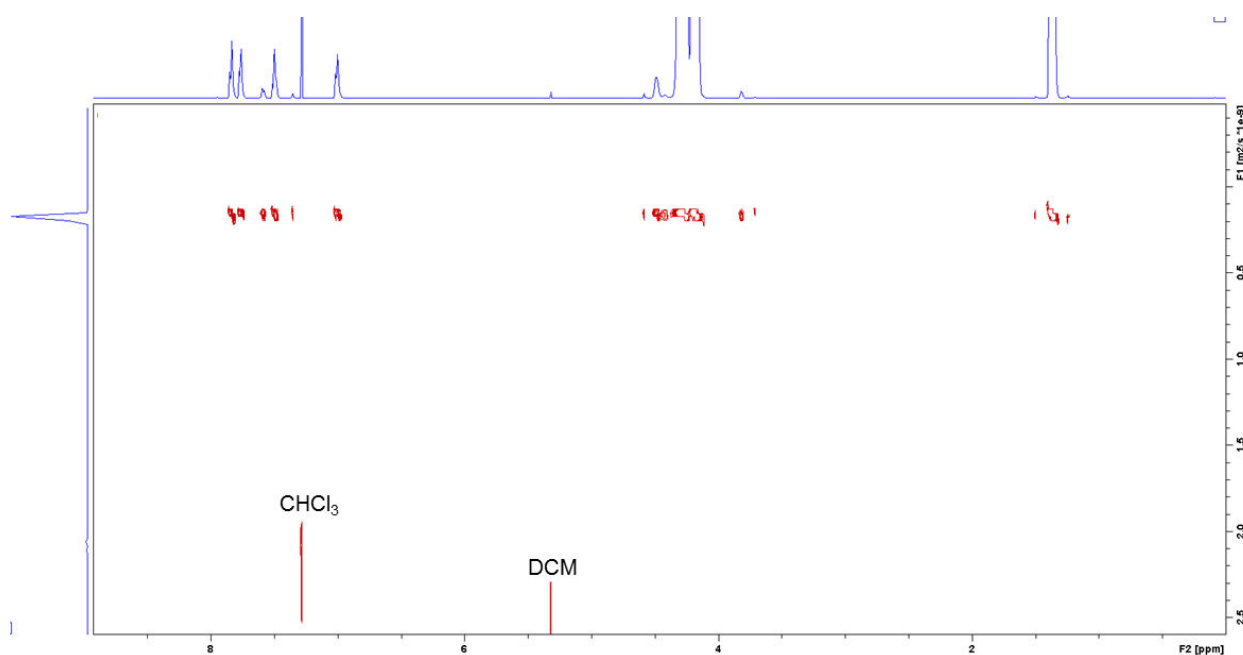


Figure S5.21.  $^1\text{H}$ -DOSY (500 MHz,  $\text{CDCl}_3$ ) of P1 at 298K.

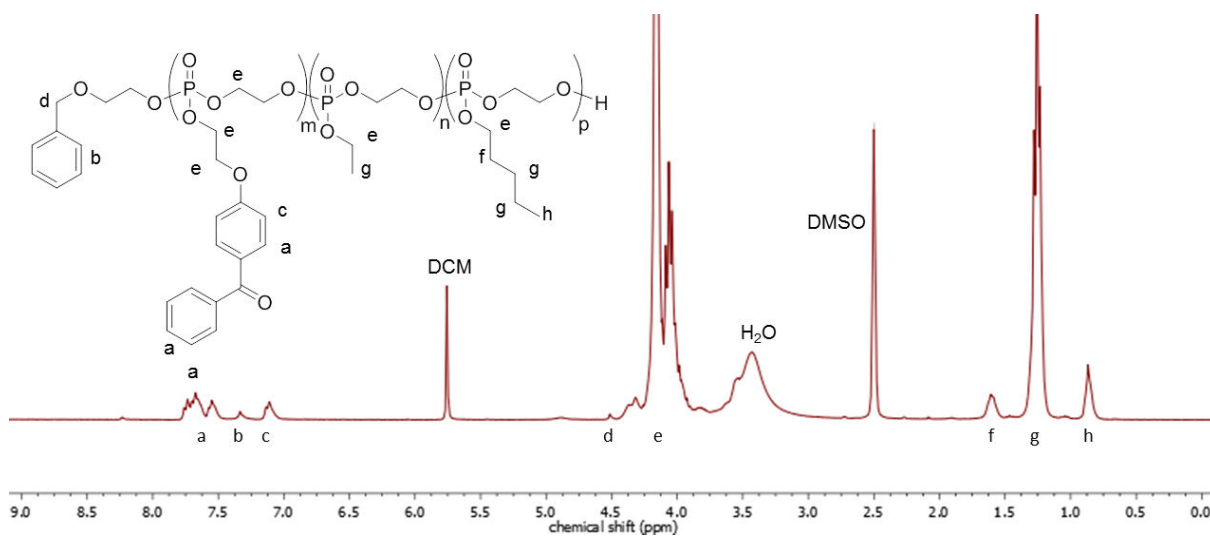
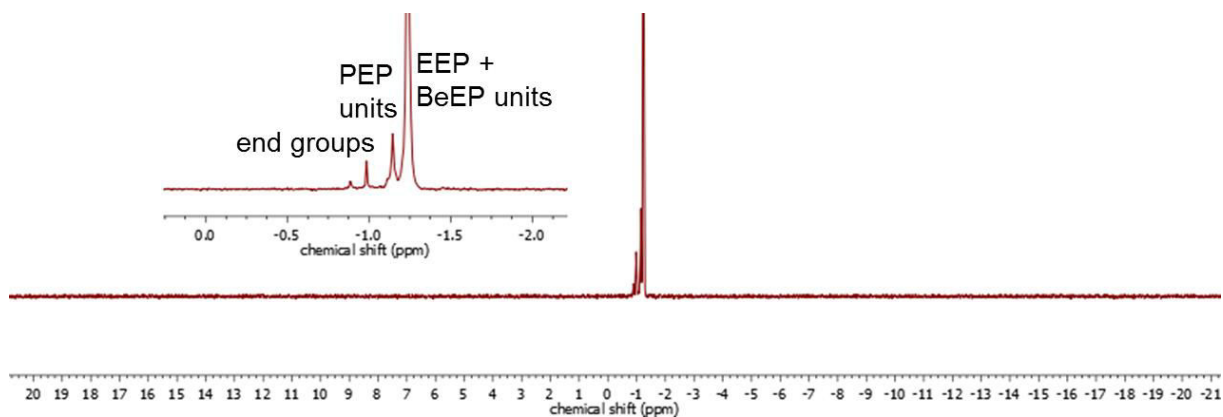
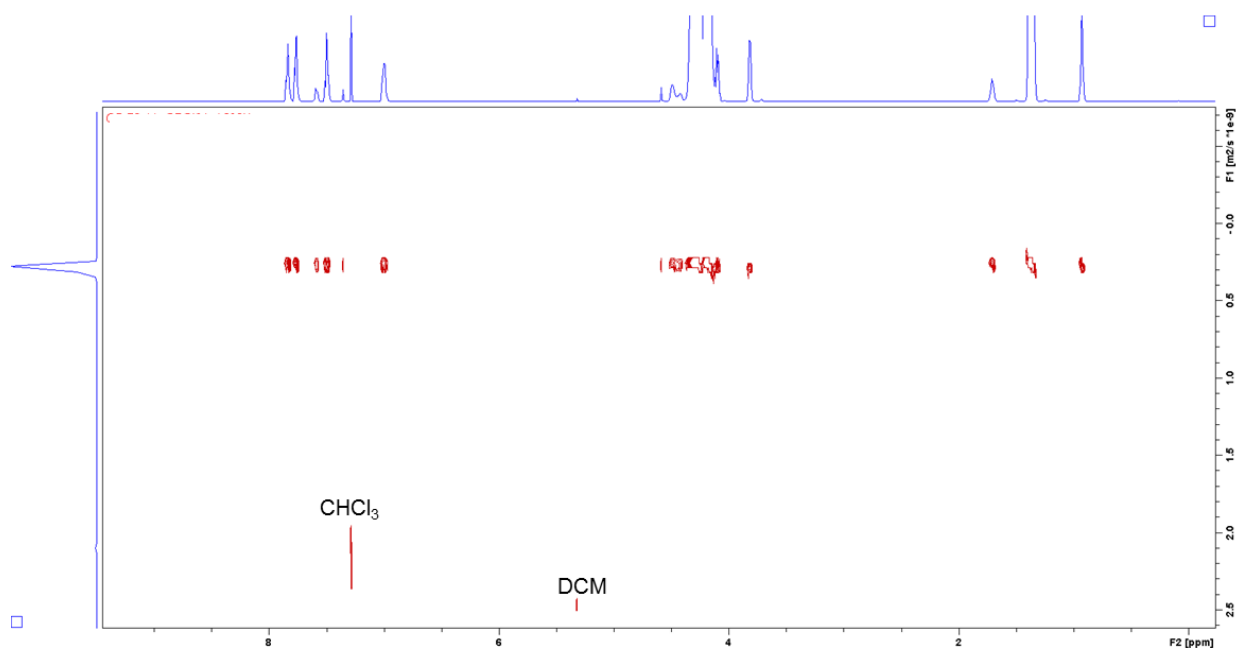


Figure S5.22.  $^1\text{H}$  NMR (300 MHz,  $\text{DMSO-d}_6$ ) of P2 at 298K.



**Figure S5.23.**  $^{31}\text{P}\{\text{H}\}$  NMR (121 MHz,  $\text{DMSO-d}_6$ ) of **P2** at 298K.



**Figure S5.24.**  $^1\text{H}$ -DOSY (500 MHz,  $\text{CDCl}_3$ ) of **P2** at 298 K.

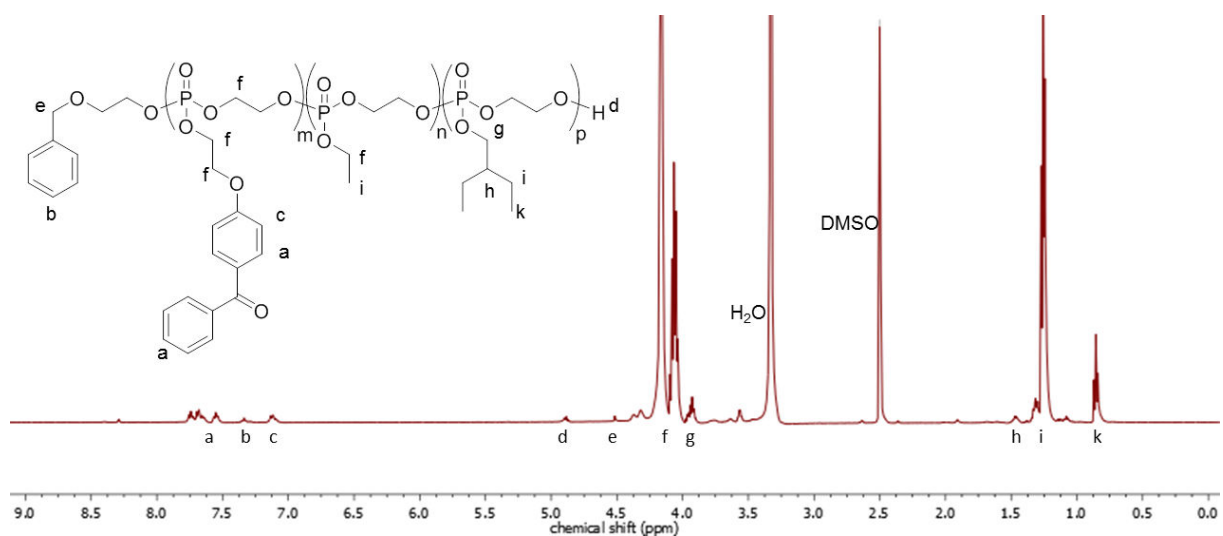


**Figure S5.26.**  $^1\text{H}$  NMR (500 MHz,  $\text{DMSO-d}_6$ ) of **P3** at 298K.

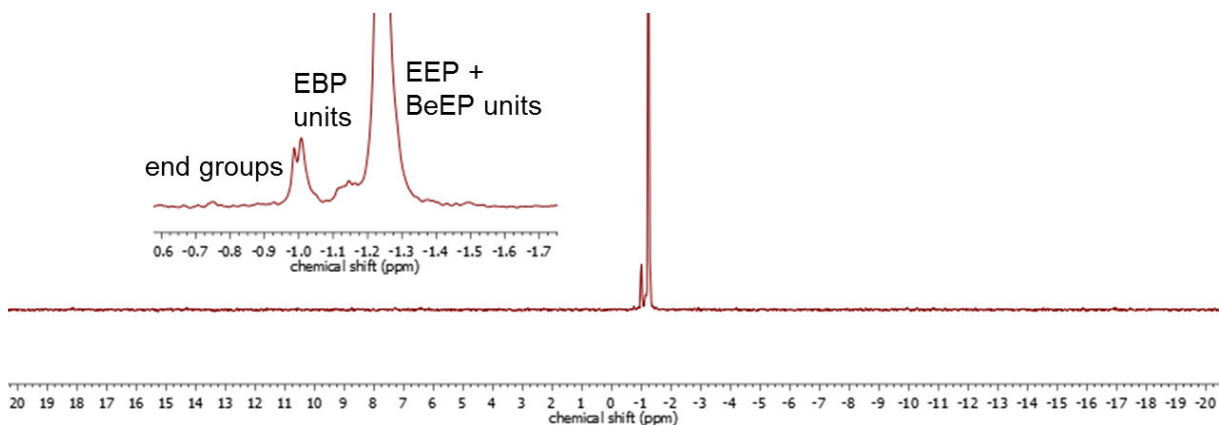


Figure S0.1.  $^{31}\text{P}\{\text{H}\}$  NMR (202 MHz, DMSO- $d_6$ ) of P3 at 298K.

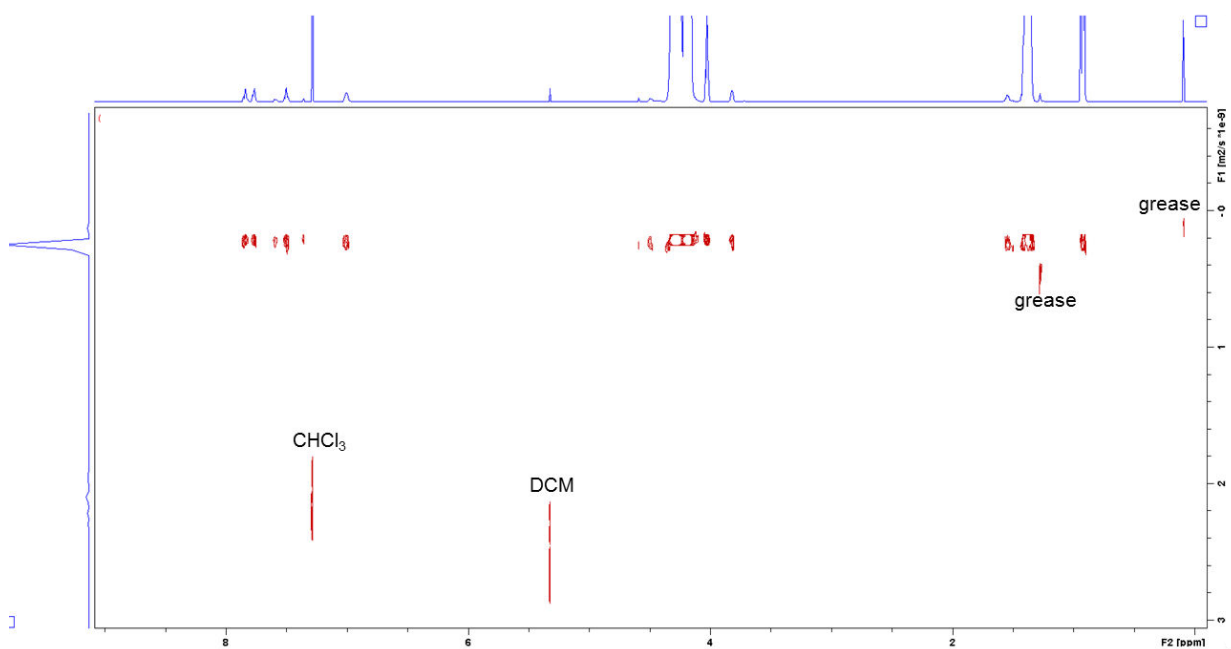


Figure S5.27.  $^1\text{H}$ -DOSY (500 MHz,  $\text{CDCl}_3$ ) of P3 at 298 K.

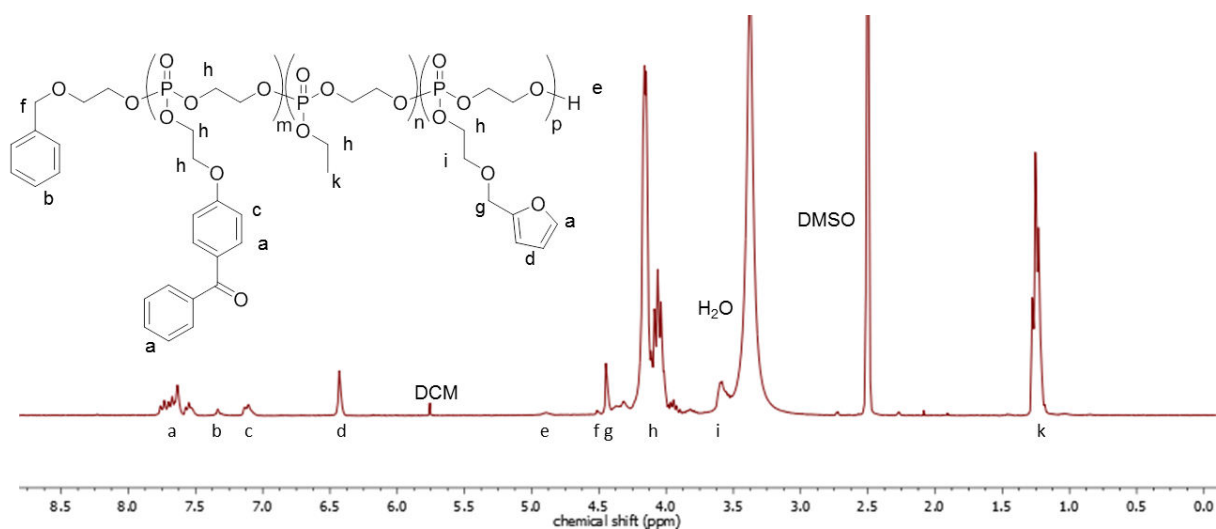


Figure S5.28.  $^1\text{H}$  NMR (300 MHz, DMSO- $d_6$ ) of P4 at 298K.

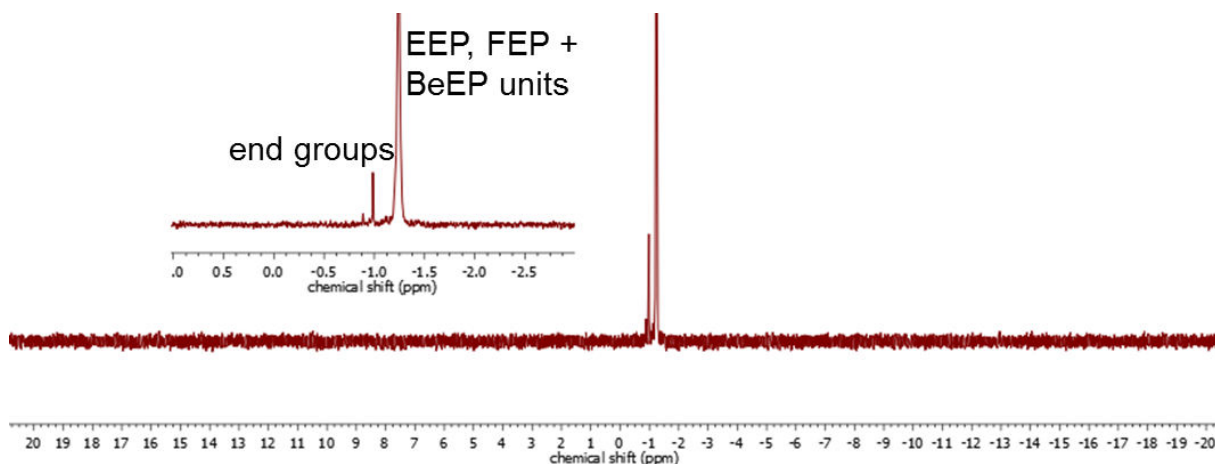


Figure S5.29.  $^{31}\text{P}\{\text{H}\}$  NMR (121 MHz,  $\text{DMSO-d}_6$ ) of **P4** at 298K.

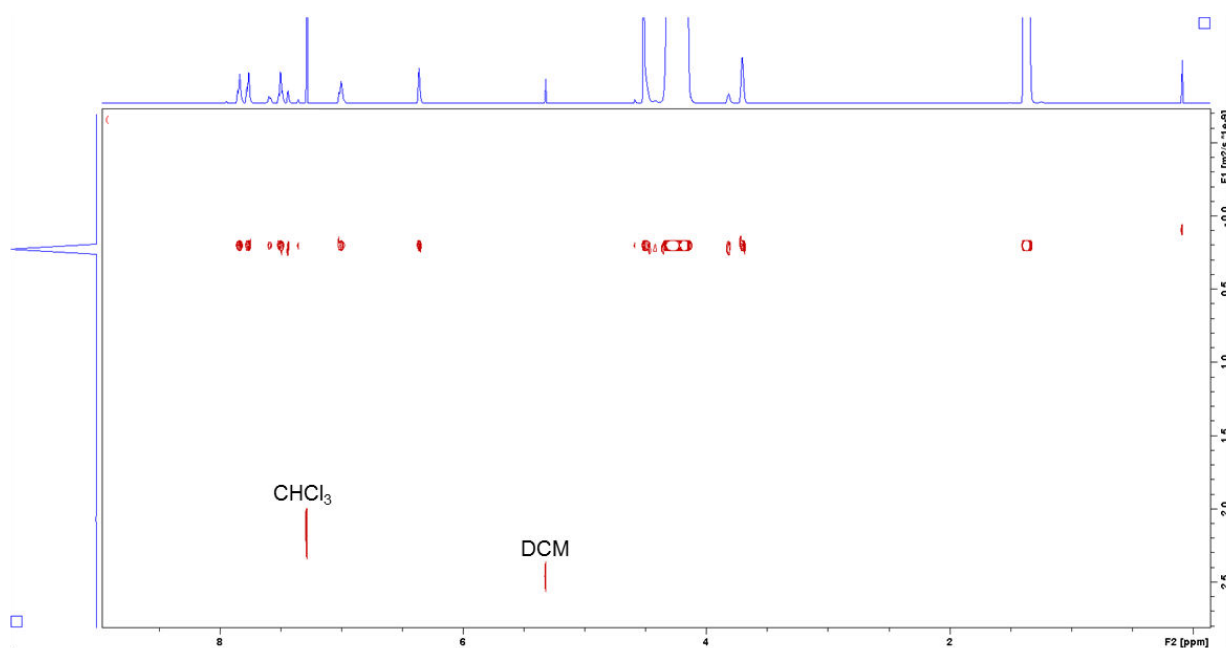


Figure S5.30.  $^1\text{H}$ -DOSY (500 MHz,  $\text{CDCl}_3$ ) of **P4** at 298 K.

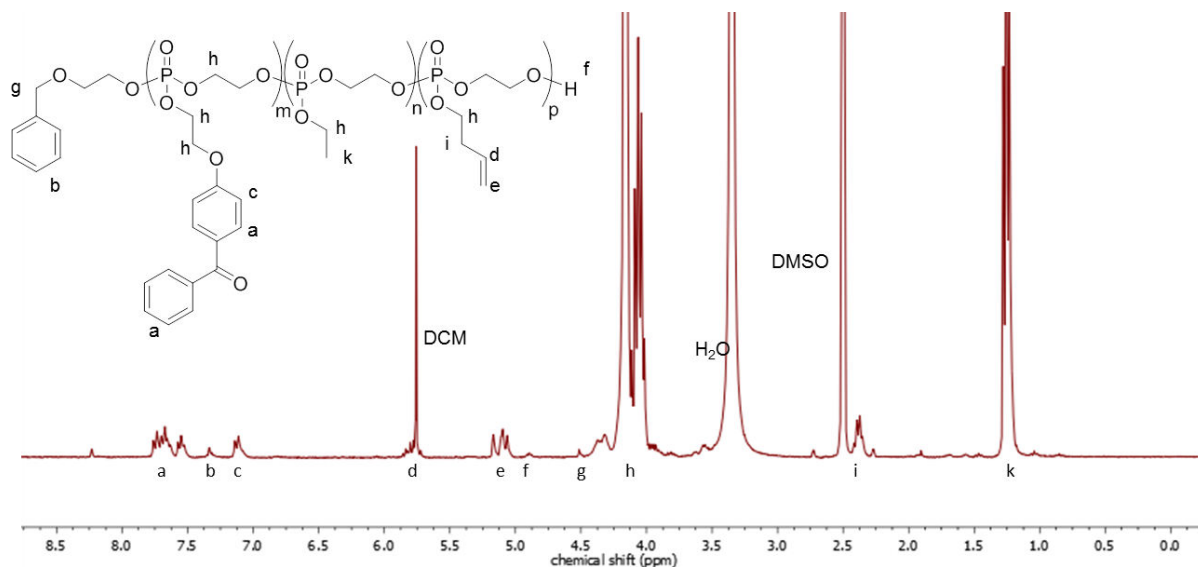


Figure S5.31.  $^1\text{H}$  NMR (300 MHz,  $\text{DMSO-d}_6$ ) of **P5** at 298K.

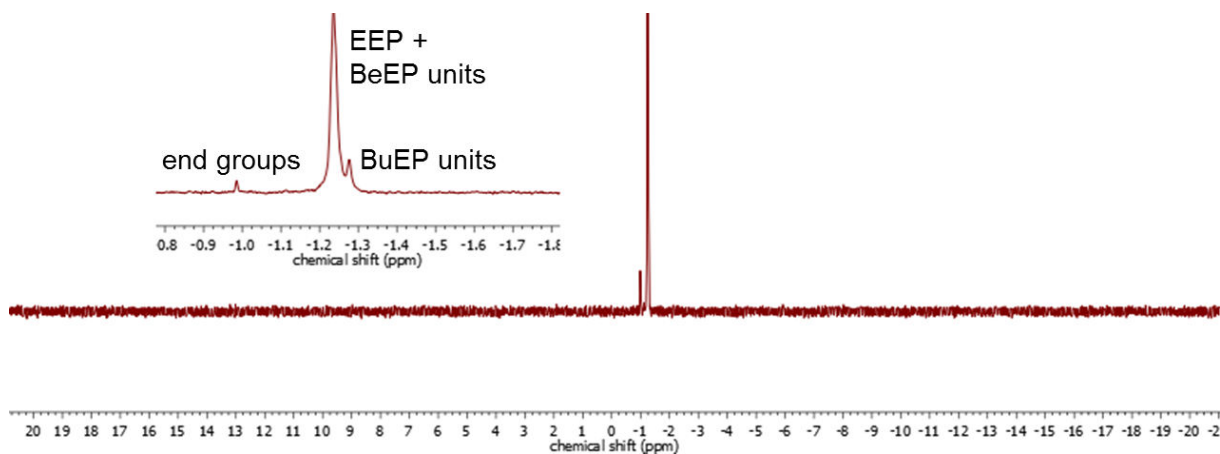


Figure S5.32.  $^{31}\text{P}\{\text{H}\}$  NMR (121 MHz,  $\text{DMSO-d}_6$ ) of **P5** at 298 K.

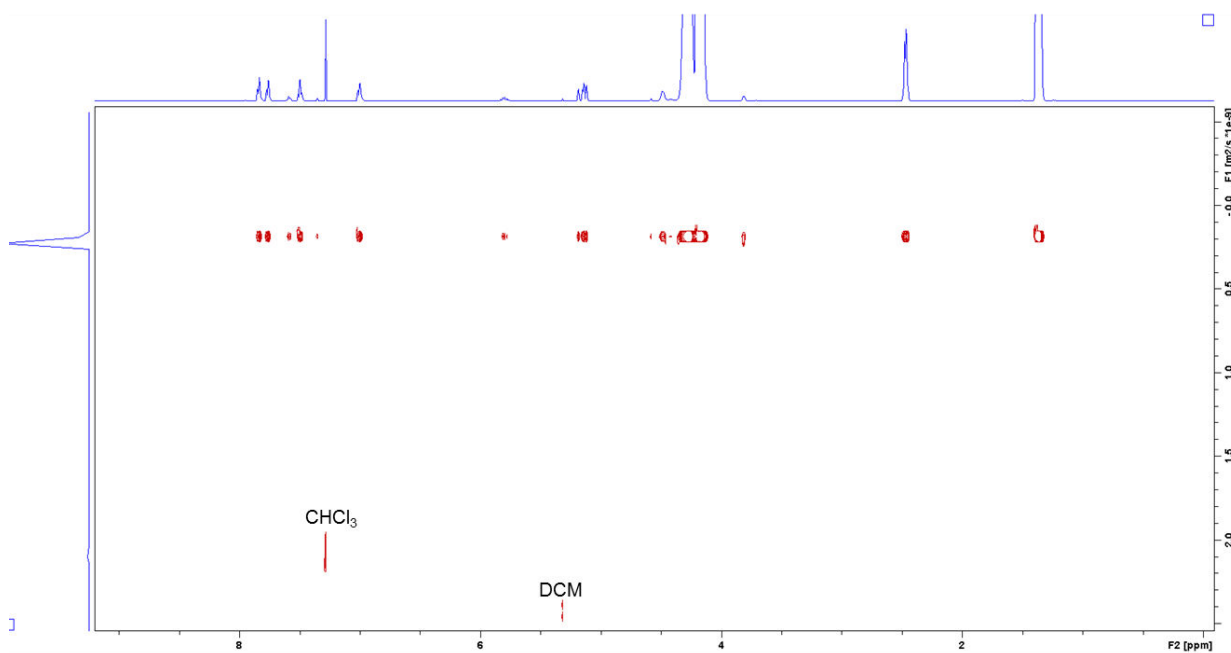


Figure S5.33.  $^1\text{H}$ -DOSY (500 MHz,  $\text{CDCl}_3$ ) of **P5** at 298 K.

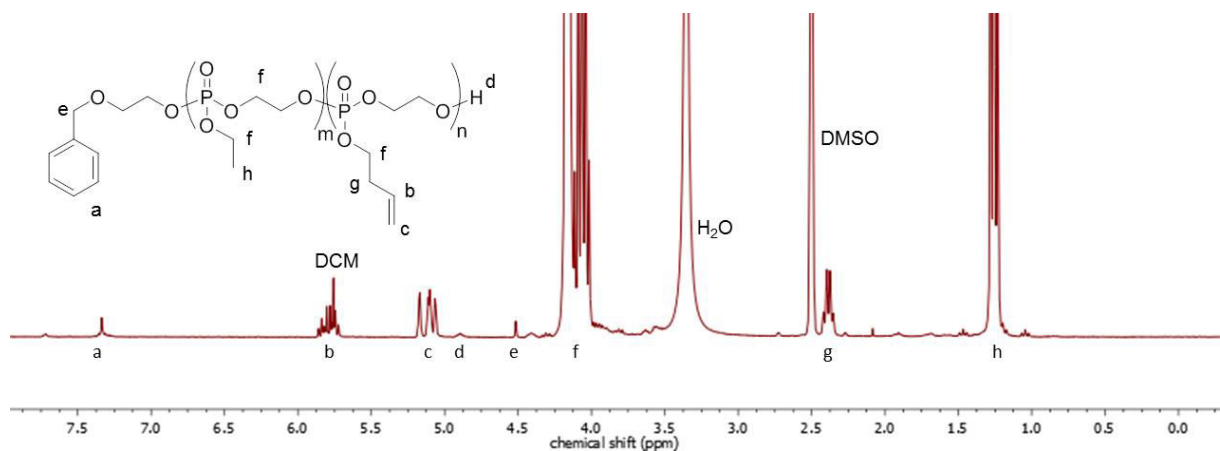
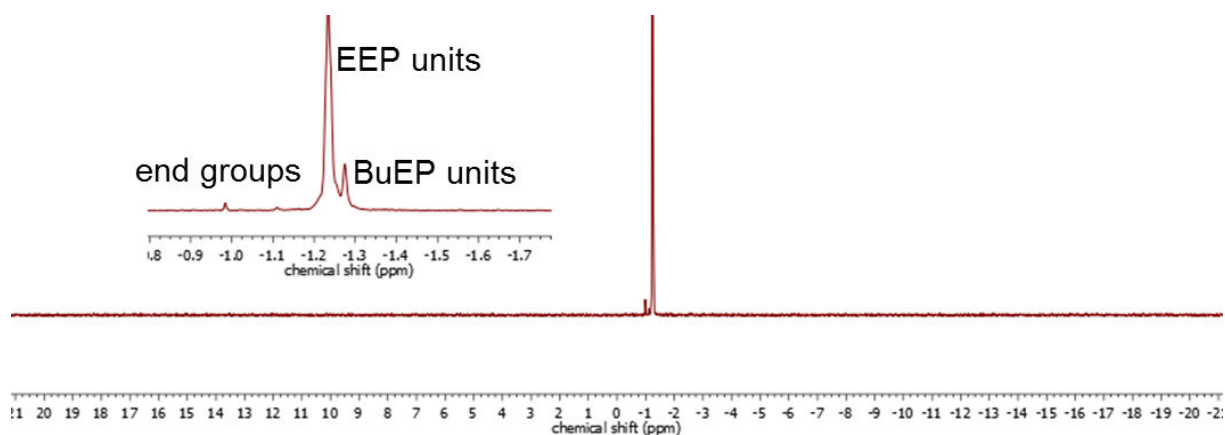
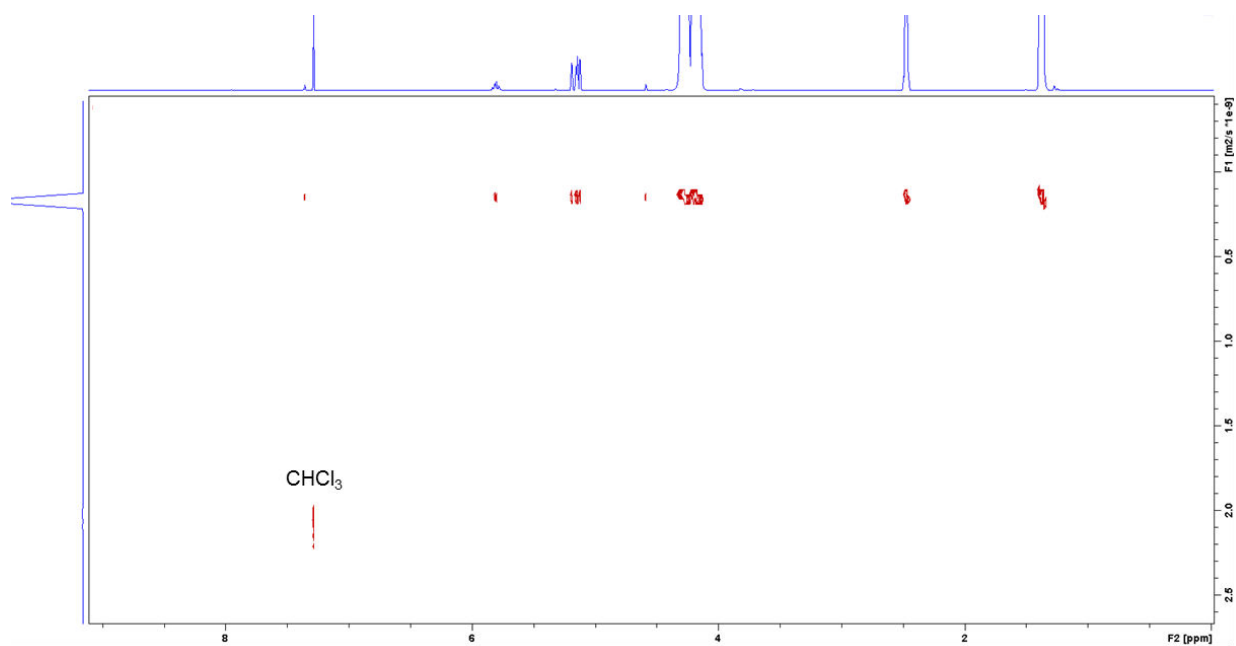


Figure S5.34.  $^1\text{H}$  NMR (300 MHz,  $\text{DMSO-d}_6$ ) of **P6** at 298 K.



**Figure S5.35.**  $^{31}\text{P}\{\text{H}\}$  NMR (121 MHz,  $\text{DMSO-d}_6$ ) of **P6** at 298K.



**Figure S5.36.**  $^1\text{H}$ -DOSY (500 MHz,  $\text{CDCl}_3$ ) of **P6** at 298 K.

**b. IR spectra**

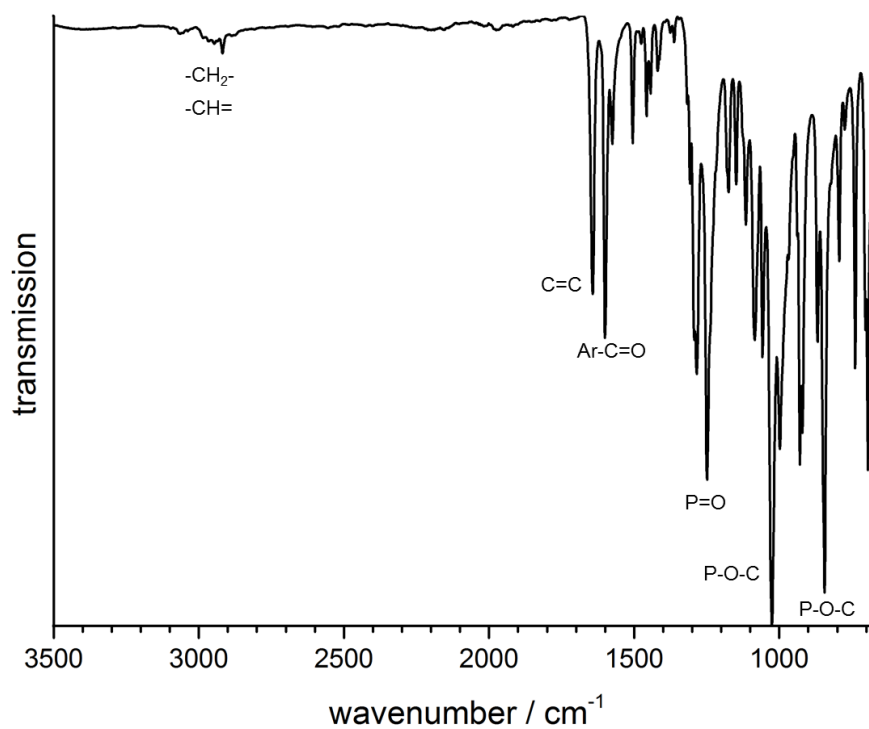


**Figure S5.37.** FT-IR spectrum of **BeEP (1)** at 298 K.

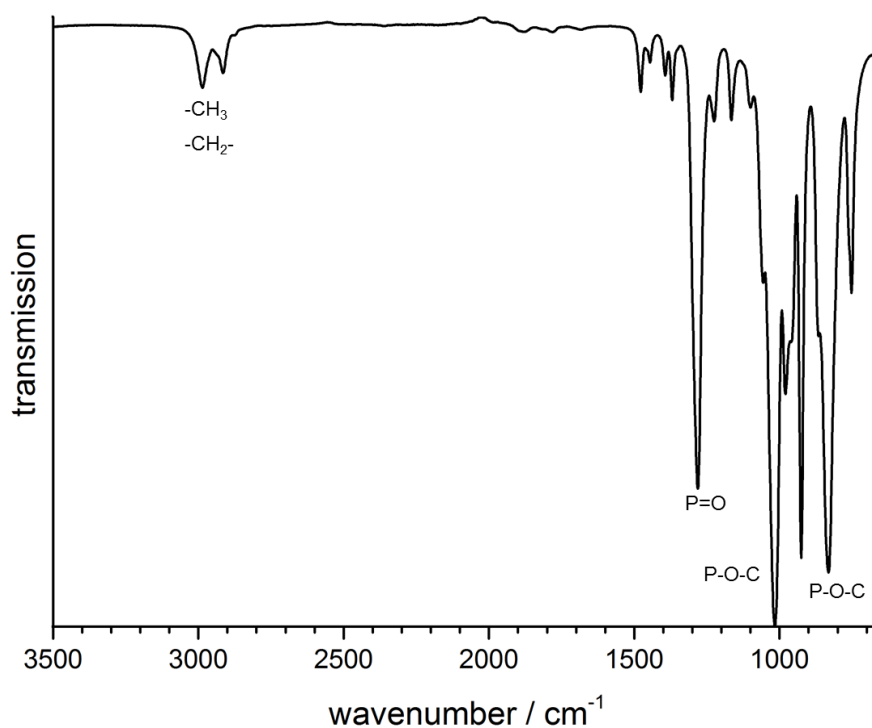


**Figure S5.38.** FT-IR spectrum of **EEP (2)** at 298 K.

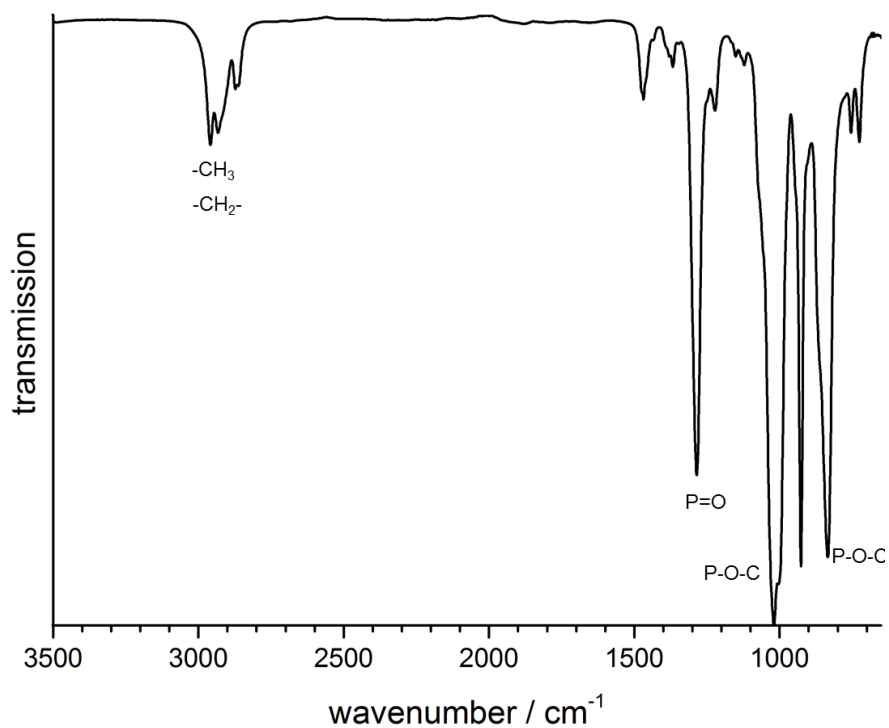


**Figure S5.39.** FT-IR spectrum of **PEP (3)** at 298 K.

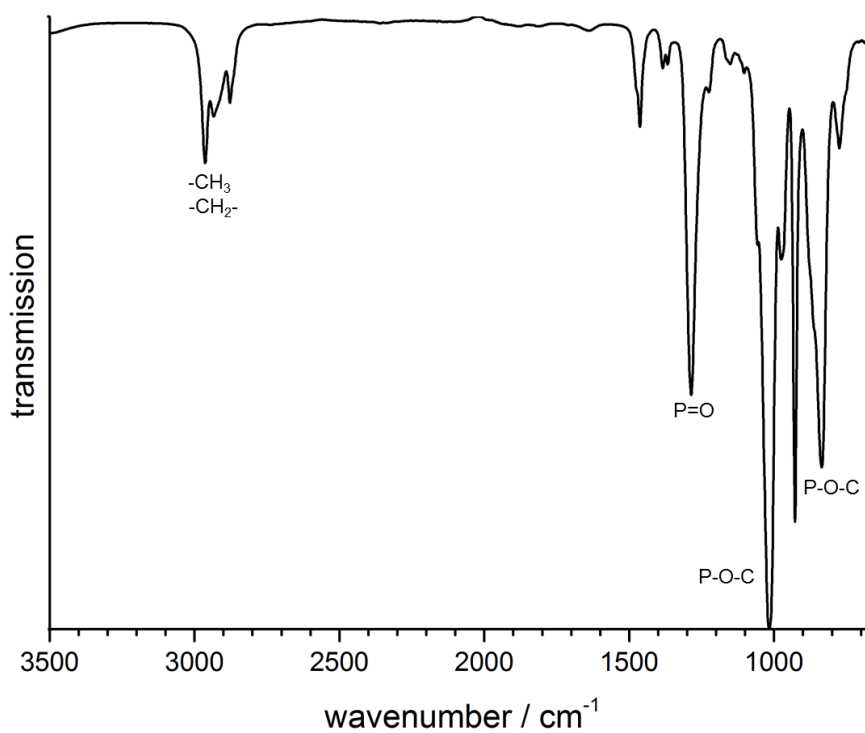


**Figure S5.40.** FT-IR spectrum of **EBP (4)** at 298 K.

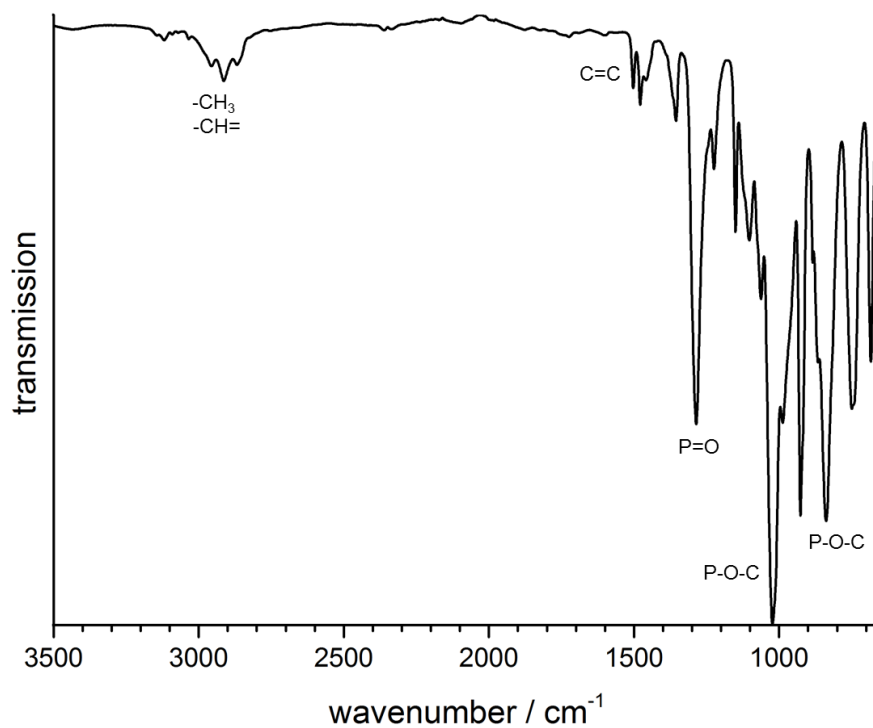


**Figure S5.41.** FT-IR spectrum of **FEP (5)** at 298 K.

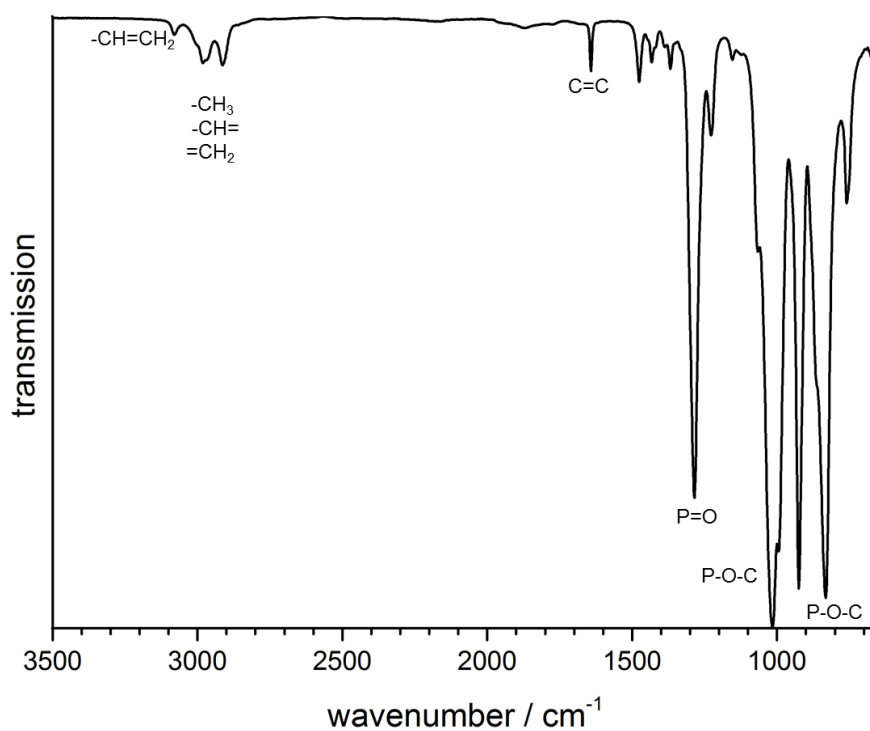


**Figure S5.42.** FT-IR spectrum of **BuEP (6)** at 298 K.

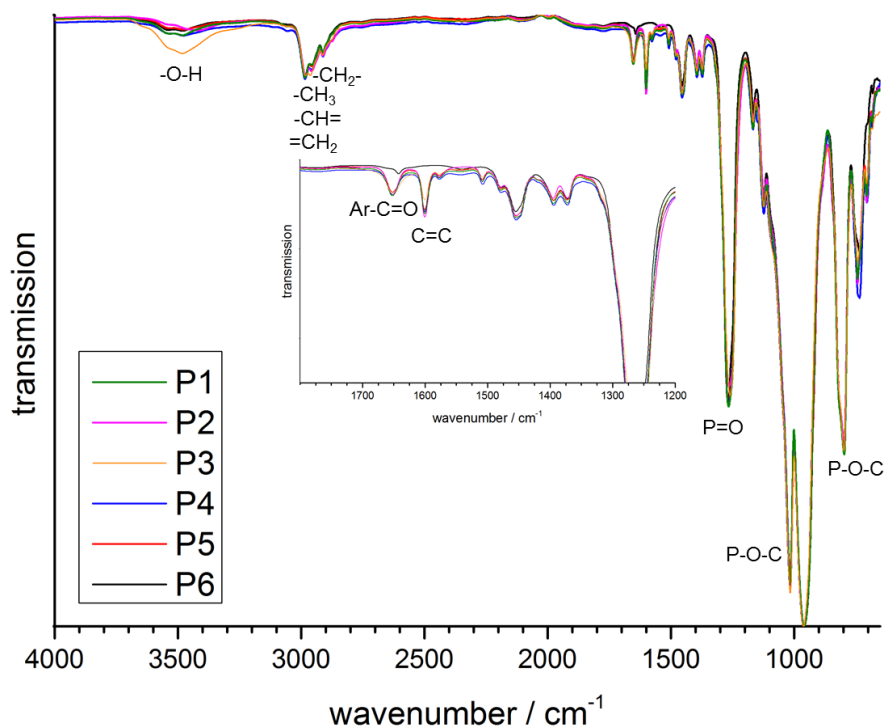


Figure S5.43. FT-IR spectra of polymers **P1-P6** at 298 K.

### 5.7.3 Kinetic measurements of copolymerizations

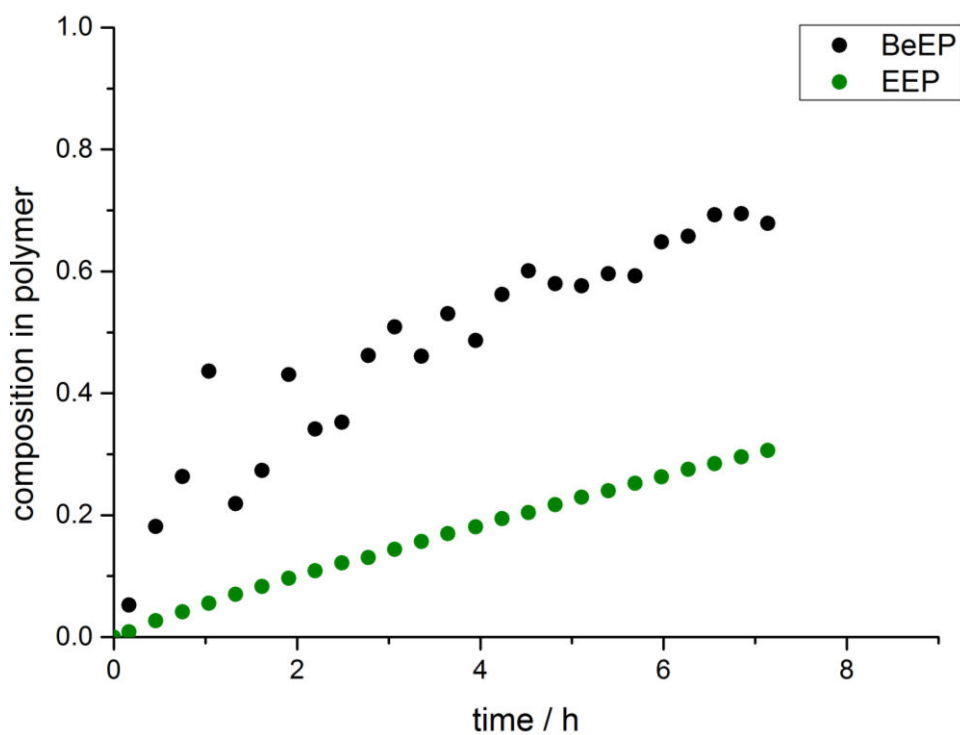
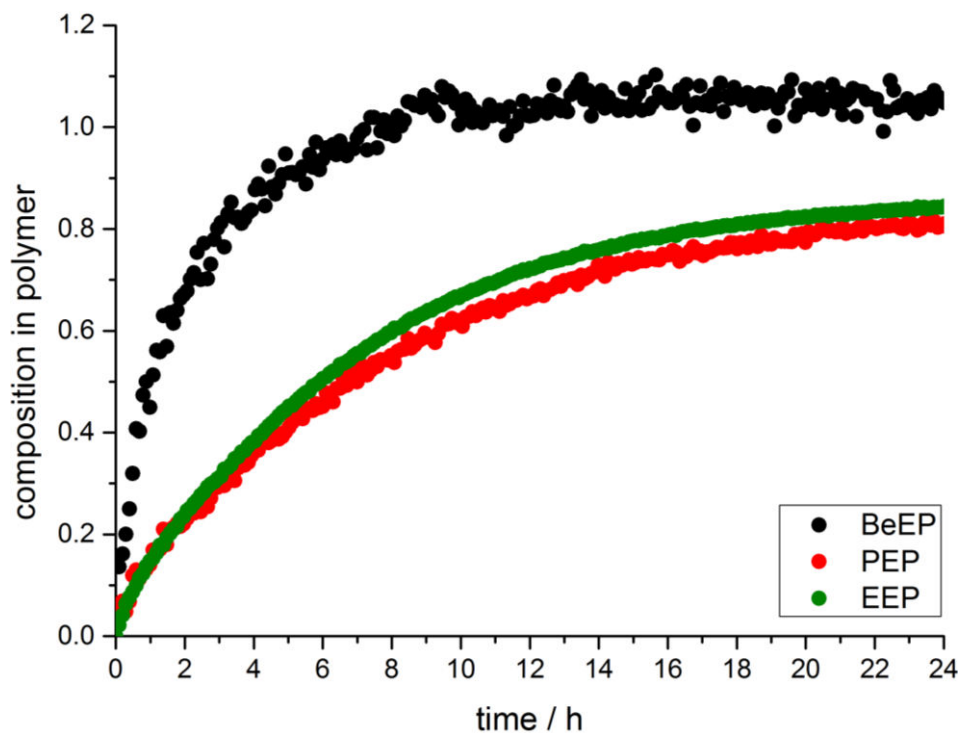
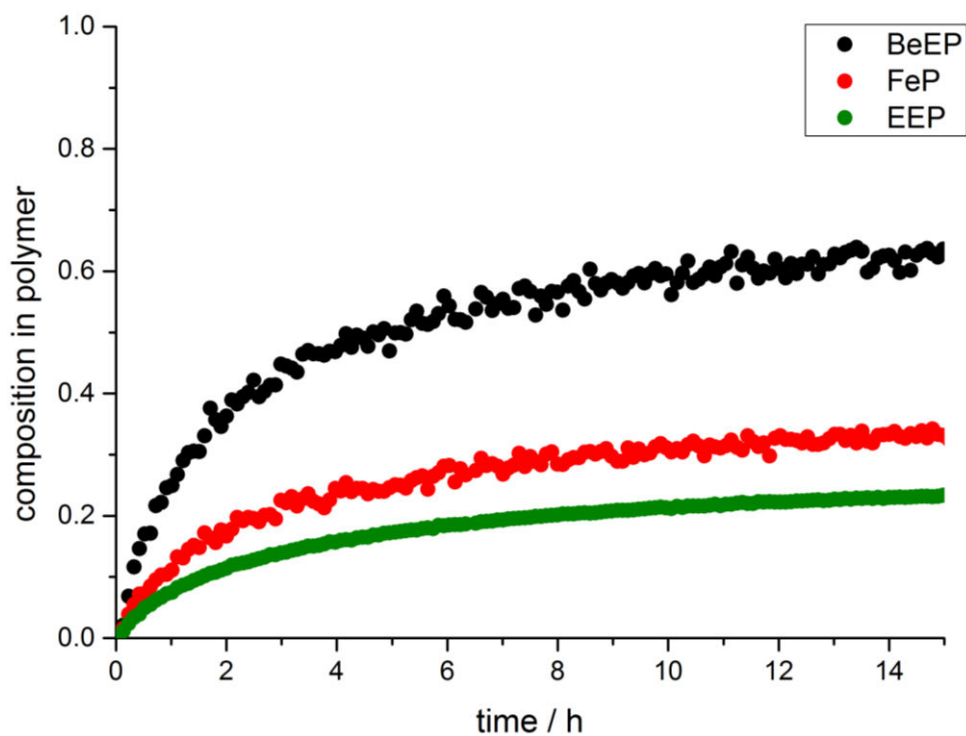


Figure S5.44. Simultaneous copolymerization: the monomer composition in polymer vs time (analog to polymer **P1**).



**Figure S5.45.** Simultaneous terpolymerization: the monomer composition in polymer vs time (analog to polymer **P2**).



**Figure S5.46.** Simultaneous terpolymerization: the monomer composition in polymer vs time (analog to polymer **P5**).

### 5.7.4 Network characterization

**Table S5.1.** Overview of layer thicknesses of PPE-networks of **P4** on silicon substrates in dependence of the concentration of used polymer solution.

polymer concentration / mg/mL	layer thickness / nm
50	199±2
30	61±1
20	54±1
10	24±1

**Table S5.2.** Contact angles of the polymer networks.

sample	static / °		advancing / °		receding / °	
	left	right	left	right	left	right
P2	20±1	21±0	21±4	22±4	11±1	10±1
P4	26±3	26±3	29±2	29±3	16±1	16±1
P5	26±1	25±1	34±3	35±3	8±1	8±1

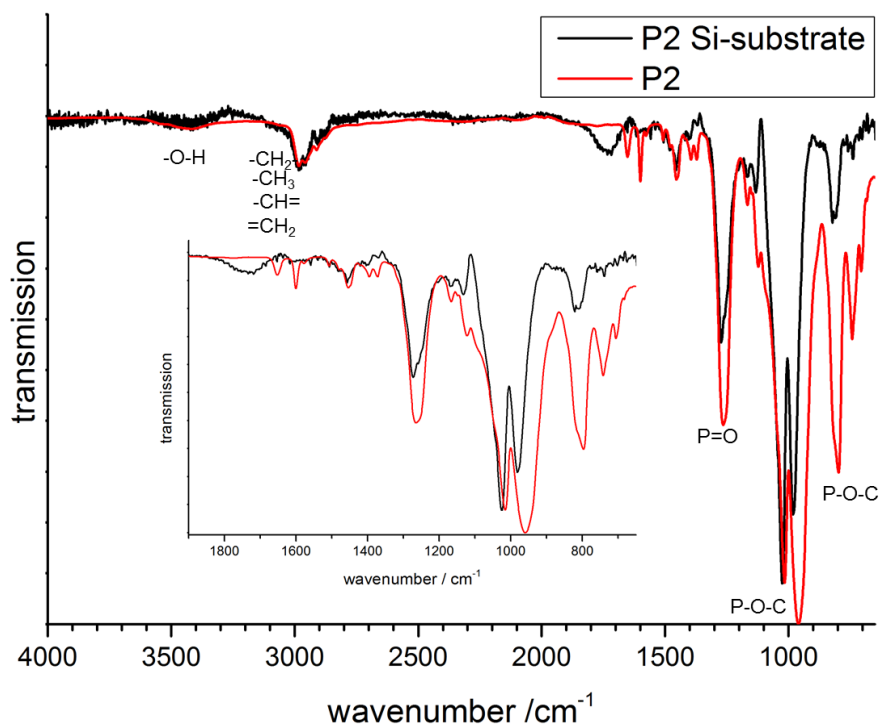


**Figure S5.47.** FT-IR spectra of **P2** and **P2** on Si-substrate.

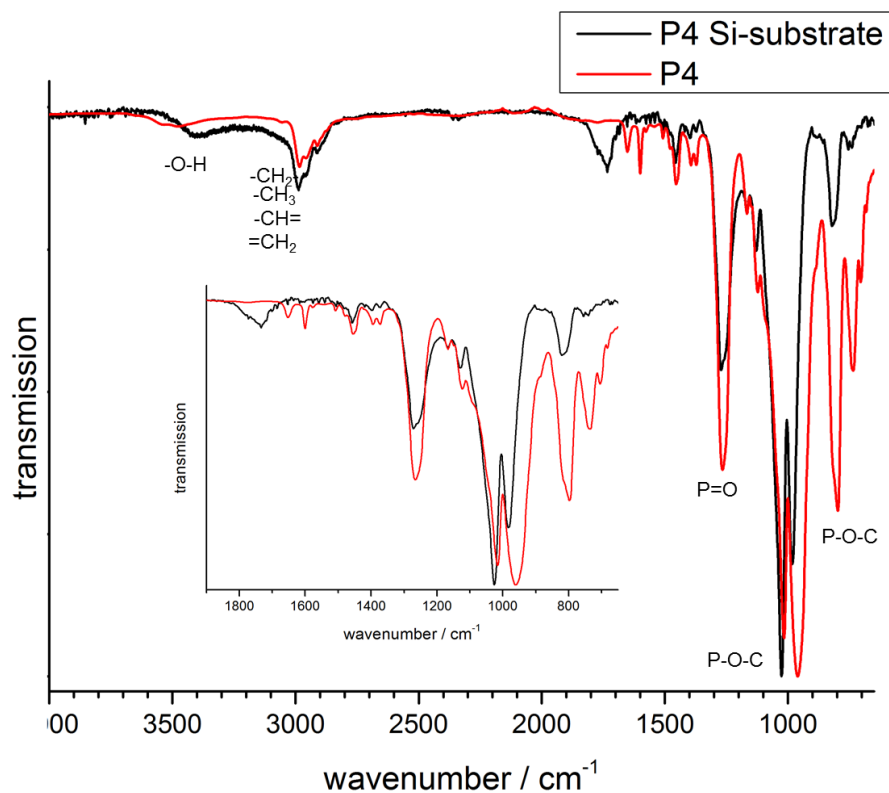


Figure S5.48. FT-IR spectra of P4 and P4 on Si-substrate.

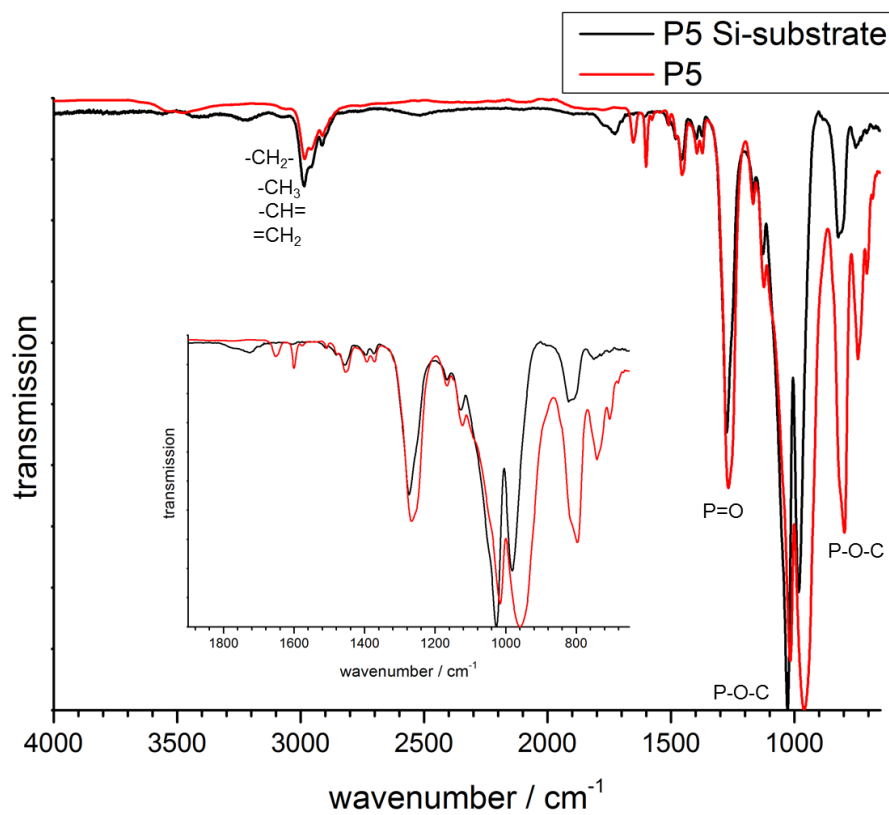
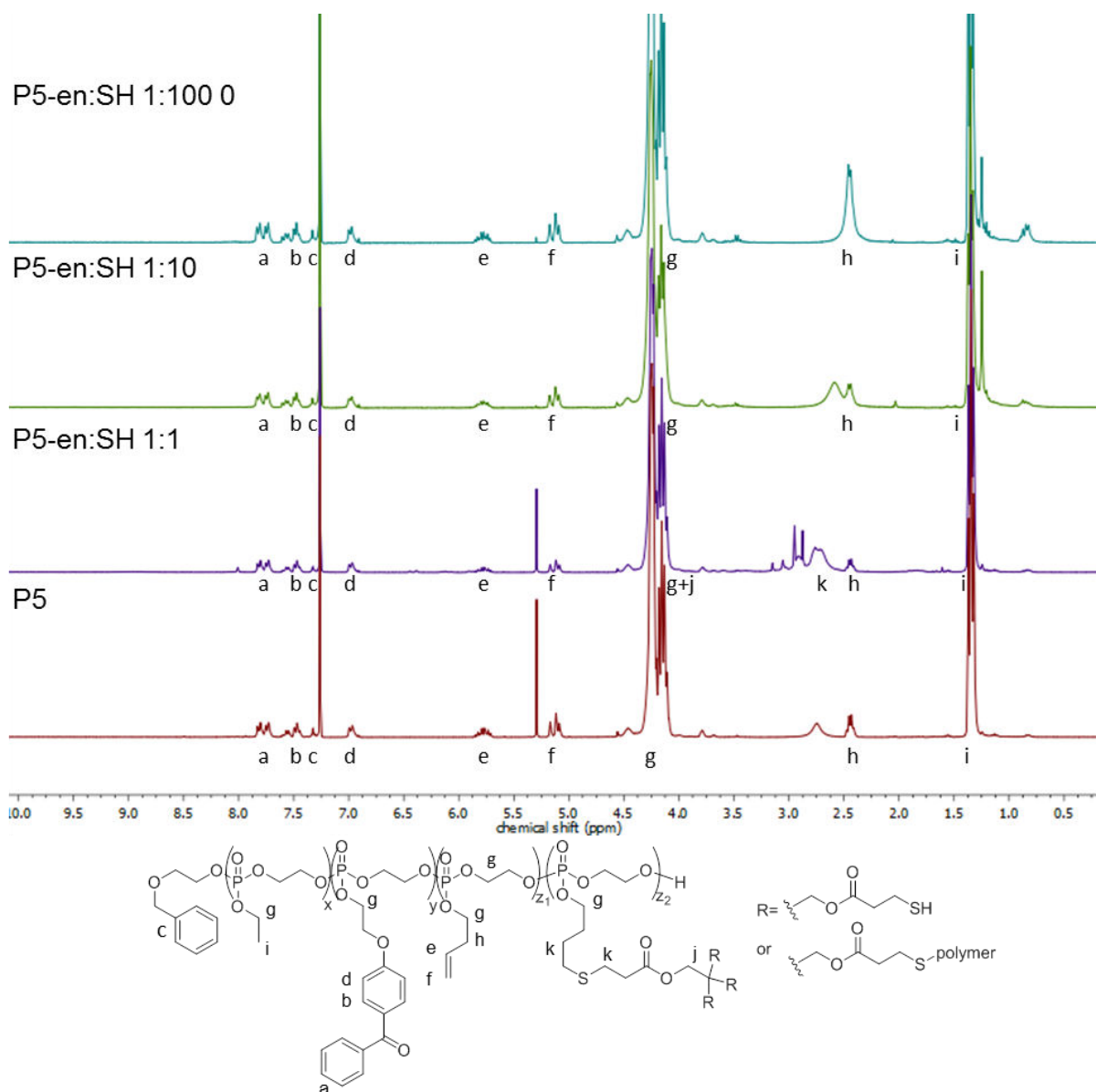
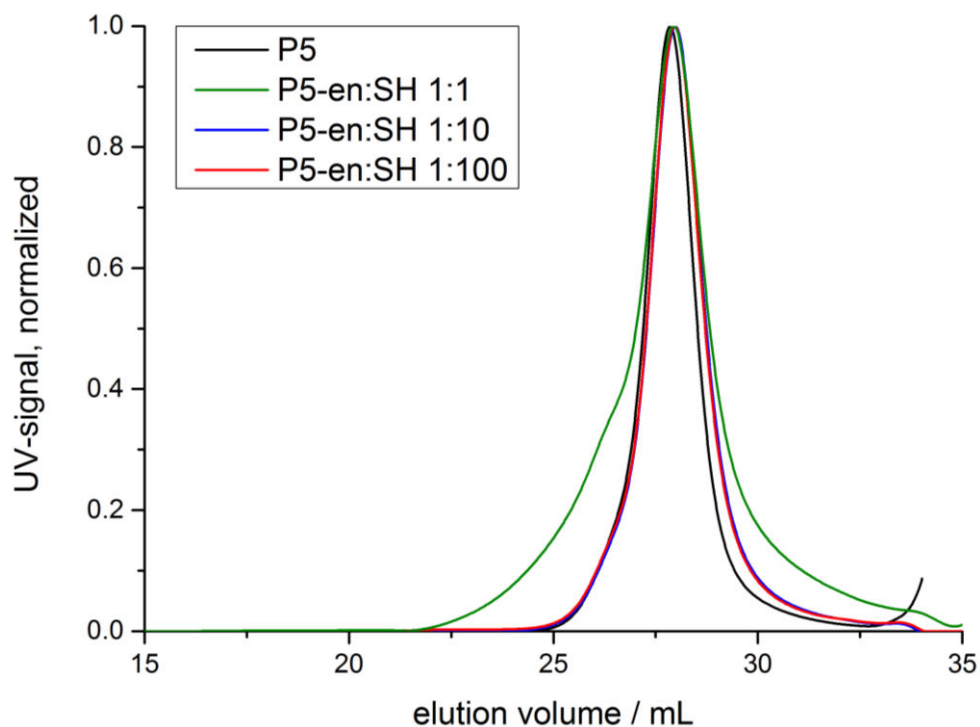


Figure S5.49. FT-IR spectra of P5 and P5 on Si-substrate.

5.7.5 Alternative networks



**Figure S5.50.** <sup>1</sup>H NMR (300 MHz, CDCl<sub>3</sub>) overlay of **P5** and precrosslinking with different ratios of tetrathiol crosslinker.



**Figure S5.51.** GPC elugrams of **P5** and precrosslinked **P5** with different ratios of tetrathiol crosslinker, in DMF, PEO standard, UV signal.

### 5.7.6 Post-modification of networks

**Table S5.3.** Contact angles and layer thicknesses before and after post-polymerization modification.

sample	static / °		advancing / °		receding / °		layer thickness / nm
	left	right	left	right	left	right	
<b>P4</b>	26±3	26±3	29±2	29±3	16±1	16±1	110±2
<b>P4-C<sub>12</sub></b>	37±1	38±1	63±3	64±4	11±1	10±1	77±1
<b>P5-</b>	26±1	25±1	34±3	35±3	8±1	8±1	263±1
<b>P5-C<sub>12</sub></b>	28±1	29±1	42±2	42±1	8±1	8±1	77±1

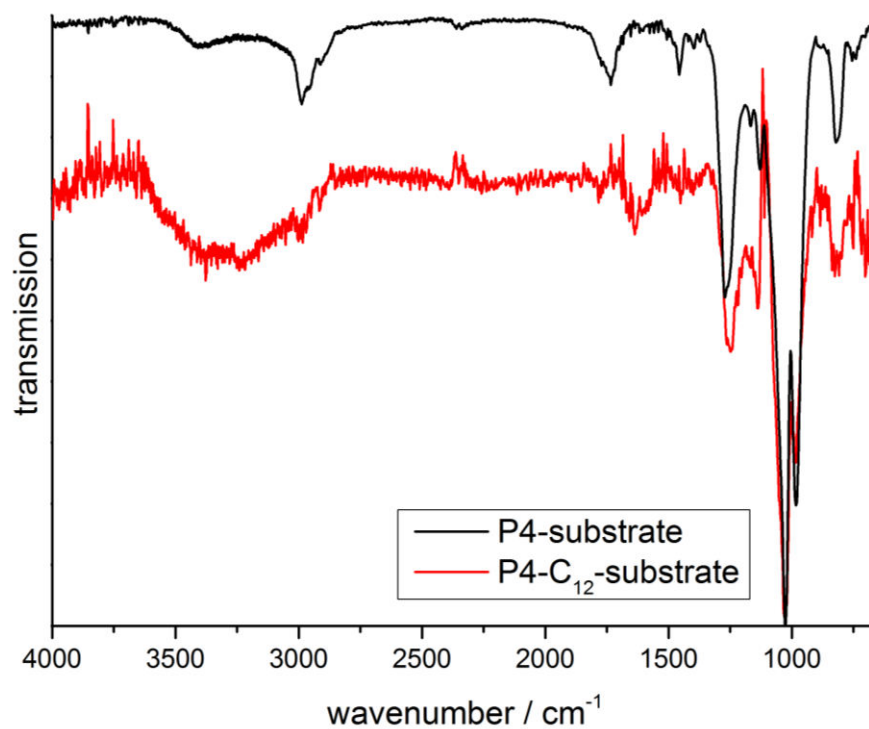


**Figure S5.52.** FT-IR spectra of **P4** on Si-substrate before and after functionalization. Note: Due to mass loss, **P4-C<sub>12</sub>**-substrate did not exhibit enough material for a significant IR measurement.

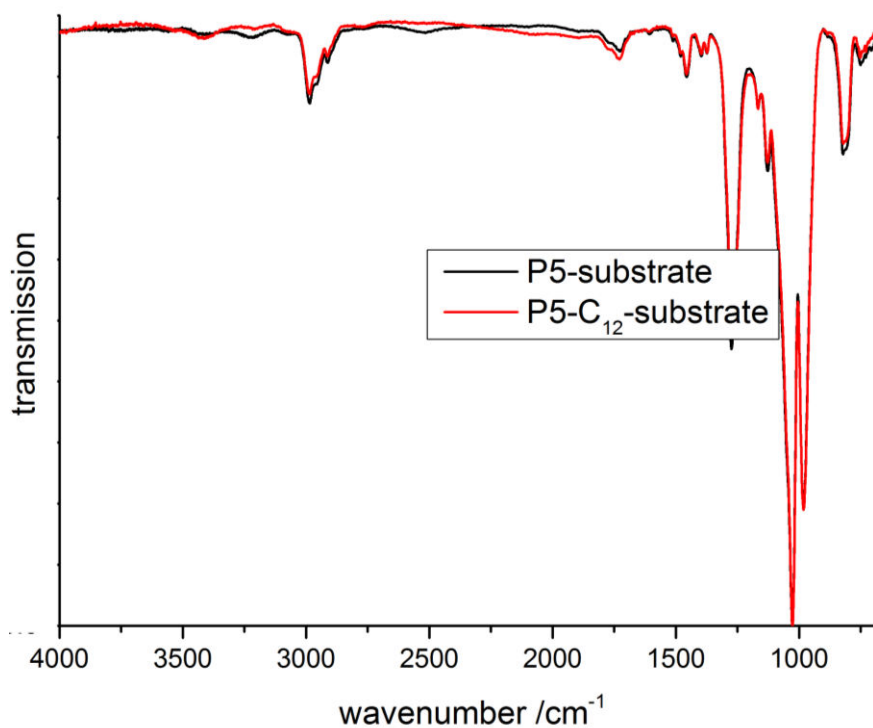


**Figure S5.53.** FT-IR spectra of **P5** on Si-substrate before and after functionalization. Note: The IR spectrum of **P4-C<sub>12</sub>**-substrate did not show any change of band intensities.

## 5.8 References

1. Hartleb, W.; Saar, J. S.; Zou, P.; Lienkamp, K., *Macromol. Chem. Phys.* **2016**, *217* (2), 225-231.
2. Damodaran, V. B.; Murthy, N. S., *Biomater. Res.* **2016**, *20* (1), 18.
3. Banerjee, I.; Pangule, R. C.; Kane, R. S., *Adv. Mater.* **2011**, *23* (6), 690-718.
4. Ekin, A.; Webster, D. C.; Daniels, J. W.; Stafslin, S. J.; Cassé, F.; Callow, J. A.; Callow, M. E., *J. Coat. Technol. Res.* **2007**, *4* (4), 435.
5. Yarbrough, J. C.; Rolland, J. P.; DeSimone, J. M.; Callow, M. E.; Finlay, J. A.; Callow, J. A., *Macromolecules* **2006**, *39* (7), 2521-2528.
6. Krishnan, S.; Weinman, C. J.; Ober, C. K., *J. Mater. Chem.* **2008**, *18* (29), 3405-3413.
7. Kurowska, M.; Eickenscheidt, A.; Guevara-Solarte, D.-L.; Widyaya, V. T.; Marx, F.; Al-Ahmad, A.; Lienkamp, K., *Biomacromolecules* **2017**.
8. Steinbach, T.; Wurm, F. R., *Angew. Chem. Int. Ed.* **2015**, *54* (21), 6098-6108.
9. Schöttler, S.; Becker, G.; Winzen, S.; Steinbach, T.; Mohr, K.; Landfester, K.; Mailänder, V.; Wurm, F. R., *Nat. Nano.* **2016**, *11* (4), 372-377.
10. Pandiyarajan, C. K.; Prucker, O.; Rühle, J., *Macromolecules* **2016**, *49* (21), 8254-8264.
11. Körner, M.; Prucker, O.; Rühle, J., *Macromolecules* **2016**, *49* (7), 2438-2447.
12. Prucker, O.; Naumann, C. A.; Rühle, J.; Knoll, W.; Frank, C. W., *J. Am. Chem. Soc.* **1999**, *121* (38), 8766-8770.
13. Toomey, R.; Freidank, D.; Rühle, J., *Macromolecules* **2004**, *37* (3), 882-887.
14. Freeman, R.; Hill, H. D. W.; Kaptein, R., *J. Magn. Reson.* **1972**, *7* (3), 327-329.
15. Clément, B.; Grignard, B.; Koole, L.; Jérôme, C.; Lecomte, P., *Macromolecules* **2012**, *45* (11), 4476-4486.
16. Leahaf, A. M.; Moussallem, M. D.; Schlenoff, J. B., *Langmuir* **2011**, *27* (8), 4756-4763.
17. Lim, Y. H.; Tiemann, K. M.; Heo, G. S.; Wagers, P. O.; Rezenom, Y. H.; Zhang, S.; Zhang, F.; Youngs, W. J.; Hunstad, D. A.; Wooley, K. L., *ACS Nano* **2015**, *9* (2), 1995-2008.
18. Zhao, Z.; Wang, J.; Mao, H.-Q.; Leong, K. W., *Adv. Drug Delivery Rev.* **2003**, *55* (4), 483-499.
19. Zhang, S.; Zou, J.; Zhang, F.; Elsabahy, M.; Felder, S. E.; Zhu, J.; Pochan, D. J.; Wooley, K. L., *J. Am. Chem. Soc.* **2012**, *134* (44), 18467-18474.
20. Steinbach, T.; Schroder, R.; Ritz, S.; Wurm, F. R., *Polym. Chem.* **4** (16), 4469-4479.
21. Samuel, J. D. J. S.; Brenner, T.; Prucker, O.; Grumann, M.; Ducree, J.; Zengerle, R.; Rühle, J., *Macromol. Chem. Phys.* **2010**, *211* (2), 195-203.
22. Moschallski, M.; Baader, J.; Prucker, O.; Rühle, J., *Anal. Chim. Acta* **2010**, *671* (1), 92-98.
23. Shapovalov, V.; Zaitsev, V. S.; Strzhemechny, Y.; Choudhery, F.; Zhao, W.; Schwarz, S. A.; Ge, S.; Shin, K.; Sokolov, J.; Rafailovich, M. H., *Polym. Int.* **2000**, *49* (5), 432-436.
24. Hesse, M.; Meier, H.; Zeeh, B., *Spektroskopische Methoden in der organischen Chemie*. 5th, revised ed.; Georg Thieme Verlag: Stuttgart, 1995.
25. Socrates, G., *Infrared and Raman Characteristic Group Frequencies: Tables and Charts*. 3rd ed.; Wiley: 2004.
26. Becker, G.; Marquetant, T. A.; Wagner, M.; Wurm, F. R., *submitted* **2017**.
27. Colak, S.; Tew, G. N., *Langmuir* **2012**, *28* (1), 666-675.
28. Burkholder, T. P.; Bratton, L. D.; Kudlacz, E. M.; Maynard, G. P.; Kane, J. M.; Santiago, B. US6329392 B1, 2001.
29. Pratt, R. C.; Lohmeijer, B. G. G.; Long, D. A.; Lundberg, P. N. P.; Dove, A. P.; Li, H.; Wade, C. G.; Waymouth, R. M.; Hedrick, J. L., *Macromolecules* **2006**, *39* (23), 7863-7871.
30. Gianneli, M.; Roskamp, R. F.; Jonas, U.; Loppinet, B.; Fytas, G.; Knoll, W., *Soft Matter* **2008**, *4* (7), 1443-1447.
31. Chen, X.-L.; Zhang, L.-J.; Li, F.-G.; Fan, Y.-X.; Wang, W.-P.; Li, B.-J.; Shen, Y.-C., *Pest Manage. Sci.* **2015**, *71* (3), 433-440.

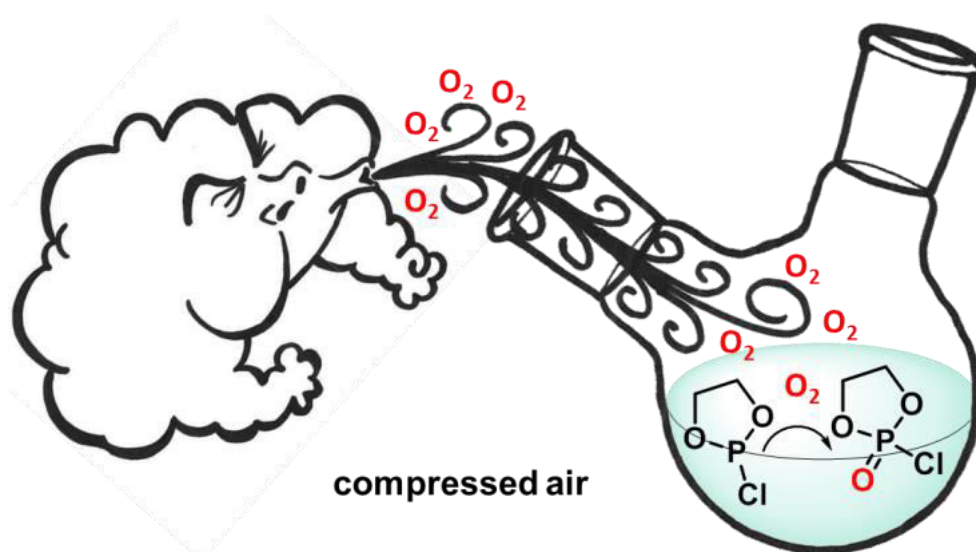
## 6. Breathing air as oxidant: Optimization of 2-chloro-2-oxo-1,3,2-dioxaphospholane synthesis as a precursor for phosphoryl choline derivatives and cyclic phosphate monomers

Greta Becker,<sup>1,2</sup> Frederik R. Wurm<sup>1</sup>

<sup>1</sup>Max Planck Institute for Polymer Research, Ackermannweg 10, 55128 Mainz, Germany,

<sup>2</sup>Graduate School Materials Science in Mainz, Staudinger Weg 9, 55128 Mainz, Germany

Reprinted with permission from "Tetrahedron, **2017**, 73 (25), 3536-3540". Copyright 2017 Elsevier.



**Keywords:** 2-chloro-1,3,2-dioxaphospholane, 2-chloro-2-oxo-1,3,2-dioxaphospholane, COP, poly(phosphoester), phosphorylcholine derivative, oxidation with air.

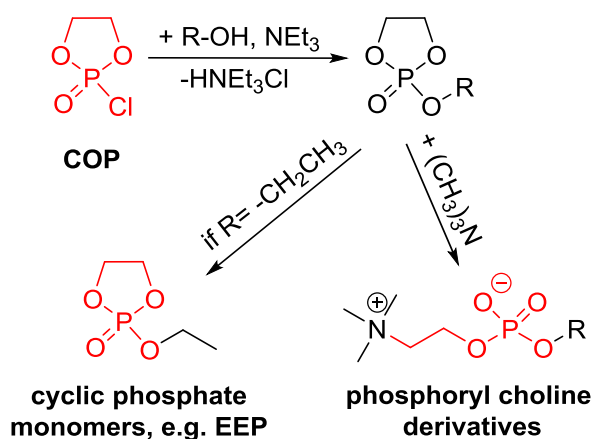
## 6.1 Abstract

Phosphoryl choline derivatives are important compounds used in drug development. Also other phosphoesters have received increased demand in recent years. Many of such compounds rely on the cyclic 2-chloro-2-oxo-1,3,2-dioxaphospholane (COP) intermediate. COP is available in a two-step reaction from the cyclic adduct of phosphorus chloride and ethylene glycol after oxidation. Although commercially available, in-house synthesis of COP is often still required due to several reasons: pricing, purity, and delivery issues. Molecular oxygen from air is a convenient and economical oxidizing agent, yet not used for synthesis of COP so far. While slow consumption of the P(III)-precursor 2-chloro-1,3,2-dioxaphospholane with molecular oxygen from a gas bottle, high amounts of unreacted oxygen are lavished and even may cause an explosion. Oxygen from air is a reasonable and much safer alternative. Additionally, catalytic amounts of cobalt(II)chloride increase the reaction kinetics remarkably. The results presented herein allow a controlled and easy access to a variety of phosphoesters by optimized reaction conditions of COP and its derivatives.

## 6.2 Introduction

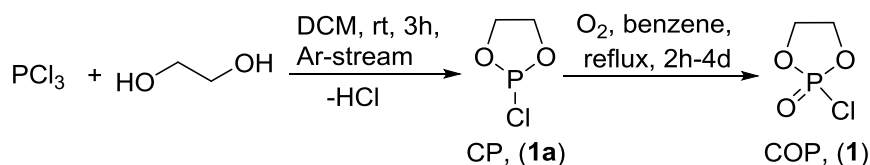
2-Chloro-2-oxo-1,3,2-dioxaphospholane (COP) (also known as ethylene chlorophosphate or ethylene phosphochloridate) is an essential precursor and a key building block for mainly two purposes: the synthesis of (i) phosphorylcholine (PC) derivatives, a polar zwitterion naturally present in phospholipids of cell membranes, which are used in diverse drug delivery applications. A popular synthetic representative is the monomer 2-methacryloyloxyethyl phosphorylcholine (MPC), which produces the water-soluble and biocompatible polymer PMPC, mimicking the phospholipids.<sup>1-5</sup> Also the synthesis of small molecule PC's for different polymers has been reported.<sup>6-9</sup> However also the preparation of (ii) cyclic phosphate monomers for the ring-opening polymerization to produce poly(phosphoester)s (PPEs)<sup>10-17, 18, 19</sup> is a valuable reaction pathway of COP (Scheme 6.1). Synthetic PPEs are inspired by desoxyribose nucleic acid (DNA) and a versatile class of polymers ranging from hydrophobic to water-soluble materials. They find currently an increased attention as potential materials for biomedical applications<sup>13, 20, 21</sup> or as flame retardant additives.<sup>22</sup>

The most common route for the synthesis of COP refers to protocols from Scully et al.<sup>23</sup> and Edmundson<sup>24</sup> from the 1950's and 1960's. Nowadays, COP is still synthesized via this route in a two-step reaction: (i) esterification of phosphorus trichloride with ethylene glycol generates 2-chloro-1,3,2-dioxaphospholane (CP) (**1a**), which is (ii) oxidized by molecular oxygen in refluxing



**Scheme 6.1.** Application examples for 2-chloro-2-oxo-1,3,2-dioxaphospholane (COP) as precursor.

organic solvent to prepare 2-chloro-2-oxo-1,3,2-dioxaphospholane (**1**) (Scheme 6.2). For the oxidation reaction slight modifications are reported, substituting the reaction solvent benzene using toluene<sup>5, 25</sup> or dichloromethane<sup>26</sup> instead. Also the reaction times from 8h-4d<sup>24, 27</sup> and temperatures from room temperature<sup>5, 26</sup> to reflux<sup>24, 27</sup> vary. However, moderate yields from 37-83%<sup>5, 27</sup> are reported so far, often lacking high purity of the product. Additionally, molecular oxygen from a gas bottle in large excess is used in all cases as reagent and bubbled through the reaction, showing only poor and slow consumption with unreacted oxygen being released in large amounts (note: in a well-ventilated fume hood this should be unproblematic, however flying sparks need to be prevented). Several attempts in our group conducting the oxidation in a closed system were sparsely satisfying and can cause unwelcome overpressure in the system due to reflux conditions.<sup>10</sup> In our search for alternative routes, reported literature protocols include the use of dinitrogen tetroxide (N<sub>2</sub>O<sub>4</sub>)<sup>28</sup> or ozone (O<sub>3</sub>)<sup>29</sup> as oxidants, also resulting in poor yields in the case of N<sub>2</sub>O<sub>4</sub> and challenging handling of reactant. Also phosphorus oxychloride, ethylene glycol and catalytic amounts of copper(I)chloride (CuCl) were reported to produce COP in a one-step reaction, but several attempts of this protocol in our group did not produce COP in reasonable yields or purity.<sup>30</sup>



**Scheme 6.2.** Typical reaction protocol for the preparation of COP.

There is a high demand in COP. Although commercially available, price, delivery time and purity of the commercial product are often unsatisfactory. Therefore an efficient, inexpensive and safer in-house preparation is indispensable. Herein, we present a facilitated synthesis protocol using the oxygen from air as oxidant, instead of molecular oxygen from a gas bottle. Still used in excess, large amounts of wasted unreacted molecular oxygen can be avoided. Additionally, cobalt(II)chloride has

been found to be an efficient catalyst that accelerates the reaction from days to several hours, resulting in COP with a very high purity and overall acceptable yields of 70%.

### 6.3 Experimental Section

**Materials.** All reagents were used without further purification, unless otherwise stated. Solvents, dry solvents (over molecular sieves) and deuterated solvents were purchased from Acros Organics, Sigma-Aldrich, Deutero GmbH (Germany) or Fluka. Ethylene glycol was purchased from Sigma-Aldrich, dried prior to use with NaH, distilled and stored over molecular sieves.  $\text{PCl}_3$  was purchased from Acros Organics. Cobalt(II)chloride hexahydrate was purchased from Sigma Aldrich, and dried at reduced pressure at  $\sim 500$  °C directly prior to use.

**Instrumentation and Characterization Techniques.** For nuclear magnetic resonance (NMR) analysis  $^1\text{H}$ ,  $^{13}\text{C}$  and  $^{31}\text{P}$  NMR spectra were recorded either on a Bruker AVANCE III 300 spectrometer operating with 300 MHz, 75 MHz and 121 MHz or a Bruker AVANCE III 700 spectrometer operating with 700 MHz, 176 MHz and 283 MHz. All spectra were measured either in  $\text{DMSO-}d_6$  or  $\text{CDCl}_3$ .  $^1\text{H}$  and  $^{13}\text{C}$  spectra were calibrated against the solvent signal,  $^{31}\text{P}$  spectra used as conducted. Spectra were analyzed using MestReNova 8 from Mestrelab Research S.L. for 1D spectra All  $^{13}\text{C}$  and  $^{31}\text{P}$ -NMR spectra are  $^1\text{H}$ -decoupled.

**Syntheses.** *2-Chloro-1,3,2-dioxaphospholane (CP, 1a)*: A flame-dried 500mL three-neck flask, equipped with a dropping funnel and a reflux condenser, was charged with phosphorus trichloride (137.3 g, 1.000 mol) in dry dichloromethane (150.0 mL). Ethylene glycol (62.07 g, 1.000 mol) was added drop-wise to the stirred solution, while argon was bubbled through the solution to remove the released hydrogen chloride. The Ar-stream with released hydrogen chloride was passed through a NaOH-solution for neutralization. The reaction was continued for additional 2h. Then, the solvent was removed and the residue purified by distillation at reduced pressure to give a fraction at 72-78°C/65-67 mbar, obtaining the clear, colorless, liquid product (84.15 g, 0.670 mol, yield: 67%). NMR data matches literature values.<sup>31</sup>  $^1\text{H}$ -NMR (700 MHz,  $\text{CDCl}_3$ ):  $\delta$  4.35-4.13 (m, 4H, O- $\text{CH}_2$ - $\text{CH}_2$ -O).  $^{13}\text{C}$  {H}NMR (76 MHz,  $\text{CDCl}_3$ ):  $\delta$  65.29.  $^{31}\text{P}$ {H}-NMR (202 MHz,  $\text{CDCl}_3$ ):  $\delta$  167.80.

*2-Chloro-2-oxo-1,3,2-dioxaphospholane (COP, 1)*: A flame-dried 500mL three-neck flask, equipped with a reflux condenser, was charged with 2-chloro-1,3,2-dioxaphospholane (20.00 g, 0.160 mol) dissolved in benzene (250.0 mL) and dry  $\text{CoCl}_2$  (20.50 mg,  $1.590 \cdot 10^{-4}$  mol) was added. A stream of dried air (passed through conc.  $\text{H}_2\text{SO}_4$ ) was passed through the solution for 3h at 80°C and for 12h at room temperature (overnight). Subsequently, the solvent was removed *in vacuo* and the residue purified by fractionated distillation at reduced pressure to give a fraction at

66-74 °C/0.13-0.15 mbar, obtaining the clear, colorless, liquid product COP in high purity (15.82 g, 0.110 mol, yield: 70%, 99% purity). NMR data matches literature values.<sup>26</sup> <sup>1</sup>H NMR (300 MHz, CDCl<sub>3</sub>): δ 4.61-4.44 (m, 4H, O-CH<sub>2</sub>-CH<sub>2</sub>-O), <sup>13</sup>C {H} NMR (76 MHz, CDCl<sub>3</sub>): δ 66.54, <sup>31</sup>P {H} NMR (121 MHz, CDCl<sub>3</sub>): δ 22.74.

*Isolation of byproduct in entry 3:* After fractionated distillation, 1.500 g of product with non-phosphorus containing byproduct was stirred in 10 mL DCM with 5.000 g silica gel for 10 min. The silica gel was removed by filtration and the solvent removed, obtaining the byproducts 1-(benzyl)-4-methylbenzene and 1-(benzyl)-2-methylbenzene (180.0 mg, 6.420\*10<sup>-4</sup> mol, yield: 12%). Ratio 1-(benzyl)-4-methylbenzene : 1-(benzyl)-2-methylbenzene from <sup>1</sup>H-NMR is 0.42 : 0.57. NMR data matches literature values<sup>32-33</sup>: *1-(benzyl)-4-methylbenzene*: <sup>1</sup>H NMR: δ 7.29-7.09, 3.93, 2.30. <sup>13</sup>C {H} NMR: δ 141.5, 138.2, 135.6, 130.4, 129.3, 129.0, 128.6, 126.0, 41.7, 21.1. *1-(benzyl)-2-methylbenzene*: <sup>1</sup>H-NMR: δ 7.35-7.11, 4.03, 2.23. <sup>13</sup>C {H} NMR: δ 140.8, 139.4, 137.1, 130.7, 130.4, 129.2, 128.8, 126.9, 126.4, 126.3, 39.9, 20.1.

*1-(benzyl)-2-methylbenzene*: <sup>1</sup>H-NMR (300 MHz, CD<sub>2</sub>Cl<sub>2</sub>): δ 7.32-7.11 (m, 8H, aromatic protons), 3.94 (s, 2H, Ar-CH<sub>2</sub>-Ar-CH<sub>3</sub>), 2.32 (s, 3H, Ar-CH<sub>2</sub>-Ar-CH<sub>3</sub>). <sup>13</sup>C{H}-NMR (75 MHz, CD<sub>2</sub>Cl<sub>2</sub>): δ 141.19, 138.86, 136.18, 130.79, 130.41, 129.33, 128.96, 126.95, 126.50, 126.44, 39.89, 19.98.

*1-(benzyl)-4-methylbenzene*: <sup>1</sup>H-NMR (300 MHz, CD<sub>2</sub>Cl<sub>2</sub>): δ 7.32-7.11 (m, 8H, aromatic protons), 4.01 (s, 2H, Ar-CH<sub>2</sub>-Ar-CH<sub>3</sub>), 2.26 (s, 2H, Ar-CH<sub>2</sub>-Ar-CH<sub>3</sub>). <sup>13</sup>C{H}-NMR (75 MHz, CD<sub>2</sub>Cl<sub>2</sub>): δ 142.27, 139.72, 137.20, 129.65, 129.27, 129.25, 128.90, 126.50, 42.04, 21.28.

FD-MS: 182.35 (calculated for C<sub>14</sub>H<sub>14</sub>: 182.11).

## 6.4 Results and Discussion

Following the protocol of Edmundson,<sup>24</sup> the oxidation of 2-chloro-1,3,2-dioxaphospholane (CP) with molecular oxygen from a gas bottle bubbled through the reaction in benzene under reflux shows slow consumption and requires several days (4d) for the reaction to reach full conversion to 2-chloro-2-oxo-1,3,2-dioxaphospholane (COP) (yields up to 83%, 98% purity, Table 6.1, **entry 1**). The major disadvantage of the set-up is the waste of unreacted molecular oxygen and the potential risk with high amounts of oxygen in the atmosphere. Previously, we reported on the conduction of the reaction in a closed system using a peristaltic pump to reuse the unreacted oxygen and to avoid wasting high amounts of oxygen.<sup>10</sup> However, care has to be taken that no over- or under pressure is produced in the set-up; also the organic solvent vapors are problematic for tubing and they have to be replaced regularly.

**Table 6.1.** Overview on the reaction conditions for the oxidation of 2-chloro-1,3,2-dioxaphospholane (CP) to 2-chloro-2-oxo-1,3,2-dioxaphospholane (COP).

entry	reactant	catalyst	solvent	T / °C	t / h	conv. <sup>a</sup> / %	yield COP / %	purity <sup>b</sup> / %
1	O <sub>2</sub>	-	benzene	80	96	>90	83	98
2	air	-	benzene	80/rt	96/72	98	86	97
3	air	-	toluene	111	23	98	-	93
4	air	CoCl <sub>2</sub>	benzene	80/rt	3/12	97	70	99
5	air	CoCl <sub>2</sub>	PC <sup>c</sup>	80/120/rt	3/10/14	100	8 <sup>d</sup>	-
6	air	CoCl <sub>2</sub>	EA <sup>e</sup>	80	13	10	5 <sup>d</sup>	-
7	air	CoCl <sub>2</sub>	ACN <sup>f</sup>	80	25	17	15 <sup>d</sup>	-
8	air	CoCl <sub>2</sub>	MCB <sup>g</sup>	80	16	69	10 <sup>d</sup>	-

<sup>a</sup>Conversion of reagent 2-chloro-1,3,2-dioxaphospholane. <sup>b</sup>Determined by <sup>31</sup>P {H} NMR. <sup>c</sup>PC: propylene carbonate. <sup>d</sup>Not distilled. <sup>e</sup>EA: ethyl acetate. <sup>f</sup>ACN: acetonitrile. <sup>g</sup>MCB: monochlorobenzene

The use of oxygen from air would be a cheap, easy, and safer alternative, however has not been reported in literature before and also previous attempts in our laboratory remained unsatisfactory in terms of reaction time and product purity. Detailed optimization of this oxidation step allowed us to prepare COP by a set-up with dried air bubbled through the reaction (**entry 2**), but turned out to be very slow (similar to the one with pure oxygen): in benzene 4d at reflux temperatures and 3d at room temperature were necessary to reach almost full conversion (98%) (Figure 6.1). Small amounts of ring-opened side-product were also found in the reaction mixture. After fractionated distillation, an overall yield of 86% can be reached with typically ca. 97% purity of the product.

Instead, the reaction is much faster in refluxing toluene (<1d) reaching a conversion of starting material of >98% (**entry 3**, Figure 6.2). After fractionated distillation, <sup>31</sup>P{H}-NMR spectroscopy shows purity of 93% of product and 7% opened ring as byproduct. However, a second, non-phosphorus-containing byproduct can be observed in <sup>1</sup>H-NMR spectroscopy (Figure S7). The second byproduct was isolated by filtration over silica gel and identified as 1-(benzyl)-4-methylbenzene and 1-(benzyl)-2-methylbenzene (Figure S6.8-S6.11), resulting from coupling of the

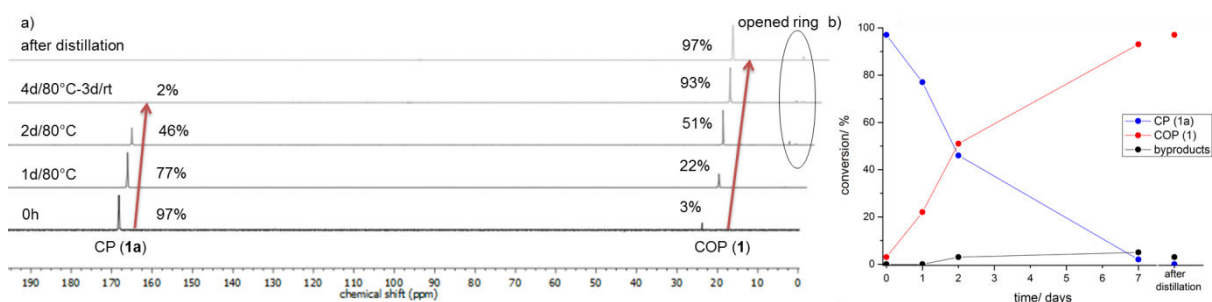


**Figure 6.1.** a) <sup>31</sup>P {H} NMR spectra (121MHz, CDCl<sub>3</sub>, 298K) of the oxidation reaction of CP to COP in benzene (Table 1, **entry 2**), b) plotted conversion of reagent and formation of COP in **entry 2**, measured by <sup>31</sup>P NMR spectroscopy.

solvent during reaction. The product COP cannot be purified from the byproduct by distillation due to very similar boiling points. However, for the purpose of COP as precursor for cyclic phosphate monomers, the byproduct disturbs neither the synthesis of the monomers nor their ring-opening polymerization.

A modified reaction in benzene with air and 0.1 mol% of anhydrous  $\text{CoCl}_2$  as catalyst shows high conversions (>98%) within 15h (3h under reflux and 12h at room temperature (**entry 4**)). After fractionated distillation, purity of 99% of the desired product and 1% opened ring as a byproduct (yields: 70-75%, Figures S6.4-6.6).

Several other solvents were screened for the reaction to substitute benzene. While the reaction in the “green” solvent propylene carbonate (PC) with air and 0.1 mol% of dry  $\text{CoCl}_2$  (**entry 5**) shows 21% product after 13h at high temperature (3h at 80 °C and 10h at 120 °C), further 14h at room temperature does not lead to an increase in the COP amount, but instead opening of the ring was detected in NMR kinetics (Figure S6.12). Since  $^{31}\text{P}$  {H}NMR shows 92% byproduct and only 8% COP product at that point, purification was not attempted. The reaction in ethyl acetate (**entry 6**) after 13h at 80°C also shows low conversion of CP, only 5% formed product COP and 5% byproduct. Two solvents suitable for radical reactions were further investigated: acetonitrile and chlorobenzene. The reaction in acetonitrile (**entry 7**) after 25h at 80 °C shows only 15% formation of COP. Although the solvent is generally suitable for the reaction and only 2% byproduct is formed, conversion is very slow and time consuming. Finally, the reaction in chlorobenzene (**entry 8**, Figure S6.13) at 80 °C shows after 7h 49% product, but also 10% opened ring byproduct. Longer reaction times do not show any increase in the yields, but instead degradation of COP was detected (51%).

In summary, from the solvent studied, benzene and toluene remain the most suitable reaction media. However, as toluene is not inert in radical reactions, the coupling products might be

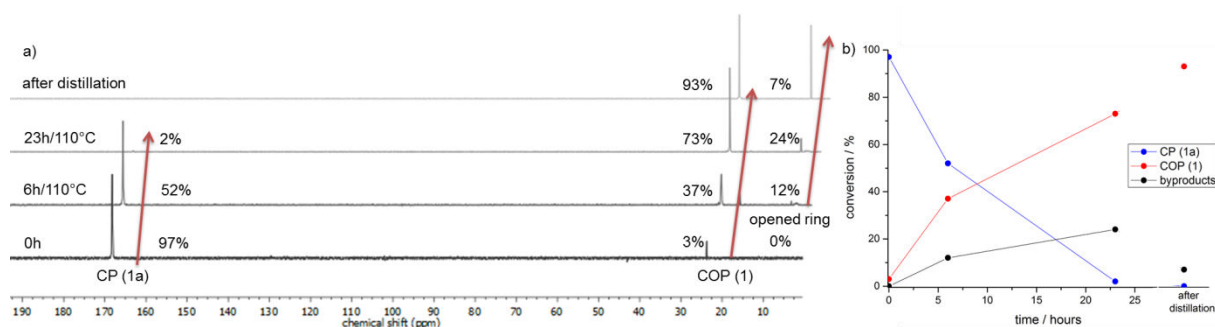


**Figure 6.2.** a)  $^{31}\text{P}$  {H} NMR spectra (121MHz,  $\text{CDCl}_3$ , 298K) of the oxidation reaction of CP to COP in toluene (Table 1, **entry 3**), b) plotted conversion of reagent and formation of COP in **entry 3**, measured by  $^{31}\text{P}$  NMR spectroscopy. Note: only phosphorus-containing byproducts are considered.

contaminants of the product. Greener solvents, such as ethyl acetate and propylene carbonate<sup>34</sup> were suitable for the oxidation of CP, but lower yields are accessible. For radical reactions generally only few inert solvents are convenient, e.g. benzene, chlorobenzene, acetonitrile, carbon tetrachloride or tetrachloroethane. The less hazardous-ranked solvents chlorobenzene and acetonitrile might be used, but both did not show satisfying results in our studies. Therefore, we consider benzene still to be the most eligible solvent for this reaction.

## 6.5 Conclusions

High demands on purity, pricing and delivery issues of COP still require in-house synthesis of this precursor molecule. Using oxygen from air instead of pure oxygen from a gas tank, has a strong economical impact, is easy to perform and avoids wasting of oxygen. Additionally, this is the first report on the acceleration of this reaction by the addition of catalytic amounts of  $\text{CoCl}_2$  to reduce the reaction times from days to hours. A screening of different solvents revealed that the highest conversions can be achieved in toluene and benzene, while other “greener” solvents might be used, but are hampered by low reaction kinetics and the ring-opening of the product over prolonged reaction times. This minor, but crucial replacement of the oxygen source dramatically facilitates the synthesis of COP (at least in the university lab), which is required in high and pure amounts for the preparation of phosphoryl choline derivatives and cyclic monomers for poly(phosphoester)s. Further issues might include the further dilution of air (or oxygen) with inert gas, but we considered the ease of air beneficial. Also conducting the reaction in a continuous reactor setup in a green solvent might be a strategy for future industrial relevance that might be considered. Our strategy presented herein overcomes the commercial availability and establishes easy access to this important precursor molecule.

## 6.6 Acknowledgments

G.B. is recipient of a fellowship through funding of the Excellence Initiative (DFG/GSC 266) in the context of the graduate school of excellence “MAINZ” (Material Sciences in Mainz). F.R.W. is grateful to the Max Planck Graduate School (MPGC) for support.

## 6.7 Supporting Information

The Supporting Information contains NMR spectra of 2-chloro-1,3,2-dioxaphospholane, 2-chloro-2-oxo-1,3,2-dioxaphospholane, the byproduct and for entries 5 and 8 .

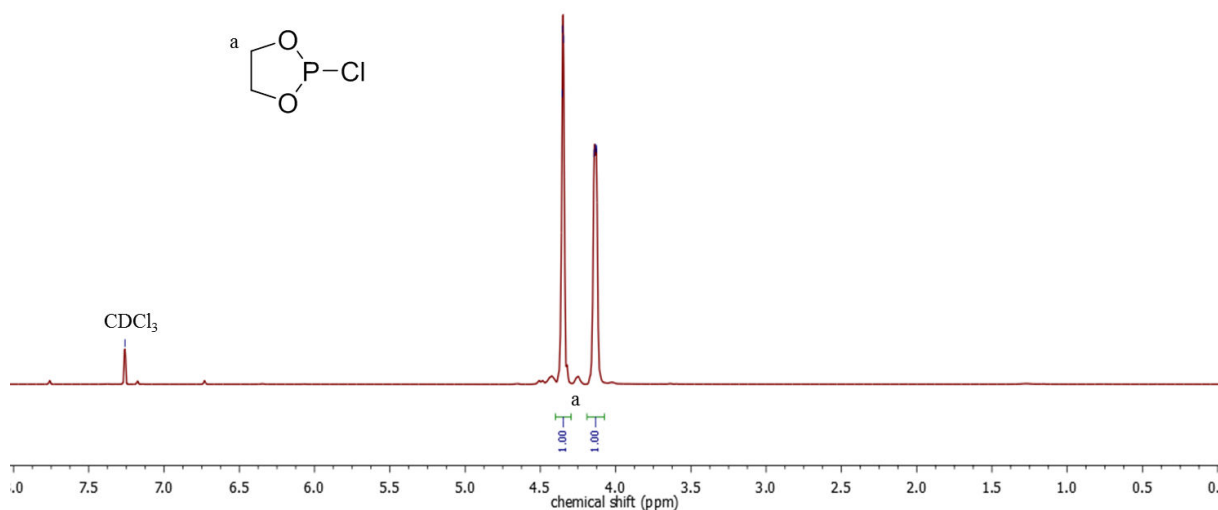


**Figure S6.1.** <sup>1</sup>H NMR (700 MHz, CDCl<sub>3</sub>) of 2-chloro-1,3,2-dioxaphospholane.

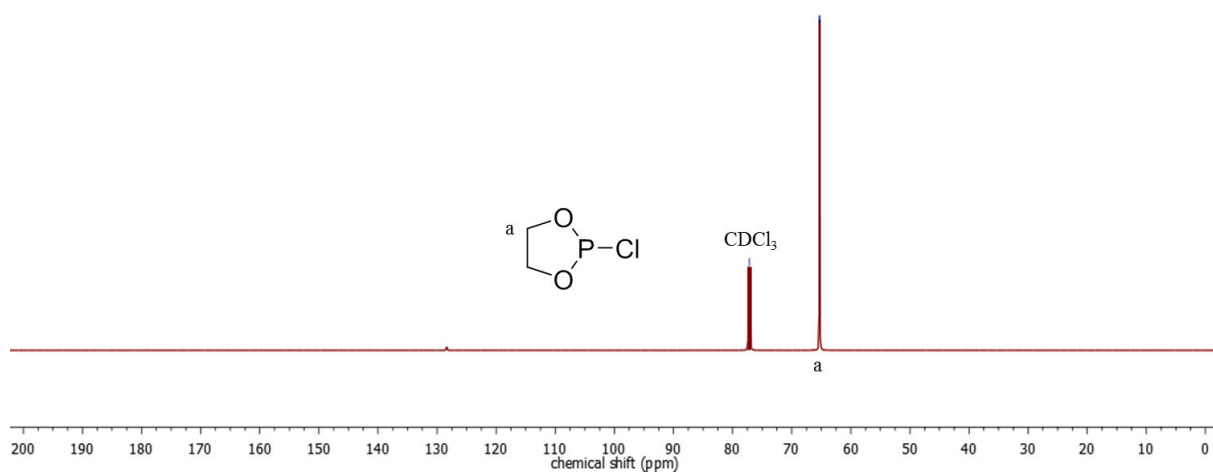


**Figure S6.2.** <sup>13</sup>C {<sup>1</sup>H} NMR (76 MHz, CDCl<sub>3</sub>) of 2-chloro-1,3,2-dioxaphospholane.

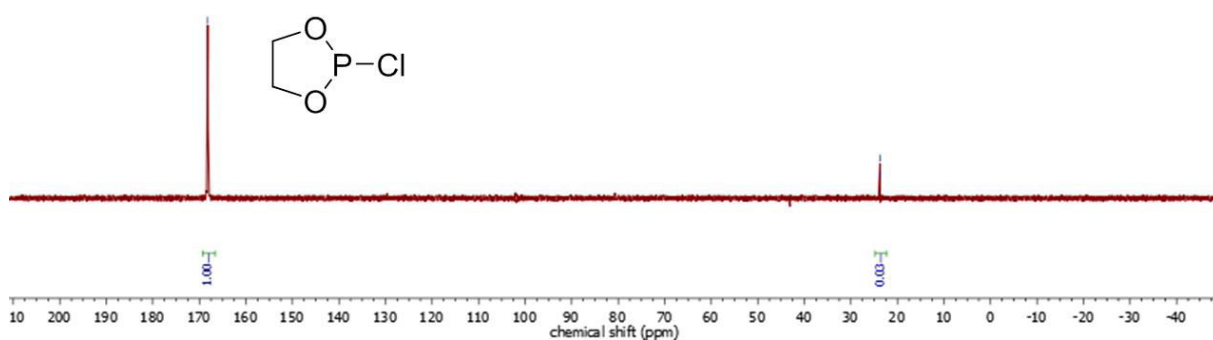


**Figure S6.3.** <sup>31</sup>P {<sup>1</sup>H} NMR (202 MHz, CDCl<sub>3</sub>) of 2-chloro-1,3,2-dioxaphospholane.

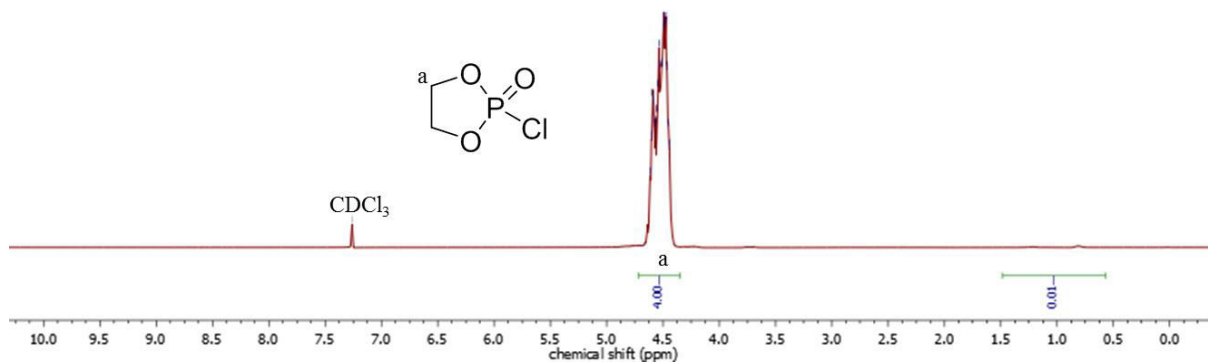


**Figure S6.4.** <sup>1</sup>H NMR (300 MHz, CDCl<sub>3</sub>) of 2-chloro-2-oxo-1,3,2-dioxaphospholane.

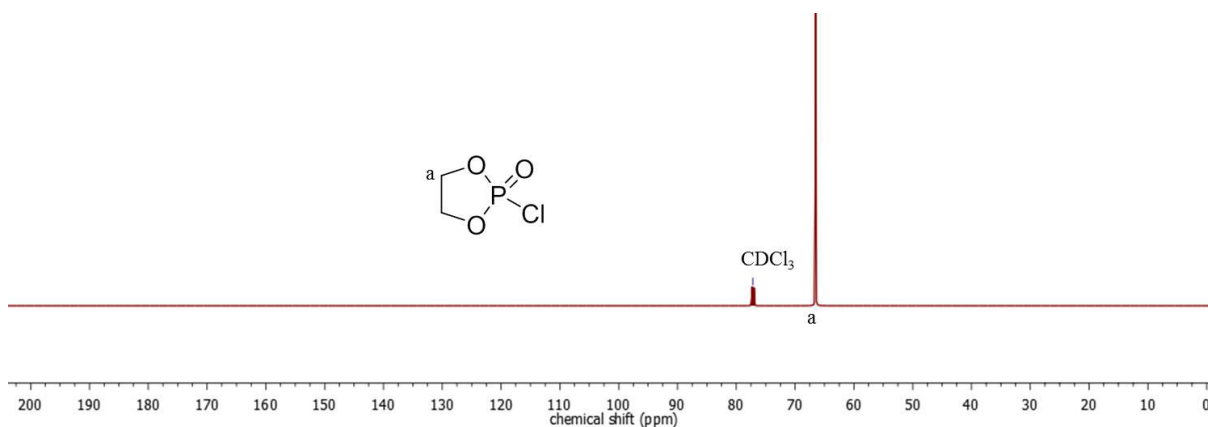


**Figure S6.5.** <sup>13</sup>C {<sup>1</sup>H} NMR (76 MHz, CDCl<sub>3</sub>) of 2-chloro-2-oxo-1,3,2-dioxaphospholane.

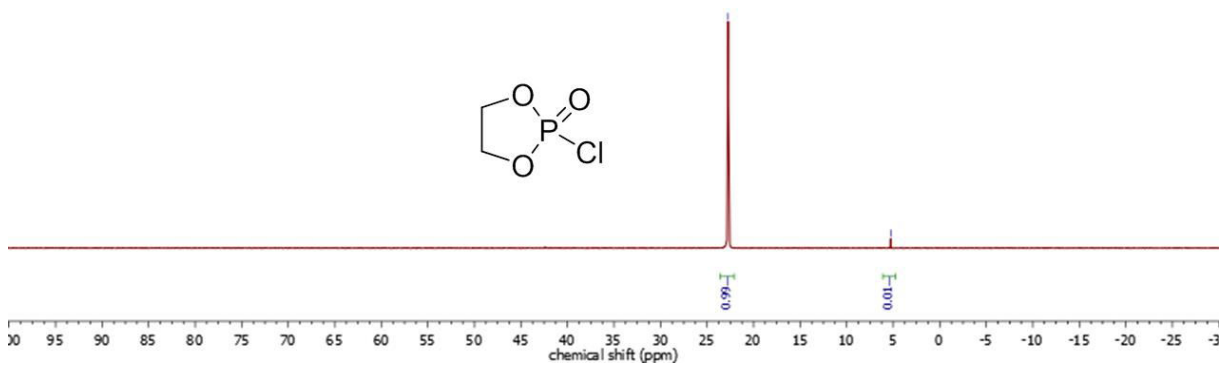


**Figure S6.6.** <sup>31</sup>P {<sup>1</sup>H} NMR (121 MHz, CDCl<sub>3</sub>) of 2-chloro-2-oxo-1,3,2-dioxaphospholane.

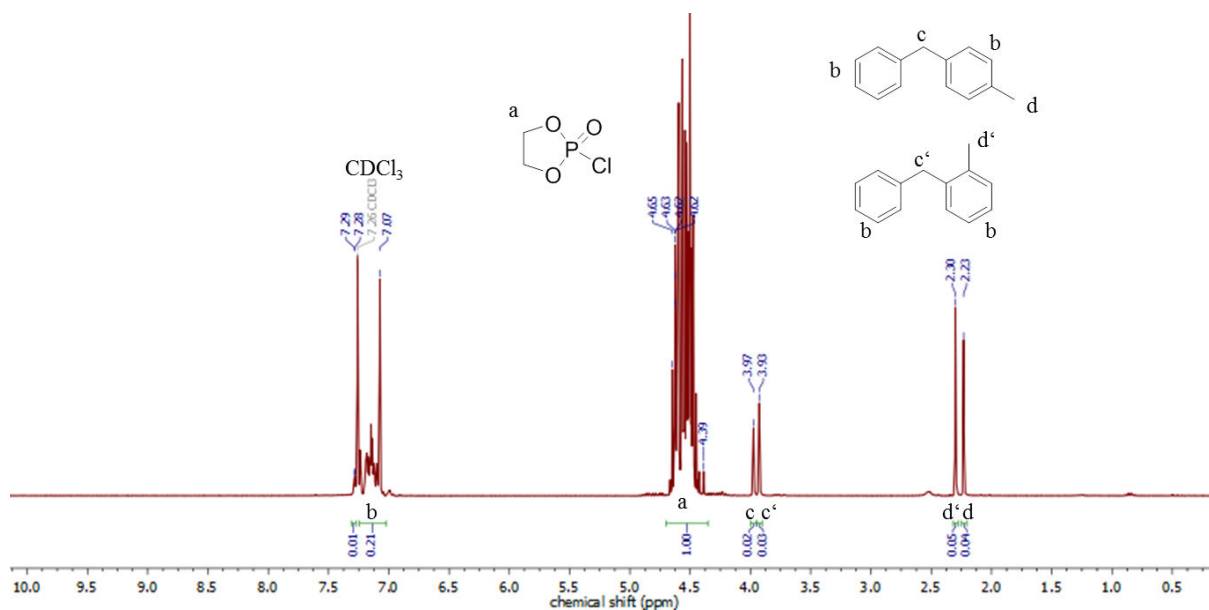


**Figure S6.7.**  $^1\text{H}$  NMR (300 MHz,  $\text{CDCl}_3$ ) of entry 3 after distillation: presence of COP and byproducts 1-(benzyl)-4-methylbenzene and 1-(benzyl)-2-methylbenzene.

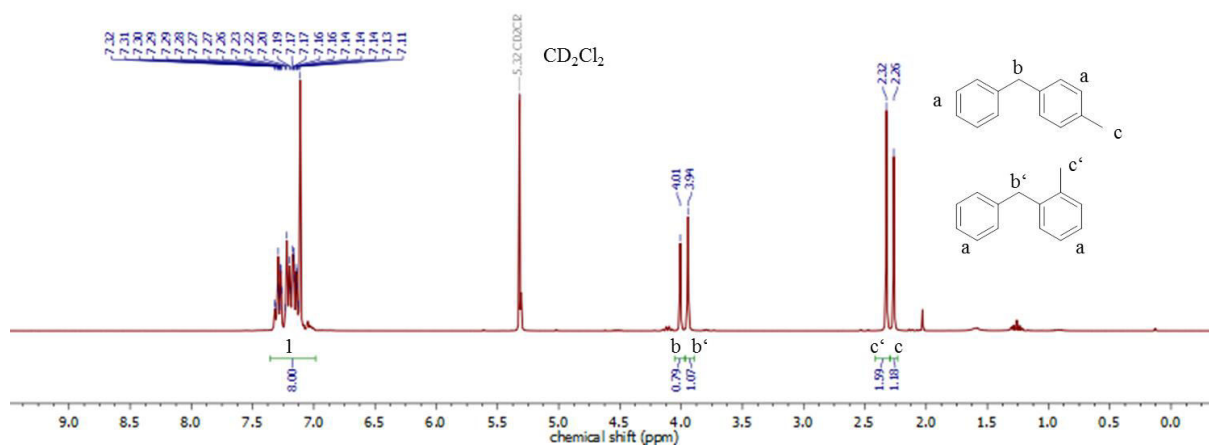


**Figure S6.8.**  $^1\text{H}$  NMR (300 MHz,  $\text{CD}_2\text{Cl}_2$ ) of isolated non-phosphorus containing byproduct of entry 3: 1-(benzyl)-4-methylbenzene and 1-(benzyl)-2-methylbenzene.

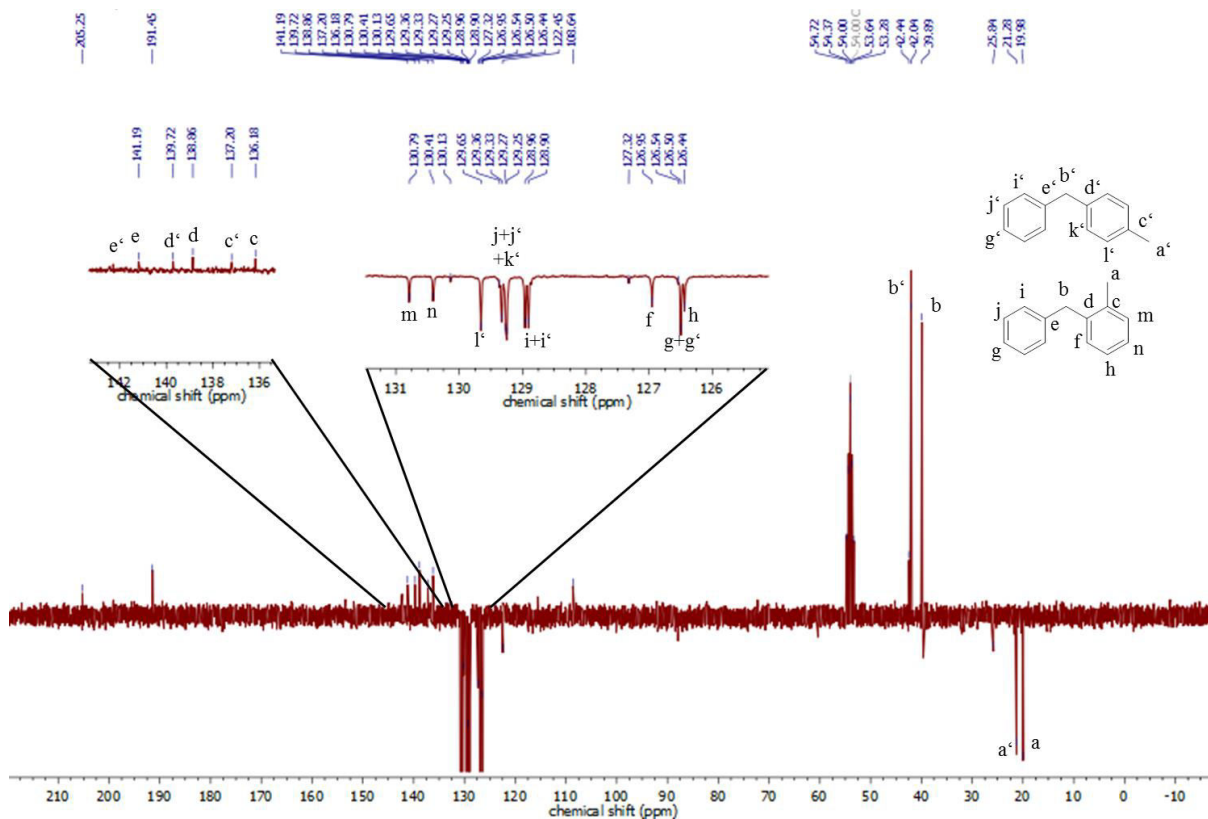


**Figure S6.9.**  $^{13}\text{C}$  {H} NMR (76 MHz,  $\text{CD}_2\text{Cl}_2$ ) of isolated non-phosphorus containing byproduct of entry 3: 1-(benzyl)-4-methylbenzene and 1-(benzyl)-2-methylbenzene.

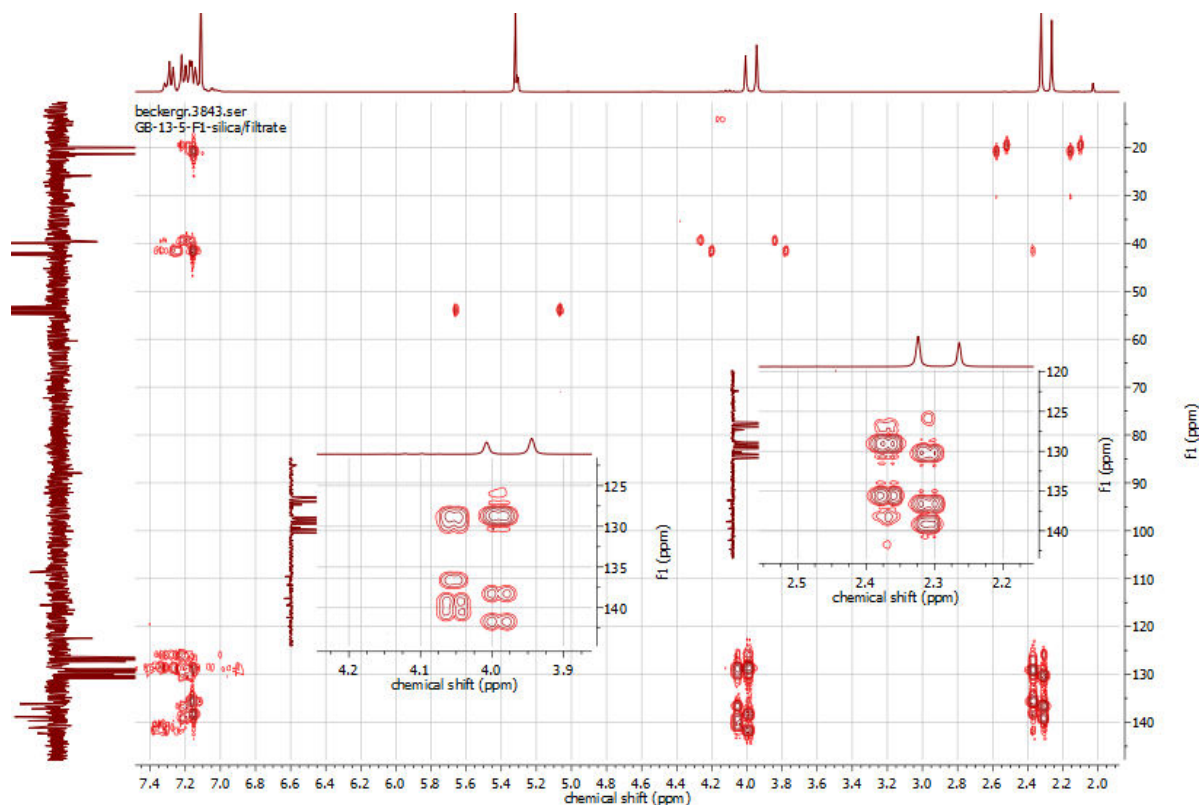


**Figure S6.10.**  $^1\text{H}$ - $^{13}\text{C}$ -HMBC NMR of isolated non-phosphorus containing byproduct of entry 3: 1-(benzyl)-4-methylbenzene and 1-(benzyl)-2-methylbenzene.

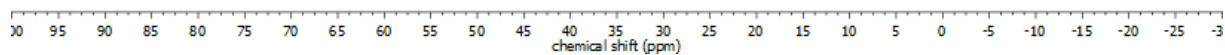


**Figure S6.11.**  $^{31}\text{P}$  {H} NMR (121 MHz,  $\text{CD}_2\text{Cl}_2$ ) of isolated non-phosphorus containing byproduct of **entry 3**: 1-(benzyl)-4-methylbenzene and 1-(benzyl)-2-methylbenzene.

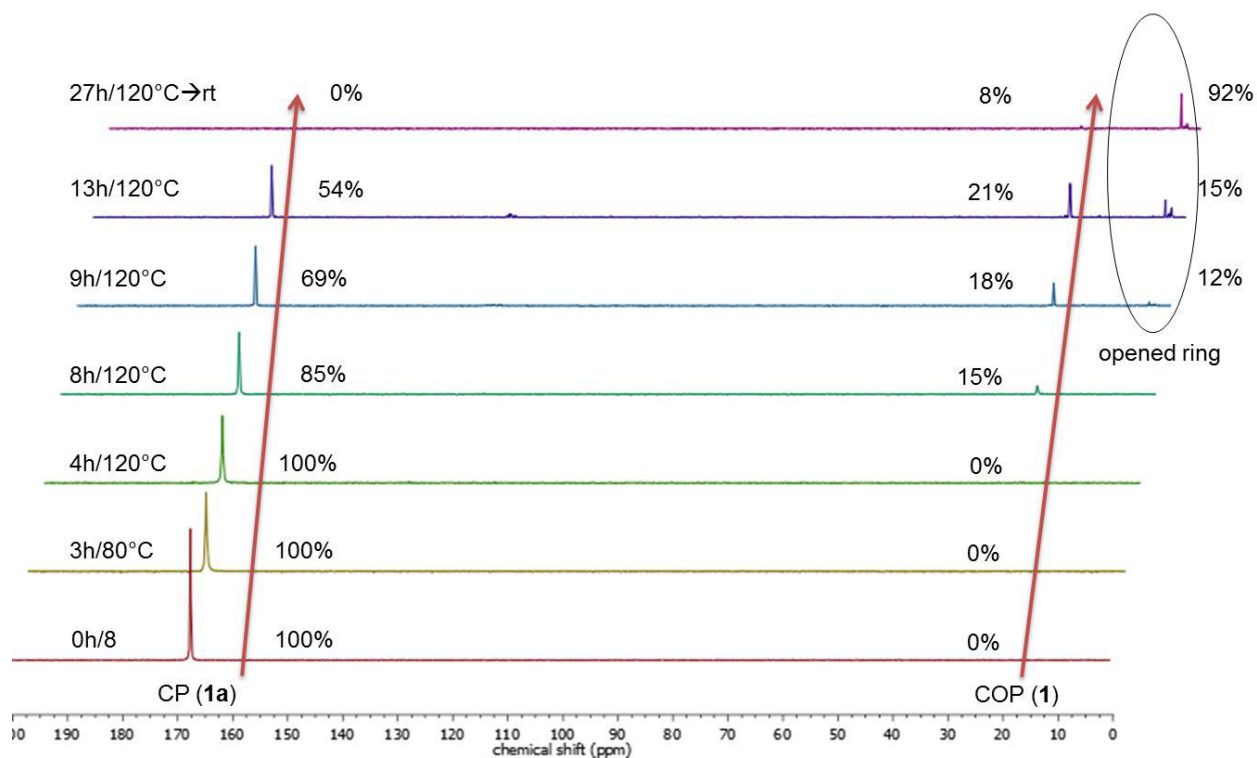


**Figure S6.12.**  $^{31}\text{P}$  {H} NMR spectra (121MHz,  $\text{CDCl}_3$ , 298K) of the oxidation reaction of CP to COP in propylene carbonate (**entry 5**).

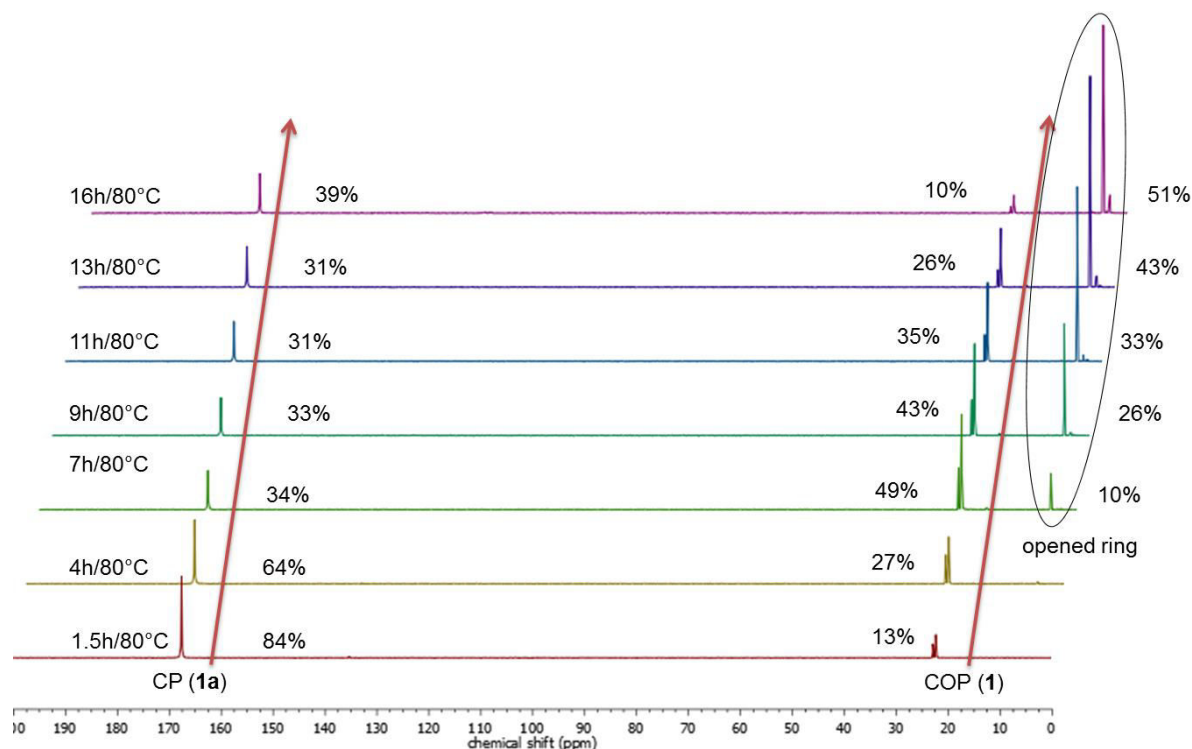


**Figure S6.13.**  $^{31}\text{P}$   $\{^1\text{H}\}$  NMR spectra (121MHz,  $\text{CDCl}_3$ , 298K) of the oxidation reaction of CP to COP in chlorobenzene (**entry 8**).

## 6.8 References

1. Feng, W.; Zhu, S.; Ishihara, K.; Brash, J. L., *Langmuir* **2005**, *21* (13), 5980-5987.
2. Goda, T.; Ishihara, K.; Miyahara, Y., *J. Appl. Polym. Sci.* **2015**, *132* (16), n/a-n/a.
3. Lewis, A.; Tang, Y.; Brocchini, S.; Choi, J.-w.; Godwin, A., *Bioconjugate Chem.* **2008**, *19* (11), 2144-2155.
4. Lobb, E. J.; Ma, I.; Billingham, N. C.; Armes, S. P.; Lewis, A. L., *J. Am. Chem. Soc.* **2001**, *123* (32), 7913-7914.
5. Kamon, Y.; Inoue, N.; Mihara, E.; Kitayama, Y.; Ooya, T.; Takeuchi, T., *Appl. Surf. Sci.* **2016**, *378*, 467-472.
6. Nederberg, F.; Bowden, T.; Hilborn, J., *Macromolecules* **2004**, *37* (3), 954-965.
7. Brazeau, G. A.; Attia, S.; Poxon, S.; Hughes, J. A., *Pharm. Res.* **1998**, *15*, 680.
8. Yakovlev, I.; Deming, T. J., *J. Am. Chem. Soc.* **2015**, *137* (12), 4078-4081.
9. Papillon, J. P. N.; Pan, M.; Brousseau, M. E.; Gilchrist, M. A.; Lou, C.; Singh, A. K.; Stawicki, T.; Thompson, J. E., *Bioorg. Med. Chem. Lett.* **2016**, *26* (15), 3514-3517.
10. Steinbach, T.; Schroder, R.; Ritz, S.; Wurm, F. R., *Polym. Chem.* **4** (16), 4469-4479.
11. Zhang, F.; Smolen, J. A.; Zhang, S.; Li, R.; Shah, P. N.; Cho, S.; Wang, H.; Raymond, J. E.; Cannon, C. L.; Wooley, K. L., *Nanoscale* **2015**, *7* (6), 2265-2270.
12. Clément, B.; Molin, D. G.; Jérôme, C.; Lecomte, P., *J. Polym. Sci., Part A: Polym. Chem.* **2015**, *53* (22), 2642-2648.
13. Zhao, Z.; Wang, J.; Mao, H.-Q.; Leong, K. W., *Adv. Drug Delivery Rev.* **2003**, *55* (4), 483-499.
14. Li, Q.; Wang, J.; Shahani, S.; Sun, D. D. N.; Sharma, B.; Elisseff, J. H.; Leong, K. W., *Biomaterials* **2006**, *27* (7), 1027-1034.
15. Zhang, S.; Zou, J.; Elsabahy, M.; Karwa, A.; Li, A.; Moore, D. A.; Dorshow, R. B.; Wooley, K. L., *Chem. Sci.* **2013**.

16. Wang, Y.-C.; Tang, L.-Y.; Sun, T.-M.; Li, C.-H.; Xiong, M.-H.; Wang, J., *Biomacromolecules* **2007**, *9* (1), 388-395.
17. Penczek, S.; Duda, A.; Kaluzynski, K.; Lapienis, G.; Nyk, A.; Szymanski, R., *Makromol. Chem., Macromol. Symp.* **1993**, *73* (1), 91-101.
18. Iwasaki, Y.; Yamaguchi, E., *Macromolecules* **2010**, *43* (6), 2664-2666.
19. Lim, Y. H.; Tiemann, K. M.; Heo, G. S.; Wagers, P. O.; Rezenom, Y. H.; Zhang, S.; Zhang, F.; Youngs, W. J.; Hunstad, D. A.; Wooley, K. L., *ACS Nano* **2015**, *9* (2), 1995-2008.
20. Steinbach, T.; Wurm, F. R., *Angew. Chem. Int. Ed.* **2015**, *54* (21), 6098-6108.
21. Wang, Y.-C.; Yuan, Y.-Y.; Du, J.-Z.; Yang, X.-Z.; Wang, J., *Macromol. Biosci.* **2009**, *9* (12), 1154-1164.
22. Tauber, K.; Marsico, F.; Wurm, F. R.; Schartel, B., *Polym. Chem.* **2014**.
23. Lucas, H. J.; Mitchell, F. W.; Scully, C. N., *J. Am. Chem. Soc.* **1950**, *72* (12), 5491-5497.
24. Edmundson, R. S., *Chem. Ind. (London)* **1962**, 1828.
25. Yao, X.; Du, H.; Xu, N.; Sun, S.; Zhu, W.; Shen, Z., *J. Appl. Polym. Sci.* **2015**, *132* (42), n/a-n/a.
26. Svenningsen, S. W.; Janaszewska, A.; Ficker, M.; Petersen, J. F.; Klajnert-Maculewicz, B.; Christensen, J. B., *Bioconjugate Chem.* **2016**, *27* (6), 1547-1557.
27. Schöttler, S.; Becker, G.; Winzen, S.; Steinbach, T.; Mohr, K.; Landfester, K.; Mailänder, V.; Wurm, F. R., *Nat. Nano.* **2016**, *11* (4), 372-377.
28. Cox, J. R.; Westheimer, F. H., *J. Am. Chem. Soc.* **1958**, *80* (20), 5441-5443.
29. Ding, J. S.; Xiaofeng; Shi, Xiaoqing; Qian, Qing; Gu, Ye CN 102424692, 2012.
30. Jiang, H. CN 103421039, 2013.
31. National Institute of Advanced Industrial Science and Technology (AIST). Spectral Database for Organic Compounds (SDBS). [http://sdb.sdb.aist.go.jp/sdb/cgi-bin/direct\\_frame\\_disp.cgi?sdbno=8452](http://sdb.sdb.aist.go.jp/sdb/cgi-bin/direct_frame_disp.cgi?sdbno=8452).
32. Sun, G.; Wang, Z., *Tetrahedron Lett.* **2008**, *49* (33), 4929-4932.
33. Krüger, T.; Vorndran, K.; Linker, T., *Chem. - Eur. J.* **2009**, *15* (44), 12082-12091.
34. Prat, D.; Hayler, J.; Wells, A., *Green Chem.* **2014**, *16* (10), 4546-4551.



## 7. Triazolinedione-“clicked” poly(phosphoester)s: Systematic adjustment of thermal properties

Greta Becker,<sup>1,2</sup> Laetitia Vlamincx,<sup>3</sup> Maria M. Velencoso,<sup>1</sup> Filip E. Du Prez,<sup>3</sup> Frederik R. Wurm<sup>1</sup>

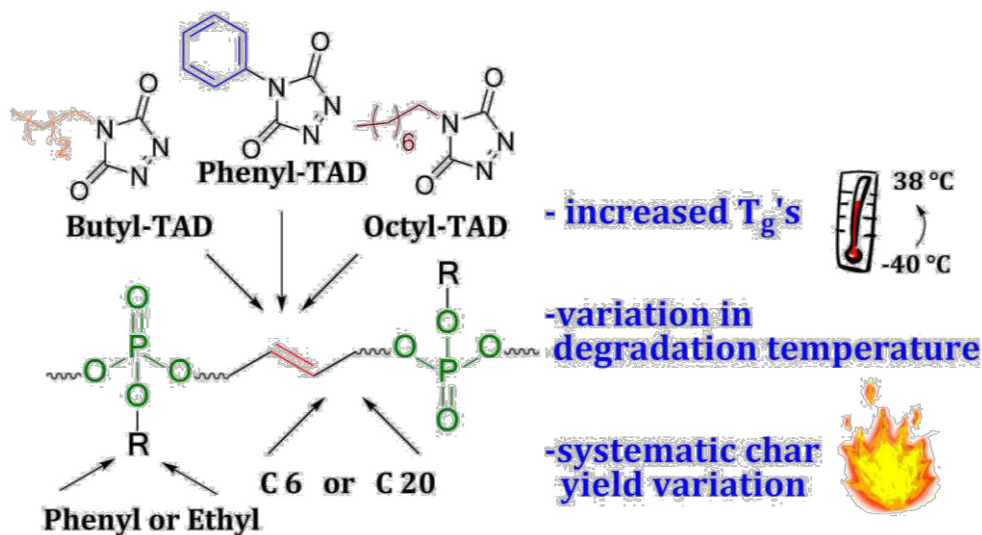
<sup>1</sup>Max Planck Institute for Polymer Research, Ackermannweg 10, 55128 Mainz, Germany

<sup>2</sup>Graduate School Materials Science in Mainz, Staudinger Weg 9, 55128 Mainz, Germany

<sup>3</sup>Department of Organic and Macromolecular Chemistry, Polymer Chemistry Research Group, Ghent University, Krijgslaan 281 S4-bis, 9000 Ghent, Belgium

Reproduced with permission from “Polymer Chemistry Communication, **2017**, 8, 4074-4078”.  
Copyright 2017, published by The Royal Society of Chemistry.

Poly(phosphoester)s were synthesized and characterized by Greta Becker, 1,2,4-triazoline-3,5-dione derivatives by Laetitia Vlamincx. Post-modification of the polymers and characterization have been conducted together by Greta Becker and Laetitia Vlamincx. Interpretation of TGA results have been done together by Greta Becker and Maria M. Velencoso.



**Keywords:** 1,2,4-triazoline-3,5-dione, TAD, post-modification, phosphorus, poly(phosphoester), PPE, thermal stability, polymer degradation, flame retardant, flame retardancy.

## 7.1 Abstract

The thermal properties of halogen-free flame retardant poly(phosphoester)s from acyclic diene metathesis polycondensation have been optimized by a systematic post-modification using 1,2,4-triazoline-3,5-dione derivatives. The straightforward modification not only increased their glass transition temperatures significantly but also improved the thermal stability with respect to their char yields.

## 7.2 Introduction

Poly(phosphoester)s (PPEs) can be prepared via both ring-opening polymerization<sup>1</sup> or polycondensation. We recently applied the ADMET polycondensation to prepare a variety of PPEs.<sup>2-5</sup> Today, PPEs are studied in biomedical applications for their biocompatibility,<sup>6</sup> biodegradability and adjustable hydrophilicity.<sup>6-7</sup> Furthermore, PPEs are also currently under discussion as potent flame retardant additives, as many halogenated compounds are banned from the market.<sup>2</sup> PPEs show higher resistance to leaching and migration, compared to low molecular weight additives.<sup>8</sup> Indeed, phosphorus is an efficient char promoter forming an accumulated protective layer on the materials surface, which limits the release of fuel to the flame.<sup>9-10</sup> Additionally, PPEs typically show low toxicity or almost smoke-free burning.<sup>11-12</sup> Recently, the combination of phosphorus-containing flame retardants with nitrogen compounds has attracted much attention. The combination of both elements physically and chemically can dramatically improve the action of the phosphorus species in the condensed phase upon combustion.<sup>13-14</sup> Nitrogen compounds are believed to act by release of inert gases or by promotion of char formation as a result of a condensation reaction. Besides phosphorus and nitrogen, the introduction of aromatic structures is also often mentioned to promote the charring.<sup>15</sup>

As a systematic study on the thermal properties and char yield, with structural variation of the main- and side chain of PPEs, is missing in the current literature, the main goal of this research was the preparation of modified PPEs via ADMET polycondensation, both as a result of the variation of the backbone and side chains. Furthermore, we used the efficient, recently revisited “click chemistry” of 1,2,4-triazoline-3,5-diones (TAD)<sup>16-17</sup> to modify the double bonds along the PPE backbone to further adjust the material properties. This TAD-ene chemistry can not only be applied as a reliable and convenient post-modification reaction of unsaturated polymers but will also introduce additional nitrogen atoms to the PPEs, which is expected to have a positive influence on their flame retardant performance. TADs are one of the most reactive (di)enophiles and show quantitative conversions at room temperature with isolated alkenes or conjugated dienes,

respectively in an Alder-ene or Diels-Alder reaction. TAD has recently been applied in a wide range of applications, such as self-healing,<sup>18</sup> surface chemistry,<sup>19-21</sup> and post-modification of unsaturated ADMET polymers.<sup>22</sup>

This is the first report on the post-modification of PPEs via their internal double bonds for tuning of their thermal properties. Supposing that TAD-modification can increase the glass transition temperature ( $T_g$ ), this would undoubtedly broaden the range of application for PPEs, which typically exhibit low  $T_g$ 's between -40 to -60°C.<sup>3</sup> Finally, the introduced nitrogen atoms and additional aromatic structures will alter the degradation behavior of the polymers during combustion, making it a useful and straightforward modification for the design of novel PPE-based flame retardants.

### 7.3 Experimental Section

**Materials.** All reagents were used without further purification, unless otherwise stated. Solvents, dry solvents (over molecular sieves) and deuterated solvents were purchased from Acros Organics, Sigma-Aldrich, Deutero GmbH or Fluka. Bromine, butyl isocyanate, phenyl isocyanate and potassium hydroxide, 3-buten-1-ol, 10-undecen-1-ol, phenol, HCl (37%), tris(hydroxymethyl)phosphine (90%), catalyst Grubbs 1<sup>st</sup> generation were purchased from Sigma-Aldrich. POCl<sub>3</sub> (phosphoryl chloride, 99%), 1-chloronaphthalene, ethyl carbazate and aluminium oxide (neutral, for chromatography) were purchased from Acros Organics. 1,4-diazabicyclo[2.2.2]octane was purchased from TCI chemicals. Triethylamine (Et<sub>3</sub>N, 99.5%) was purchased from Roth, dried with CaH<sub>2</sub>, distilled and stored over molecular sieves.

**Instrumentation and Characterization Techniques.** For the poly(phosphoester)s, size exclusion chromatography (SEC) measurements were performed in THF with a PSS SecCurity system (Agilent Technologies 1260 Infinity). Sample injection was performed by a 1260-ALS autosampler (Waters) at 30 °C. SDV columns (PSS) with dimensions of 300 × 80 mm, 10 μm particle size, and pore sizes of 106, 104, and 500 Å were employed. The DRI Shodex RI-101 detector (ERC) and UV-vis 1260-VWD detector (Agilent) were used for detection. Calibration was achieved using PS standards provided by Polymer Standards Service. For nuclear magnetic resonance analysis <sup>1</sup>H, <sup>13</sup>C, and <sup>31</sup>P NMR spectra were recorded on a Bruker AVANCE III 300 MHz spectrometer. All spectra were measured in either *d*<sub>6</sub>-DMSO or CDCl<sub>3</sub> at 298 K. The spectra were calibrated against the solvent signal (CDCl<sub>3</sub> (7.26 ppm) or *d*<sub>6</sub>-DMSO (2.50 ppm)) and analyzed using MestReNova 8 from Mestrelab Research S.L. The thermal properties of the synthesized polymers have been measured by differential scanning calorimetry (DSC) on a Mettler Toledo instrument 1/700 under nitrogen atmosphere at a heating rate of 10 °C min<sup>-1</sup>. The glass transition temperatures were determined

from midpoints in the second heating using the STARE software of Mettler-Toledo. Thermogravimetric analysis (TGA) was performed using a Mettler-Toledo TGA/SDTA851e equipment. Samples (5 to 10 mg) were heated in a nitrogen atmosphere with a heating rate of 10 K min<sup>-1</sup> going from 25°C to 800°C. For the analysis of the thermograms, the STARE software of Mettler-Toledo was used. All curves are blank corrected.

**Syntheses.** *General procedure for ADMET Polymerization (C6-Et, C6-Ph, C20-Ph):* The respective monomer, 3 mol% catalyst Grubbs 1<sup>st</sup> generation and ca. 50wt% 1-chloronaphthalene were mixed under argon atmosphere. Polymerization was carried out at reduced pressure to remove the evolving ethylene at 60-80°C for up to 72h until reaction was completed. Reaction progress was monitored with <sup>1</sup>H NMR spectroscopy and a spatula tip of additional catalyst added after measurement if necessary until reaction was completed. The reaction was cooled down, 7 mL of DCM, ca. 10 mg of tris(hydroxymethyl)phosphine and 3 drops of Et<sub>3</sub>N were added to deactivate the catalyst. After 1 h, 5 mL distilled water was added and the mixture was stirred overnight. The organic phase was extracted with aqueous HCl (5 wt%) and brine. The mixture was concentrated at reduced pressure and the polymer precipitated into hexane twice. Yields 50-90%.

**C6-Et:** <sup>1</sup>H NMR (300 MHz, CDCl<sub>3</sub>): δ [ppm] 5.83-5.72 (m, CH<sub>2</sub>=CH-CH<sub>2</sub>-CH<sub>2</sub>-O-P), 5.54-5.50 (m, -CH<sub>2</sub>-CH=CH-CH<sub>2</sub>-), 5.17-5.08 (m, CH<sub>2</sub>=CH-CH<sub>2</sub>-CH<sub>2</sub>-O-P), 4.12-3.98 (m, -CH<sub>2</sub>-O-P), 2.46-2.36 (m, CH<sub>2</sub>=CH-CH<sub>2</sub>-CH<sub>2</sub>-O-P), 1.33 (t, CH<sub>3</sub>-). <sup>13</sup>C NMR (176 MHz, CDCl<sub>3</sub>): δ [ppm] 128.28, 127.31, 122.02, 67.07, 33.71, 16.34. <sup>31</sup>P{H} NMR (121 MHz, CDCl<sub>3</sub>): δ [ppm] -1.00.

**C6-Ph:** <sup>1</sup>H NMR (300 MHz, CDCl<sub>3</sub>): δ [ppm] 7.36-7.12 (m, Ph-O-P), 5.80-5.71 (m, CH<sub>2</sub>=CH-CH<sub>2</sub>-CH<sub>2</sub>-O-P), 5.56-5.38 (m, -CH<sub>2</sub>-CH=CH-CH<sub>2</sub>-), 5.15-5.06 (m, CH<sub>2</sub>=CH-CH<sub>2</sub>-CH<sub>2</sub>-O-P), 4.20-4.06 (m, -CH<sub>2</sub>-O-P), 2.46-2.25 (m, CH<sub>2</sub>=CH-CH<sub>2</sub>-CH<sub>2</sub>-O-P). <sup>31</sup>P{H} NMR (121 MHz, CDCl<sub>3</sub>): δ [ppm] -6.39.

**C20-Ph:** <sup>1</sup>H NMR (300 MHz, CDCl<sub>3</sub>): δ [ppm] 7.36-7.13 (m, Ph-O-P), 5.40-5.30 (m, -CH<sub>2</sub>-CH=CH-CH<sub>2</sub>-), 4.16-4.09 (m, -CH<sub>2</sub>-O-P), 1.99-1.92 (m, -CH=CH-CH<sub>2</sub>-CH<sub>2</sub>-), 1.69-1.62 (m, -CH<sub>2</sub>-CH<sub>2</sub>-O-P), 1.36-1.25 (m, 12H, -CH<sub>2</sub>-). <sup>31</sup>P{H} NMR (121 MHz, CDCl<sub>3</sub>): δ [ppm] -6.10.

*General procedure for TAD functionalization of polymers:* The polymers were solubilized in DCM (approx. 1ml) and 1 eq. of the corresponding TAD component, solubilized in ca. 0.5 mL DCM (Bu-TAD, Oct-TAD) or THF (Ph-TAD) was added in order to obtain full functionalisation (for detailed amounts see Table 7.1). The reaction was stirred overnight to obtain full conversion and was precipitated in hexane. During reaction the colour changes from pink to colourless for C11-Ph or brownish for C4-Et and C4-Ph. After drying (overnight, vacuum, 40°C), a variation of glassy to sticky polymers was obtained in quantitative yields.

**Table 7.1.** Overview of amounts of polymers and TADs used for functionalization.

	<b>C6-Ph</b>	<b>C6-Et</b>	<b>C20-Ph</b>
<b>amount polymer</b>	250 mg	100 mg	250 mg
<b>mass repeating unit</b>	254,22 g/mol	206,17 g/mol	450,60 g/mol
<b>n</b>	0,9834 mmol	0,4850 mmol	0,5548 mmol
<b>PhTAD</b>	172 mg	127 mg	97 mg
<b>Bu-TAD</b>	152 mg	113 mg	86 mg
<b>Oct-TAD</b>	208 mg	154 mg	117 mg

**C6-Et-Bu:** <sup>1</sup>H NMR (300 MHz, d<sub>6</sub>-DMSO): δ [ppm] 10.35 (s, trans, -N-NH-C(=O)-), 10.01 (s, cis, -N-NH-C(=O)-), 5.77 (s, trans, -CH(N)-CH=CH-CH<sub>2</sub>-), 5.51 (s, cis, -CH(N)-CH=CH-CH<sub>2</sub>-), 4.61 (s, trans, -CH(N)-CH=CH-CH<sub>2</sub>-O-P), 4.44 (s, -CH<sub>2</sub>-CH(N)-CH=CH-), 4.10-3.88 (m, cis, -CH(N)-CH=CH-CH<sub>2</sub>-O-P; m, -CH<sub>2</sub>-CH<sub>2</sub>-O-P; m, CH<sub>3</sub>-CH<sub>2</sub>-O-P), 2.31 (s, -CH<sub>2</sub>-CH<sub>2</sub>-O-P), 2.12-1.82 (m, CH<sub>3</sub>-CH<sub>2</sub>-CH<sub>2</sub>-CH<sub>2</sub>-N-), 1.59-1.44 (m, CH<sub>3</sub>-CH<sub>2</sub>-CH<sub>2</sub>-CH<sub>2</sub>-N-), 1.38-1.16 (m, CH<sub>3</sub>-CH<sub>2</sub>-CH<sub>2</sub>-CH<sub>2</sub>-N-; t, CH<sub>3</sub>-CH<sub>2</sub>-O-P), 0.92-0.77 (m, CH<sub>3</sub>-CH<sub>2</sub>-CH<sub>2</sub>-CH<sub>2</sub>-N-). <sup>31</sup>P{H} NMR (121 MHz, CDCl<sub>3</sub>): δ [ppm] -1.40.

**C6-Et-Oct:** <sup>1</sup>H NMR (300 MHz, d<sub>6</sub>-DMSO): δ [ppm] 10.54 (s, trans, -N-NH-C(=O)-), 10.21 (s, cis, -N-NH-C(=O)-), 5.86 (s, trans, -CH(N)-CH=CH-CH<sub>2</sub>-), 5.59 (s, cis, -CH(N)-CH=CH-CH<sub>2</sub>-), 4.67 (s, trans, -CH(N)-CH=CH-CH<sub>2</sub>-O-P), 4.50 (s, -CH<sub>2</sub>-CH(N)-CH=CH-), 4.24-3.92 (m, cis, -CH(N)-CH=CH-CH<sub>2</sub>-O-P; m, -CH<sub>2</sub>-CH<sub>2</sub>-O-P; m, CH<sub>3</sub>-CH<sub>2</sub>-O-P), 2.29 (s, -CH<sub>2</sub>-CH<sub>2</sub>-O-P), 2.06-1.79 (m, CH<sub>3</sub>-(CH<sub>2</sub>)<sub>5</sub>-CH<sub>2</sub>-CH<sub>2</sub>-N-), 1.47 (m, CH<sub>3</sub>-(CH<sub>2</sub>)<sub>5</sub>-CH<sub>2</sub>-CH<sub>2</sub>-N-), 1.35-0.94 (m, CH<sub>3</sub>-(CH<sub>2</sub>)<sub>5</sub>-CH<sub>2</sub>-CH<sub>2</sub>-N-; t, CH<sub>3</sub>-CH<sub>2</sub>-O-P), 0.83-0.58 (m, CH<sub>3</sub>-(CH<sub>2</sub>)<sub>5</sub>-CH<sub>2</sub>-CH<sub>2</sub>-N-). <sup>31</sup>P{H} NMR (121 MHz, CDCl<sub>3</sub>): δ [ppm] -1.39.

**C6-Et-Ph:** <sup>1</sup>H NMR (300 MHz, d<sub>6</sub>-DMSO): δ [ppm] 10.46 (s, trans, -N-NH-C(=O)-), 9.79 (s, cis, -N-NH-C(=O)-), 7.67-7.34 (m, *Ph*-), 5.86 (s, trans, -CH(N)-CH=CH-CH<sub>2</sub>-), 5.50 (s, cis, -CH(N)-CH=CH-CH<sub>2</sub>-), 4.73 (s, trans, -CH(N)-CH=CH-CH<sub>2</sub>-O-P), 4.48 (s, -CH<sub>2</sub>-CH(N)-CH=CH-), 4.09-3.87 (m, cis, -CH(N)-CH=CH-CH<sub>2</sub>-O-P; m, -CH<sub>2</sub>-CH<sub>2</sub>-O-P; m, CH<sub>3</sub>-CH<sub>2</sub>-O-P), 2.30 (s, -CH<sub>2</sub>-CH<sub>2</sub>-O-P), 1.22 (t, CH<sub>3</sub>-CH<sub>2</sub>-O-P). <sup>31</sup>P{H} NMR (121 MHz, CDCl<sub>3</sub>): δ [ppm] -1.04.

**C6-Ph-Bu:** <sup>1</sup>H NMR (300 MHz, d<sub>6</sub>-DMSO): δ [ppm] 10.32 (s, trans, -N-NH-C(=O)-), 10.01 (s, cis, -N-NH-C(=O)-), 7.40-7.19 (m, *Ph*-), 5.76 (s, trans, -CH(N)-CH=CH-CH<sub>2</sub>-), 5.44 (s, cis, -CH(N)-CH=CH-CH<sub>2</sub>-), 4.58 (s, trans, -CH(N)-CH=CH-CH<sub>2</sub>-O-P; s, -CH<sub>2</sub>-CH(N)-CH=CH-), 4.05 (s, cis, -CH(N)-CH=CH-CH<sub>2</sub>-O-P; s, -CH<sub>2</sub>-CH<sub>2</sub>-O-P), 2.28 (s, -CH<sub>2</sub>-CH<sub>2</sub>-O-P), 2.14-1.85 (m, CH<sub>3</sub>-CH<sub>2</sub>-CH<sub>2</sub>-CH<sub>2</sub>-N-), 1.57-1.39 (m, CH<sub>3</sub>-CH<sub>2</sub>-CH<sub>2</sub>-CH<sub>2</sub>-N-), 1.35-1.11 (m, CH<sub>3</sub>-CH<sub>2</sub>-CH<sub>2</sub>-CH<sub>2</sub>-N-), 0.95-0.70 (m, CH<sub>3</sub>-CH<sub>2</sub>-CH<sub>2</sub>-CH<sub>2</sub>-N-). <sup>31</sup>P{H} NMR (121 MHz, CDCl<sub>3</sub>): δ [ppm] -6.71.

**C6-Ph-Oct:** <sup>1</sup>H NMR (300 MHz, d<sub>6</sub>-DMSO): δ [ppm] 10.31 (s, trans, -N-NH-C(=O)-), 10.00 (s, cis, -N-NH-C(=O)-), 7.38-7.18 (m, *Ph*-), 5.75 (s, trans, -CH(N)-CH=CH-CH<sub>2</sub>-), 5.43 (s, cis, -CH(N)-CH=CH-CH<sub>2</sub>-), 4.57 (s, trans, -CH(N)-CH=CH-CH<sub>2</sub>-O-P; s, -CH<sub>2</sub>-CH(N)-CH=CH-), 4.08 (s, cis, -CH(N)-CH=CH-CH<sub>2</sub>-O-P; s, -CH<sub>2</sub>-CH<sub>2</sub>-O-P), 2.28 (s, -CH<sub>2</sub>-CH<sub>2</sub>-O-P), 2.14-1.85 (m, CH<sub>3</sub>-(CH<sub>2</sub>)<sub>5</sub>-CH<sub>2</sub>-CH<sub>2</sub>-N-), 1.63-1.40

(m, CH<sub>3</sub>-(CH<sub>2</sub>)<sub>5</sub>-CH<sub>2</sub>-CH<sub>2</sub>-N-), 1.34-1.06 (m, CH<sub>3</sub>-(CH<sub>2</sub>)<sub>5</sub>-CH<sub>2</sub>-CH<sub>2</sub>-N-), 0.91-0.74 (m, CH<sub>3</sub>-(CH<sub>2</sub>)<sub>5</sub>-CH<sub>2</sub>-CH<sub>2</sub>-N-). <sup>31</sup>P{H} NMR (121 MHz, CDCl<sub>3</sub>): δ [ppm] -6.72.

**C6-Ph-Ph:** <sup>1</sup>H NMR (300 MHz, d<sub>6</sub>-DMSO): δ [ppm] 10.79 (s, trans, -N-NH-C(=O)-), 10.45 (s, cis, -N-NH-C(=O)-), 7.60-7.18 (m, *Ph*-), 5.84 (s, trans, -CH(N)-CH=CH-CH<sub>2</sub>-), 5.42 (s, cis, -CH(N)-CH=CH-CH<sub>2</sub>-), 4.73 (s, trans, -CH(N)-CH=CH-CH<sub>2</sub>-O-P), 4.61 (s, -CH<sub>2</sub>-CH(N)-CH=CH-), 4.16 (s, cis, -CH(N)-CH=CH-CH<sub>2</sub>-O-P), 4.04 (s, -CH<sub>2</sub>-CH<sub>2</sub>-O-P), 2.29 (s, -CH<sub>2</sub>-CH<sub>2</sub>-O-P). <sup>31</sup>P{H} NMR (121 MHz, CDCl<sub>3</sub>): δ [ppm] -6.70.

**C20-Ph-Bu:** <sup>1</sup>H NMR (300 MHz, d<sub>6</sub>-DMSO): δ [ppm] 10.24 (s, trans, -N-NH-C(=O)-), 9.97 (s, cis, -N-NH-C(=O)-), 7.49-7.11 (m, *Ph*-), 5.57 (s, trans, -CH(N)-CH=CH-CH<sub>2</sub>-), 5.35 (s, cis, -CH(N)-CH=CH-CH<sub>2</sub>-), 4.28 (m, -CH<sub>2</sub>-CH(N)-CH=CH-), 4.05 (m, -CH<sub>2</sub>-CH<sub>2</sub>-O-P), 1.92 (m, CH<sub>3</sub>-CH<sub>2</sub>-CH<sub>2</sub>-CH<sub>2</sub>-N-), 1.67-1.39 (m, CH<sub>3</sub>-CH<sub>2</sub>-CH<sub>2</sub>-CH<sub>2</sub>-N-; m, -CH<sub>2</sub>-CH<sub>2</sub>-O-P), 1.37-1.01 (m, CH<sub>3</sub>-CH<sub>2</sub>-CH<sub>2</sub>-CH<sub>2</sub>-N-; -CH<sub>2</sub>-backbone), 0.83 (t, CH<sub>3</sub>-CH<sub>2</sub>-CH<sub>2</sub>-CH<sub>2</sub>-N-). <sup>31</sup>P{H} NMR (121 MHz, CDCl<sub>3</sub>): δ [ppm] -6.26.

**C20-Ph-Oct:** <sup>1</sup>H NMR (300 MHz, d<sub>6</sub>-DMSO): δ [ppm] 10.12 (s, trans, -N-NH-C(=O)-), 10.00 (s, cis, -N-NH-C(=O)-), 7.44-7.06 (m, *Ph*-), 5.54 (s, trans, -CH(N)-CH=CH-CH<sub>2</sub>-), 5.36 (s, cis, -CH(N)-CH=CH-CH<sub>2</sub>-), 4.21 (m, -CH<sub>2</sub>-CH(N)-CH=CH-), 4.01 (m, -CH<sub>2</sub>-CH<sub>2</sub>-O-P), 1.88 (m, CH<sub>3</sub>-(CH<sub>2</sub>)<sub>5</sub>-CH<sub>2</sub>-CH<sub>2</sub>-N-), 1.51 (m, CH<sub>3</sub>-(CH<sub>2</sub>)<sub>5</sub>-CH<sub>2</sub>-CH<sub>2</sub>-N-; m, -CH<sub>2</sub>-CH<sub>2</sub>-O-P), 1.20-1.15 (m, CH<sub>3</sub>-(CH<sub>2</sub>)<sub>5</sub>-CH<sub>2</sub>-CH<sub>2</sub>-N-; -CH<sub>2</sub>-backbone), 0.83 (t, CH<sub>3</sub>-(CH<sub>2</sub>)<sub>5</sub>-CH<sub>2</sub>-CH<sub>2</sub>-N-). <sup>31</sup>P{H} NMR (121 MHz, CDCl<sub>3</sub>): δ [ppm] -6.25.

**C20-Ph-Ph:** <sup>1</sup>H NMR (300 MHz, d<sub>6</sub>-DMSO): δ [ppm] 10.72 (s, trans, -N-NH-C(=O)-), 10.45 (s, cis, -N-NH-C(=O)-), 7.62-7.09 (m, *Ph*-), 5.65 (s, trans, -CH(N)-CH=CH-CH<sub>2</sub>-), 5.49 (s, cis, -CH(N)-CH=CH-CH<sub>2</sub>-), 4.40 (m, -CH<sub>2</sub>-CH(N)-CH=CH-), 4.04 (m, -CH<sub>2</sub>-CH<sub>2</sub>-O-P), 1.96 (m, -CH(N)-CH=CH-CH<sub>2</sub>-), 1.70 (m, -CH<sub>2</sub>-CH<sub>2</sub>-O-P), 1.55 (m, -CH<sub>2</sub>- backbone), 0.121 (m, -CH<sub>2</sub>- backbone). <sup>31</sup>P{H} NMR (121 MHz, CDCl<sub>3</sub>): δ [ppm] -6.30.

## 7.4 Results and Discussion

Di(but-3-en-1-yl) ethyl phosphate (**1**), di(but-3-en-1-yl) phenyl phosphate (**2**) and di(undec-10-en-1-yl) phenyl phosphate (**3**) (Figure 7.1a) have been used as the respective monomers for the ADMET polycondensation,<sup>3,4</sup> yielding PPEs with different alkyl spacers between the phosphate centers along the backbone (6 or 20 methylene groups) and different pendant groups (ethoxy or phenoxy; **C6-Et**, **C6-Ph** and **C20-Ph**). Successful polycondensation of the monomers can be determined from the <sup>1</sup>H NMR spectra by the decrease of signals for terminal double bonds at 5.10 and 5.80 ppm and the appearance of a new signal at ca. 5.40-5.50 ppm for the internal double bonds formed during the metathesis reaction (Figures 7.1b bottom and S7.1-7.6). The obtained polymers are viscous oils with molecular weights of 29,700 g/mol and 7,100 g/mol for **C6-Et** and **C6-Ph** polymers, respectively, determined via end-group analysis of the ratio between signals for

terminal and internal double bonds. Molecular weight dispersities show values of 1.46 (**C6-Et**) and 1.84 (**C6-Ph**), up to 2.21 (**C20-Ph**).

Subsequently, all polymers were post-modified via TAD click chemistry. The double bonds were reacted fast in solution at room temperature with three TAD derivatives, **Ph-TAD**, **Bu-TAD** or **Oct-TAD** (Figure 7.1a).

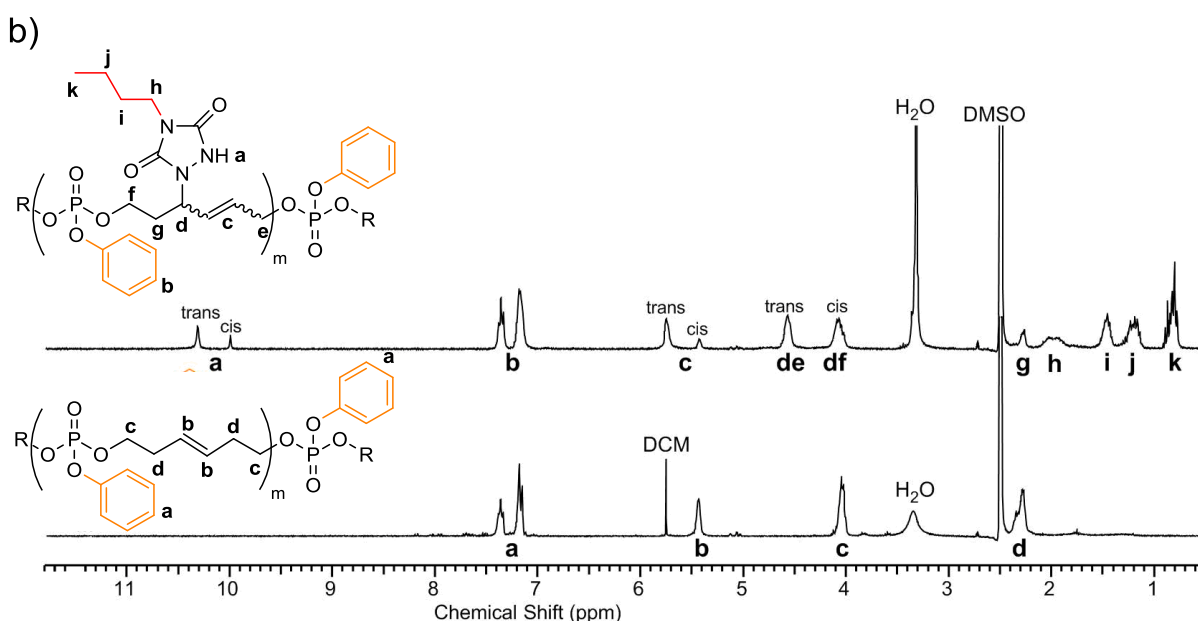
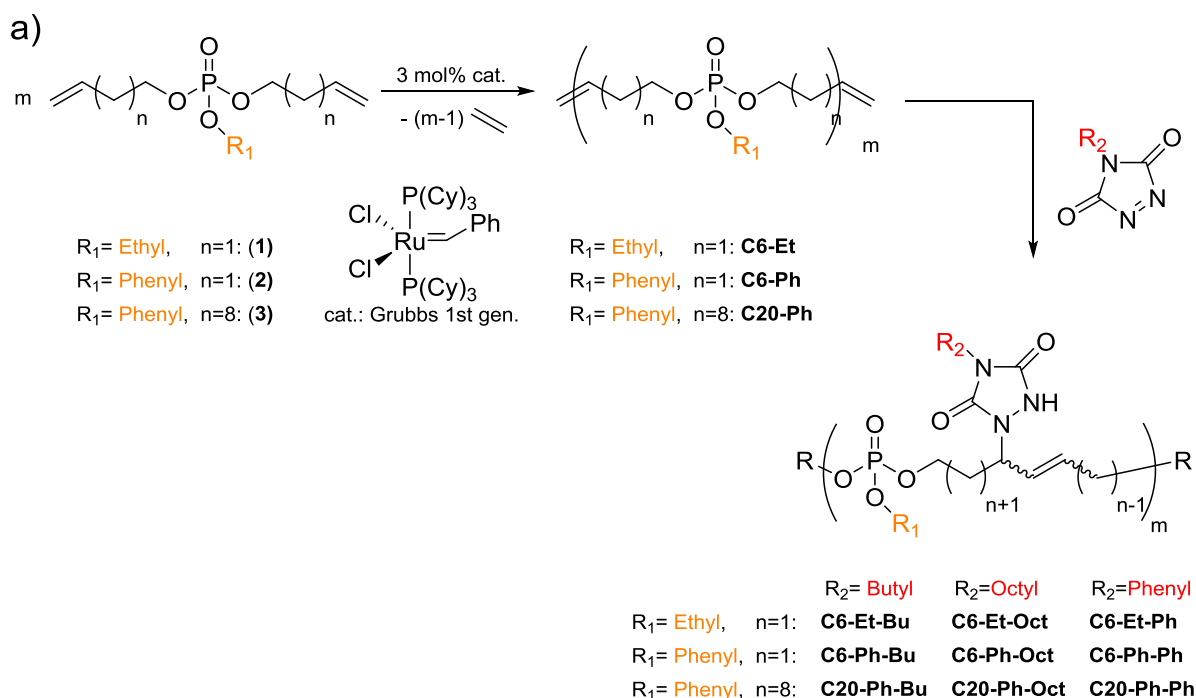


**Figure 7.1.** a) Synthesis scheme of **C6-Et**, **C6-Ph** and **C20-Ph** and post-modification with **Bu-TAD**, **Oct-TAD** or **Ph-TAD**; b)  $^1\text{H}$  NMR spectra of polymers **C6-Ph** (bottom) and **C6-Ph-Bu** (top) (300 MHz,  $d_6$ -DMSO).

$^1\text{H}$  NMR spectroscopy reveals full modification in all cases, as the original resonance attributed to the unsaturations (b at 5.47 ppm, Figure 7.1b bottom) is completely replaced by two new resonances as a result of the newly formed double bond (c at 5.44 and 5.76 ppm Figure 7.1b top). For all polymers, a cis-trans split-up of the internally moved double bonds can be observed. In case of the modified shorter chain polymers (**C6-Et** and **C6-Ph**), a split-up of the P-O neighbouring methylene group for cis and trans isomers can additionally be observed, due to the allylic position to the phosphate groups in the backbone. In case of the modified **C20-Ph** polymers, the split-up for the P-O neighbouring methylene group is not observed, because the internal double bonds are too distant. Additional proof of full modification is given via  $^{31}\text{P}$  {H}NMR, which is a sensitive probe to assess the modification of the polymers. Also in this case, the spectra reveal full modification of all polymers and show a clear upfield shift (for **C6-Et** polymers from -1.00 to -1.39 ppm, exemplarily shown in Figures 7.2b and S7.10-S7.12). After modification, a broader signal emerges due to an increased stiffness of the backbone as a result of the allylic position of P-O and the double bond. As SEC analysis for all modified polymers show similar dispersities after TAD-modification, as well as unmodified shape of the SEC-curves, it can be concluded that no degradation takes place after the straightforward chemical procedure (shown in Figures 7.2a and S7.13, and Table S7.1).

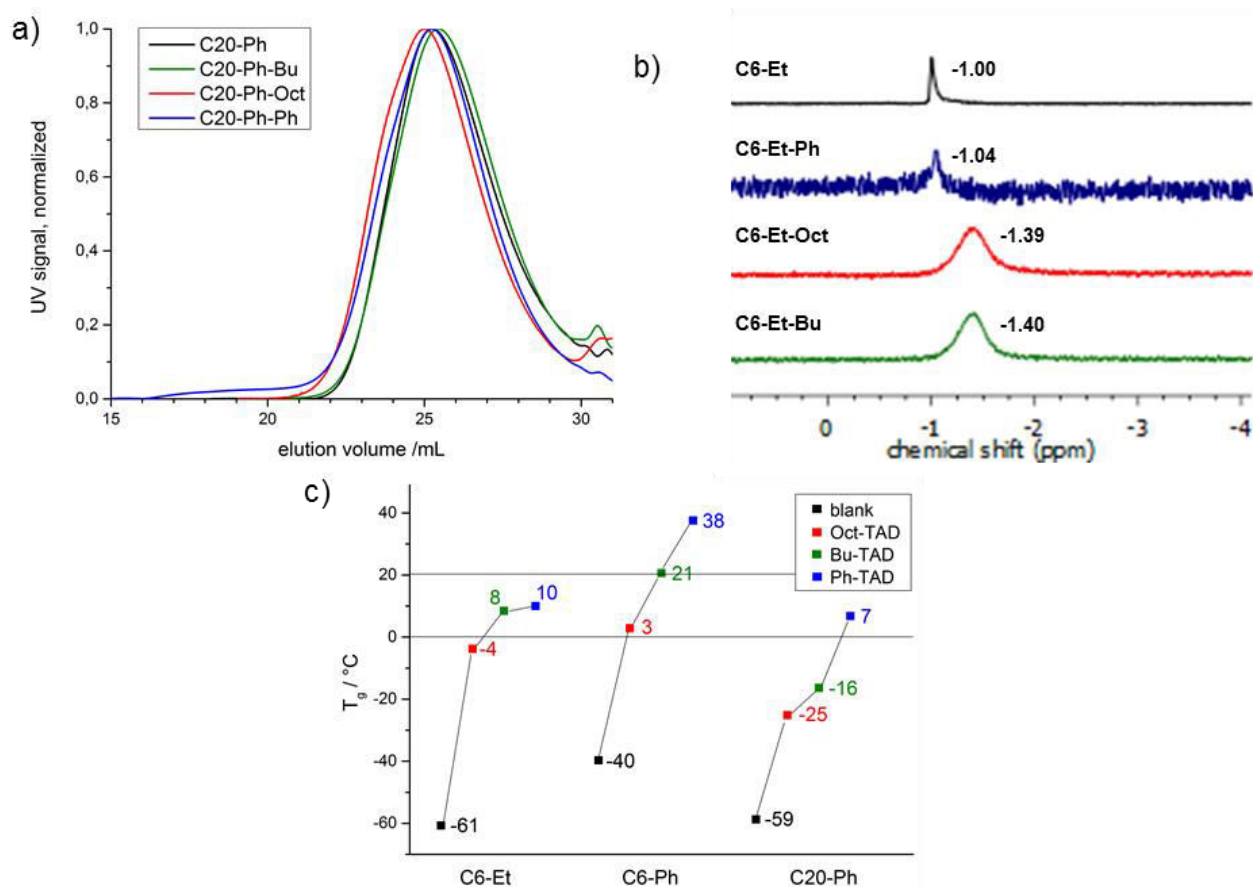


**Figure 7.2.** a) SEC curves of **C20-Ph**, **C20-Ph-Bu**, **C20-Ph-Oct** and **C20-Ph-Ph** in THF, UV signal; b)  $^{31}\text{P}$  {H} NMR spectra of **C6-Et**, **C6-Et-Bu**, **C6-Et-Oct** and **C6-Et-Ph**; c)  $T_g$ 's of all PPE's.

As mentioned earlier, aliphatic PPEs typically exhibit  $T_g$ 's below 0 °C.<sup>3</sup> The polymers used in this study exhibit  $T_g$ 's of -40 °C (**C6-Ph**), -59 °C (**C20-Ph**) and -61 °C (**C6-** modified polymers show an increased  $T_g$  with  $\Delta T_g$  ranging from 34 to 77 °C compared to unmodified polymers, which could be expected from the observations with previously reported polymers after TAD modification.<sup>22</sup> The highest increase of  $T_g$  was found for the modification with the rigid Ph-TAD, yielding  $T_g$ 's of 38 °C (**C6-Ph**), 10 °C (**C6-Et**) and 7 °C (**C20-Ph**). For the two alkyl-containing TADs, the more flexible Oct-TAD shows the lowest effect on the  $T_g$ 's: 3 °C (**C6-Ph**), -4 °C (**C6-Et**) and 25 °C (**C20-Ph**).

The thermal stability and degradation of the PPE and the TAD-modified polymers was investigated via thermogravimetric analysis (TGA). Figure 7.3 shows the TGA thermograms of the polymers (detailed TGA data are summarized in Table S7.2) and shows a large difference in the thermal stabilities and the char yields of the non-modified PPEs with varying backbone length. Note that **C6-Et** and **C6-Ph** show onset degradation temperatures (at 95wt%) at 231 and 222 °C, respectively, which are considerably lower in comparison to **C20-Ph** (291 °C). Additionally, the char yields at 700°C for **C6-Et** (29 wt%) and **C6-Ph** (28 wt%) are higher than for **C20-Ph** (13 wt%). Both effects can be explained by the increased amount of phosphorus in **C6-Et** and **C6-Ph** (15 and 12 wt%) compared to **C20-Ph** (7 wt%). It is known that the P-O-C bond decomposes at ca. 180 °C and is less stable than the C-C-bonds.<sup>23-25</sup> This lower bonding strength stimulates the degradation of the phosphate to phosphoric acids, which can form stable phosphorus-carbon structures, enhancing the charring of the polymer in the condensed phase and therefore increasing the residual mass.<sup>2, 23, 25-26</sup>

Also, the length of the alkyl chain in the backbone of the PPE was found to have a more significant effect on the thermal stability than the nature of the substituent in the side chain (Et or Ph). Thus, although **C6-Ph** shows a less pronounced decomposition than **C6-Et** between 250-350 °C, probably because of a charring effect of the aromatic side group, the degradation profile for both polymers is very similar at temperatures above 400 °C.

For all TAD-modified **C6-Et** and **C6-Ph** polymers (Figure 7.3), a similar degradation profile in comparison to their unmodified polymers can be observed. They show a similar residual mass at 700 °C (Table S7.2) and a similar onset degradation temperature as the unmodified one. From previous studies of TAD derivatives,<sup>22</sup> it is known that the urazole moiety degrades around 300 °C ( $T_{\text{onset}} = 250$  °C) by scission of the carbon-nitrogen linkage to the polymer chain, followed by further degradation to provide aniline and phenyl isocyanate in the gas phase. This indicates that the degradation of the PPE backbone takes place at lower temperatures than the degradation of the TAD moieties, which can explain the limited effect of these nitrogen containing moieties on the thermal degradation of the PPEs. Only the pending Ph-urazole moiety is found to have a significant effect on the thermal degradation of the **C6-Ph** polymer, as the residual mass at 700 °C increases from 28 wt% (**C6-Ph**) to 39 wt% (**C6-Ph-Ph**).

For the modified **C20-Ph** polymers (Figure 7.3d), the results are the most striking. All modified polymers show an earlier degradation temperature between 262-268 °C instead of 291 °C (**C20-Ph**), probably attributed to the urazole moieties cleavage from the polymers. Furthermore, while **C20-Ph** degrades in one step with a weight loss of 55 wt% at 295 °C, the modified polymers degrade over an improved temperature range of around 200 °C and show a weight loss of only 27 wt% at 295 °C. Therefore, in this case, the simultaneous degradation of the PPE and TAD group shows a notable improvement on the thermal stability from 300 °C to 450 °C. However, contrary to what might be expected, there is no notable increase in the char yield, except again for the **C20-Ph-Ph**, which leaves a final residue of 16 wt% compared to the 13 wt% of the **C20-Ph**. This modified polymer shows a similar pattern like **C6-Ph-Ph**. The increased degradation temperature of the modified **C20-Ph** polymers is situated in the range of the ones of epoxy resins, which makes them interesting as flame-retardant additives for such resins.

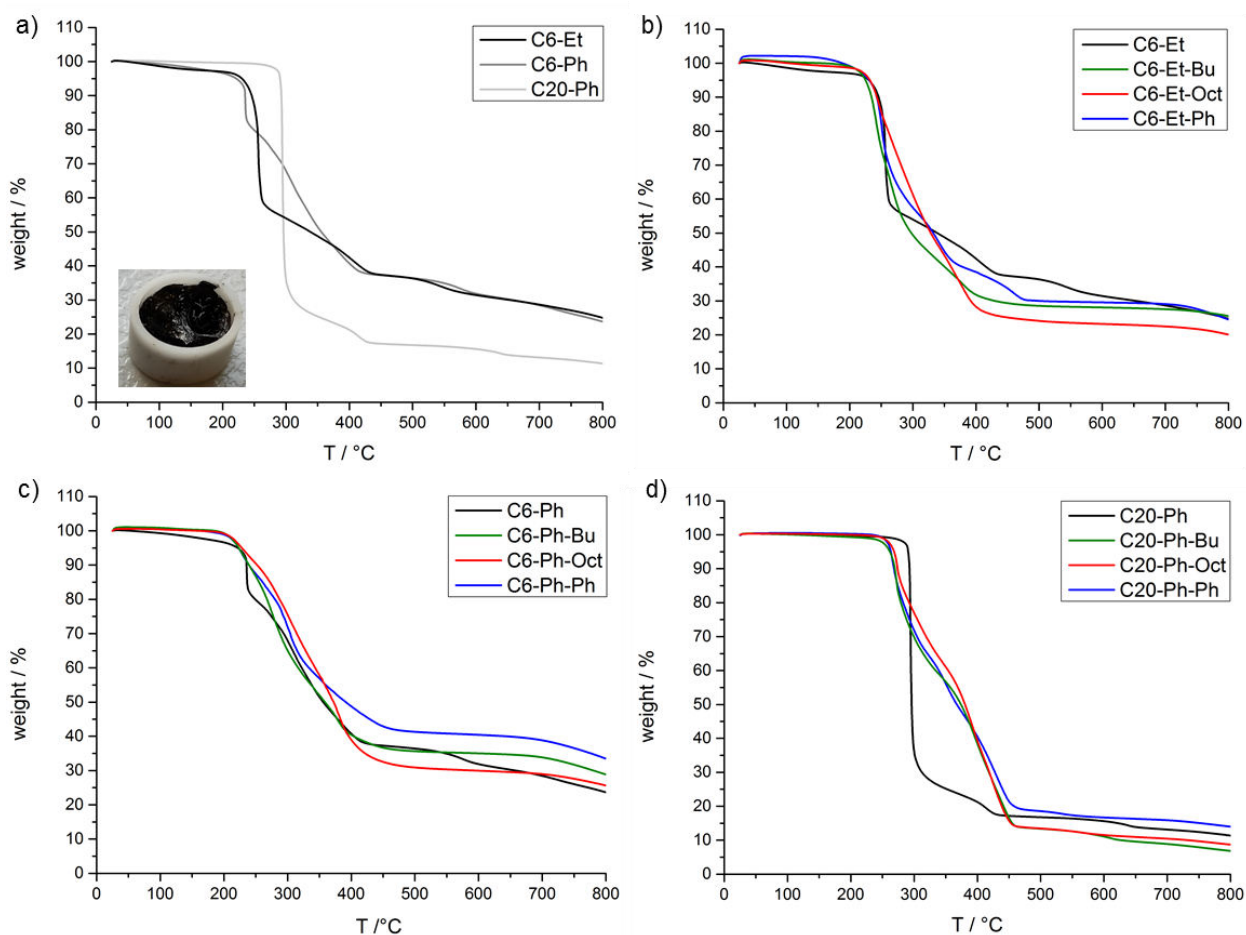


**Figure 7.3.** TGA-curves of unmodified and modified PPEs. Picture in Fig. 7.3a shows TGA residue at 800 °C.

## 7.5 Conclusions

ADMET-derived PPEs with a variation of chain-lengths (C6 or C20) and side chains (aliphatic or aromatic), could be quantitatively post-modified in an ultrafast way with both aliphatic and aromatic TADs for the first time. The post-modification improves the polymer properties, as PPEs with  $T_g$ 's above room temperature were obtained. Additionally, the modification led to an increase in decomposition temperature, because of enhanced charring behaviour, especially for the long-chain polymers. Moreover, the modification results in a rise of the residual mass for short-chain polymers with aromatic side chains. Taking these interesting findings into account, we strongly believe that the functionalized PPEs can find applications as flame retardant additives for materials in numerous applications.

## 7.6 Acknowledgments

G. Becker is a recipient of a fellowship through funding of the Excellence Initiative (DFG/GSC 266) in the graduate school of excellence “MAINZ” (Material Sciences in Mainz). The authors thank the Deutsche Forschungsgemeinschaft for funding. M.M. Velencoso thanks the Marie Skłodowska-Curie fellowship 705054-NOFLAME (Flame Retardant Nanocontainers) project. L. Vlamincx acknowledges the Special Research Fund (BOF) of Ghent University for funding of her PhD project.

## 7.7 Supporting Information

The Supporting Information contains additional synthetic procedures, NMR spectra, SEC and TGA diagrams and curves.

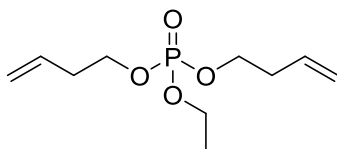
### Content

- 7.7.1 Synthetic procedures
- 7.7.2 NMR spectra
- 7.7.3 Size Exclusion Chromatography
- 7.7.4 Thermogravimetric Analysis

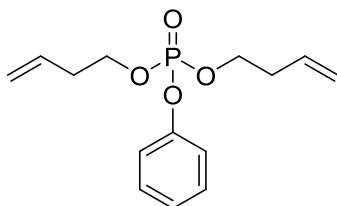
### 7.7.5 Synthetic procedures

*Representative Procedure for Monomer Synthesis:* The monomers were synthesized according to literature<sup>3</sup>. To a stirred solution of POCl<sub>3</sub> (10.00 g, 65.22 mmol, 1 eq.) in 100 mL dry DCM a mixture of a 3-buten-1-ol (9.41 g, 130.44 mmol, 2 eq.) and Et<sub>3</sub>N (13.20 g, 130.44 mmol, 2 eq.) in 20 mL dry DCM at 0°C was added dropwise. After 18 h, a mixture of dry ethanol (6.01 g, 130.44 mmol, 2 eq.) and Et<sub>3</sub>N (13.20 g, 130.44 mmol, 2 eq.) in 20 mL dry DCM was added dropwise at 0°C. After 24 h, the solvent was concentrated, diethyl ether added and Et<sub>3</sub>N·HCl as a white solid removed by filtration. Remaining di(but-3-en-1-yl) phosphorochloridate was removed by flushing the crude product over neutral Al<sub>2</sub>O<sub>3</sub> with DCM to give the pure product, a clear oil.

*Di(but-3-en-1-yl) ethyl phosphate (1):* DCM/ethyl acetate = 10:1, R<sub>f</sub>=0,53. Yield: 73% (11.15 g). <sup>1</sup>H NMR (300 MHz, CDCl<sub>3</sub>): δ [ppm] 5.83-5.70 (m, 2H, CH<sub>2</sub>=CH-CH<sub>2</sub>-CH<sub>2</sub>-O-P), 5.14-5.04 (m, 4H, CH<sub>2</sub>=CH-CH<sub>2</sub>-CH<sub>2</sub>-O-P), 4.13-4.01 (m, 6H, -CH<sub>2</sub>-O-P), 2.45-2.37 (dd, 4H, CH<sub>2</sub>=CH-CH<sub>2</sub>-CH<sub>2</sub>-O-P), 1.30 (t, 3H, CH<sub>3</sub>-). <sup>13</sup>C {H} NMR (76 MHz, CDCl<sub>3</sub>): δ [ppm] 133.51 (CH<sub>2</sub>=CH-CH<sub>2</sub>-CH<sub>2</sub>-O-P), 117.81 (CH<sub>2</sub>=CH-CH<sub>2</sub>-CH<sub>2</sub>-O-P), 66.83 (CH<sub>2</sub>=CH-CH<sub>2</sub>-CH<sub>2</sub>-O-P), 63.97 (-CH<sub>2</sub>-O-P), 34.77 (CH<sub>2</sub>=CH-CH<sub>2</sub>-CH<sub>2</sub>-O-P), 16.22 (-CH<sub>3</sub>). <sup>31</sup>P {H} NMR (121 MHz, CDCl<sub>3</sub>): δ [ppm] -1.03. ESI-MS: *m/z* 257.07 [M + Na]<sup>+</sup>, 491.17 [2M + Na]<sup>+</sup> (calculated for C<sub>10</sub>H<sub>19</sub>O<sub>4</sub>P: 234.10). FTIR (cm<sup>-1</sup>): 3080, 2981, 2933, 2904, 1642, 1473, 1432, 1391, 1369, 1264 (P=O), 1165, 1013 (P-O-C), 988 (P-O-C), 914, 860, 799, 734, 701.

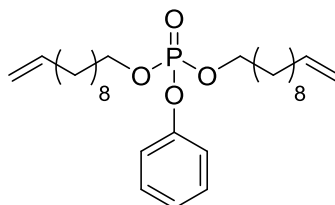


*Di(but-3-en-1-yl) phenyl phosphate (2):* Following the general procedure described above and using phenol instead of ethanol, **2** was obtained after column chromatography over silica using as eluent dichloromethane. DCM, R<sub>f</sub> = 0.3. Yield: 70%. <sup>1</sup>H NMR (300 MHz, CDCl<sub>3</sub>): δ [ppm] 7.33–7.16 (m, 5H, Ph-O-P), 5.79–5.73 (m, 2H, CH<sub>2</sub>=CH-CH<sub>2</sub>-CH<sub>2</sub>-O-P), 5.11-5.08 (m, 4H, CH<sub>2</sub>=CH-CH<sub>2</sub>-CH<sub>2</sub>-O-P), 4.20–4.13 (m, 4H, -CH<sub>2</sub>-O-P), 2.44–2.42 (m, 4H, CH<sub>2</sub>=CH-CH<sub>2</sub>-CH<sub>2</sub>-O-P). <sup>13</sup>C {H} NMR (76 MHz, CDCl<sub>3</sub>): δ [ppm] 150.69, 150.65, 133.12, 129.70, 125.05, 120.04, 120.01, 117.91, 67.54, 67.50, 34.60, 34.56. <sup>31</sup>P {H} NMR (121 MHz, CDCl<sub>3</sub>): δ [ppm] -6.40.



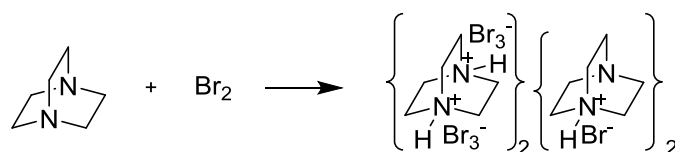
*Di(undecen-10-en-1-yl) phenyl phosphate (3):* Following the general procedure described above and using phenol instead of ethanol and 10-undecen-1-ol instead of 3-buten-1-ol, **3** was obtained after column chromatography over silica using as eluent dichloromethane. DCM, R<sub>f</sub>=0.5. Yield: 80%.

$^1\text{H}$  NMR (300 MHz,  $\text{CDCl}_3$ ):  $\delta$  [ppm] 7.32-7.16 (m, 5H, *Ph*-O-P), 5.83–5.77 (m, 2H,  $\text{CH}_2=\text{CH}-\text{CH}_2-$ ), 5.00–4.91 (m, 4H,  $\text{CH}_2=\text{CH}-\text{CH}_2-$ ), 4.16–4.09 (m, 4H,  $-\text{CH}_2-\text{O}-\text{P}$ ), 2.04–2.01 (m, 4H,  $\text{CH}_2=\text{CH}-\text{CH}_2-\text{CH}_2-$ ), 1.69–1.65 (m, 4H,  $-\text{CH}_2-\text{CH}_2-\text{O}-\text{P}$ ), 1.39–1.26 (m, 12H,  $-\text{CH}_2-$ ).  $^{13}\text{C}$  {H} NMR (76 MHz,  $\text{CDCl}_3$ ):  $\delta$  [ppm] 150.98, 150.94, 139.29, 129.77, 125.02, 120.10, 114.27, 68.69, 68.66, 33.93, 30.37, 30.33, 29.55, 29.04.  $^{31}\text{P}$  {H} NMR (121 MHz,  $\text{CDCl}_3$ ):  $\delta$  [ppm] –6.11.



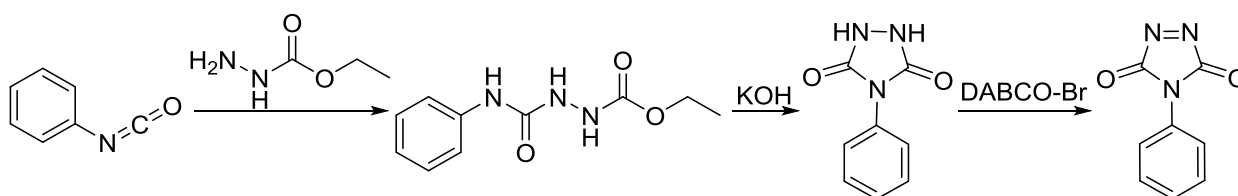
#### Synthesis of TAD compounds:

**DABCO-Br:** In a 500 mL two-neck flask, 1,4-diazabicyclo[2.2.2]octane (6.73 g, 60.0 mmol, 1 eq.) was dissolved in chloroform (100 mL). In a next step, a solution of  $\text{Br}_2$  (20.0 g, 0.125 mol, 2.1 eq.) in chloroform (100 mL) was added dropwise using an addition funnel. The resulting mixture was stirred under inert atmosphere for 1 hour. The yellow precipitate was filtered off, washed with chloroform (50 mL) and dried overnight in a vacuum oven at 40 °C to obtain 23.3 g of yellow powder (14.8 mmol, 99%).

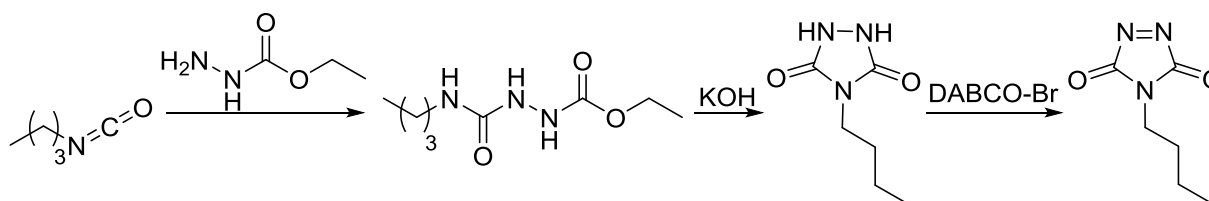


**4-phenyl-1,2,4-triazoline-3,5-dione (Ph-TAD):** A mixture of ethyl carbazate (10 g, 96.1 mmol, 1 eq.) and toluene (105 mL) was placed in a three neck flask (250 mL) and cooled in an ice bath. The flask was equipped with an addition funnel, containing 10.44 mL phenylisocyanate (96.1 mmol, 1 eq.), a mechanical stirrer and a bulb condenser. The mixture was put under inert atmosphere and the isocyanate was added slowly under vigorous stirring. After addition the mixture was stirred at room temperature for two hours, followed by 2 hours at 90°C. After cooling the reaction to room temperature, 4-phenyl-1-(ethoxycarbonyl) semicarbazide was filtered off and washed with toluene (96 %). Subsequently, the obtained 4-phenyl-1-(ethoxycarbonyl) semicarbazide (12.2 g, 60.0 mmol) was dissolved in 30 mL of an aqueous potassium hydroxide solution (4M) in a 50 mL flask under inert atmosphere. This mixture was refluxed for 1.5 hour (100°C), warm filtered, cooled to room temperature and acidified to pH 1 by addition of HCl. This mixture was cooled to room temperature to yield a white powder that was filtered off (95%). In a last step, a mixture of the just obtained 4-phenyl-1,2,4-triazolidine-3,5-dione (1 g, 5.64 mmol, 1 eq.), DABCO-Br (2 g, 1.27 mmol, 0.2 eq.) and dichloromethane (30 mL) was put in a flask (100 mL) under inert atmosphere and stirred for 2 hours at room temperature. The reaction mixture was filtered off, the residue washed

with dichloromethane (2 × 30 mL) and the filtrate was concentrated in vacuo to obtain 4-phenyl-1,2,4-triazoline-3,5-dione (**Ph-TAD**) as dark red crystals (92%). The temperature of the cooling bath should not exceed 50°C due to the volatility of the obtained compound. <sup>1</sup>H-NMR (300 MHz, d<sub>6</sub>-DMSO): δ [ppm] 7.60–7.45 (m, 5H, Ar-).

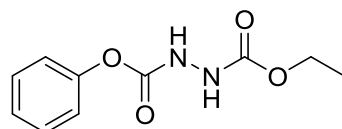


**4-butyl-1,2,4-triazoline-3,5-dione (Bu-TAD):** A mixture of ethyl carbazate (10 g, 96.1 mmol, 1 eq.) and toluene (105 mL) was placed in a three neck flask (250 mL) and cooled in an ice bath. The flask was equipped with an addition funnel, containing 10.8 mL butylisocyanate (96.1 mmol, 1 eq.), a mechanical stirrer and a bulb condenser. The mixture was put under inert atmosphere and the isocyanate was added slowly under vigorous stirring. After addition, the mixture was stirred at room temperature for two hours, followed by 2 hours at 90°C. After cooling the reaction to room temperature, 4-butyl-1-(ethoxycarbonyl) semicarbazide (96%) was filtered off and washed with toluene. In a 50 mL flask, 4-butyl-1-(ethoxycarbonyl) semicarbazide (12.2 g, 60.0 mmol) was dissolved in 30 mL of an aqueous potassium hydroxide solution (4M) under inert atmosphere. This mixture was refluxed for 1.5 hour (100°C), warm filtered, cooled to room temperature and acidified until pH 1 by addition of hydrogen chloride. This mixture was cooled to room temperature to yield 4-butyl-1,2,4-triazolidine-3,5-dione (62%) as a solid white powder, that was filtered off. A mixture of 4-butyl-1,2,4-triazolidine-3,5-dione (1 g, 6.36 mmol, 1 eq.), DABCO-Br (2 g, 1.27 mmol, 0.2 eq.) and dichloromethane (30 mL) was put in a flask (100 mL) under inert atmosphere and stirred for 2 hours at room temperature. The reaction mixture was filtered off, the residue washed with dichloromethane (2 × 30 mL) and the filtrate was concentrated in vacuo to obtain 4-butyl-1,2,4-triazoline-3,5-dione (72%). The temperature of the heating bath cannot exceed 50°C due to the volatility of the obtained compound. <sup>1</sup>H-NMR (300 MHz, d<sub>6</sub>-DMSO): δ [ppm] 3.47 (t, 2H, N-CH<sub>2</sub>-), 1.56 (m, 2H, N-CH<sub>2</sub>-CH<sub>2</sub>-), 1.30 (m, 2H, CH<sub>3</sub>-CH<sub>2</sub>-CH<sub>2</sub>-), 0.88 (t, 3H, CH<sub>3</sub>-(CH<sub>2</sub>)<sub>3</sub>-).

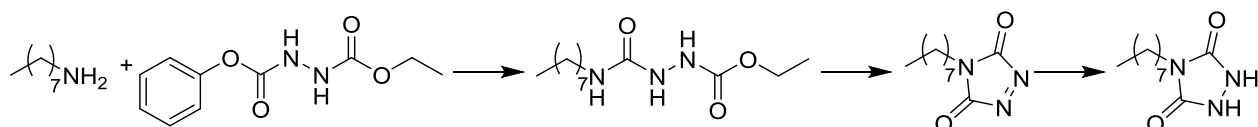


**1-ethyl 2-phenyl hydrazine-1,2-dicarboxylate:** The compound was synthesized according to literature.<sup>27</sup> 10.0 g of ethylcarbrazate (96.1 mmol, 1 eq.) and 20.0 mL di-isopropylethylamine (DIPEA) (115 mmol, 1.2 eq) were solubilized in 100 mL dichloromethane under inert atmosphere.

The reaction mixture was cooled with an ice bath and 12.1 mL phenyl chloroformate (96.1 mmol, 1 eq.) was added dropwise. After overnight stirring, the reaction mixture was extracted with 0.5M HCl solution (3 x 30.0 mL) and washed with 50.0 mL saturated NaCl-solution. The organic phase was dried on MgSO<sub>4</sub> and the solvent was removed in vacuo to obtain 19.6 g 1-ethyl 2-phenyl hydrazine-1,2-dicarboxylate (87.4 mmol, 91 %). <sup>1</sup>H-NMR (300 MHz, d<sub>6</sub>-DMSO): δ [ppm] 7.40 (t, 2H, aromatic), 7.25 (t, 1H, aromatic), 7.18 (d, 2H, aromatic), 6.85 (s (br), 1H, NH), 6.56 (s (br), 1H, NH), 4.27 (q, 2H, O-CH<sub>2</sub>-CH<sub>3</sub>), 1.32 (O-CH<sub>2</sub>-CH<sub>3</sub>).



**4-octyl-1,2,4-triazoline-3,5-dione (Oct-TAD):** In a 50 mL of acetonitrile, 1 mL (0.78 g, 6.03 mmol, 1 eq.) of octyl amine was added to 2.03 g ethylphenyl hydrazine dicarboxylate (9.05 mmol, 1 eq.) and this reaction mixture was stirred overnight at room temperature, after which the solvent was removed under reduced pressure. The product was purified via column chromatography (eluent EtOAc:Hexane 2:1), yielding 1.14g of pure semicarbazide (4.40 mmol, 73%). Subsequently, ring closure of the semicarbazide was performed in basic environment. The semicarbazide (1.14g, 4.40 mmol, 1 eq.) was solubilized in 30 mL of methanol and potassium carbonate (2.43 g, 17.60 mmol, 4 eq.) was added. The mixture was refluxed overnight, cooled to room temperature and acidified until pH 1 by addition of hydrogen chloride. The salts were filtered off and the solvent was removed in vacuo to yield 4-octyl-1,2,4-triazolidine-3,5-dione (0.84 g, 3.92 mmol, 89%) as a solid white powder. In the last step, 0.84 g of 4-octyl-1,2,4-triazolidine-3,5-dione was solubilized in dichloromethane (25 mL) and 1.23 g of DABCO-Br (0.78 mmol, 0.2 eq.) was added. This mixture was filtered off after one hour and the filtrate was concentrated in vacuo to yield 0.79 g of 4-octyl-1,2,4-triazoline-3,5-dione (3.72 mmol, 95%). 4-octyl-semicarbazide: <sup>1</sup>H-NMR (300 MHz, d<sub>6</sub>-DMSO): δ [ppm] 8.70 (s, 1H, NH), 7.60 (s, 1H, NH), 6.27 (s, 1H, NH), 4.01 (q, 2H, O-CH<sub>2</sub>-CH<sub>3</sub>), 2.97 (q, 2H, NH-CH<sub>2</sub>-CH<sub>2</sub>-), 1.36 (quin, 2H, NH-CH<sub>2</sub>-CH<sub>2</sub>-), 1.24 (m, 10H, alkyl), 1.17 (t, 3H, O-CH<sub>2</sub>-CH<sub>3</sub>), 0.86 (t, 3H, -CH<sub>2</sub>-CH<sub>2</sub>-CH<sub>3</sub>). 4-octyl-1,2,4-triazolidine-3,5-dione: <sup>1</sup>H-NMR (300 MHz, d<sub>6</sub>-DMSO): δ [ppm] 10.00 (s, 2H, NH-NH), 3.33 (t, 2H, N-CH<sub>2</sub>-CH<sub>2</sub>-), 1.52 (quin, 2H, N-CH<sub>2</sub>-CH<sub>2</sub>-), 1.24 (m, 10H, alkyl), 0.86 (t, 3H, -CH<sub>2</sub>-CH<sub>2</sub>-CH<sub>3</sub>). 4-octyl-1,2,4-triazoline-3,5-dione: <sup>1</sup>H-NMR (300 MHz, d<sub>6</sub>-DMSO): 3.45 (q, 2H, N-CH<sub>2</sub>-CH<sub>2</sub>-), 1.56 (quin, 2H, N-CH<sub>2</sub>-CH<sub>2</sub>-), 1.24 (m, 10H, alkyl), 0.86 (t, 3H, -CH<sub>2</sub>-CH<sub>2</sub>-CH<sub>3</sub>).



### 7.7.2 NMR spectra

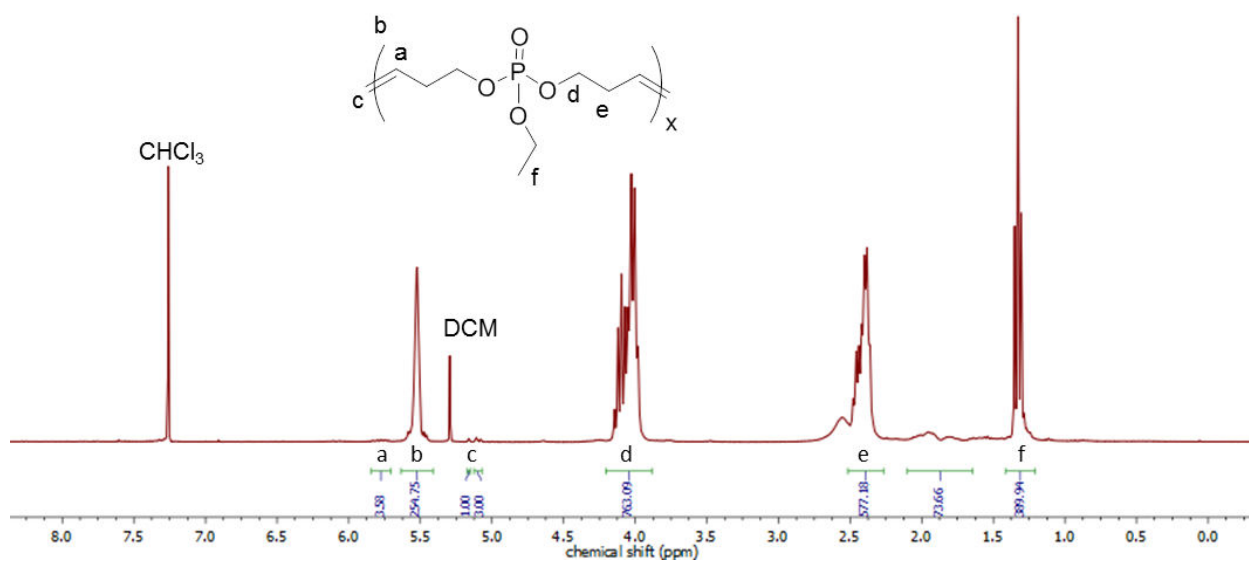


**Figure S7.1.** <sup>1</sup>H NMR (300 MHz, CDCl<sub>3</sub>) of polymer C6-Et.

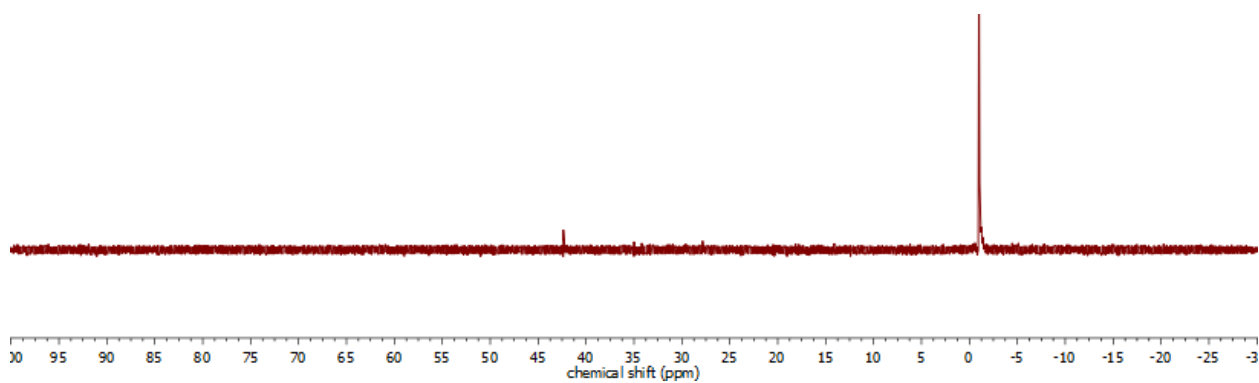


**Figure S7.2.** <sup>31</sup>P {<sup>1</sup>H}NMR (202 MHz, CDCl<sub>3</sub>) of polymer C6-Et.

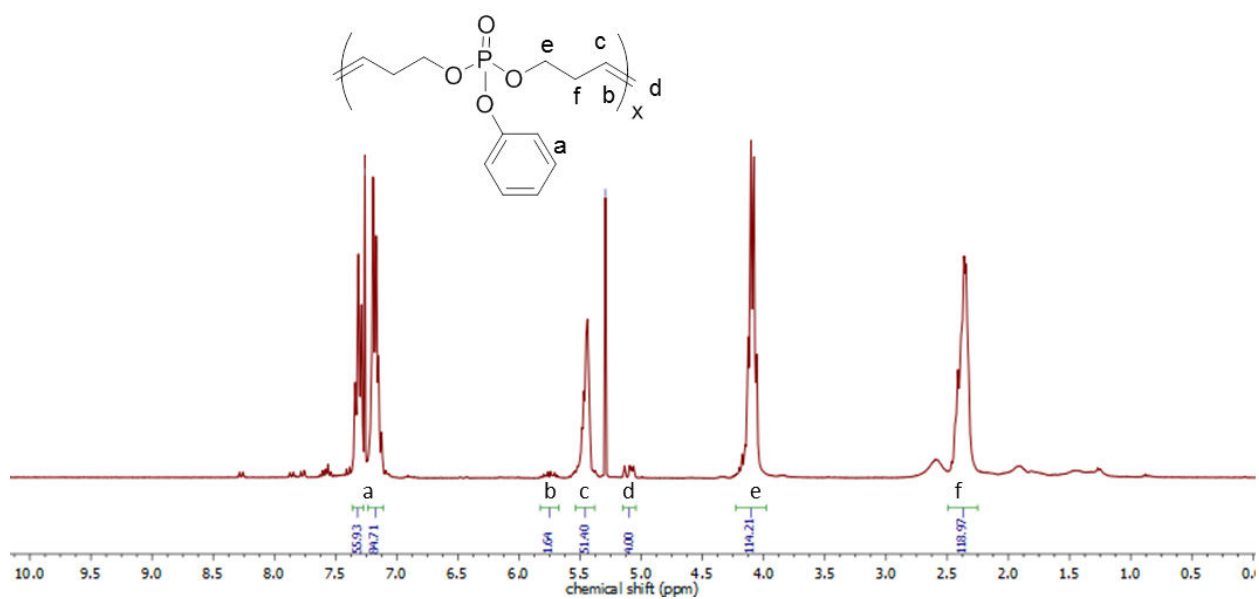


**Figure S7.3.**  $^1\text{H}$  NMR (300 MHz,  $\text{CDCl}_3$ ) of polymer **C6-Ph**.

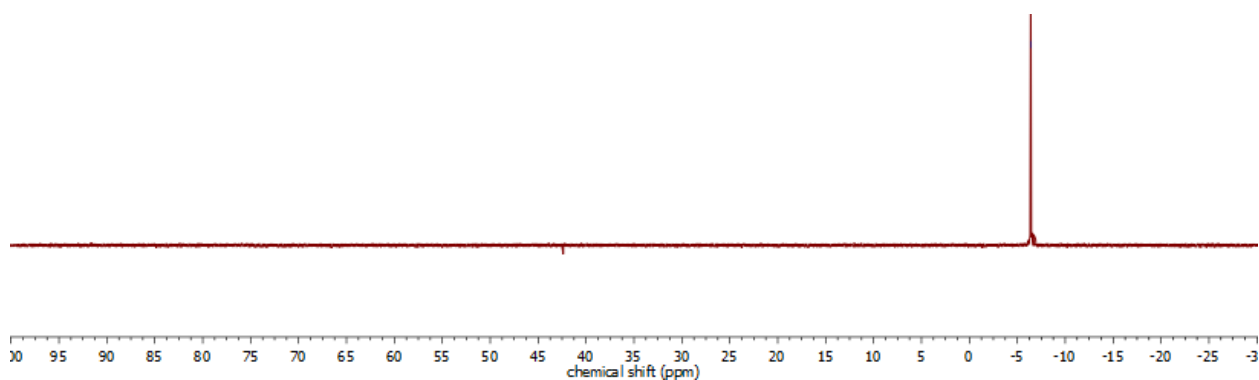


**Figure S7.4.**  $^{31}\text{P}$  {H}NMR (121 MHz,  $\text{CDCl}_3$ ) of polymer **C6-Ph**.

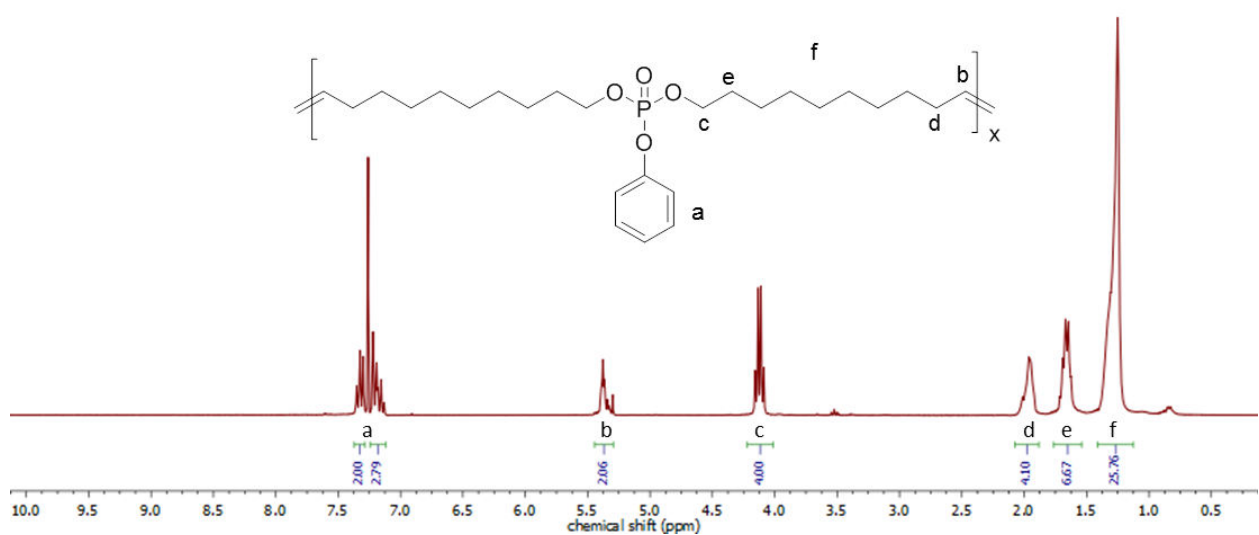


**Figure S7.5.**  $^1\text{H}$  NMR (300 MHz,  $\text{CDCl}_3$ ) of polymer **C20-Ph**.

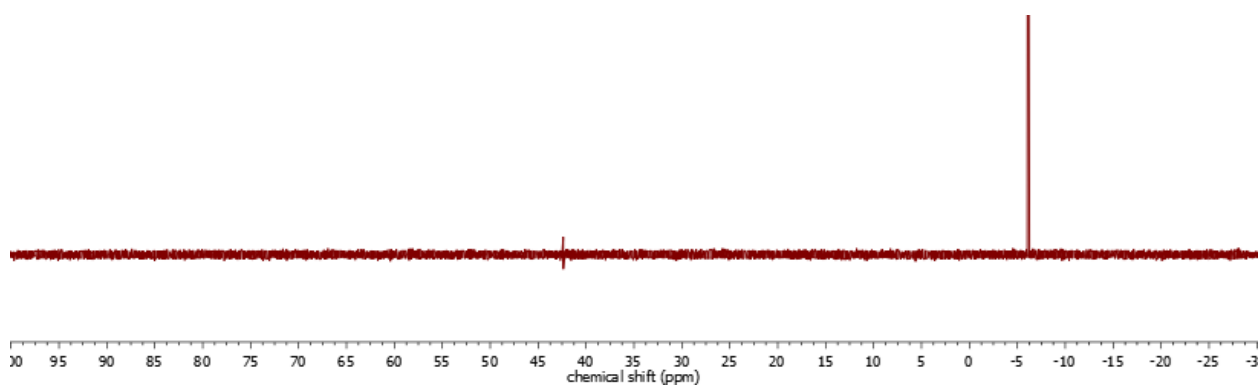


**Figure S7.6.**  $^{31}\text{P}$  {H}NMR (121 MHz,  $\text{CDCl}_3$ ) of polymer **C20-Ph**.

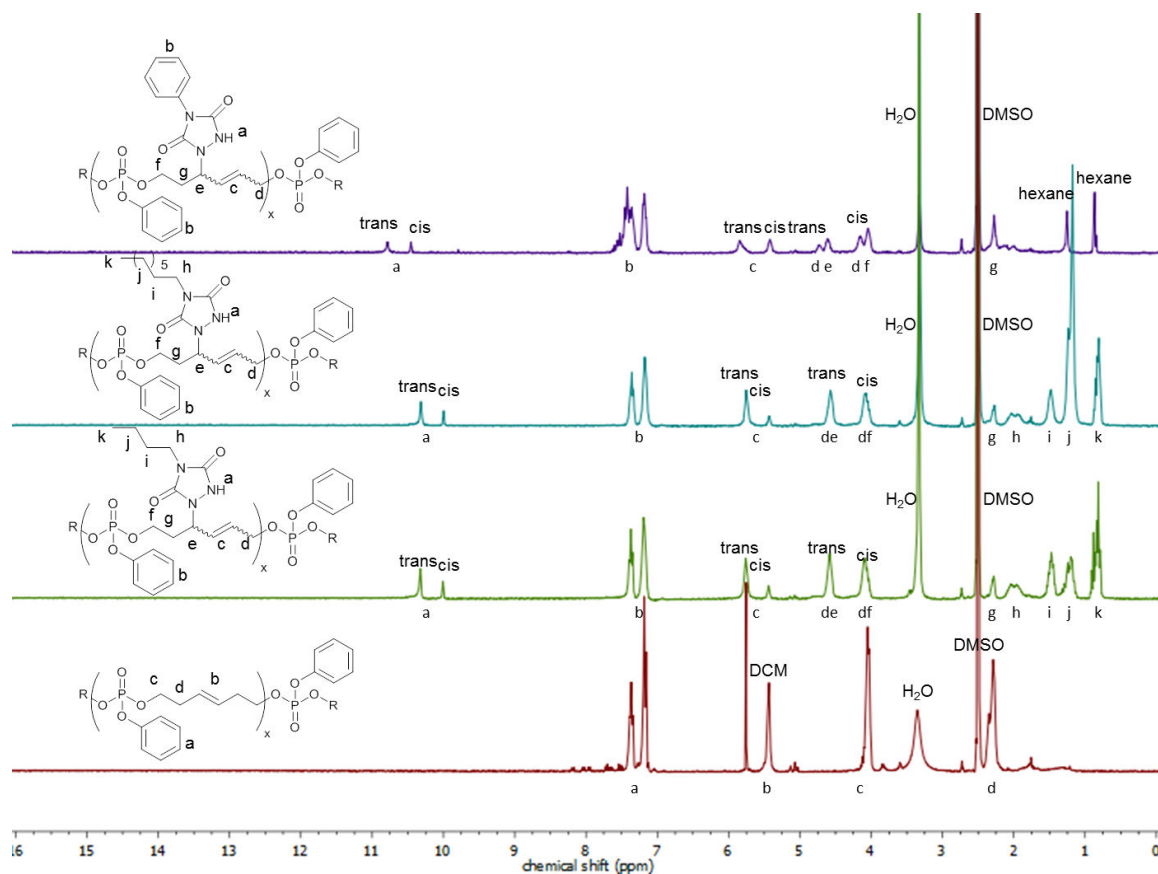


**Figure S7.7.**  $^1\text{H}$  NMR (300 MHz,  $d_6$ -DMSO) of polymers C6-Ph, C6-Ph-Bu, C6-Ph-Oct, C6-Ph-Ph.

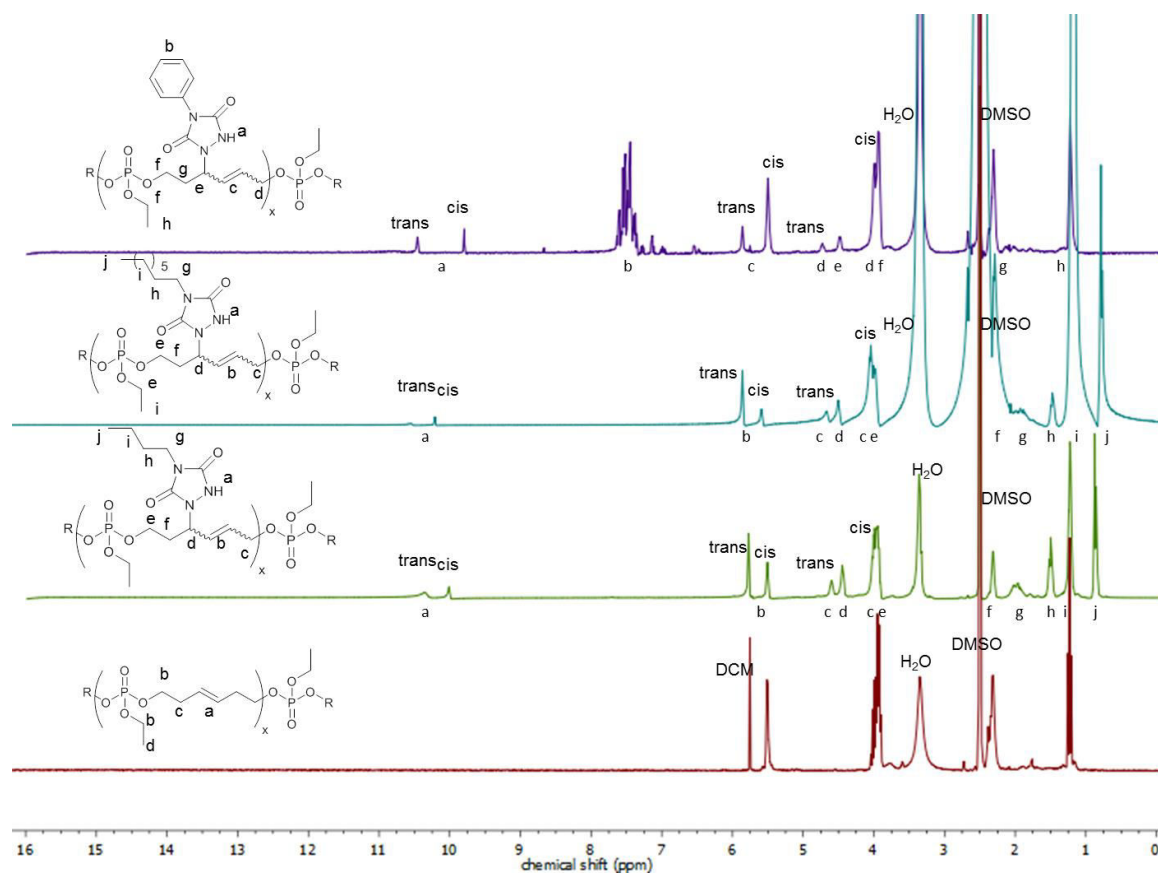


**Figure S7.8.**  $^1\text{H}$  NMR (300 MHz,  $d_6$ -DMSO) of polymers C6-Et, C6-Et-Bu, C6-Et-Oct, C6-Et-Ph.

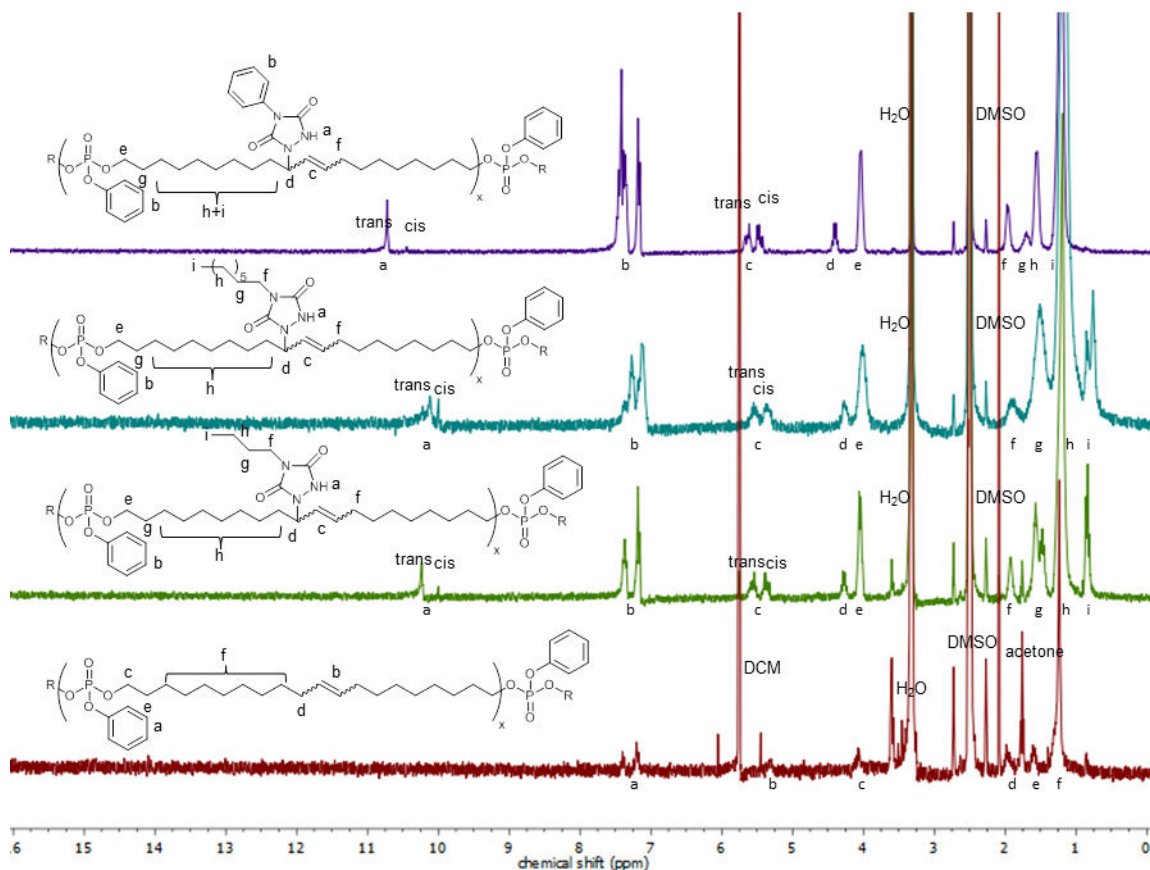


**Figure S7.9.**  $^1\text{H}$  NMR (300 MHz,  $d_6$ -DMSO) of polymers C20-Ph, C20-Ph-Bu, C20-Ph-Oct, C20-Ph-Ph.

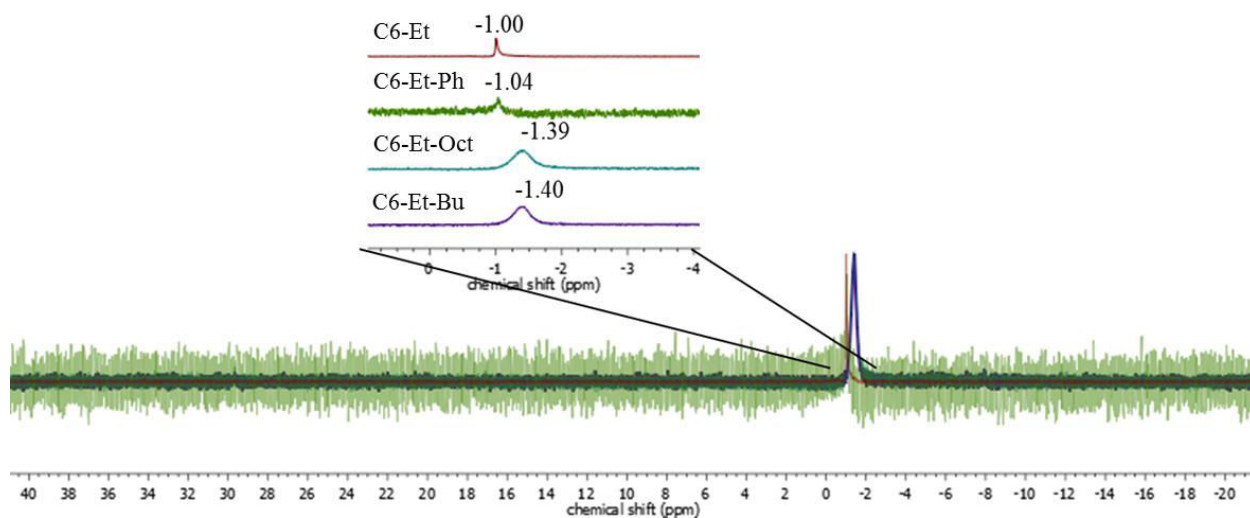


**Figure S7.10.**  $^{31}\text{P}$  { $^1\text{H}$ } NMR (121 MHz,  $\text{CDCl}_3$ ) of polymers C6-Et, C6-Et-Bu, C6-Et-Oct, C6-Et-Ph.

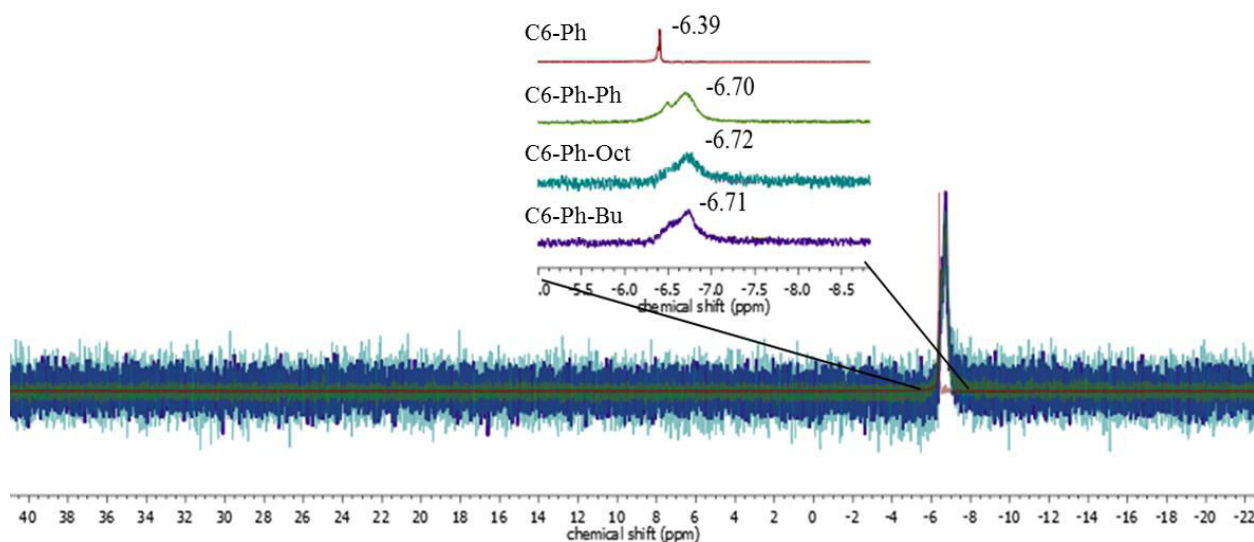


**Figure S7.11.**  $^{31}\text{P}$  {H}NMR (121 MHz,  $\text{CDCl}_3$ ) of polymers **C6-Ph**, **C6-Ph-Bu**, **C6-Ph-Oct**, **C6-Ph-Ph**.

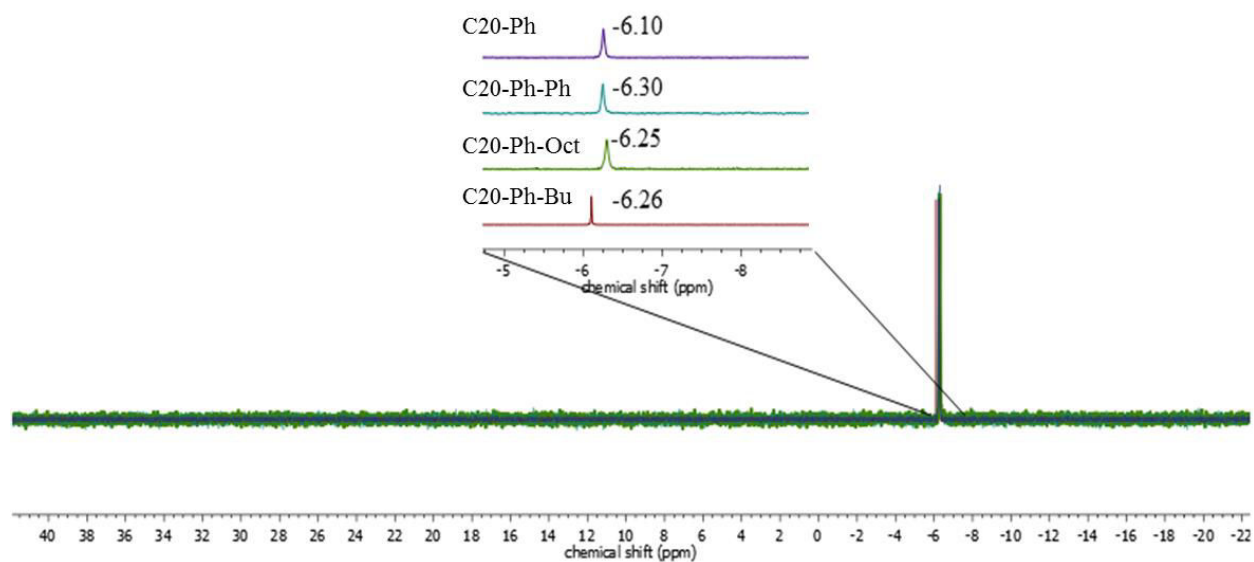


**Figure S7.12.**  $^{31}\text{P}$  {H}NMR (121 MHz,  $\text{CDCl}_3$ ) of polymers **C20-Ph**, **C20-Ph-Bu**, **C20-Ph-Oct**, **C20-Ph-Ph**.

### 7.7.3 Size Exclusion Chromatography

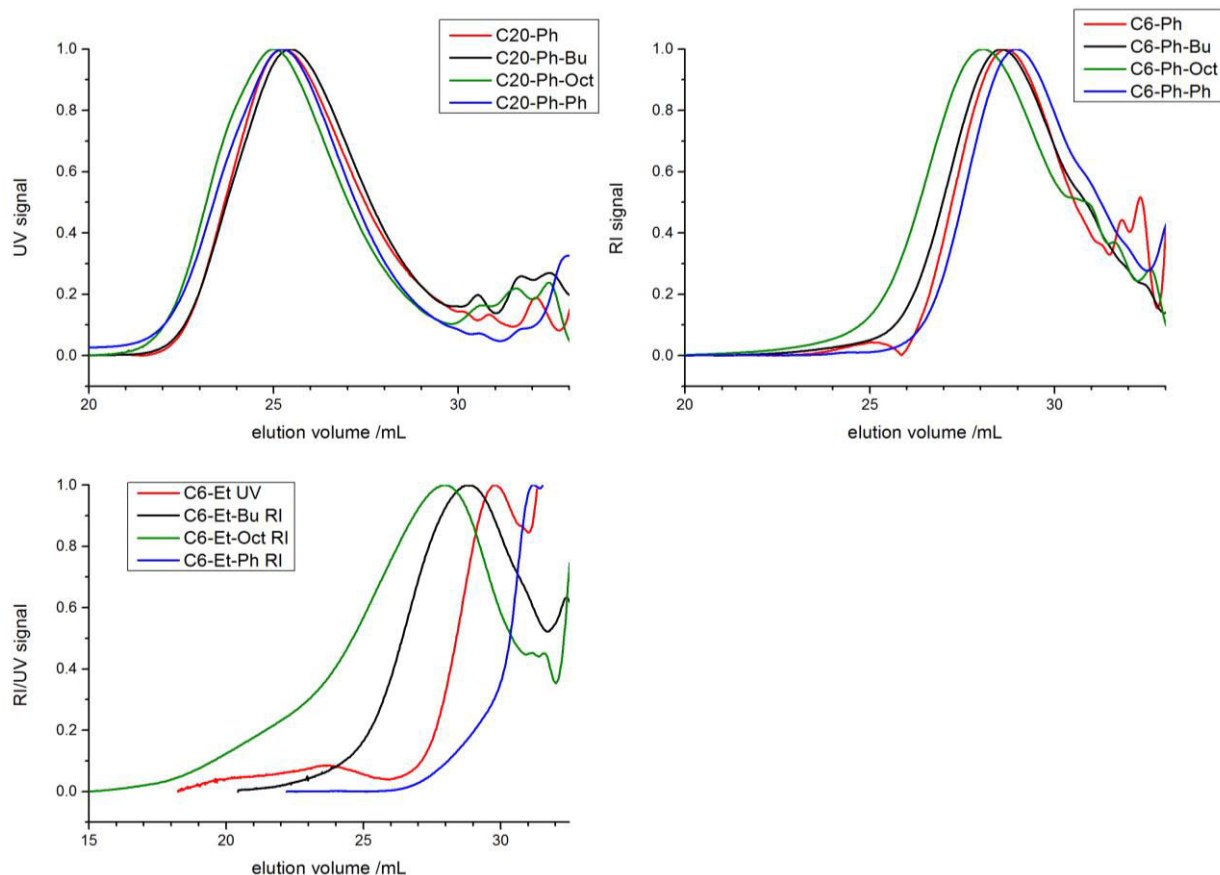


**Figure S7.13.** SEC curves of all polymers and functionalized polymers, in THF with UV-signal for **C20-Ph**, RI-signal for **C6-Ph** and UV or RI-signal for **C6-Et**.

**Table S7.1.** Overview of SEC results.

sample	signal	$M_n$ / g/mol	$M_w$ / g/mol	$\bar{D}$	$V_{max}$ / mL
<b>C20-Ph</b>	UV	10,100	22,400	2.21	25.26
<b>C20-Ph-Bu</b>	UV	11,000	21,800	1.99	25.45
<b>C20-Ph-Oct</b>	UV	14,500	28,500	1.97	25.01
<b>C20-Ph-Ph</b>	UV	12,800	28,200	2.20	25.24
<b>C6-Ph</b>	RI	2,300	4,300	1.84	28.68
<b>C6-Ph-Bu</b>	RI	2,300	4,700	2.00	28.54
<b>C6-Ph-Oct</b>	RI	4,200	8,100	1.95	28.06
<b>C6-Ph-Ph</b>	RI	2,000	3,600	1.83	28.96
<b>C6-Et</b>	UV	1,700	2,500	1.46	29.83
<b>C6-Et-Bu</b>	RI	3,300	7,500	2.22	28.83
<b>C6-Et-Oct</b>	RI	4,500	10,600	2.35	27.99
<b>C6-Et-Ph</b>	RI	1,000	1,700	1.66	31.22

### 7.7.4 Thermogravimetric Analysis

**Table S7.2.** Overview of TGA results.

sample	wt% P <sub>th</sub>	wt% N <sub>th</sub>	T <sub>onset</sub> (95wt%) /°C	T <sub>max</sub> /°C	Char (wt%) at 700°C	Yield
C6-Et	15.02	-	230.5	257	29	
C6-Et-Bu	8.57	11.63	225	242	26	
C6-Et-Oct	7.42	10.07	232	247	22	
C6-Et-Ph	8.12	11.02	231	281	29	
C6-Ph	12.18	-	221.5	236	28	
C6-Ph-Bu	7.57	10.26	223	~275	34	
C6-Ph-Oct	6.65	9.03	228	~310	29	
C6-Ph-Ph	7.21	9.79	223	~310	39	
C20-Ph	6.87	-	290.5	295	13	
C20-Ph-Bu	5.11	6.94	261.5	272	9	
C20-Ph-Oct	4.68	6.35	268	273	10	
C20-Ph-Ph	4.95	6.72	263	267	16	

## 7.8 References

- Zhang, F.; Smolen, J. A.; Zhang, S.; Li, R.; Shah, P. N.; Cho, S.; Wang, H.; Raymond, J. E.; Cannon, C. L.; Wooley, K. L., *Nanoscale* **2015**, 7 (6), 2265-2270.
- Tauber, K.; Marsico, F.; Wurm, F. R.; Schartel, B., *Polymer Chemistry* **2014**, 5 (24), 7042-7053.
- Marsico, F.; Wagner, M.; Landfester, K.; Wurm, F. R., *Macromolecules* **2012**, 45 (21), 8511-8518.
- Bauer, K. N.; Tee, H. T.; Lieberwirth, I.; Wurm, F. R., *Macromolecules* **2016**, 49 (10), 3761-3768.
- Steinmann, M.; Markwart, J.; Wurm, F. R., *Macromolecules* **2014**, 47 (24), 8506-8513.
- Zhao, Z.; Wang, J.; Mao, H.-Q.; Leong, K. W., *Adv. Drug Delivery Rev.* **2003**, 55 (4), 483-499.
- Steinbach, T.; Wurm, F. R., *Angew. Chem. Int. Ed.* **2015**, 54 (21), 6098-6108.
- Bourbigot, S.; Duquesne, S., *J. Mater. Chem.* **2007**, 17 (22), 2283-2300.
- Joseph, P.; Tretsiakova-Mcnally, S., *Polym. Adv. Technol.* **2011**, 22 (4), 395-406.
- Chattopadhyay, D. K.; Webster, D. C., *Prog. Polym. Sci.* **2009**, 34 (10), 1068-1133.
- Ma, H.-Y.; Tong, L.-F.; Xu, Z.-B.; Fang, Z.-P., *Adv. Funct. Mater.* **2008**, 18 (3), 414-421.
- Borreguero, A. M.; Sharma, P.; Spiteri, C.; Velencoso, M. M.; Carmona, M. S.; Moses, J. E.; Rodríguez, J. F., *React. Funct. Polym.* **2013**, 73 (9), 1207-1212.
- Nguyen, T.-M.; Chang, S.; Condon, B.; Slopek, R.; Graves, E.; Yoshioka-Tarver, M., *Ind. Eng. Chem. Res.* **2013**, 52 (13), 4715-4724.
- Gaan, S.; Sun, G.; Hutches, K.; Engelhard, M. H., *Polym. Degrad. Stab.* **2008**, 93 (1), 99-108.
- Costes, L.; Laoutid, F.; Aguedo, M.; Richel, A.; Brohez, S.; Delvosalle, C.; Dubois, P., *Eur. Polym. J.* **2016**, 84, 652-667.
- Houck, H. A.; De Bruycker, K.; Billiet, S.; Dhanis, B.; Goossens, H.; Catak, S.; Van Speybroeck, V.; Winne, J. M.; Du Prez, F. E., *Chem. Sci.* **2017**, 8 (4), 3098-3108.
- De Bruycker, K.; Billiet, S.; Houck, H. A.; Chattopadhyay, S.; Winne, J. M.; Du Prez, F. E., *Chem. Rev.* **2016**, 116 (6), 3919-3974.
- Billiet, S.; De Bruycker, K.; Driessen, F.; Goossens, H.; Van Speybroeck, V.; Winne, J. M.; Du Prez, F. E., *Nat Chem* **2014**, 6 (9), 815-821.
- Roling, O.; De Bruycker, K.; Vonhören, B.; Stricker, L.; Körsgen, M.; Arlinghaus, H. F.; Ravoo, B. J.; Du Prez, F. E., *Angew. Chem. Int. Ed.* **2015**, 54 (44), 13126-13129.
- van der Heijden, S.; Daelemans, L.; De Bruycker, K.; Simal, R.; De Baere, I.; Van Paeppegem, W.; Rahier, H.; De Clerck, K., *Compos. Struct.* **2017**, 159, 12-20.

21. De Bruycker, K.; Delahaye, M.; Cools, P.; Winne, J.; Prez, F. E. D., *Macromolecular Rapid Communications* **2017**.
22. Vlaminck, L.; De Bruycker, K.; Turunc, O.; Du Prez, F. E., *Polymer Chemistry* **2016**, 7 (36), 5655-5663.
23. Sun, D.; Yao, Y., *Polym. Degrad. Stab.* **2011**, 96 (10), 1720-1724.
24. Velencoso, M. M.; Ramos, M. J.; Klein, R.; De Lucas, A.; Rodriguez, J. F., *Polym. Degrad. Stab.* **2014**, 101, 40-51.
25. Xing, W.; Song, L.; Lv, P.; Jie, G.; Wang, X.; Lv, X.; Hu, Y., *Mater. Chem. Phys.* **2010**, 123 (2-3), 481-486.
26. Wang, H.; Wang, Q.; Huang, Z.; Shi, W., *Polym. Degrad. Stab.* **2007**, 92 (10), 1788-1794.
27. Breton, G. W.; Turlington, M., *Tetrahedron Lett.* **2014**, 55 (33), 4661-4663.



## 8. Conclusions

The side chains of poly(phosphoester)s are well-accessible to introduce functionalities which can react in polymer analogous reactions to further tune their properties or to obtain smart materials for potential biomedical or flame-retardant applications.

The joining of two natural adhesives, the catechol motif and phosphate units, produces PPEs which may be interesting for nanocarrier functionalization, e.g. magnetite nanoparticles, or for the formation of adhesive gels for drug delivery or (soft) tissue engineering.

The versatile furan functionality in PPEs allows thermoreversible Diels-Alder reaction with maleimides and may allow the development of reversible gels and novel drug carriers. Furan-containing PPEs are interesting materials for thermoresponsive applications. The solubility of PPEs can be altered from waterinsoluble to completely watersoluble, depending of the used maleimide derivative. Furthermore, PPE-electrolytes are accessible by the polymer analogous reaction.

Degradation of PEEP, furfuryl-containing copolymers, and DA-modified copolymers under basic conditions take predominantly place in the backbone of the polymer. This finding is important and favorable, when degradation of the material is desired.

Surface-attached poly(phosphoester)-networks, obtained from benzophenone-containing PPEs, show highly hydrophilic properties and might be interesting (protein-repellent) coatings for biomedical devices.

The optimization of the synthetic protocol of 2-chloro-2-oxo-1,3,2-dioxaphospholane, using oxygen from air instead of molecular oxygen from a gasbottle, establishes easy access to this important precursor molecule and avoids wasting of oxygen. The use of catalytic amounts of  $\text{CoCl}_2$  reduces the reaction times from days to hours.

Post-modification of the internal double bonds of ADMET-derived PPEs by TAD-chemistry allows the improvement of their thermal properties: increased decomposition temperatures, because of enhanced charring behaviour, and  $T_g$ 's above room temperature are obtained. The modification of PPEs results in a rise of the residual mass. Improvement of the thermal properties is promising for futuristic applications of PPE as flame-retardant additives.

## 9. Appendix

### 9.1 List of Publications

1. "Triazolinedione-"clicked" poly(phosphoester)s: Systematic adjustment of thermal properties"  
**Greta Becker**, Laetitia Vlaminc, Maria M. Velencoso, Filip du Prez, Frederik R. Wurm, *Polym. Chem.*, 2017, 8, 4074-4078. DOI: 10.1039/C7PY00813A.
2. "Breathing air as oxidant: Optimization of 2-chloro-2-oxo-1,3,2-dioxaphospholane synthesis as a precursor for phosphoryl choline derivatives and cyclic phosphate monomers"  
**Greta Becker**, Frederik R. Wurm, *Tetrahedron*, 2017, 73(25), 3536-3540. DOI:10.1016/j.tet.2017.05.037.
3. "Joining two natural motifs: catechol-containing poly(phosphoester)s"  
**Greta Becker**, Lisa-Maria Ackermann, Eugen Schechtel, Markus Klapper, Wolfgang Tremel, Frederik R. Wurm, *Biomacromolecules*, 2017, 18(3), 767-777. DOI: 10.1021/acs.biomac.6b01613.
4. "Reversible bioconjugation: biodegradable poly(phosphate)-protein conjugates"  
Tobias Steinbach, **Greta Becker**, Alina Spiegel, Tamiris Figueiredo, Daniela Russo, Frederik R. Wurm, *Macromolecular Bioscience*, 2017. DOI: 10.1002/mabi.201600377.
5. "Protein adsorption is required for stealth effect of poly(ethylene glycol) and poly(phosphoester)-coated nanocarriers"  
Susanne Schöttler, **Greta Becker**, Svenja Winzen, Tobias Steinbach, Kristin Mohr, Katharina Landfester, Volker Mailänder, Frederik R. Wurm, *Nature Nanotechnology*, 2016, 11(4), 372-377. DOI:10.1038/nnano.2015.330.
6. "Multifunctional poly(phosphoester)s for reversible Diels-Alder postmodification to tune the LCST in water"  
**Greta Becker**, Tristan Alexei Marquetant, Frederik R. Wurm, *submitted*.

## 9.2 Curriculum Vitae

### PERSÖNLICHES

Geburtsdatum 6. Februar 1988  
Geburtsort Goslar  
Nationalität deutsch



### AUSBILDUNG

07/2014 -09/2017 Doktorandin am **Max-Planck-Institut für Polymerforschung** und in der **Graduierten Schule "Material Science in Mainz" (MAINZ)** (Exzellenzinitiative), *Mainz, Deutschland*  
Arbeitskreis: Prof. Dr. Katharina Landfester  
Projektgruppe: Dr. habil. Frederik R. Wurm  
Promotion: "Functional poly(phosphoester)s: Variation of solubility, thermal stability, film formation and gelation"

04/2008 - 10/2013 **Johannes-Gutenberg Universität Mainz, Deutschland**  
Studium der biomedizinischen Chemie  
Abschluss Diplom-Chemiker, Abschlussnote: 1.0

08/2011 - 03/2012 **University of Massachusetts, Amherst, USA**  
Fachbereich: Polymer Science and Engineering  
Arbeitskreis: Prof. Gregory N. Tew  
Synthese und Evaluierung zellpenetrierender Peptide und dem Effekt der Polymerarchitektur auf deren Membraninteraktion

08/2000 - 06/2007 **Ratsgymnasium Goslar, Deutschland**  
Abschluss Allgemeine Hochschulreife (Abschlussnote: 1.9)

### PRAKTISCHE ERFAHRUNGEN

01 - 03/2014 **BASF South East Asia Pte. Ltd., Singapur**  
Praktikum im Rahmen des "Explore Together"-Programms im globalen Forschungszentrum in Singapur  
Synthese organischer Moleküle für optoelektronische Anwendungen

10 - 11/2013 & 09 - 10/2010 **H.C. Starck, Goslar, Deutschland**  
Studentische Hilfskraft in der Gasanalytik der zentralen Analytik und Qualitätsprüfung  
Kontrolle der Betriebsproben auf deren Gasgehalt zur Produktionsüberprüfung

01 - 10/2013 **Max-Planck-Institut für Polymerforschung, Mainz, Deutschland**  
Arbeitskreis: Prof. Dr. Katharina Landfester  
Diplomarbeit: "The Stealth Effect of Poly(phosphoester)s"

10/2012 - 01/2013 **Max-Planck-Institut für Polymerforschung, Mainz, Deutschland**  
Arbeitskreis: Prof. Dr. Klaus Müllen  
Studentische Hilfskraft  
Synthese phosphor- und borhaltiger Dendrimere

## STIPENDIEN UND AUSZEICHNUNGEN

09/2016	1. Preis im <b>Springer Oral Award</b> Kontest auf der APA'16
09/2015	Posterpreis <b>Wiley Polymers Poster Award</b> auf dem ACS workshop "Polymers in Medicine and Biology" 2015
07/2015	Posterpreis <b>MDPI Polymers Poster Award</b> auf der IP'15
seit 07/2014	Stipendiatin der <b>Graduierten Schule MAINZ</b> (Exzellenzinitiative)
10/2014	<b>Procter&amp;Gamble Award</b> , Förderpreis für eine ausgezeichnete Diplomarbeit
08/2011 - 03/2012	<b>ISAP-Stipendium</b> (DAAD) für internationale Studien- und Ausbildungspartnerschaften

## WEITERE QUALIFIKATIONEN

09/2016	1-wöchige GDCh-Fortbildung: "Geprüfter Projektmanager Wirtschaftschemie"
01/2016 - 01/2017	Promovierendensprecherin der <b>Graduierten Schule MAINZ</b>
2-tägige Workshops	Projektmanagement Kommunikation und Konfliktmanagement Selbstpräsentation und Körpersprache Präsentationsseminar Interkulturelles Bewusstsein BWL für Nicht-BWLER
01/2015 - 08/2016	Mentee im Programm <b>MentMainz</b> der Graduierten Schule MAINZ
09/2007 - 02/2008	<b>Europäischer Freiwilligendienst</b> (EFD), Kattegatcentret, <i>Grenaa, Dänemark</i>
2002 - 2007	Ehrenamtliches Engagement in den <b>ev. Kirchengemeinden Schlewecke-Göttingerode</b> und <i>Immenrode</i> Mitarbeiterin in der Jugendarbeit und beim Kindergottesdienst, Betreuung der Konfirmandenseminarfahrten
Forschungsinteresse	Polymerchemie, bioabbaubare Polymere, Poly(phosphoester), Kolloidchemie, Catechole, Phosphorchemie
Tech. Kenntnisse	Ringöffnende Polymerisation (ROP) und -Metathesepolymerisation (ROMP), Acyclische Dienmetathese-Polymerisation (ADMET), Spin-coating, Miniemulsionspolymerisation, fortgeschrittene organische Synthesetechniken
Analyt. Methoden	NMR, GPC, IR, UV-VIS, DLS, Zeta-Potential, Partikelladungsdetektion, Massenspektrometrie, Ellipsometrie, Kontaktwinkel
Fremdsprachen	englisch (fließend), dänisch (Grundkenntnisse), französisch (Grundkenntnisse), latein (Latinum)
EDV Kenntnisse	MS Office (sehr gut), ChemDraw (sehr gut), EndNote (sehr gut), Origin (gut), MestReNova (gut), ImageJ (gut), ChemSketch (gut), GIMP (gut), LaTeX (Grundkenntnisse)

## LEHRE

- 04/2015 - 03/2016 Leitung des Tutoriums begleitend zur Vorlesung "Einführung in die organische makromolekulare Chemie" und Betreuung der Vorlesungsexperimente
- 2015-2016 wissenschaftliche und praktische Betreuung einer studentischen Hilfskraft, Bachelorstudent, Erasmusstudent, Auftragspräparat im student. Fortgeschrittenenpraktikum organische Chemie

## AUSLANDSAUFENTHALTE

- 08/2016 Forschungsaufenthalt an der **Universität Gent, Gent, Belgien**  
Arbeitskreis: Prof. Filip du Prez
- 06/2014 Forschungsaufenthalt am **Paul Scherrer Institut (PSI), Villigen, Schweiz**
- 01/2014 - 03/2014 **BASF South East Asia Pte. Ltd., Singapur**  
Auslandspraktikum
- 08/2011 - 03/2012 **University of Massachusetts, Amherst, USA**  
Auslandssemester
- 09/2007 - 02/2008 **Kattegatcentret, Grenaa, Dänemark**  
Europäischer Freiwilligendienst (EFD)

## KONFERENZEN UND SOMMERSCHULEN

- 2017 MAINZ Master Class on "Supramolecular functional Materials", *Budenheim, Deutschland*- Posterpräsentation
- 2016 APA'16 - International Conference on Advanced Polymers, Biomaterials, Bioengineering & Nano Drug Delivery, *Flic-en-Flac, Mauritius* - Vortrag
- 132th BASF International Summer Course 2016, *Ludwigshafen, Deutschland*  
- Posterpräsentation
- Bayreuth International Summer School on "Advanced Polymers in Engineering and Energy" 2016, *Bayreuth, Deutschland*
- Seminarfahrt der Graduierten Schule MAINZ, *Dublin, Irland* - Vortrag
- 2015 ACS workshop - Polymers in Medicine and Biology, *Santa Rosa (CA), USA*  
- Posterpräsentation
- IP'15 - International Symposium on Ionic Polymerization, *Bordeaux, Frankreich*  
- Posterpräsentation
- Makromolekulares Kolloquium 2015, *Freiburg, Deutschland*
- Seminarfahrt der Graduierten Schule MAINZ, *Lissabon, Portugal*  
- Posterpräsentation
- 2014 Seminarfahrt der Graduierten Schule MAINZ, *Prag, Tschechische Repu*